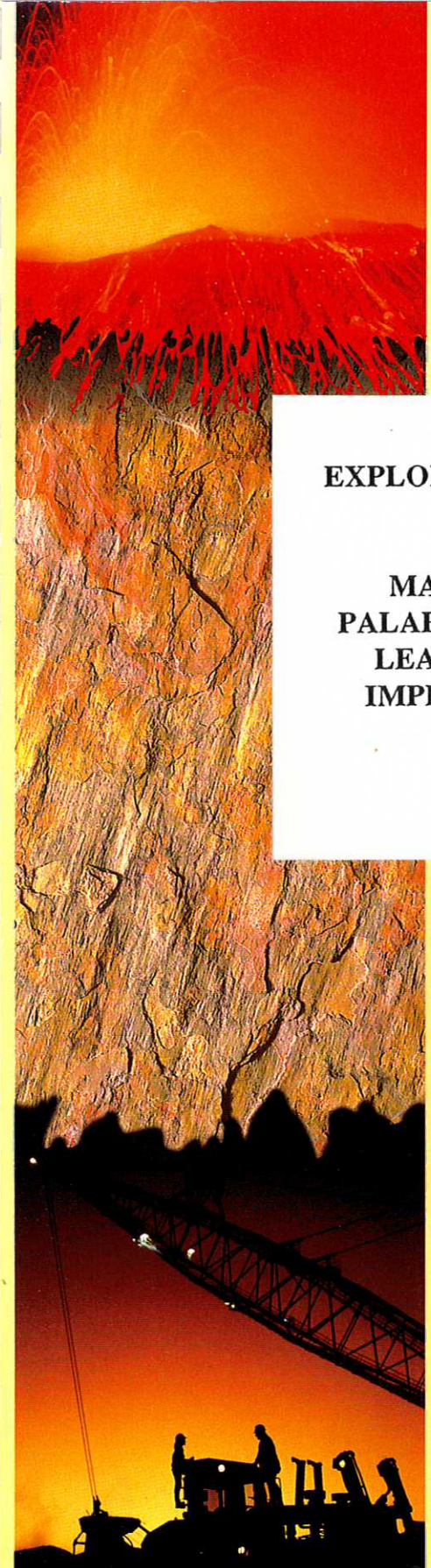

EXPLORATION AND MINING REPORT 6C

MAGNETIC PETROPHYSICS AND PALAEOMAGNETISM OF THE FITZROY LEASES, CENTRAL QUEENSLAND - IMPLICATIONS FOR EXPLORATION (QMC/CSIRO-8)

D.A. Clark

CSIRO
AUSTRALIA

EXPLORATION
DIVISION OF
AND MINING

Institute of Minerals, Energy & Construction

CSIRO
AUSTRALIA

DIVISION OF EXPLORATION AND MINING
Institute of Minerals, Energy and Construction

EXPLORATION AND MINING REPORT 6C

MAGNETIC PETROPHYSICS AND PALAEOMAGNETISM OF THE FITZROY LEASES, CENTRAL QUEENSLAND - IMPLICATIONS FOR EXPLORATION (QMC/CSIRO-8)

D.A. Clark

Prepared for QMC Ltd

March 1994

CSIRO Division of Exploration and Mining
PO Box 136, North Ryde, NSW, Australia 2113

THIS IS A CONFIDENTIAL REPORT TO
QUEENSLAND METALS CORPORATION LTD
AS PART OF THE FITZROY PROJECT

NO PART OF THIS REPORT IS TO BE MADE PUBLIC OR DISTRIBUTED
WITHOUT THE PERMISSION OF BOTH
THE EXPLORATION MANAGER, QMC LTD

and

The Chief, CSIRO Division of Exploration and Mining

Distribution List

	No. of Copies
Mr D. Horton, Queensland Metals Corporation	2
Dr B.E. Hobbs, Chief, CSIRO Division of Exploration and Mining	1
Mr D.A. Clark, CSIRO Division of Exploration and Mining	1
Dr P.W. Schmidt, CSIRO Division of Exploration and Mining	1
Records Section (North Ryde)	1

Copy No. 3 of 6 copies

LIST OF TABLES

LIST OF FIGURES

APPENDICES

EXECUTIVE SUMMARY

A sampling programme (243 oriented samples from 97 sites, plus 41 partially oriented drill core samples) has been carried out to provide a database of magnetic properties for the QMC Fitzroy Leases. The objectives of this study were to assist and constrain interpretation of the detailed aeromagnetic survey and to use palaeomagnetism to correlate volcanic units within the area and to provide structural information on local tilting. All major rock units within the area were sampled, with particular emphasis on the Rookwood Volcanics. As part of this project a preliminary interpretation of the aeromagnetic data was commissioned from S. Webster of Austirex International Ltd.

The magnetic property data from this study have been entered into a Paradox 4.0 database and the resulting table has been imported into the MIPS system, along with the digital version of the preliminary magnetic interpretation map. This allows direct comparison of local magnetic signatures with "ground truth" magnetic property data and will assist continuing interpretation of the magnetics.

The main features of the magnetic property database are:

• Representative susceptibilities, natural remanent magnetisations and Koenigsberger ratios have been established for major rock types and their variability across the area has been characterised. These data constrain qualitative geological interpretation of magnetics images and will provide essential input to quantitative modelling of magnetic anomalies.

• All sedimentary rocks sampled have very low susceptibilities. The general order of susceptibilities according to rock type is: sediments < felsic volcanics < intermediate/mafic volcanics < mafic intrusives < ultramafics. Both weakly magnetic and strongly magnetic felsic intrusions are present. Devlin Creek sulphide mineralisation has very low susceptibility and remanent magnetisation.

• The Rookwood Volcanics have very variable magnetic properties at all scales. This tends to produce a characteristic busy texture in suitably processed magnetics images. There is a bimodal susceptibility distribution for the Rookwood Volcanics, reflecting distinct magnetite-poor and magnetite-rich populations. The occurrence of extensive zones of relatively weakly magnetic Rookwood Volcanics that are indistinguishable in the field from magnetic Rookwoods in other areas (e.g. South of Devlin Creek) may be due to weak but pervasive alteration in these zones. Within the weakly magnetic Rookwood Volcanics there is still sufficient variability in susceptibility that the volcanics can be mapped beneath superficial cover using high-pass filtered magnetics images (vertical derivatives or downward continued magnetics).

• For most rock types, remanence makes a subsidiary contribution to the total magnetisation, compared to induced magnetisation. Representative Q values are typically 0.2-0.5, indicating remanent intensities 20-50% of the induced magnetisation. Magnetic Rookwood Volcanics have remanent magnetisations that are slightly subordinate to, or comparable to, induced magnetisations. In pre-Cretaceous rocks, the remanence is generally dominated by a Cretaceous overprint of normal polarity, which is steeper than the present field. The effect of remanence in most cases is to augment the effective susceptibility of the rocks by 20-50% above the measured susceptibilities (up to ~100% for the Rookwood Volcanics).

• Measured susceptibility anisotropies are low (<5%), implying that magnetic anisotropy can be ignored in magnetic modelling. However the weak anisotropy defines a magnetic fabric (foliation and lineation) that provides structural information.

Palaeomagnetic study of the samples has shown that palaeomagnetism is a useful tool for correlation and structural analysis in this area. Thermal demagnetisation has isolated stable palaeomagnetic components in many samples. Rookwood Volcanics, Connors Volcanics and a number of other igneous rocks are good palaeomagnetic recorders. The main findings of the palaeomagnetic study are:

• The Rookwood Volcanics carry a stable primary Permian remanance of reversed polarity, usually strongly overprinted by a Cretaceous magnetisation of normal polarity. The primary remanence is directed very steeply downwards for flat-lying units, but is rotated away from the reference field direction for tilted units. Where the bedding attitude of the Rookwood Volcanics is unknown, it can be inferred from the characteristic Permian remanence.

• The Connors Volcanics and associated intrusions carry an apparently primary reversed polarity remanence, which is directed SW with moderate positive (downward inclination). This characteristic remanence suggests a mid-Carboniferous age for upper parts of the Connors Volcanics. Most of these units are also extensively overprinted by a Cretaceous normal component, which is directed north and steeply upwards. Where the structure of Connors Volcanic units is unknown, it should be deducible from the palaeomagnetic directions.

The main implications of this study for exploration in the Fitzroy Leases are:

• Remapping of the extent of the Rookwood Volcanics from the magnetics defines new areas, mostly under superficial cover, that are prospective for Devlin Creek type mineralisation, including a western extension of the Devlin Creek Belt beneath the Duaringa Formation..

• The magnetic property data and observed magnetic signatures suggest that the magnetic signature of Devlin Creek mineralisation should be anomalously smooth zones of lower base level within a more magnetically active background typical of normal Rookwood Volcanics. The southern portion of the Devlin Creek belt contains a magnetically quiet zone similar to that around the Devlin Creek mineralisation.

• Structural breaks within the Rookwood Volcanics are evident within high-pass filtered magnetics images. Features detected by the magnetics may be related to structural controls on mineralisation, as suggested in S. Webster's interpretation. Faulting detected in the magnetics images may constrain locations of extensions of known mineralisation.

• Contact metamorphism and alteration associated with granitoids may affect the magnetic character of Rookwood Volcanics and sulphide mineralisation in the Ohio Prospect. Sulphide mineralisation in the Ohio area may be magnetic due to the presence of monoclinic pyrrhotite, in contrast to the Devlin Creek mineralisation.

• The Langdale Hill intrusion lies along a linear NNW-trending belt of porphyry intrusions that is associated with a magnetic anomaly, although the altered sulphide-bearing porphyry samples collected at Langdale Hill have very weak magnetisations. High-resolution magnetics could indicate potentially mineralised alteration zones within porphyry intrusions in this belt as local areas of smooth magnetic relief within magnetically active zones associated with unaltered portions of intrusions.

• The palaeomagnetism of the Langdale Hill intrusion indicates a westerly plunge of ~55° for the intrusion. Tilting of the intrusion could have implications for drill targetting and for interpretation of drilling data in terms of zoning models.

• A more complete interpretation of the magnetic survey, including anomaly modelling constrained by magnetic property data, is now possible and should produce more definitive maps of the surface and solid geology, particularly if integrated with radiometric and remote sensing data and recent mapping. Detailed analysis and modelling of the magnetic responses over the Devlin Creek, Ohio and Langdale Hill Prospects is required to define signatures of mineralisation and/or alteration that can be used for identification of prospective areas elswhere within the Fitzroy Leases. The magnetic petrology of the Rookwood Volcanics requires further study, to define the processes that create and destroy magnetic minerals in these rocks. This would assist interpretation of the magnetics in terms of geology and allow the significance of magnetic responses over mineralised areas to be assessed. Correlations and structural information derived from paleomagnetic data should be incorporated into the regional tectonic model that is being developed for the area.

1. INTRODUCTION

This report details and summarises results of a pilot magnetic petrophysical/palaeomagnetic study of rocks from the QMC Fitzroy Leases and discusses implications for interpretatation of the Austirex aeromagnetic survey of this area. Applications of this study to exploration and recommendations for further work are discussed at the end of this report.

The objectives of this study were to assist and constrain interpretation of the detailed aeromagnetic survey and to use palaeomagnetism to correlate volcanic units within the area and to provide structural information on local tilting. The aeromagnetic data can be used to improve the outdated regional mapping of this area, which was carried out by the BMR in the 1960s, in order to provide a framework for exploration. More specifically, delineation of all possible occurrences of Rookwood Volcanics within the leases is important, because these rocks host the Devlin Creek mineralisation and are therefore prospective for similar, perhaps more economic, deposits. The detailed aeromagnetic data also have the potential to indicate prospective areas within the Rookwood Volcanics and to guide drilling, once there is sufficient understanding of the magnetic signatures of mineralisation and the mineralised environment within the background signature of the host rocks.

Although magnetic surveys provide an extremely cost-effective tool for regional mapping and, in favourable circumstances, for drill targetting, interpretation of magnetic surveys is afflicted with ambiguity. This ambiguity includes the fundamental non-uniqueness of source geometry in potential field modelling and the weak correlation between rock type and magnetisation, which often confuses qualitative interpretation when "ground truth" control is lacking. This leads to the situation where magnetics images indicate a wealth of geological information, but extraction of this information is equivocal. The most practical solution to the problem of ambiguity is to constrain the interpretation with reliable magnetic property data. This study has assisted preliminary analysis of the aeromagnetic data and the quantitative information that has been entered into the MIPS GIS can provide essential input to more detailed interpretation, including modelling of anomalies in key areas.

2. SAMPLING

A sampling programme (243 oriented samples from 97 sites, plus 41 partially oriented drill core samples) was carried out to provide a database of magnetic properties for the QMC Fitzroy Leases. All major rock units and lithologies in the study area were sampled to some extent, but sampling concentrated on the economically important Rookwood Volcanics and other volcanic units that are potentially mineralised or could be confused with the Rookwood Volcanics.

Rookwood Volcanics of the Devlin Creek belt were sampled along a west-east traverse to the east of Sulphide City, and along traverses extending from the southern parts of the Devlin Creek grid to the southern extremity of the belt. Drill core samples were obtained from DDH3, 16, 18, 19 and 27 in the Devlin Creek area. A north-south traverse in the Ohio Leases extended along most of the Ohio belt of Rookwood Volcanics. Other major occurrences of Rookwood Volcanics that were sampled include the Glenroy-Rosewood belt and the Gogango-Westwood belt. The Back Creek - Comanche belt was not sampled in this study.

Connors Volcanics and associated intrusions were sampled in the Mount McKenzie area and along the type-section (the Croydon-St Lawrence road), which is to north of the aeromagnetic survey area. Other rock types sampled include ultramafics of the Marlborough Province, Siluro-Devonian volcanics and sediments, Carboniferous sediments and volcanics, Permian sediments, Triassic Native Cat Andesite, Cretaceous trachytes and basalts, and a variety of intrusions, mainly of Permo-Triassic age.

3. METHODS

3.1 Rock Magnetic Techniques

Palaeomagnetic sampling was carried out where possible using a portable petrol-powered drill, supplemented by occasional block sampling. In most cases samples were oriented with a sun compass as well as a magnetic compass, in order to avoid errors due to local declination anomalies in the vicinity of strongly magnetised rocks. Several standard palaeomagnetic specimens were prepared from each oriented sample. Natural remanent magnetisations were measured using a CTF cryogenic magnetometer and bulk susceptibilities were measured using the CSIRO transformer bridge. A modified Digico anisotropy delineator was used for measuring susceptibility anisotropies.

Limited alternating field demagnetisation of remanence was carried out. Representative specimens from all samples were thermally demagnetised to unravel the magnetic history and define palaeomagnetic compoments acquired at various stages of the rocks' history. The resulting unblocking temperature spectra were analysed to provide information on magnetic mineralogy. Principal component analysis (Kirschvink, 1980) was used to define discrete palaeomagnetic components.

Magnetic property data were entered into a Paradox 4.0 database (QMCMAG.DB) that was then incorporated into the MIPS GIS. A database containing sampling site information (Mag_Sites) was imported into the 8 bit raster file (MAGNETIC.RVF) that contains the processed magnetic survey data, and was converted to a vector set (Mag_Sites). The magnetic properties database was also imported into MAGNETIC.RVF (dbf Mag_Res) and converted to a link vector set (Mag_Res).

3.2 Interpretation Methods

The total magnetic intensity (TMI) contour map and image provided a framework for preliminary interpretation of the gross distribution of magnetic rocks and their relative magnetisations. The distribution of the main units of economic interest and many subtle geological features were only apparent in high-pass filtered images (first vertical derivative or downward-continued). The preliminary interpretation of the disposition of Rookwood Volcanics, Connors Volcanics and Siluro-Devonian volcanics by S. Webster was based mainly on reduced-to-the-pole TMI and first vertical derivative images, in conjunction with existing geological mapping and radiometrics, and some preliminary data on magnetic properties. Other aspects of the magnetics discussed in this report reflect field observations during the sampling programme, Dr B. Dickson's analysis of the radiometric data, and results of the magnetic property study. However, definitive interpretation of the magnetics, incorporating magnetic property information into modelling and integrating with other data sets , would be the objective of a follow-up project.

4. MAGNETIC PETROPHYSICS

4.1 Magnetic Property Databases

For the outcrop samples site locations, rock unit assignments and lithological descriptions were entered into a Paradox database file along with magnetic property information. Both sample mean and site mean properties are included in the database. All locations are based upon AMG co-ordinates for zone 55, which contains the majority of sampling sites, although some sites lie east of longitude 150°E and are therefore in zone 56. The following properties are included in the database:

- bulk susceptibility in μG/Oe (to convert to SI, multiply by $4\pi \times 10^{-6}$) and some information on variability (maximum and minimum values, standard deviation),

- NRM intensity (in μG or mA/m) and direction (declination and inclination), with information on variability (maximum, minimum and standard deviation for intensities; α_{95} for directions),

- Koenigsberger ratio or Q value, which is the remanent intensity/induced intensity. This paramater indicates the relative importance of remanent and induced magnetisations.

- Anisotropy parameter A, which is equal to the major susceptibility/minor susceptibility and indicates the importance of anisotropic susceptibility.

A separate database file (QMCDDH.DB) was created for magnetic property data on drill core samples from the Devlin Creek area. Table 1 summarises the locations of magnetic sampling sites and relates these to radiometric sampling sites. Table 2 provides more information on rock types at the magnetic sampling sites. Magnetic properties of outcrop samples are listed in Table 3 and Table 4 gives magnetic properties of the drill core samples.

4.2 Susceptibilities

The most important factor affecting the susceptibility of rocks is magnetite content. Although other minerals, notably monoclinic pyrrhotite, occasionally dominate the susceptibility, for the majority of rocks magnetite is the most important magnetic mineral.The relationship between susceptibility and amount of magnetite content is almost linear for magnetite contents between ~0.1% and ~10% by volume. In this range the susceptibility is given by: $k \approx 2760v$ (μG/Oe) = $34.7v \times 10^{-6}$ SI, where v is the percentage of magnetite by volume. Thus 1% magnetite produces a fairly strong susceptibility, capable of producing large anomalies. When magnetite is absent or present in only trace amounts the relatively weak susceptibility is predominantly due to paramagnetic minerals, mainly iron-bearing silicates. The relationship between magnetic susceptibility and total iron in a rock for which all iron is contained in paramagnetic minerals (silicates, carbonates etc.) is: k (μG/Oe) $\approx 5 \times$ wt% FeO^T ($\sim 60 \times 10^{-6} \times$ wt% FeO^T, SI). Before the advent of high resolution magnetic surveys, paramagnetic rocks were regarded as "non-magnetic". However even the very small susceptibiltiy contrasts between different paramagnetic rock units produce anomalies that can be detected in modern aeromagnetic surveys.

A stacked bar histogram showing the distribution of susceptibilities, grouped according to rock type is shown in Fig. 4.1. A very broad range of susceptibilities is represented in the area,

Fig.4.1. Susceptibility distributions grouped according to rock type.

SUSCEPTIBILITY HISTOGRAMS

All Rock Types

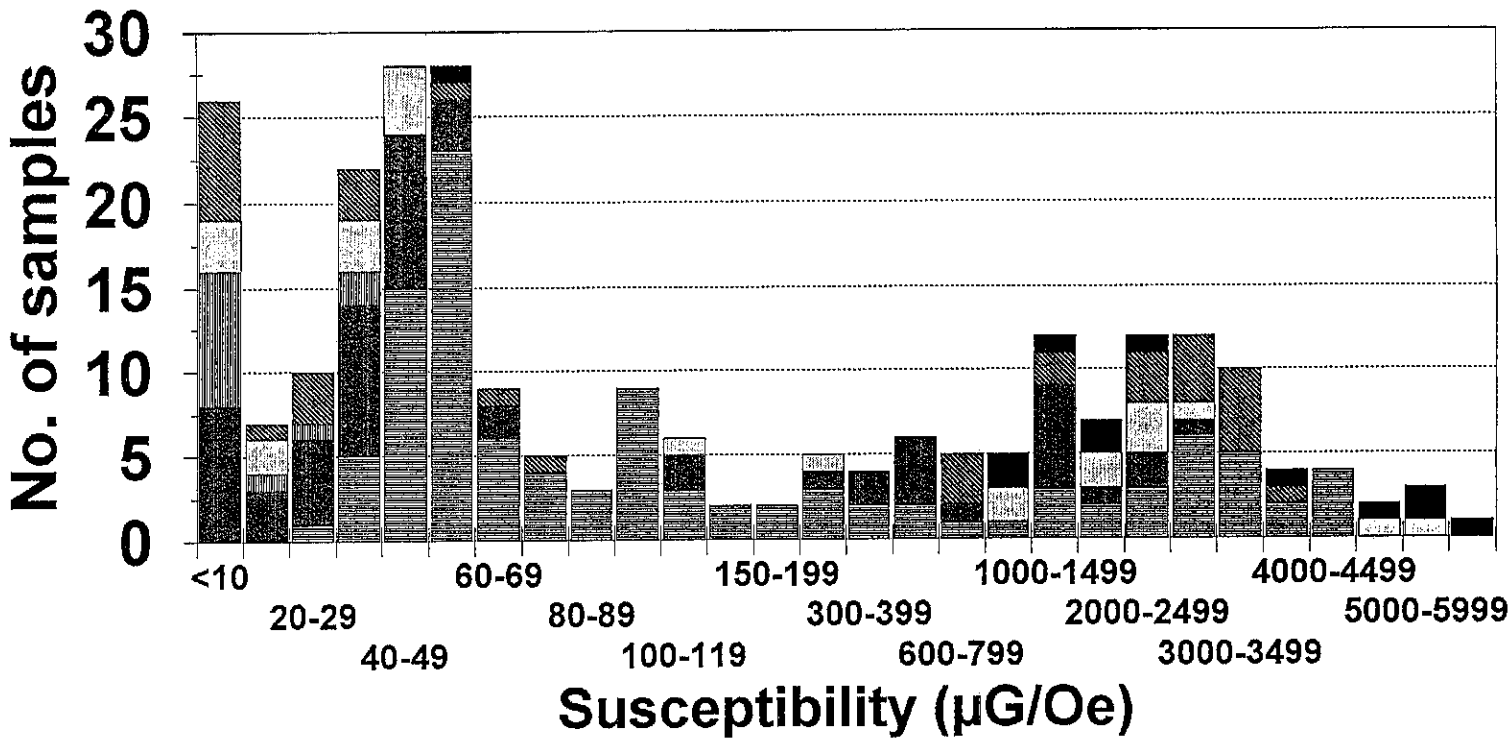

Fig.4.2. Susceptibility histogram for outcrop samples of Rookwood Volcanics.
(1 μG/Oe = 12.6×10^{-6} SI)

SUSCEPTIBILITY HISTOGRAM

Rookwood Volcanics

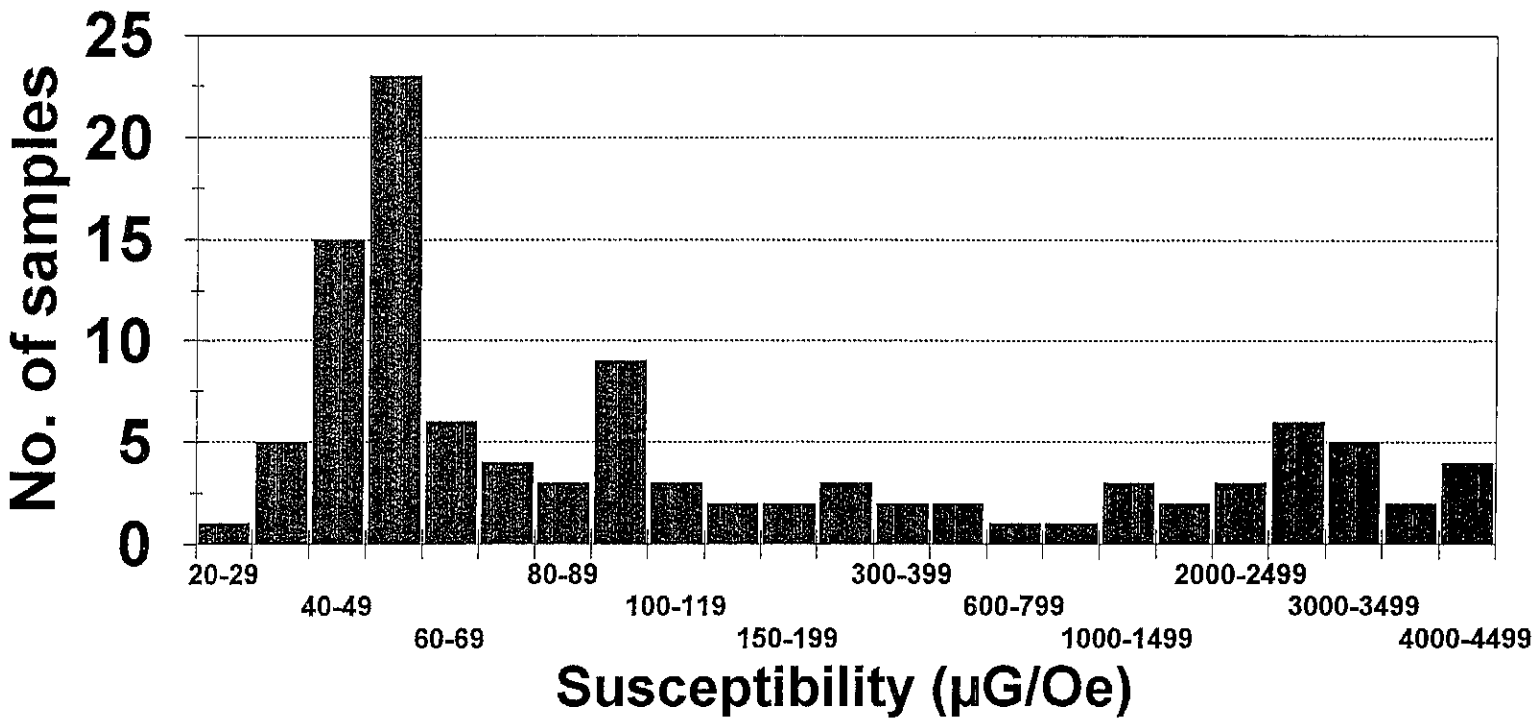

Fig.4.3. Susceptibility histogram for DDH samples of Rookwood Volcanics.

DEVLIN CREEK DDH SAMPLES

Susceptibility Histogram

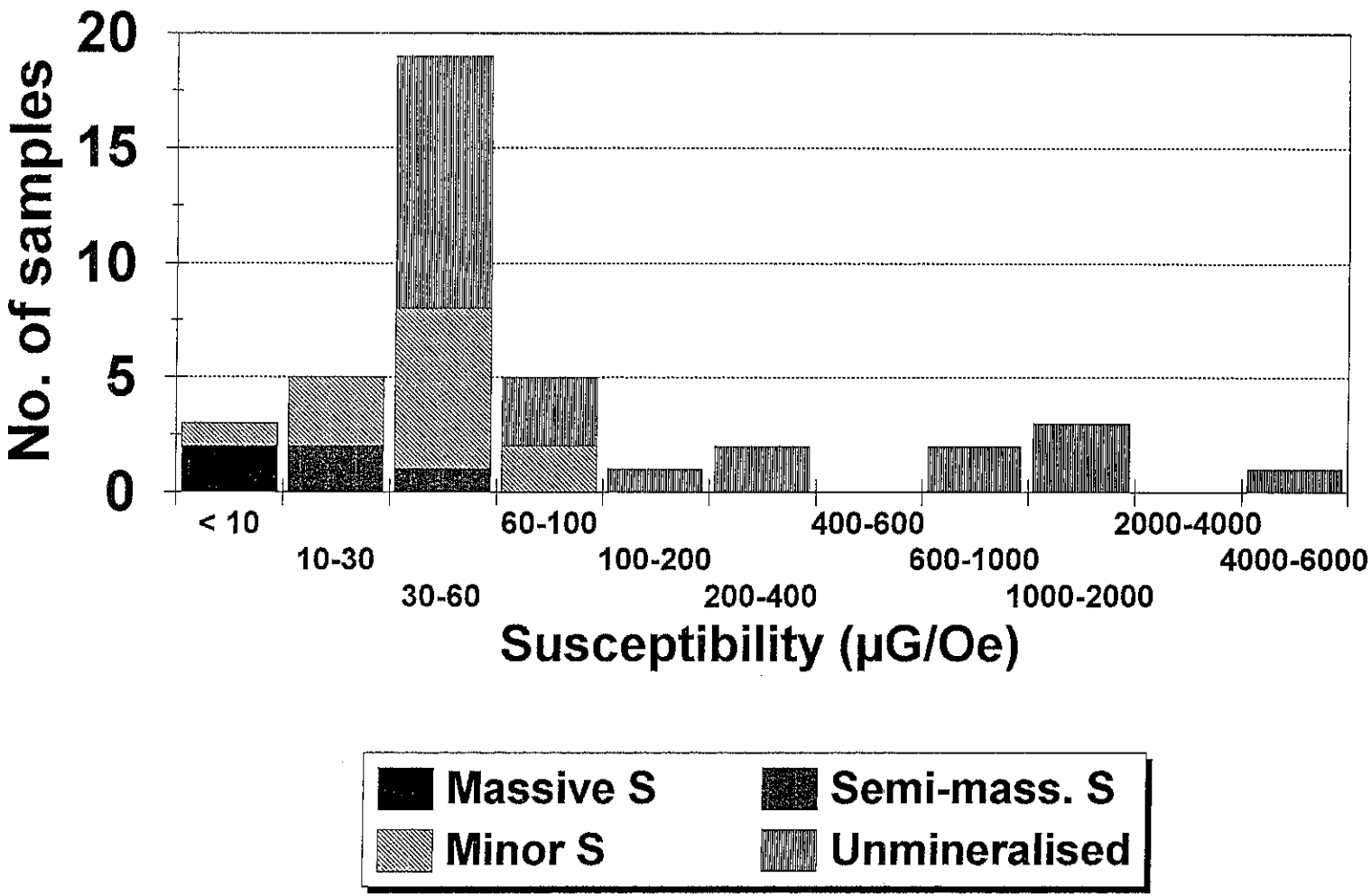

Fig.4.4. Susceptibility histogram for samples of Connors Volcanics and associated intrusions.

SUSCEPTIBILITY HISTOGRAM

Connors Volcanics

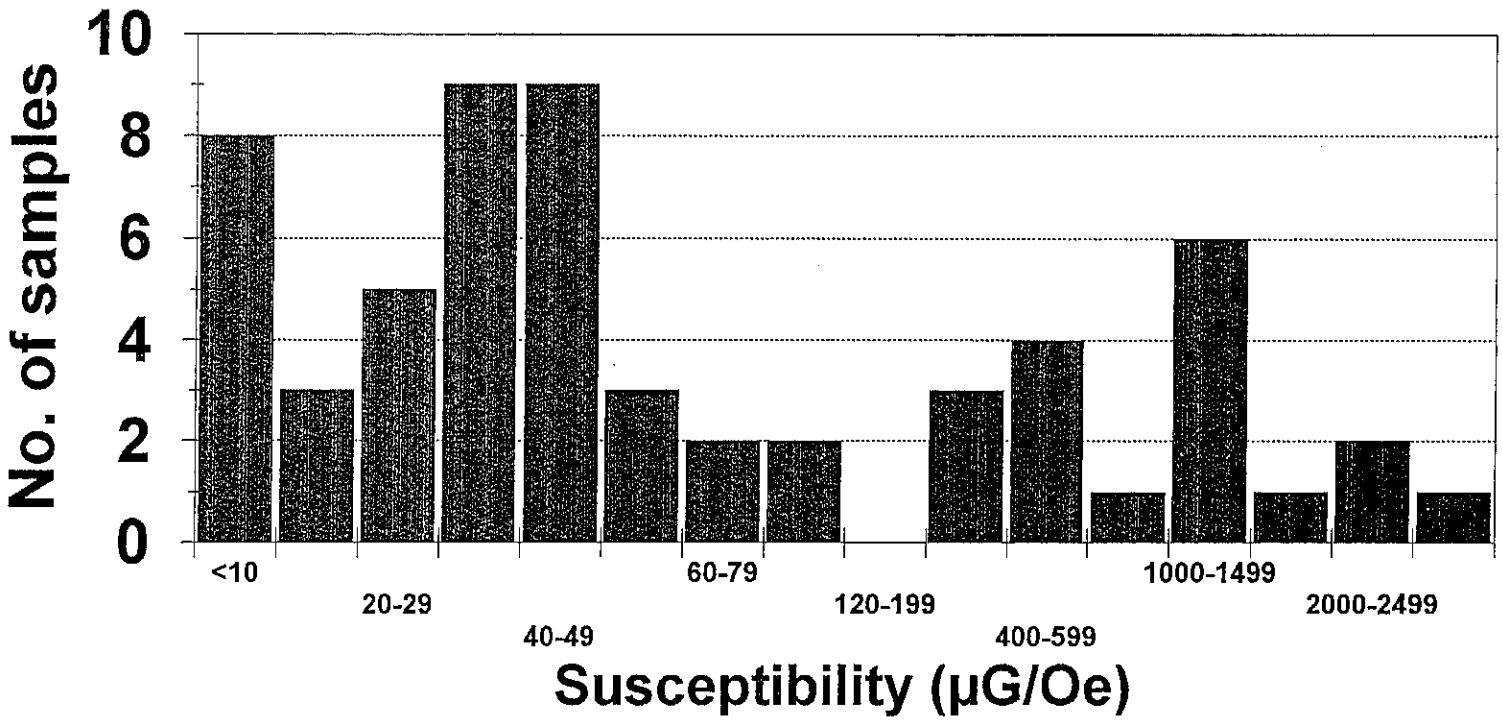

Fig.4.5. Susceptibility histogram for samples other than Rookwood Volcanics and Connors Volcanics.

SUSCEPTIBILITY HISTOGRAM

All Other Samples

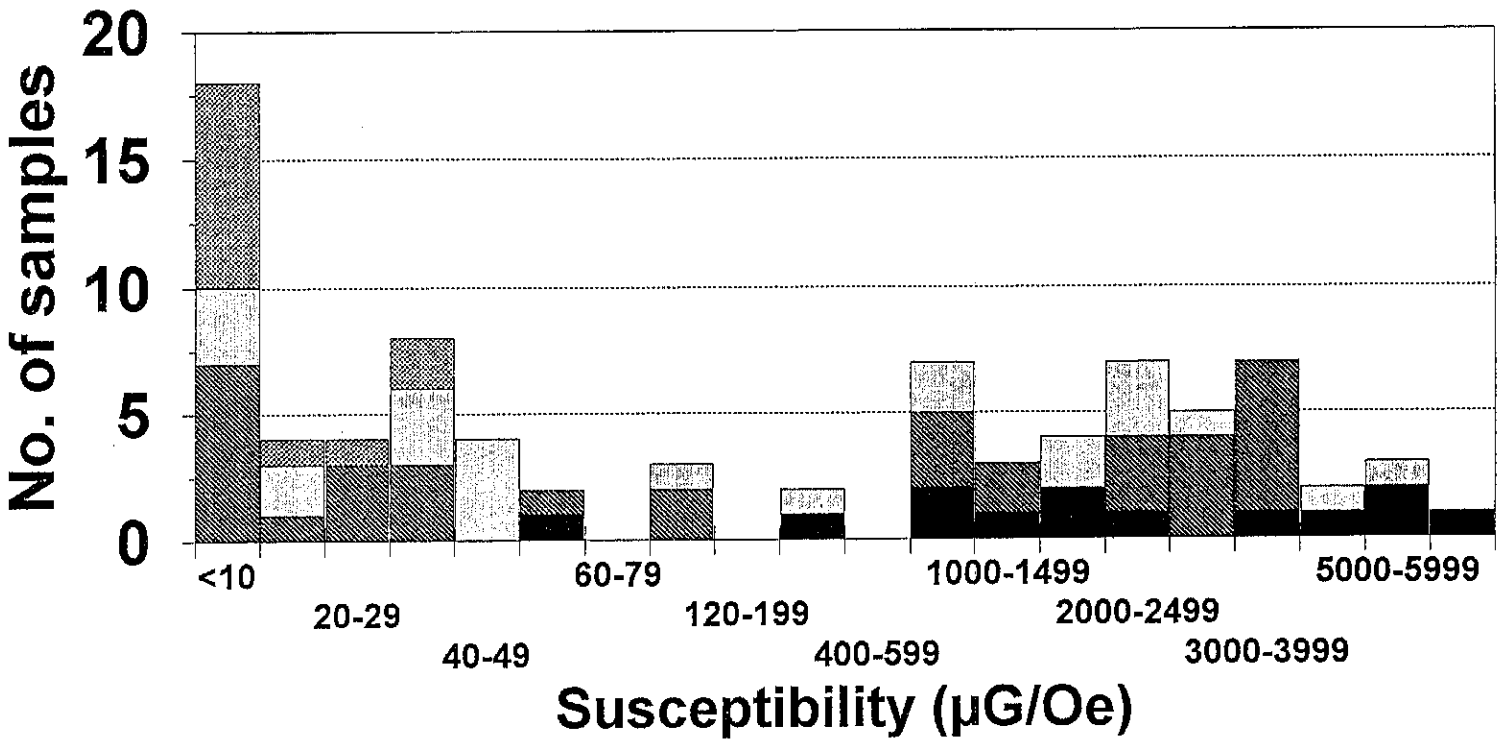

ranging from sediments with very low susceptibilities, to ultramafic rocks, which generally have the highest susceptibilities. There are three main populations within the overall distribution. A subpopulation with very low susceptibility (< 10 μG/Oe = 126 × 10^{-6} SI) comprises the majority of the sedimentary samples, and some felsic igneous rocks that contain no magnetite and have low total iron. The largest subpopulation comprises rocks with susceptibilities of 30-60 μG/Oe (380-750 × 10^{-6} SI), which have no more than trace amounts of magnetite. For these rocks the susceptibility largely reflects the paramagnetic iron content. Mafic/intermediate igneous rocks depleted in magnetite comprise most of this subpopulation.

Rocks for which magnetite dominates the susceptibility have a very broad range of susceptibilities, reflecting widely varying magnetite contents. However there is a peak in the histogram in the range 1000-4000 μG/Oe (13-50 × 10^{-6} SI), corresponding to magnetite contents of ~0.4-1.5 % by volume. The distinctly bimodal susceptibility distribution is typical for igneous and metamorphic rocks, as varying petrogenetic conditions produce distinct magnetite-poor and magnetite-rich populations. In volcanic piles it is common for individual lavas to have relatively consistent properties, but with large variations from unit to unit. Variable intensity and style of alteration and differing grades of metamorphism of magnetic rock types are also responsible for producing a bimodal susceptibility distribution.The magnetic heterogeneity occurs on a small to medium scale in many magnetic rock types, producing a characteristically variable magnetic response, which appears as a "busy" texture in high resolution magnetics images.

A susceptibility histogram for outcrop samples of Rookwood Volcanics is shown in Fig.4.2 and for drill core samples from the Devlin Creek area in Fig.4.3. Figure 4.2 illustrates a classic bimodal susceptibility distribution. The magnetite-poor subpopulation peaks at about 50 μG/Oe (60 × 10^{-6} SI), suggesting that a total iron content of ~10 wt% is typical of the Rookwood Volcanics. The magnetite-bearing population has a wide range of susceptibilities, but exhibits a mode at about 3000 μG/Oe (~40 × 10^{-3} SI), corresponding to about 1% magnetite content. The distribution of susceptibilities is not uniform across the study area. There are distinctly less magnetic and more magnetic zones within individual belts of Rookwood Volcanics and also systematic variations from belt to belt. For example the Devlin Creek belt is much more magnetic on average to the east of Sulphide City than around the mineralised area. The zone south of Sulphide Suburb contains rocks that are almost all in the paramagnetic population. These variations may reflect regional alteration systems or facies changes within the Rookwood Volcanics that may act as marker horizons.

The susceptibilities of drill core samples (Fig.4.3) show that mineralised samples are less magnetic than unmineralised samples. Massive sulphides have very low susceptibilities, as they consist largely of pyrite, with no magnetite or pyrrhotite. Although only two massive sulphide samples were collected, measurements with a hand-held susceptibility meter confirmed that sulphide-rich rocks in this area are very weakly magnetic. Semi-massive sulphides are only slightly more magnetic than massive mineralisation and Rookwood Volcanics with minor sulphides have slightly higher susceptibilities on average than more mineralised samples. Barren Rookwood Volcanics intersected in this area have a broad range of susceptibilties, but the paramagnetic samples are slightly more magnetic than sulphide-bearing rocks and the strongly magnetic subpopulation is restricted to barren volcanics. Overall the data suggest that the mineralised zone has relatively low susceptibility and the barren volcanics are significantly more magnetic overall and more heterogeneous. Relatively weakly altered grey-green lavas are

the most magnetic samples in this collection. Some purple epidote- and jasper-bearing lavas are also quite strongly magnetic.

These remarks may not translate to the Ohio leases, however, because preliminary observations of susceptibilities of drill core samples at the Ohio Prospect suggest the presence of magnetic sulphides, probably monoclinic pyrrhotite, within weakly magnetic andesites. Pyrrhotite has been logged at this prospect, suggesting that mineralisation in this area may be magnetic. Cursory hand-held susceptibility meter measurements indicate that pale massive andesites generally were paramagnetic, unless they contained sulphides, epidote-veined pillow lavas had higher susceptibilities (~500-2500 μG/Oe = 6-30 × 10^{-3} SI) and medium-grained darker basalts had susceptibilities of ~1500-2500 μG/Oe (20-30 × 10^{-6} SI).

Figure 4.4 shows the susceptibility histogram for the Connors Volcanics samples, including associated intrusions. Again there is a bimodal susceptibility distribution. Overall the Connors Volcanics tend to be somewhat less magnetic than the Rookwood Volcanics, reflecting their more felsic average composition. The very low susceptibilities correspond to rhyolitic compositions with total iron contents of < 2 wt%. Andesitic volcanics have paramagnetic and ferromagnetic subpopulations. Green alteration within the andesitic volcanics appeared to be associated with lower susceptibilities.The sampled diorites and quartz monzonite intrusions in this suite had moderate to high susceptibility, except for the altered diorite within the Mount McKenzie alteration system, which had an extremely low susceptibility (6 μG/Oe = 75 × 10^{-6} SI).

Figure 4.5 shows the susceptibility histograms for other rock units in the Fitzroy Leases. All sedimentary samples (Siluro-Devonian limestones, Carboniferous limestones and a variety of Permian sedimentary rocks) have susceptibilities less than 40 μG/Oe (500 × 10^{-6} SI), and the majority, including the limestones, have k < 10 μG/Oe (130 × 10^{-6} SI). At the other extreme, the ultramafic rocks, although very heterogeneous at all scales, generally have high susceptibilities and are the most magnetic rocks on average in the study area. The magnetite in the Marlborough Province ultramafics is not primary, but results from serpentinisation. Variable serpentinisation, controlled by structure and proximity of intrusions, acting on heterogeneous protoliths is responsible for the wide range of measured susceptibilities. Volcanic rocks exhibit a wide range of susceptibilities with a slightly bimodal distribution. Felsic volcanics of various ages are generally weakly magnetic in this area, whereas mafic/intermediate volcanics are more variable. Cretaceous basalts have high susceptibility, Triassic Native Cat Andesites have very variable susceptibility, but are quite magnetic on average. Both mafic and felsic intrusions had bimodal susceptibility distributions. Ridgelands Granodiorite, Bouldecombe Complex Granite and Permo-Triassic adamellites to diorites in the Ohio Leases are moderately to strongly magnetic, whereas a granite intruding the Marlborough Province south of Marlborough is very weakly magnetic. An associated gabbro is strongly magnetic. There is a general tendency for more mafic members of each intrusive suite to be more magnetic than felsic members.

4.3 Remanence Properties

Magnetic anomalies are caused by variations in total magnetisation within the subsurface. The induced magnetisation is the product of the susceptibility and the geomagnetic field intensity. The regional geomagnetic field is virtually constant over a limited area, such as the Fitzroy Leases, so variations in induced magnetisation correspond to changes in susceptibility. The

induced magnetisation is essentially parallel to the geomagnetic field, unless the rocks are highly anisotropic. Remanent magnetisation adds vectorially to the induced magnetisation. The presence of strong remanence complicates interpretation because the direction of magnetisation can depart substantially from the field direction and is often unknown, in the absence of remanence measurements on representative samples.. For this reason, it is important to assess the contribution of remanence and to characterise remanence directions to provide input to modelling of magnetic anomalies. Remanence measurements also provide palaeomagnetic information, which can be used for indirect dating, for correlation and for structural analysis.

Remanent magnetisation is an important contributor to magnetic anomalies when substantial volumes of rock carry remanence with a reasonably consistent direction and with intensity comparable to, or greater than, the induced magnetisation. The Koenigsberger ratio, or Q value, indicates the relative contributions of remanent and induced magnetisation for a sample or magnetic body. The geomagnetic field intensity in the Fitzroy Leases is about 52,000 nT or 0.52 Oe. Thus the Koenigsberger ratio can be calculated from the tabulated susceptibilities and remanent intensities by:

$$Q = J/kF,$$

where J is the remanent intensity in μG, k is the susceptibility in μG/Oe (i.e. 10^{-6} CGS) and F = 0.52 Oe. If Q < 1, induced magnetisation dominates, whereas Q > 1 indicates that remanent magnetisation is stronger than induced magnetisation. Some generalisations about Koenigsberger ratios are given below:

- Remanence of thermal, chemical or recent viscous origin that is carried by multidomain magnetite is characterised by Q values less than unity, typically 0.2-0.5. Multidomain magnetite has a grain size greater than ~10 μm and is the main remanence carrier in most magnetite-bearing felsic plutonic rocks, ultramafic rocks and metamorphic rocks.

- Multidomain magnetite-bearing rocks with Q values that are substantially greater than unity carry remanence that is paleomagnetic noise and is unrepresentative of the bulk *in situ* remanence. In outcrop samples lightning strikes are the main cause of anomalously high Q values. In drill core, drilling-induced magnetisation and logging with pencil magnets are common causes of unrepresentative remanence. When this occurs remanence directions tend to be very scattered. Palaeomagnetic cleaning can sometimes remove these spurious effects.

- Remanence carried by very fine-grained magnetite is often associated with high Q. Pseudosingle domain magnetite grains, a few microns in size, generally exhibit Q values in the range 1-10, and submicron single domain grains can give rise to Q values greater than 10. Rapidly cooled magnetite-bearing volcanic rocks often have high Koenigsberger ratios, as do some gabbros and diorites that contain ultrafine magnetite particles exsolved in silicates (olivines, pyroxenes or plagioclase).

- Remanence carried by monoclinic pyrrhotite or haematite usually has high Koenigsberger ratios, often much greater than one.

As discussed in the section on palaeomagnetism, the remanence of many rock types in the study area comprises superimposed components acquired at different times. A viscous

magnetisation acquired in the recent field overprints to varying degrees more ancient magnetisations. Most pre-Cretaceous rocks carry a prominent ancient component, directed steeply upward with approximately northerly declination, which overprints older, often primary, remanence. The almost ubiquitous steep up overprint component is attributed to a Cretaceous thermal event, which appears to have affected the study area and surrounding regions. The primary remanence of Permo-Carboniferous rocks has reversed polarity. Rocks of this age can have reversed NRMs, provided the remanence is sufficiently stable to prevent substantial overprinting. If the Koenigsberger ratio of such rocks is greater than unity, the total magnetisation is reversed.

Prominent magnetic lows can be produced by magnetic Permo-Carboniferous intrusions and volcanic rocks that have very fine-grained magnetite as the main remanence carrier. It is far more common, however, for the NRM of rocks in the study area to be dominated by viscous and Cretaceous components of normal polarity. In this case the remanent magnetisation is subparallel to the induced magnetisation and therefore the effect of remanence is essentially to augment the effective susceptibility to ~k(1+Q). Quantitative modelling should allow for this effect, even where the anomaly form suggests magnetisation parallel to the Earth's field, as the susceptibilities measured with a hand-held meter or in the laboratory do not fully account for the total magnetisation.

Figure 4.6 illustrates this point by plotting NRM directions for specimens from Rookwood Volcanics samples. The sterograms show that there is considerable scatter, but there is a general bias towards north and up directions. A number of specimens have downward-pointing NRMs, however, reflecting remanence dominated by a primary reversed component. Variable overprinting of reversed primary components by normal secondary components produces much of the observed scatter. The overall mean direction has normal polarity and is slightly steeper than the present field, due to the prominence of the steep Cretaceous component.

Figure 4.7 shows a histogram of Koenigsberger ratios for Rookwood Volcanics samples, grouped according to susceptibility. Magnetite is the only important remanence carrier for most Rookwood Volcanics samples. Paramagnetic samples, which have $k < 100$ μG/Oe, tend to have particularly low Q values, because they contain very little magnetite and therefore have weak remanence. Their susceptibilities are not proportionately reduced, however, because paramagnetic silicates contribute to the susceptibility, but carry no remanence. As a result, the Q value of the rock is much less than the Q value of the magnetite grains. Ferromagnetic samples, on the other hand, have susceptibilities dominated by magnetite. The Q of these samples is therefore almost equal to the Q of the magnetite grains. More than 50% of the paramagnetic samples have $Q < 0.3$ and 94% have $Q < 1$, whereas none of the ferromagnetic samples have Q below 0.3, about 40% of the ferromagnetic samples have Q in the range 0.3-1 and 60% have $Q > 1$.

The very high Koenigsberger ratios, above 3-4, however, are not representative of bulk properties, as the NRM directions from these sites are very scattered. The larger Q values, particularly those greater than 10, are attributable to lightning effects. The very intense remanence produced locally around lightning strikes can produce spiky anomalies that are prominent in ground magnetic surveys, but have negligible effects at airborne survey heights. Ignoring unrepresentative values from lightning-affected sites, typical Koenigsberger ratios for relatively magnetic portions of the Rookwood Volcanics are ~1.0 ± 0.5. Taking the scatter of NRM directions into account, an effective Q value of ~0.5-0.8 for substantial volumes of rock

Fig.4.6. NRM directions of Rookwood Volcanics samples that are unaffected by lightning.
(a) NE Devlin Creek belt, (b) S Devlin Creek belt, (c) N Ohio belt,
(d) Rannes Beds (site 70) and S Ohio belt, (e)and (f) Glenroy-Rosewood
and Gogango-Westwood belts.

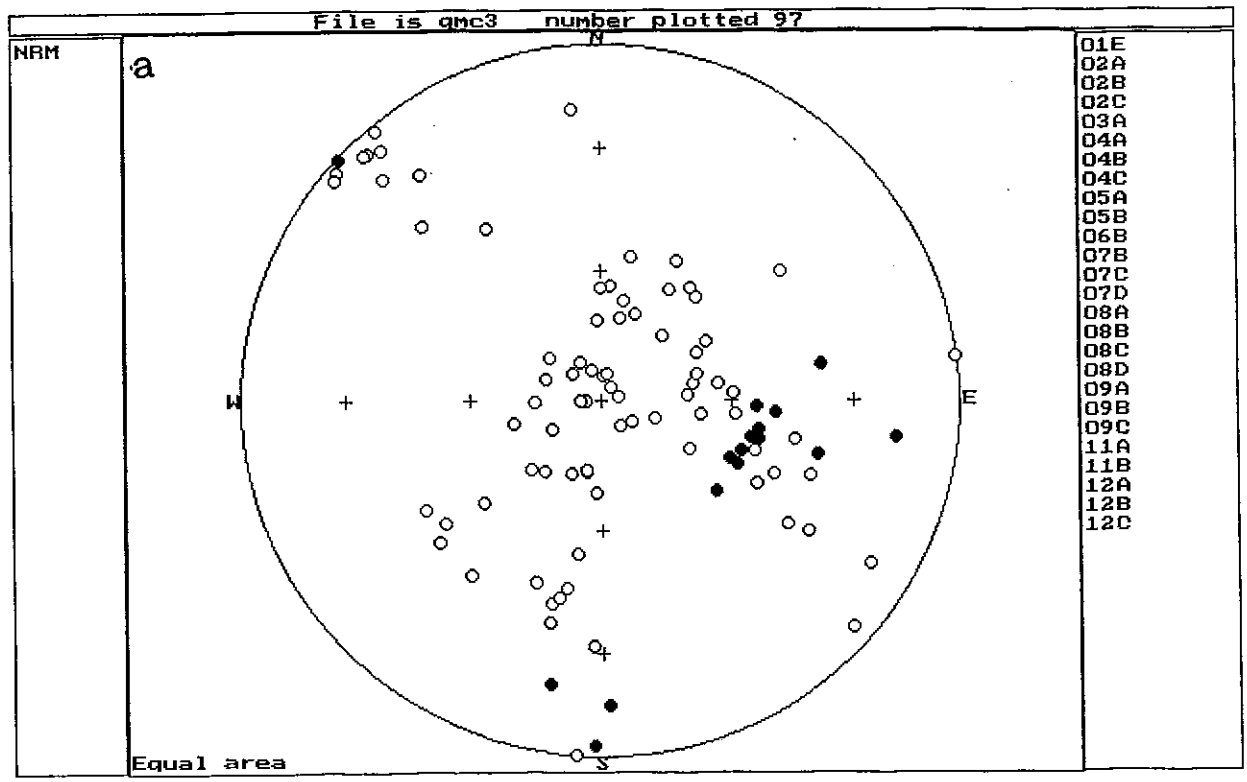
File is qmc3 number plotted 97
NRM
a
N
W
E
S
Equal area
01E
02A
02B
02C
03A
04A
04B
04C
05A
05B
06B
07B
07C
07D
08A
08B
08C
08D
09A
09B
09C
11A
11B
12A
12B
12C

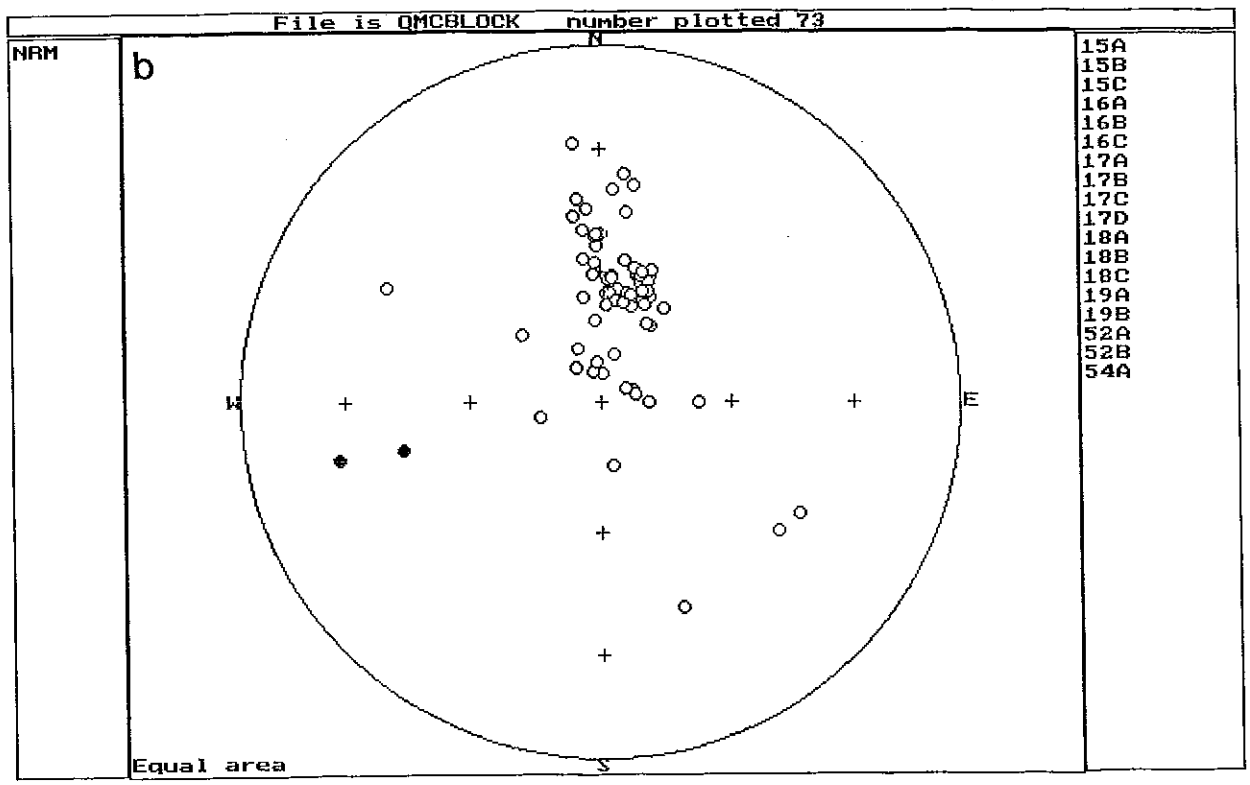
File is QMCBLOCK number plotted 73
NRM
b
N
W
E
S
Equal area
15A
15B
15C
16A
16B
16C
17A
17B
17C
17D
18A
18B
18C
19A
19B
52A
52B
54A

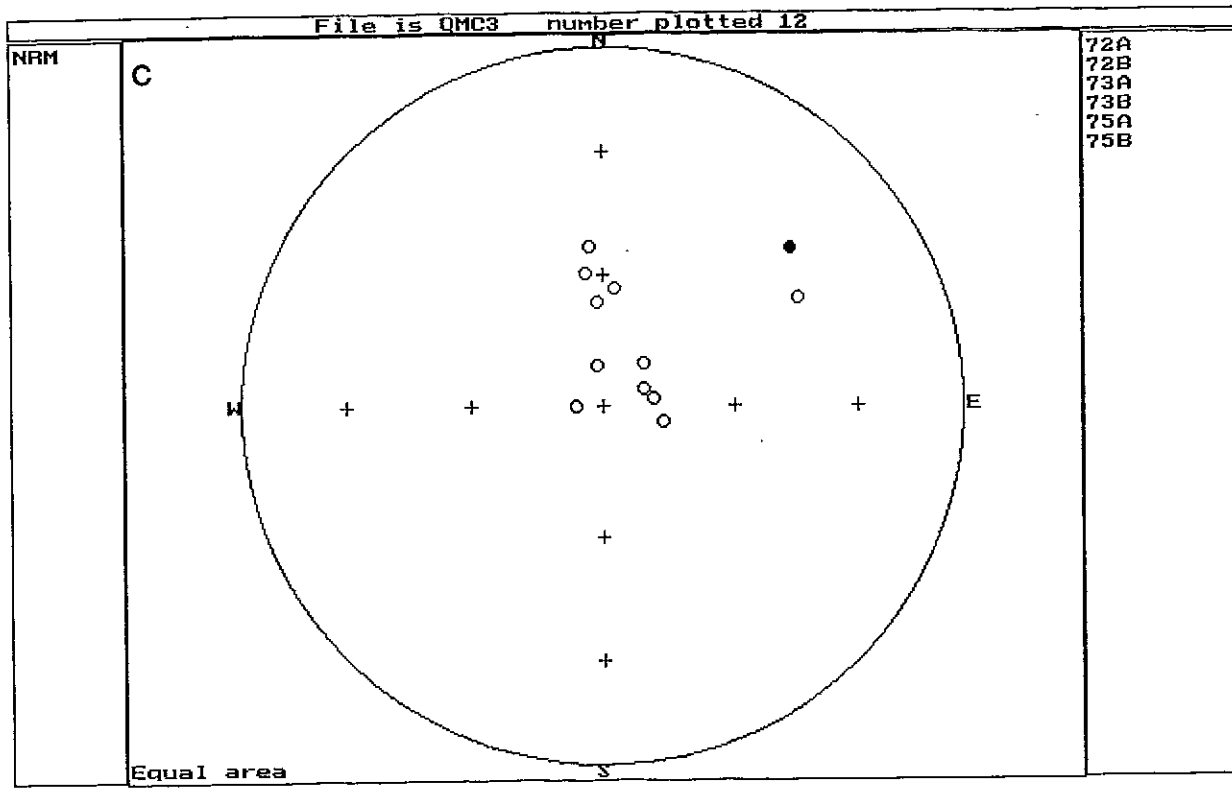
File is QMC3 number plotted 12
NRM
c
N
W
E
S
Equal area
72A
72B
73A
73B
75A
75B

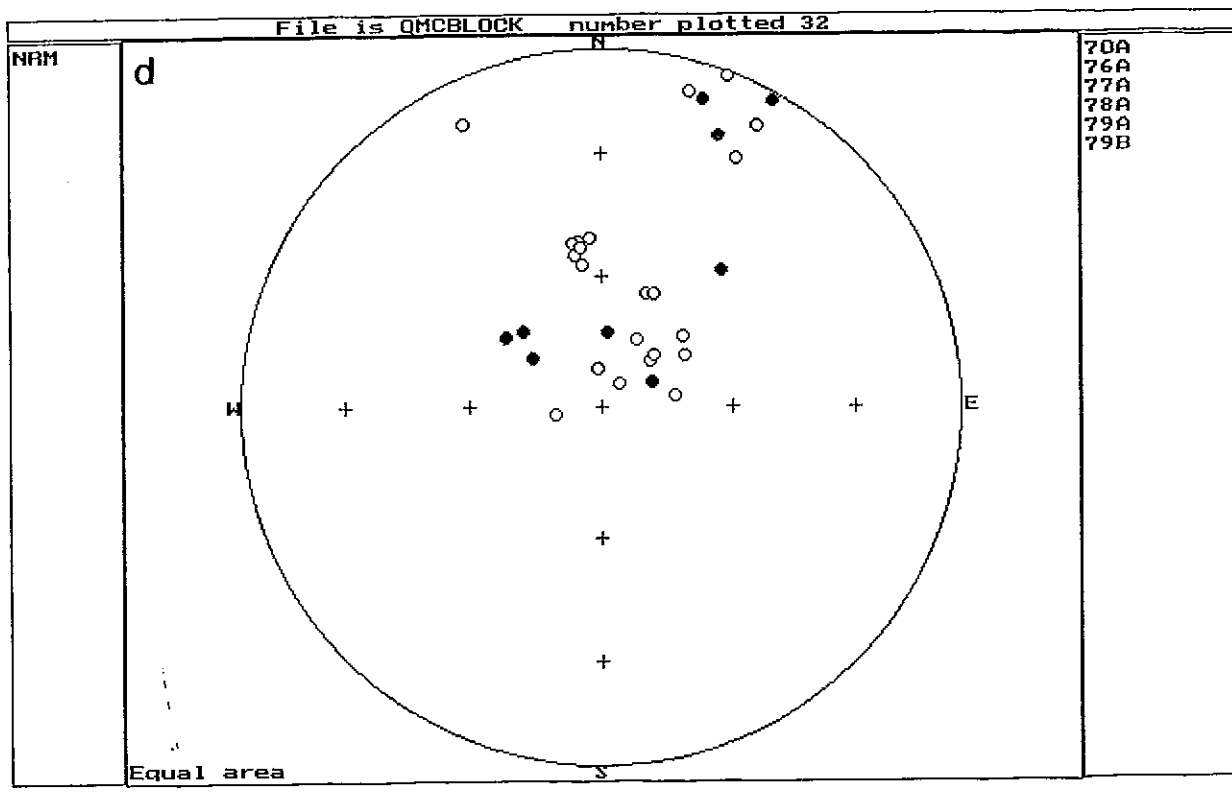
File is QMCBLOCK number plotted 32
NRM
d
N
W
E
S
Equal area
70A
76A
77A
78A
79A
79B

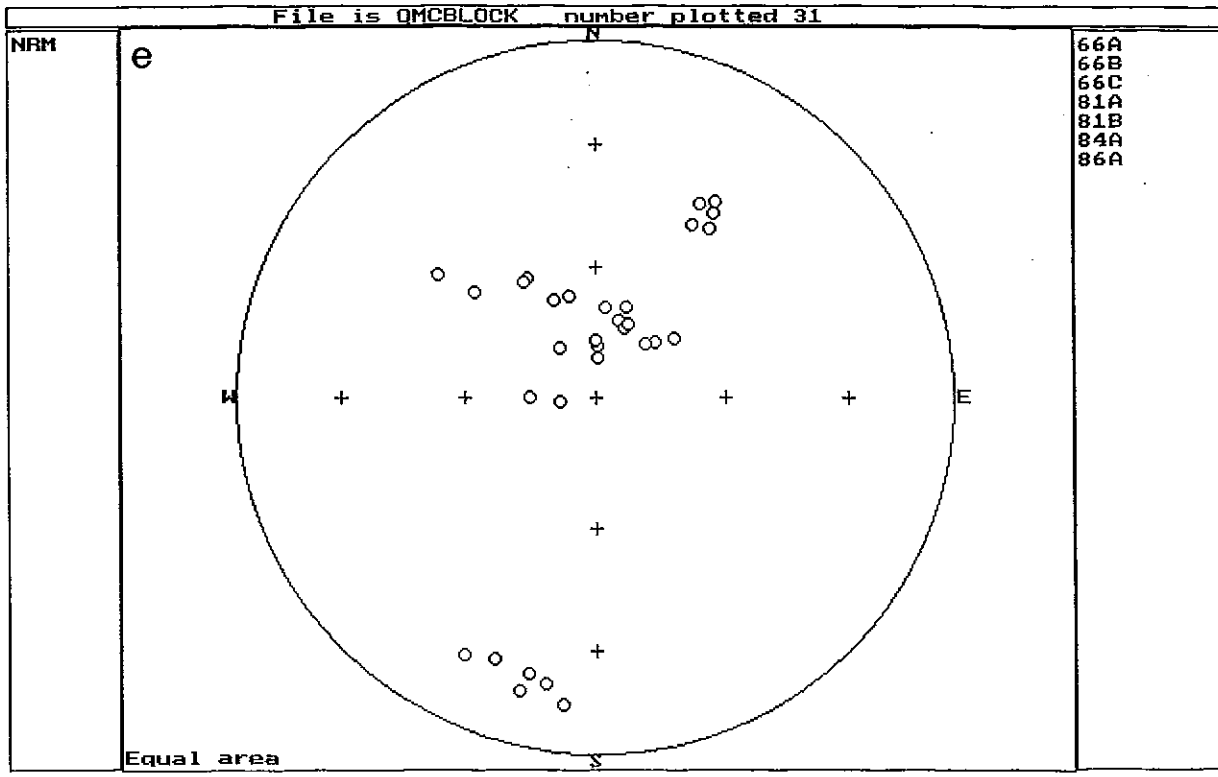
File is QMCBLOCK number plotted 31
NRM
e
N
W
E
S
Equal area
66A
66B
66C
81A
81B
84A
86A

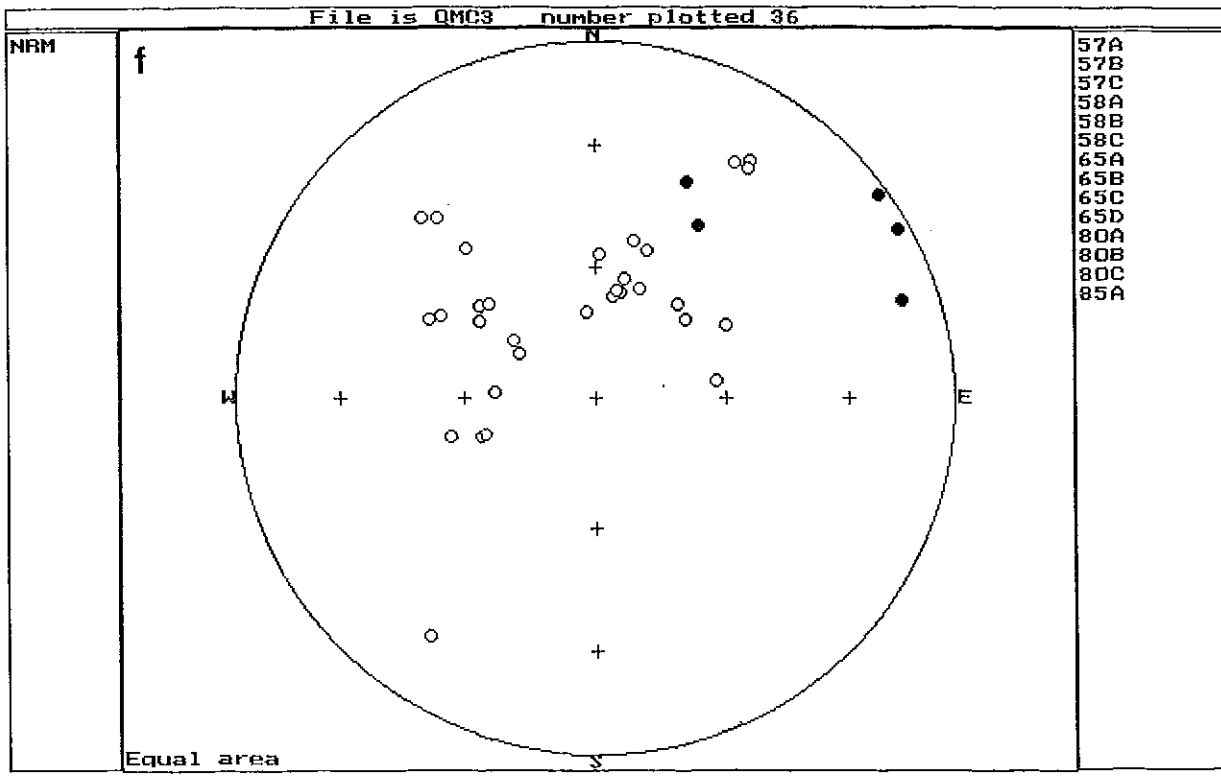
File is QMC3 number plotted 36
NRM
f
N
W
E
S
Equal area
57A
57B
57C
58A
58B
58C
65A
65B
65C
65D
80A
80B
80C
85A

Fig.4.7. Koenigsberger ratios (Q values) of outcrop samples from the Rookwood Volcanics. Paramagnetic samples have susceptibilities less than 100 μG/Oe (1.3×10^{-3} SI) and ferromagnetic samples have susceptibilities greater than this value.

KOENIGSBERGER RATIOS

Rookwood Volcanics

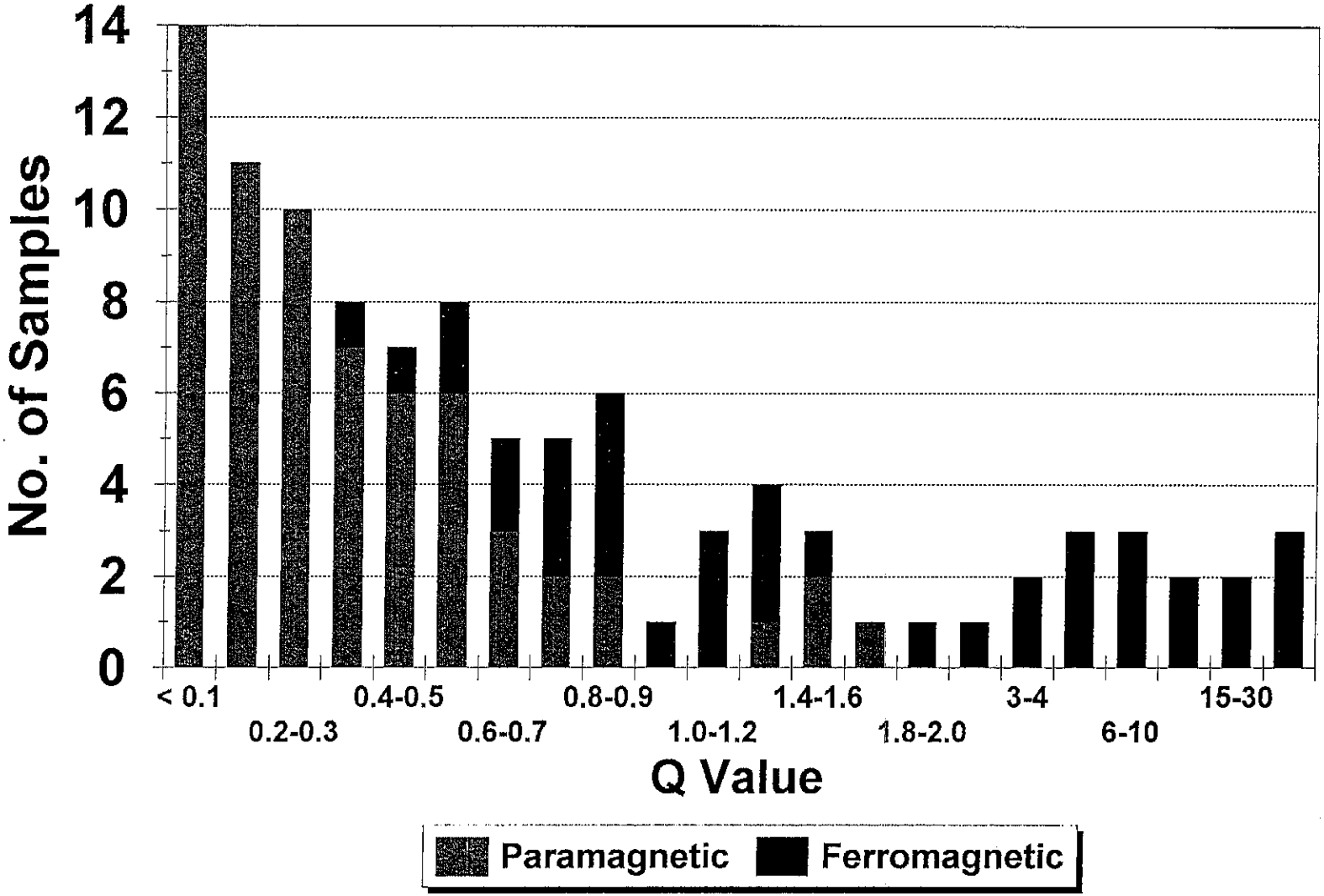

Fig.4.8. Koenigsberger ratios (Q values) of drill core samples from the Rookwood Volcanics, grouped according to their susceptibilities.

KOENIGSBERGER RATIOS

Rookwood Volcanics - DDH Samples

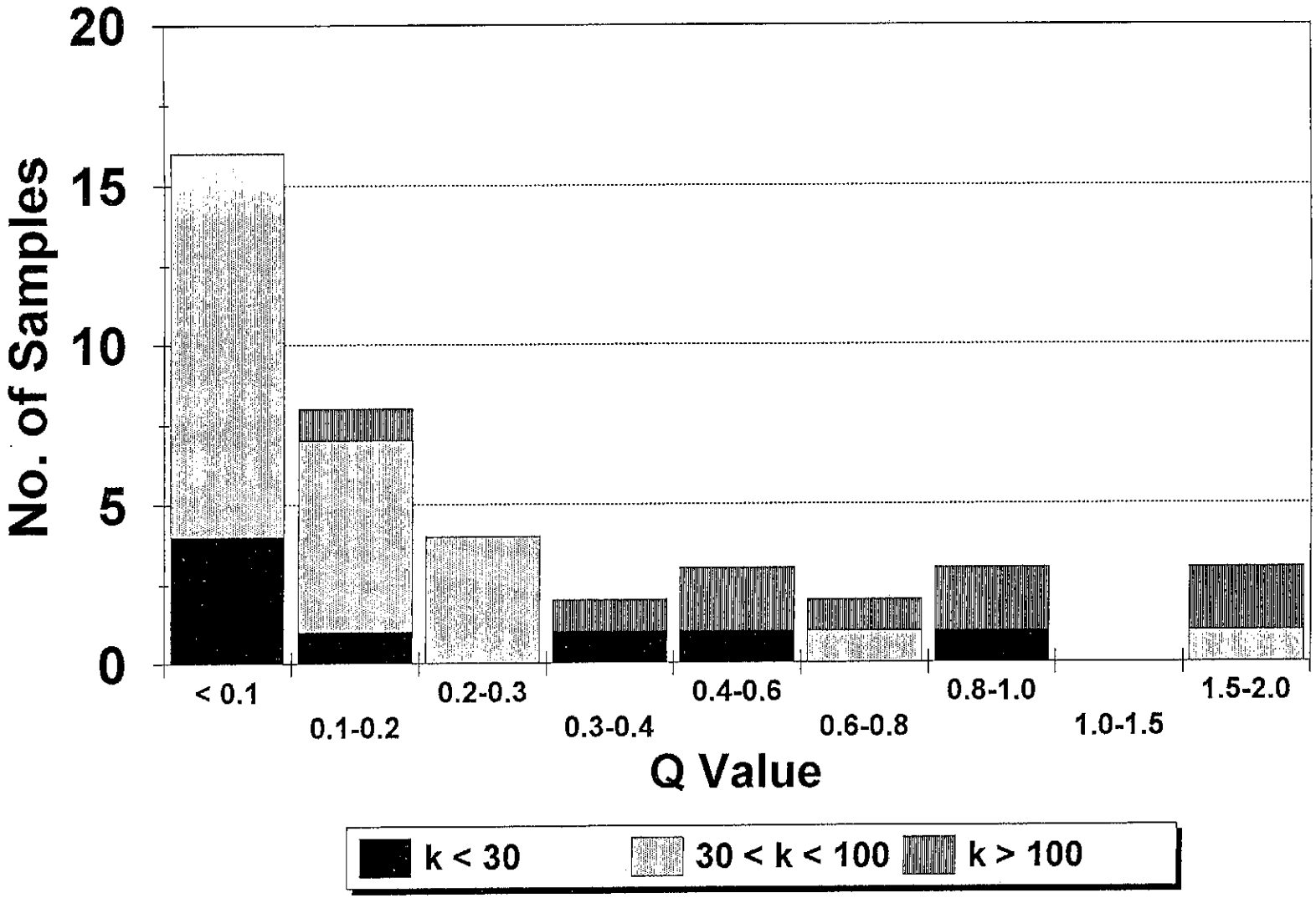

Fig.4.9. Koenigsberger ratios (Q values) of samples from the Connors Volcanics and associated intrusions, grouped according to their susceptibilities and intrusive or extrusive nature.

KOENIGSBERGER RATIOS

Connors Volcanics

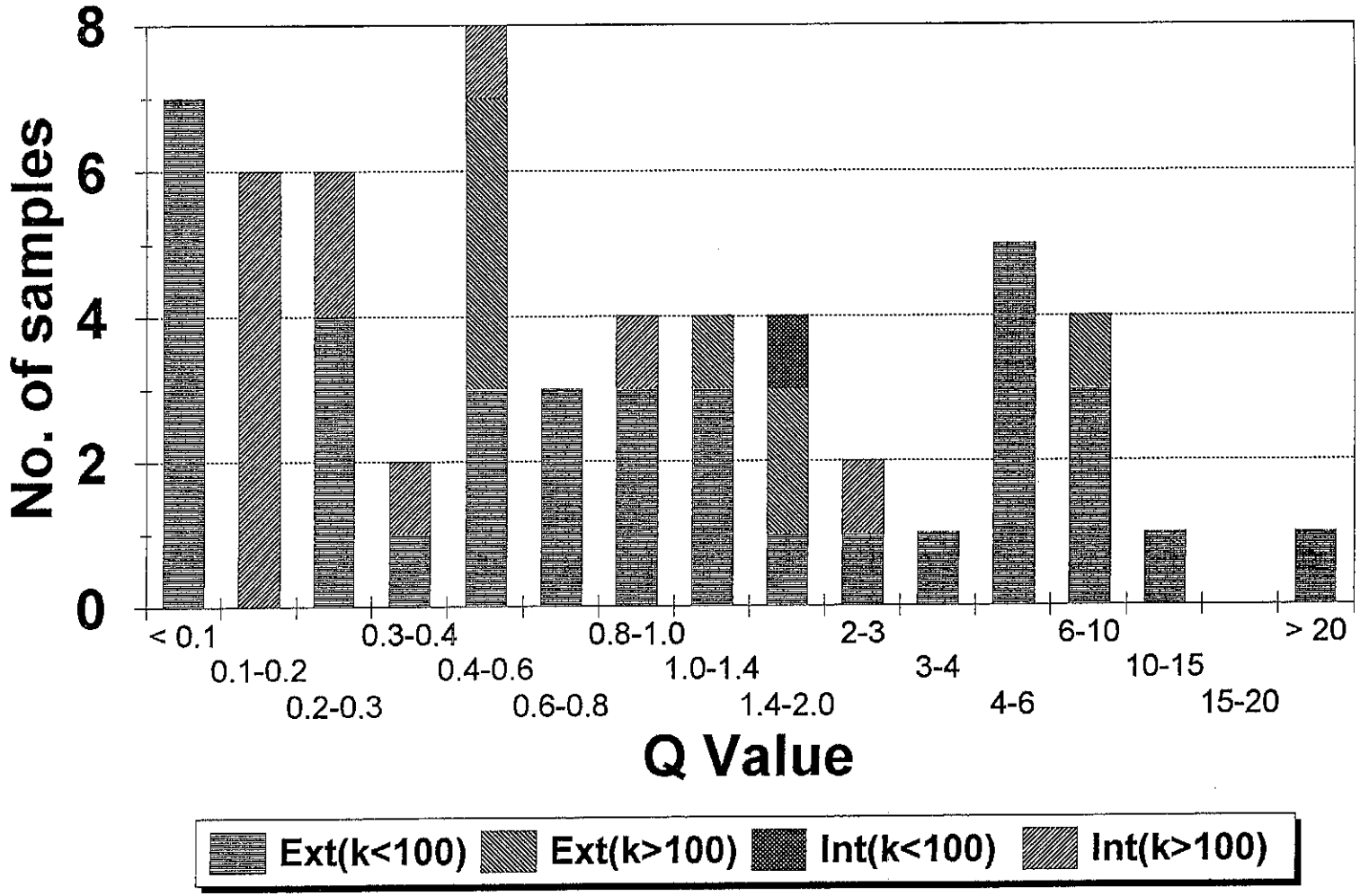

Fig.4.10. Koenigsberger ratios (Q values) of rocks other than Rookwood Volcanics or Connors Volcanics, grouped according to their susceptibilities and rock type. Susceptibility units are μG/Oe.

KOENIGSBERGER RATIOS

Other Rock Units

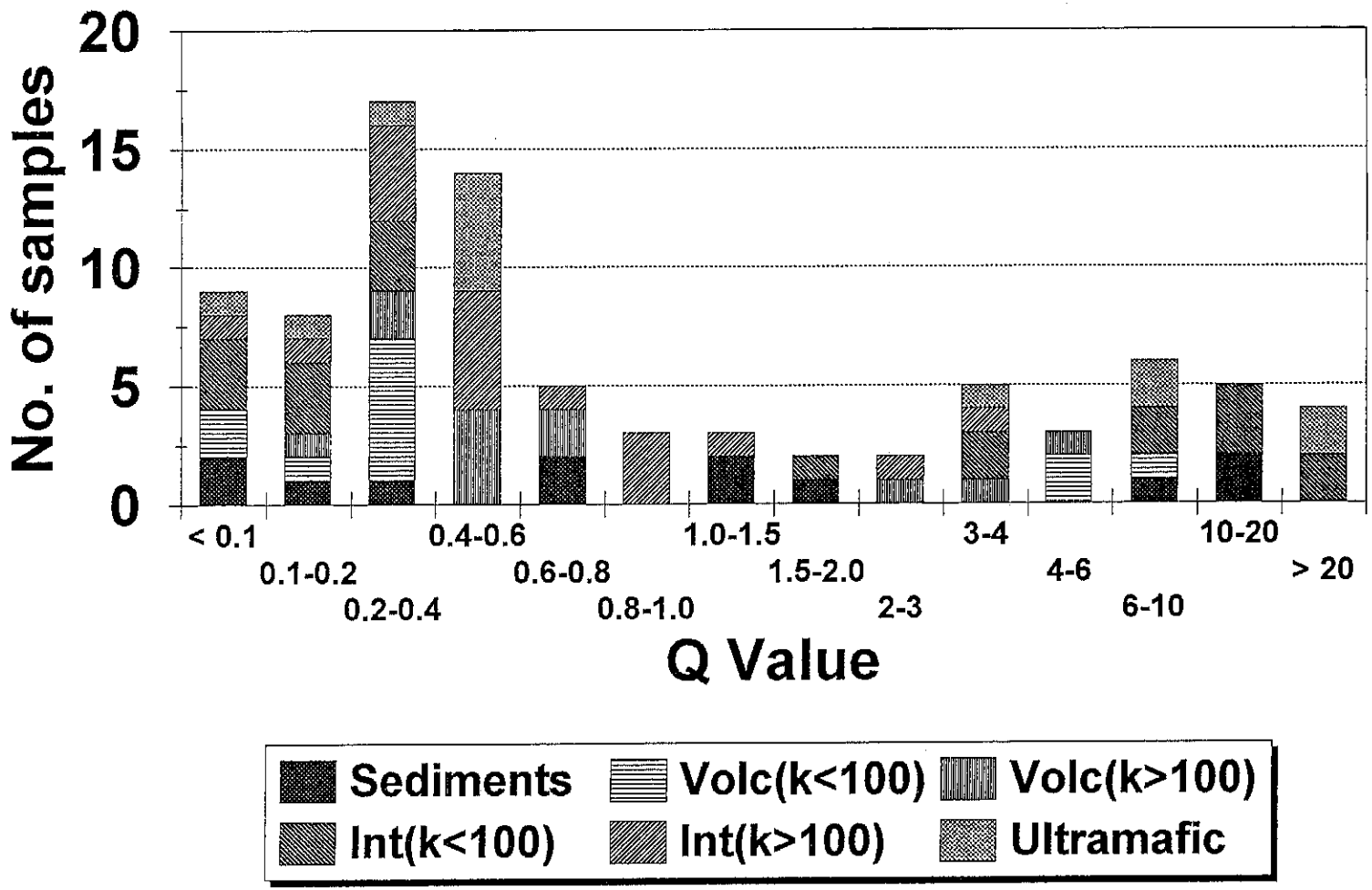

is indicated. Thus contrasts in remanence intensity and variations in average direction probably contribute substantially to the short wavelength magnetic texture of magnetic Rookwood Volcanics. The overall contribution of remanence is to increase the effective susceptibility substantially.

Figure 4.8 shows the distribution of Koenigsberger ratios for DDH samples from the Devlin Creek area. The very weakly magnetic massive and semi-massive sulphides have low Q values, as do the paramagnetic, mostly altered, Rookwood Volcanics. Ferromagnetic samples, however, tend to have slightly higher Q, mostly in the range 0.4-1.0 but with values up to 2. The drill core samples are azimuthally unoriented, but the NRM directions are mostly within 30°-40° of the up-hole directions, indicating predominantly normal polarity. A remanence component caused by drilling may contribute to the measured remanence of some samples, but contamination of the NRMs is probably minor, because their directions depart significantly from the drilling axis and the intensities, inclinations and Q values are comparable to those of typical outcrop samples.

Connors Volcanics and associated coeval intrusives exhibit a wider range of Koenigsberger ratios than the Rookwood Volcanics (see Fig.4.9). This reflects a wider range of compositions and emplacement conditions. Although many paramagnetic extrusives in this suite have low Q (20% less than 0.1, 50% less than 0.8), some have substantially higher Koenigsberger ratios because the remanence is carried by haematite. Haematite has very low susceptibility, but carries relatively intense remanence and therefore has a very high intrinsic Q. Felsic extrusives of the Connors Volcanics have relatively low paramagnetic susceptibilities, because of their low iron contents, and the Q value for the rock is not greatly diminished by the contribution of paramagnetic susceptibility. Magnetite-bearing Connors Volcanics and intrusions have similar Q values to the Rookwood Volcanics. A few very high Q values are attributable to lightning.

Figure 4.10 shows histograms of Q values for other rock types. Ultramafics have low Q (< 0.6), except for lightning-struck samples from site 40, which have very high, but unrepresentative, Q values and scattered NRM directions. Some very weakly magnetic haematite-bearing sediments and felsic volcanics have high Q, similar to those of haematite-bearing felsic Connors Volcanics. Some sedimentary and most felsic volcanic rocks have Q < 0.4. Ferromagnetic igneous rocks tend to have Q values less than unity, unless affected by lightning. Sampling concentrated on the rocks that contribute most to the aeromagnetic anomalies, which contain predominantly multidomain magnetite. This accounts for the preponderance of Koenigsberger ratios in the range 0.2-0.6.

4.3 Susceptibility Anisotropy and Magnetic Fabric

In magnetic interpretation it is generally assumed that the induced magnetisation is parallel to the geomagnetic field. This is strictly true only if the susceptibilitiy is isotropic. Magnetic grains in rocks usually have a preferred dimensional or crystallographic orientation due to forces that acted during formation of the rock and during its subsequent history. The petrofabric arising from these forces produces anisotropy of susceptibilitity. For example, inequidimensional magnetite grains exhibit higher susceptibilities parallel to their long axes than along other directions. Preferred orientation of long axes of magnetite grains therefore leads to higher susceptibility parallel to the preferred direction than along orthogonal directions. Monoclinic pyrrhotite has much higher susceptibility within the basal plane than along the c-axis. Thus

preferred crystallographic orientation of pyrrhotite produces pronounced susceptibility anisotropy.

In undeformed igneous rocks the susceptibility anisotropy is generally very weak, but measurable. The effect of anisotropy on magnetic anomalies is negligible for such rocks, but the magnetic fabric defined by the weak anisotropy reflects magma flow and can provide useful geological information. The plane of higher susceptibility (magnetic foliation) is generally parallel to intrusive contacts and to flow units in extrusives. The maximum susceptibility axis (magnetic lineation) is generally parallel to the flow direction.

In deformed rocks tectonic fabrics overprint primary fabrics and provide information on finite strain. Anisotropy associated with deformed rocks is usually stronger than that of undeformed rocks. Magnetic foliations are generally parallel to fold axial planes and magnetic lineations often indicate directions of maximum extension.

Magnetic fabric data from this collection are plotted in Appendix II. Anisotropy ratios (maximum susceptibility/minimum susceptibilty) are listed in Table 3. These data show that anisotropy ratios are less than 1.05, implying directional variation in susceptibility of less than 5%. Anisotropy variations of about 2% are typical of most samples. Thus anisotropy effects can be neglected for anomaly modelling.

Detailed interpretation of the magnetic fabric data in terms of structure was not attempted. When reliable structural information becomes available at some key sampling localities the significance of the magnetic fabric data at these sites should be re-assessed and the information applied to structural interpretation of the magnetic fabric data at other sites that do not have good structural control. I confine myself to a number of observations about the data:

- Magnetic fabric axes are rather scattered for pillow lavas and breccias of the Rookwood Volcanics, whereas massive flows show a more coherent fabric.

- In the Devlin Creek belt, subvertical foliations containing steeply plunging lineations predominate. Lineation generally dominates foliation. The strike of the magnetic foliation varies significantly from site to site and is often poorly defined.. NE and NW strikes are common, but sites 5 and 6, which have the best-defined foliations, have approximately E-W striking vertical foliations.The overall impression is of intersecting steeply dipping foliations generating a subvertical lineation.

- In the Ohio Leases the "pepperite" in the Rannes Beds (site 70) has a N-S vertical foliation, subparallel to the nearby intrusive contact, containing a subhorizontal lineation that is parallel to the N-S strike of the beds. This fabric probably results from emplacement of the intrusion. Magnetic foliations in the Rookwood Volcanics have variable strikes (NW, N, NE) and moderately to steeply plunging lineations. The magnetic foliations appear to broadly parallel regional trends and may indicate orientations of fold axial planes.

- At two Siluro-Devonian volcanics sites (59 and 60) for which the structure could be determined, the magnetic foliation was parallel to bedding and the magnetic lineations were down-dip.

• Sites 42 and 43, Devonian-Carboniferous volcanics north of the Devlin Creek belt, both have N-S striking, east dipping magnetic foliations with a N-S subhorizontal magnetic lineation that is probably parallel to the fold axes in this area.

• The Macksford Volcanics (upper Connors Volcanics) and associated intrusions exhibit relatively well-defined magnetic fabrics of tectonic origin. In the Mount McKenzie area the magnetic foliations are quite consistent between and within sites and have NW strike and steep dips. Foliations generally dominate lineations and minor susceptibility axes (magnetic foliation poles) are better grouped than lineations, which tend to be distributed around a girdle normal to the mean foliation pole. The fabric of the only site in the Clement Creek Volcanics (site 30) is distinctly different, with an ESE-dipping foliation and a well-defined lineation with shallow NE plunge. The lineation lies along the intersection of the magnetic foliation and the bedding plane at site 30. The magnetic fabric of the Macksford Volcanics appears to reflect flattening in response to NE-SW compression.

• Along the Connors Volcanics type section N to NW-striking subvertical magnetic foliations predominate. This foliation may have resulted from E-W compression and is consistent with the northerly strike of the volcanic units in this area. Site 39, at the eastern edge of this traverse, has a distinctly different fabric, with an E-W subvertical foliation. The palaeomagnetic results from this site also indicate a different structural attitude for this locality (see section 5.3).

5. PALAEOMAGNETISM

5.1 Palaeomagnetic Poles and Reference Field Directions

Interpretation of palaeomagnetic data is based upon the axial geocentric dipole model, the validity of which is well established, particularly for Phanerozoic time. This model states that the geomagnetic field at any locality, if averaged over several thousand years to remove secular variation, coincides closely with that of a dipole located at the Earth's centre and aligned with the rotation axis. Thus the time-averaged geomagnetic poles coincide with the geographic poles, which allows the pole position to be calculated from the field direction at any location. Continental motion caused by plate tectonic forces can be detected by the changes in geomagnetic field direction, as recorded by rocks of different ages. With respect to the continent the pole appears to be moving. The track traced out by the pole with respect to the continent is the apparent polar wander path (APWP).

Many rocks record the geomagnetic field direction faithfully at the time of their formation. The primary magnetic remanence may be subsequently overprinted by thermal events or chemical alteration. Palaeomagnetic cleaning techniques, such as alternating field demagnetisation and thermal demagnetisation, are designed to selectively and sequentially remove remanence components acquired at different times, allowing the palaeomagnetic directions to be determined for each of the geological events recorded by the magnetic minerals in the rocks.

Palaeomagnetic poles calculated from magnetisations with well-defined ages are used to define a reference APWP. Palaeomagnetic poles calculated from rocks of unknown age can be compared with the reference track as a means of indirect dating. If the age of magnetisation is known, comparison of the calculated pole with the APWP allows tectonic movements to be defined.

The apparent polar wander path for Australia is well defined for the Late Palaeozoic, Mesozoic and Tertiary periods, but is less certain for earlier times. There is still controversy over the interpretation of poles obtained from rocks of Silurian and Devonian age in particular. For the purposes of this report the APWP favoured by the CSIRO and UWA palaeomagnetic groups (Schmidt *et al* (1994), Lackie and Schmidt (1994) , Chen *et al* (1994) and Li (1994), Exploration Geophysics, in press) is taken as the reference track for comparison with poles derived from the present study and for calculation of reference field directions. Figure 5.1 shows the Mesozoic and Tertiary APWP and Fig.5.2 shows the Devonian to Permian track. The key poles and the corresponding reference directions at 23°S, 150°E are listed below.

The geomagnetic field maintained a fixed polarity for two extended periods in the Mesozoic and Palaeozoic: the Cretaceous Normal Superchron (83-118 Ma) and the Permo-Carboniferous Kiaman Reversed Superchron (~250-310 Ma). At all other times the field was reversing relatively frequently and palaeomagnetic directions recorded outside the two polarity superchrons may therefore have either normal or reversed polarity. For this reason both normal and reversed senses of the reference directions are given, in that order, for relevant ages.

EPOCH	AGE (Ma)	POLE POSITION Lat	Long	REFERENCE DIRECTION Dec	Inc
				Normal	
Late Cretaceous	90	58°S	141°E	008°	-70°
				Normal	
Late Cretaceous	100	52°S	157°E	351°	-74°
				N/R	
Early Cretaceous	130	23°S	151°E	270°	-89°
				090°	+89°
				N/R	
Early-mid Jurassic	190	47°S	181°E	322°	-71°
				142°	+71°
				N/R	
Early Triassic	240	33°S	150°E	000°	-85°
				180°	+85°
				Reversed	
Early Permian	280	44°S	144°E	192°	+79°
				Reversed	
Late Carboniferous	305	41°S	130°E	218°	+77°
				N/R	
Early Carboniferous	340	42°S	063°E	051°	-32°
				231°	+32°
				N/R	
Late Devonian	370	58°S	029°E	027°	-09°
				207°	+09°
				N/R	
Middle Devonian	380	77°S	331°E	000°	-19°
				180°	+19°
				N/R	
Early Devonian	400	74°S	223°E	343°	-45°
				163°	+45°

Fig.5.1. Mesozoic and Tertiary apparent polar wander path for Australia.

Fig.5.2. Mid to Late Palaeozoic apparent polar wander path for Australia.

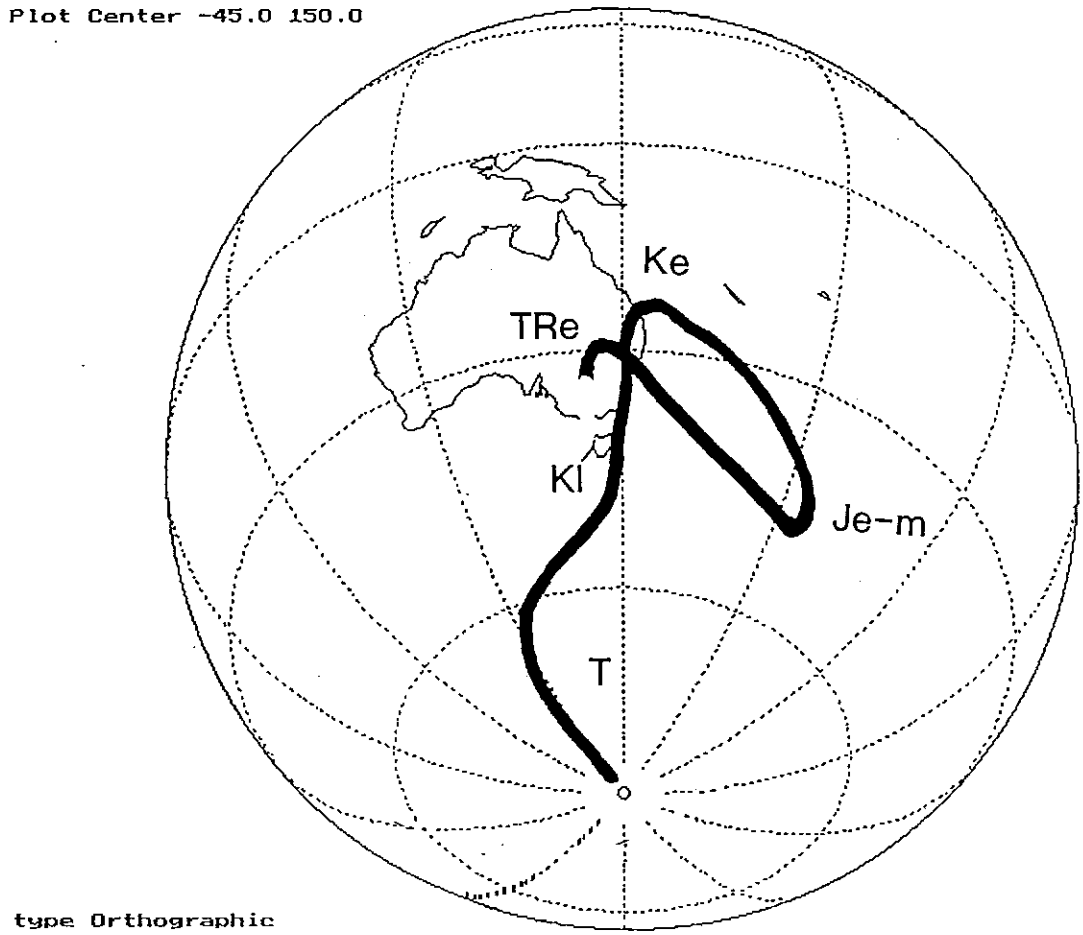
Plot Center -45.0 150.0
Ke
TRe
Kl
Je-m
T
type Orthographic

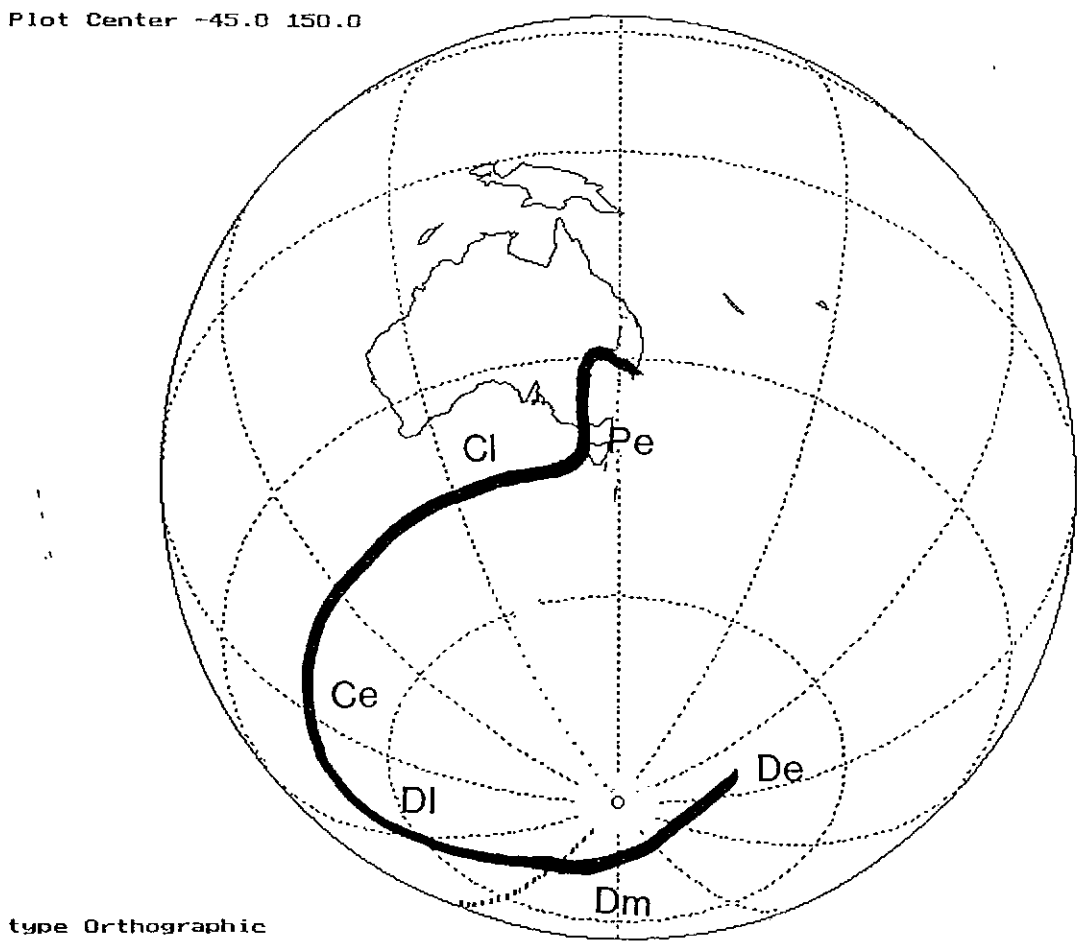
Plot Center -45.0 150.0
Cl
Pe
Ce
Dl
De
Dm
type Orthographic

Fig.5.3. Reference field directions for the Fitzroy Leases from the present to 190 Ma.
PF = present field, PDF = present dipole field, numbers indicate ages in Ma.
For mixed polarity chrons both normal (N) and reversed polarity (R) directions are plotted. According to standard palaeomagnetic conventions, open symbols indicate directions on the upper hemisphere and closed symbols indicate lower hemisphere directions. The movement of the normal polarity direction through time is indicated.

Fig.5.4. Reference field directions for the Fitzroy Leases from 240 Ma to 400 Ma.
For mixed polarity chrons both normal (N) and reversed polarity (R) directions are plotted. The movement of the reversed polarity direction through time is indicated.

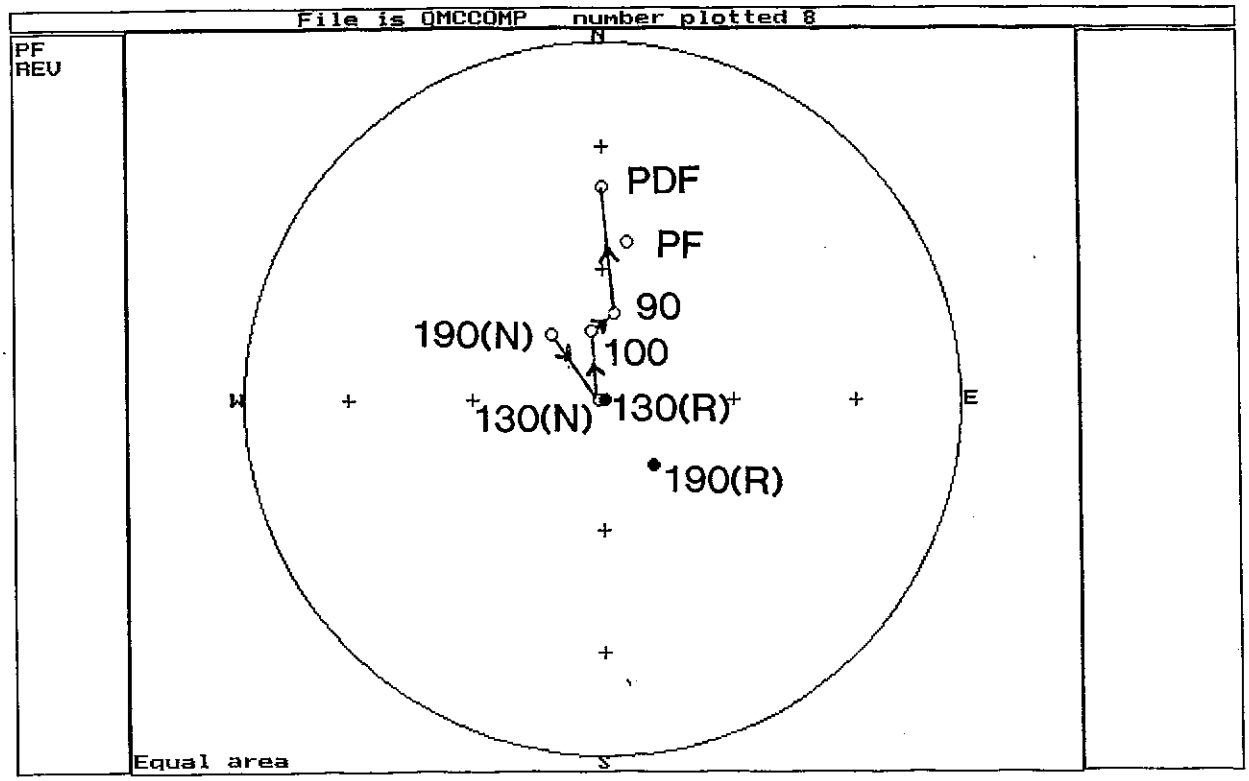
File is QMCCOMP number plotted 8
PF
REV
N
PDF
PF
90
190(N)
100
W
130(N)
130(R)
E
190(R)
S
Equal area

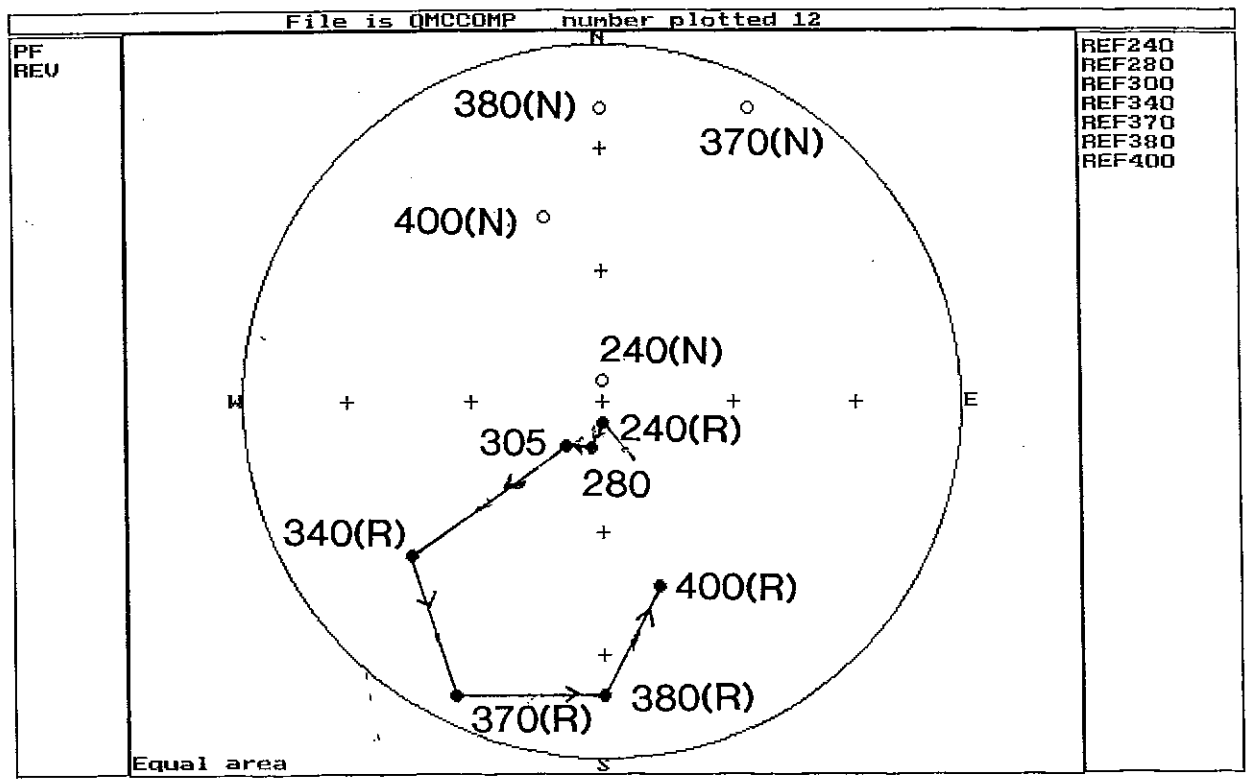
File is QMCCOMP number plotted 12
PF
REV
N
380(N)
370(N)
400(N)
240(N)
W
E
240(R)
305
280
340(R)
400(R)
380(R)
370(R)
S
Equal area
REF240
REF280
REF300
REF340
REF370
REF380
REF400

The reference field directions for the 90-240 Ma and ≥240 Ma intervals are plotted in Fig.5.3 and Fig.5.4 respectively. For comparison, the present field direction (dec = 9°, inc = -53°) and the present dipole field direction (dec = 0°, inc = -40°) are also shown in Fig.5.3. The dipole field direction represents the average recent field direction over the last several thousand years.

In order to interpret palaeomagnetic data it is important to determine if a remanent magnetisation was acquired before or after folding of the units. Pre-folding components from units with different structural attitudes agree only after the units are restored to the horizontal. This establishes that the remanence was acquired before folding and may therefore be primary. If the remanence components from different fold limbs agree *in situ*, but diverge upon structural correction, they were acquired after folding and are therefore secondary. Sometimes palaeomagnetic directions from different limbs agree only after partial unfolding, but exhibit distinct "crossing over"" upon full structural correction. This demonstrates that the remanence is synfolding. Once it is established that a remanence component was acquired before folding, structural correction of the direction must be carried out before calculating a palaeomagnetic pole for comparison with the APWP. On the other hand, the *in situ* direction is used to calculate poles for post-folding components.

Well-resolved palaeomagnetic components isolated by progressive thermal demagnetisation correspond to linear trends traced out by successive vector end-points, representing removal of a single component over an extended temperature interval. If several consecutive linear trends are present, each linear segment represents a remanence component acquired at a different time.When these vector end-points are projected onto the horizontal plane and either the E-W or N-S vertical planes, well-resolved components correspond to segments that are linear on both projections, over a common temperature interval. Different remanence components with overlapping unblocking temperature spectra are identifiable by curved segments on the vector plots. Purely thermal overprinting of primary remanence often produces minimal overlap of unblocking temperatures, allowing clean separation of the overprint component from the primary magnetisation. Chemical overprinting, on the other hand, often produces overlapped unblocking temperature spectra, which may make complete separation of secondary and primary components difficult. Lightning strikes may also remagnetise nearby rocks and preclude determination of geologically meaningful components.

Once the distinct remanence components are recognised, their directions are determined by finding least-squares best-fit lines to each component. This procedure is carried using a principal component analysis (PCA) algorithm based on the method of Kirschvink, (1980).

5.2 Palaeomagnetism of the Rookwood Volcanics

Some representative demagnetisation plots for Rookwood Volcanics samples are shown in Fig.5.5. Application of PCA to the thermal demagnetisation data for the Rookwood Volcanic samples led to recognition of three distinct components:

A: removed at low temperatures (generally less than 300°C), directed north with moderate negative (i.e. upward) inclination, close to the present field direction,

B: removed at low to intermediate temperatures (generally 300-500°C), directed north with steep negative inclination, and

C: a high temperature component of reversed polarity, generally isolated above ~500°C.

Figure 5.6 plots directions of site mean A and B components for all sites within the Rookwood Volcanics for which these components could be fully resolved.

Traverse East of Sulphide City

Figure 5.7 shows stereoplots of the well-defined components found in Rookwood Volcanic samples from sites 1-13. The directions evidently fall into three distinct clusters, which correlate with their thermal demagnetisation characteristics. In some samples a relatively shallow component (A) is removed initially, followed by removal of the distinctly steeper B component, but in most specimens only one of these components is well-defined. A few samples were clearly affected by lightning and were not included in the analysis. For some specimens components could not be fully resolved and results from these specimens were therefore excluded from calculations of mean directions. The site-mean directions and directional statistics for the three populations of directions are:

Component A: dec = 359°, inc = -55°, N = 6, α_{95} = 6.5°, K = 108.1

Component B: dec = 1.5°, inc = -76°, N = 8, α_{95} = 11.6°, K = 23.6

Component C: dec = 183°, inc = +36°, N = 9, α_{95} = 14.3°, K = 13.91.

N is the number of unit vectors combined to calculate the mean directions, α_{95} is the half-angle of the 95% cone of confidence about the mean direction, and K is the invariance or precision parameter.

The directions of component A and the present field are indistinguishable. Component A is interpreted as a viscous magnetisation acquired in the recent field, although in a few cases recent weathering may contribute. Component B has a consistent orientation, irrespective of the present bedding attitude of Rookwood Volcanic units, and is also present in a wide range of rock types of different ages across the study area, as well as throughout the southern and central Bowen Basin (M. Lackie, pers. comm.). This implies that the B component is post-folding. Comparison with the reference field directions given above suggests that the B component was acquired during the Cretaceous, around 110±10 Ma. This age also explains the consistent normal polarity of the B component, as this period occurs within the Cretaceous Normal Superchron.

The B component probably represents a regional low grade thermal overprint that has affected the study area and a considerable surrounding region, although it has apparently not affected the northern Bowen Basin (M. Lackie, pers. comm.). The inferred Cretaceous thermal event may be related to the emplacement of Cretaceous syenites, trachyte plugs and flows, and mafic intrusives and extrusives. In coastal areas of SE Australia a Cretaceous thermal event related to the opening of the Tasman Sea has produced pervasive palaeomagnetic overprinting at ~90 Ma (Schmidt and Embleton, 1981) and resetting of apatite fission track ages, which record cooling through ~100°C at about 80 Ma (Morley *et al.*, 1981). Thus Cretaceous overprinting appears to have occurred extensively along the eastern seaboard of Australia.

Fig.5.5. Representative examples of thermal demagnetisation plots for Rookwood Volcanics samples. The top left plot shows remanence intensity versus temperature and the corresponding unblocking temperature spectrum (rate of change of remanence vector with respect to temperature). The bottom left plot is a stereonet showing remanence directions after each demagnetisation step. The right hand plot is a Zijderveld plot, which depicts both intensity and directional changes of remanenc during demagnetisation. Vector end-points after each demagnetisation step are plotted on two orthogonal projections: open symbols are the projections onto a vertical plane (either E-W or N-S as indicated) and closed symbols are the projections onto the horizontal plane. Segments that are linear on both projections over the same temperature interval indicate removal of a single remanence component. Each remanence component is acquired parallel to the field acting at the time of acquisition. Thermal overprint components unblock at lower temperatures than primary remanence.

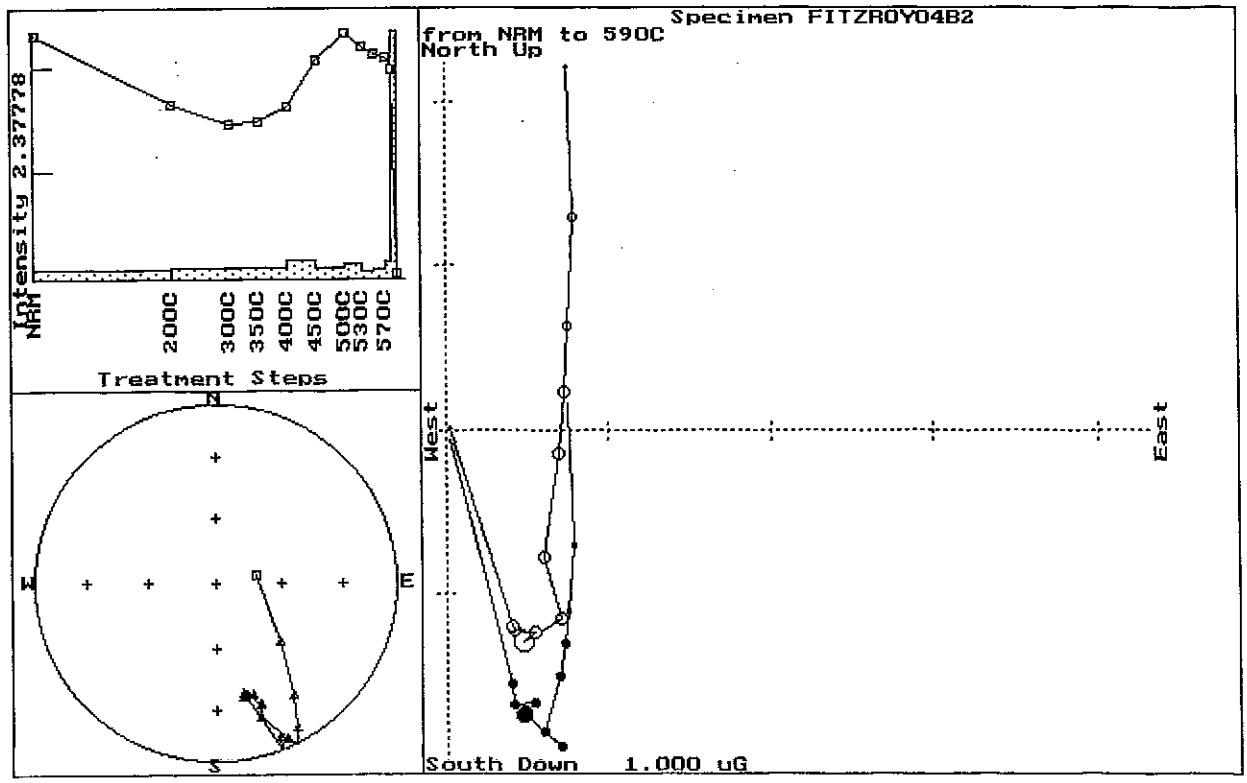
Specimen FITZROY04B2
from NRM to 590C
North Up
Intensity 2.37778
NRM
200C
300C
350C
400C
450C
500C
530C
570C
Treatment Steps
N
E
S
W
West
East
South Down 1.000 uG

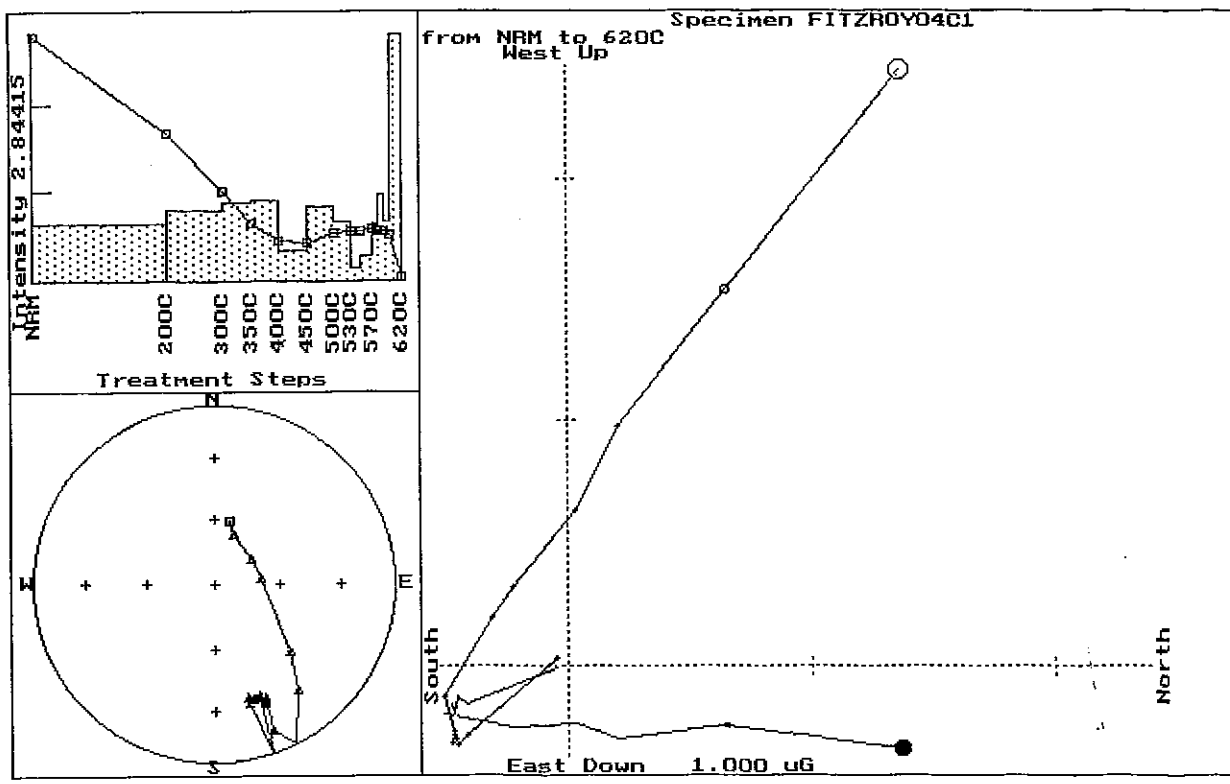
Specimen FITZROY04C1
from NRM to 620C
West Up
Intensity 2.84415
NRM
200C
300C
350C
400C
450C
500C
530C
570C
620C
Treatment Steps
N
E
S
W
South
North
East Down 1.000 uG

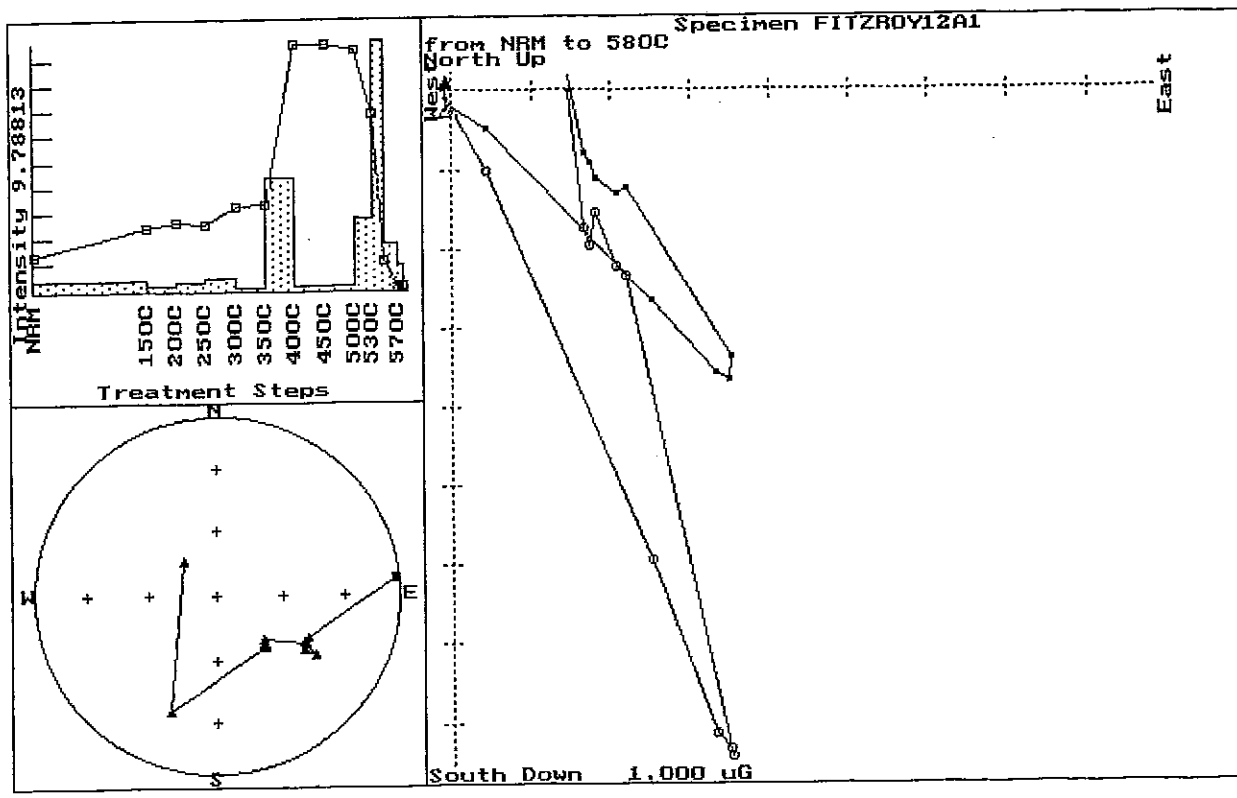
Specimen FITZROY12A1
from NRM to 580C
North Up
West
East
Intensity 9.78813
NRM
150C 200C 250C 300C 350C 400C 450C 500C 530C 570C
Treatment Steps
N
W
E
S
South Down 1.000 uG

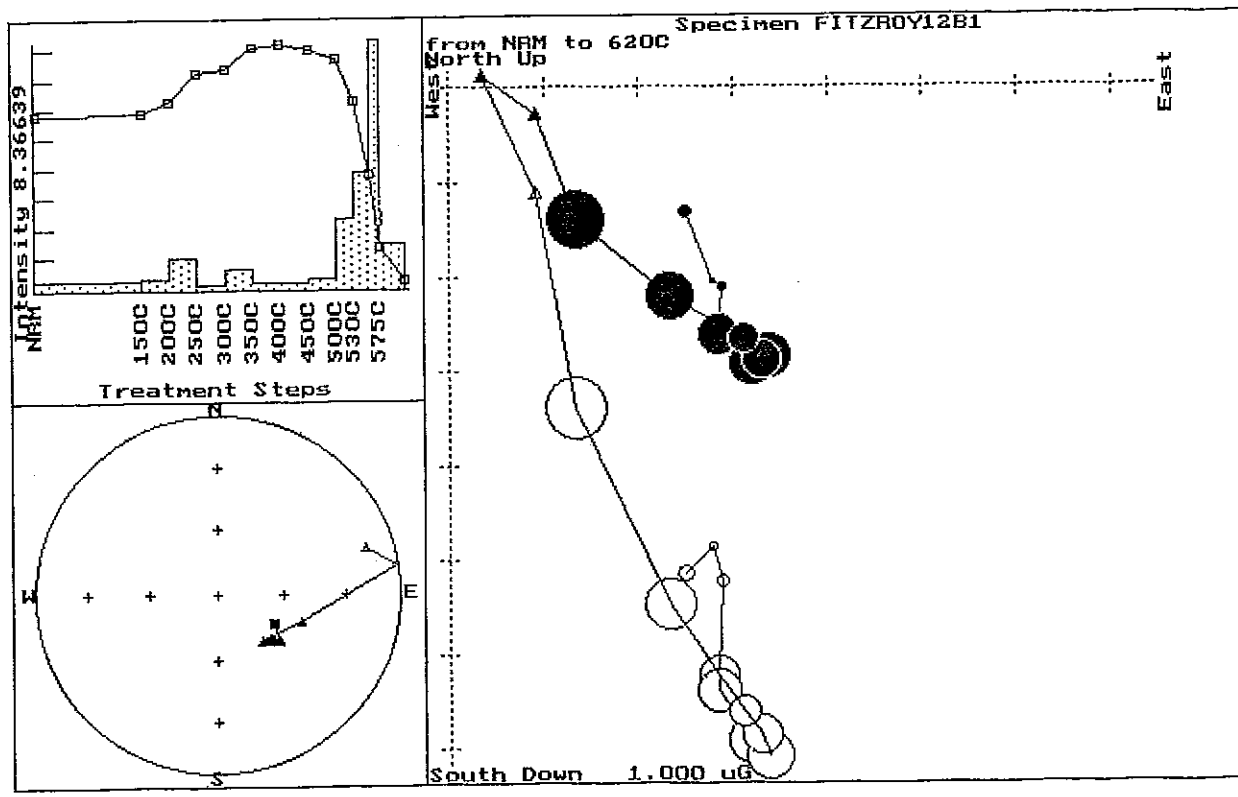
Specimen FITZROY12B1
from NRM to 620C
North Up
West
East
Intensity 8.36639
NRM
150C 200C 250C 300C 350C 400C 450C 500C 530C 575C
Treatment Steps
N
W
E
S
South Down 1.000 uG

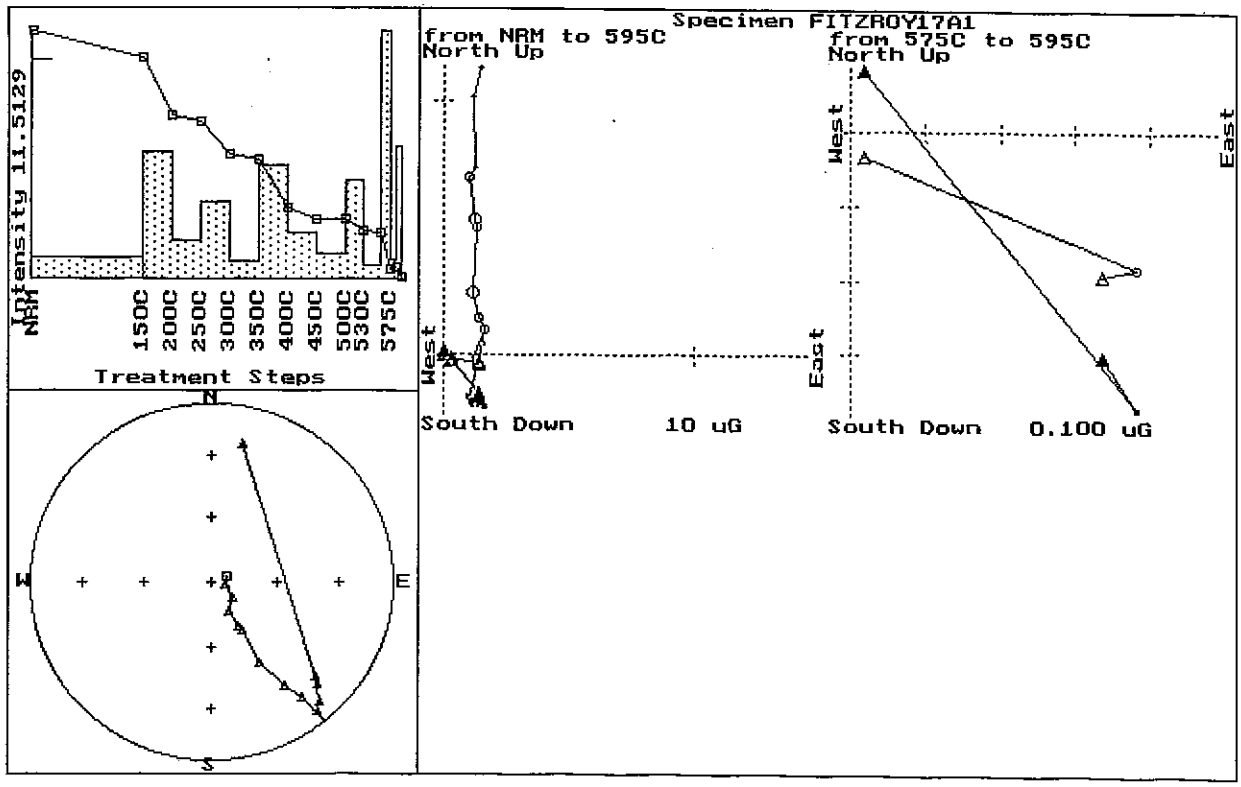
Intensity 11.5129
NRM
150C
200C
250C
300C
350C
400C
450C
500C
530C
575C
Treatment Steps
N
E
S
W
Specimen FITZROY17A1
from NRM to 595C
North Up
West
East
South Down
10 uG
from 575C to 595C
North Up
West
East
South Down
0.100 uG

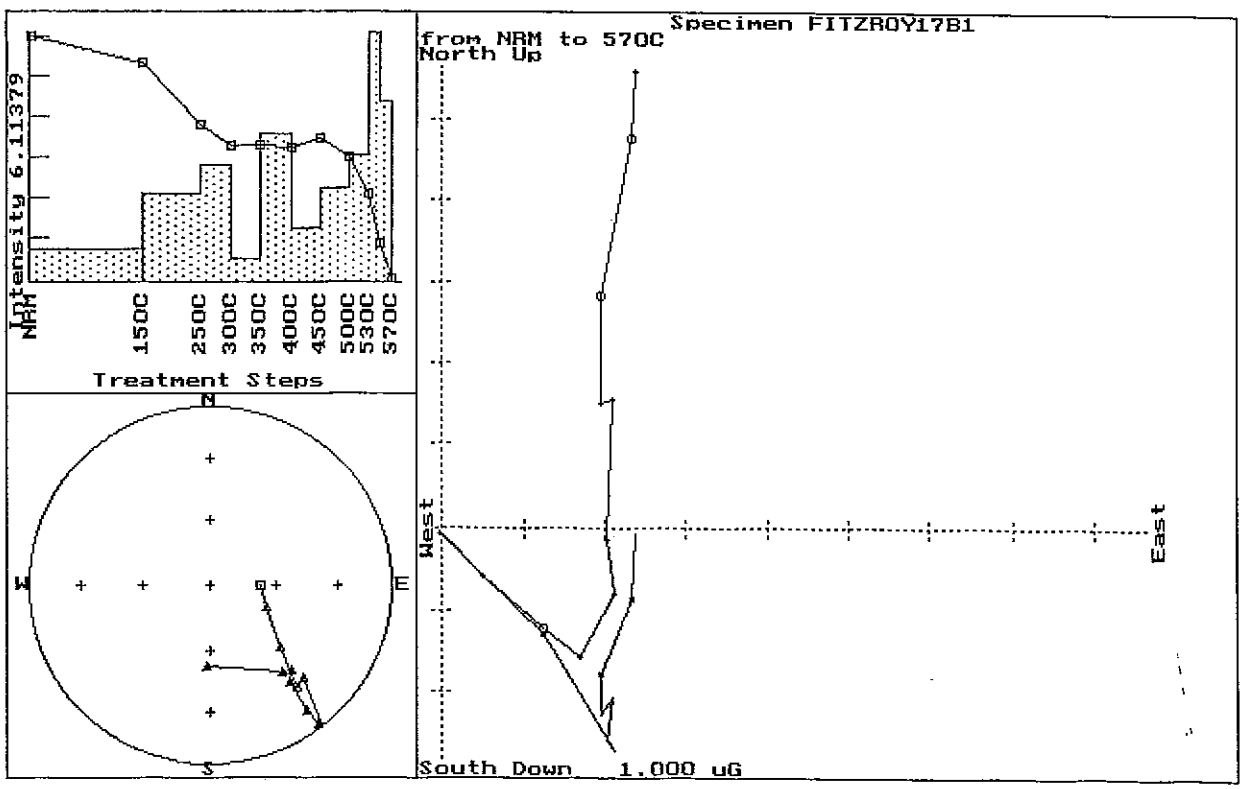
Intensity 6.11379
NRM
150C
250C
300C
350C
400C
450C
500C
530C
570C
Treatment Steps
N
E
S
W
Specimen FITZROY17B1
from NRM to 570C
North Up
West
East
South Down
1.000 uG

Fig.5.6. Overprint components revealed by thermal demagnetisation of Rookwood Volcanics samples, (a) present field components, (b) Cretaceous overprint components.

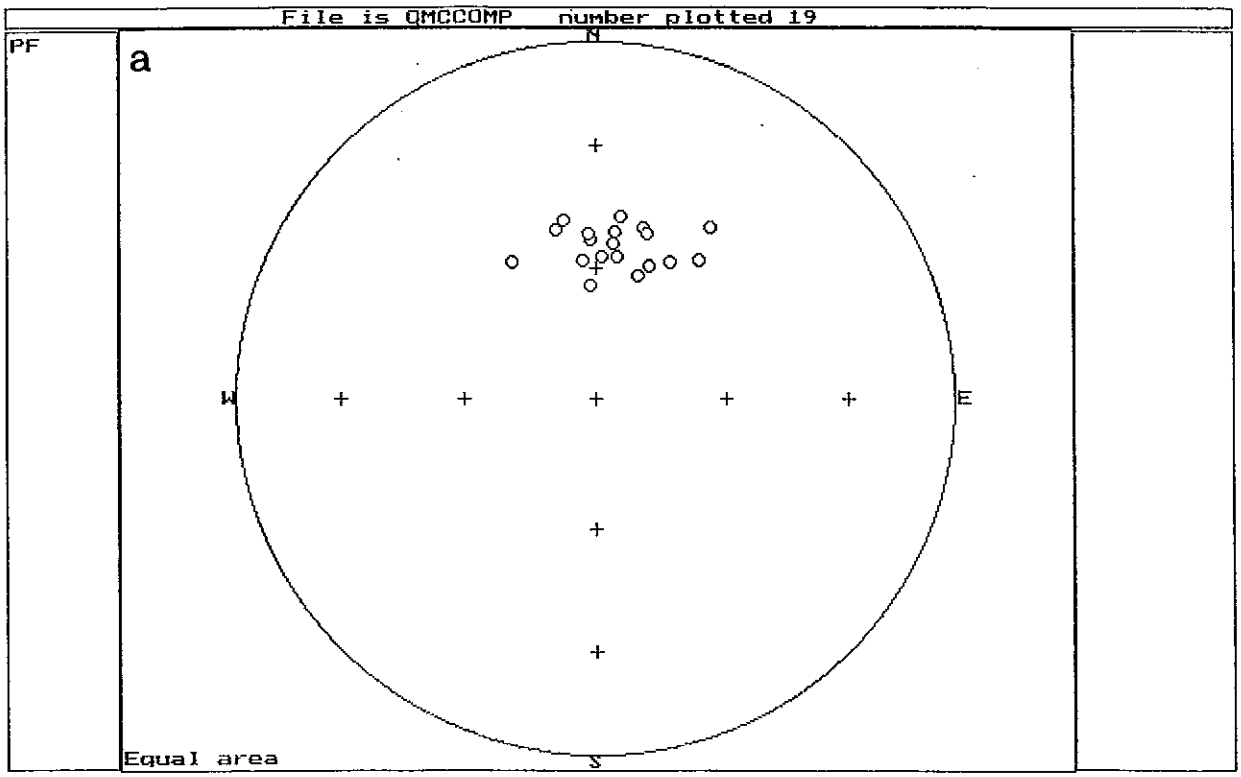
File is QMCCOMP number plotted 19
PF
a
N
W
E
S
Equal area

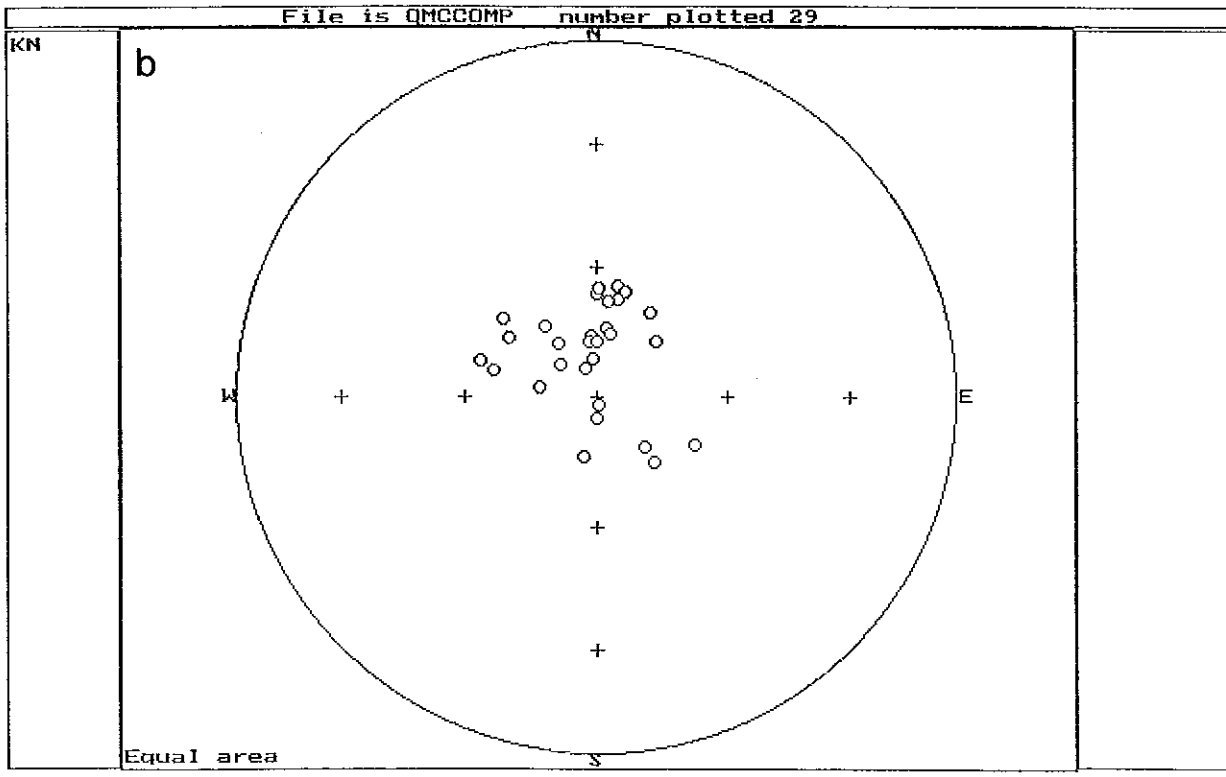
File is QMCCOMP number plotted 29
KN
b
N
W
E
S
Equal area

Fig.5.7. Well-defined remanence components isolated by thermal demagnetisation of Rookwood Volcanics samples from the NE Devlin Creek belt. Note three groups of directions: a cluster of low temperature components close to the present field direction, a steep up cluster (Cretaceous overprint) and high temperature components of reversed polarity.

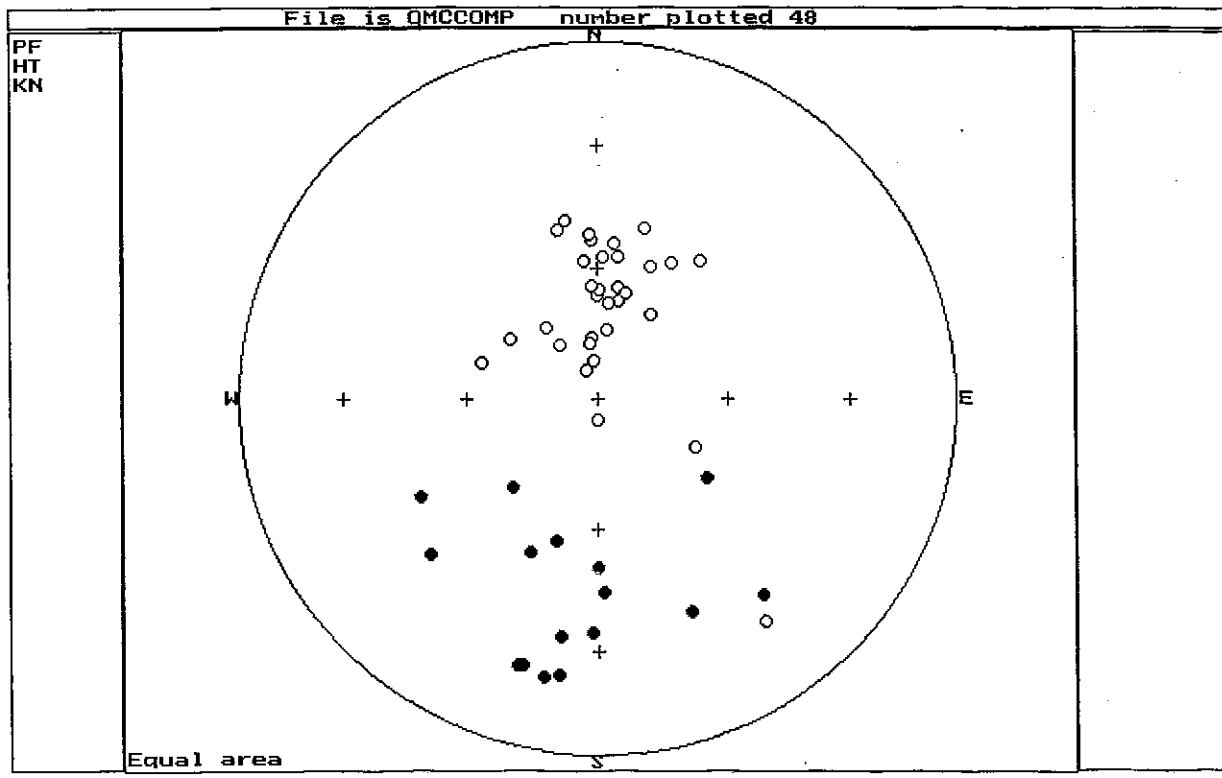
File is QMCCOMP number plotted 48
PF
HT
KN
N
W
E
S
Equal area

Fig.5.8. Reversed high temperature components interpreted as primary from the Devlin Creek belt of Rookwood Volcanics, (a) NE Devlin Creek, (b) South Devlin Creek.

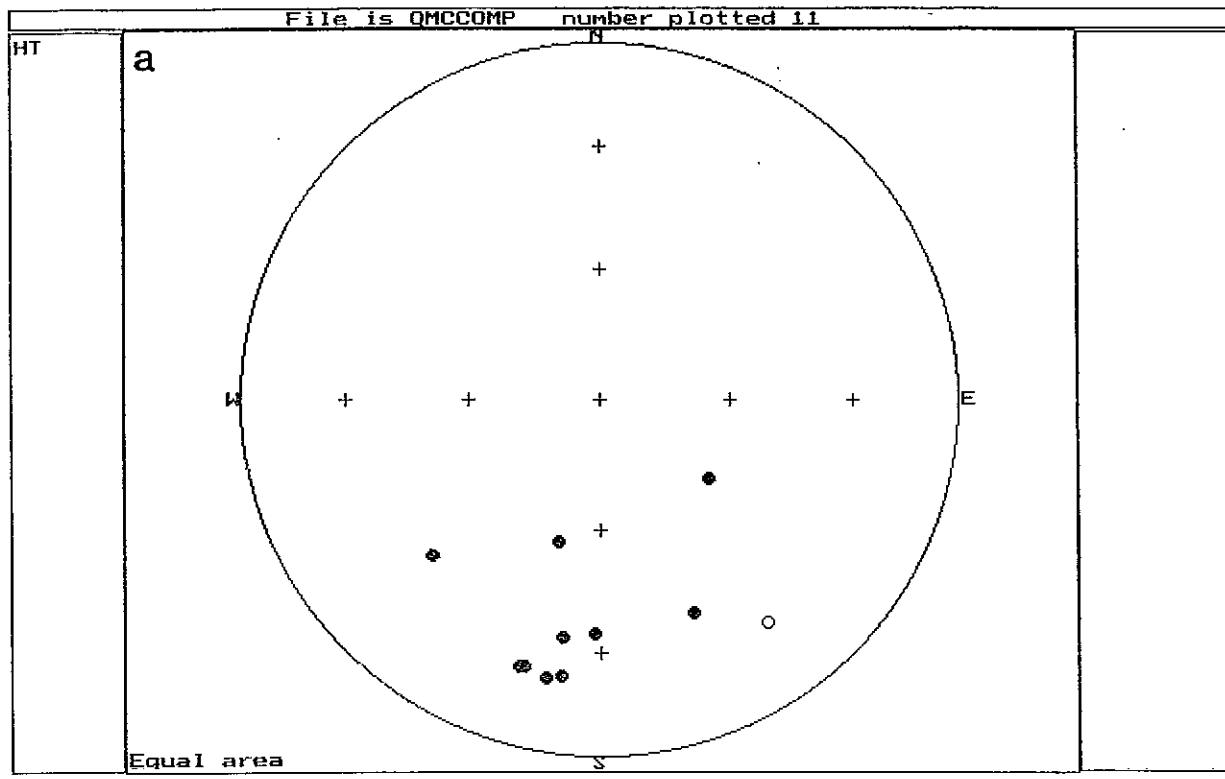
File is QMCCOMP number plotted 11
HT
a
N
W
E
S
Equal area

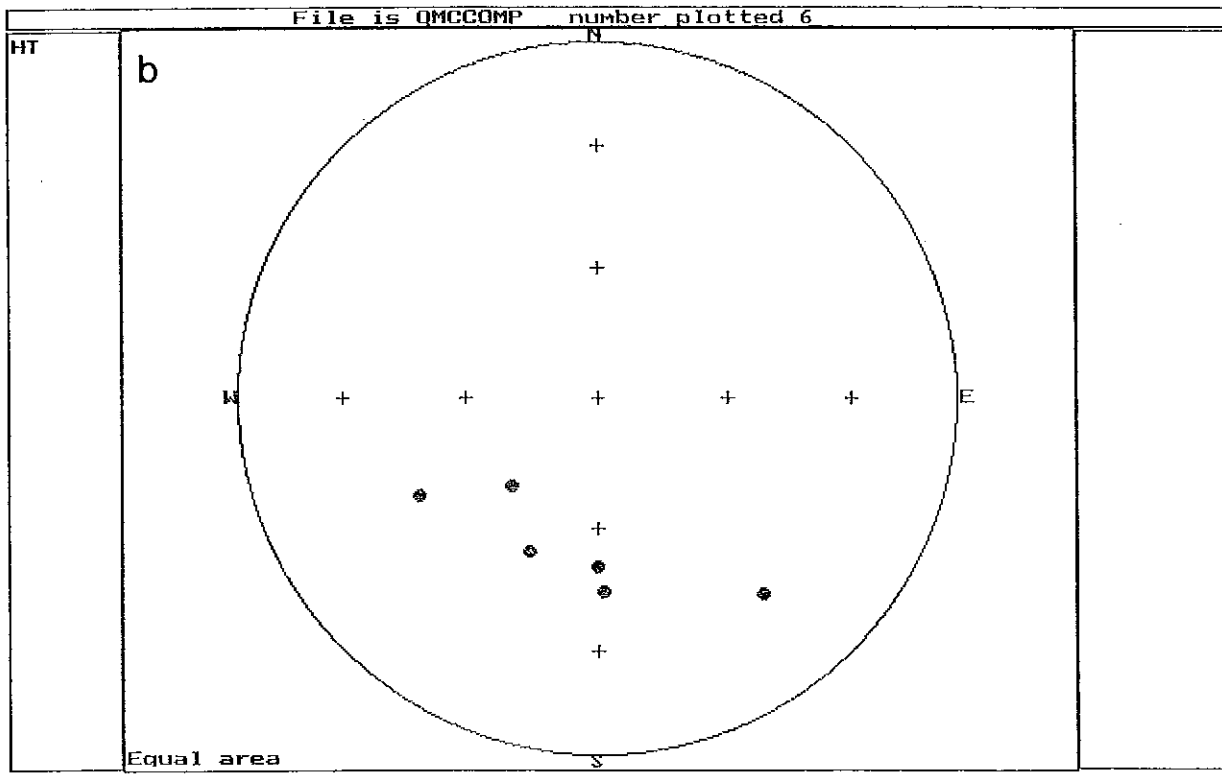
File is QMCCOMP number plotted 6
HT
b
N
W
E
S
Equal area

Figure 5.8(a) plots C component directions for sites 1-13. Without structural correction the C component does not coincide with any reference field direction for the Permian or younger periods. However, the units are known to dip ~35°N at the western end of the traverse. Restoring these units to the horizontal rotates the C component to a direction similar to the Early Permian reference direction. The similarity of C component directions from sites farther east along the traverse suggests that this bedding attitude is reasonably consistent along the traverse. The moderate scatter of C component directions probably reflects, at least in part, small local departures from the regional bedding attitude. Assuming the same structural correction is applicable to all sites in this traverse, the bedding-corrected mean direction becomes

Component C (structurally corrected):
dec = 199°, inc = +71°, N = 9, α_{95} = 14.3°, K = 13.91.

The corresponding palaeomagnetic pole lies at 55°S, 132°E (dp = 22°, dm = 25°). This direction, and therefore the corresponding pole, are consistent with an Early Permian age of magnetisation. This suggests that the C component is primary. Alternatively it could be a relatively early secondary magnetisation acquired before the folding, which occurred during the Permo-Triassic Hunter-Bowen orogeny (Henderson *et al*, 1993). The consistent reversed polarity of the C component, both for this traverse and at all other Rookwood Volcanics localities, indicates that the C component was acquired before the end of the Kiaman Reversed Superchron, i.e. it is pre-Triassic.

Regional metamorphism of the sampled Rookwood Volcanics is very low grade and would not have obliterated primary thermoremanence. Given the great stability of the C component, its near ubiquity in units of varying lithology and alteration, the common occurrence of primary magnetite in basaltic to andesitic lavas and the particularly good palaeomagnetic recording characteristics of subaqueous lavas, the C component is interpreted as essentially primary thermoremanence, acquired during initial cooling of the lavas. This magnetisation is carried by magnetite and, in some cases, also by haematite. In this context the "primary" magnetic carriers may be either primary magmatic minerals or products of deuteric alteration, as remanence carried by magnetite is only blocked in after cooling below 580°C (680°C for haematite). It is possible that some of the C component may be attributable to magnetic minerals formed during sea-floor alteration or during initial burial, however this does not affect the utility of the palaeomagnetic method for correlation of volcanic units or detection of tectonic tilting.

Comparable results were obtained from Rookwood Volcanics samples collected from elsewhere in the study area, although the magnetic mineralogy shows some variability. These other localities will now be discussed individually.

Sites 15-19

Sites 15-19 lie along an approximately NE-SW traverse extending from about 3 km east of Sulphide Suburb to about 2 km south of South Yards, within a reasonably magnetically active zone of the Rookwood Volcanics. The lava flows dip ~60°NNW at Sulphide City. Figure 5.8(b) plots C component directions for the southern Devlin Creek Belt of Rookwood Volcanics (sites 15-19 and 49-54). The mean C component for these sites is dec = 181°,

inc = +48° (N = 4, α_{95} = 39°, K = 6.67) before structural correction. In all cases the inclinations of the C components are substantially lower than expected for the Permian. The low K and consequent large angular error probably reflects variable structural attitude, rather than imperfect isolation of remanence components, because the thermal demagnetisation data suggest clean resolution of discrete well-defined low temperature and high temperature components.

The C component at site 15, which lies closest to Sulphide Suburb, has a similar direction (dec = 178°, inc = +45°) to the mean for the traverse. Applying the structural correction appropriate for Sulphide Suburb to the direction from site 15 yields a direction (dec = 296°, inc = +68°) that is more consistent with the Permian direction, although it appears to be somewhat overcorrected. Assuming a dip of 40° rather than 60°, corrects the *in situ* direction to dec = 235°, inc = +75°, which is within 10° of the expected Early Permian direction. Given the 3 km distance from the mapped structure to the sampling site, a 20° difference in dip is not surprising. The simplest interpretation of the C component for this traverse is that it represents a Permian remanence that has been tilted away from the reference field direction.

North Yards - South Yards - Muldoon Area

These sites lie along an approximately N-S traverse about 8 km long and about 3 km west of sites 15-19. The interpolated traverse passes close to Sulphide Suburb, but the closest sites, 49 and 54, are ~2.5 km N and ~ 3 km S of Sulphide Suburb respectively. Site 49 is close to the North Yards Prospect. Sites 49-54 lie within a very magnetically quiet zone of the Rookwood Volcanics and have low susceptibilities and weak NRMs. Well-defined characteristic components of reversed polarity could only be isolated from sites 49 and 51. The mean direction of the C component for samples from these sites is dec = 210°, inc = +56° (N = 7, α_{95} = 10°, K = 38.9). Without structural correction this direction is not consistent with any known palaeofield direction for the Permian or Mesozoic (see Fig.5.8(b)). If we assume that this component is pre-folding, the divergence from the Permian reference field indicates a present bedding dip of ~25° N. The sense of tilt is consistent with that found at Sulphide Suburb, although the magnitude is lower. Assuming a substantially larger dip would overcorrect the observed direction and move it away from the palaeofield direction for the Permian or later times. Thus the preferred interpretation is that the C component is also a Permian remanence that has been tilted with the volcanic units during the folding event and that the bedding dip is shallower to the west of Sulphide Suburb.

Whilst the C component is carried by magnetite at site 51, at site 49 its remanence is largely unblocked between 300°C and 400°C. This indicates a different magnetic carrier, either maghaemite, which breaks down chemically in this temperature range, or monoclinic pyrrhotite, which has a Curie temperature of ~330°C. In spite of the much lower unblocking temperatures for the C component in samples from site 49, the B component, possibly contaminated with some A component, is also recorded and is removed between room temperature and ~300°C. The other sites that record only A or B components also exhibit low unblocking temperatures, suggesting that the reason for the failure to record a primary magnetisation is the lack of magnetite in these samples. The magnetic carrier with low unblocking temperatures is easily overprinted and in most cases has been remagnetised during the Cretaceous.

Fig.5.9. Reversed high temperature components from the Rookwood Volcanics, (a) Ohio belt, (b) Gogango-Westwood belt.

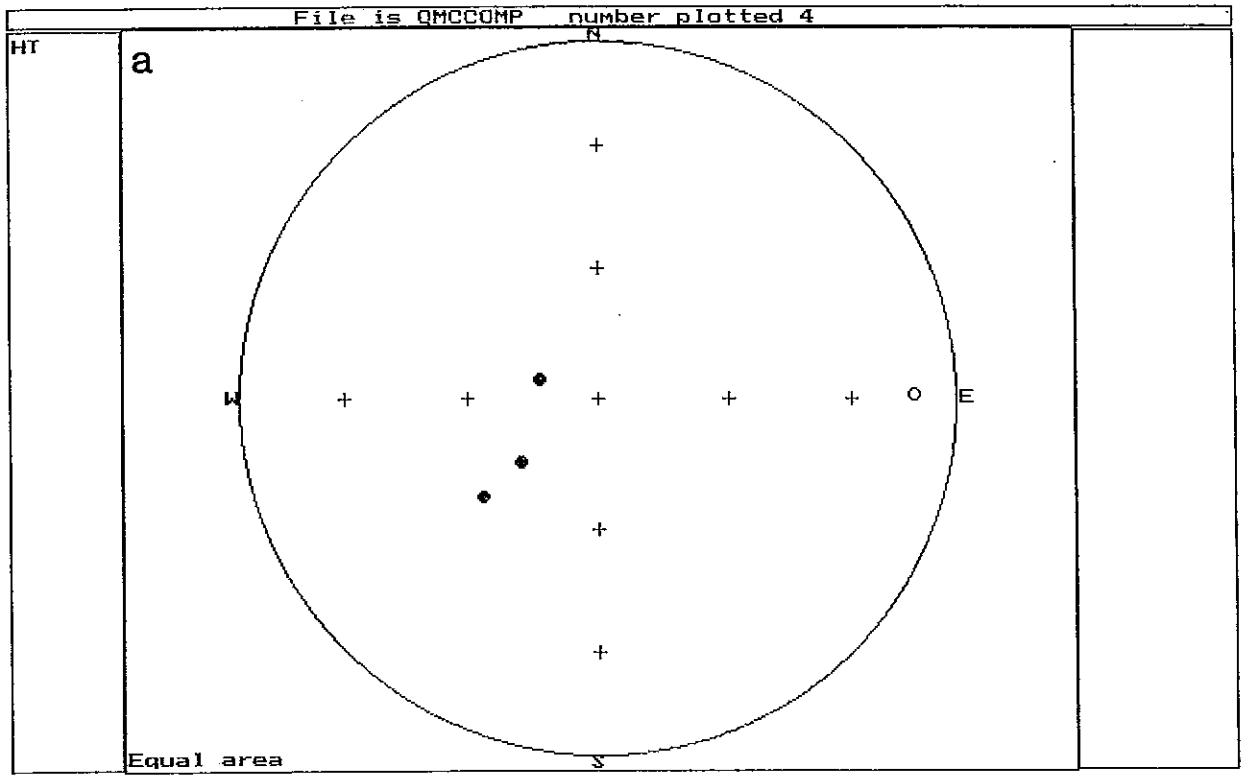
File is QMCCOMP number plotted 4
HT
a
N
W
E
S
Equal area

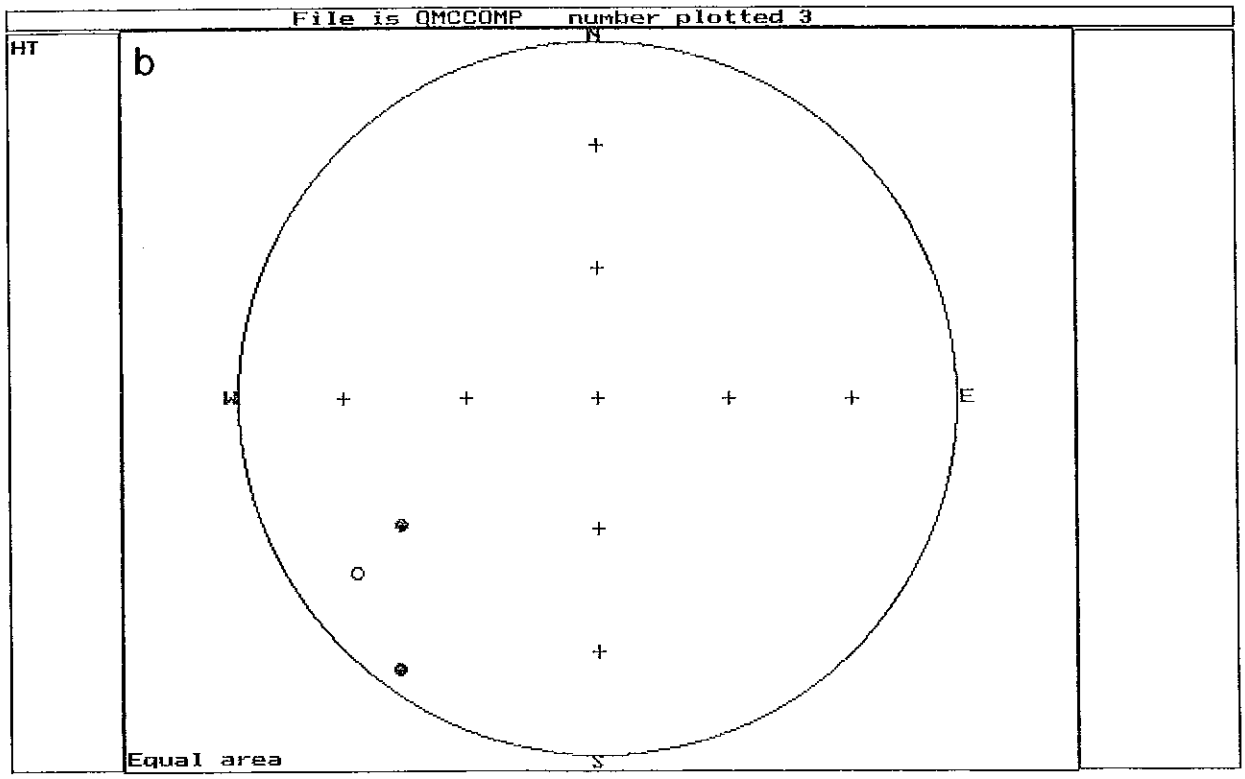
File is QMCCOMP number plotted 3
HT
b
N
W
E
S
Equal area

Ohio Leases

Sites 72,73 and 75-79 lie along a traverse from NW to SE within the Rookwood Volcanics of the Ohio leases. Site 70 lies within altered Rannes Beds immediately west of the northern end of this traverse. C components were isolated from sites 70, 76 and 78, yielding a formation mean direction of dec = 227°, inc = +69° (N =3, α_{95} = 29°), which lies within 13° of the Early Permian direction (see Fig.5.9(a)). A components were present at sites 70 and 79 and all of the Rookwood Volcanics sites, except site 76, yielded well-defined B components with a formation mean direction of dec = 115°, inc = -86° (N = 5, α_{95} = 14°).

It is possible that the Rookwood Volcanics in this belt have been locally overprinted by contact metamorphism or alteration associated with Permo-Triassic adamellites to diorites, which are exposed within the volcanics and sediments and which the magneticanomalies suggest are more extensive beneath cover than shown in the maps. The C component may therefore represent a Late Permian -Early Triassic remagnetisation rather than an Early Permian primary magnetisation. There was little apparent polar wander during the Permian and it would be difficult to distinguish between Late and Early Permian directions, particularly without detailed structural information. If the local resetting occurred in the Early Triassic, the polarity could be normal (with ~50% probability) and the steep up direction would be difficult to distinguish from the subsequent Cretaceous overprint. The intrusion sampled at site 71 does carry a primary Early Triassic magnetisation of normal polarity. The sites which did not yield a recognisable C component may in fact be carrying a normal Triassic component overprinted by the Cretaceous B component.

The unblocking temperature spectra of some of the weakly magnetic samples from the Ohio leases indicate that a low unblocking temperature phase (maghaemite or pyrrhotite) is the main magnetic carrier. These samples have similar characteristics to samples from sites 49-54 (the magnetic quiet zone south of Devlin Creek) and may reflect local alteration similar to that postulated for sites 49-54. The presence of monoclinic pyrrhotite in Rookwood Volcanics intersected by diamond drilling at the Ohio Prospect is indicated by the presence of higher susceptibility zones associated with sulphide patches within otherwise weakly magnetic andesite. Pyrrhotite has been logged in this area, although it is apparently absent from the sulphide mineralisation at Devlin Creek. This suggests that, at least in the Ohio area, traces of pyrrhotite may be the main magnetic carrier in Rookwood Volcanics for which alteration has destroyed magnetite.

Glenroy -Rosewood Belt

Sites 57 and 58 lie towards the northern end of the arcuate belt of relatively magnetic Rookwood Volcanics that stretches from Glenroy Homestead in the north to the Rosewood Gold and Mineral Field in the south. Site 65 lies within a weakly magnetic lobe or dismembered block of Rookwood Volcanics at the southeastern end of this belt and site 66 lies within the southern, SE trending portion of the main belt. The Rookwood Volcanics are flanked to the east by Siluro-Devonian volcanic rocks, which have rather similar magnetic character to the Rookwood Volcanics in this area. Site 57 was affected by lightning and yielded no useful results. Site 58 carried the B component, but the C component could not be resolved. Sites 65 and 66 exhibited well-defined B components, but the C component could only be isolated successfully from site 65. The site mean directions for well-defined components from this belt are:

B component (site 58): dec = 285°, inc = -66°
B component (site 65): dec = 47°, inc = -71°
B component (site 66): dec = 12°, inc = -75°

C component (site 65): dec = 288°, inc = +75°.

The direction of the C component diverges from the reference field direction by ~20°, suggesting that the Rookwood Volcanics dip ~20° SE at site 65.

Gogango-Rookwood Crossing-Westwood Area

Sites 80, 81, and 84-86 lie within a magnetically active zone of Rookwood Volcanics between Gogango and Westwood, which extends north to the Fitzroy River at Rookwood Crossing. Thermal demagnetisation revealed the presence of A components at sites 81, 84 and 86, and B components at sites 80 and 81. The C component could only be fully resolved at site 84, where it has the direction dec = 237°, inc = +35°. Figure 5.9(b) shows this direction and, for comparison, incompletely resolved directions of high temperature components from two other sites. The direction from site 84 suggests a dip of ~45°NE at this locality, which lies near the Fitzroy River in the NW portion of this belt.

5.3 Palaeomagnetism of the Connors Volcanics and Associated Intrusives

Since the original BMR mapping of the 1:250,000 sheet areas straddled by the study area, more detailed mapping carried out by exploration companies has revealed the presence of unconformities within the intermediate to felsic volcanic sequences that were mapped as the Connors Volcanics. Before the remapping and subdivision of these volcanics reported by Dear (1986), the Connors Volcanics were assigned to the Devonian or Carboniferous periods, on stratigraphic grounds. The oldest rocks of the Connors Arch are the felsic to intermediate Clement Creek Volcanics. They are intruded by intermediate and felsic plutons of the Clive Creek Igneous Complex, which are nonconformably overlain by the predominantly andesitic Macksford Volcanics. Alteration zones at Mount McKenzie and Clive Creek are associated with subvolcanic quartz-feldspar porphyries and dacites in the basal part of the Macksford Volcanics. These intrusives appear to be feeders to the Bald Hill Tuff, which is a locally prominent series of felsic volcanics within the lower part of the Macksford Volcanics (Dear, 1986). The Macksford Volcanics are intruded by the Late Carboniferous Burswood Complex and are unconformably overlain by the Early Permian Carmila Beds.

For this study "Connors Volcanics" and coeval intrusives were sampled around Mount McKenzie and also along the type section, which lies along the Croydon-St Lawrence road to the north of the QMC leases. In the Mount McKenzie area there is a substantial angular unconformity between the Clement Creek Volcanics, which dip ~30°NE, and the overlying Macksford Volcanics, which dip ~15°SW. The regional dip of the Macksford Volcanics along the type section is ~20°E, although the dip is somewhat variable (J. Dear, pers. comm.). Only one site (site 30) was within the Clement Creek Volcanics.

Thermal demagnetisation of specimens from most sites in these areas revealed the presence of a normal polarity component, overprinting a high temperature component of reversed polarity. Representative demagnetisation diagrams for some of these sites are shown in Fig.5.10.

Fig.5.10. Representative examples of thermal demagnetisation plots for samples of Connors Volcanics and associated intrusions. The top left plot shows remanence intensity versus temperature and the corresponding unblocking temperature spectrum (rate of change of remanence vector with respect to temperature). The bottom left plot is a stereonet showing remanence directions after each demagnetisation step. The right hand plot is a Zijderveld plot, which depicts both intensity and directional changes of remanence during demagnetisation. Vector end-points after each demagnetisation step are plotted on two orthogonal projections: open symbols are the projections onto a vertical plane (either E-W or N-S as indicated) and closed symbols are the projections onto the horizontal plane. Segments that are linear on both projections over the same temperature interval indicate removal of a single remanence component. Each remanence component is acquired parallel to the field acting at the time of acquisition. Thermal overprint components unblock at lower temperatures than primary remanence.

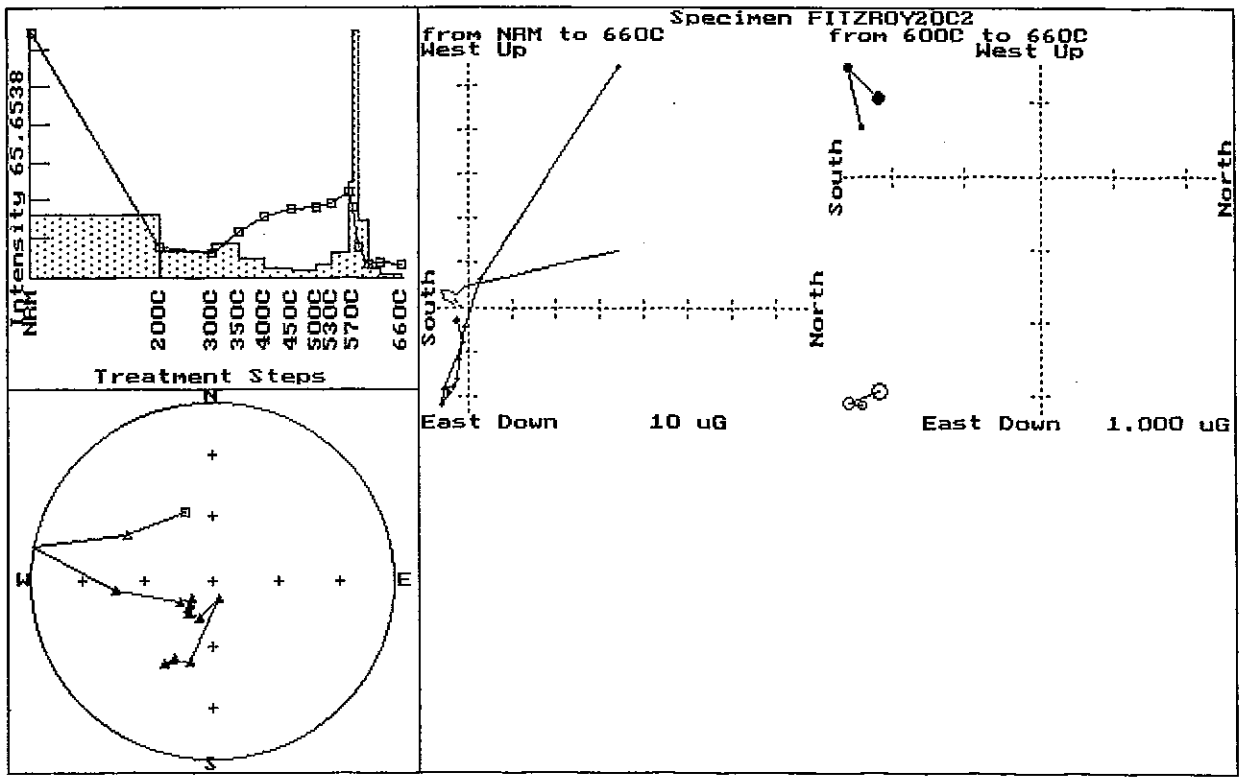
Specimen FITZROY20C2
from NRM to 660C
West Up
from 600C to 660C
West Up
Intensity 65.6538
NRM
200C
300C
350C
400C
450C
500C
530C
570C
660C
Treatment Steps
South
North
East Down
10 uG
East Down
1.000 uG

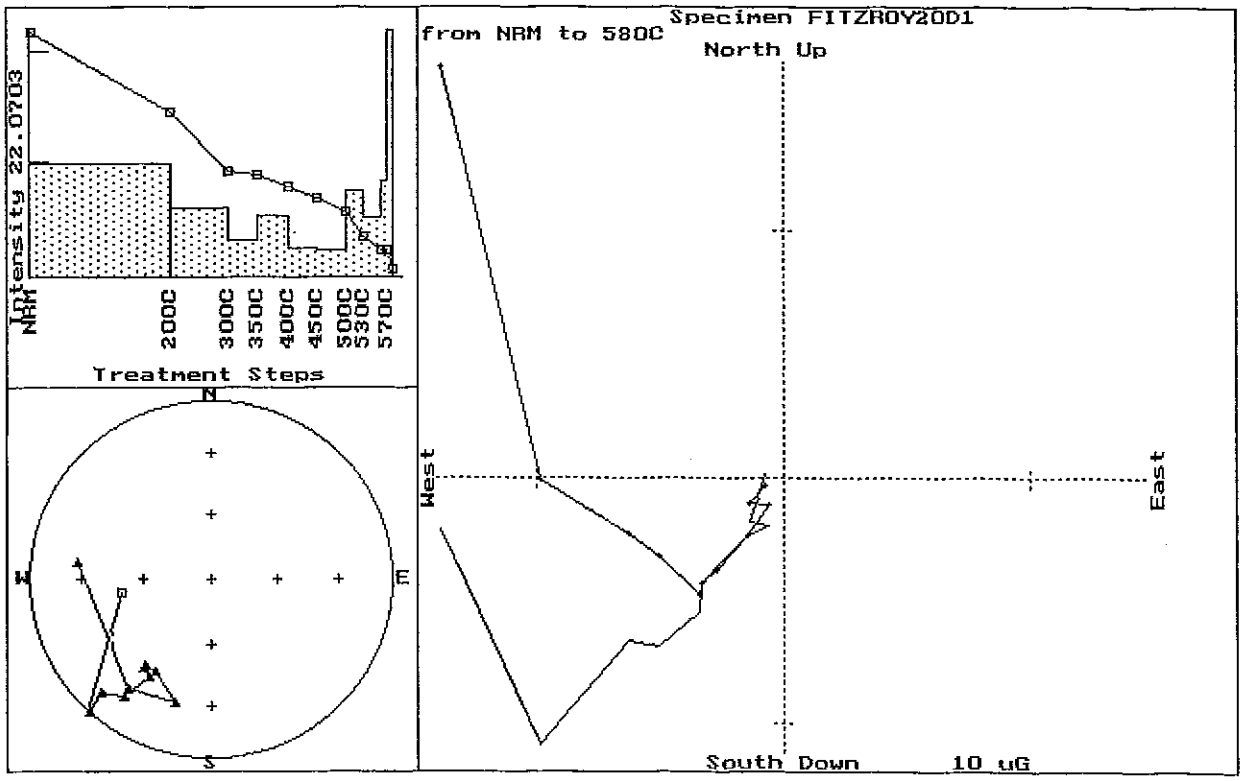
Specimen FITZROY20D1
from NRM to 580C
North Up
Intensity 22.0703
NRM
200C
300C
350C
400C
450C
500C
530C
570C
Treatment Steps
West
East
South Down
10 uG

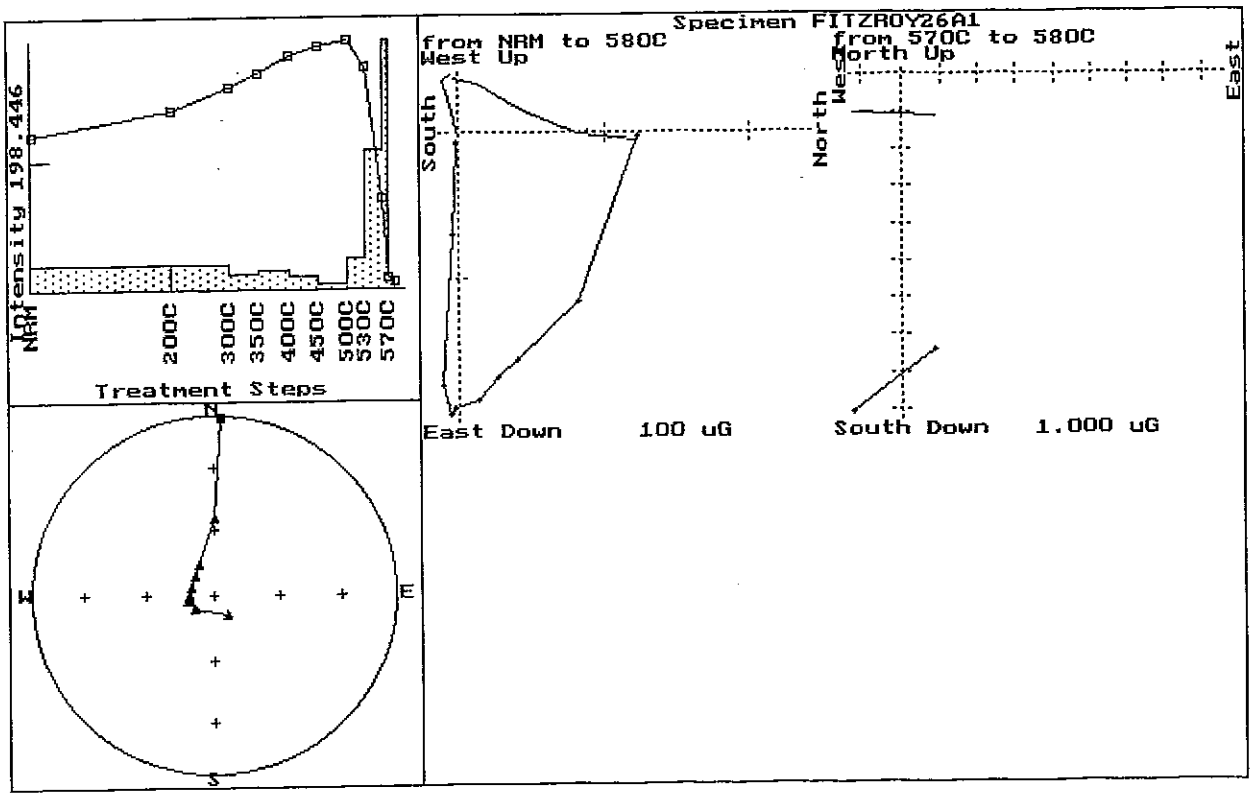
Specimen FITZROY26A1
from NRM to 580C
West Up
from 570C to 580C
North Up
Intensity 198.446
NRM
200C
300C
350C
400C
450C
500C
530C
570C
Treatment Steps
South
North
West
East
East Down 100 uG
South Down 1.000 uG
N
E
S

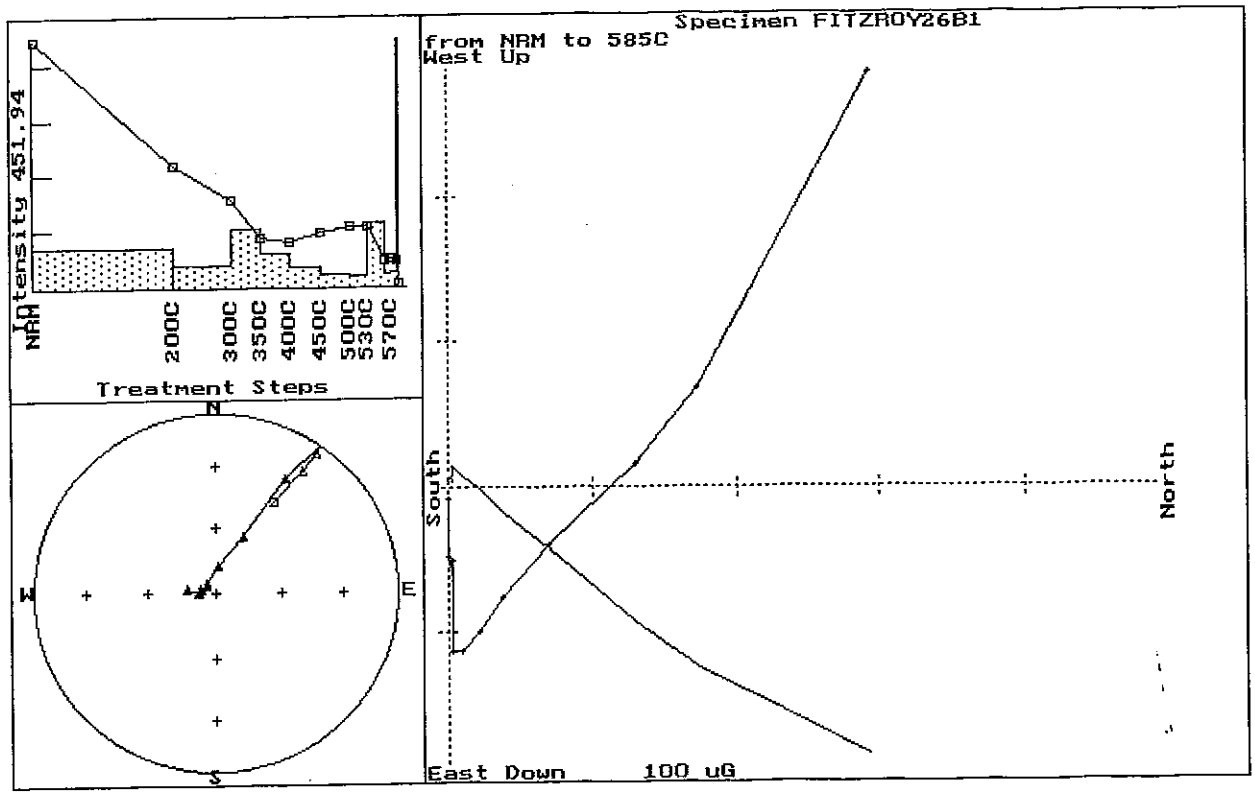
Specimen FITZROY26B1
from NRM to 585C
West Up
Intensity 451.94
NRM
200C
300C
350C
400C
450C
500C
530C
570C
Treatment Steps
South
North
East Down 100 uG
N
E
S

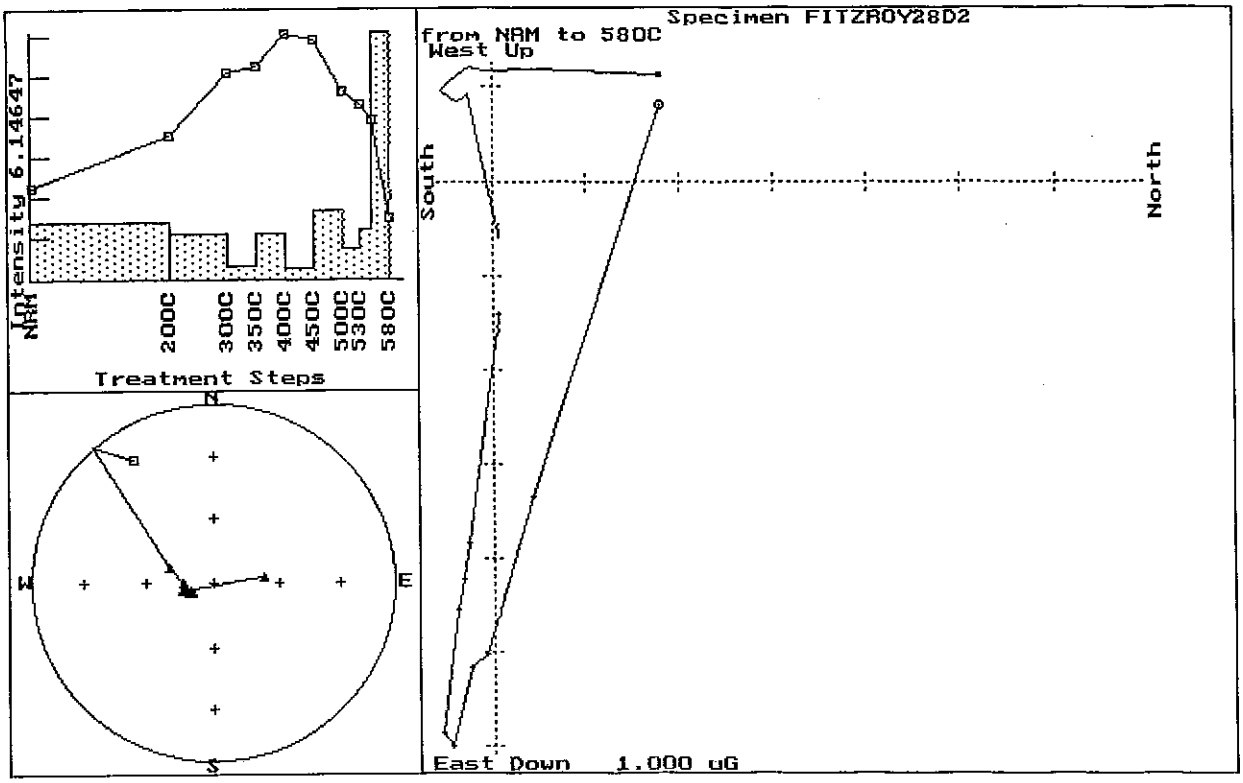
Specimen FITZROY28D2
from NRM to 580C
West Up
South
North
Intensity 6.14647
NRM
200C
300C
350C
400C
450C
500C
530C
580C
Treatment Steps
N
W
E
S
East Down 1.000 uG

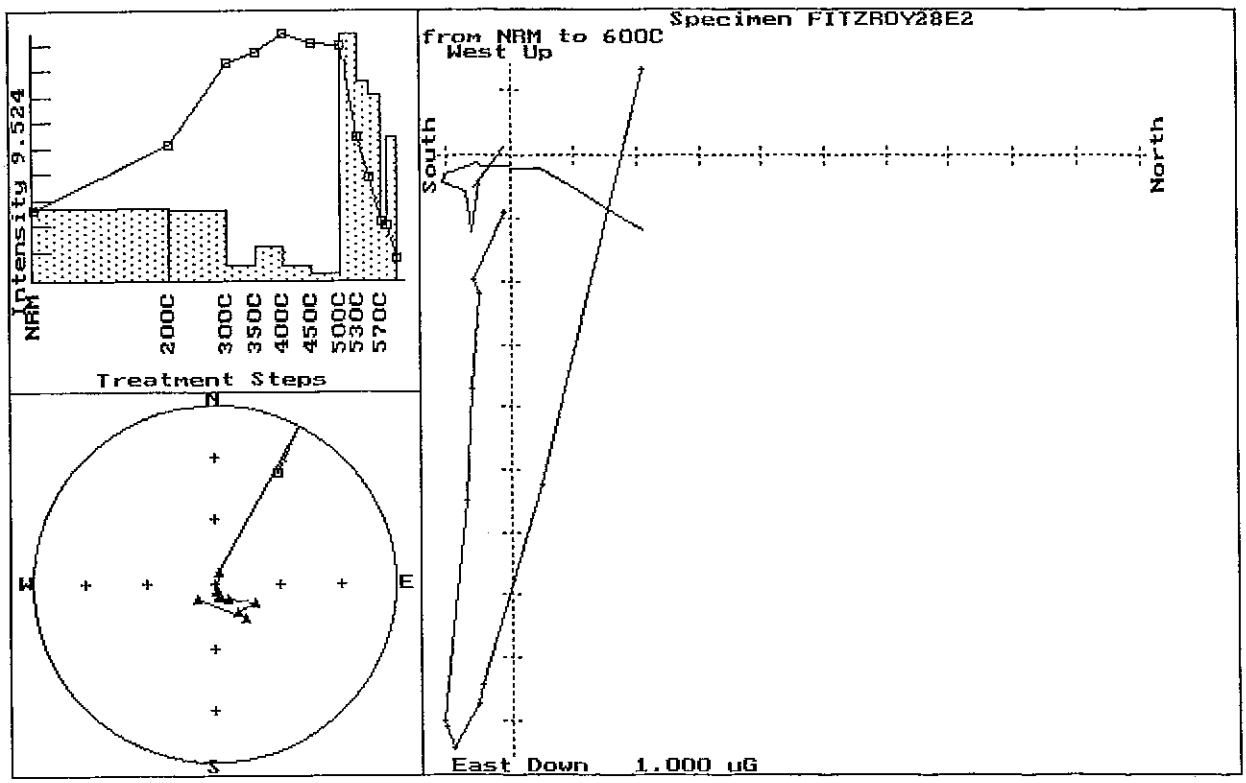
Specimen FITZROY28E2
from NRM to 600C
West Up
South
North
Intensity 9.524
NRM
200C
300C
350C
400C
450C
500C
530C
570C
Treatment Steps
N
W
E
S
East Down 1.000 uG

5.11. Overprint components revealed by thermal demagnetisation of samples of Connors Volcanics and associated intrusions, (a) present field, (b) Cretaceous overprint.

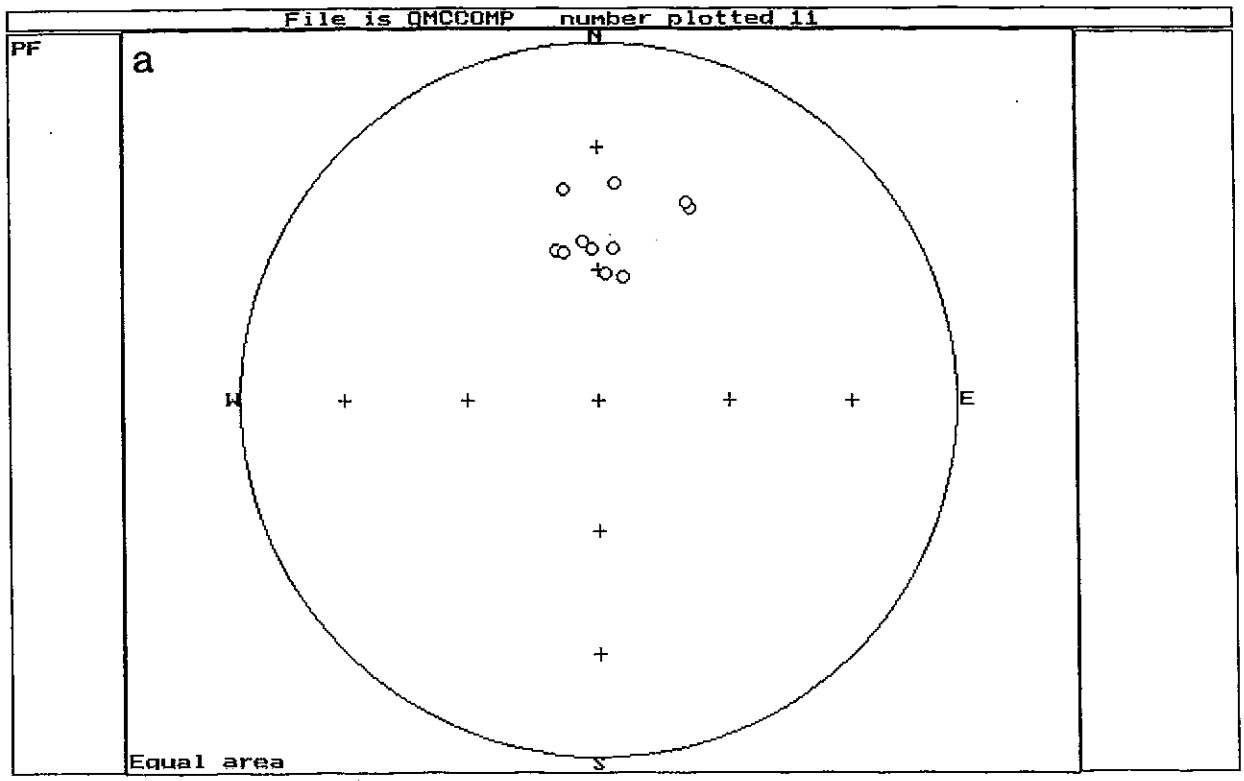
File is QMCCOMP number plotted 11
PF
a
N
W
E
S
Equal area

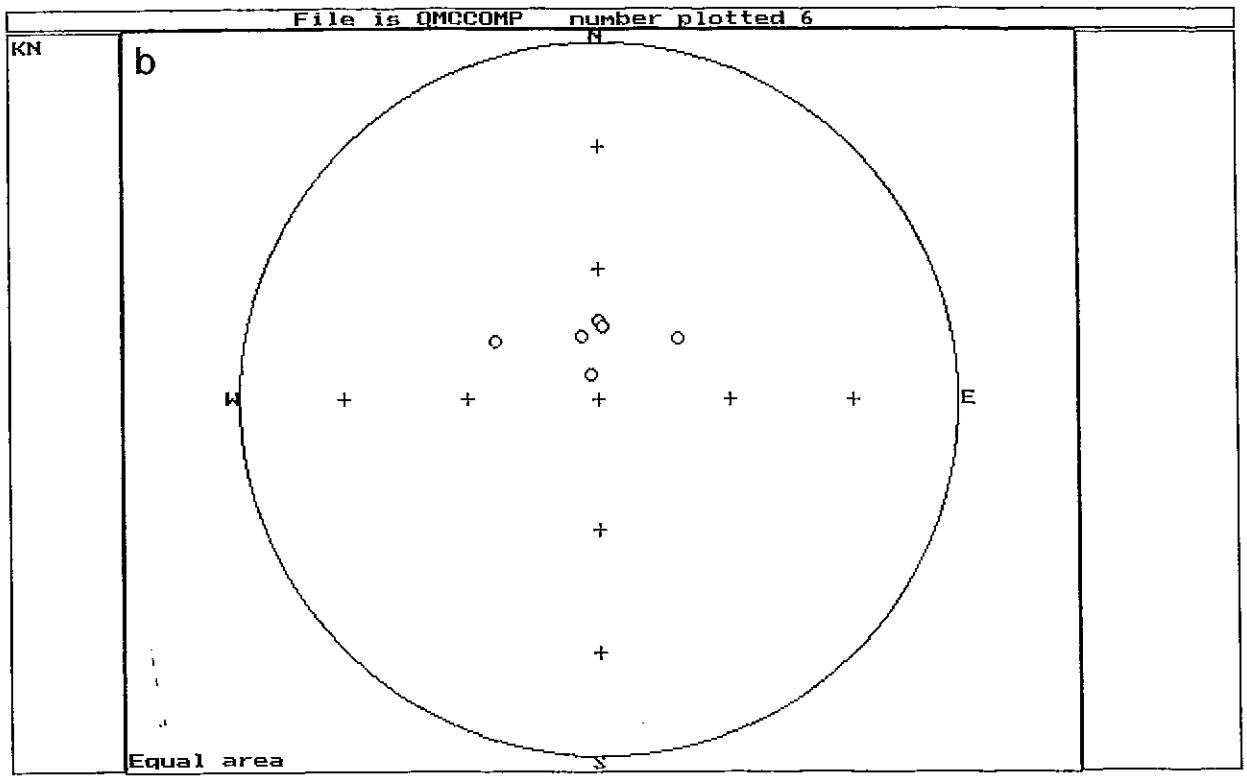
File is QMCCOMP number plotted 6
KN
b
N
W
E
S
Equal area

Fig.5.12. Reversed high temperature components interpreted as primary from the Connors Volcanics and associated intrusions, (a) Mount McKenzie area, (b) type section. Note the disparity of *in situ* directions from the two areas. After structural correction the mean directions from the two areas are similar, indicating that this magnetisation was acquired before folding.

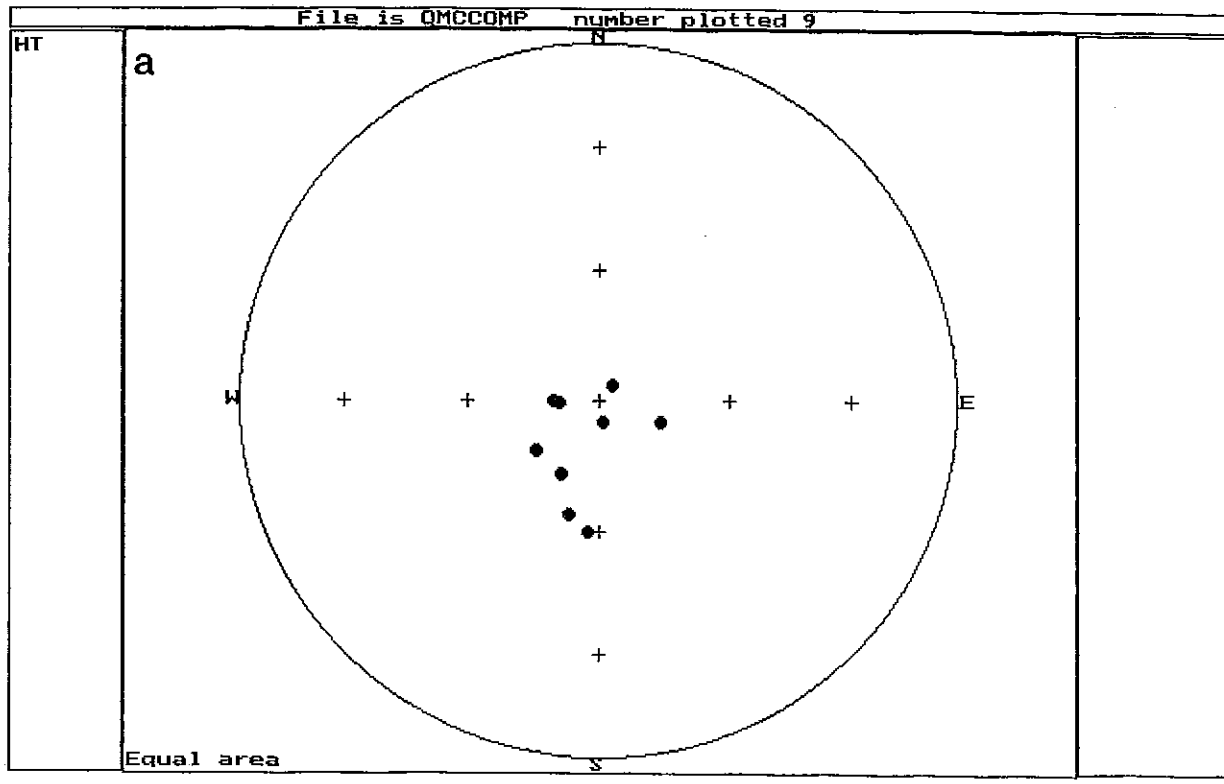
File is QMCCOMP number plotted 9
HT
a
N
W
E
S
Equal area

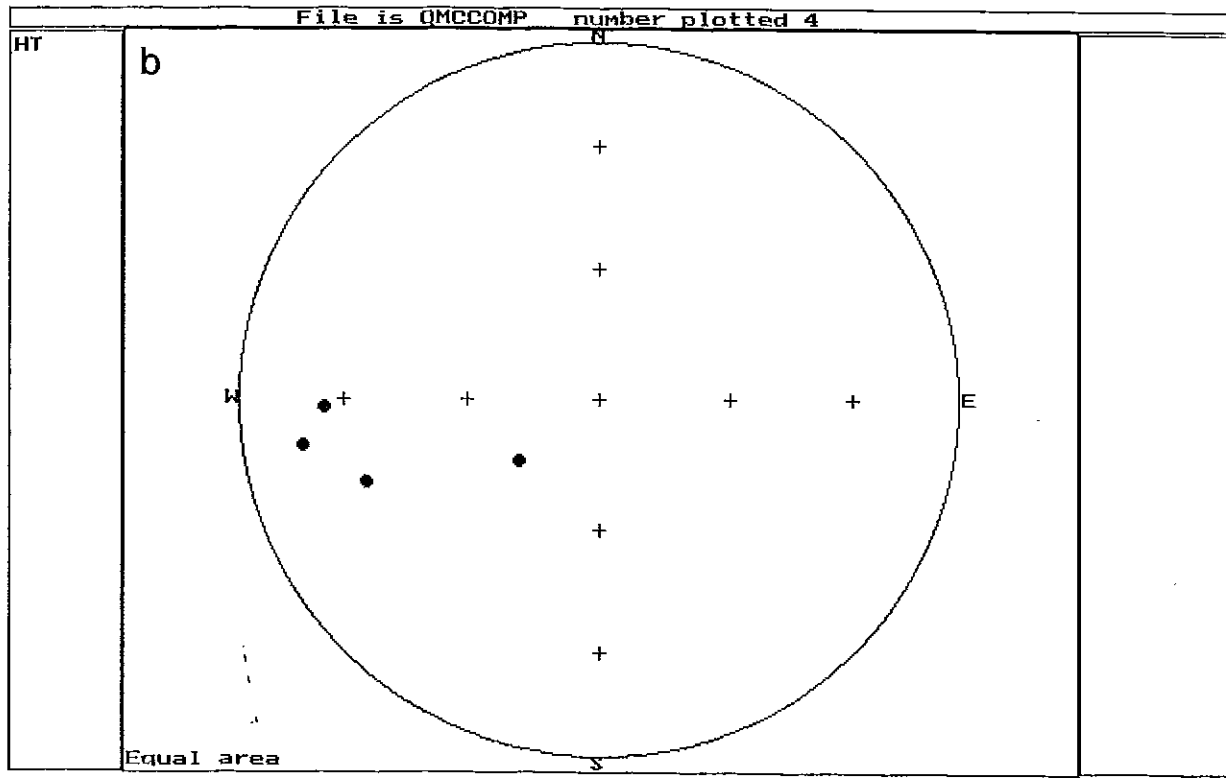
File is QMCCOMP number plotted 4
HT
b
N
W
E
S
Equal area

Demagnetisation data from all sites are plotted in Appendix I. As for the Rookwood Volcanics, directions of the lower temperature components fall into two categories: those indistinguishable from the present field direction (A components) and steeper, clearly ancient, B components. Figure 5.11 plots A and B components for all sites for which these components were resolved. In a few cases a present field A component was removed initially, followed by removal of a steep up B component. The reversed polarity high temperature C components are considered to be primary thermoremanent magnetisations. There was no discernible difference in directions of corresponding components from extrusive and associated intrusive rocks, so the results have been combined.

C component directions for sites of the Mount McKenzie area are shown in Fig.5.12(a). For the Macksford Volcanics and intrusives in this area the formation mean directions for each of the components are:

A component: dec = 3°, inc = -51° (N = 7, α_{95} = 8.5°, K = 51.8)

B component: dec = 356°, inc = -79° (N = 7, α_{95} = 11°, K = 29.3)

C component: dec = 200°, inc = +79° (uncorrected for tilting)
dec = 215°, inc = +65° (structurally corrected)
(N = 9, α_{95} = 9.5°, K = 30.6).

For the type section the corresponding results are:

A component: dec = 4°, inc = -52° (N = 5, α_{95} = 14°, K = 30.1)

B component: dec = 4.5°, inc = -76° (N = 5, α_{95} = 16°, K = 25.2)

C component: dec = 257°, inc = +38° (uncorrected for tilting)
dec = 251°, inc = +55° (structurally corrected)
(N = 5, α_{95} = 28°, K = 11.4).

The C component directions from the type section are shown in Fig.5.12(b).The *in situ* A and B components from the two areas are in good agreement, but are discrepant if the units are restored to the horizontal. This establishes that they are post-folding overprints. The A component is interpreted as a viscous remanence acquired in the recent field and the B component is interpreted as a Cretaceous overprint, acquired at ~110±10 Ma, on the basis of the corresponding pole position and the consistent normal polarity of the B component.

The *in situ* C components from the two areas are significantly different, with >95% confidence, whereas after structural correction they are indistinguishable at the 95% confidence level. This constitutes a positive fold test, demonstrating that the C component was acquired before the Permo-Triassic folding. Given the very high thermal stability of the C component and its consistent direction for all sampled lithologies with a given structural attitude, this component is probably a primary thermoremance.

Site 39 is the easternmost sampling locality of the type section, near the mapped eastern margin of the Connors Volcanics, and has a C component direction (dec = 126°, inc = +74°;, N = 3, α_{95} = 26°) that departs significantly from the corresponding directions from other

sites along the type section. This suggests a significant departure from the regional bedding attitude at this locality. If the C component from site 39 is rejected as an outlier, the site mean directions from 13 sites for which the structure is known with reasonable confidence may be combined to calculate the bedding-corrected formation mean C direction for the Macksford Volcanics and associated intrusives:

Structurally-corrected C component:
dec = 228°, inc = +63° (N = 13, α_{95} = 10°, K = 17.6).

The relatively low precision parameter for the C component probably reflects undetected variation of bedding attitudes that are not taken into account in the structural correction. Improved definition of the C component and the corresponding pole should result from accurate determination of bedding dips at sampling sites.

The mean direction of the B component for sites from both areas is:

B component (not structurally corrected):
dec = 3°, inc = -78°, N = 8, α_{95} = 10°, K = 30.9).

The corresponding pole positions for the B and C components are:

B component: 45°S, 148°E (dp = 18°, dm = 19°),

C component: 46°S, 100°E (dp = 13°, dm = 16°).

Based on the APWP, the age of the C component is interpreted to be ~320±10 Ma. This accords well with the age of the Macksford Volcanics deduced from field relationships. The B component in the Connors Arch is identical to the B component found in a wide range of rock types in the QMC leases, in the Rockhampton area and in the south and central Bowen Basin. This demonstrates the regional extent of the inferred Cretaceous thermal event. Many rock types record the Cretaceous overprint, because magnetic carriers exhibiting a wide range of blocking temperatures below 500°C, extending to ≤ 200°C in many cases, are commonly present.

In rocks that only exhibit blocking temperatures above 500°C, however, the low grade Cretaceous thermal event was incapable of overprinting the primary remanence. The trachyandesites that conformably overlie the Mount McKenzie alteration system (site 27) are good examples. The remanence of these samples is unaffected by thermal demagnetisation to ~530°C, but is progressively unblocked, without any change in direction, over two narrow temperature ranges, 550°C-580°C and 660°C-680°C. This shows that the primary remanence in these rocks is carried approximately equally by magnetite and haematite grains that are optimal palaeomagnetic recorders and are extremely resistant to overprinting. The NRM of this rock type is a pure primary remanence with a steep down direction. The high Koenigsberger ratio of the samples from this site indicates the single domain nature of the magnetic carriers, which is consistent with the excellent palaeomagnetic recording characteristics.

The Macksford Volcanics are generally good palaeomagnetic recorders and primary component directions can be determined for most samples. This suggests that, where the bedding attitude is unknown, the tilt can be estimated by comparison with the structurally

corrected formation mean C component given above. For example the inferred dip of the units at site 39 is ~40° to the WSW. At site 32, which is a disused quarry about 5 km east of Mount McKenzie, the inferred dip is ~30° to the ESE (if the single sample collected there is representative). Another site mapped as Connors Volcanics (site 69) lies well to the south of the Mount McKenzie area and exhibits very noisy behaviour on thermal demagnetisation. This precludes palaeomagnetic determination of bedding attitude for this site.

The only sampling locality within the Clement Creek Volcanics (site 30) gave results that differ distinctly from the Macksford Volcanics. The results from two cleaned samples, only one of which produced well-resolved high temperature components, do not allow any firm conclusions. It is worth noting, however, that the well-defined high temperature magnetite and haematite components isolated by thermal demagnetisation of the only well-behaved specimen, which are directed east subhorizontal and north shallow up respectively, are quite unlike the C component of the younger rocks and appear to be more ancient. Much more sampling is needed within the Clement Creek Volcanics to define the palaeomagnetic components carried by this formation.

5.4 Palaeomagnetism of the Langdale Hill Intrusion

Altered quartz-feldspar porphyry of the Langdale Hill Prospect was sampled at two sites. The three samples from site 48 are more altered than the four samples from site 47. All specimens have NRMs of reversed polarity. Demagnetisation diagrams for specimens from these sites are shown in Appendix I. The thermal demagnetisation behaviour is similar for all specimens. After removal of minor upward-directed low temperature components that are not fully resolved, a directionally stable west down component is removed mainly above 500°C. By analogy with results from other rocks sampled for this study the low temperature components may represent recent field viscous magnetisation, Cretaceous overprinting, or combination of the two. The high temperature component is carried by magnetite and haematite in samples 47C and 47D and by magnetite alone in all other samples. The high temperature directions are well grouped and clearly represent a stable ancient magnetisation that was recorded during emplacement, being either primary thermoremanence or a chemical remanence associated with the alteration, which Graham (1993) attributes to autometasomatism during crystallisation of the porphyry. The mean direction of this component is:

Langdale Hill High T Component: dec = 275°C, inc = +57° (N = 7, α_{95} = 12°).

The Langdale Hill body intrudes rocks mapped as Early Permian Carmila Beds, so the magnetisation is Permian or younger. The high temperature direction diverges significantly from all post-Carboniferous reference fields, suggesting that it has been tilted away from the original direction. However, the *in situ* direction does lie within 30°-40° of the Early and Late Permian reference field directions. The simplest interpretation of the stable remanence recorded by the Langdale Hill intrusion is that it is an effectively primary magnetisation of Permian age that has been tilted along with the intrusion away from its originally subvertical orientation to its present west-plunging direction. If the magnetisation had been acquired substantially later (Late Triassic or younger) it would be post-tilting and its present direction would be inexplicable.

The preferred interpretation of the Langdale Hill results is tilting of the porphryry stock through 35°±15° so that it is plunging ~55° to the west. This interpretation is consistent with moderate easterly dips within the Carmila Beds to the north, west and south of Langdale Hill that are indicated on the 1:250,000 St Lawrence Sheet Geology.

5.5 Other Palaeomagnetic Results

Appendix I shows demagnetisation plots for specimens from all sampling sites. Results from particular localities or formations will now be discussed individually.

Site 10 (DCa-p)

A felsic porphyritic igneous rock apparently underlying Rookwood Volcanics was sampled at site 10, about 40 metres NW of Rookwood Volcanics at site 11. A normal polarity component overprints a horizontal high temperature component that is directed ENE. The normal overprint is probably composed of a Cretaceous B component, somewhat contaminated by the high temperature component. The high temperature component, if representative of this unit, appears to be much more ancient than the Early Permian C component of the Rookwood Volcanics and may represent a tilted Late Devonian or Early Carboniferous magnetisation.

Site 31 (?Late Carboniferous Granite)

Three samples were collected from a moderately magnetic granitoid that intrudes the Connors Volcanics about 4 km east of Mt McKenzie. This exposure appears to have been affected by lightning and remanence directions were accordingly scattered. Koenigsberger ratios were greater than unity, whereas thermoremanent magnetisation of coarse-grained felsic plutonic rocks is normally associated with Q values less than ~0.5. For this reason this site did not yield any palaeomagnetic results.

Ultramafic Rocks of the Marlborough Province

Weathered, but strongly magnetic, serpentinised ultramafic rocks were collected beside the access road to the Chrysoprase Mine (site 40) and fresher samples were collected at site 41 in a stream bed beside the track from Marlborough to the Devlin Creek Prospect. Scattered remanence directions and very high Q values for the site 40 samples indicate lightning effects and these samples did not give useful palaeomagnetic data. At site 41, however, much lower Q values and consistent directions indicate little or no contamination of the NRM by lightning. Present field A components and Cretaceous overprint B components were recorded by some samples, and all five samples from this locality recorded high temperature components that were directed consistently ENE with moderate positive (downward) inclination. The site mean direction for this component is:

Site 41 High Temperature Component: dec = 60°, inc = +48° (N = 5, α_{95} = 9.4°).

This direction does not agree with any reference field direction for the Late Palaeozoic or younger times. The stability and directional consistency of this component, however, suggests that it is an ancient remanence, possibly dating from the serpentinisation event that produced magnetite, which carries this component. This event is thought to be associated with intrusion of the Marlborough ultramafics by the Ridgelands Granodiorite and other Permian granitoids.

If the high temperature component at site 41 is indeed a Permian magnetisation it would originally have been directed very steeply downwards. Assuming the remanence is Permian, its present attitude indicates subsequent tilting of site 41 through ~45°. The inferred sense of tilting is down to the WSW. Given the complex tectonic history of the Marlborough Province, substantial rotations of ancient remanence components are to be expected.

Site 89 was a roadcut along the Marlborough-Rockhampton highway. The ultramafic rocks exposed at this locality have very variable magnetic susceptibilities, reflecting heterogeneous serpentinisation. A Cretaceous B component was isolated from one sample overprinting a steep down high temperature component. This reversed polarity thermally stable component was also found in another sample from site 89 and from the only sample at site 90, about 30 km SE of site 89. The site mean direction of the high temperature component at site 89 is dec = 248°, inc = +78° and the corresponding component at site 90 is dec = 189°, inc = +68°. These *in situ* directions are close to the Permian field direction and support the assumption that the ultramafics may record a Permian serpentinisation event that is locally rotated by tectonic movements.

Intrusions within the Marlborough Province

Two plutons that intrude the ultramafic rocks and schists of the Marlborough Province south of Marlborough were sampled: a magnetic diorite or gabbro at site 87 and a weakly magnetic hornblende-biotite-quartz granite at site 88. Both intrusions are assigned to the Pui intrusions, which have K-Ar hornblende and biotite ages of ~235 Ma (Malone, 1970). The diorite exhibits well-defined high temperature components of reversed polarity, overprinted by normal components which appear to be hybrid present field and Cretaceous overprints with overlapping unblocking temperature spectra. The granite exhibits only minor overprinting of the steep down high temperature component because most of the magnetite grains that carry the remanence have unblocking temperatures close to the Curie point of magnetite and unblock mainly above 500°C. However the subordinate overprint components could be resolved by the thermal demagnetisation. The site mean directions are:

Pui Diorite High Temperature Component: dec = 181°, inc = +79° (N = 5, α_{95} = 11°)

Pui Granite Overprint Component: dec = 311°, inc = -71° (N = 3, α_{95} = 4.4°)

Pui Granite High Temperature Component: dec = 323°, inc = +80° (N = 3, α_{95} = 8°)

The high temperature directions are consistent with Late Permian primary magnetisations and the overprint direction is consistent with the ubiquitous Cretaceous overprint.

The Ridgelands Granodiorite, which intrudes the SE portion of the Marlborough Province was also sampled (site 97). The radiometric age of the Ridgelands Granodiorite is 280 Ma (Murray, 1975). The remanence of the magnetic granodiorites at site 97 is almost completely overprinted with only a hint of an unresolved high temperature component. The site mean overprint direction from the two samples is:

Ridgelands Granodiorite Overprint Component: dec = 77°, inc = -83° .

The complex magnetic pattern of the Marlborough Province is partly attributable to the influence of granitoids that intrude the ultramafic rocks, causing heterogeneous serpentinisation and imparting thermoremanent magnetisation by contact metamorphism and thermochemical remanence by contact metasomatism. The remanence associated with Permian intrusions has reversed polarity. Varying degrees of overprinting of this reversed remanence by a Cretaceous normal component and by viscous remanence produces highly variable contributions of remanence to the total magnetisations of the serpentinised ultramafics. Variability on a large scale produces substantial base level shifts in the TMI map, whereas smaller scale variability contributes to the characteristic busy texture of the magnetic pattern over the ultramafics.

Siluro-Devonian Rocks

Massive flows mapped as Siluro-Devonian volcanics were sampled in the Fitzroy River bed at site 59. Five samples were collected from four separate flows. The measured dip of the flows is 36° to 235°. Thermal demagnetisation revealed well-defined Cretaceous overprints, in one case itself overprinted by a present field component. High temperature components appeared to be defined for each sample, but the directions varied from sample to sample. This scatter may reflect the presence of both polarities of the high temperature remanence, although not enough samples were collected to be definite. One possible interpretation of the high temperature directions is that two flows have recorded a SW down component and a third flow has recorded the antipodal NE up field. these directions appear to be very ancient, but further sampling is required to define possible primary components in these rocks. The site mean Cretaceous overprint direction is dec = 44°, inc = -70° (N = 4, α_{95} = 11°).

At site 60 Siluro-Devonian sediments are intruded by narrow veins of mafic igneous rock. Two samples of the igneous rocks were collected. Both carried steep up Cretaceous components (mean direction dec = 6°, inc = -76°) overprinting very steep high temperature components. One sample had a high temperature component that was directed steeply upwards, whereas the other sample had an almost antipodal steep down high temperature component. Converting the reversed direction to normal polarity and combining with the normal component gives a mean *in situ* direction of dec = 299°, inc = -83°. These directions suggest dual polarity remanence acquired during the Triassic. On the other hand, assuming that the high temperature components predate folding and restoring the steeply dipping enclosing sediments to the horizontal rotates the high temperature directions to NNE shallow up/SSW shallow down directions, which are consistent with Devonian magnetisations. Without further data it is impossible to be definite about the age of magnetisation. However, these very preliminary results suggest that good palaeomagnetic recorders are present within the Siluro-Devonian belt.

Very weakly magnetic Siluro-Devonian limestones were sampled near the entrance to "Melrose". A high temperature magnetisation of reversed polarity was weakly overprinted by a normal component that was removed up to 200-300°C. The overprint component was only resolved in one case, but appears to be Cretaceous. The reversed magnetisation unblocks principally between 300°C and 350°C, suggesting that trace quantities of either monoclinic pyrrhotite or maghaemite carry most of the magnetisation. The mean direction of the component carried by this low unblocking temperature mineral is dec = 46°, inc = +63°. There is also a hint of a distinct, very weak, high temperature component carried by magnetite that cannot be fully resolved, but appears to be directed ~S with moderate positive inclination.

Correcting the lower unblocking temperature direction for the bedding dip rotates it to a SW-directed component with an inclination of ~60°, which could be interpreted as a Carboniferous magnetisation. With more sampling, unravelling the magnetic and structural history of the ?Siluro-Devonian sediments of the Yarrol Terrane should prove possible.

Sites 42-43 (DCa-p)

Volcanic rocks exposed to the northeast of the Rookwood Volcanics of the Devlin Creek Prospect were sampled at sites 42 and 43. The NRM of the site 43 sample is suspected to be lightning affected because of the high Koenigsberger ratio. NE-directed directions with moderate negative inclination were isolated by thermal demagnetisation of specimens from site 43, after initial removal of a minor, poorly resolved overprint component. The mean direction of the high temperature component is dec = 50°, inc = -39°, which is consistent with an unrotated Early Carboniferous magnetisation. Further sampling, in conjunction with determination of structural attitudes, should define the significance of this component.

Permian Sediments (Sites 44-46)

Permian sediments from site 44 carry a reversed polarity high temperature remanence, slightly overprinted by a normal polarity component, whereas site 46 is totally overprinted by a steep up component. Site 45 did not yield interpretable components, probably due to normal and reversed components with highly overlapped unblocking temperatures. Permian sediments from the Bowen Basin are strongly overprinted by a steep up magnetisation, indistinguishable from the overprint found throughout this study area, and primary Permian magnetisations can only occasionally be isolated (M. Lackie, pers. comm.).

Carboniferous Limestones (Sites 55-56)

Both present field and Cretaceous overprinting could be recognised in weakly magnetic limestones exposed south of Muldoon. These rocks are mapped mapped as Cl. Site 56 samples also carry a thermally stable magnetisation, carried by haematite, directed ~N with moderate negative inclination (Dec = 7°, inc = -38°), which upon structural correction changes to dec = 312°, inc = -40°. This direction is within 23° of the Early Devonian field direction, raising the possibility that these rocks are actually mismapped S-D limestones, which are lithologically similar to Carboniferous limestones. However, the high temperature direction is close to the present dipole field direction and could represent a component produced by recent weathering.

P-Mi Granite and Mafic Dyke at Mount Wallace (Sites 62-64)

Granite denoted as P-Mi was sampled either side of a 10 metre wide mafic dyke at Mount Wallace. Sample 62A, 3m from the dyke margin has an NRM dominated by a steep up overprint, whereas sample 62B, which is only 1m from the dyke contact also has a steep down high temperature component. The dyke carries a high temperature component of reversed polarity that is not fully resolved due to overlapped unblocking temperatures with a normal overprint, but has steep inclination.

These results are interpreted as local remagnetisation of the granite in the baked zone adjacent to the dyke, probably during the Permian. Both rock types were subsequently overprinted

during the Cretaceous, particularly the granite, which is not as good a palaeomagnetic recorder. The primary magnetisation of the granite does not appear to have survived.

Diorite (Site 68)

A diorite intrusion, mapped as P-Mi but possibly related to intrusions of the Clive Creek Complex, was sampled beside the Bruce Highway-Duaringa Road. The Cretaceous overprint direction dominated the NRM of these samples. The mean direction of this component was dec = 348°, inc = -70° (N = 3, α_{95} = 18°). Only one sample had a well-defined high temperature component (dec = 168°, inc = +67°). This direction is consistent with a Permian or Carboniferous primary magnetisation, slightly rotated by tectonic tilting.

Pui Diorite (Sites 71 and 74)

Diorite to adamellite intrusions into the Rookwood Volcanics near the Ohio prospect were sampled at sites 71 and 74. Weakly magnetic site 71 samples carried a monocomponent remanence with a steep up direction. The remanence is extremely stable to thermal demagnetisation, unblocking almost entirely between 570°C and 580°C. This is presumably a primary thermoremanence carried by palaeomagnetically optimal magnetite grains that cannot be overprinted by low grade thermal events. The site mean direction is:

Site 71 Diorite: dec = 226°, -81° (N = 3, α_{95} = 17°). Pole 9.9°S; 162°E (31.6, 32.8)

Because of its normal polarity, this direction suggests an Early Triassic age of magnetisation, rather than Late Permian. This intrusion has an approximate radiometric age of 240 Ma (Kirkegaard, 1970), which is consistent with the inferred palaeomagnetic age.

Site 74 samples had scattered directions and yielded no interpretable palaeomagnetic results. These samples are much more magnetic than the site 71 samples, because they contain abundant multidomain magnetite. They exhibit very broad unblocking temperature spectra and do not have the ideal palaeomagnetic characteristics of the site 71 samples, which contain single domain magnetite as the only magnetic mineral, albeit in trace amounts.

Site 82 Trachyte

A trachytic plug intruding Rookwood Volcanics of the Gogango-Westwood belt was sampled at site 82, near Rookwood Crossing. This intrusion is associated with a prominent radiometric anomaly. Trachytes in the region are restricted to the Cretaceous period. Thermal demagnetisation revealed an essentially monocomponent magnetisation with direction dec = 349°, inc = -70°, which is consistent with a Cretaceous age of magnetisation.

Site 83 Diorite

Two samples were collected from an unmapped intrusion at site 83 within the Rookwood Volcanics of the northern portion of the Gogango-Westwood belt. One sample was lightning-affected and had a very high Q value. The other sample had a Q value in the normal range and exhibited a monocomponent remanence with direction dec = 324°, inc = -57°, which may represent a Cretaceous overprint, although it diverges from the reference field directions by

~25°. Some contamination of the remanence by lightning is possible, given the proximity of a lightning-affected sample.

Cretaceous Igneous Rocks (Sites 91, 94, 95)

An unmapped mafic igneous rock exposed beneath the Alligator Creek bridge on the Bruce Highway was sampled at site 91. A flow banded rhyolite mapped as Kut was sampled at site 94 and Cretaceous basalt (Kub) was sampled in a roadcut on the Capricorn Highway at site 95. All these sites carried almost monocomponent remanence directed steep up, consistent with a Cretaceous age of magnetisation. This magnetisation is carried by magnetite only at site 95, by both magnetite and haematite at site 91 and predominantly by haematite, with only a minor magnetite contribution, at site 94. There is no evidence of a reversed high temperature component at site 91, which should be present if this rock is a Permian basalt and it is therefore assigned to Kub, rather than Pub.

Bouldercombe Complex Intrusion (Site 96)

A moderately magnetic ?granodiorite of the Bouldercombe Complex (Puo) was sampled in a quarry beside the Capricorn Highway. Subparallel, steep up, intermediate temperature and high temperature components were defined by thermal demagnetisation. The high temperature component is carried by magnetite and haematite. The data can be interpreted as a Cretaceous overprint of a steep up primary magnetisation, or as a single component that recorded minor secular variation during cooling of the pluton. The broad unblocking temperature spectrum implies that a pre-Cretaceous primary magnetisation would have been partially overprinted during the Cretaceous event. The Bouldercombe Complex intrudes the Rookwood Volcanics and Late Permian sediments and is overlain by Cretaceous basalts and trachytes.Its radiometric age is 235 Ma (Murray, 1975), i.e. Middle Triassic. Thus the remanence of this intrusion is interpreted as a primary Triassic magnetisation of normal polarity, partially overprinted in a subparallel field during the Cretaceous. The directions of the two components are:

Middle Triassic Primary Component: dec = 304°, inc = -76°, (Pole 34.9°S, 176.1°E)

Cretaceous Overprint Component: dec = 6°, inc = -78°.

Native Cat Andesite (Sites 92, 93)

Post-orogenic, variably magnetic samples of Triassic Native Cat Andesite were sampled at sites 92 and 93. The two site 92 samples carried remanence comprised of minor present field components overprinting more thermally stable normal polarity components directed ~NE with steep negative inclination. Directions from site 93 were scattered and thermal demagnetisation yielded no consistent thermally stable component. The mean direction from site 92 (dec = 56°, inc = -68°) is about 20° from Triassic or Cretaceous field directions. This could simply reflect secular variation, as individual lava flows record only spot readings of the palaeofield at the time of extrusion. However the broad unblocking temperature spectrum suggests that this unit should have been overprinted in the Cretaceous. The slightly anomalous direction may arise from contamination of the ancient component(s) by a shallower recent field component with an overlapping unblocking temperature spectrum.

5.5 Synthesis of Palaeomagnetic results

The most striking feature of the palaeomagnetic data from pre-Cretaceous rocks is the pervasive presence of low to intermediate temperature components that are consistently directed steeply upwards, irrespective of the age of the rocks and their structural attitude. This evidently post-folding remanence agrees with overprint components found throughout the south and central Bowen Basin (M. Lackie, pers. comm.) and is similar to a Cretaceous magnetisation that consistently overprints sedimentary and pre-Tertiary igneous rocks of the Sydney Basin (Schmidt and Embleton, 1981). The site mean directions from all sites that recorded this component, apart from the Connors Volcanics, were combined to yield the following estimate of the palaeofield direction during acquisition of this magnetisation:

Mean Cretaceous Overprint Component: dec = 5.3°, inc = -78.6°
(N = 42, α_{95} = 4.2°, K = 28.0).

This mean direction is indistinguishable from the corresponding component found in the Connors Volcanics and associated intrusives in the far NW corner of the study area, demonstrating that the overprinting is of regional extent and is penecontemporaneous across the study area.

The mean high temperature direction from the Cretaceous rocks sampled in this study is:

Mean Cretaceous Primary Component: dec = 20°, inc = -75°
(N = 4, α_{95} = 20°, K = 21.0).

This direction lies only 5° from the mean overprint direction. The overprint direction is therfore indistinguishable from the interpreted primary magnetisations of the Cretaceous rocks, suggesting that the overprinting event occurred close in time to the Cretaceous igneous activity.

The corresponding palaeomagnetic pole position for the overprint magnetisation is:

Cretaceous Overprint Pole: 44.8°S, 147.2°E (dp = 7.5°, dm = 8.0°).

The age of overprinting is estimated as 110 ± 10 Ma from the APWP. This interval is within the Cretaceous Normal Superchron, accounting for the consistent normal polarity of the overprint magnetisation.

The cause of the overprinting is uncertain, but an elevated geothermal gradient accompanying Cretaceous magmatism appears to be the most likely explanation, given the coincidence of overprinting with Cretaceous igneous activity. Elevated temperatures acting for geologically significant periods can reset magnetic grains, particularly multidomain magnetite grains, which have laboratory unblocking temperatures far higher than the ambient temperature. Primary remanence is retained only by grains with very high unblocking temperatures. Thus a low grade thermal event in the Cretaceous could have remagnetised all the less thermally stable magnetic grains in the rocks, producing a remanence consisting of two components: a primary magnetisation retained by grains with high unblocking temperatures and an overprint component carried by grains with low to intermediate unblocking temperatures.

Fission track studies or Ar-Ar analyses could characterise the thermal history of the area in detail. There is evidence of substantial resetting of K-Ar and Rb-Sr systems in rocks from SE Queensland, which causes low apparent ages in the Triassic North Arm Volcanics and other igneous rocks of similar age (Ashley and Shaw, 1993). These authors suggest overprinting associated either with emplacement of the Noosa intrusive suite or with a pervasive low-temperature alteration event, related to a period of high heat flow. It is possible that an event similar to the overprinting detected in this study is responsible for the overprinting of isotopic systems in SE Queensland. Variable degrees of Cretaceous overprinting could produce the hybrid apparent ages (187-152 Ma) found in rocks dated at ~213 Ma.

In many cases Rookwood Volcanic units retain a probably primary Permian magnetisation which is isolated by thermal demagnetisation above ~500°C. The remanence component is invariably of reversed polarity and has been rotated with the volcanic units during folding. The high temperature stable remanence of the Rookwood Volcanics can therefore be used to infer the local bedding attitude where the structure is unknown. The current best estimate of the palaeofield direction during extrusion of the Rookwood Volcanics is:

Rookwood Volcanics Primary Component: dec = 199°, inc = +71°
($N = 9$, $\alpha_{95} = 14°$, $K = 13.9$).

Approximate estimates of semi-regional bedding attitudes were used to derive this bedding-corrected direction. Better definition of the mean direction should result from accurate determination of the local structure at key sampling sites. In the interim, it may be more reliable to use departures of primary remanence directions from the Early Permian reference field direction (dec = 192°, inc = +79°) for estimating local structure, although the difference between the two directions is only 8°.

The Macksford Volcanics (upper portion of the "Connors Volcanics") and associated intrusions generally retain an apparently primary remanence of reversed polarity, which can be resolved by thermal demagnetisation above ~500°C. The age of magnetisation, and therefore probably the age of emplacement, is inferred to be ~310 Ma from the palaeomagnetic pole position. The estimated palaeofield direction recorded by these rocks is:

Macksford Volcanics Primary Component: dec = 228°, inc = +63°
($N = 13$, $\alpha_{95} = 10°$, $K = 17.6$).

Where the local structure is unknown, comparison of high temperature directions from Macksford Volcanic units with this paleofield direction should enable estimation of the bedding attitude.

Many other pre-Cretaceous rocks retain a primary remanence, in most cases overprinted by the Cretaceous component. In some cases the age of undated or poorly dated rocks may be inferred or refined palaeomagnetically, using the directions and polarities of the remanence isolated at high temperatures. For example, a normal polarity primary component in a Permo-Triassic intrusion implies an Early Triassic age, rather than Late Permian. When the age of the rock is reasonably constrained, departure of the primary component direction from the known palaeofield field direction at the time of formation can define tectonic tilting of the site. This method has been used to detect tilting of the Langdale Hill intrusion, which is now plunging to the west.

6. IMPLICATIONS FOR MAGNETIC INTERPRETATION

6.1 Major Features of the TMI Data

Figure 6.1 shows the total magnetic intensity (TMI) map for the QMC Fitroy Leases survey, with sampling sites indicated. Although the unprocessed TMI map is not the most suitable basis for interpretation of fine geological detail or for mapping subtle magnetic features associated with the less weakly magnetic units, it does preserve anomaly amplitudes and places gross geological features in context. There are some approximate rules of thumb that are useful in relating observed anomaly amplitudes to magnetisations of sources. This relationship depends on the source geometry, geomagnetic field strength and field direction. Examples applicable to this study area are:

Laterally Extensive Bodies with Great Depth Extent/Steep Geological Contacts

Susceptibility Contrast		Magnetisation Contrast	Anomaly Amplitude
μG/Oe	10^{-6} SI	μG or mA/m	nT
10	126	5.2	~3
100	1256	52	~30
1000	12560	520	~300

Subcropping dykes or thin steeply dipping units (thickness comparable to flying height)

Susceptibility Contrast		Magnetisation Contrast	Anomaly Amplitude
μG/Oe	10^{-6} SI	μG or mA/m	nT
10	126	5.2	~0.4
100	1256	52	~4
1000	12560	520	~40

A susceptibility contrast of 1000 μG/Oe corresponds to a change in magnetite content of only about 0.3 vol%. Variations in average magnetite content of this order produce large magnetic anomalies, typically hundreds of nT. In weakly magnetic rocks trace amounts of magnetite can produce susceptibility differences of ~100 μG/Oe. This is quite sufficient to produce detectable anomalies (several nT to several tens of nT) in airborne surveys. Even in the total absence of magnetite or other ferromagnetic minerals, coherent differences in iron content can be detected from the air. The relationship between magnetic susceptibility and total iron in a rock for which all iron is contained in paramagnetic minerals (silicates, carbonates etc.) is: k (μG/Oe) $\approx 5 \times$ wt% FeO^T. Thus a difference in paramagnetic iron contents of 2 wt% across a geological contact produces a susceptibility contrast of 10 μG/Oe, which gives rise to an anomaly of ~3 nT. Larger differences in total iron give rise to correspondingly larger susceptibility contrasts and anomalies.

Although large homogeneous bodies produce larger TMI responses than narrow dyke-like bodies, long narrow sources near the surface produce much stronger vertical derivative responses than broad or deep sources. Thus filtering of the TMI data to produce first vertical derivative images greatly enhances the response of shallow and narrow features with respect to broad and deep sources. The amplitude (in nT/m) of the first verical derivative anomalies associated with subcropping dykes of width equal to the flying height can be estimated by dividing the anomaly amplitudes given above by the sensor height.

Fig.6.1. Total magnetic intensity image for the Fitzroy Leases aeromagnetic survey, with sampling sites indicated.

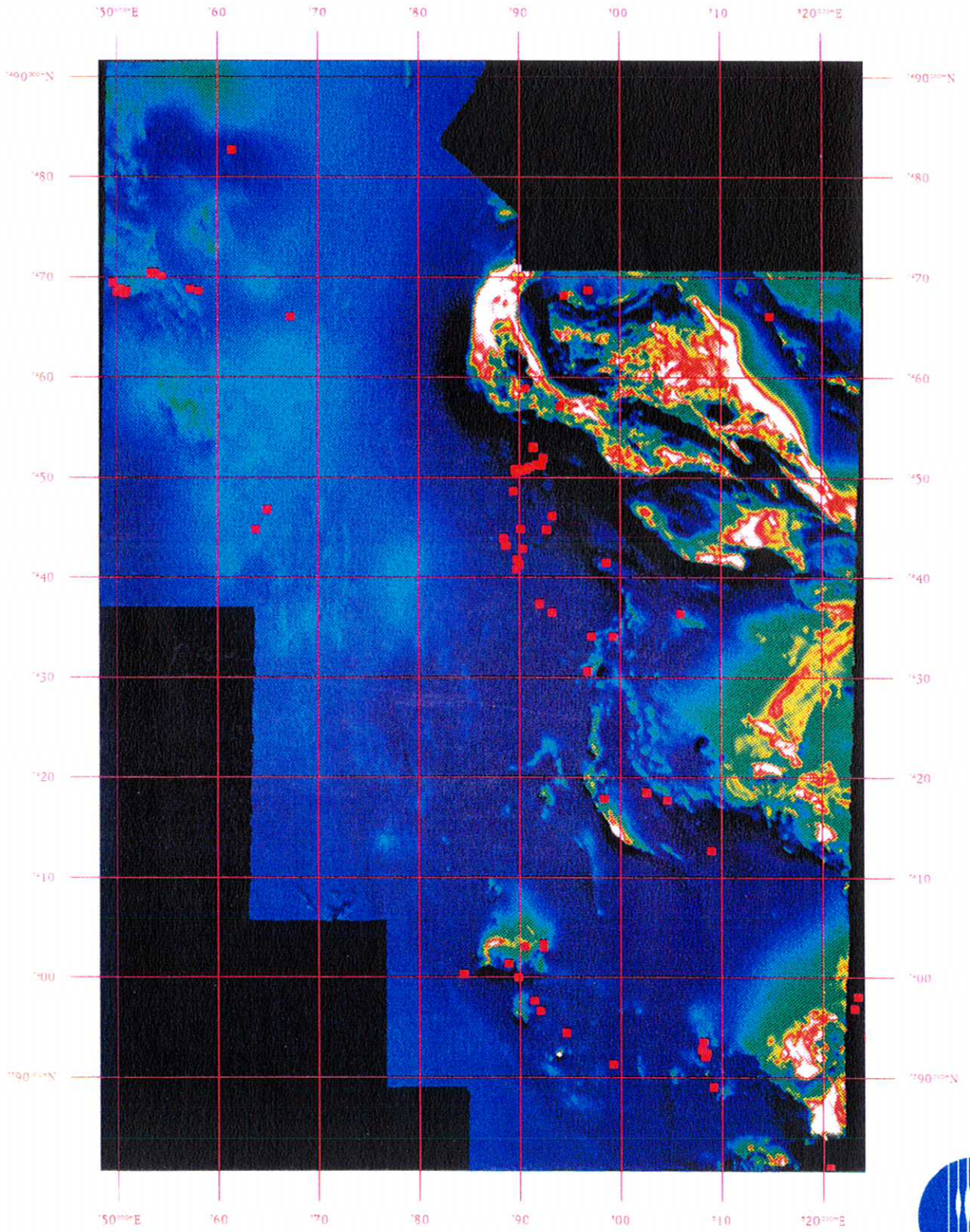

Division of Exploration and Mining

Total Magnetic Intensity
Red squares indicate sample sites.

CSIRO
AUSTRALIA

The most prominent signature in the survey area is associated with serpentinised ultramafic rocks of the Marlborough Province. The overall anomaly of the Marlborough Province is a magnetic high, about 1000 nT above the regional base level, corresponding to an average effective susceptibility contrast of ~3000 μG/Oe (0.038 SI). Within this high, however, there are prominent linear and arcuate relative magnetic lows with very smooth character associated with belts of non-magnetic Palaeozoic metamorphic rocks. These smooth low zones are traversed by many low amplitude, narrow, linear anomalies, which are clearly displayed in the high-pass filtered versions of the data, and which probably represent dykes intruding the Marlborough Block. Felsic volcanics of the Berserker Beds wthin the Marlborough Province correspond to a relative magnetic low, but exhibit a "busy" magnetic pattern that is typical of moderately magnetic volcanic rocks.

In detail, the ultramafic rocks are associated with a very busy magnetic texture, with rapid variations of hundreds of nT. This pattern is characteristic of magnetic rocks that are very heterogeneous over distances comparable to the flying height. The susceptibility and NRM measurements confirm that the ultramafics are the most magnetic rocks in the study area on average, but have very variable properties. As well as the small scale variations in the field there are larger zones of higher and lower base level, reflecting larger scale changes in average magnetisation. Intrusions into the Marlborough Block, and their aureoles, also show distinctive signatures. It seems likely that local overprinting of remanent magnetisation of the ultramafics by contact metamorphism may account for some of the variation in magnetic base level within the ultramafics. Analysis of remanence components from ultramafic samples confirms that these rocks are capable of retaining stable ancient magnetisations, variably overprinted by later events. Serpentinisation fronts around plutons intruding the ultramafics may also produce extensive zones of differing average magnetite content, producing relative magnetic highs over more intensely serpentinised zones. Some intrusions are inferred from the magnetic pattern but are not exposed, suggesting that they lie in the subsurface. The noisy magnetic texture is explicable by heterogeneous protolith composition and small scale variability in serpentinisation, which lead to large variations in magnetite content. Spatially coherent linear and arcuate structures are evident within the overall noisy magnetic pattern of the ultramafics, suggesting that detailed mapping of structures in the Marlborough Province is possible using the aeromagnetic data.

Large intrusions of various ages and Cretaceous volcanic rocks are also associated with prominent anomalies. The Ridgelands Granodiorite, which intrudes the Marlborough Block, is exposed in the central portion of the eastern edge of the survey area and probably extends beneath part of the Marlborough Province. This intrusion is associated with a positive magnetic anomaly of several hundred nT, reflecting its high magnetic susceptibility and overprinted remanence of normal polarity. The Eulogie Park gabbro, which was not sampled, has a weaker magnetic high. A large granitic intrusion intrudes metamorphic rocks of the Marlborough Block in the NE corner of the survey area. This body produces a magnetic high with an amplitude of several hundred nT. A dioritic to granitic intrusion in the Rookwood Area that intrudes the Rookwood Volcanics also produces a prominent magnetic high with an amplitude up to ~1000 nT above the regional background.

Other prominent zones of higher magnetisation evident in the TMI data correspond to Cretaceous volcanics and the edge of the Triassic Native Cat Andesite. These areas exhibit speckled textures characteristic of heterogeneous magnetic lavas, superimposed on larger scale

Fig.6.2. Calculated first vertical derivative anomaly map for the Fitzroy Leases. A local area gain enhancement has been used to emphasise areas of relatively low magnetic relief.

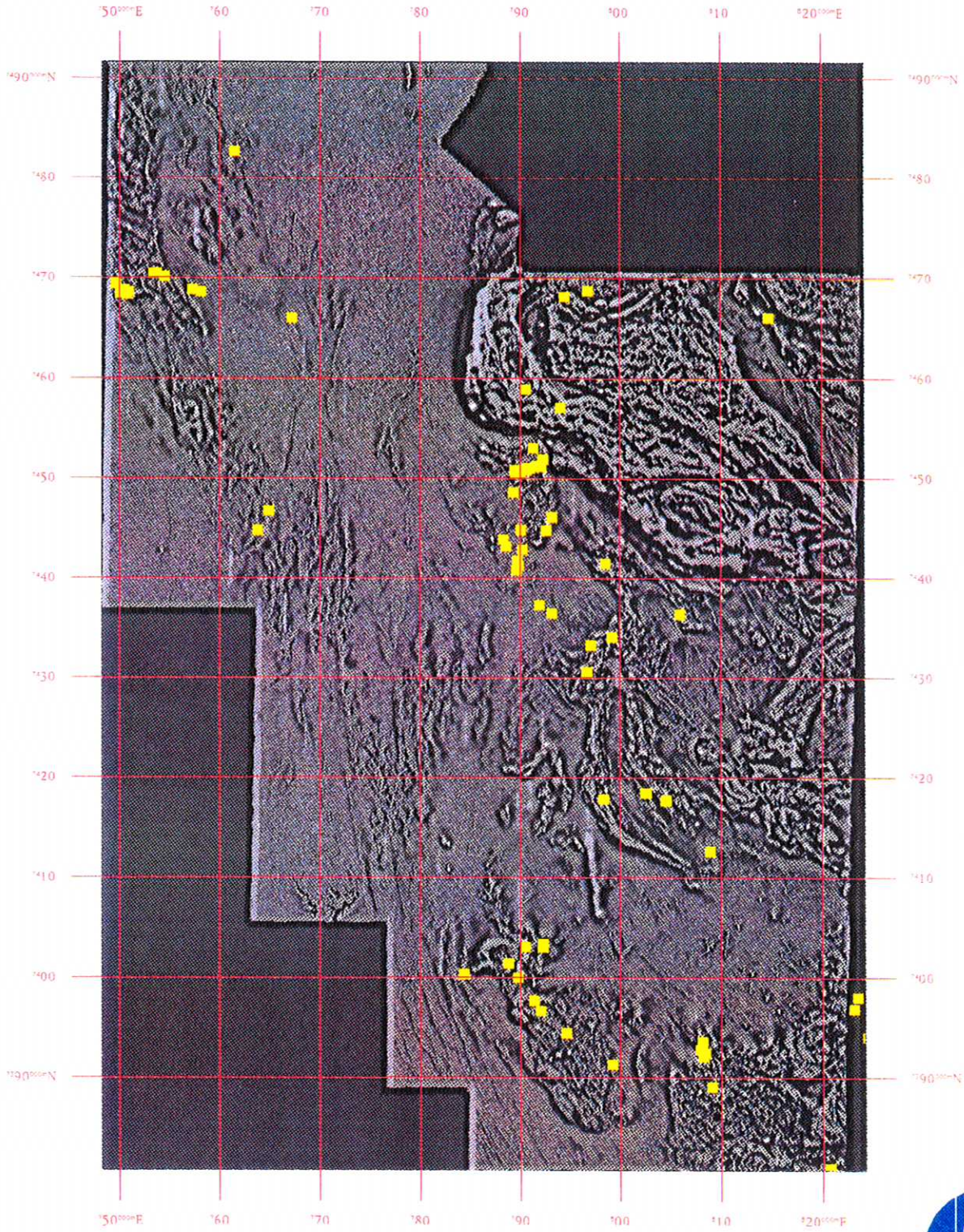

First vertical derivative of magnetic intensity with local area gain enhancement. Yellow squares indicate sample sites.

CSIRO
AUSTRALIA
Division of Exploration and Mining

variations in base level. Variations in thickness of the volcanic piles, as well as changes in average magnetisation, may be responsible for these broader variations in magnetic response.

In the TMI image the Connors Volcanics are generally associated with relatively subdued magnetic highs, averaging up to ~100 nT above the regional field. Within these belts of higher TMI, however, high frequency variations are evident. Within the relatively magnetic portions of the Connors Volcanics local variations of 100-200 nT are common. Less magnetic zones have correspondingly lower amplitude small-scale variations, but the texture is qualitatively similar.

6.2 Features of the First Vertical Derivative Map

Figure 6.2 shows an image of the calculated first vertical derivative of TMI for the QMC survey. As discussed above this type of data emphasises small scale shallow features relative to broader deeper features and shows much higher resolution of narrow units and fine detail of structure. Furthermore these data were subjected to a local gain enhancement to compensate for their large dynamic range and to preserve subtle features. Although the scale of presentation is not suitable for detailed analysis, it is evident from the image that much more geological detail is discernible in this data set than in the TMI image.

Sedimentary rocks of all ages in this area are characterised by very smooth, flat, magnetic lows in the TMI image and by the smoothest areas in the derivative map. The very low susceptibilities and remanent intensities of sampled sedimentary units account for this almost featureless background magnetic response. Because of this smooth, flat background, subtle linear anomalies due to narrow, moderately magnetic units are easily seen in the image. These features generally form swarms of subparallel linears. Examples include NNW-trending features within the Rannes Beds west of the Ohio Leases, swinging to northerly trends to the north of the Ohio Leases. In the western half of the survey area these subtle magnetic linears mostly trend NNW to N and they become sparser and less prominent towards the north. NW-trending linears predominate in the eastern half of the survey area. These features are prominent within the Late Permian sediments that lie between the Glenroy-Scrub Creek and Gogango-Westwood belts of Rookwood Volcanics, within the fault-bounded block of Siluro-Devonian limestones east of the Glenroy-Scrub Creek belt, in the Carboniferous limestones SE of the Devlin Creek grid. NW to NNW-trending dyke-like features also cut across belts of metamorphic rocks of the Marlborough Province. The magnetic linears probably represent thin, post-tectonic dykes, which are generally not exposed.

In the northern Ohio Leases narrow curvlilinear anomalies with amplitudes up to 200 nT occur within the Rannes Beds, immediately west of granitoids intruding Rookwood Volcanics. These anomalies are produced by narrow bands of igneous rock injected into and contaminating Rannes Bed sediments. At site 70 this has produced a "pepperite" with moderate susceptibility.

Belts of volcanic rocks are characterised by active zones in the 1st vertical derivative map, with mottled textures and numerous narrow linear or curvilinear features of short strike length. The magnetic patterns over Rookwood Volcanics, Connors Volcanics, Siluro-Devonian Volcanics, Cretaceous volcanics and Native Cat Andesite are qualitatively similar, but there are substantial variations in anomaly amplitudes and some discernible differences in texture between different belts of volcanics.

6.3 Magnetic Signatures of the Rookwood Volcanics

Belts of Rookwood Volcanics correspond to magnetic highs in the TMI image, averaging up to ~100 nT above the regional field. As for the Connors Volcanics, short wavelength variations are apparent. Within the relatively magnetic portions local variations of 100-200 nT are common. Less magnetic zones within the Rookwood Volcanics have qualitatively similar textures, but the magnetic variations have correspondingly lower amplitudes. The most magnetic belt of Rookwood Volcanics, stretching from Glenroy to Scrub Creek has amplitudes up to ~500 nT above regional background.

The belt of Rookwood Volcanics to the west and south of South Yards Prospect is anomalously weakly magnetic and is barely detectable in the TMI data. In high-pass filtered data (1st vertical derivative or downward continued), however, the local inhomogeneity of magnetic properties is evident in a weak, but discernible, busy texture with sparse stronger features (corresponding to 10-20 nT TMI anomalies). The volcanics in this zone contain only traces of magnetite, supplemented by very small amounts of another magnetic phase, which is either maghaemite or monoclinic pyrrhotite, and accordingly have low susceptibilities. In outcrop these rocks appear to be very similar to more magnetic Rookwood Volcanics from other areas. This suggests that magnetite may originally have been present in these rocks, as in other areas, but has been destroyed by weak but pervasive alteration. This regional alteration event may have some exploration significance, particularly if the trace magnetic phase is identified as pyrrhotite, as this would imply alteration by sulphur-bearing fluids. Similar thermomagnetic behaviour has been observed in some samples from the Ohio Leases. Pyrrhotite has been noted in mineralised Rookwood Volcanics of the Ohio Prospect, suggesting that the minor magnetic phase in altered Rookwood Volcanics may be pyrrhotite.

Fig.6.2 shows that typically active volcanic signatures are exhibited by belts of Rookwood Volcanics. The magnetic character of the Rookwood Volcanics in different belts shows similarities, but also some systematic differences. For example, the southern portion of the Glenroy-Scrub Creek belt shows subparallel extended linear anomalies produced by continuous magnetic units with relatively constant or slowly varying magnetisation. Similar features are absent from other belts, which are characterised by a much more speckled texture, suggesting very patchy magnetisation, and magnetic units with variable orientations and short strike lengths. These features suggest a more complex structure with small scale folding and pervasive faulting, whereas the linear features of the Scrub Creek area suggest a relatively consistent bedding attitude over a considerable strike length and little disruption by faulting. A noisy texture in volcanics is also more characteristic of units that have shallow average dips, whereas long linear features are often associated with more steeply dipping units.

Susceptibilities of Rookwood Volcanic samples show substantial variability within sites and large systematic differences between sites and between volcanic belts. This reflects distinct populations of paramagnetic rocks, which contain almost no magnetite and have susceptibilities less than ~100 μG/Oe (~1260 × 10^{-6} SI), and ferromagnetic rocks, for which the susceptibility is dominated by the presence of up to 2% magnetite by volume. Except for sites that have been struck by lightning, Koenigsberger ratios are mostly less than unity. For moderately to strongly magnetic Rookwood Volcanic samples Q values are typically 0. 2-0.5, and NRM directions are generally of normal polarity. This means that the total magnetisation is subparallel to the induced magnetisation, but augmented by the contribution of remanence. Thus the effective

susceptibilities of the ferromagnetic Rookwood Volcanics are ~20-50% higher than the measured susceptibilities.

A preliminary qualitative interpretation of the magnetics has been commissioned from S. Webster of Austirex International Ltd. This interpretation focussed on the initial objectives of defining the distribution and extent of the Rookwood Volcanics within the QMC leases, particularly under cover. The interpretation also maps the distribution of Connors Volcanics, Carmila Beds, Rannes Beds and subcropping and deeper intrusions using the magnetics, particularly the reduced-to-the-pole and first vertical derivative images, in conjunction with the existing geology maps. Interpretation of the magnetics was hampered in some cases by errors in the original BMR mapping. The resulting regional interpretation map is shown in Fig.6.3. Enlargements of this interpretation map superimposed on the 1st vertical derivative image are shown for the Devlin Creek and Ohio areas in Fig.6.4.

The magnetic interpretation suggests several modifications to the existing regional mapping:

• S. Webster interprets considerable extensions of Rookwood Volcanics beneath cover, linking isolated mapped occurrences into an almost continuous belt to the west of the Glenroy-Scrub Creek belt (see Fig.6.3). These two belts appear to join in the north, in an area of poor exposure. This interpretation represents a substantial addition to known occurrences of Rookwood Volcanics. In the north, the eastern margin of the Glenroy-Scrub Creek belt represents the contact with Siluro-Devonian volcanics of similar magnetic character and its location is therefore somewhat ambiguous and may require field checking. The interpreted "tail" of Rookwood Volcanics extending south towards Tynan beneath cover is associated with a relatively smooth continuous linear anomaly. The smoothness of the anomaly suggests these magnetic rocks may be under a considerable depth of cover, which may prevent easy testing of the anomaly source.

• The interpreted lobe of Rookwood Volcanics south of Back Creek, within the western belt shown on the magnetic interpretation map, contains a magnetically quiet core. This corresponds to an anticlinal structure mapped as Siluro-Devonian on the Duaringa 1:250,000 Geology Sheet. Although this area was not sampled during this study, the structural detail shown in the geology map suggests good exposure and reliable mapping. Thus the magnetic interpretation may need modification to incorporate an anticlinal core of Siluro-Devonian rocks within the Rookwood Volcanics. However, Dear (1985) remarks that the volcanic rocks mapped as Plr and S-D in this area are difficult to distinguish in the field. Differing magnetic character may therefore define the boundary between these units more reliably than the cursory mapping. From the magnetics, the rim of Rookwood Volcanics appears to be continuous, although mapped exposures are patchy.

• In Fig.6.3 the southeastern portion of the Devlin Creek belt of Rookwood Volcanics, is shown as continuous adjacent to the major NNE-trending fault. However, the Duaringa 1:250,000 Geology shows a wedge-shaped patch of fossiliferous sediments (DCa) encroaching into the Rookwood Volcanics in this area. Examination of Fig.6.4 suggests that the magnetic texture associated with the Rookwood Volcanics terminates abruptly at the northern mapped boundary of the DCa unit, but the magnetic quiet zone associated with the non-magnetic sediments does not extend as far south as the mapped boundary of DCa. Thus the extent of the DCa unit is probably less than appears on the geology map.

Fig.6.3. S. Webster's preliminary magnetic interpretation map, showing the inferred distribution of Rookwood Volcanics, Connors Volcanics, Siluro-Devonian volcanics, Rannes Beds, Carmila Beds, and subcropping and buried intrusions.

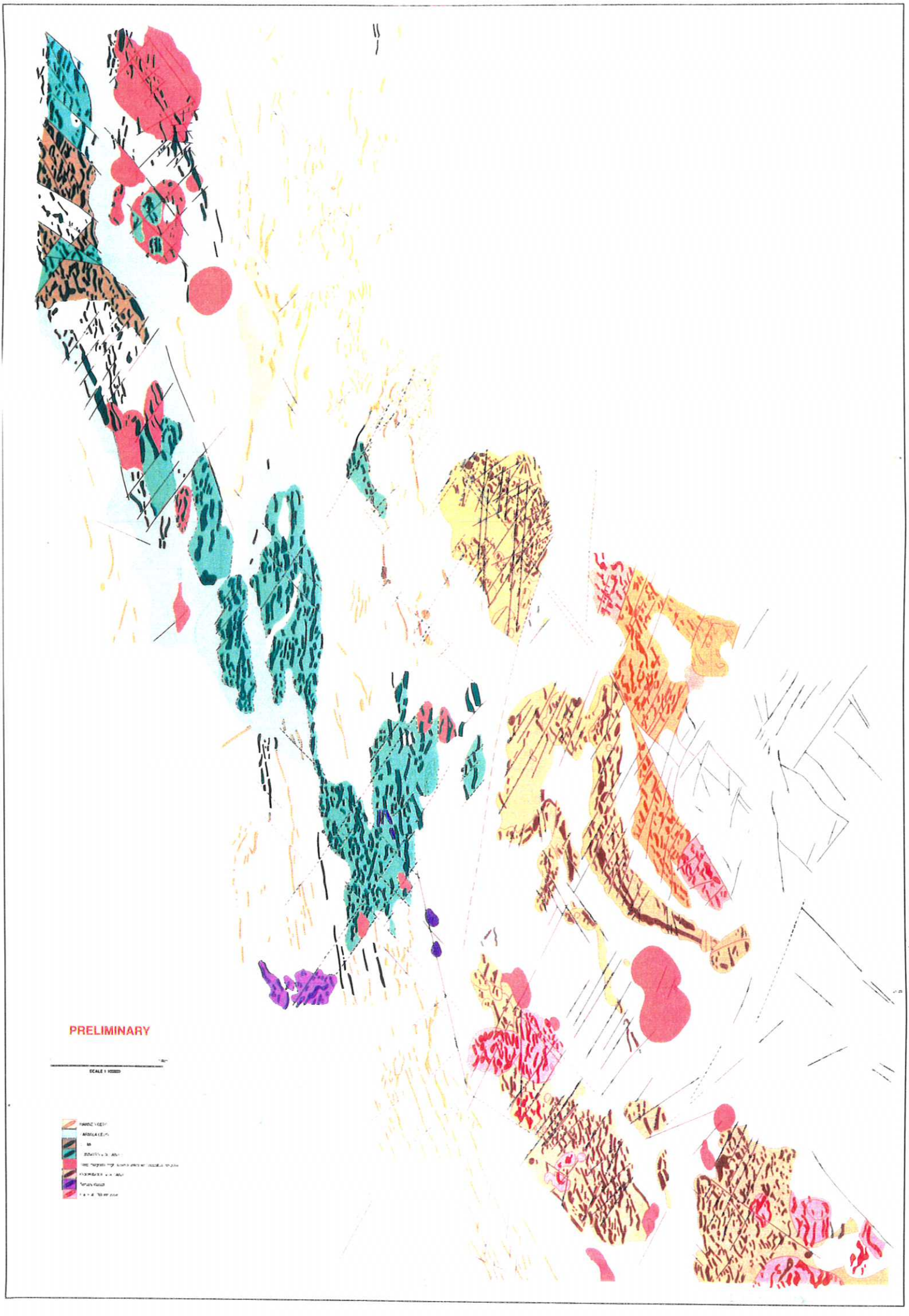
PRELIMINARY

• There is an area shown on the geology map as Youlambie Conglomerate lying to the west of Rookwood Volcanics in the southern portion of the Devlin Creek belt. The magnetic interpretation suggests that part of this area is in fact Rookwood Volcanics.

The magnetic interpretation has several implications for exploration in the Fitzroy Leases:

• Continuity of the magnetic character of the Rookwood Volcanics SE of Devlin Creek across the DCa/Plr boundary shown on the Duaringa 1:250,000 Geology Sheet is consistent with the QMC re-interpretation of geology, which corrects mismapping by the BMR. The radiometric signature is also identical either side of this putative "contact". Since the Devlin Creek mineralisation is now known to be hosted by Rookwood Volcanics, all belts of Rookwood Volcanics are prospective for similar mineralisation.

• The magnetic interpretation infers a contact between the Rookwood Volcanics and the Rannes Beds under Tertiary Cover well to the west of current drilling in the Devlin Creek area, suggesting a western extension of the prospective area under cover. Because the magnetic signature of the Rookwood Volcanics becomes weaker around and to the west of the area of known mineralisation, the location of this boundary should be regarded as only approximate. Detailed examination of original aeromagnetic data and modelling of profiles may allow this boundary to be located more accurately.

• The magnetically quiet zone of the Rookwood Volcanics to the south of the Sulphide Suburb, which is thought to result from pervasive alteration, appears in the first vertical derivative image as a southern continuation of a relatively smooth magnetic corridor stretching from the Sulphide City area, and immediately west of the known mineralisation, to the southern end of this belt of Rookwood Volcanics The known mineralisation appears to extend along the boundary between magnetically active Rookwood Volcanics to the east and much less magnetic units to the west. This may reflect an alteration front, perhaps related to mineralisation. Alternatively, this magnetic boundary may correspond to a facies change within the Rookwood Volcanics, which could be used as a marker horizon stratigraphically close to mineralisation.

• Within the Devlin Creek Prospect, magnetic properties of drill core samples confirm that sulphide mineralisation is very weakly magnetic, altered Rookwood Volcanics associated with mineralisation have slightly higher, but still weak, magnetisations and unmineralised, relatively unaltered lavas have variable properties, with substantially higher susceptibilities and remanent magnetisations on average. This suggests that the magnetic signature of Devlin Creek mineralisation should be anomalously smooth zones of lower base level within a more magnetically active background typical of normal Rookwood Volcanics. The ground magnetic contour map shown by Deakin (1993) confirms that the known mineralisation lies within a relatively quiet magnetic zone. This signature may be very subtle if the host volcanics have been subjected to pervasive magnetite-destructive alteration. Data processing specifically designed for highlighting such textural contrasts may be required to detect the signature of mineralisation.

Fig.6.4. Enlargements of portions of Fig.6.3, overlain on the first vertical derivative map, for the Devlin Creek and Ohio Prospects. Sampling sites are indicated by yellow squares.

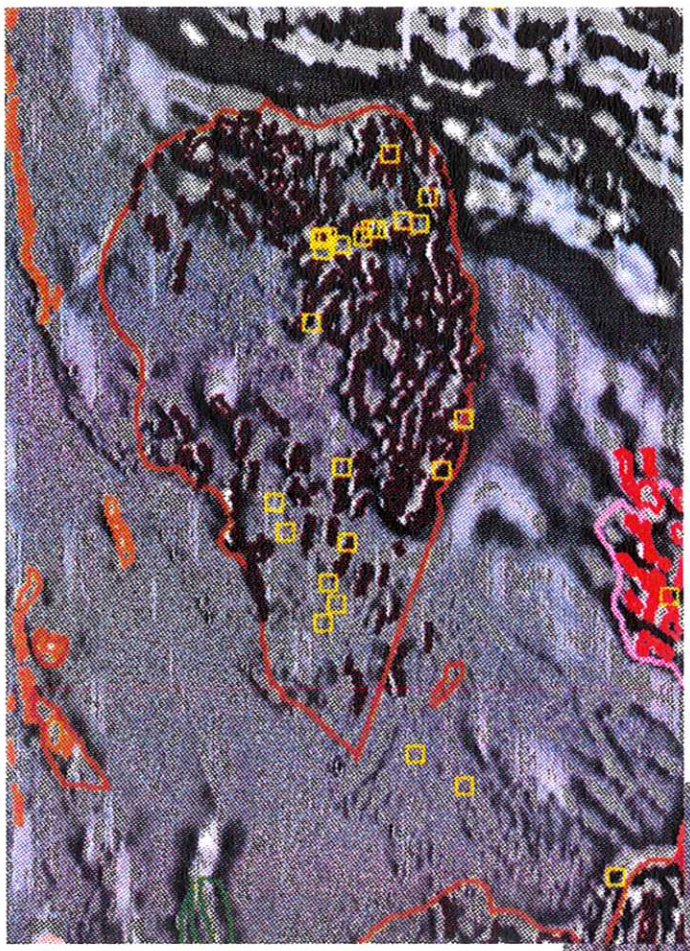

(a) Develin Creek area

0 5 kms

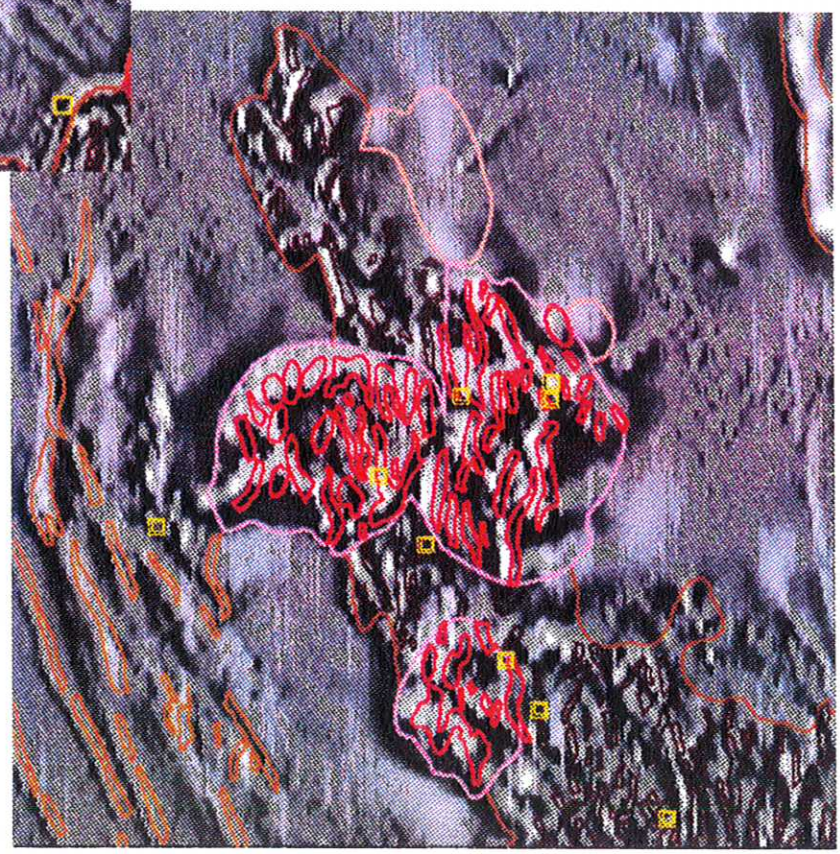

(b) Rookwood area

0 5 kms

• Structural breaks within the Rookwood Volcanics are evident within high-pass filtered magnetics images. Structural details interpreteted by S. Webster should be integrated with current geological models of the Devlin Creek mineralisation to determine if features detected by the magnetics constitute structural controls on mineralisation. Faulting detected in the magnetics images may constrain locations of extensions of known mineralistion.

• The magnetic data imply that the intermediate to felsic intrusions into Rookwood Volcanics and Rannes Beds in the northern portion of the Ohio Leases are more extensive than mapped. Nearby deeper intrusions are also indicated by the magnetics. Thus the Rookwood Volcanics in this area are likely to be affected by contact metamorphism/metasomatism. The Rannes Beds have demonstrably been baked and altered adjacent to the intrusions and magnetic images suggest aureole effects within the Rookwood Volcanics. Sulphide mineralisation in the Ohio Prospect could conceivably be intrusive-related and therefore differ profoundly from Devlin Creek-style VMS deposits. On the other hand, if the Ohio mineralisation is also VMS type, it may have been modified by the intrusions. This may account for the presence of pyrrhotite in the Ohio mineralisation, whereas pyrite is the characteristic iron sulphide at Devlin Creek. As a result, sulphide mineralisation in the Ohio area may be magnetic, in contrast to the Devlin Creek mineralisation.

6.4 Magnetics of the Langdale Hill Prospect

The Langdale Hill intrusion lies along a linear NNW-trending belt of porphyry intrusions. This line of intrusions lies within a broad smooth magnetic low on the TMI image, but shows up as string of anomalies elongated parallel to the overall trend in the first vertical derivative image. This implies that the intrusions are generally more magnetic than the surrounding sediments. The altered sulphide-bearing porphyry samples collected at Langdale Hill, however, have very weak magnetisations, comparable to those of Permian sediments, and much less than the inferred magnetisations of other intrusions along the belt. The more altered samples from site 48 are even less magnetic than the less altered equivalents from site 47. This suggests that alteration has demagnetised an originally magnetic intrusive rock at Langdale Hill. If this is so, high-resolution magnetics could indicate alteration zones within porphyry intrusions in this belt as local areas of smooth magnetic relief within magnetically active zones associated with unaltered portions of intrusions. Detailed examination of the magnetic data in the Langdale Hill area, with follow up field work, could test this hypothesis.

The palaeomagnetism of the Langdale Hill intrusion indicates a westerly plunge for the intrusion. Detailed modelling of magnetic profiles over the Langdale Hill area could enable dips of volcanic units and plunges of intrusions to be determined, if interpretation is constrained by magnetic property data. Tilting of the intrusion could have implications for drill targetting and for interpretation of drilling data in terms of zoning models.

7. CONCLUSIONS AND IMPLICATIONS FOR EXPLORATION

7.1 General Outcomes

The magnetic property data from this study have been entered into a Paradox 4.0 database and the resulting table has been imported into the MIPS system, along with the digital version of the preliminary magnetic interpretation map. This allows direct comparison of local magnetic signatures with "ground truth" magnetic property data and will assist continuing interpretation of the magnetics.

Given the outdated and inadequate regional mapping in the study area, preliminary interpretation of the magnetic survey data has substantially improved knowledge of the gross distribution of major rock units in the Fitzroy Leases, particularly when radiometric data are incorporated into the interpretation. Some misidentifications of rock units have been corrected and magnetic signatures have allowed tracing of poorly exposed units beneath cover. Magnetic anomalies also indicate the presence of some buried intrusions and volcanic units. The magnetic anomaly patterns define major structures and prominent structural trends, some unrecognised hitherto. These data should be reconciled with and incorporated into regional tectonic interpretations. There is considerable scope for more detailed qualitative interpretations of suitably processed magnetic data and for modelling of specific anomalies, constrained by magnetic property data, to provide quantitative estimates of depths, dips and source geometries.

Representative susceptibilities, natural remanent magnetisations and Koenigsberger ratios have been established for major rock types and their variability across the area has been characterised. These data constrain qualitative geological interpretation of magnetics images and will provide essential input to quantitative modelling of magnetic anomalies.

7.2 Magnetic Petrophysics

The main results of the magnetic petrophysical study are:

- All sedimentary rocks sampled have very low susceptibilities. The general order of susceptibilities according to rock type is: sediments < felsic volcanics < intermediate/mafic volcanics < mafic intrusives < ultramafics. Both weakly magnetic and strongly magnetic felsic intrusions are present.

- The Rookwood Volcanics have very variable magnetic properties at all scales. This tends to produce a characteristic busy texture in suitably processed magnetics images. There is a bimodal susceptibility distribution for the Rookwood Volcanics, reflecting distinct magnetite-poor and magnetite-rich populations. The paramagnetic subpopulation has susceptibilities clustering around the range 40-60 μG/Oe (500-750 $\times 10^{-6}$ SI). For the ferromagnetic subpopulation, susceptibilities in the range 2000-4000 μG/Oe (25-50 $\times 10^{-3}$ SI) predominate.

- Magnetic property measurements on drill core samples from the Devlin Creek Grid indicate that mineralised zones are very weakly magnetic, whereas unmineralised and relatively unaltered Rookwood Volcanics are slightly to substantially more magnetic. Massive sulphides have very low susceptibilities, less than 10 μG/Oe (130 $\times 10^{-6}$ SI), semi-massive sulphides are

only slightly more magnetic, with average susceptibility ~30 μG/Oe (380 × 10^{-6} SI), and Rookwood Volcanics samples with minor sulphides have an average susceptibility of only ~40 μG/Oe (500 × 10^{-6} SI). By contrast, the average susceptibility of unmineralised Rookwood Volcanics samples is ~640 μG/Oe (8 × 10^{-3} SI). However the susceptibilities of unmineralised lavas that have been drilled are highly variable and have a bimodal distribution. This mean value results from the presence of subequal populations of paramagnetic rocks, almost devoid of magnetite, with susceptibilities of ~60 μG/Oe (750 × 10^{-6} SI) and rocks containing 0.1-1.5 % magnetite by volume, with an average susceptibility of ~1200 μG/Oe (15 × 10^{-3} SI).

• Sulphide mineralisation in the Ohio Leases may be magnetic, in contrast to the Devlin Creek mineralisation, due to the presence of monoclinic pyrrhotite as well as pyrite.

• For most rock types remanence makes a subsidiary contribution to the total magnetisation, compared to induced magnetisation. Representative Q values are typically 0.2-0.5, indicating remanent intensities 20-50% of the induced magnetisation. In pre-Cretaceous rocks, the remanence is generally dominated by a Cretaceous overprint of normal polarity, which is steeper than the present field. The effect of remanence in most cases is to augment the effective susceptibility of the rocks by 20-50% above the measured susceptibilities.

• Ignoring unrepresentative values from lightning-affected sites, typical Koenigsberger ratios for relatively magnetic portions of the Rookwood Volcanics are ~1.0 ± 0.5. Taking the scatter of NRM directions into account, an effective Q value of ~0.5-0.8 for substantial volumes of rock is indicated. Thus contrasts in remanence intensity and variations in average direction probably contribute substantially to the short wavelength magnetic texture of magnetic Rookwood Volcanics. The overall contribution of remanence is to increase the effective susceptibility substantially.

• Measured susceptibility anisotropies are low (<5%), implying that magnetic anisotropy can be ignored in magnetic modelling. However the weak anisotropy defines a magnetic fabric (foliation and lineation) that provides structural information.

7.3 Palaeomagnetism

Palaeomagnetic study of the samples has shown that palaeomagnetism is a useful tool for correlation and structural analysis in this area. Thermal demagnetisation has isolated stable palaeomagnetic components in many samples. Rookwood Volcanics, Connors Volcanics and a number of intrusive rocks are good palaeomagnetic recorders. The main findings of the palaeomagnetic study are:

• The Rookwood Volcanics carry a stable primary Permian remanance of reversed polarity, usually strongly overprinted by a Cretaceous magnetisation of normal polarity. The primary remanence is directed very steeply downwards for flat-lying units, but is rotated away from the reference field direction for tilted units. Where the bedding attitude of the Rookwood Volcanics is unknown, it can be inferred from the characteristic Permian remanence.

• The Connors Volcanics carry an apparently primary reversed polarity remanence, which is directed SW with moderate positive (downward inclination), with respect to the palaeo-horizontal. This characteristic remanence suggests a mid-Carboniferous age (~320 ± 10 Ma) for the Connors Volcanics. Most of these units are also extensively overprinted by a Cretaceous normal component, which is directed north and steeply upwards. Where the structure of Connors Volcanic units is unknown, it should be deducible from the palaeomagnetic directions.

• Apart from rocks that do not contain magnetic grains capable of retaining stable remanence, and a few rocks with such stable remanence that overprinting is negligible, all pre-Cretaceous rocks sampled in the study area carry Cretaceous overprint magnetisations of normal polarity. The characteristic Cretaceous overprint direction is north and up, substantially steeper than the present field direction. This ubiquitous overprinting implies a thermal or alteration event of regional extent during the Cretaceous, at ~110 ±10 Ma. A similar overprint is found in the Sydney Basin and in the southern and central Bowen Basin.

• The sampled portions of the Langdale Hill intrusion are weakly magnetic, with more altered samples having lower susceptibilities than less altered portions. The weak remanence is very stable and is probably a primary Permian magnetisation of reversed polarity. The remanence direction departs from the reference field direction, however, suggesting that the intrusion has been tilted through ~35° and is now plunging to the west.

7.4 Magnetic Interpretation

Preliminary interpretation of the magnetic survey data has highlighted a number of deficiencies in the regional mapping, has defined the gross distribution of major rock units more accurately and has identified some major structures and structural trends within the leases. These findings should aid intepretation of the regional tectonics and structure. More detailed information has been adduced from the magnetics in some key exploration areas. The main results of the initial phase of magnetic interpretation are:

• In TMI data the Rookwood Volcanics are associated with zones of generally higher magnetic base level than surrounding sedimentary rocks. The average amplitude of the base level shift is typically ~100 nT, but ranges from 10-20 nT to ~500 nT in different belts or zones within belts. The overall magnetic highs are characterised by a "busy" magnetic texture, particularly in high-pass filtered magnetics images, which allows these units to be traced beneath shallow cover. Short wavelength TMI variations within the range from ~10 nT over weakly magnetic Rookwood Volcanics to hundreds of nanoTeslas over the strongly magnetic belts.

• The interpreted extent of the Rookwood Volcanics is greater than indicated by the regional mapping. The magnetics indicate some misidentified units are in fact Rookwood Volcanics. A considerable area of Rookwood Volcanics is interpreted to lie beneath superficial cover and some units beneath thicker cover are also inferred. Of particular interest is the inferred continuation of the Devlin Creek belt beneath Tertiary cover to the west of current drilling.

• There is evidence from the observed magnetics, supported by magnetic property measurements, that the magnetic signature of the Rookwood Volcanics is relatively subdued over the mineralised zone at Devlin Creek. Mineralisation and altered volcanics associated with mineralisation are uniformly weakly magnetic, whereas unaltered Rookwood Volcanics have variable properties, with some strongly magnetic portions, and are much more magnetic on average.

• The occurrence of extensive zones of relatively weakly magnetic Rookwood Volcanics that are indistinguishable in the field from magnetic Rookwoods in other areas (e.g. South of Devlin Creek) may be due to weak but pervasive alteration in these zones. This hypothesis needs to be tested and exploration implications assessed. Within the weakly magnetic Rookwood Volcanics there is still sufficient variability in susceptibility that the volcanics can be mapped beneath superficial cover using high-pass filtered magnetics images (vertical derivatives or downward continued magnetics). The weakly magnetic rocks contain traces of a magnetic phase not yet identified, but which is either maghaemite or monoclinic pyrrhotite. Identification of this phase may clarify the nature of the alteration in the magnetic quiet zones.

7.5 Exploration Implications

• Remapping of the extent of the Rookwood Volcanics from the magnetics defines new areas, mostly under superficial cover, that are prospective for Devlin Creek type mineralisation.

• The magnetic interpretation infers a contact between the Rookwood Volcanics and the Rannes Beds under Tertiary Cover well to the west of current drilling in the Devlin Creek area, suggesting a western extension of the prospective area under cover. Because the magnetic signature of the Rookwood Volcanics becomes weaker around and to the west of the area of known mineralisation, the location of this boundary should be regarded as only approximate. Detailed examination of original aeromagnetic data and modelling of profiles may allow this boundary to be located more accurately.

• The magnetically quiet zone of the Rookwood Volcanics to the south of the Sulphide Suburb, which is thought to result from pervasive alteration, appears in the first vertical derivative image as a southern continuation of a relatively smooth magnetic corridor stretching from the Sulphide City area, and immediately west of the known mineralisation, to the southern end of this belt of Rookwood Volcanics The known mineralisation appears to extend along the boundary between magnetically active Rookwood Volcanics to the east and much less magnetic units to the west. This may reflect an alteration front, perhaps related to mineralisation. Alternatively, this magnetic boundary may correspond to a facies change within the Rookwood Volcanics, which could be used as a marker horizon stratigraphically close to mineralisation.

• The magnetic property data and observed magnetic signatures suggest that the magnetic signature of Devlin Creek mineralisation should be anomalously smooth zones of lower base level within a more magnetically active background typical of normal Rookwood Volcanics. This signature may be very subtle if the host volcanics have been subjected to pervasive magnetite-destructive regional alteration. Data processing specifically designed for highlighting such textural contrasts may be required to detect the signature of mineralisation.

• Structural breaks within the Rookwood Volcanics are evident within high-pass filtered magnetics images. Features detected by the magnetics may be related to structural controls on mineralisation, as suggested in S. Webster's interpretation. Faulting detected in the magnetics images may constrain locations of extensions of known mineralisation.

• The magnetic data imply that the intermediate to felsic intrusions into Rookwood Volcanics and Rannes Beds in the northern portion of the Ohio Leases are more extensive than mapped. Nearby deeper intrusions are also indicated by the magnetics. Sulphide mineralisation in the Ohio Prospect could conceivably be intrusive-related and therefore differ profoundly from Devlin Creek-style VMS deposits. On the other hand, if the Ohio mineralisation is also VMS type, it may have been modified by the intrusions. This may account for the presence of pyrrhotite in the Ohio mineralisation, whereas pyrite is the characteristic iron sulphide at Devlin Creek. As a result, sulphide mineralisation in the Ohio area may be magnetic, in contrast to the Devlin Creek mineralisation.

• The Langdale Hill intrusion lies along a linear NNW-trending belt of porphyry intrusions that is associated with a magnetic anomaly, although the altered sulphide-bearing porphyry samples collected at Langdale Hill have very weak magnetisations. High-resolution magnetics could indicate potentially mineralised alteration zones within porphyry intrusions in this belt as local areas of smooth magnetic relief within magnetically active zones associated with unaltered portions of intrusions.

• The palaeomagnetism of the Langdale Hill intrusion indicates a westerly plunge of ~55° for the intrusion. Tilting of the intrusion could have implications for drill targetting and for interpretation of drilling data in terms of zoning models.

8. RECOMMENDATIONS

The results of the pilot petrophysical/palaeomagnetic study and the preliminary aeromagnetic interpretation suggest a number of follow-up studies that could improve understanding of the geology of the Fitzroy Leases and aid exploration using magnetics. Aspects that could usefully be investigated are listed below:

• A fuller interpretation of the aeromagnetic data, using the magnetic property information in the GIS and integrating radiometric and remote sensing data to discriminate between volcanic units with similar magnetic character and between non-magnetic sedimentary units, should be carried out to yield more definitive regional maps of the surface and solid geology. Structural elements derived from the magnetics and TM data should be integrated into the regional tectonic model.

• Modelling of magnetic survey data, constrained by magnetic property information, should be carried out in key areas. In particular, the airborne response over the Devlin Creek Grid should be modelled to constrain the 3D geometry of the Rookwood Volcanics and the alteration system in this area and to define the western edge of the Rookwood Volcanics under the Tertiary cover. A suite of models defining expected magnetic responses of Devlin Creek type mineralisation in different geological settings (differing structural attitudes, effect of contact metamorphism) could be generated from this initial model. Detailed interpretation of

the magnetics over the Ohio and Langdale Hill Prospects is also desirable. Dips and depth estimates should be interpreted from magnetic anomalies over covered or poorly exposed belts of Rookwood Volcanics.

• Magnetic property measurements on drill core and outcrop samples from the Ohio and Langdale Hill Prospects are desirable to facilitate intepretation of the magnetics over these areas.

• Further sampling is desirable to define characteristic magnetic properties of Siluro-Devonian volcanics in areas where field discrimination between Rookwood Volcanics and S-D volcanics is difficult. The Glenroy Creek - Comanche belt, which was not sampled for this study, is a specific example.

• Palaeomagnetic sampling of Rookwood Volcanics could be used to define the structure in areas where this is unknown. This information will then assist stratigraphic correlation within and between belts of Rookwood Volcanics. The Camboon Andesite to the south of the Study area could be sampled to test Richards' (1993) hypothesis that this unit is a correlative of the Rookwood Volcanics.

• A magnetic petrological study of unaltered, altered and mineralised Rookwood Volcanics would provide a deeper understanding of the variety of magnetic signatures associated with the Rookwood Volcanics and of the significance of observed magnetic patterns over mineralised areas. Magnetic petrology integrates petrology and rock magnetism to identify the processes that create and destroy magnetic minerals in rocks. By characterising the mineralogy, chemical composition and magnetic properties of selected samples, we can relate the observed magnetic behaviour to variations in protolith composition, metamorphic grade and hydrothermal alteration. Identification of the unknown trace magnetic phase within the magnetic quiet zones should provide information on the fluids that caused the alteration.

9. ACKNOWLEDGEMENTS

The colour images in this report were produced by Dr Bruce Dickson, whom I also thank for discussions on the radiometric and magnetic interpretations. Mr Steve Webster of Austirex International Ltd produced the preliminary interpretation of the aeromagnetic data. I thank Mr David Horton for briefings on the regional geology and mineralisation of the Fitzroy Leases and QMC for logistical support in the field. Mr Mark Huddleston and Dr Bruce Dickson assisted with field work. Dr John Dear assisted with access to the Mt McKenzie leases and information on stratigraphy and structure of the Connors Volcanics. Drs Phil Schmidt and Mark Lackie assisted the palaeomagnetic interpretation with data and discussions.

10. REFERENCES

Ashley, P.M. and Shaw, S.E., 1993. Apparent ages of hydrothermal alteration zones in the North Arm Volcanics, southeast Queensland. Aust. J. Earth Sci., 40, 415-421.

Deakin, R.C., 1993. Report on Geophysics from the Develin Creek Grid, Marlborough, Queensland. Prepared for Queensland Metals Corporation Ltd, November, 1993.

Dear, J.F., 1985. Authority to Prospect 3854M Boomer Range, Final report on exploration, including Report for Six Monthly Period 9/1184 to 9/5/85. CR14549.

Dear, J.F., 1986. Authority to Prospect 3965M Broadsound Range, Final report on exploration, including Report for Six Monthly Period 25/2/85 to 25/8/855. CR15100.

Embleton, B.J.J., 1981. A review of the paleomagnetism of Australia and Antarctica *in* McElhinny, M.W. and Valencio, D.A. (Eds), Paleoreconstruction of the Continents, American Geophysical Union, Washington.

Henderson, R.A., Fergusson, C.L., Leitch, E.C., Morand, V.J., Reinhardt, J.J. and Carr, P.F., 1993. Tectonics of the northern New England Fold Belt *in* Flood, P.G. and Aitchison, J.C. (Eds), New England Orogen, eastern Australia. Dept of Geology and Geophysics, University of New England.

Kirkegaard, A.G., 1970. Duaringa, Qld. 1:250,000 Geological Series Explanatory Notes, Bureau of Mineral Resources, Canberra.

Kirschvink, J.L., 1980. The least squares line and plane and the analysis of palaeomagnetic data, Geophys. J. R. astron. Soc., 62, 699-718.

Malone, E.J., 1970. St Lawrence, Qld. 1:250,000 Geological Series Explanatory Notes, Bureau of Mineral Resources, Canberra.

Morley, M.E., Gleadow, A.J.W. and Lovering, J.F., 1981. Evolution of the Tasman Rift: apatite fission track dating evidence from the southeastern Australian continental margin, *in* M.M. Cresswell and P. Vella (eds), Gondwana Five (Proceedings of the Fifth International Gondwana Symposium, Wellington, N.Z.), Balkema, Rotterdam, pp.289-300.

Murray, C.G., 1975. Rockhampton, Qld. 1:250,000 Geological Series Explanatory Notes, Bureau of Mineral Resources, Canberra.

Richards, D.N.G., 1993. A Literature Review of the Geology, Structure and Mineralisation of the Lower Permian Volcano-sedimentary sequences of the Grantleigh Trough. Prepared for Queensland Metals Corporation Ltd, October, 1993.

Schmidt, P.W. and Embleton, B.J.J., 1981. Magnetic overprinting in southeastern Australia and the thermal history of its rifted margin. J. Geophys. Res., 86, 3998-4008.

TABLE 1. MAGNETIC/RADIOMETRIC SITES Page

Palaeomagnetic Site	Radiometric Site	Easting	Northing	Unit-old	Unit-new
1	FR 1	789492	7450632	Plr	Plr
2		789522	7450632	Plr	Plr
3		789572	7450713	Plr	Plr
4		789734	7450713	Plr	Plr
5	FR 6	789587	7450373	Plr	Plr
6	FR17	790041	7450519	Plr	Plr
7		790635	7450688	Plr	Plr
8		790856	7450918	Plr	Plr
9	FR18	791001	7450902	Plr	Plr
10	FR19	791655	7451123	Plr	Dca-p
11	FR20	791685	7451100	Plr	Plr
12	FR21	792105	7451057	Plr?	Plr
13	FR21	792105	7451057	Plr?	Plr
14	FR22	792304	7451793	Plr	Plr
15	FR25	793213	7445984	Plr	Plr
16	FR26	792645	7444655	Plr	Plr
17	FR27	790078	7444702	Plr	Plr
18	FR 8	790233	7442761	Plr	Plr
19	FR 8	790233	7442761	Plr	Plr
20	FR30	750708	7468259	DCo	Dmb
21	FR31	750475	7468527	DCo	Dmb
22	FR32	750854	7468544	DCo	Dmb
23	FR135	749976	7468395	DCo	Dmb
24		750390	7468720	DCo	Dmb
25	FR33	750340	7468720	DCo	Dmb
26		750300	7468720	DCo	Dmb
27		749591	7469326	DCo	Dmb
28	FR34	749591	7469326	DCo	Dmb
29	FR35	753378	7470357	DCo	Dmb
29	FR36	753378	7470357	DCo	Dmb
30	FR140	753678	7470357	DCo	Dmb
31	FR36	753378	7470357	DCo	Dmb
32	FR37	754424	7470030	DCo	Dmb
33	FR39	726540	7518131	DCo	Dmb
34		727735	7518986	DCo	Dmb
35	FR40	728439	7518887	DCo	Dmb
36	FR41	730500	7519812	DCo	Dmb
37	FR42	732222	7520245	DCo	Dmb
38	FR43	732327	7521935	DCo	Dmb
39	FR44	733757	7524920	DCo	Dmb
40	FR46	790544	7458768	Px	Ta/Pzw
41	FR47	794035	7456968	Px	Pzw
42	FR49	791322	7452876	DCa?	Dca-p
43	FR141	791322	7452876	DCa?	Dca-p
44	FR57	767157	7465918	Pb	Pu3
45	FR59	757232	7468719	Pla?	Pla?

Palaeomagnetic Site	Radiometric Site	Easting	Northing	Unit-old	Unit-new
46	FR60	758077	7468512	Pla?	Pla?
47	FR62	761377	7482600	Pla	Dgc2
48		761377	7482600	Pla	Dgc2
49	FR13	789329	7448490	Plr	Tdf
50	FR68	789713	7441651	Plr	Plr
51	FR69	789901	7441122	Plr	Plr
52	FR70	789619	7440664	Plr	Plr
53	FR71	788578	7443048	Plr	Plr
54	FR142	788340	7443762	Plr	Plr
55	FR72	791951	7437176	Cl	Plr
56	FR73	793209	7436341	Cl	C?
57	FR74	797115	7433157	Plr	Plr
58	FR75	796717	7430434	Plr	Plr
59	FR76	799234	7433953	SD	SD?
60	FR82	798574	7441340	P-Mi	SD?
61		805925	7436232	SD	SD?
62	FR83	804565	7417574	P-Mi	SD-k
63	FR143	804565	7417574	P-Mi	SD-k
64	FR83	804565	7417574	P-Mi	SD-k
65	FR84	808952	7412497	Plr	Plr
66	FR89	798366	7417688	Plr	Plr
67	FR92	802556	7418309	SD	SD?
68	FR98	764846	7446628	P-Mi	Dmu
69	FR100	763742	7444664	Pla	Dmu
70	FR103	784322	7400161	Plw	Plw-k
71	FR104	790499	7402881	Pui	Cz
72	FR106	792315	7403165	Plr	Plr
73		792293	7402803	Plr	Plr
74	FR108	788808	7401226	Pui	Pui-a
75	FR136	789775	7399809	Plr	Plr
76	FR137	791371	7397492	Plr	Plr
77	FR139	792026	7396465	Plr	Plr
78	FR138	794583	7394264	Plr	Plr
79	FR144	799210	7391098	Plr	Plr
80		809096	7388877	Plr	Plr
81	FR145	807928	7392587	Plr	Plr
82	FR111	808404	7392271	Plr	Plr-i
83	FR113	808146	7393390	Plr	Plr-k
84	FR114	808274	7391901	Plr	Plr
85		815556	7379951	Plr	Plr
86	FR116	820677	7380802	Plr	Plr
87	FR14	794455	7468057	P-Mi	Pui-a
88	FR117	796818	7468619	Pui	Pui-a
89	FR118	814835	7465970	Px	Pzw
90	FR121	834919	7442345	Px	Pzw
91	FR146	847609	7437924	Pub?	Kub
92	FR123	823456	7397862	Rn	Rn

Palaeomagnetic Site	Radiometric Site	Easting	Northing	Unit-old	Unit-new
93	FR125	823089	7396706	Rn	Rn
94	FR126	824466	7393861	Kut	Kut
95	FR128	825745	7389421	Kub	Kub
96	FR129	846765	7400483	Puo	Puo
97		824669	7430299	Plg	Plg

TABLE 2. MAGNETIC SAMPLING SITES

SITE	NORTHING	EASTING	N/n	UNIT	ROCK TYPE
1	7450632	789492	6	Plr	Rookwood Volcanics - pillow lavas
2	7450632	789522	3	Plr	Rookwood Volcanics - massive lavas
3	7450713	789572	2	Plr	Rookwood Volcanics - volcanic breccia
4	7450713	789734	3	Plr	Rookwood Volcanics - massive lavas
5	7450373	789587	2	Plr	Rookwood Volcanics - massive lavas
6	7450519	790041	2	Plr	Rookwood Volcanics - pillow lavas
7	7450688	790634	4	Plr	Rookwood Volcanics - volcanic breccia, hm altered
8	7450918	790856	4	Plr	Rookwood Volcanics - massive vesicular flows
9	7450902	791001	3	Plr	Rookwood Volcanics - massive lavas
10	7451123	791655	2	DCa-p	Porphyritic felsic volcanics
11	7451100	791685	2	Plr	Rookwood Volcanics
12	7451057	792105	3	Plr?	Porphyritic massive ?lava
13	7451057	792105	1	Plr?	Felsic volcanic
14	7451793	792304	3	Plr	Rookwood Volcanics - massive lavas
15	7445984	793213	3	Plr	Rookwood Volcanics
16	7444655	792645	3	Plr	Rookwood Volcanics
17	7444702	790078	4	Plr	Rookwood Volcanics
18	7442761	790233	3	Plr	Rookwood Volcanics - porphyritic amygdaloidal lavas
19	7442761	790233	3	Plr	Rookwood volcanics - even grained lavas
20	7468259	750708	5	Dmb	Diorite intrusion; related to late phase of Clive Creek Complex
21	7468527	750475	3	DCo	Felsic pyroclastic lava
22	7468544	750854	3	DCo	Hornfelsed Connors Volcanics
23	7468395	749976		Dmb	Altered diorite, part of Mt McKenzie system
24	7468720	750390	2	Dmb	Diorite intrusion, related to late phase of Clive Creek Complex?
25	7468720	750340	2	Dmb	Quartz monzonite, related to latest phase of Clive Creek Complex?
26	7468720	750300	2	Dmb	Diorite intrusion, related to late phase of Clive Creek Complex
27	7469326	749591	3	DCo	Trachyandesite, conformably overlying Mt McKenzie system
28	7469326	749591	5	DCo	Andesite
29	7470357	753378	6	DCo	Dacitic crystal tuff of Broadsound Range Volcanics at base of DCo
30	7470357	753678	2	DCo	Clements Creek Volcanics - ignimbrite

SITE	NORTHING	EASTING	N/n	UNIT	ROCK TYPE
31	7470357	753378	3	C-Mi?	Granite (?Late Carboniferous)
32	7470030	754424	1	DCo	flow-banded rhyolite
33	7518131	726540	4	DCo	Connors Volcanics type section, felsic pyroclastic
34	7518986	727735	3	DCo	Connors Volcanics type section, intermed volcanic
35	7518887	728439	3	DCo	Connors Volcanics type section, lithic volcanic breccia
36	7519812	730500	4	DCo	Connors Volcanics type section, fine-grained, with mafic phases
37	7520245	732222	2	DCo	Connors Volcanics type section, crystal tuff
38	7521935	732327	3	DCo	Connors Volcanics type section, crystal tuff
39	7524920	733757	5	DCo	Connors Volcanics type section, variably altered
40	7458768	790544	4	Px	Weathered ultramafics, lightning struck?
41	7456968	794035	5	Px	Ultramafics, fresher than site 40
42	7452876	791322	2	DCa-p	?Andesitic metavolcanics
43	7452906	791322	1	DCa-p	?Andesitic metavolcanics
44	7465918	767157	2	Pu3	Fine-grained siltstone/mudstone
45	7468719	757232	1	Pla?	Sediments
46	7468512	758077	1	Pla?	Sediments
47	7482600	761377	4	Dgc2	Langdale Hill porphyry, relatively unaltered
48	7482600	761377	3	Dgc2	Langdale Hill porphyry, altered
49	7448490	789329	3	Plr	Rookwood Volcanics, volcanic breccia
50	7441651	789713	3	Plr	Rookwood Volcanics, in magnetic quiet zone
51	7441122	789901	4	Plr	Rookwood Volcanics, in magnetic quiet zone
52	7440664	789619	2	Plr	Rookwood Volcanics, in magnetic quiet zone
53	7443048	788578	3	Plr	Rookwood Volcanics, in magnetic quiet zone
54	7443762	788340	1	Plr	Rookwood Volcanics, in magnetic quiet zone
55	7437176	791951	3	Cl	Carboniferous limestone, flat-lying
56	7436341	793209	2	Cl	Carboniferous limestone, oolitic, E-dipping
57	7433953	797115	3	Plr	Rookwood Volcanics, magnetic
58	7430434	796717	3	Plr	Rookwood Volcanics, magnetic
59	7433953	799234	5	S-D?	Siluro-Devonian ?trachytic lavas, SW-dipping
60	7441340	798574	2	S-D?	Siluro-Devonian volcanics, interbedded with sediments
61	7436232	805925	3	S-D?	Siluro-Devonian limestone, vertically dipping, NW strike

SITE	NORTHING	EASTING	N/n	UNIT	ROCK TYPE
62	7417574	804565	2	SD-k	Granite at Mount Wallace, intruded by mafic dyke
63	7417574	804565	2	Pub?	Mafic dyke, intruding granite of sites 62, 64
64	7417574	804565	1	SD-k	Granite at Mount Wallace, intruded by mafic dyke
65	7412497	808952	4	Plr	Rookwood Volcanics, weakly magnetic
66	7417688	798366	3	Plr	Rookwood Volcanics, weakly magnetic
67	7418309	802556	1	SD?	Magnetic volcanics, unmapped, supposedly within Carboniferous seds
68	7446628	764846	3	Dmu	Diorite
69	7444640	763742	3	DCo	Connors Volcanics, weakly magnetic
70	7400161	784322	1	Plw-k	Slightly magnetic sediments of Rannes beds, baked by granite?
71	7402881	790499	3	Pui	?Diorite intruding Rookwood Volcanics
72	7403165	792315	2	Plr	Rookwood Volcanics
73	7402803	792293	2	Plr	Rookwood Volcanics, massive lavas
74	7401226	788808	3	Pui-a	Magnetic diorite intruding Rookwoods, magnetic phase of site 71?
75	7399809	789775	2	Plr	Rookwood Volcanics
76	7397492	791371	1	Plr	Rookwood Volcanics
77	7396465	792026	1	Plr	Rookwood Volcanics, silicified fine-grained, massive lavas
78	7394264	794583	1	Plr	Rookwood Volcanics
79	7391098	799210	2	Plr	Rookwood Volcanics
80	7388877	809096	3	Plr	Rookwood Volcanics, fine-grained lavas
81	7392587	807928	2	Plr	Rookwood Volcanics
82	7392271	808404	2	Kut?	?Trachyte intrusive
83	7393390	808146	2	P-Mi?	?Diorite intruding Rookwood Volcanics, lightning struck
84	7391901	808274	1	Plr	Altered Rookwood Volcanics, magnetic
85	7379951	815556	1	Plr	Rookwood Volcanics, fresh fine-grained massive lavas
86	7380802	820677	1	Plr	Rookwood Volcanics
87	7468057	794455	4	Pui	Magnetic gabbroic intrusion within Marlborough Block
88	7468619	796818	3	Pui	Hornblende-biotite-quartz granite intruding Marlborough Block
89	7465970	814835	3	Px	Ultramafics of Marlborough Block
90	7442345	834919	1	Px	Ultramafics of Marlborough Block
91	7437924	847609	1	?Kub	Mafic igneous rock
92	7397862	823456	2	TRn	Native Cat Andesite, variably magnetic

SITE	NORTHING	EASTING	N/n	UNIT	ROCK TYPE
93	7396706	823089	3	TRn	Native Cat Andesite, magnetic
94	7393861	824466	1	Kut	Flow-banded ?rhyolite
95	7389421	825745	2	Kub	Basalt
96	7400483	846765	1	Puo	Granodiorite, moderately magnetic
97	7430299	824669	2	Plg	Ridgelands Granite

TABLE 3. MAGNETIC PROPERTIES

SAMPLE	N/n	UNIT	AV. k (μG/Oe)	AV. J (μG)	AVDEC(°)	AVINC(°)	KOENIGSBERGER RATIO	ANISOTROP
1A	2	Plr	61.0	36.5	193.0	-42.0	1.2	
1B	3	Plr	169.0	1329.0	175.0	-70.0	15.1	1.016
1C	3	Plr	263.0	124406.0	22.0	19.0	910.0	1.023
1D	3	Plr	278.0	608.0	326.0	-55.0	4.2	1.027
1E	3	Plr	42.0	9.8	194.0	11.0	.5	1.018
1F	3	Plr	328.0	196.0	219.0	-1.5	1.2	1.033
2A	3	Plr	202.0	79.7	232.0	-41.0	.8	1.048
2B	3	Plr	72.0	30.0	181.0	6.5	.8	1.023
2C	4	Plr	57.0	6.3	278.0	-75.0	.2	1.013
3A	4	Plr	80.0	34.5	353.0	-38.0	.8	1.027
3B	3	Plr	297.0	1243.0	241.0	-51.0	8.1	1.029
4A	3	Plr	67.0	3.2	104.5	-42.0	.1	1.032
4B	4	Plr	45.0	2.0	93.0	-68.0	.1	1.021
4C	4	Plr	56.0	3.2	23.0	-60.0	.1	1.016
5A	4	Plr	47.0	2.4	51.0	-67.0	.1	1.018
5B	4	Plr	45.0	3.9	122.0	-27.0	.2	1.021
6A	4	Plr	63.0	47.0	145.0	-3.0	1.4	1.023
6B	3	Plr	50.0	6.4	8.0	-67.0	.3	1.023
7A	6	Plr	140.0	72.8	107.7	-64.1	1.0	1.012
7B	3	Plr	372.0	244.0	120.0	-43.0	1.3	1.029
7C	2	Plr	94.0	24.9	50.5	-61.5	.5	1.024
7D	3	Plr	129.0	32.5	47.0	-60.0	.5	1.033
8A	5	Plr	3022.0	1386.0	317.0	-4.0	.9	1.026
8B	4	Plr	2194.0	944.0	313.0	-8.0	.8	1.040
8C	3	Plr	2889.0	923.0	0.0	-84.0	.6	1.023
8D	3	Plr	3188.0	853.0	338.0	-79.0	.5	1.027
9A	4	Plr	4271.0	1488.0	183.0	-19.0	.7	1.019
9B	6	Plr	4024.0	1091.0	93.0	-82.0	.5	1.038
9C	5	Plr	1309.0	224.0	200.0	-69.0	.3	1.037
10A	3	DCa-p	17.1	1.5	55.5	-51.0	.2	1.009
10B	3	DCa-p	16.2	1.7	43.5	-51.0	.2	1.016
11A	3	Plr	55.5	6.4	191.0	-47.0	.2	1.024
11B	4	Plr	53.9	6.5	228.0	-74.0	.2	1.020
12A	4	Plr?	92.8	2.3	91.0	24.5	.1	1.018
12B	5	Plr?	91.2	5.2	115.0	56.0	.1	1.015
12C	4	Plr?	97.1	15.4	99.0	52.5	.3	1.021
13A	2	Plr?	113.0	143.0	228.0	14.0	2.4	1.014
14A	2	Plr	1680.0	3744.0	108.5	26.0	4.3	1.030
14B	3	Plr	2924.0	9032.0	44.0	-39.0	5.9	1.031
14C	4	Plr	2907.0	15086.0	117.0	74.0	10.0	1.040
15A	4	Plr	57.6	9.8	2.0	-41.0	.3	1.026
15B	5	Plr	45.8	10.8	357.0	-56.0	.5	1.024
15C	4	Plr	44.3	11.9	7.0	-65.0	.5	1.009
16A	4	Plr	85.0	14.1	13.0	-59.0	.3	1.019
16B	6	Plr	188.0	98.2	359.0	-51.0	1.0	1.022
16C	5	Plr	76.0	13.5	358.0	-42.0	.3	1.015
17A	3	Plr	56.7	10.9	70.0	-82.3	.4	1.016
17B	2	Plr	56.7	8.2	113.6	-48.2	.3	1.023
17C	2	Plr	53.6	6.4	122.5	-52.6	.3	1.023
17D	3	Plr	55.8	7.7	355.7	-82.3	.3	1.018
18A	3	Plr	37.8	3.8	20.6	-63.2	.2	1.015
18B	4	Plr	36.5	4.4	22.0	-60.4	.2	1.017

TABLE 3. MAGNETIC PROPERTIES

SAMPLE	N/n	UNIT	AV. k (μG/Oe)	AV. J (μG)	AVDEC(°)	AVINC(°)	KOENIGSBERGER RATIO	ANISOTROP
18C	2	Plr	36.1	3.0	256.7	34.4	.2	1.021
19A	2	Plr	55.7	.7	19.8	-70.8	.0	1.036
19B	4	Plr	49.5	7.5	346.4	-73.7	.3	1.021
19C	3	Plr	113.0	3447.0	226.9	46.7	59.0	1.053
20A	3	Dmb	1195.0	105.0	351.0	-64.0	.2	1.031
20B	3	Dmb	1487.0	100.0	346.0	-68.0	.1	1.033
20C	4	Dmb	1325.0	83.0	344.0	-63.0	.1	1.032
20D	3	Dmb	216.0	19.9	253.0	-68.0	.2	1.038
20E	3	Dmb	361.0	39.3	286.0	-68.0	.2	1.034
21A	4	DCo	2.4	49.0	283.7	80.1	39.0	1.022
21B	1	DCo	1.8	13.4	322.6	33.1	14.0	1.033
21C	5	DCo	7.2	26.6	321.6	56.1	7.1	
22A	3	DCo	112.0	86.3	165.7	-72.5	1.5	1.060
22B	4	DCo	102.0	54.0	323.3	42.9	1.0	1.060
22C	4	DCo	582.0	434.0	168.3	74.5	1.4	1.050
23A	5	Dmb	6.0	4.3	200.9	53.2	1.4	1.017
24A	4	Dmb	2111.0	482.0	258.0	-24.5	.4	1.023
24B	2	Dmb	529.0	230.0	331.0	-48.0	.8	1.018
25A	3	Dmb	1469.0	138.0	138.0	-14.0	.2	1.032
25B	4	Dmb	1173.0	72.0	113.0	-43.0	.1	1.027
26A	3	Dmb	1455.0	166.0	2.0	-8.0	.2	1.031
26B	4	Dmb	2213.0	448.0	145.0	-53.0	.4	1.018
27A	3	DCo	32.4	114.0	208.0	85.0	6.8	1.014
27B	2	DCo	33.9	99.0	171.0	83.0	5.6	1.017
27C	4	DCo	32.2	100.0	141.0	80.0	6.0	1.015
28A	2	DCo	64.8	36.5	340.0	-28.0	1.1	1.025
28B	2	DCo	41.3	10.0	341.0	78.0	.5	1.017
28C	3	DCo	49.3	23.8	39.0	-28.0	.9	1.025
28D	3	DCo	43.7	2.0	351.5	16.0	.1	1.017
28E	4	DCo	50.6	2.2	358.0	-1.5	.1	1.015
29A	5	DCo	46.6					1.013
29B	6	DCo	42.5	121.0	87.4	76.5	5.7	1.025
30A	7	DCo	5.6	.8	352.0	-55.4	.3	1.020
30B	6	DCo	11.5	2.9	54.6	-27.6	.5	1.017
31A	2	Dmb	565.0	645.0	0.0	-21.0	2.2	1.040
31B	4	C-Mi?	611.0	728.0	76.0	-53.0	2.3	1.041
31C	3	C-Mi?	711.0	429.0	72.0	-32.5	1.2	1.032
32A	6	DCo	42.8	86.5	268.1	46.9	3.9	1.051
33A	4	DCo	34.7	79.3	262.0	24.0	4.4	1.014
33B	4	DCo	27.7	74.8	259.0	21.0	5.2	1.014
33C	3	DCo	25.8	9.0	278.0	-11.0	.7	1.011
33D	3	DCo	24.2	9.8	283.0	-10.0	.8	1.007
34A	3	DCo	32.4	16.5	27.0	-49.0	1.0	1.016
34B	2	DCo	350.0	168.0	83.0	-70.0	.5	1.025
34C	3	DCo	1600.0	372.0	45.0	-65.0	.5	1.026
35A	2	DCo	47.7	25.6	266.0	13.0	1.0	1.024
35B	3	DCo	28.4	35.6	269.0	-15.0	2.4	1.036
35C	3	DCo	26.6	8.7	276.0	-13.0	.6	1.013
36A	3	DCo	18.4	14.1	229.0	56.0	1.5	1.015
36B	3	DCo	19.2	.7	219.0	64.0	.1	1.015
36C	3	DCo	33.3	73.5	251.0	69.0	4.2	1.016
36D	4	DCo	2536.0	8084.0	195.0	-67.0	6.1	1.037
37A	2	DCo	655.0	143.0	305.0	-60.5	.4	1.044

TABLE 3. MAGNETIC PROPERTIES

SAMPLE	N/n	UNIT	AV. k (μG/Oe)	AV. J (μG)	AVDEC(°)	AVINC(°)	KOENIGSBERGER RATIO	ANISOTROP
37B	2	DCo	424.0	94.2	317.0	-57.5	.4	1.029
38A	2	DCo	7.2	3.3	78.0	-52.0	.9	1.011
38B	3	DCo	8.5	1.0	48.0	-85.0	.2	1.020
38C	3	DCo	8.1	1.7	105.0	-22.0	.4	1.016
39A	3	DCo	61.0	7.4	1.0	-44.0	.2	1.012
39B	2	DCo	55.0	35.9	62.0	86.0	1.3	1.012
39C	2	DCo	48.0	1.1	279.0	-46.0	.0	1.011
39D	3	DCo	47.0	4.5	49.0	0.0	.2	1.007
39E	3	DCo	53.0	8.2	358.5	-62.0	.3	1.007
40A	1	Px	866.0	3346.0	93.0	26.7	7.4	1.064
40B	3	Px	2075.0	10189.0	64.9	23.3	9.4	1.064
40C	1	Px	1935.0	36420.0	254.2	-44.1	36.0	1.097
40D	2	Px	1557.0	41598.0	309.2	17.9	51.0	1.036
41A	1	Px	903.0	1792.0	9.1	-52.3	3.8	1.373
41B	2	Px	4894.0	1492.0	4.7	-51.9	.6	1.062
41C	2	Px	5297.0	1296.0	17.8	-52.4	.5	1.038
41D	1	Px	5130.0	637.0	18.3	-36.8	.2	1.051
41E	1	Px	6253.0	1390.0	11.5	-53.4	.4	1.037
42A	3	DCa-p	910.0	223.0	33.9	-45.5	.5	1.054
42B	3	DCa-p	914.0	250.0	34.9	-45.0	.5	1.056
43A	3	DCa-p	287.0	603.0	192.3	-27.6	4.0	1.098
44A	2	Pu3	13.2	33.0	197.7	48.6	.1	1.030
44B	1	Pu3	23.5	2.6	192.9	39.3	.2	1.019
45A	4	Pla?	32.3	.8	11.5	-8.2	.0	
46A	7	Pla?	39.4	1.3	307.8	-83.7	.1	
47A	2	Dgc2	13.6	44.3	268.5	44.6	6.3	1.019
47B	2	Dgc2	7.0	42.0	265.7	45.9	11.5	1.017
47C	2	Dgc2	3.2	23.1	284.5	56.3	13.9	1.033
47D	4	Dgc2	3.5	24.0	350.1	47.4	3.0	1.025
48A	3	Dgc2	4.8	.5	284.4	35.6	.2	1.003
48B	2	Dgc2	.5	.5	267.6	42.1	1.9	1.143
48C	2	Dgc2	.1	.8	285.2	39.1	21.4	2.974
49A	3	Plr	50.0	17.0	244.9	48.5	.7	1.026
49B	2	Plr	44.4	13.5	227.0	58.8	.6	1.008
49C	1	Plr	48.6	18.9	220.2	61.0	.8	1.031
50A	1	Plr	42.8	1.4	8.5	.8	.1	1.020
50B	2	Plr	39.5	7.3	340.2	-24.6	.4	1.011
50C	2	Plr	54.9	3.0	2.5	-21.7	.1	1.012
51A	3	Plr	47.8	4.0	89.2	-40.0	.2	1.014
51B	2	Plr	48.9	1.0	41.5	-23.0	.0	1.012
51C	2	Plr	54.2	2.4	76.8	-38.1	.1	1.012
51D	3	Plr	53.2	46.9	266.2	-3.4	1.7	1.014
52A	2	Plr	25.2	1.2	355.6	-75.0	.1	1.034
52B	5	Plr	50.2	3.1	16.7	-63.0	.1	1.021
53A	3	Plr	50.7	.4	7.2	-67.4	.0	1.009
53B	1	Plr	52.5	1.6	338.6	-78.2	.1	1.013
53C	2	Plr	51.6	3.6	18.2	-68.2	.1	1.016
54A	6	Plr	50.6	3.8	26.6	-65.6	.1	
55A	3	Cl	2.5	1.3	322.3	-51.9	1.0	1.023
55B	2	Cl	1.8	.6	328.4	-70.1	.6	1.070
55C	1	Cl	1.1	.7	309.2	-71.4	1.2	1.058
56A	2	Cl	.2	2.0	349.2	-63.0	17.0	1.113
56B	2	Cl	2.6	1.0	3.3	-62.0	.7	1.032

TABLE 3. MAGNETIC PROPERTIES

SAMPLE	N/n	UNIT	AV. k (μG/Oe)	AV. J (μG)	AVDEC(°)	AVINC(°)	KOENIGSBERGER RATIO	ANISOTROP
57A	3	Plr	2702.0	83165.0	61.9	5.3	59.0	
57B	3	Plr	2070.0	759.0	54.0	-64.7	.7	1.028
57C	2	Plr	415.0	2606.0	296.1	-48.0	12.0	1.032
58A	3	Plr	3778.0	2197.0	257.1	-64.4	1.1	1.034
58B	3	Plr	3737.0	6410.0	307.9	-57.1	3.3	1.038
58C	2	Plr	4437.0	4187.0	27.8	39.7	1.8	1.047
59A	2	S-D?	42.0	7.7	28.7	-69.8	.4	1.025
59B	2	S-D?	35.3	6.8	32.2	-66.2	.4	1.026
59C	1	S-D?	40.8	7.8	23.0	*****	.4	1.015
59D	2	S-D?	39.0	7.8	27.7	-58.3	.4	1.020
59E	2	S-D?	39.7	7.2	326.5	-76.7	.4	1.019
60A	4	S-D?	44.8	1.5	352.0	-68.5	.1	1.036
60B	5	S-D?	41.8	1.0	322.4	-54.0	.1	
61A	1	S-D?	.8	2.4	36.6	55.6	6.2	1.043
61B	2	S-D?	.9	.8	33.6	60.2	1.8	1.052
61C	2	S-D?	.4	2.8	48.6	45.8	15.0	1.125
62A	2	SD-k	81.4	7.9	120.3	-61.7	.2	1.041
62B	2	SD-k	1291.0	58.8	325.1	-70.7	.1	1.045
63A	2	Pub?	2869.0	587.0	358.8	40.5	.4	1.008
63B	6	Pub?	80.3	13.9	272.3	-32.3	.3	1.008
64A	2	SD-k	1070.0	157.0	273.9	-9.1	.3	1.054
65A	3	Plr	69.3	17.3	8.1	-62.7	.5	1.018
65B	2	Plr	77.7	24.4	3.6	-67.9	.6	1.033
65C	2	Plr	66.8	15.3	17.4	-53.4	.4	1.024
65D	3	Plr	73.5	23.1	43.0	-60.7	.6	1.026
66A	4	Plr	41.8	6.9	36.1	-71.4	.3	
66B	3	Plr	37.3	7.9	2.8	-71.6	.4	
66C	6	Plr	44.1	11.4	12.1	-73.9	.5	
67A	6	SD?	2043.0	538.0	355.4	-65.0	.5	
68A	2	Dmu	30.8	1.4	102.0	68.5	.1	1.011
68B	2	Dmu	37.9	.9	61.1	-79.4	.1	1.008
68C	3	Dmu	34.3	1.4	41.0	-72.3	.1	1.017
69A	1	DCo	36.7	.3	357.9	-23.3	.0	1.025
69B	2	DCo	31.6	.4	334.3	-78.7	.0	1.018
69C	2	DCo	35.6	.5	119.5	-74.1	.0	1.030
70A	6	Plw-k	128.0	11.4	25.8	-7.4	.2	
71A	2	Pui	68.4	256.0	293.3	-80.5	7.2	1.022
71B	2	Pui	74.3	388.0	287.6	-82.0	10.0	1.024
71C	2	Pui	58.4	113.0	218.6	-81.6	3.7	1.039
72A	1	Plr	96.8	2.7	6.3	-63.1	.1	1.070
72B	2	Plr	86.5	65.7	58.3	-24.0	1.5	1.069
73A	1	Plr	722.0	10894.0	325.7	-84.1	29.0	1.056
73B	3	Plr	1149.0	422.0	355.3	-60.4	.7	
74A	2	Pui-a	3049.0	1430.0	306.5	-11.0	.9	1.127
74B	3	Pui-a	3310.0	784.0	238.5	8.5	.5	1.050
74C	2	Pui-a	3153.0	819.0	218.7	-32.7	.5	1.105
75A	2	Plr	838.0	413.0	51.4	-78.0	1.0	1.041
75B	2	Plr	440.0	278.0	93.7	-77.5	1.2	1.018
76A	5	Plr	53.6	2.0	40.5	49.9	.1	1.022
77A	3	Plr	53.0	1.5	341.7	-76.8	.1	1.016
78A	2	Plr	57.3	15.3	308.4	65.1	.5	1.012
79A	6	Plr	1336.0	4422.0	352.3	-52.0	6.4	1.030
79B	6	Plr	1677.0	727.0	51.3	-72.8	.8	1.054

TABLE 3. MAGNETIC PROPERTIES

SAMPLE	N/n	UNIT	AV. k (μG/Oe)	AV. J (μG)	AVDEC(°)	AVINC(°)	KOENIGSBERGER RATIO	ANISOTROP
80A	3	Plr	2616.0	1128.0	302.9	-68.6	.8	1.026
80B	2	Plr	2397.0	926.0	318.0	-35.7	.7	1.040
80C	3	Plr	2706.0	4777.0	32.9	-22.8	3.4	1.026
81A	2	Plr	93.6	3.5	293.1	-79.5	.1	1.017
81B	4	Plr	68.0	7.8	193.7	-18.7	.2	1.023
82A	3	Kut?	3.0	9.7	3.3	-66.5	6.2	1.023
82B	3	Kut?	3.7	7.7	354.1	-68.3	4.0	1.013
83A	2	P-Mi?	2680.0	1396.0	331.1	-55.9	.5	1.031
83B	3	P-Mi?	2918.0	74667.0	303.0	14.6	49.0	1.029
84A	2	Plr	4372.0	1125.0	318.1	-53.6	.5	1.032
85A	2	Plr	3096.0	2360.0	229.9	-39.8	1.5	1.017
86A	5	Plr	107.0	27.6	31.3	-37.9	.5	1.026
87A	3	Pui	2150.0	1046.0	338.1	5.1	.9	1.028
87B	1	Pui	2332.0	621.0	35.7	16.8	.5	1.035
87C	1	Pui	2431.0	1141.0	164.9	-67.7	.9	1.027
87D	3	Pui	2585.0	275.0	316.8	22.1	.2	1.034
88A	3	Pui	24.5	1.9	334.6	83.9	.2	1.022
88B	3	Pui	27.8	1.9	298.8	76.7	.1	1.025
88C	3	Pui	26.0	5.1	327.5	74.0	.4	1.029
89A	3	Px	3587.0	764.0	93.8	-31.7	.4	1.082
89B	3	Px	59.1	.1	44.8	-28.3	0.0	1.016
89C	4	Px	300.0	16.1	141.1	-3.2	.1	1.032
90A	3	Px	1453.0	345.0	284.2	-49.5	.5	1.060
91A	4	?Kub	3960.0	991.0	82.8	-62.4	.5	1.036
92A	3	TRn	2035.0	300.0	105.7	-77.0	.3	1.042
92B	4	TRn	2979.0	343.0	28.2	-55.0	.2	1.024
93A	2	TRn	2483.0	680.0	345.9	-58.0	.5	1.046
93B	2	TRn	1927.0	598.0	226.5	-23.6	.6	1.051
93C	2	TRn	1998.0	653.0	.2	-42.3	.6	1.042
94A	5	Kut	9.3	25.3	23.7	-69.7	5.2	1.013
95A	3	Kub	5294.0	6845.0	344.0	-56.9	2.5	1.039
95B	1	Kub	4711.0	8791.0	4.3	-52.7	3.6	1.036
96A	4	Puo	601.0	190.0	60.0	-80.6	.6	1.073
97A	2	Plg	3472.0	356.0	85.5	-67.3	.2	1.134
97B	2	Plg	3189.0	294.0	33.2	-79.1	.2	1.093

TABLE 4. MAGNETIC PROPERTIES OF DDH SAMPLES

DDH	DEPTH(m)	N	ROCK TYPE	AV. k (μG/Oe)	AV. J (μG)	AVINC(°)	Q
DDH3	129.0	3	Buff-greyish fine-grained pillow lava, unweathered	57.30	2.8	-81.5	.09
DDH3	156.5	2	Volcanic hyaloclastic breccia, sulphide rich	33.60	2.7	46.2	.15
DDH3	191.6	2	Volcanic hyaloclastic breccia, disseminated sulphide, pale	59.30	5.2	-53.9	.20
DDH3	205.4	3	Pillow lava/VHB with minor sulphides	68.70	6.5	-40.3	.18
DDH3	225.4	2	Pillow lava, grey, sulphide-rich, chloritic amygdules	90.10	22.1	36.0	.77
DDH3	238.0	3	Pillow lava, grey, minor sulphides, chloritic amygdules	44.80	1.7	-81.3	.07
DDH3	269.5	3	Siliceous breccia, grey-white silica replacement veins, minor sulphides	7.70	1.2	-51.7	.30
DDH3	305.5	3	Pillow lava, grey, very fine-grained, minor pyrite, strong silica alteration	65.40	1.5	-57.0	.04
DDH16	107.8	3	Pillow lava? Pale grey altered zone, numerous buff very fine-grained veinlets	43.90	2.5	-67.7	.11
DDH16	121.8	2	Massive sulphides, in pale grey bleached zone with abundant sulphides	.78	.2	-60.6	.59
DDH16	157.3	3	VHB, pale grey siliceous rock with sulphide-rich fractures	19.30	.5	-67.0	.05
DDH16	227.2	3	Pillow lava with strong pyrite veining and stockwork	39.60	.7	-37.2	.03
DDH16	256.2	3	Andesite. Amygdaloidal grey rock, fine to medium grained massive flow	39.70	1.6	-53.9	.08
DDH16	258.0	2	Grey, siliceous, sulphide-rich volcanic hyaloclastic breccia	30.20	.3	-36.9	.02
DDH16	265.5	3	Pillow lava? Siliceous amygdaloidal, medium grey, with irregular sulphide veins	35.60	.2	-60.6	.01
DDH16	270.7	4	Andesite. Dark, unaltered, medium grained with irregular sulphide veinlets	43.40	.2	-73.7	.01
DDH16	282.0	3	Pillow lava andesite, more altered than 270.7m, pale grey siliceous with strong sulphide stockwork	39.40	.8	-59.9	.04
DDH16	290.5	1	Andesite, medium grained, darker than 282m, with semi-massive sulphides	50.50	.7	-66.9	.03
DDH16	314.4	2	Pillow lavas, altered, siliceous, light grey, fine-grained with stockwork pyritic veins	54.90	3.4	-67.7	.12
DDH18	83.3	4	Pillow lava, pale grey, green alteration with much pale veining	56.50	5.8	-80.9	.20
DDH18	101.0	2	Pillow lava, altered, pale grey, with silica-sulphide veining, sulphide-rich	29.40	.8	-81.0	.05
DDH18	103.0	1	Pillow lava, altered, pale grey, with silica-sulphide veining, less sulphide than 101m	47.60	1.9	-77.3	.08
DDH18	124.8	1	Pillow lava, very fine-grained, milky, with coarse semi-massive sulphide veins and fine stockwork	19.50	1.3	-68.0	.13
DDH18	148.0	3	Massive sulphide, within sulphide-rich zone with faint brecciated texture	3.10	1.6	76.4	.81
DDH18	166.0	1	Semi-massive sulphide in silica	8.60	.1	-69.8	.02
DDH18	240.9	1	Semi-massive sulphide in silica	25.40	.2	-62.6	.01
DDH18	342.8	2	Pillow lavas? Stockwork alteration zone, pale grey, with disseminated and stockwork sulphides	44.80	.9	40.1	.04
DDH19	117.0	4	Pillow lava, med. grey green, scattered white amygdules, dark chloritic rims (green var, jasper)	1181.00	497.0	-84.9	.81
DDH19	126.2	2	Pillow lava, med. grey green, scattered white amygdules, dark chloritic rims (green var, jasper)	217.00	57.3	-75.6	.51
DDH19	130.3	2	Pillow lava, med. grey green, scattered white amygdules, dark chloritic rims (green var, jasper)	4262.00	958.0	-82.9	.43

TABLE 4. MAGNETIC PROPERTIES OF DDH SAMPLES

DDH	DEPTH(m)	N	ROCK TYPE	AV. k (μG/Oe)	AV. J (μG)	AVINC(°)	Q
DDH19	166.8	1	Pillow lava, green var., jasper	69.90	9.0	-85.5	.25
DDH19	176.0	5	Pillow lava, green var., jasper	383.00	183.0	-81.0	.92
DDH19	244.0	1	Pillow lava, green var., jasper	71.40	7.0	-25.8	.19
DDH19	253.8	2	Pillow lava, green var., jasper	51.80	4.8	-63.5	.18
DDH27	262.0	1	Andesite pillow lavas, grey-green, amygdaloidal, abundant epidote	1376.00	436.0	83.6	.61
DDH27	263.0	3	Andesite pillow lavas, fine-grained grey-green to purplish, amygdaloidal, abundant epidote	51.80	55.1	-21.0	2.00
DDH27	279.0	2	Andesite, massive, medium-grained, grey-green, within moderately magnetic zone	661.00	501.0	-72.4	1.50
DDH27	280.3	7	Andesite, massive, medium-grained, grey-green, with jasper/epidote, within moderately magnetic zone	1243.00	1318.0	-80.3	2.00
DDH27	282.0	3	Pillow lava, grey-green, amygdaloidal, with epidote-altered rim at one end	51.50	7.3	-67.2	.27
DDH27	285.3	3	Pillow lava, medium-grained, grey-green to purplish	106.00	19.1	-64.1	.35
DDH27	288.5	3	Pillow lava, purple, with abundant epidote	986.00	95.0	-35.3	.19

Appendix I

Representative examples of thermal demagnetisation plots for all sites. Refer to caption for Fig.5.5 for explanation of plots.

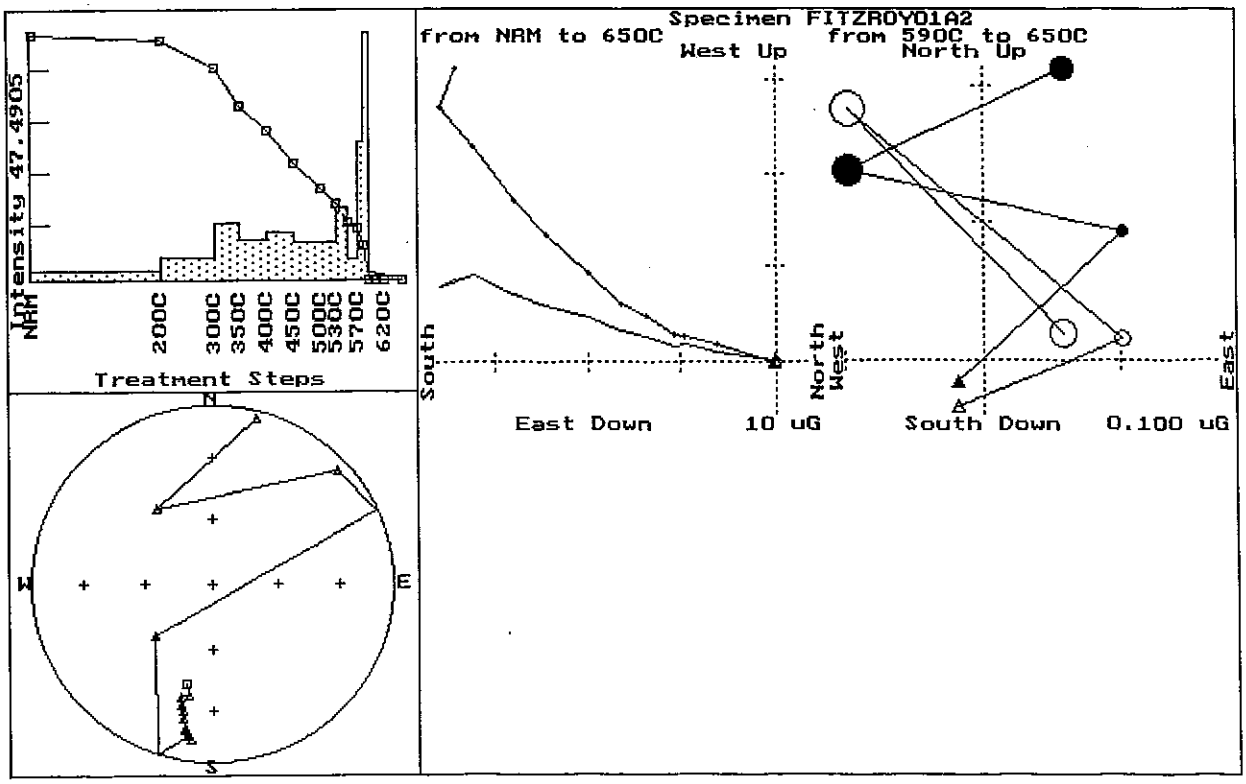
Specimen FITZROY01A2
from NRM to 650C
West Up
from 590C to 650C
North Up
Intensity 47.4905
NRM
200C
300C
350C
400C
450C
500C
530C
570C
620C
Treatment Steps
N
W
E
S
South
North
West
East
East Down
10 uG
South Down
0.100 uG

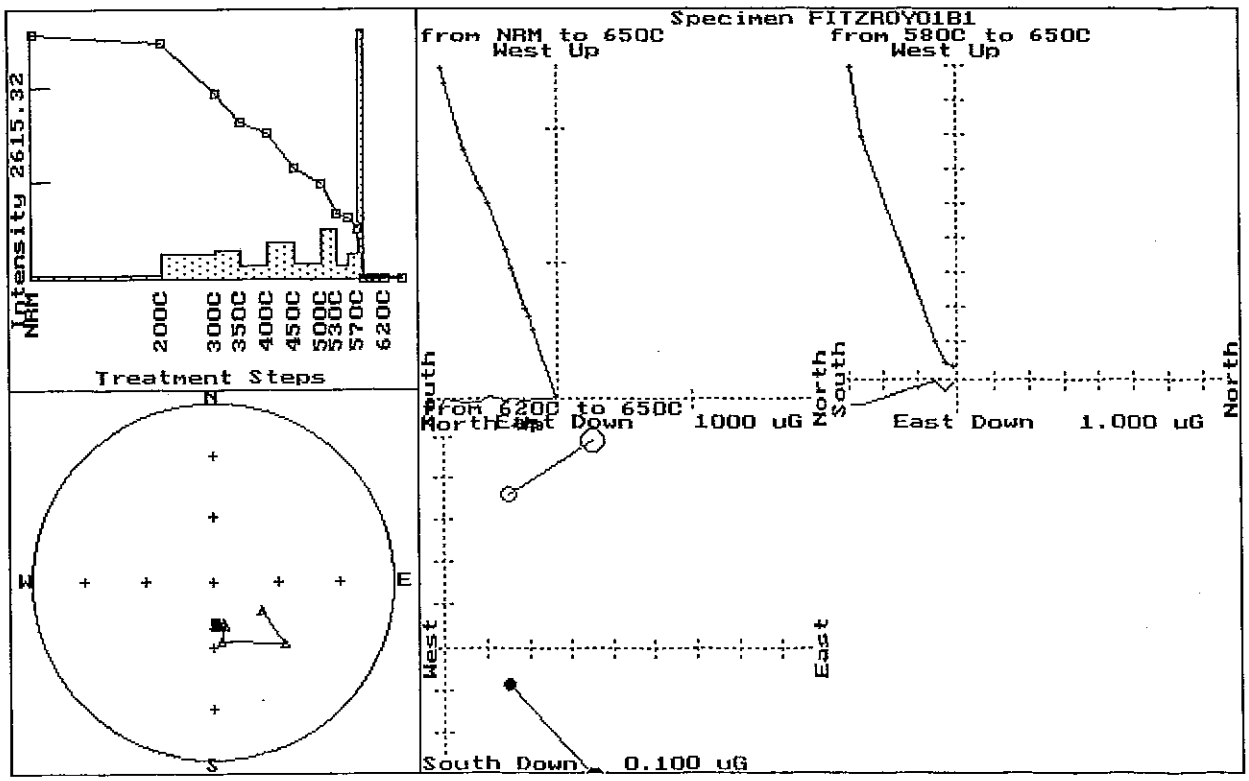
Specimen FITZROY01B1
from NRM to 650C
West Up
from 580C to 650C
West Up
Intensity 2615.32
NRM
200C
300C
350C
400C
450C
500C
530C
570C
620C
Treatment Steps
N
W
E
S
South
North
from 620C to 650C
East Down
1000 uG
East Down
1.000 uG
West
East
South Down
0.100 uG

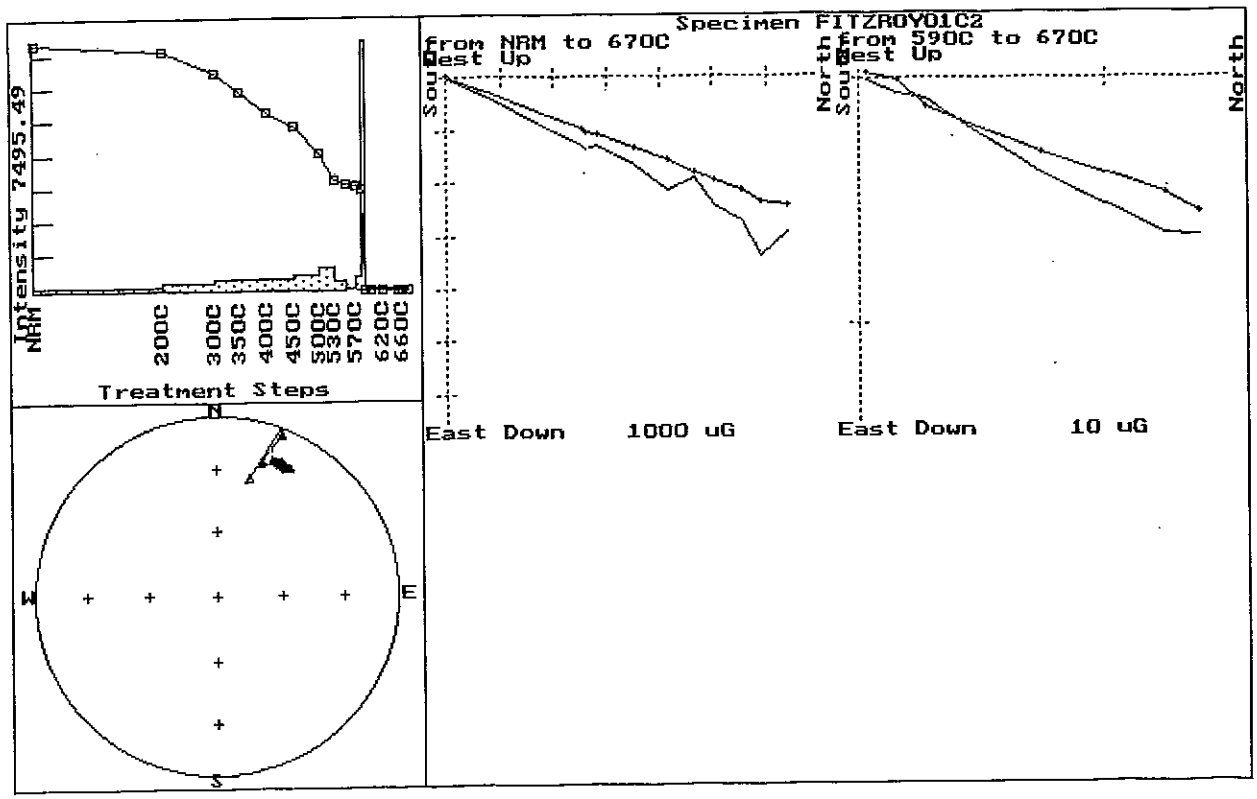
Intensity 7495.49
NRM
200C
300C
350C
400C
450C
500C
530C
570C
620C
660C
Treatment Steps
N
E
S
W
Specimen FITZROY01C2
from NRM to 670C
West Up
South
East Down
1000 uG
from 590C to 670C
West Up
North
South
East Down
10 uG

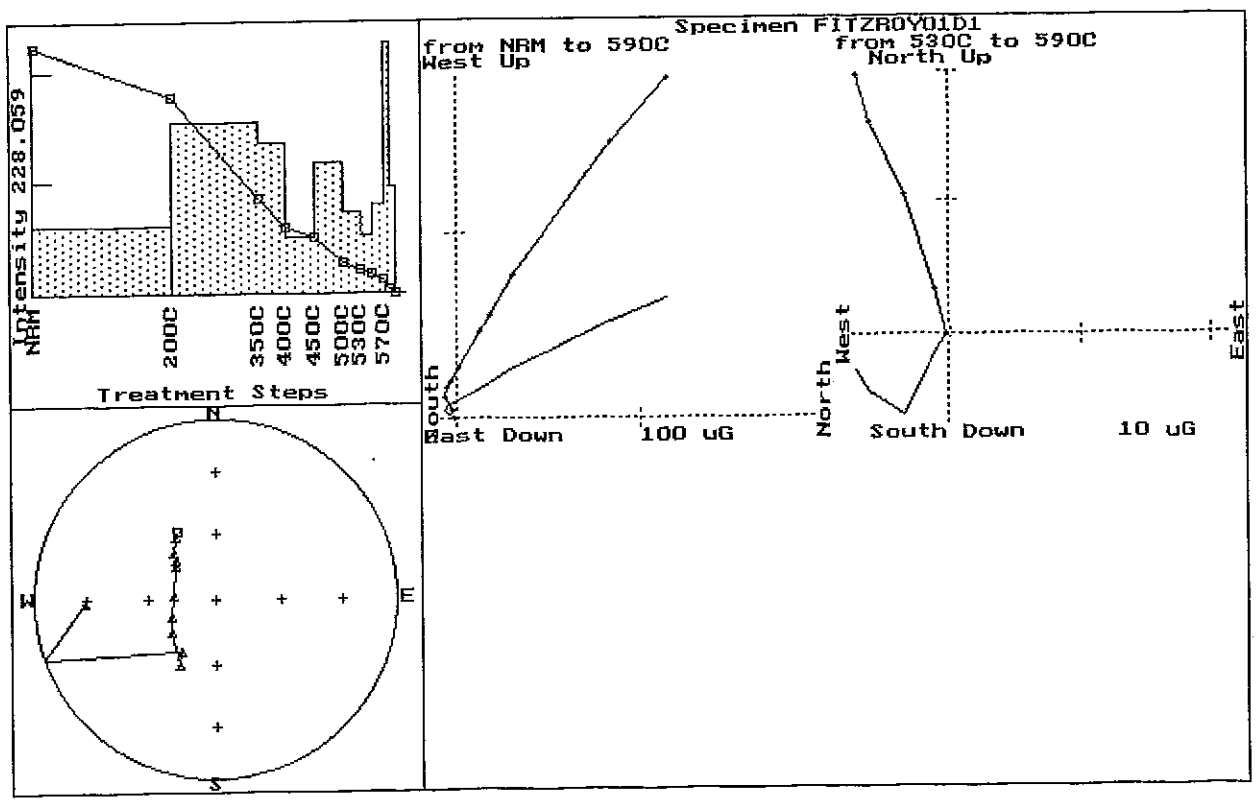
Intensity 228.059
NRM
200C
350C
400C
450C
500C
530C
570C
Treatment Steps
N
E
S
W
Specimen FITZROY01D1
from NRM to 590C
West Up
South
East Down
100 uG
from 530C to 590C
North Up
West
North
East
South Down
10 uG

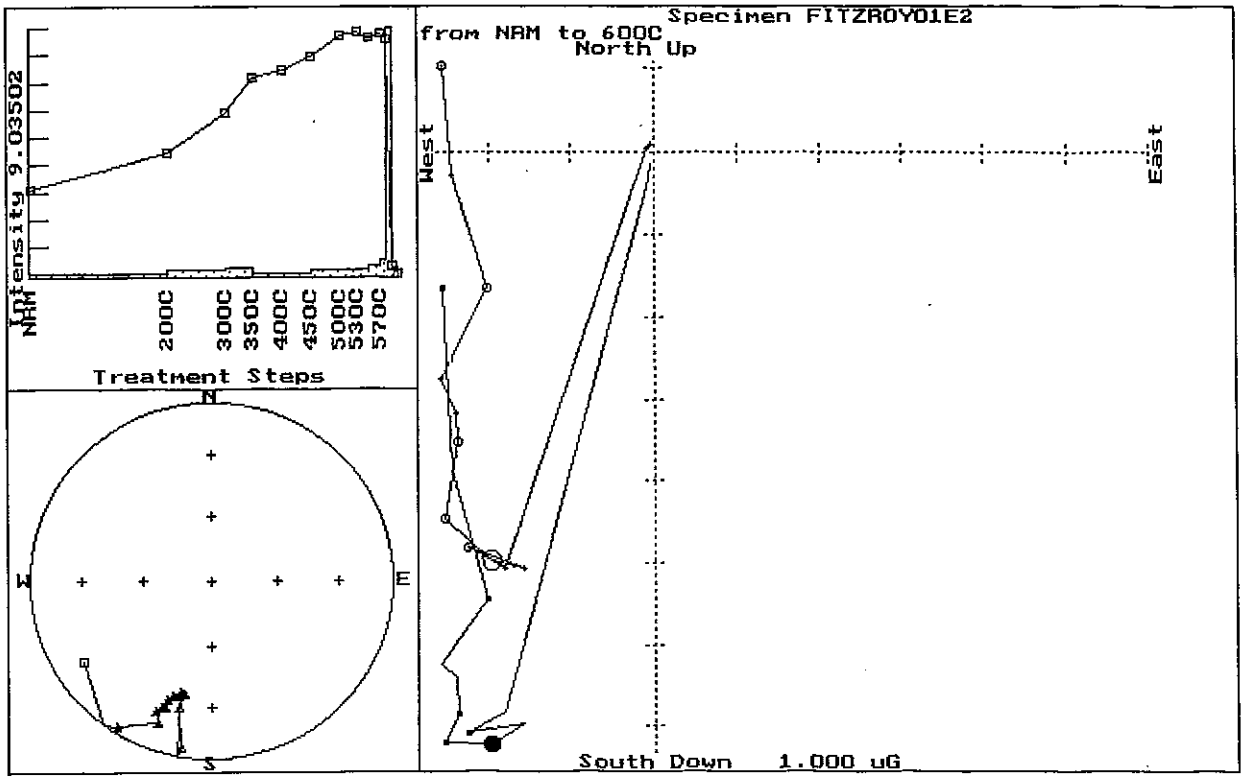
Specimen FITZROY01E2
from NRM to 600C
North Up
West
East
Intensity 9.03502
NRM
200C
300C
350C
400C
450C
500C
530C
570C
Treatment Steps
N
W
E
S
South Down
1.000 uG

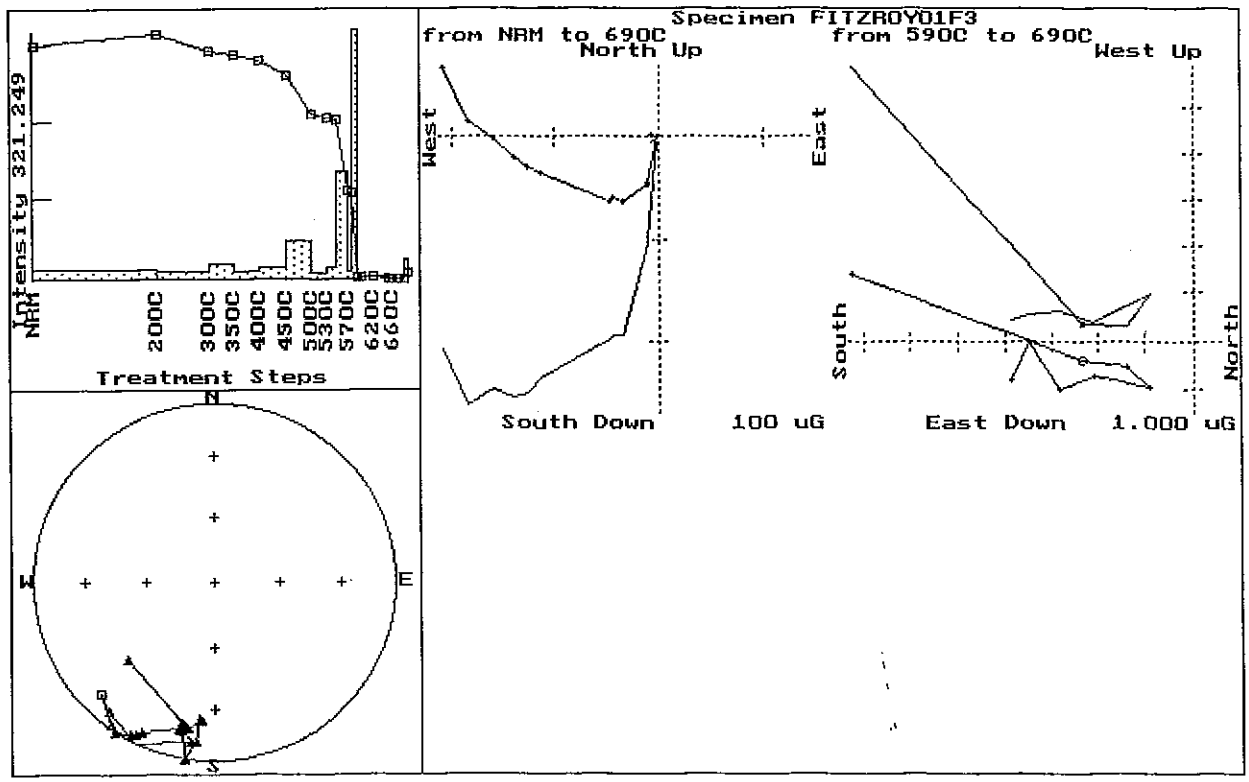
Specimen FITZROY01F3
from NRM to 690C
North Up
from 590C to 690C
West Up
West
East
South
North
Intensity 321.249
NRM
200C
300C
350C
400C
450C
500C
530C
570C
620C
660C
Treatment Steps
N
W
E
S
South Down
100 uG
East Down
1.000 uG

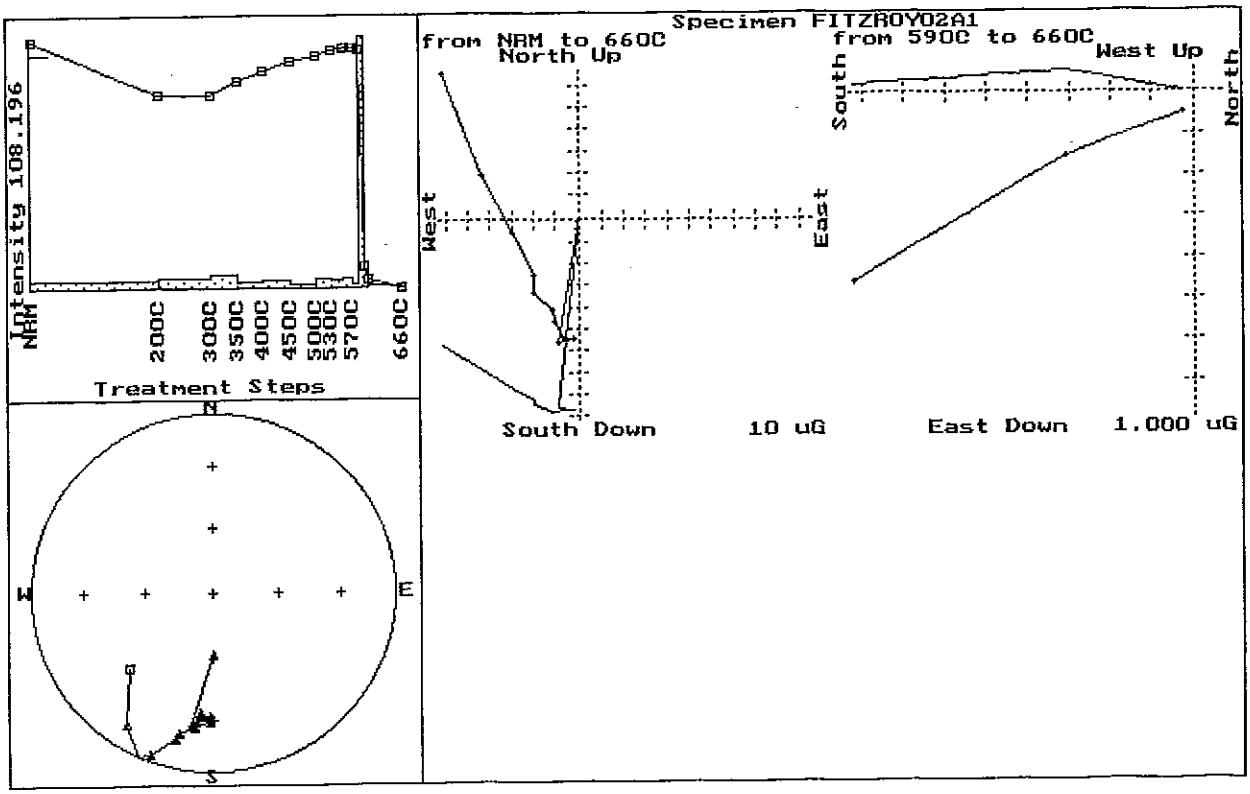
Intensity 108.196
NRM
200C
300C
350C
400C
450C
500C
530C
570C
660C
Treatment Steps
N
W
E
S
Specimen FITZROY02A1
from NRM to 660C
North Up
West
East
South Down
10 uG
from 590C to 660C
West Up
South
North
East Down
1.000 uG

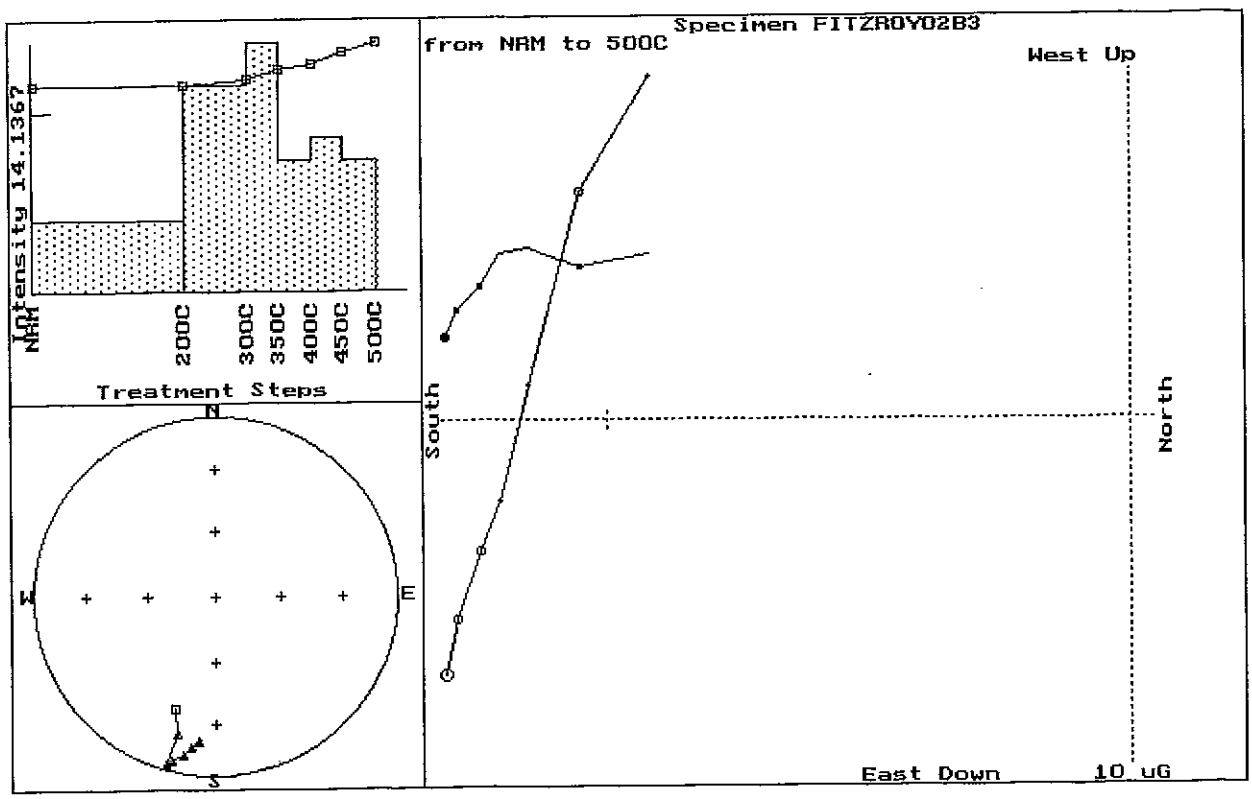
Intensity 14.1367
NRM
200C
300C
350C
400C
450C
500C
Treatment Steps
N
W
E
S
Specimen FITZROY02B3
from NRM to 500C
West Up
South
North
East Down
10 uG

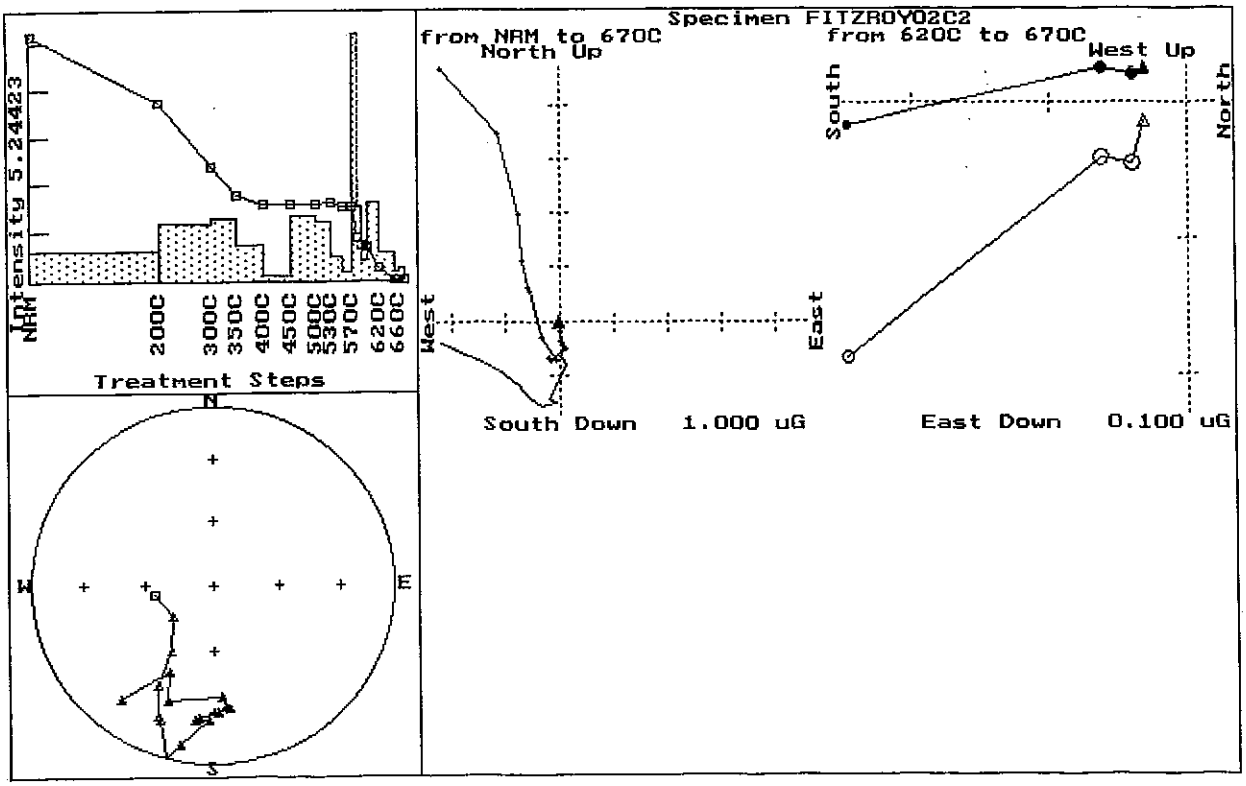
Specimen FITZROY02C2
from NRM to 670C
North Up
from 620C to 670C
West Up
Intensity 5.24423
NRM
200C
300C
350C
400C
450C
500C
530C
570C
620C
660C
Treatment Steps
West
East
South
North
South Down 1.000 uG
East Down 0.100 uG
N
E
S
W

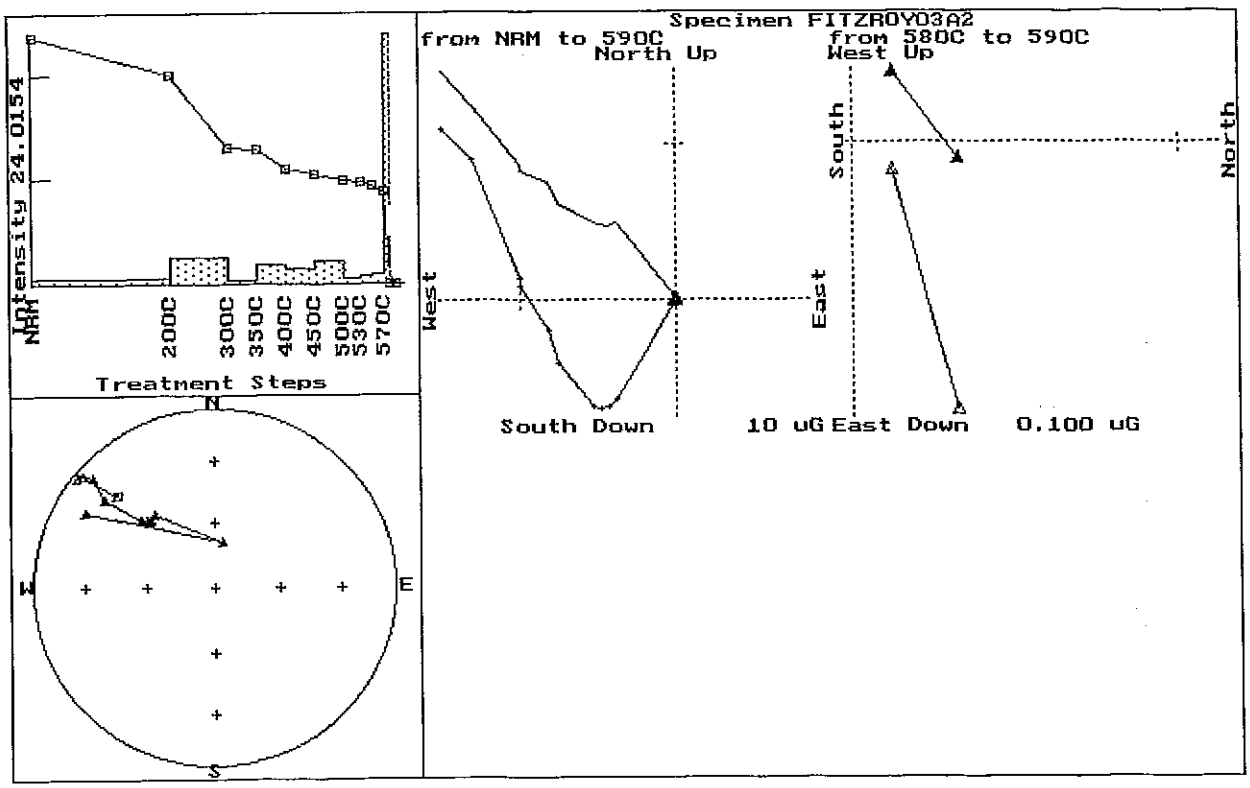
Specimen FITZROY03A2
from NRM to 590C
North Up
from 580C to 590C
West Up
Intensity 24.0154
NRM
200C
300C
350C
400C
450C
500C
530C
570C
Treatment Steps
West
East
South
North
South Down 10 uG
East Down 0.100 uG
N
E
S
W

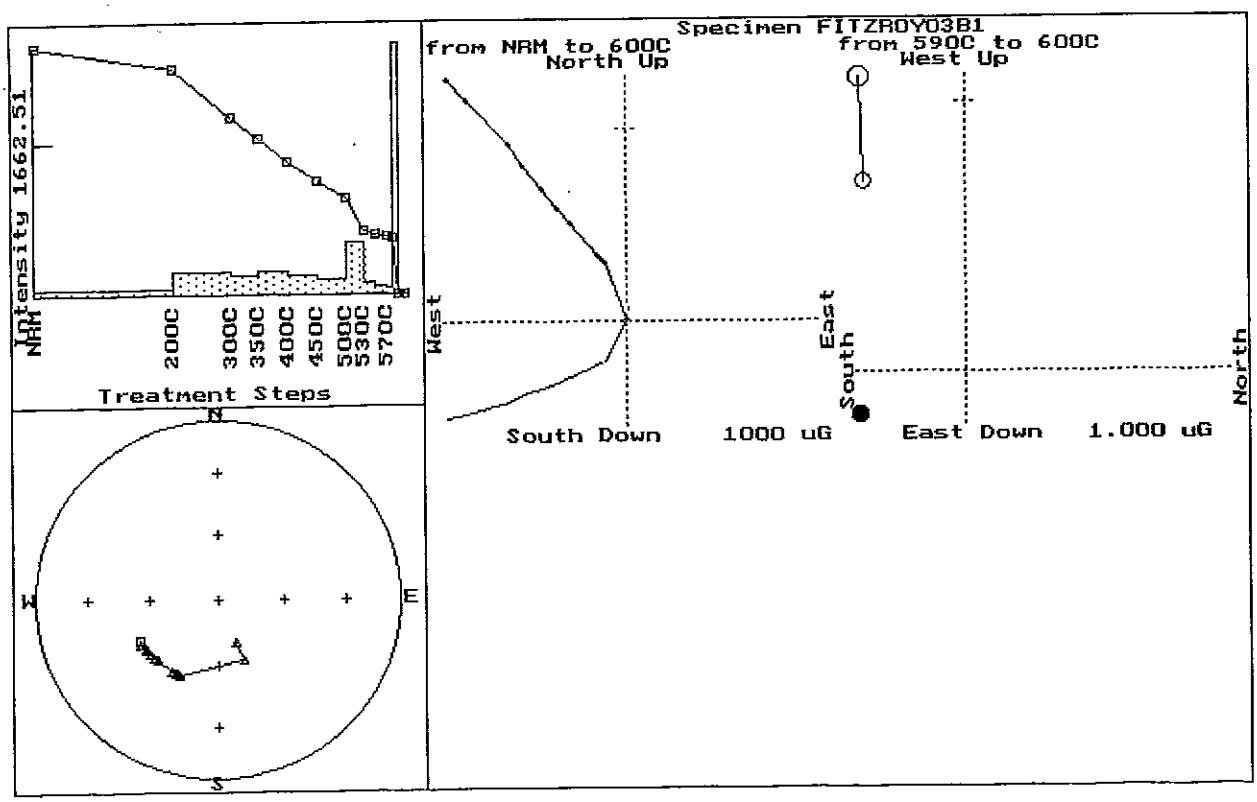
Specimen FITZROY03B1
from NRM to 600C
North Up
from 590C to 600C
West Up
Intensity 1662.51
NRM
200C
300C
350C
400C
450C
500C
530C
570C
Treatment Steps
West
East
South
North
South Down
1000 uG
East Down
1.000 uG
N
E
S
W

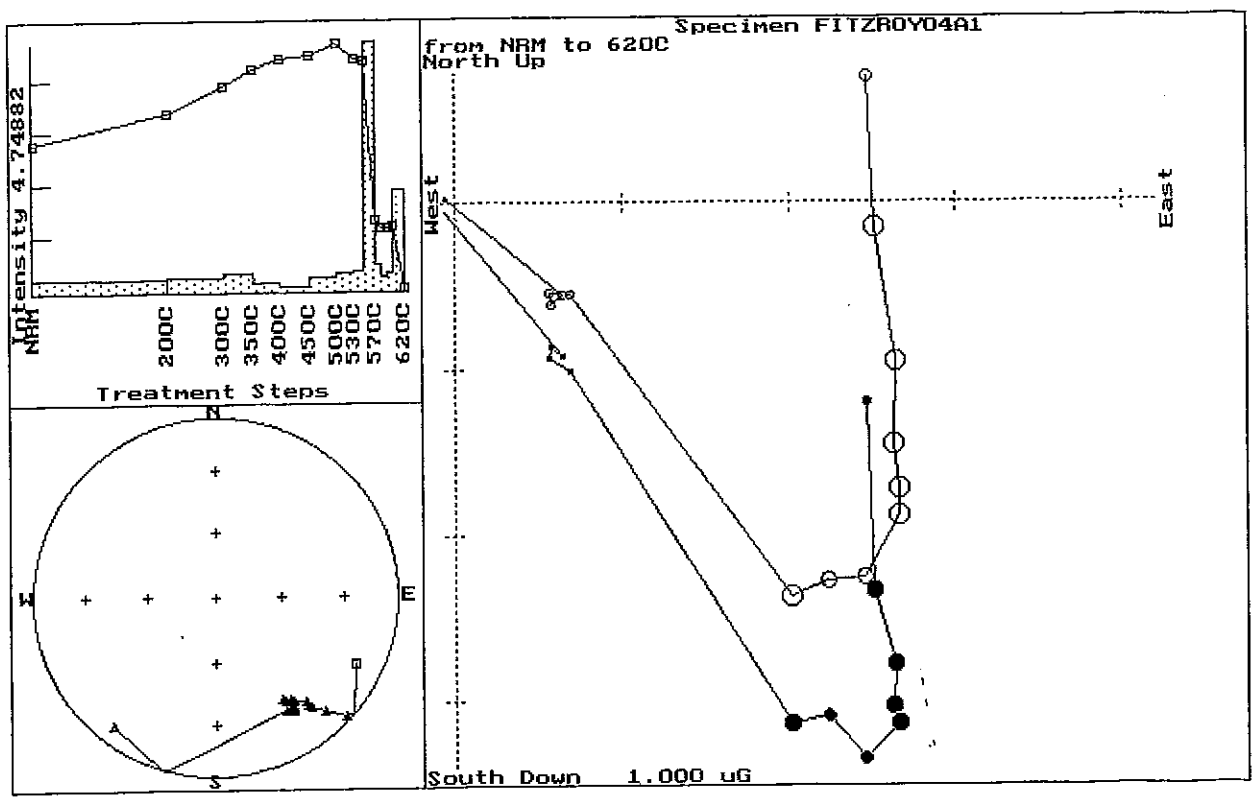
Specimen FITZROY04A1
from NRM to 620C
North Up
Intensity 4.74882
NRM
200C
300C
350C
400C
450C
500C
530C
570C
620C
Treatment Steps
West
East
South Down
1.000 uG
N
E
S
W

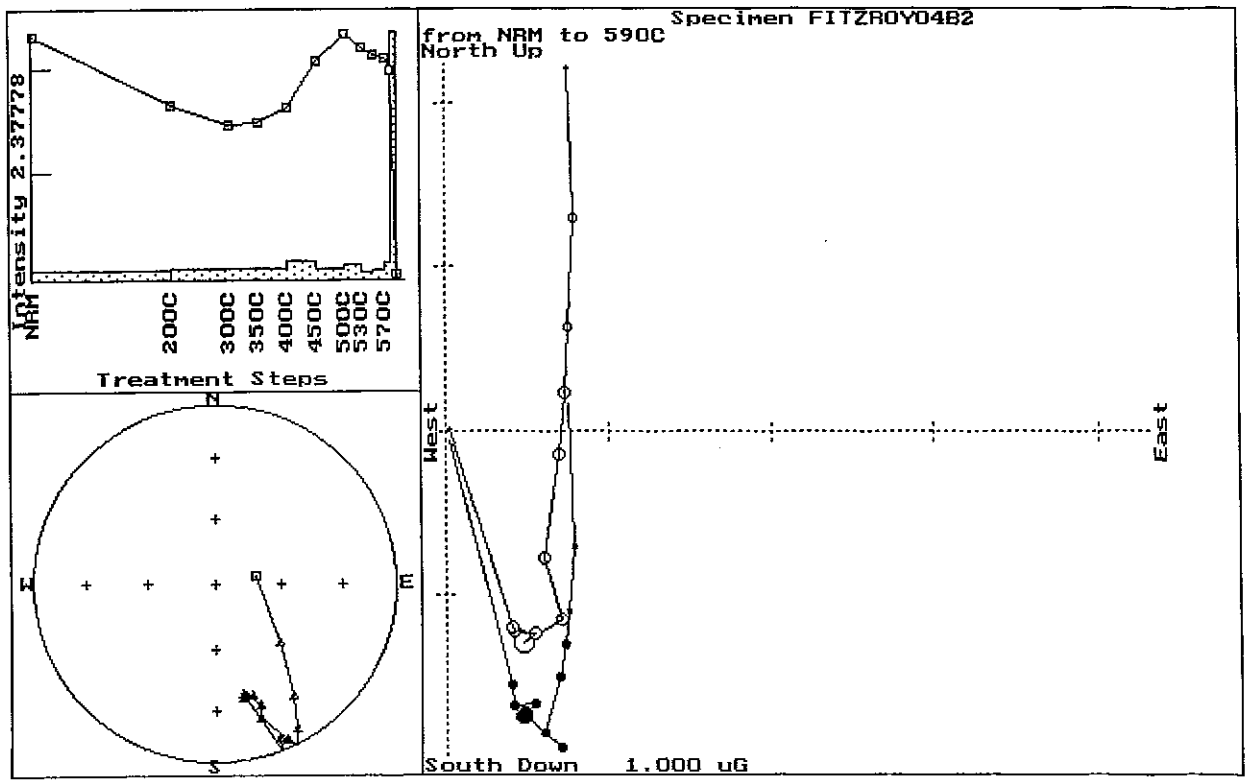
Specimen FITZROY04B2
from NRM to 590C
North Up
Intensity 2.37778
NRM
200C
300C
350C
400C
450C
500C
530C
570C
Treatment Steps
N
W
E
S
West
East
South Down 1.000 uG

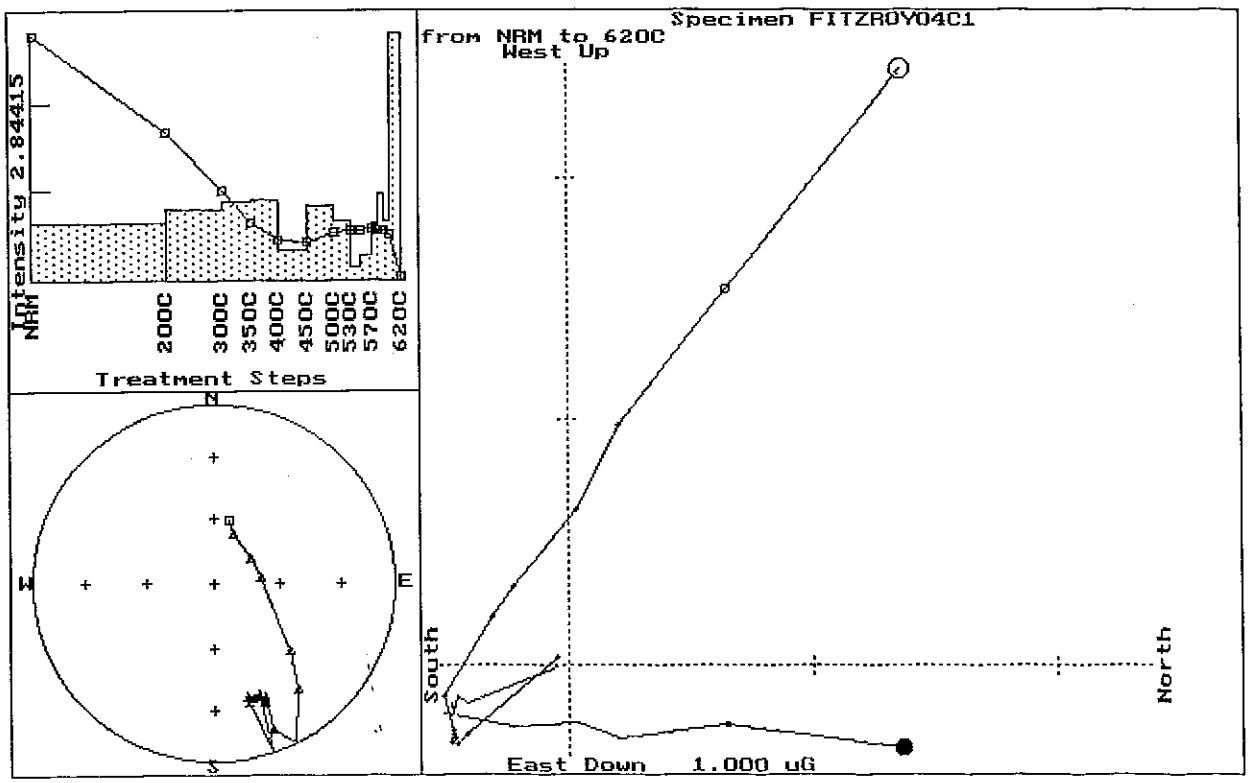
Specimen FITZROY04C1
from NRM to 620C
West Up
Intensity 2.84415
NRM
200C
300C
350C
400C
450C
500C
530C
570C
620C
Treatment Steps
N
W
E
S
South
North
East Down 1.000 uG

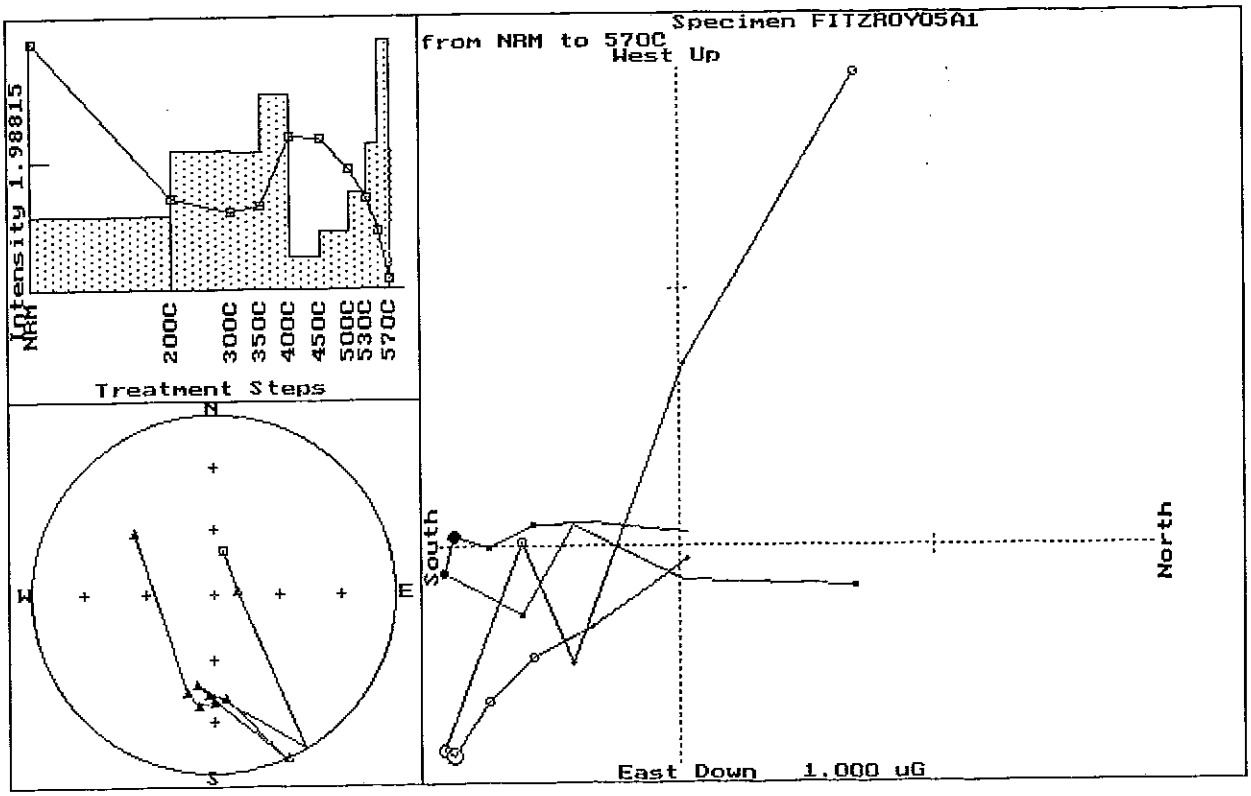
Specimen FITZROY05A1
from NRM to 570C
West Up
Intensity 1.98815
NRM
200C
300C
350C
400C
450C
500C
530C
570C
Treatment Steps
N
E
S
W
South
North
East Down 1.000 uG

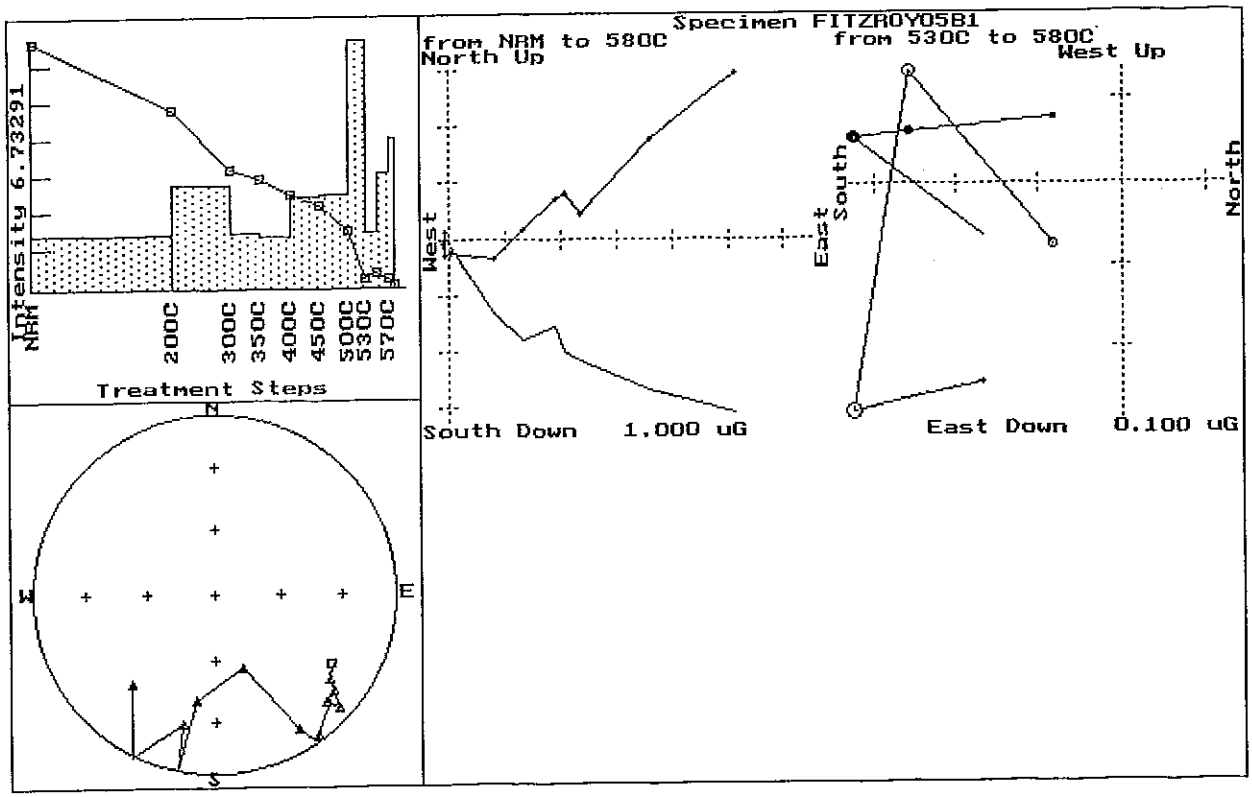
Specimen FITZROY05B1
from NRM to 580C
North Up
from 530C to 580C
West Up
Intensity 6.73291
NRM
200C
300C
350C
400C
450C
500C
530C
570C
Treatment Steps
N
E
S
W
West
East
South
North
South Down 1.000 uG
East Down 0.100 uG

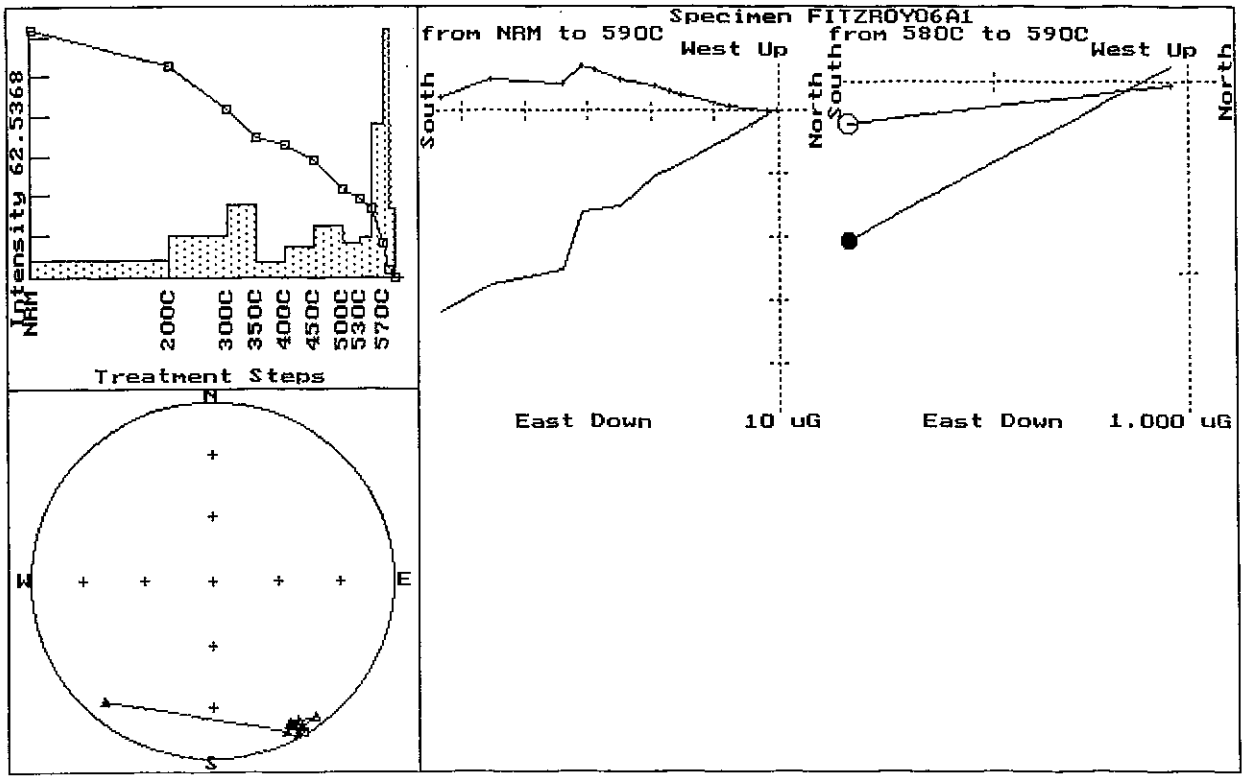
Specimen FITZROY06A1
from NRM to 590C
West Up
South
East Down
10 uG
from 580C to 590C
West Up
North
South
East Down
1.000 uG
Intensity 62.5368
NRM
200C
300C
350C
400C
450C
500C
530C
570C
Treatment Steps
N
E
S
W

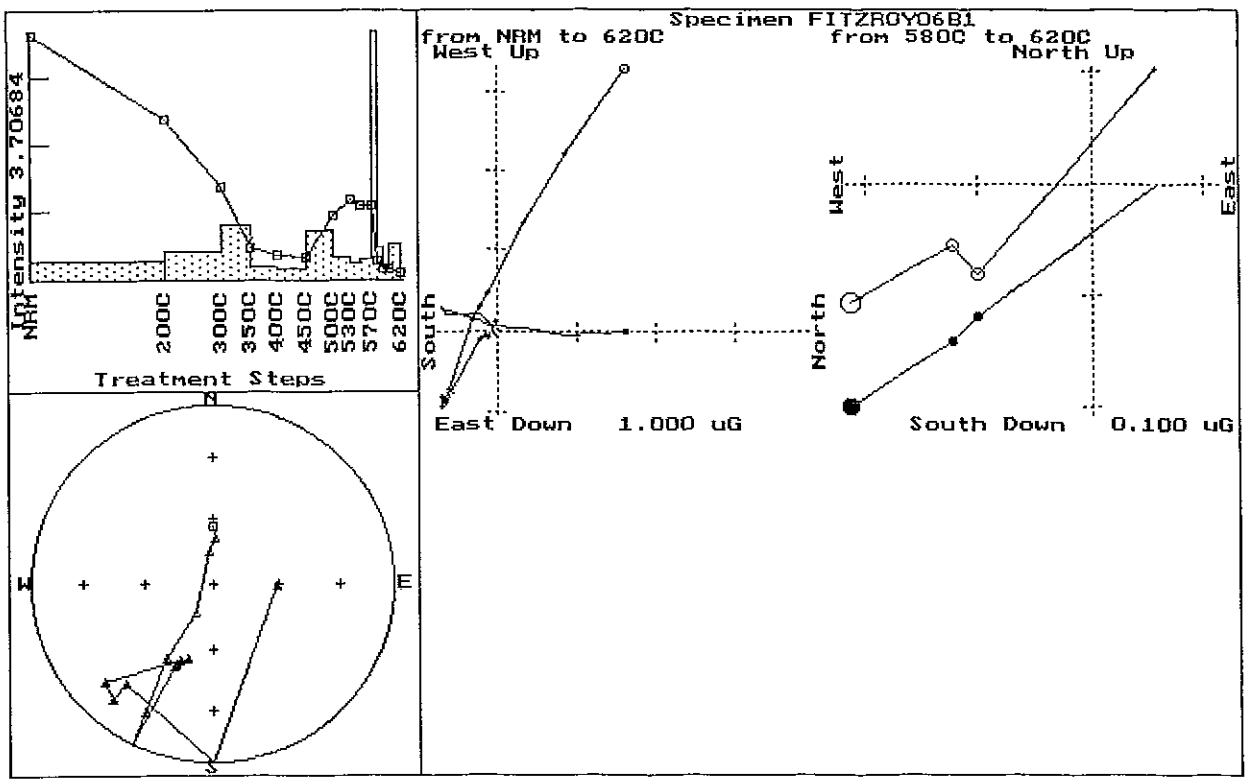
Specimen FITZROY06B1
from NRM to 620C
West Up
South
East Down
1.000 uG
from 580C to 620C
North Up
West
East
North
South Down
0.100 uG
Intensity 3.70684
NRM
200C
300C
350C
400C
450C
500C
530C
570C
620C
Treatment Steps
N
E
S
W

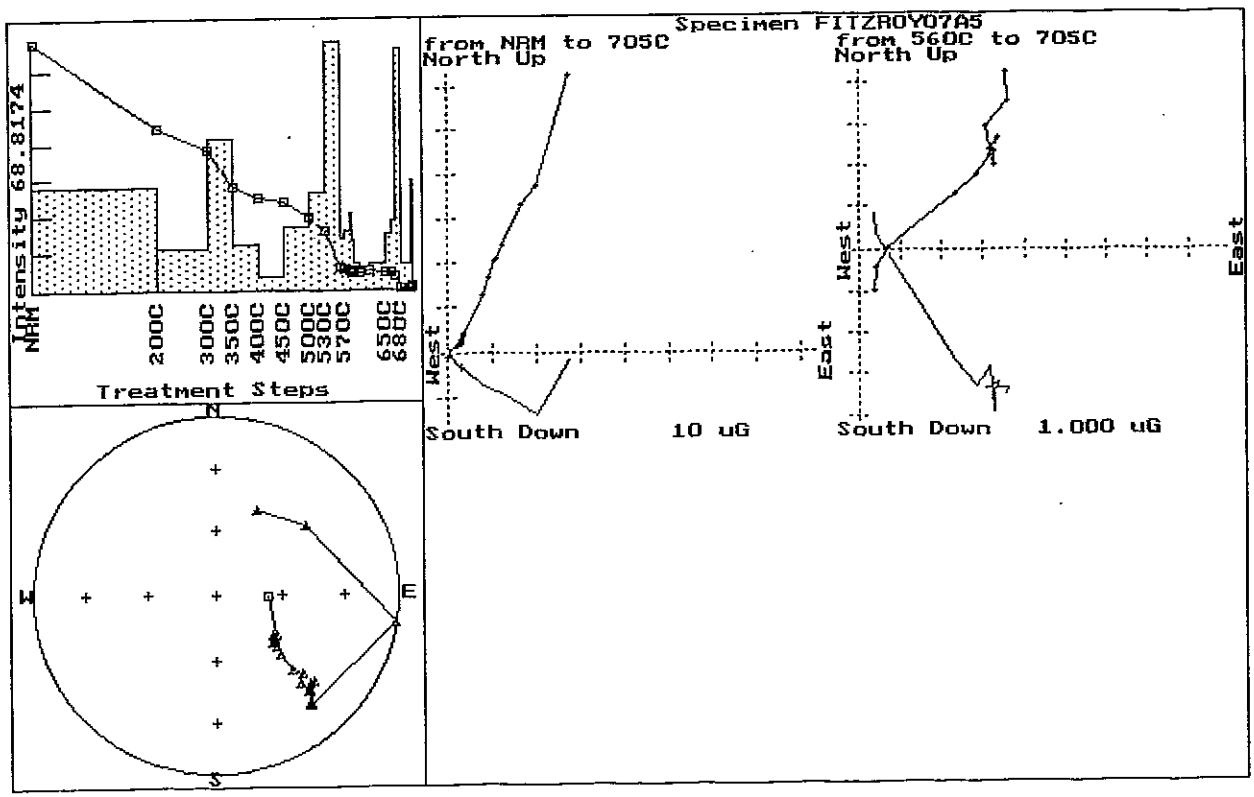
Specimen FITZROY07A5
Intensity 68.8174
NRM
200C
300C
350C
400C
450C
500C
530C
570C
650C
680C
Treatment Steps
N
E
S
W
from NRM to 705C
North Up
West
East
South Down
10 uG
from 560C to 705C
North Up
West
East
South Down
1.000 uG

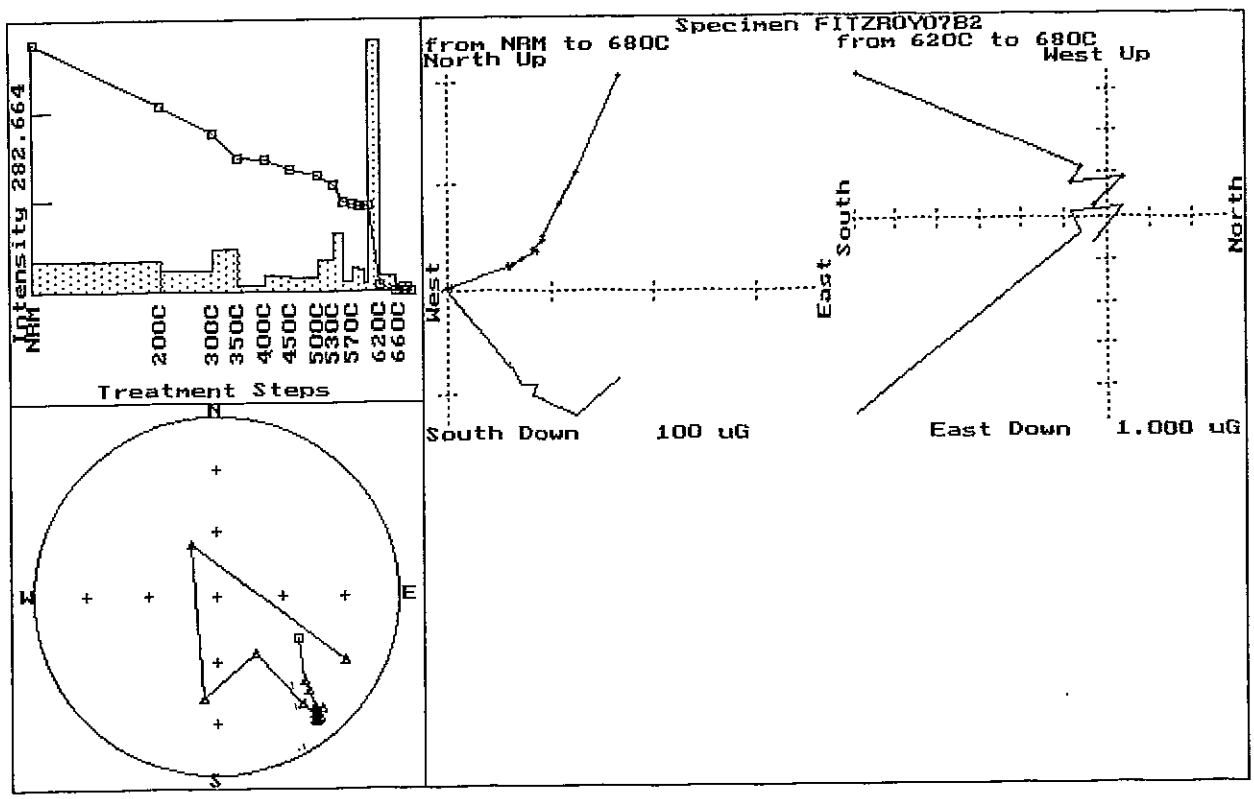
Specimen FITZROY07B2
Intensity 282.664
NRM
200C
300C
350C
400C
450C
500C
530C
570C
620C
660C
Treatment Steps
N
E
S
W
from NRM to 680C
North Up
West
East
South Down
100 uG
from 620C to 680C
West Up
South
North
East Down
1.000 uG

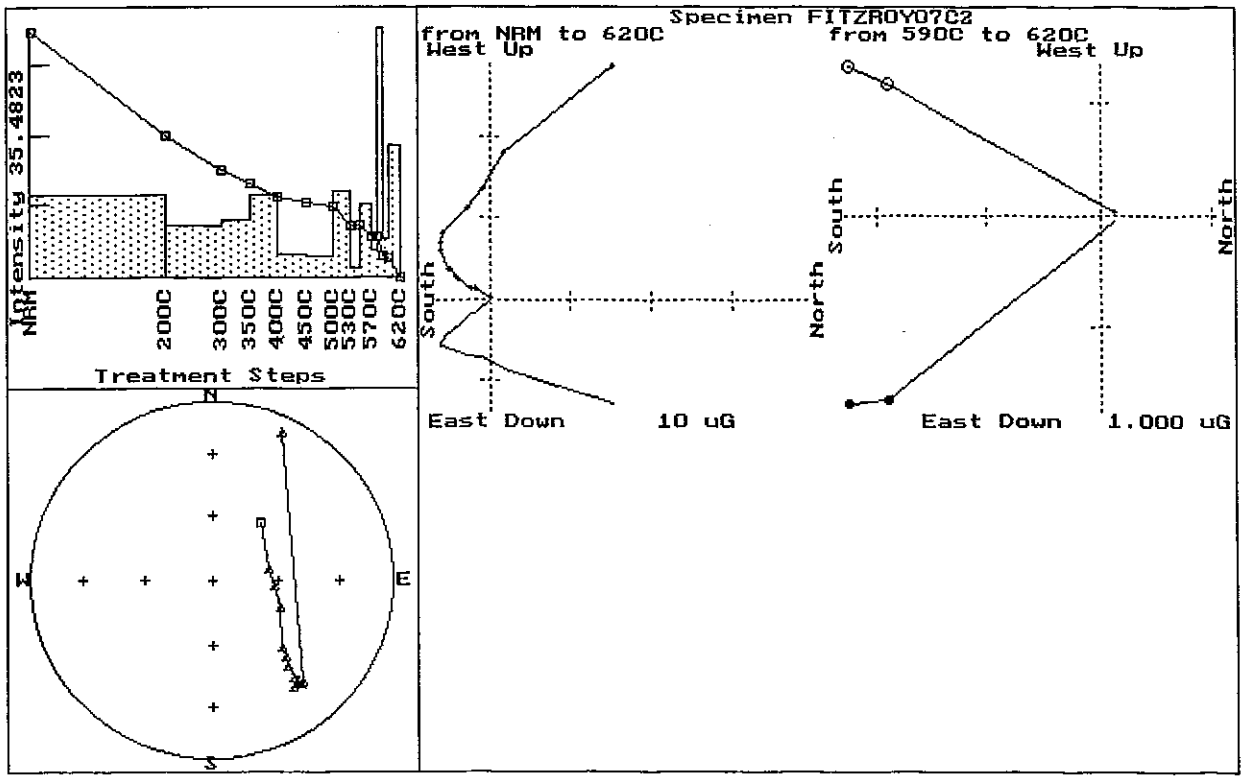
Intensity 35.4823
NRM
200C
300C
350C
400C
450C
500C
530C
570C
620C
Treatment Steps
N
W
E
S
Specimen FITZROY07C2
from NRM to 620C
West Up
South
East Down
10 uG
from 590C to 620C
West Up
South
North
East Down
1.000 uG

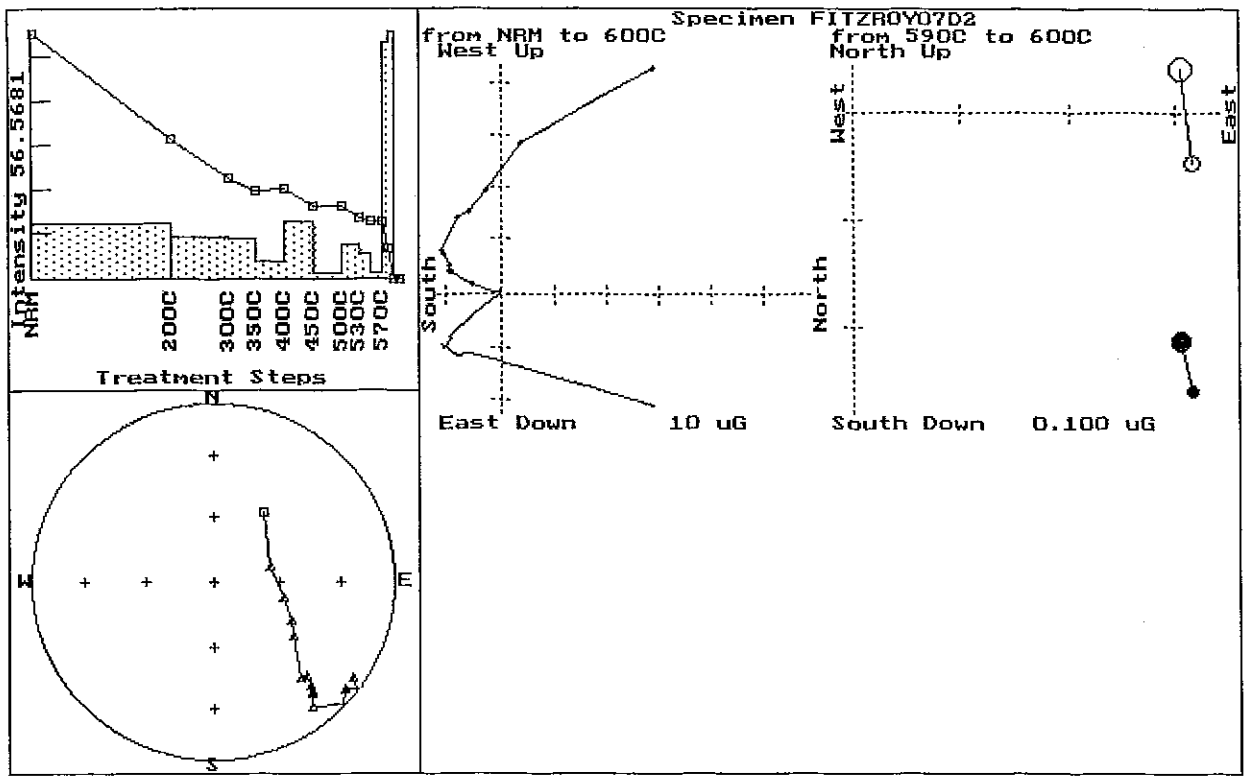
Intensity 56.5681
NRM
200C
300C
350C
400C
450C
500C
530C
570C
Treatment Steps
N
W
E
S
Specimen FITZROY07D2
from NRM to 600C
West Up
South
East Down
10 uG
from 590C to 600C
North Up
West
East
North
South Down
0.100 uG

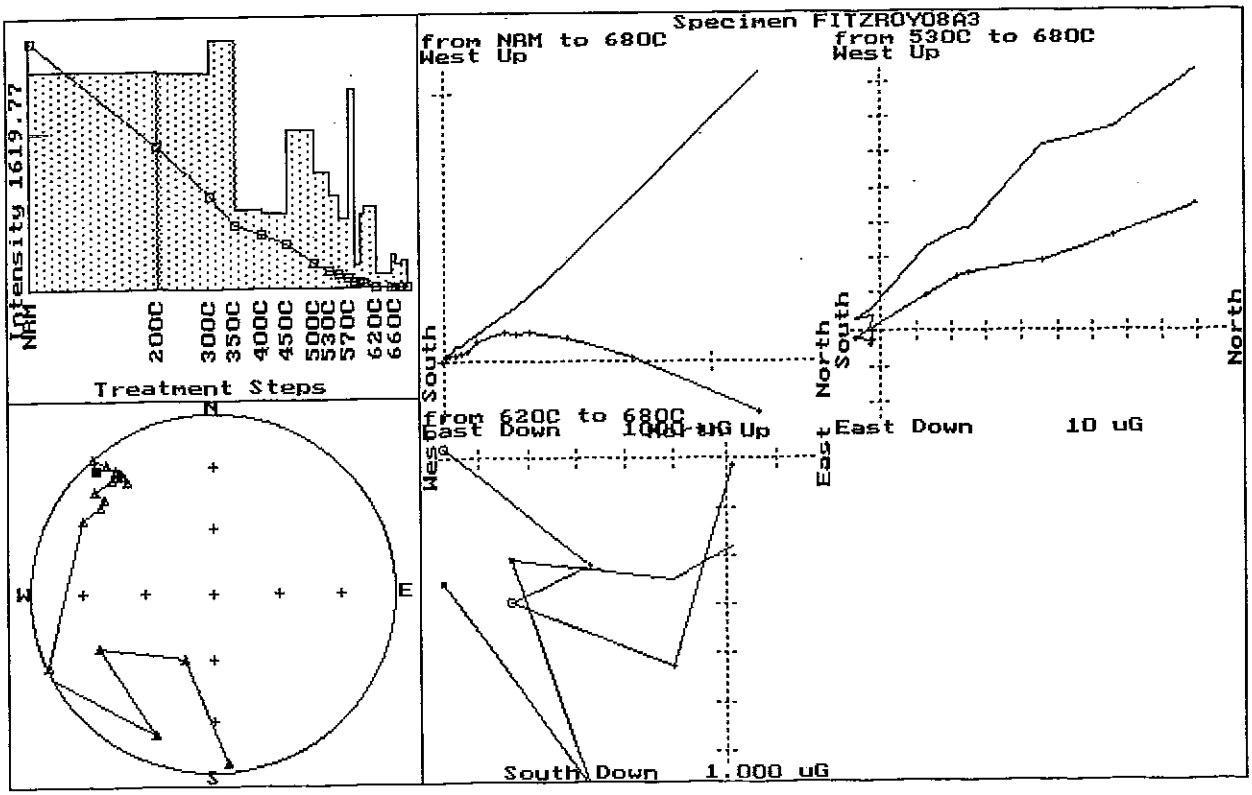
Specimen FITZROY08A3
Intensity 1619.77
NRM
200C
300C
350C
400C
450C
500C
530C
570C
620C
660C
Treatment Steps
N
W
E
S
from NRM to 680C
West Up
South
North
from 530C to 680C
West Up
South
North
East Down
10 uG
from 620C to 680C
East Down
West
East
South Down
1.000 uG

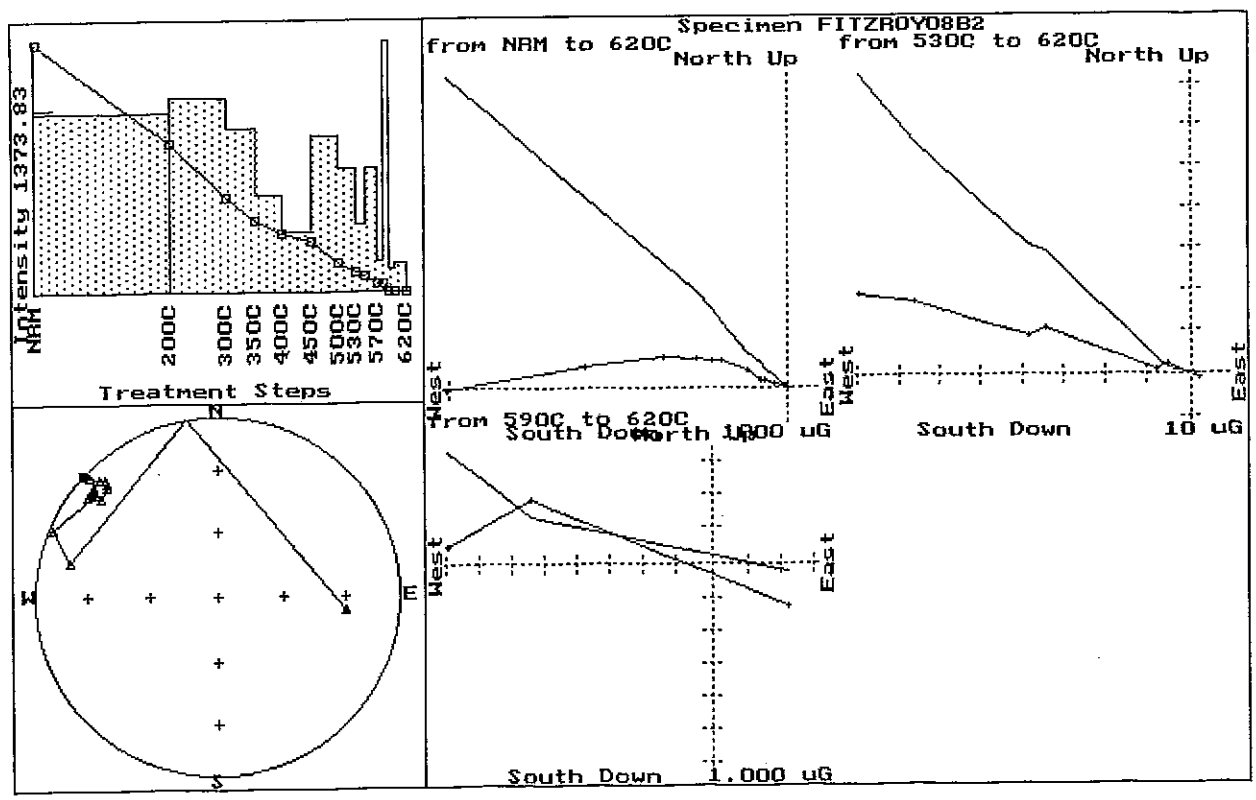
Specimen FITZROY08B2
Intensity 1373.83
NRM
200C
300C
350C
400C
450C
500C
530C
570C
620C
Treatment Steps
N
W
E
S
from NRM to 620C
North Up
West
East
from 530C to 620C
North Up
West
East
South Down
10 uG
from 590C to 620C
West
East
South Down
1.000 uG

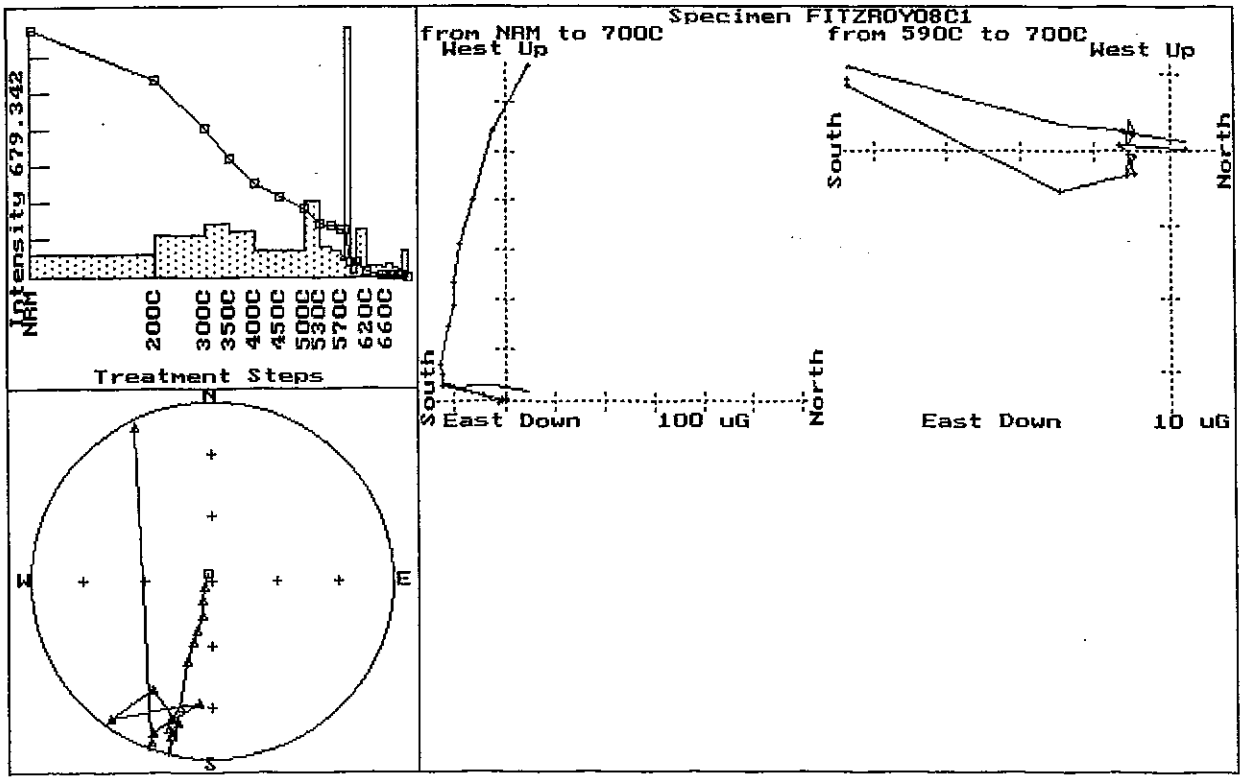
Specimen FITZROY08C1
from NRM to 700C
West Up
from 590C to 700C
West Up
Intensity 679.342
NRM
200C
300C
350C
400C
450C
500C
530C
570C
620C
660C
Treatment Steps
N
E
S
W
South
North
East Down
100 uG
East Down
10 uG

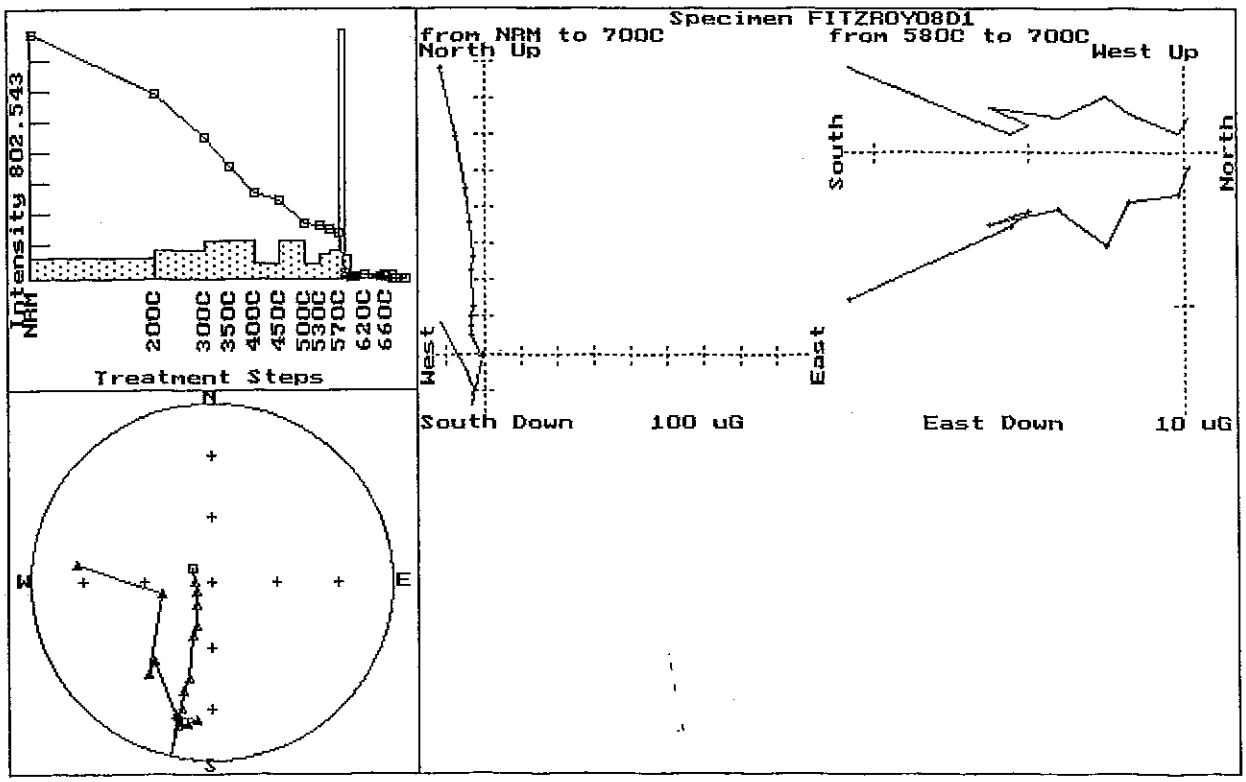
Specimen FITZROY08D1
from NRM to 700C
North Up
from 580C to 700C
West Up
Intensity 802.543
NRM
200C
300C
350C
400C
450C
500C
530C
570C
620C
660C
Treatment Steps
N
E
S
W
South
North
West
East
South Down
100 uG
East Down
10 uG

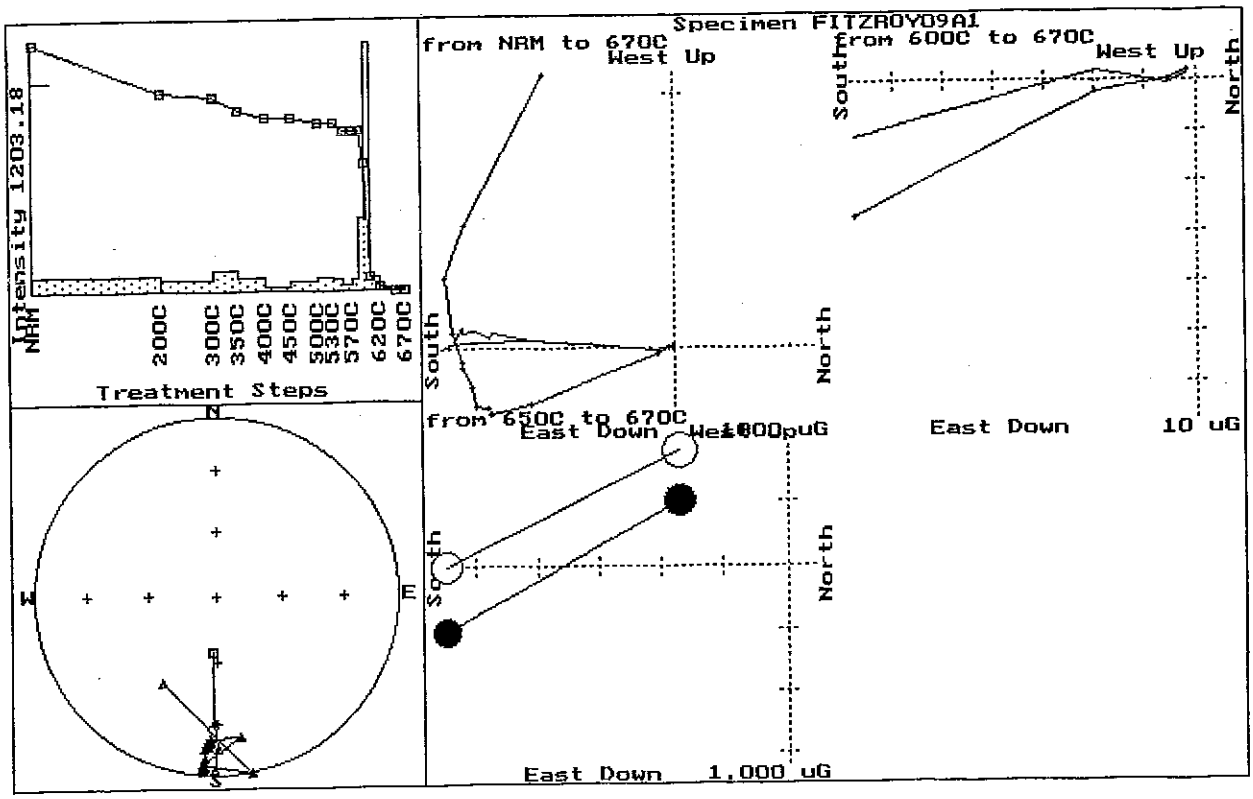
Specimen FITZROY09A1
Intensity 1203.18
NRM
200C
300C
350C
400C
450C
500C
530C
570C
620C
670C
Treatment Steps
from NRM to 670C
West Up
South
North
East Down
1,000 uG
from 600C to 670C
West Up
South
North
East Down
10 uG
from 650C to 670C
East Down
West
South
North
East Down
1,000 uG
N
E
S
W

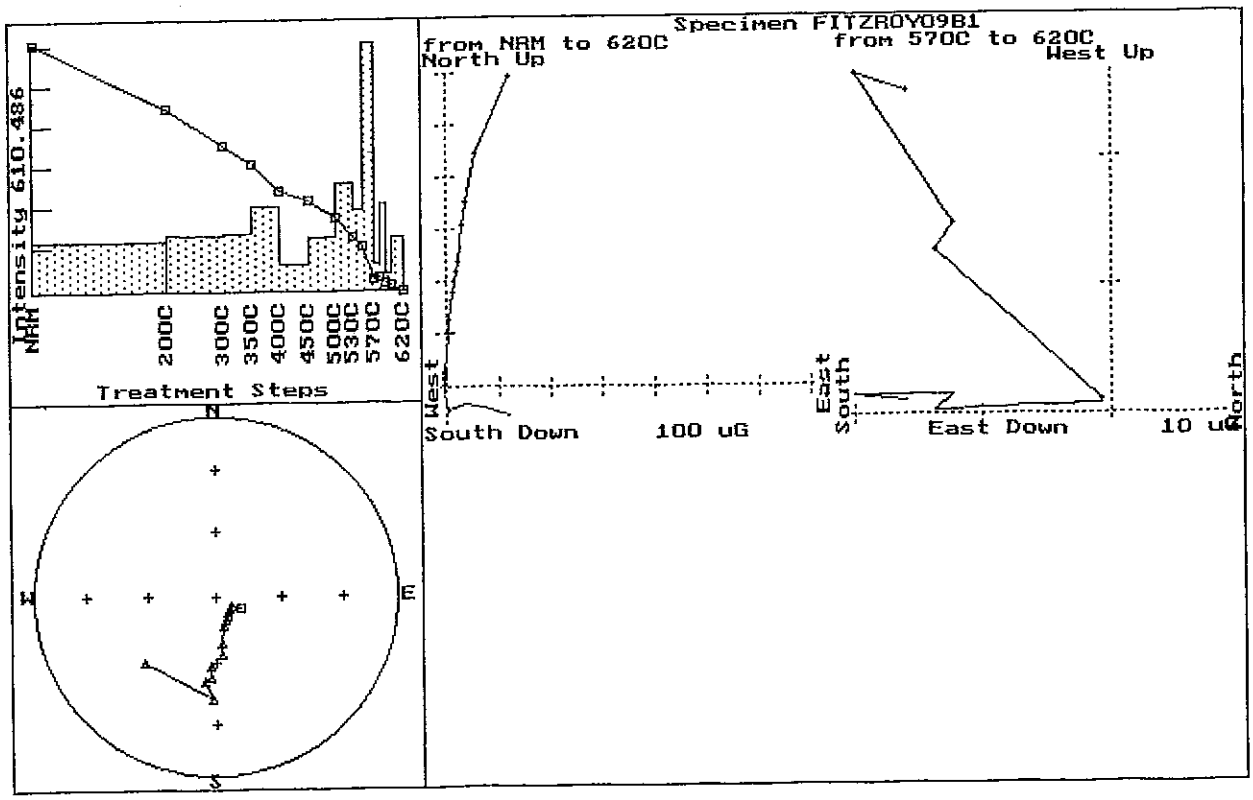
Specimen FITZROY09B1
Intensity 610.486
NRM
200C
300C
350C
400C
450C
500C
530C
570C
620C
Treatment Steps
from NRM to 620C
North Up
West
South
South Down
100 uG
from 570C to 620C
West Up
East
South
North
East Down
10 uG
N
E
S
W

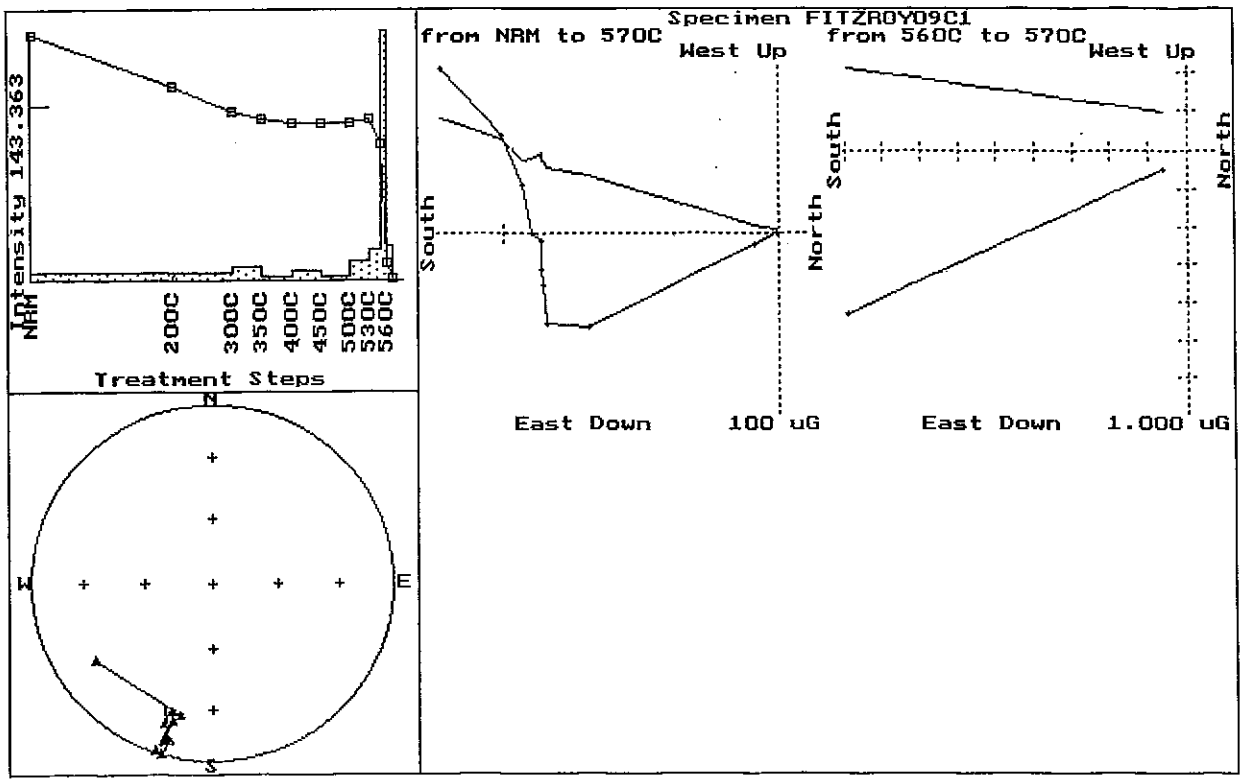
Specimen FITZROY09C1
from NRM to 570C
West Up
from 560C to 570C
West Up
Intensity 143.363
NRM
200C
300C
350C
400C
450C
500C
530C
560C
Treatment Steps
N
W
E
S
South
North
East Down
100 uG
East Down
1.000 uG

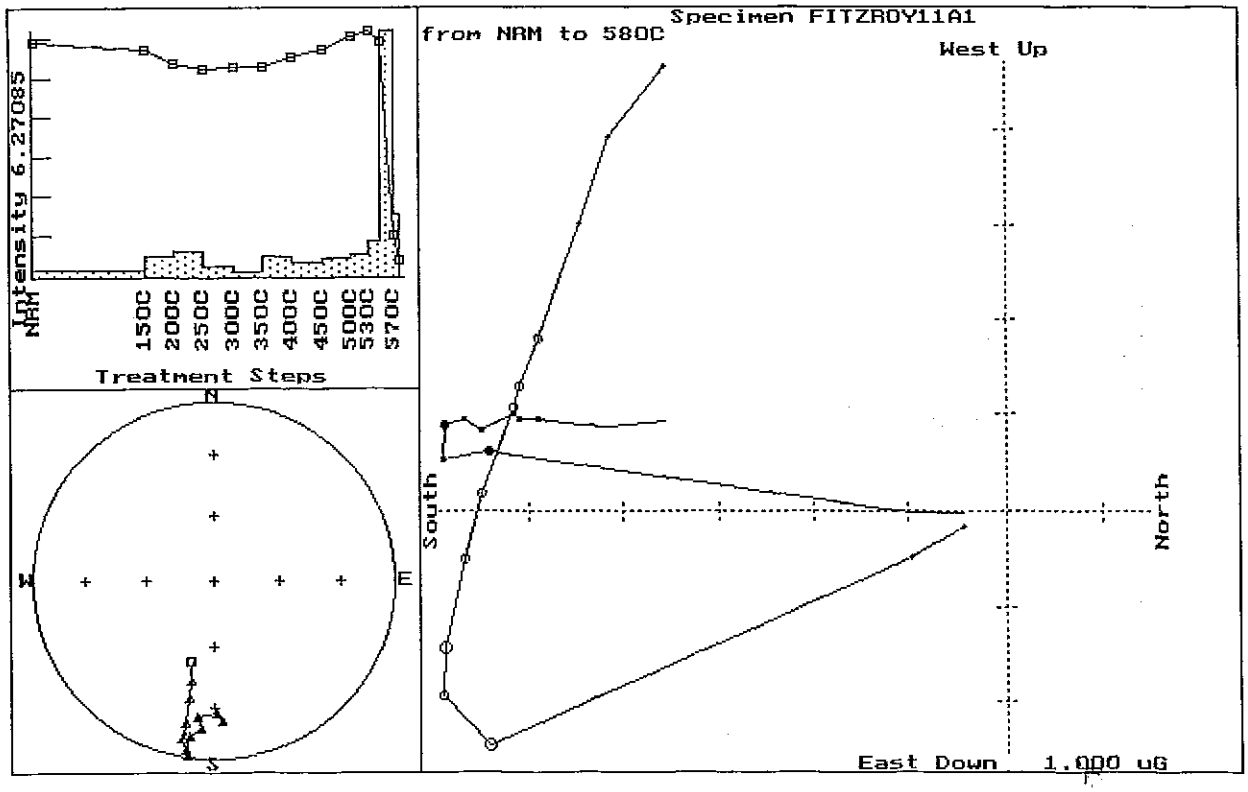
Specimen FITZROY11A1
from NRM to 580C
West Up
Intensity 6.27085
NRM
150C
200C
250C
300C
350C
400C
450C
500C
530C
570C
Treatment Steps
N
W
E
S
South
North
East Down
1.000 uG

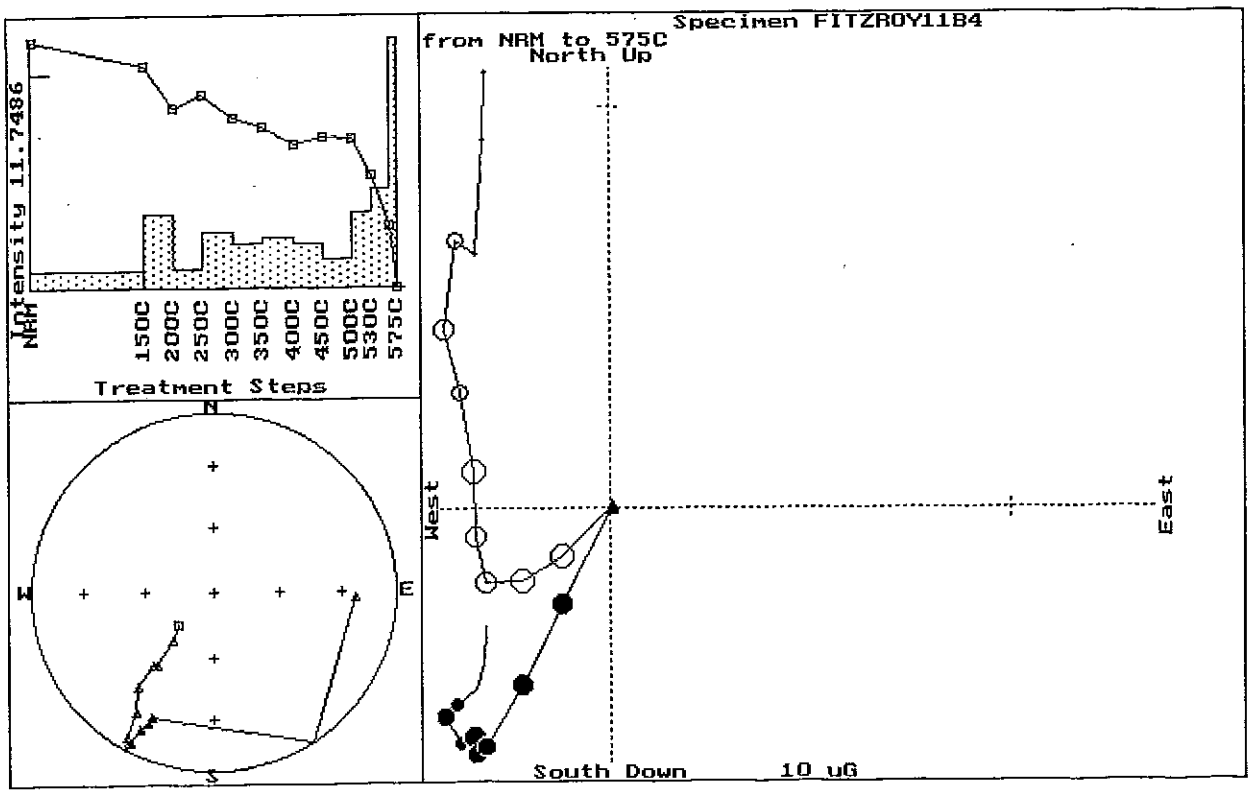
Specimen FITZROY11B4
from NRM to 575C
North Up
Intensity 11.7486
NRM
150C 200C 250C 300C 350C 400C 450C 500C 530C 575C
Treatment Steps
N
W
E
S
West
East
South Down
10 uG

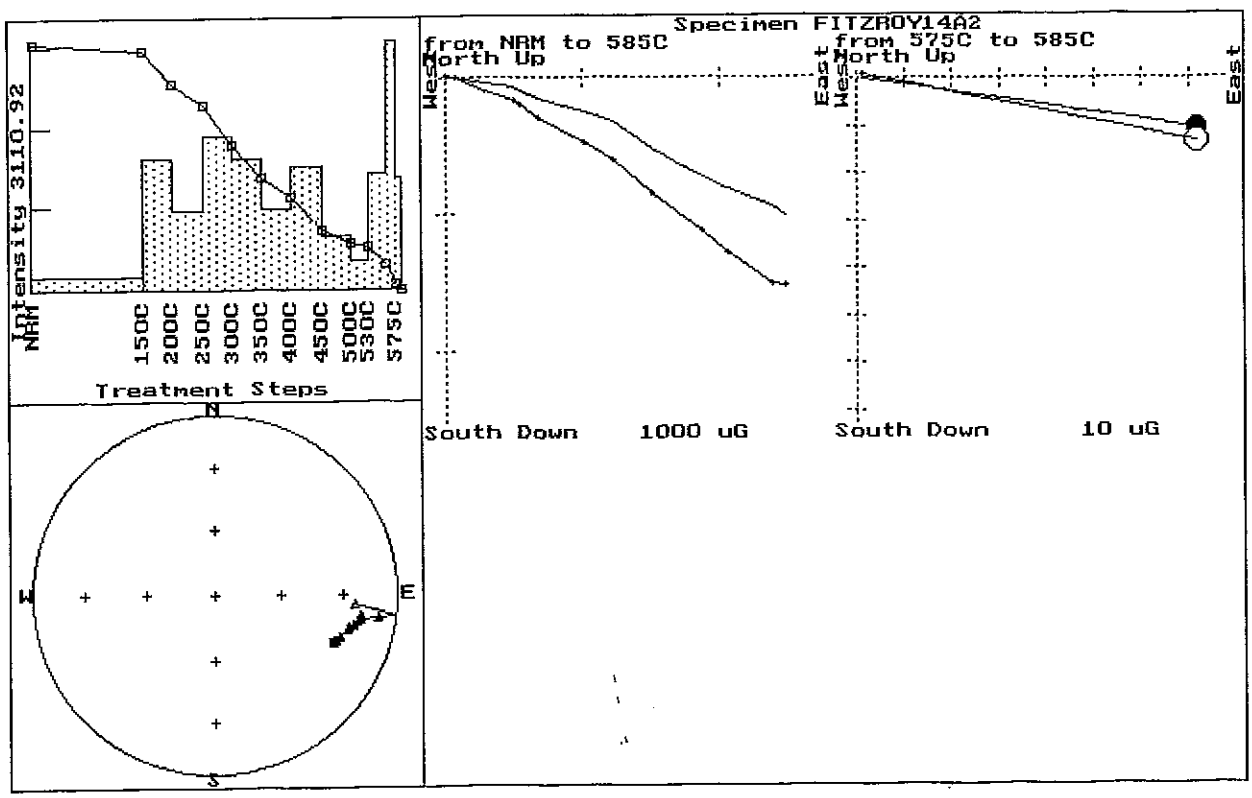
Specimen FITZROY14A2
from NRM to 585C
North Up
from 575C to 585C
North Up
Intensity 3110.92
NRM
150C 200C 250C 300C 350C 400C 450C 500C 530C 575C
Treatment Steps
N
W
E
S
West
East
West
East
South Down
1000 uG
South Down
10 uG

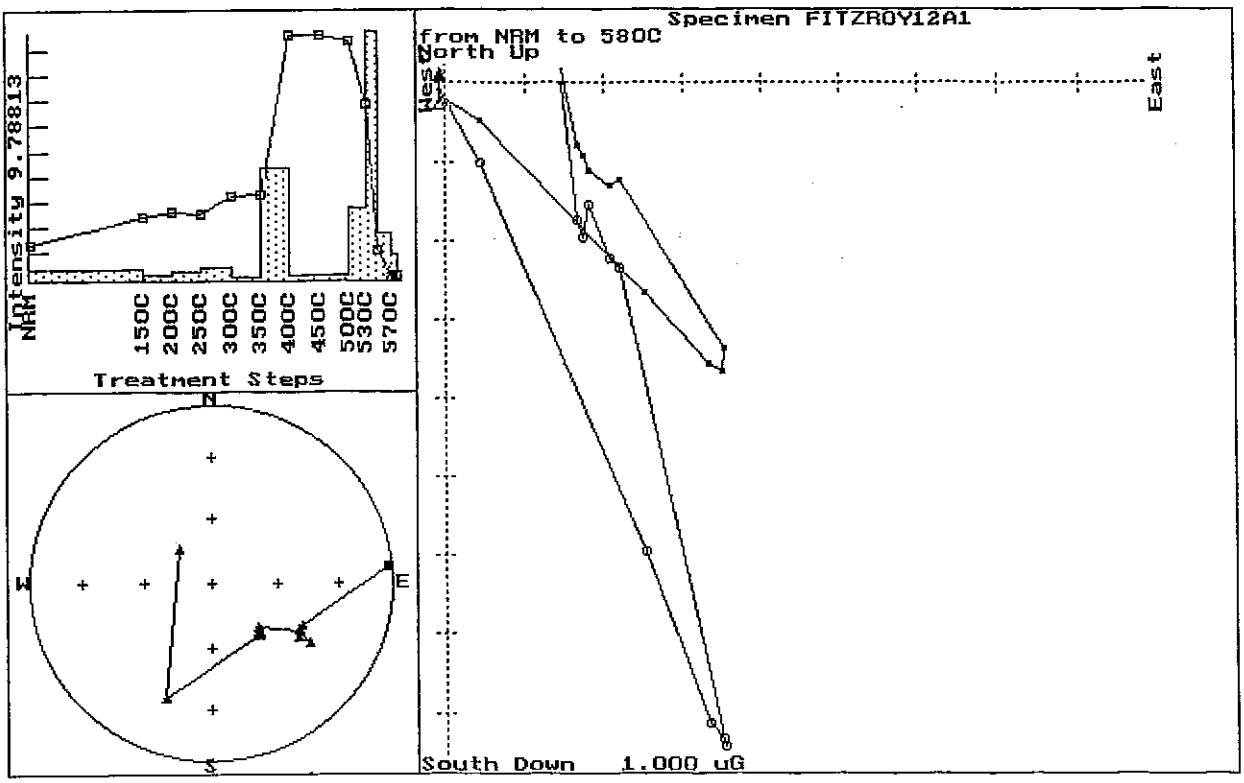
Specimen FITZROY12A1
from NRM to 580C
North Up
West
East
Intensity 9.78813
NRM
150C
200C
250C
300C
350C
400C
450C
500C
530C
570C
Treatment Steps
N
E
S
South Down 1.000 uG

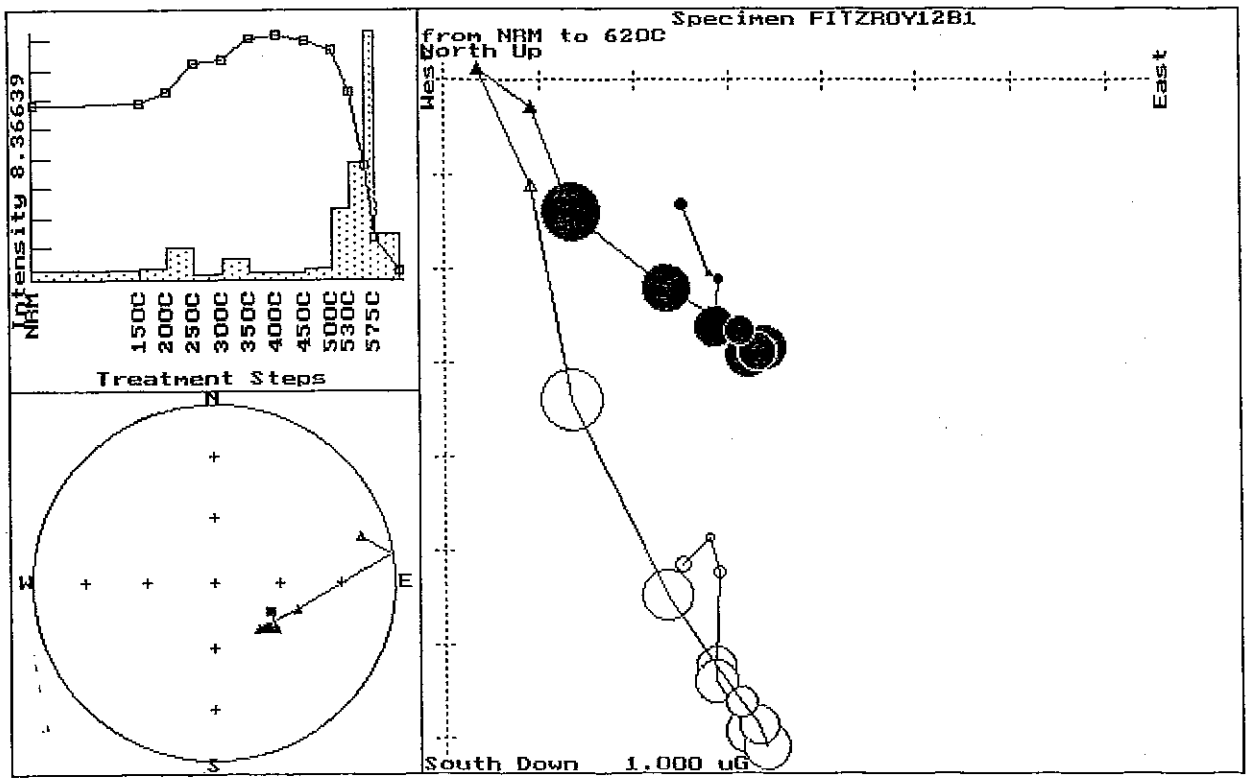
Specimen FITZROY12B1
from NRM to 620C
North Up
West
East
Intensity 8.36639
NRM
150C
200C
250C
300C
350C
400C
450C
500C
530C
575C
Treatment Steps
N
E
S
South Down 1.000 uG

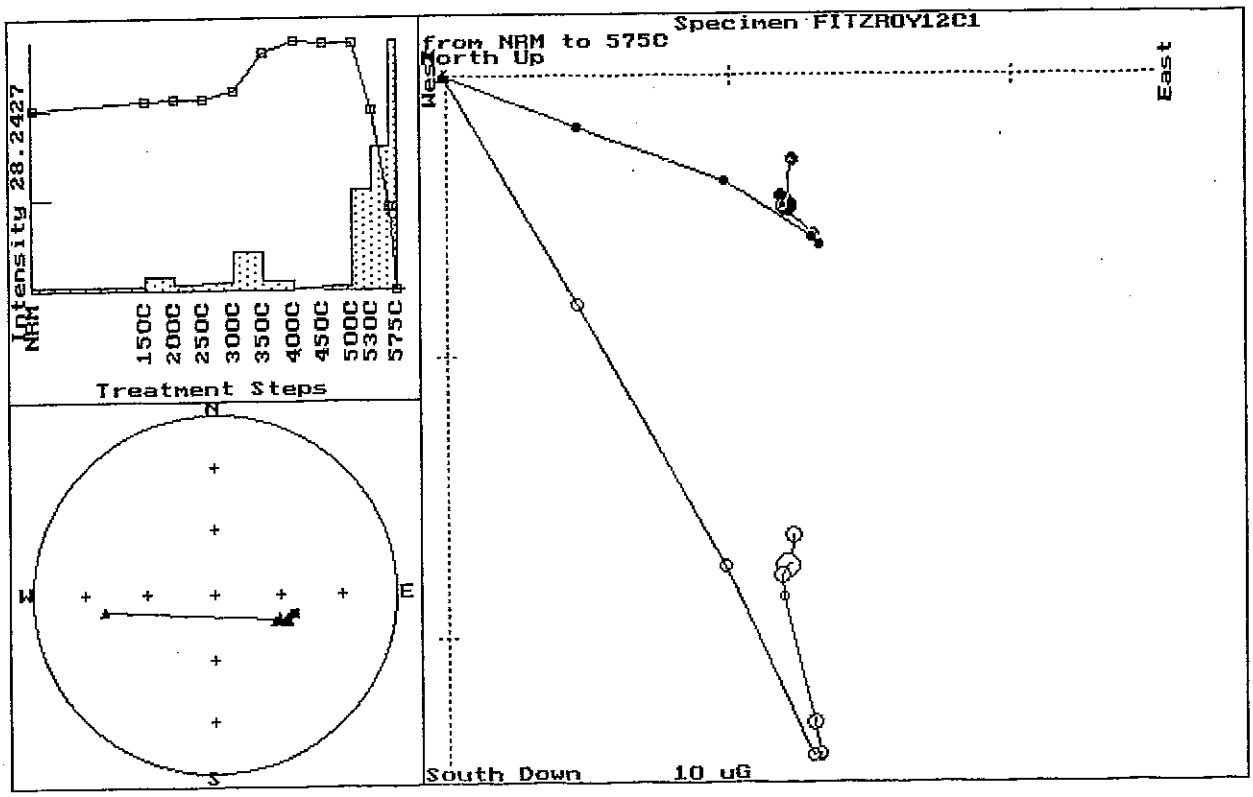
Specimen FITZROY12C1
from NRM to 575C
North Up
West
East
Intensity 28.2427
NRM
150C
200C
250C
300C
350C
400C
450C
500C
530C
575C
Treatment Steps
N
W
E
S
South Down
10 uG

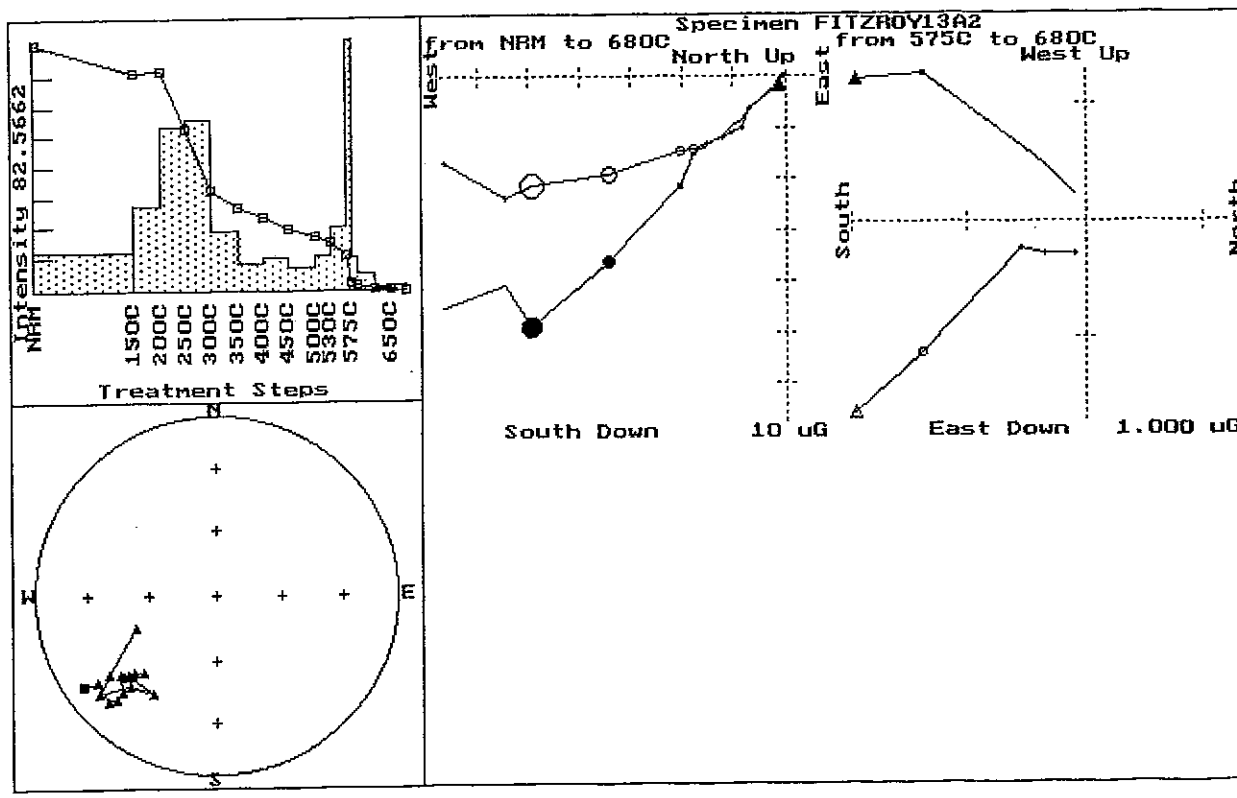
Specimen FITZROY13A2
from NRM to 680C
North Up
from 575C to 680C
West Up
West
East
South
North
Intensity 82.5662
NRM
150C
200C
250C
300C
350C
400C
450C
500C
530C
575C
650C
Treatment Steps
N
W
E
S
South Down
10 uG
East Down
1.000 uG

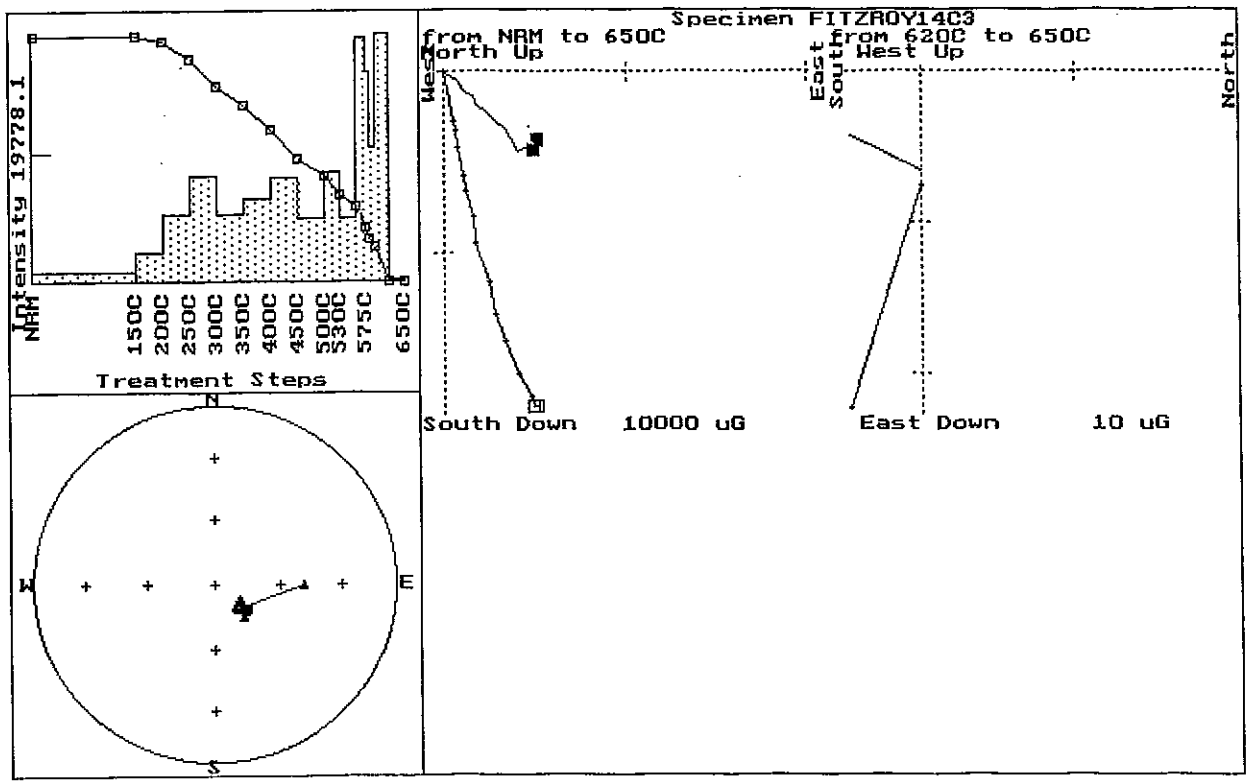
Specimen FITZROY14C3
from NRM to 650C
North Up
from 620C to 650C
West Up
West
East
South
North
Intensity 19778.1
NRM
150C 200C 250C 300C 350C 400C 450C 500C 530C 575C 650C
Treatment Steps
N
W
E
S
South Down 10000 uG
East Down 10 uG

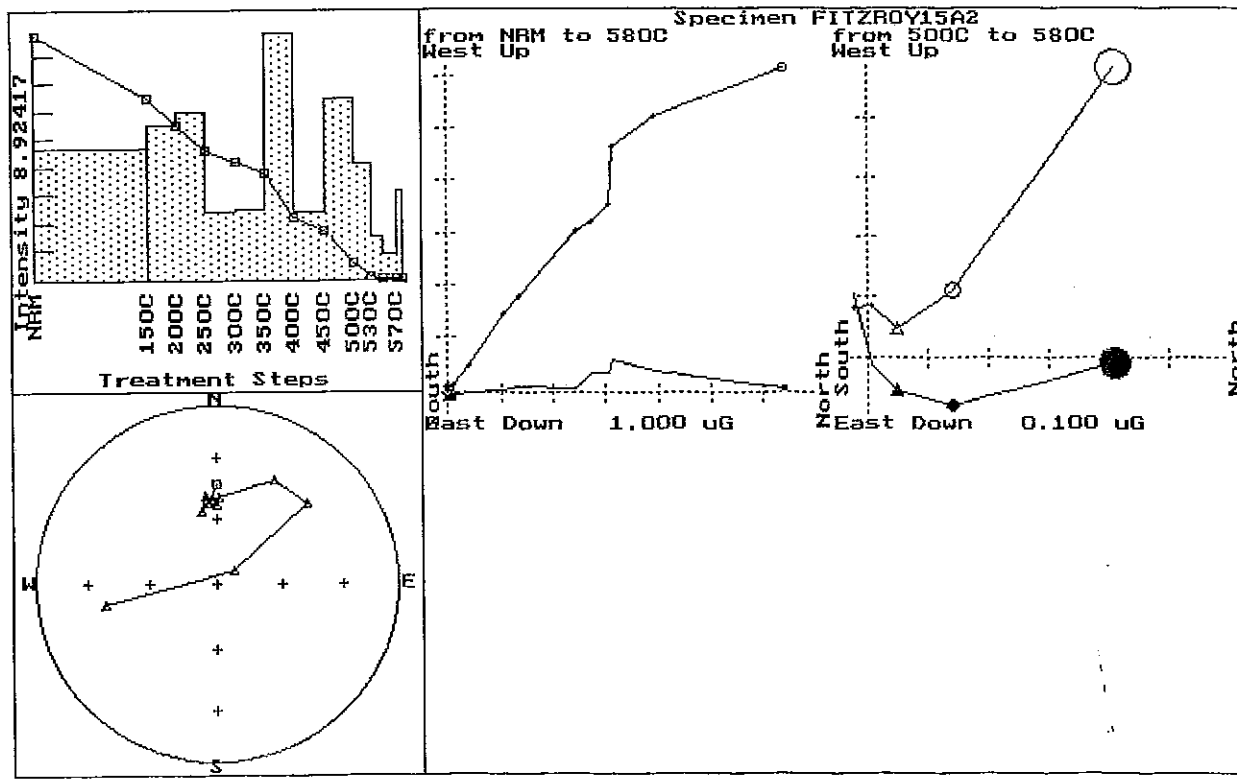
Specimen FITZROY15A2
from NRM to 580C
West Up
from 500C to 580C
West Up
Intensity 8.92417
NRM
150C 200C 250C 300C 350C 400C 450C 500C 530C 570C
Treatment Steps
N
W
E
S
East Down 1.000 uG
North
South
East Down 0.100 uG

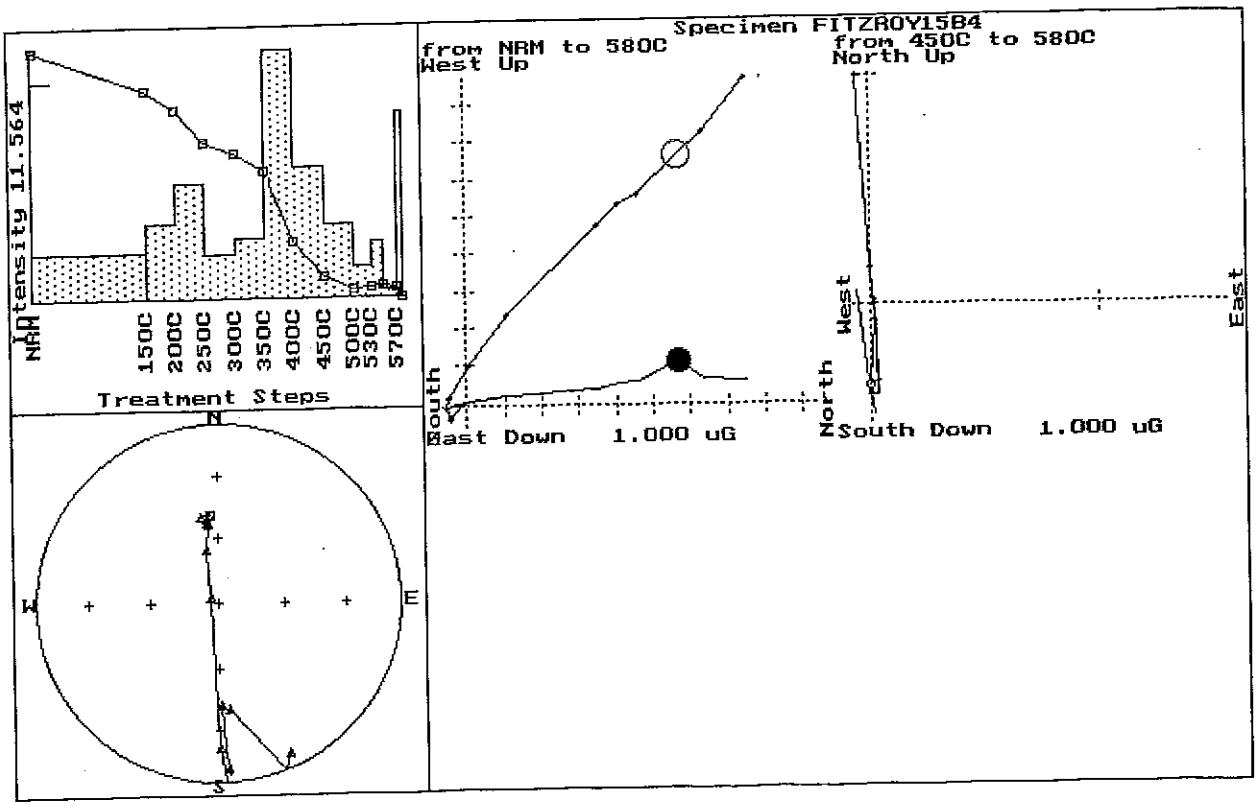
Specimen FITZROY15B4
from NRM to 580C
West Up
from 450C to 580C
North Up
Intensity 11.564
NRM
150C
200C
250C
300C
350C
400C
450C
500C
530C
570C
Treatment Steps
N
W
E
S
South
East Down 1.000 uG
North
West
East
South Down 1.000 uG

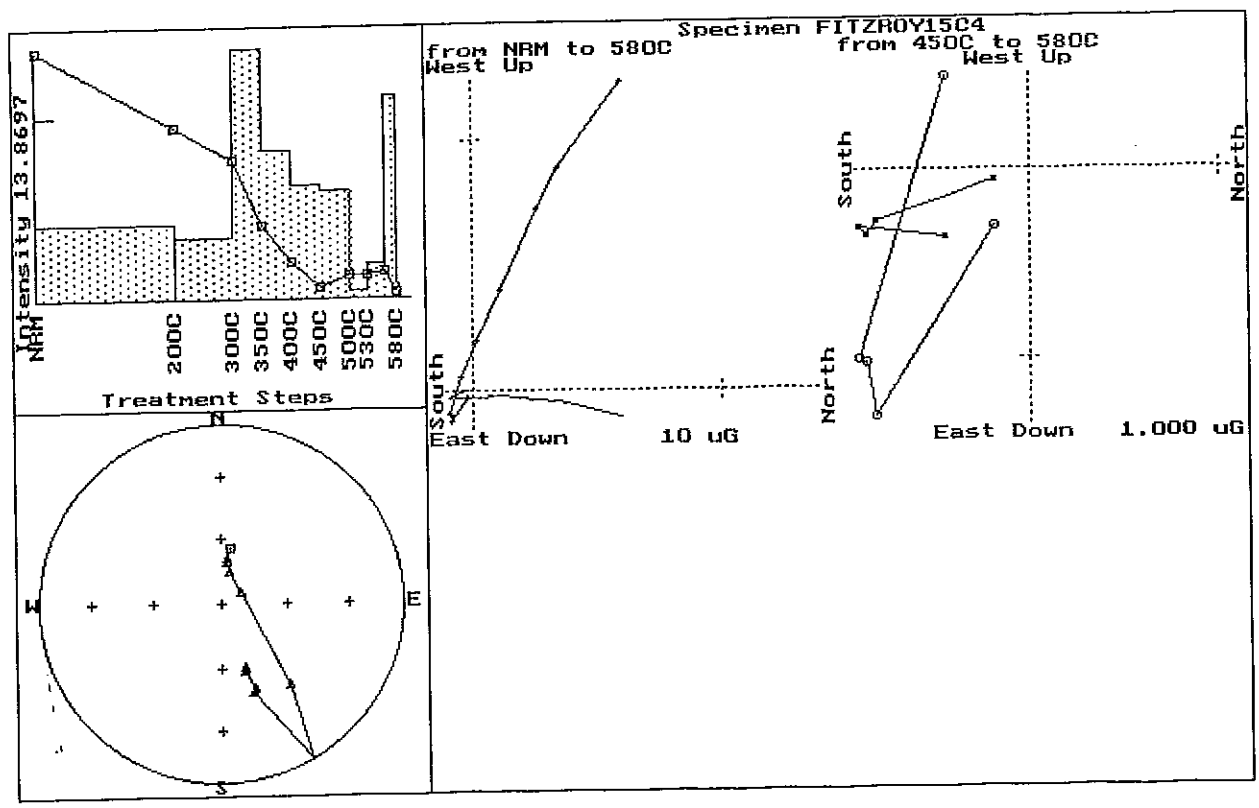
Specimen FITZROY15C4
from NRM to 580C
West Up
from 450C to 580C
West Up
Intensity 13.8697
NRM
200C
300C
350C
400C
450C
500C
530C
580C
Treatment Steps
N
W
E
S
South
East Down 10 uG
North
South
East Down 1.000 uG
North

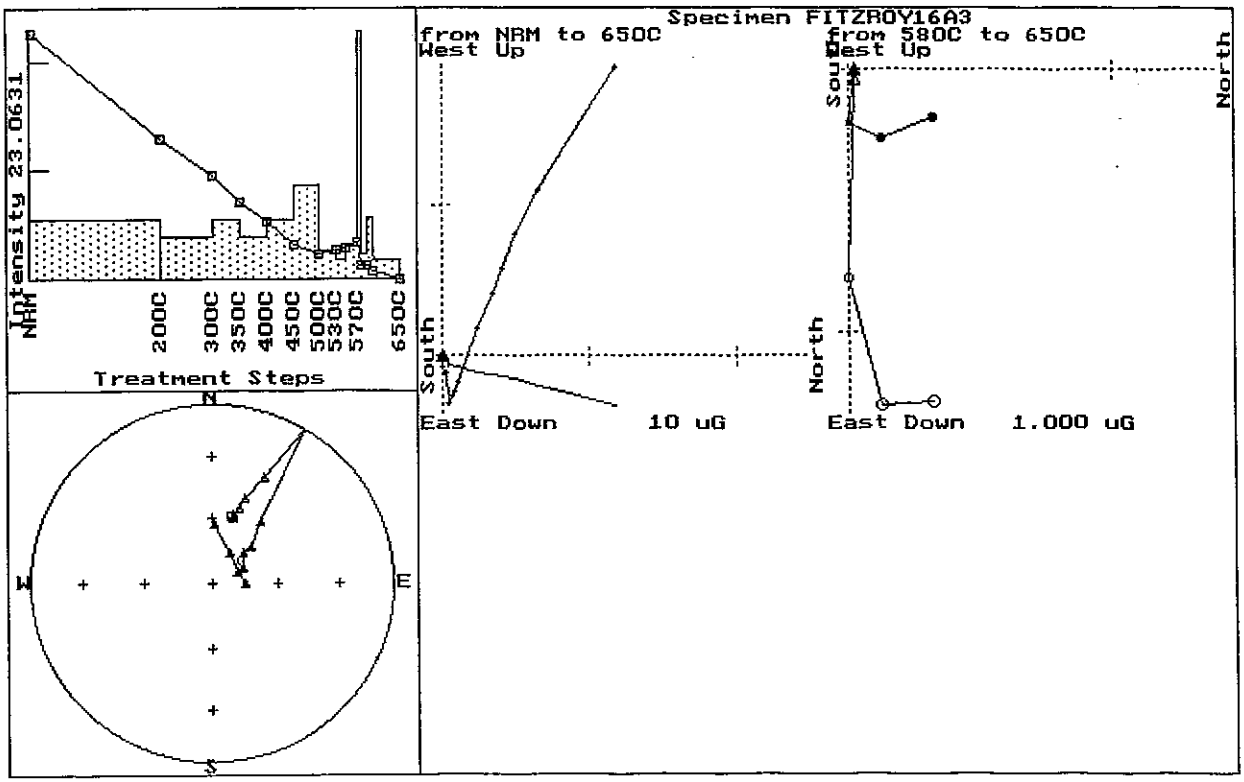
Specimen FITZROY16A3
from NRM to 650C
West Up
from 580C to 650C
West Up
Intensity 23.0631
NRM
200C
300C
350C
400C
450C
500C
530C
570C
650C
Treatment Steps
N
W
E
S
South
North
East Down
10 uG
East Down
1.000 uG

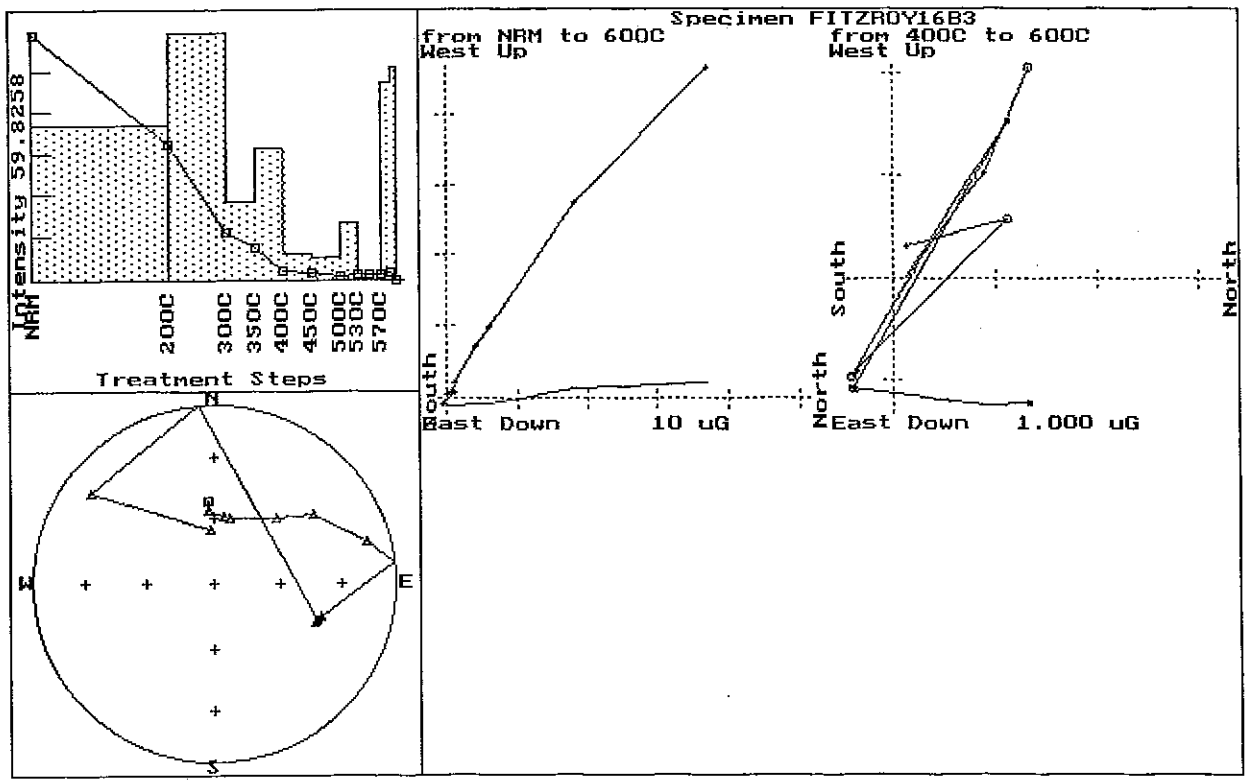
Specimen FITZROY16B3
from NRM to 600C
West Up
from 400C to 600C
West Up
Intensity 59.8258
NRM
200C
300C
350C
400C
450C
500C
530C
570C
Treatment Steps
N
W
E
S
South
North
East Down
10 uG
East Down
1.000 uG

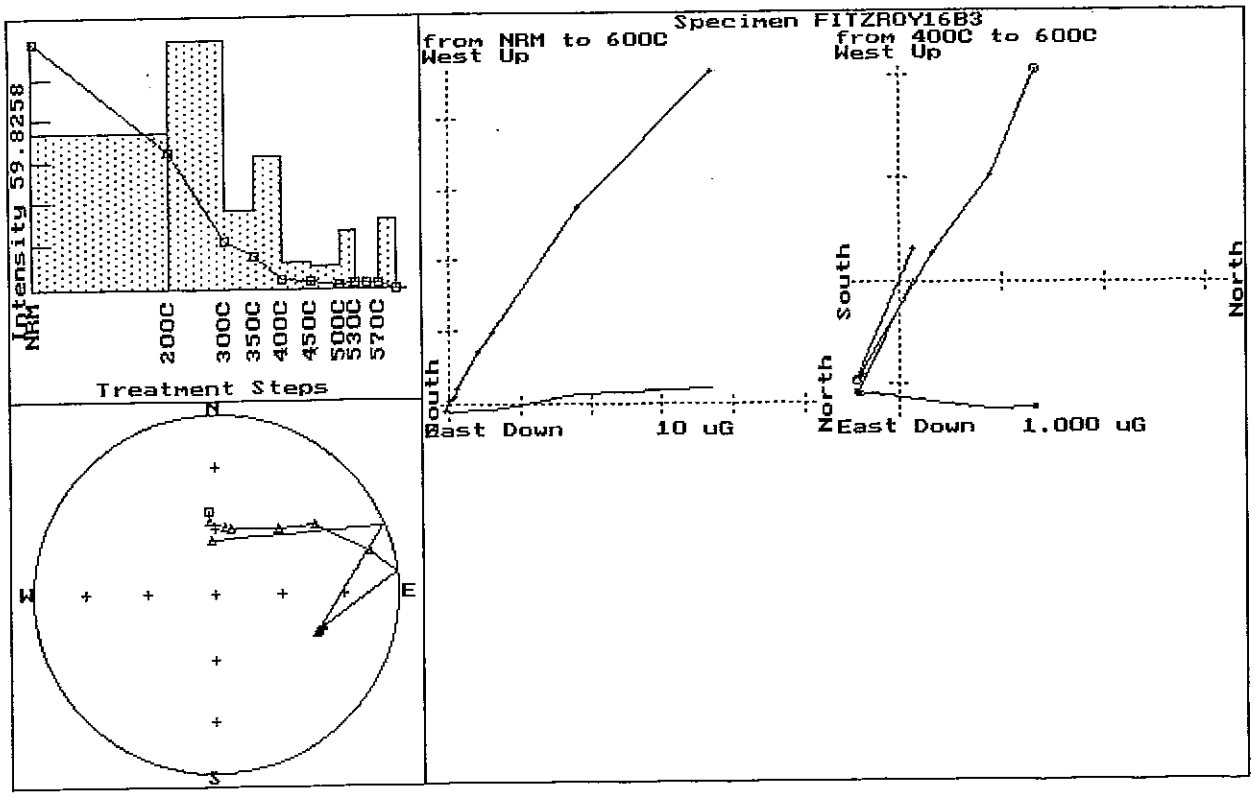
Intensity 59.8258
NRM
200C
300C
350C
400C
450C
500C
530C
570C
Treatment Steps
N
E
S
W
Specimen FITZROY16B3
from NRM to 600C
West Up
South
East Down
10 uG
from 400C to 600C
West Up
South
North
East Down
1.000 uG

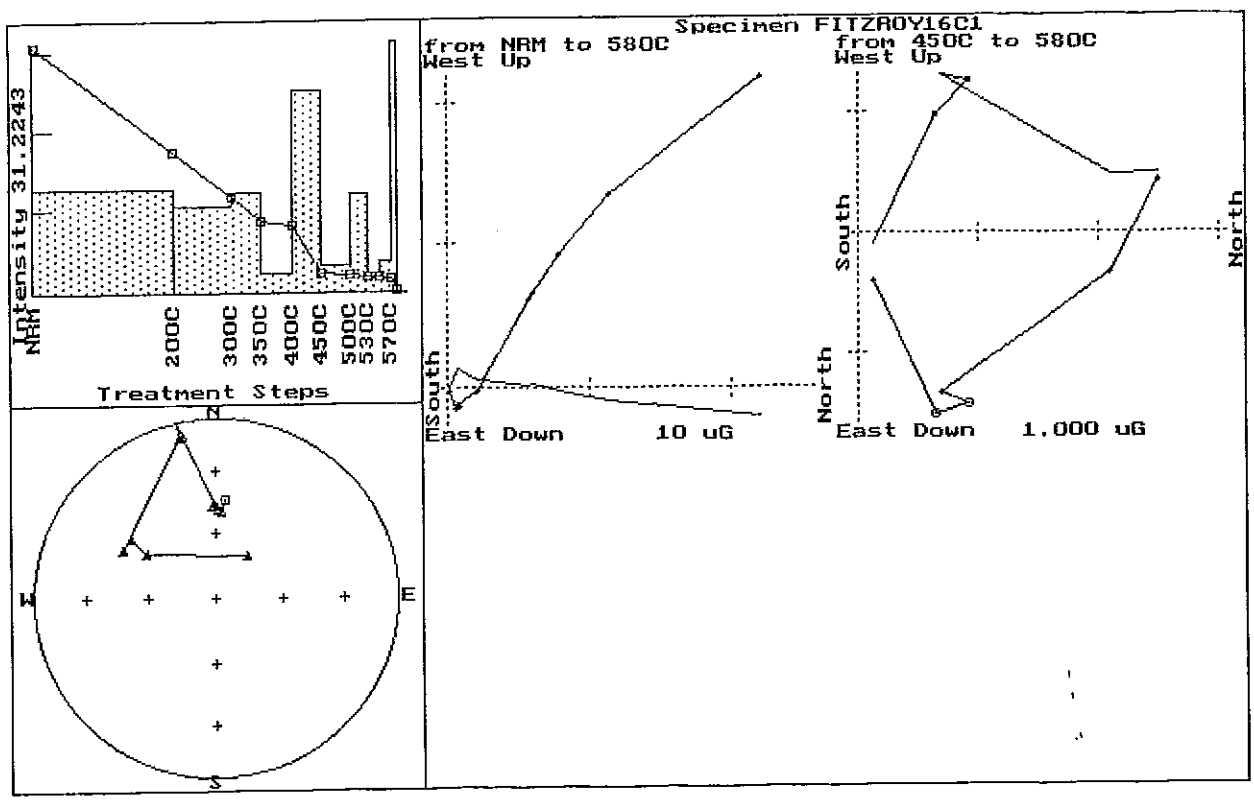
Intensity 31.2243
NRM
200C
300C
350C
400C
450C
500C
530C
570C
Treatment Steps
N
E
S
W
Specimen FITZROY16C1
from NRM to 580C
West Up
South
East Down
10 uG
from 450C to 580C
West Up
South
North
East Down
1.000 uG

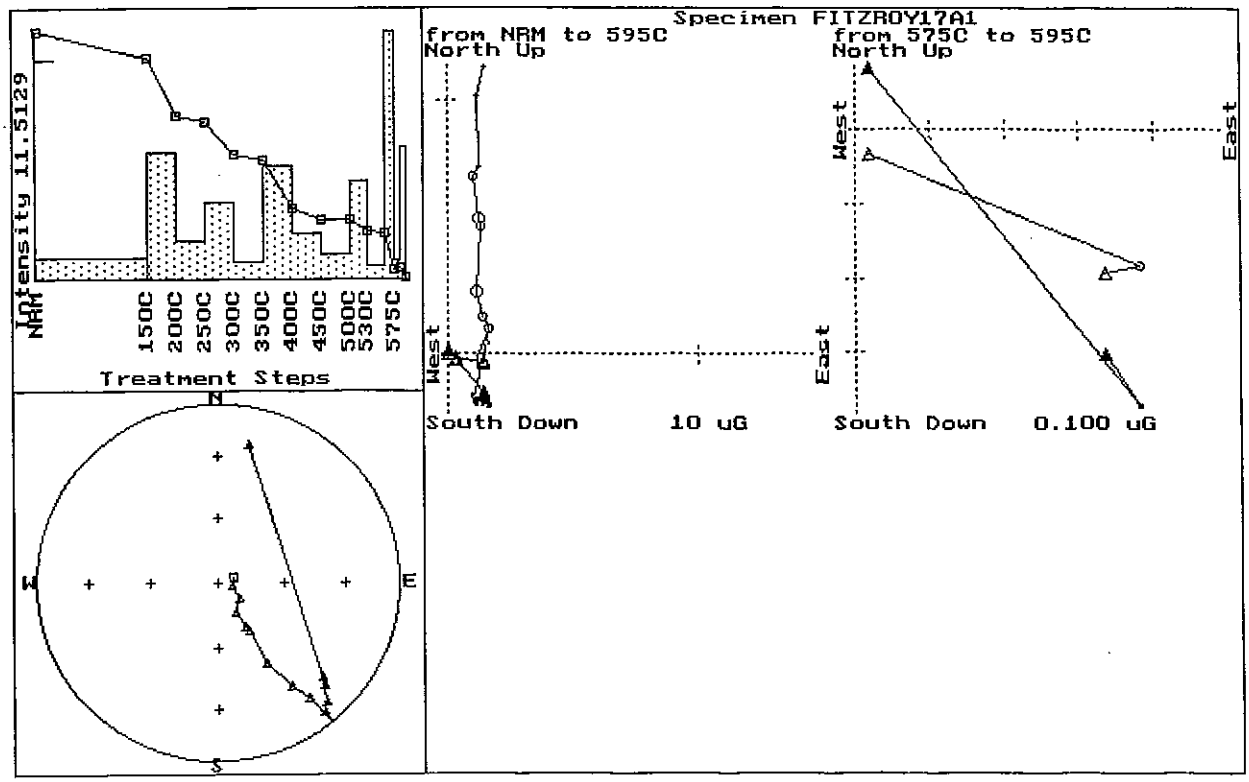
Intensity 11.5129
NRM
150C
200C
250C
300C
350C
400C
450C
500C
530C
575C
Treatment Steps
N
W
E
S
Specimen FITZROY17A1
from NRM to 595C
North Up
West
East
South Down
10 uG
from 575C to 595C
North Up
West
East
South Down
0.100 uG

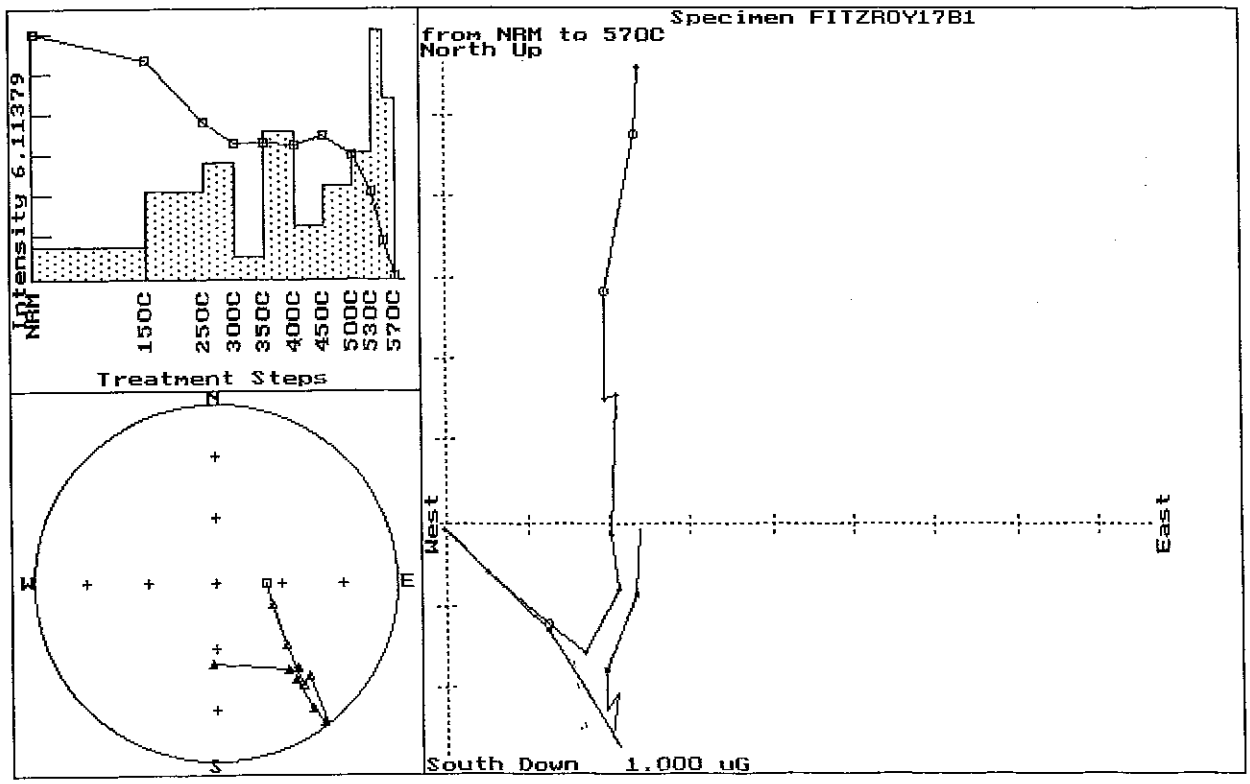
Intensity 6.11379
NRM
150C
250C
300C
350C
400C
450C
500C
530C
570C
Treatment Steps
N
W
E
S
Specimen FITZROY17B1
from NRM to 570C
North Up
West
East
South Down
1.000 uG

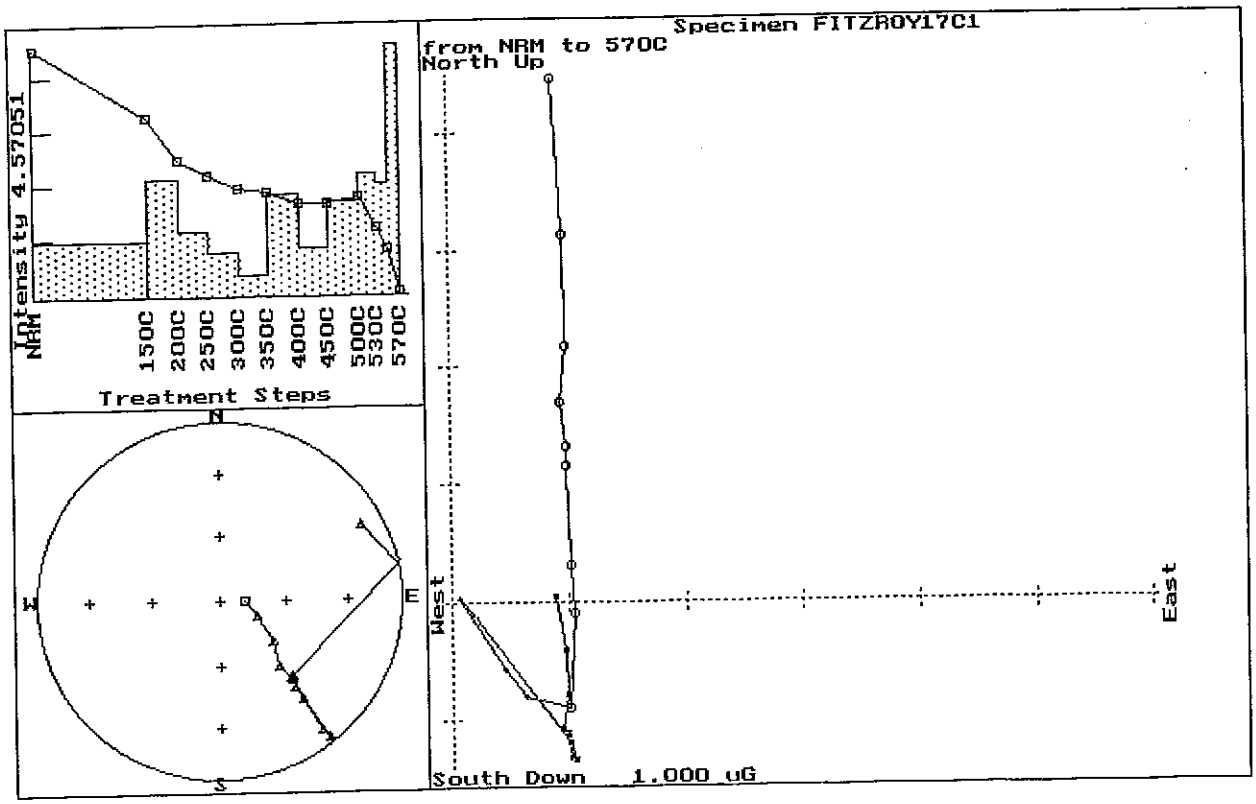
Specimen FITZROY17C1
from NRM to 570C
North Up
Intensity 4.57051
NRM
150C
200C
250C
300C
350C
400C
450C
500C
530C
570C
Treatment Steps
N
E
S
W
West
East
South Down
1.000 uG

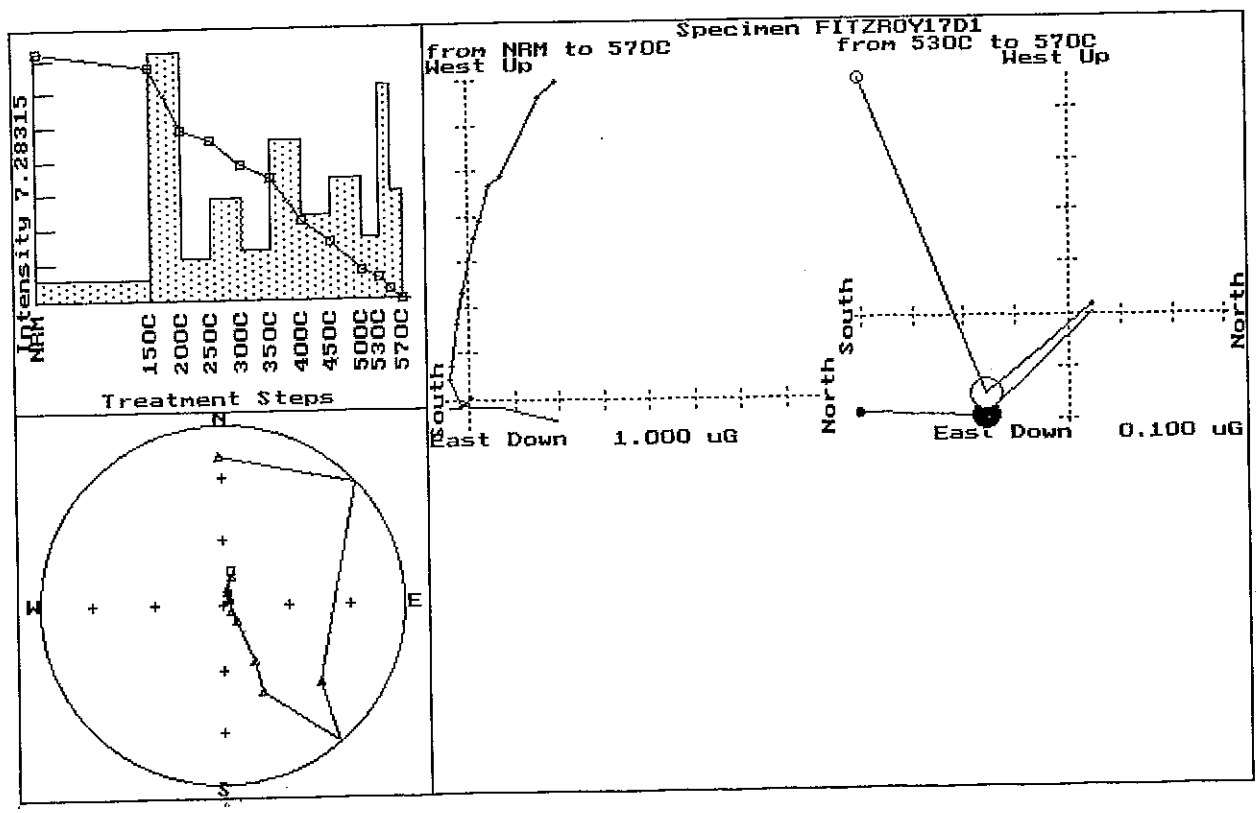
Specimen FITZROY17D1
from NRM to 570C
West Up
from 530C to 570C
West Up
Intensity 7.28315
NRM
150C
200C
250C
300C
350C
400C
450C
500C
530C
570C
Treatment Steps
N
E
S
W
South
East Down
1.000 uG
North
South
North
East Down
0.100 uG

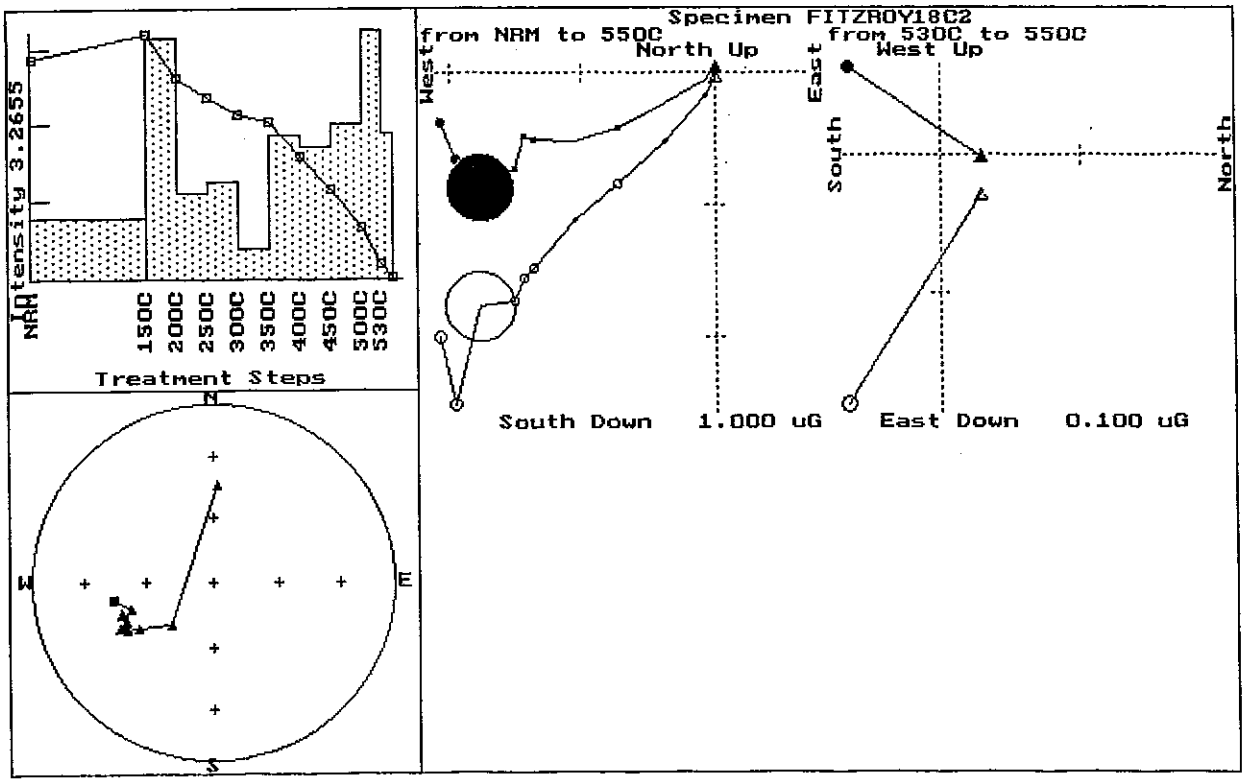
Intensity 3.2655
NRM
150C
200C
250C
300C
350C
400C
450C
500C
530C
Treatment Steps
N
W
E
S
Specimen FITZROY18C2
from NRM to 550C
North Up
West
East
South
North
from 530C to 550C
West Up
South Down 1.000 uG
East Down 0.100 uG

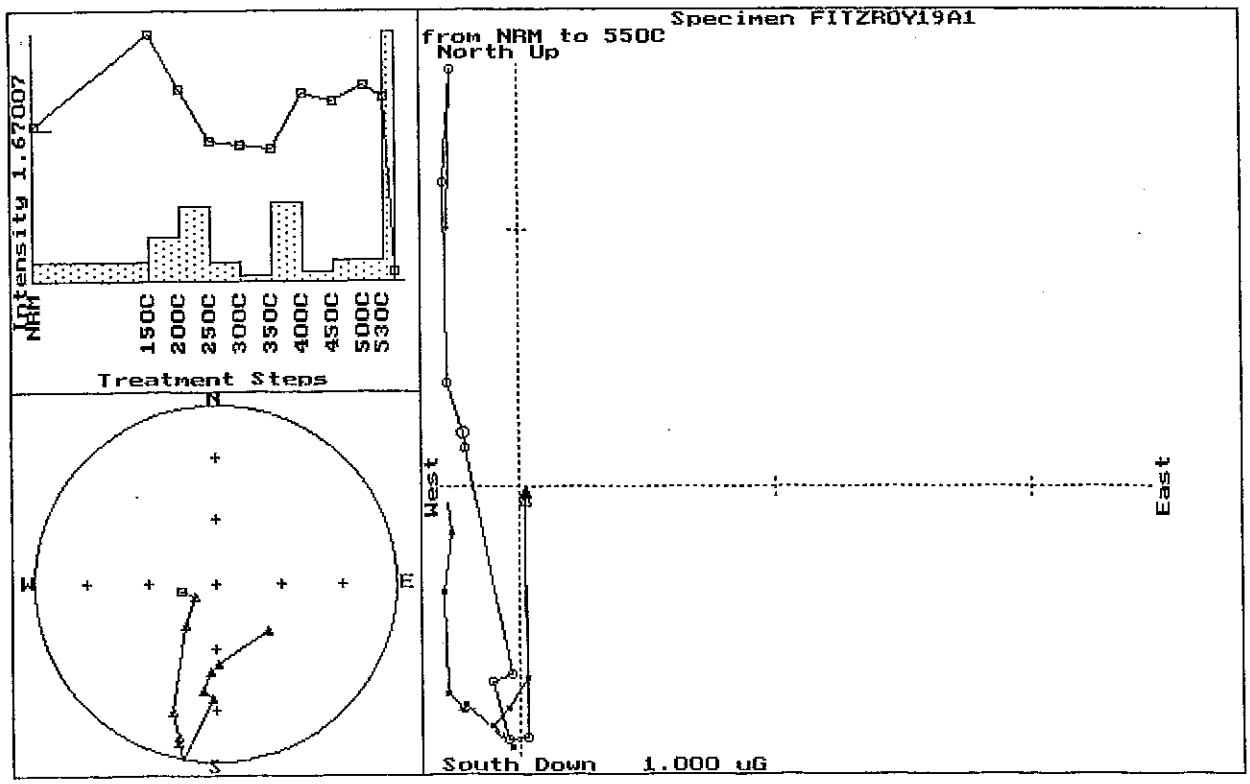
Intensity 1.67007
NRM
150C
200C
250C
300C
350C
400C
450C
500C
530C
Treatment Steps
N
W
E
S
Specimen FITZROY19A1
from NRM to 550C
North Up
West
East
South Down 1.000 uG

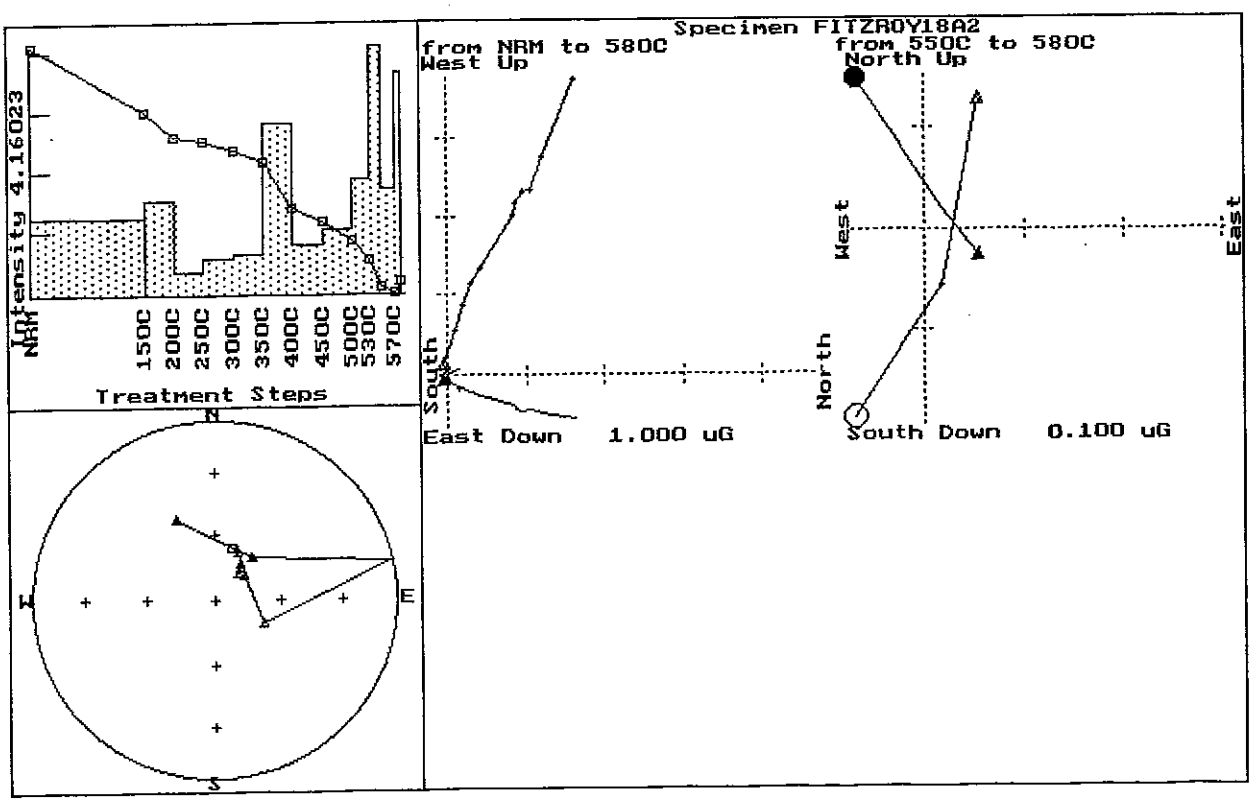
Specimen FITZROY18A2
from NRM to 580C
West Up
from 550C to 580C
North Up
Intensity 4.16023
NRM
150C
200C
250C
300C
350C
400C
450C
500C
530C
570C
Treatment Steps
N
W
E
S
South
North
West
East
East Down 1.000 uG
South Down 0.100 uG

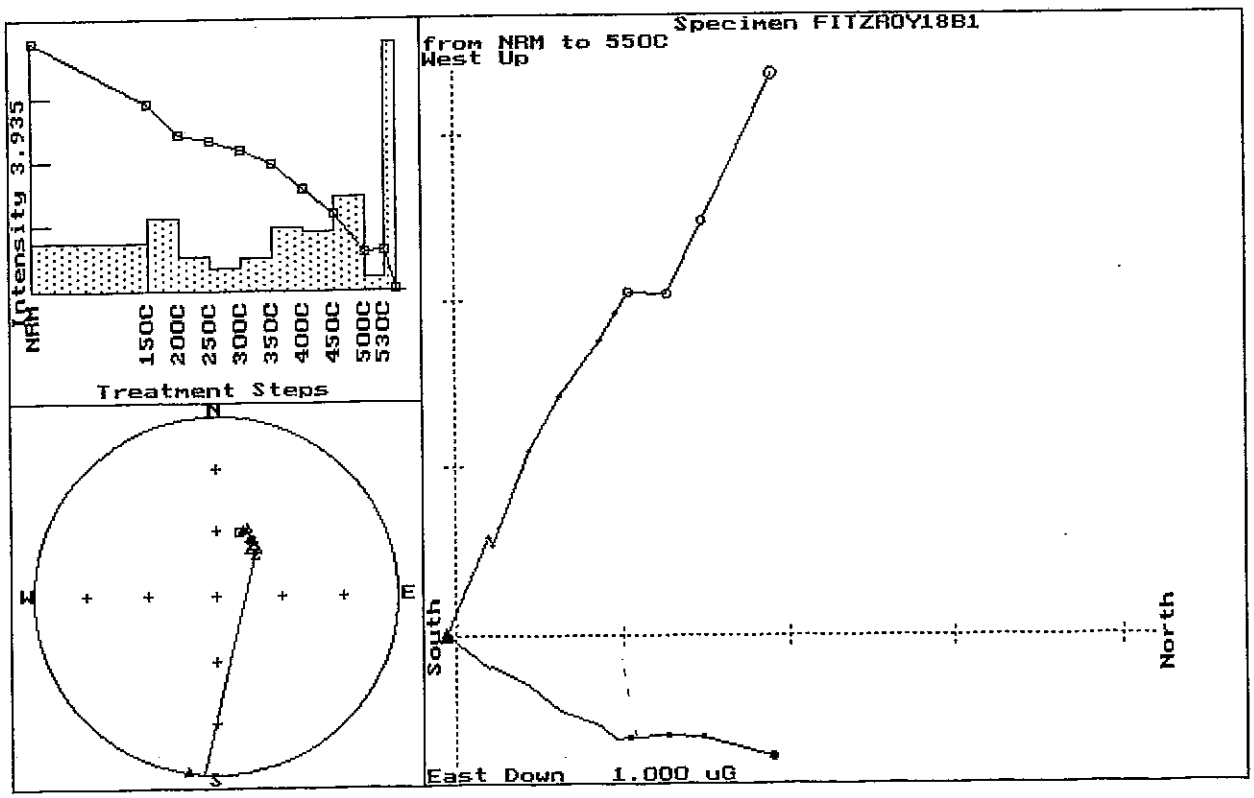
Specimen FITZROY18B1
from NRM to 550C
West Up
Intensity 3.935
NRM
150C
200C
250C
300C
350C
400C
450C
500C
530C
Treatment Steps
N
W
E
S
South
North
East Down 1.000 uG

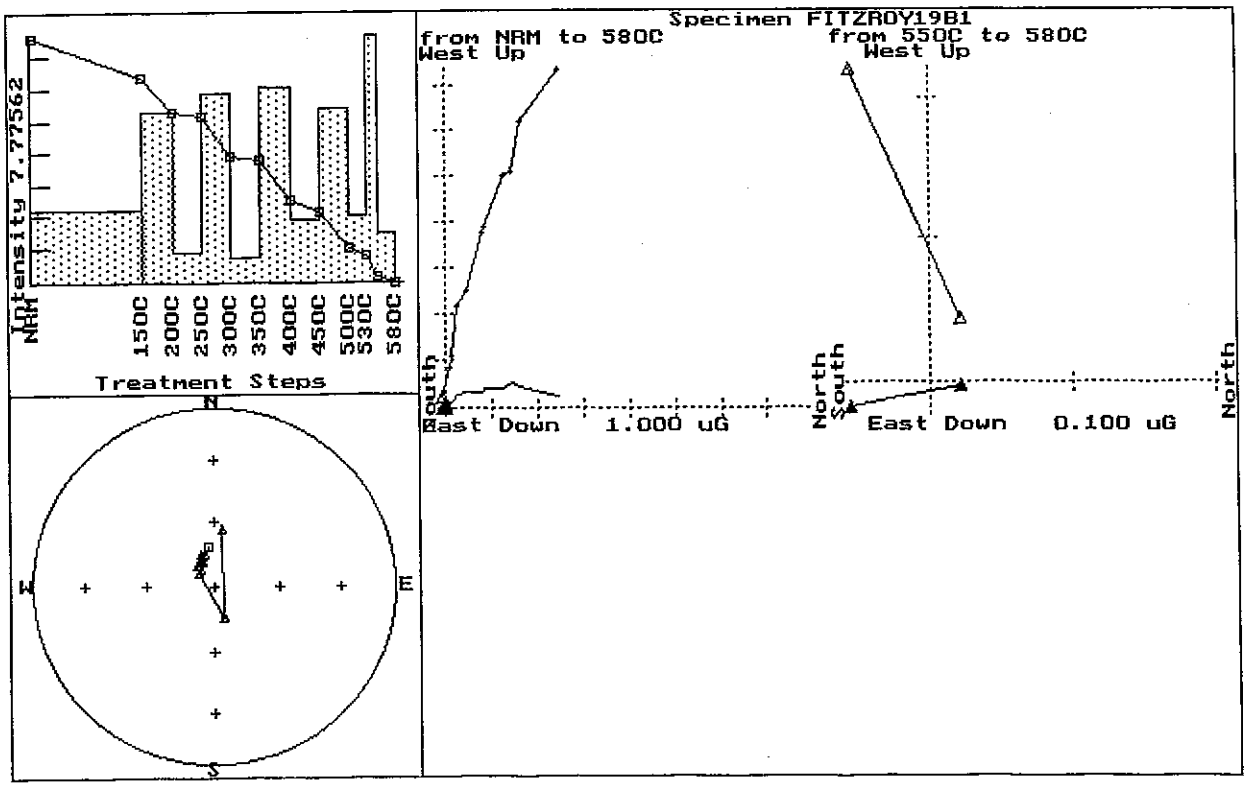
Intensity 7.77562
NRM
150C
200C
250C
300C
350C
400C
450C
500C
530C
580C
Treatment Steps
N
W
E
S
Specimen FITZROY19B1
from NRM to 580C
West Up
South
East Down
1.000 uG
from 550C to 580C
West Up
North
South
East Down
0.100 uG
North

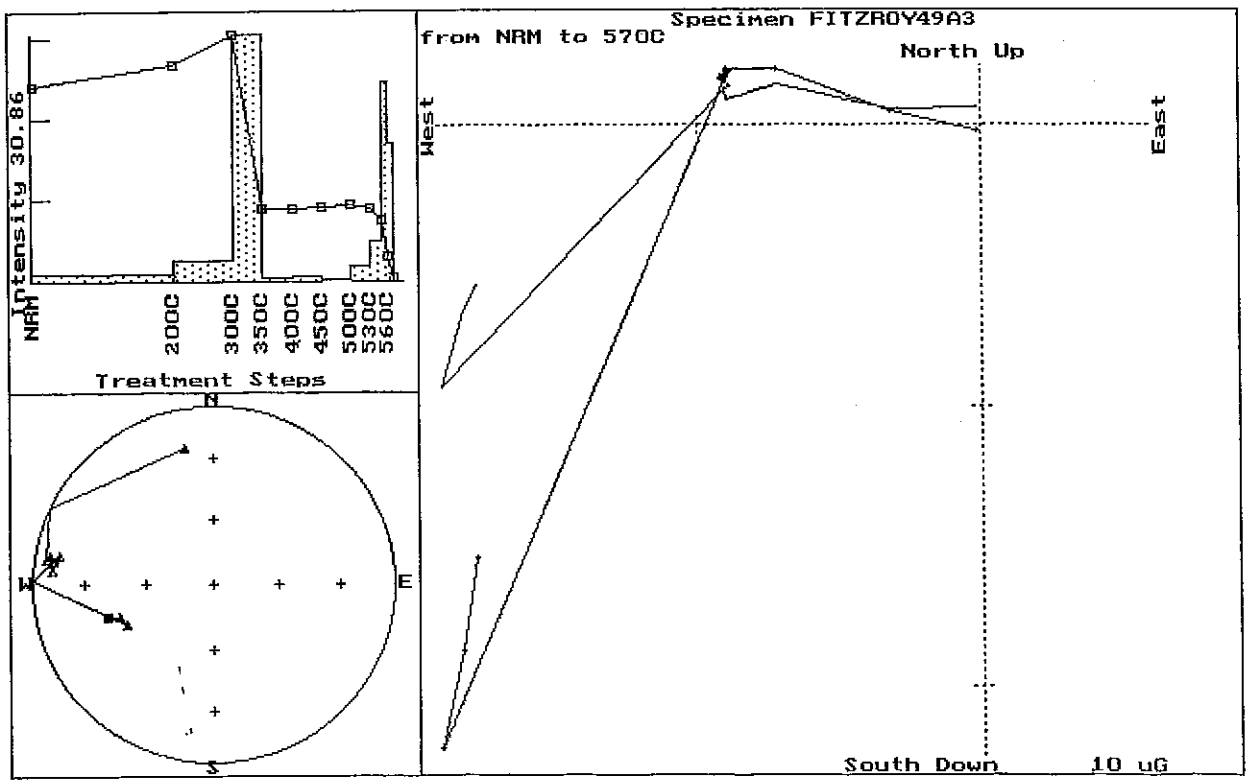
Intensity 30.86
NRM
200C
300C
350C
400C
450C
500C
530C
560C
Treatment Steps
N
W
E
S
Specimen FITZROY49A3
from NRM to 570C
North Up
West
East
South Down
10 uG

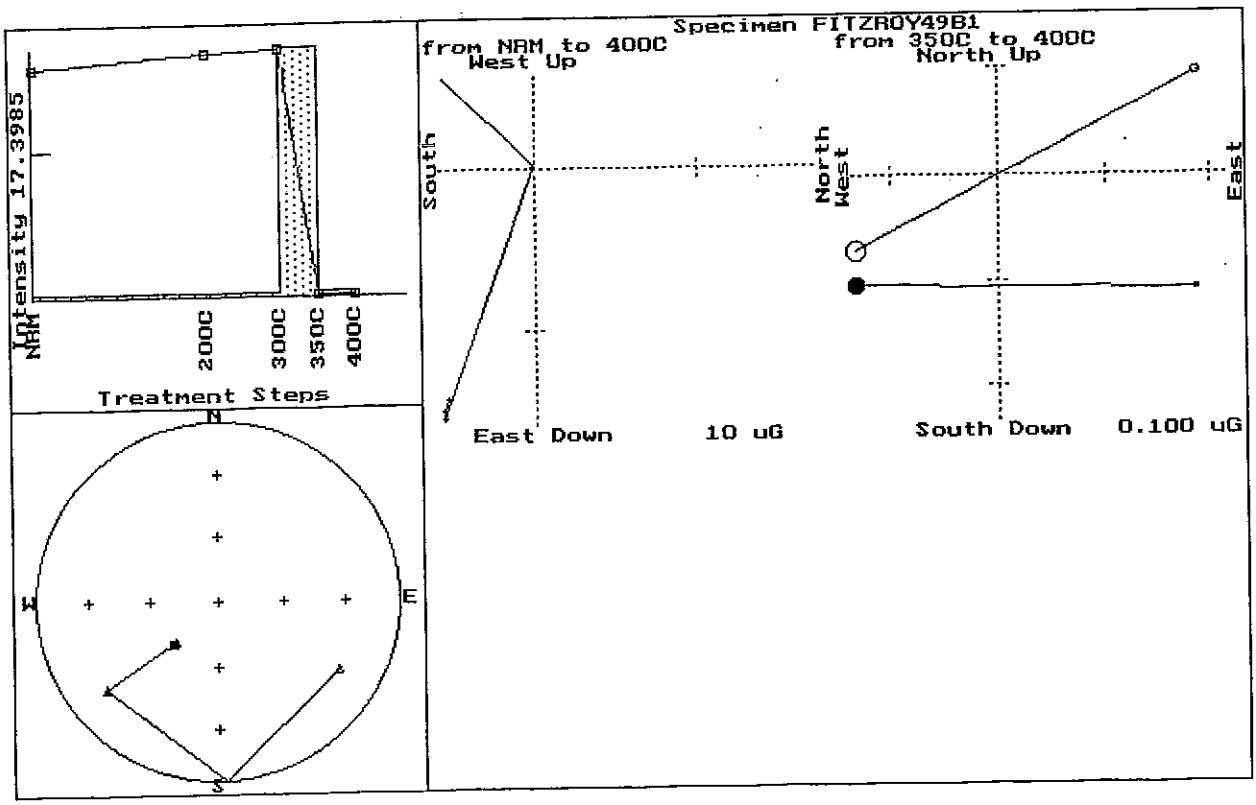
Intensity 17.3985
NRM
200C
300C
350C
400C
Treatment Steps
N
W
E
S
Specimen FITZROY49B1
from NRM to 400C
West Up
South
East Down
10 uG
from 350C to 400C
North Up
North
West
East
South Down
0.100 uG

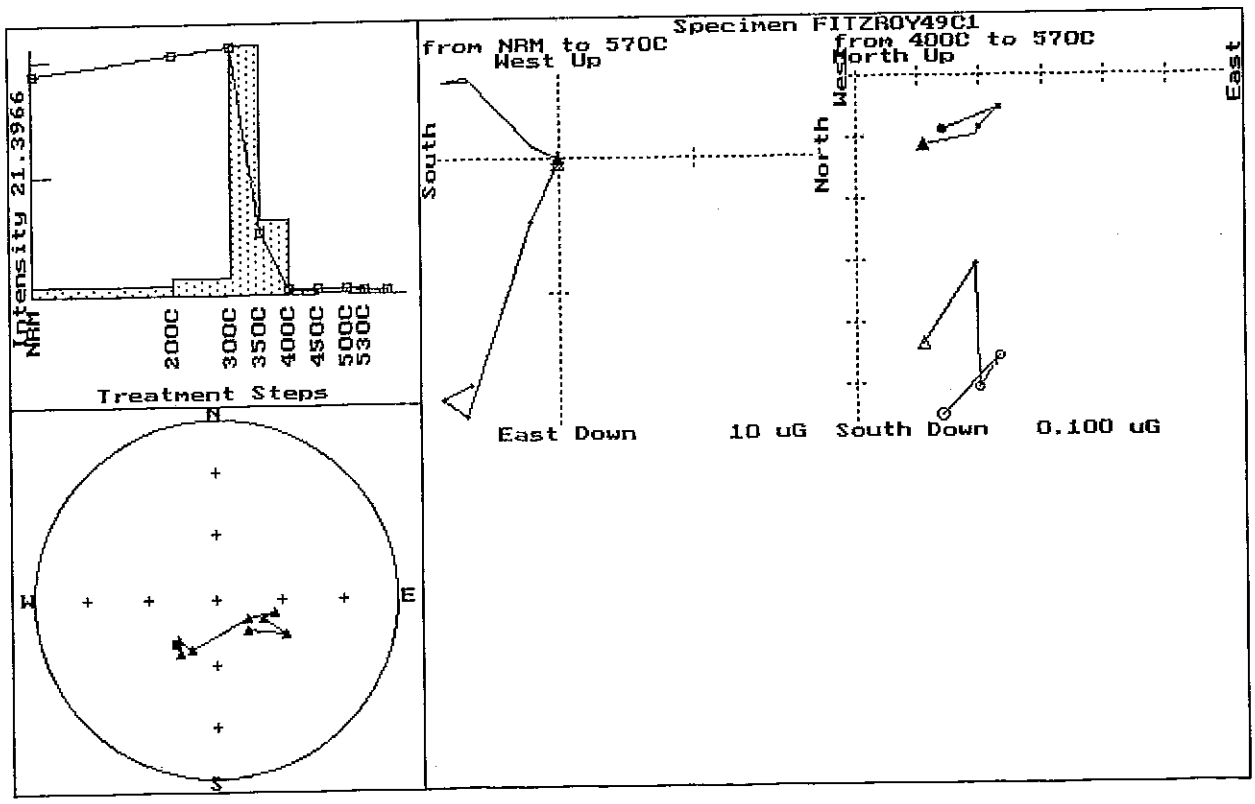
Intensity 21.3966
NRM
200C
300C
350C
400C
450C
500C
530C
Treatment Steps
N
W
E
S
Specimen FITZROY49C1
from NRM to 570C
West Up
South
East Down
10 uG
from 400C to 570C
North Up
West
North
East
South Down
0.100 uG

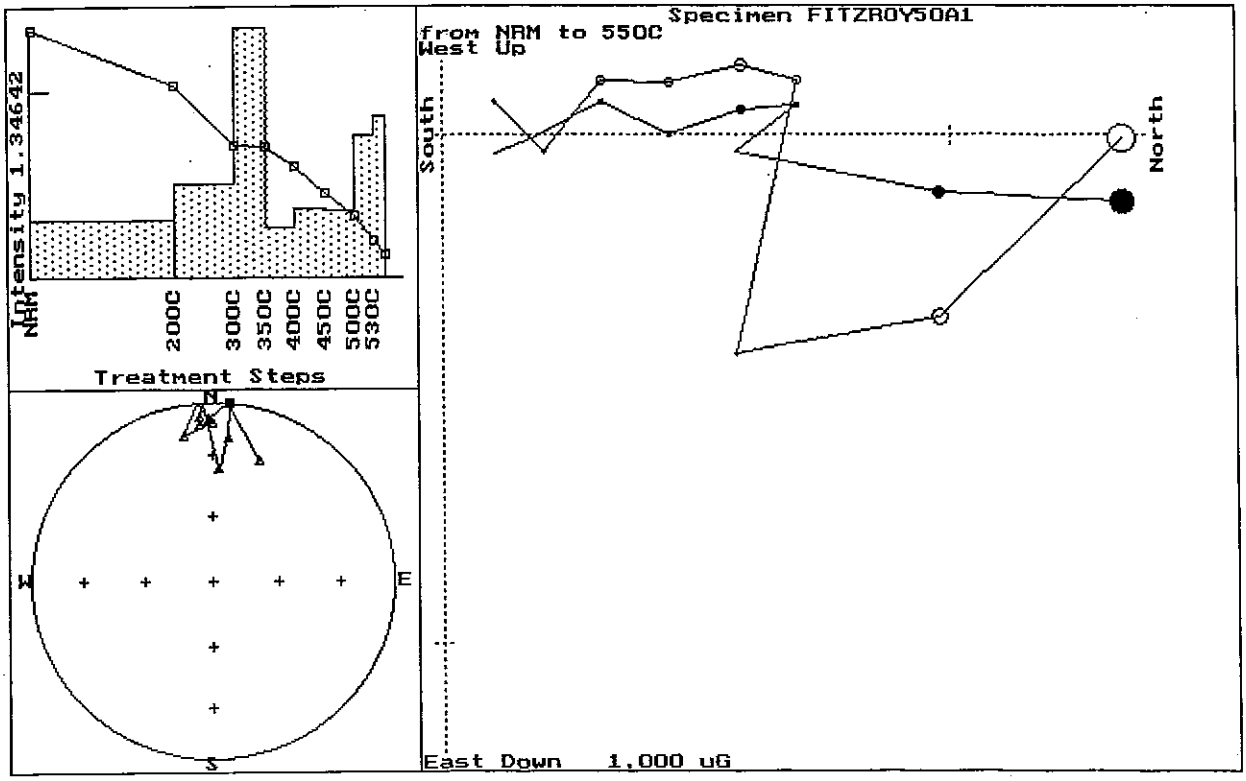
Specimen FITZROY50A1
from NRM to 550C
West Up
South
North
East Down 1.000 uG
Intensity 1.34642
NRM
200C
300C
350C
400C
450C
500C
530C
Treatment Steps
N
E
S
W

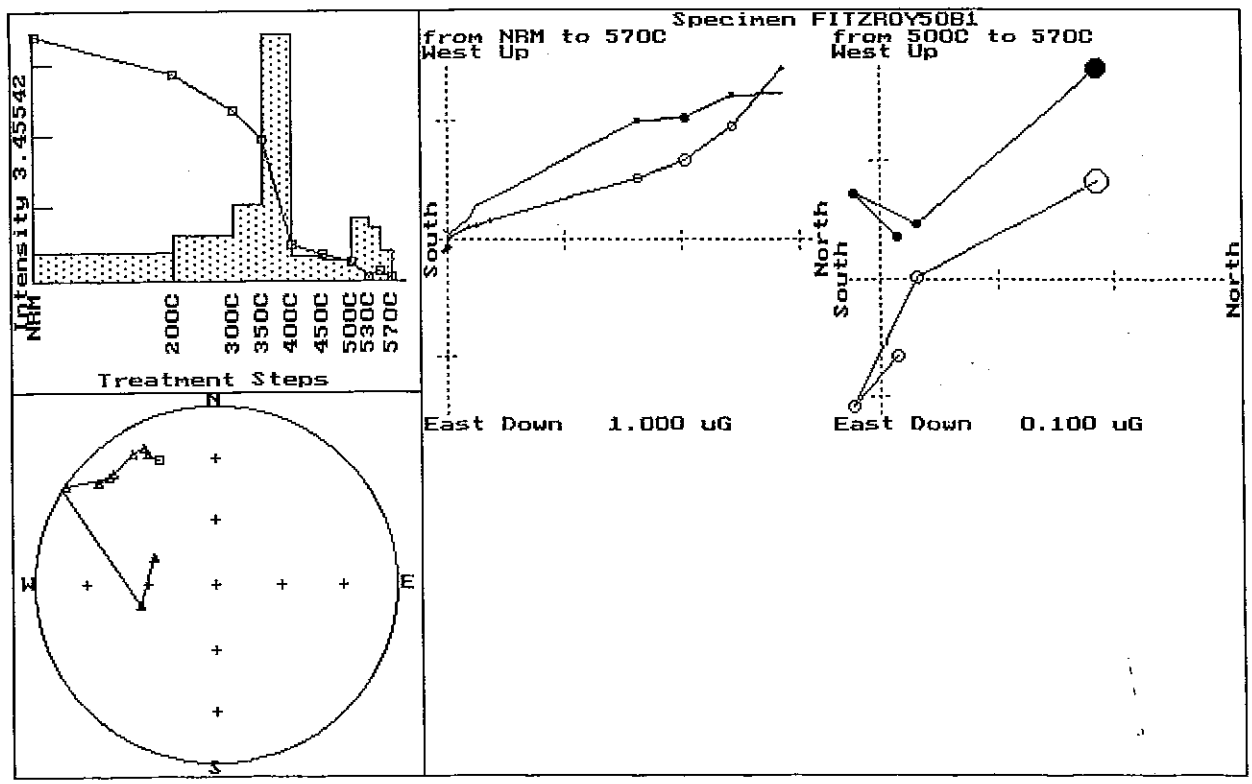
Specimen FITZROY50B1
from NRM to 570C
West Up
from 500C to 570C
West Up
South
North
South
North
East Down 1.000 uG
East Down 0.100 uG
Intensity 3.45542
NRM
200C
300C
350C
400C
450C
500C
530C
570C
Treatment Steps
N
E
S
W

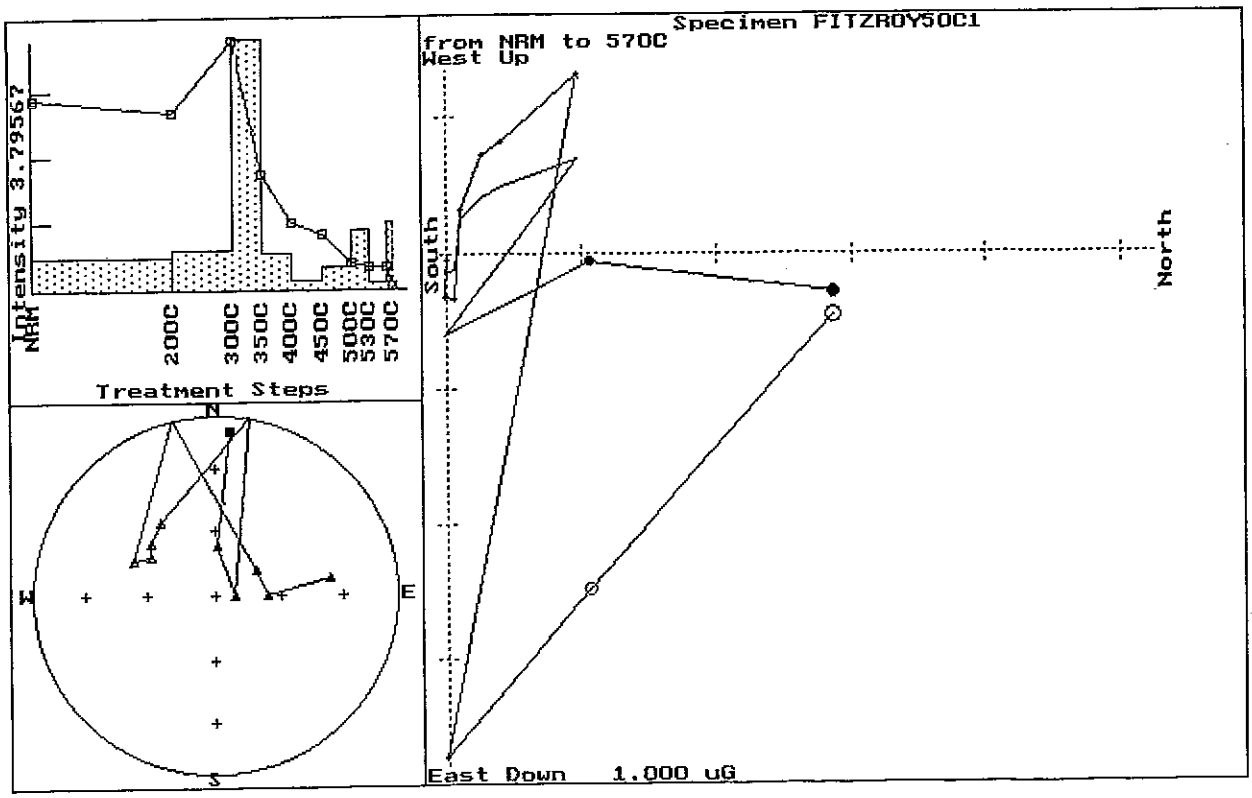
Specimen FITZROY50C1
from NRM to 570C
West Up
Intensity 3.79567
NRM
200C
300C
350C
400C
450C
500C
530C
570C
Treatment Steps
N
E
S
W
South
North
East Down
1.000 uG

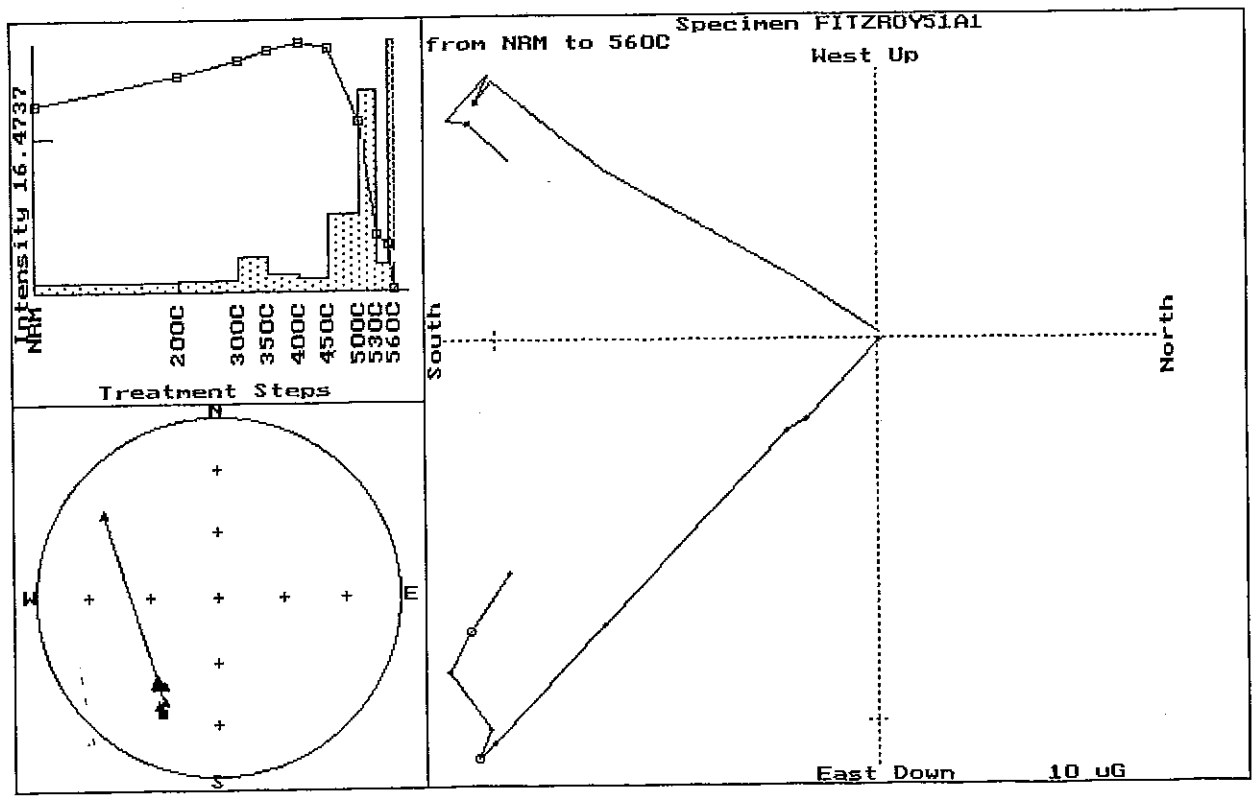
Specimen FITZROY51A1
from NRM to 560C
West Up
Intensity 16.4737
NRM
200C
300C
350C
400C
450C
500C
530C
560C
Treatment Steps
N
E
S
W
South
North
East Down
10 uG

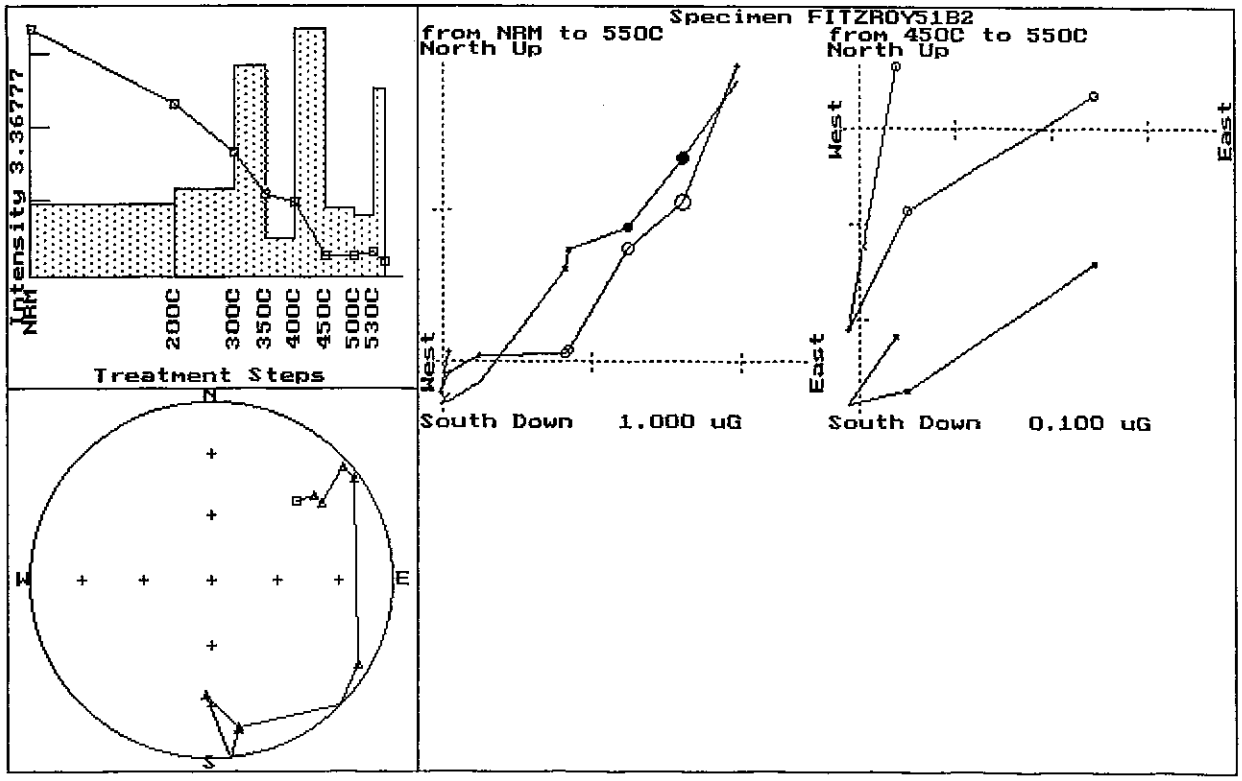
Specimen FITZROY51B2
from NRM to 550C
North Up
from 450C to 550C
North Up
Intensity 3.36777
NRM
200C
300C
350C
400C
450C
500C
530C
Treatment Steps
West
East
South Down 1.000 uG
South Down 0.100 uG
N
W
E
S

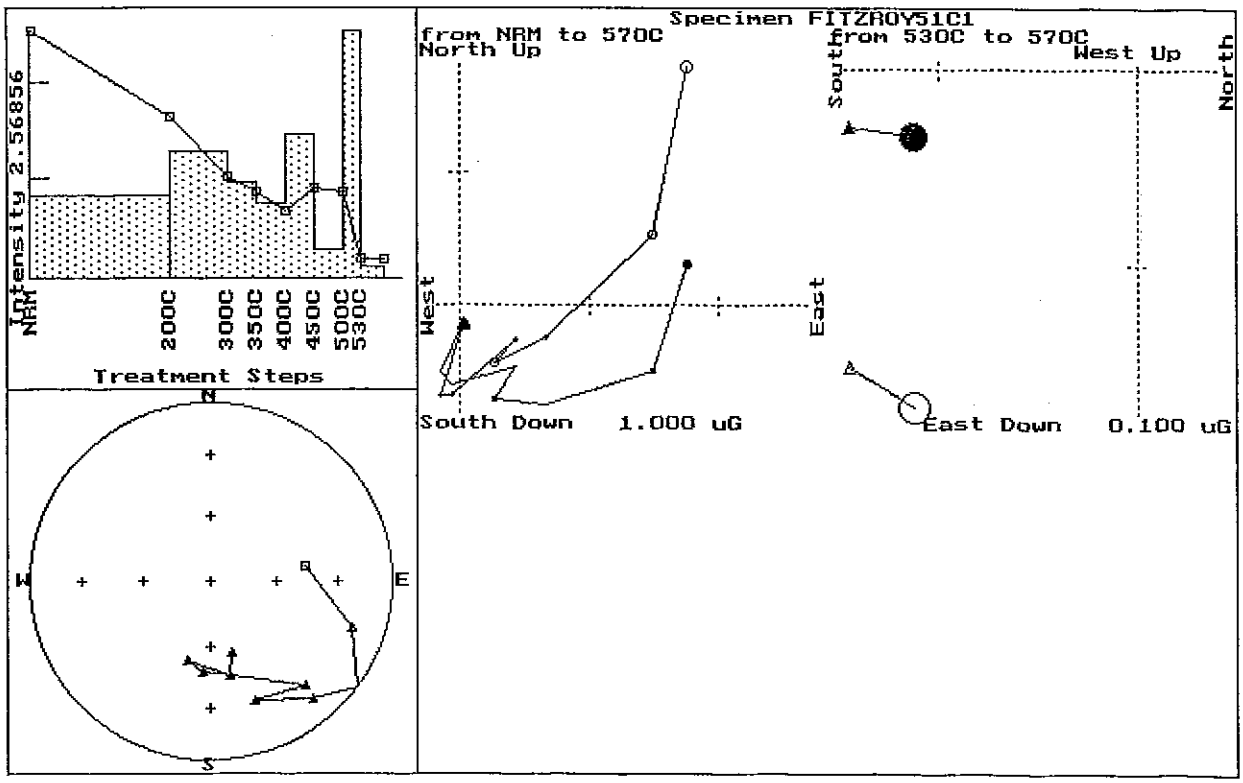
Specimen FITZROY51C1
from NRM to 570C
North Up
from 530C to 570C
West Up
South
North
Intensity 2.56856
NRM
200C
300C
350C
400C
450C
500C
530C
Treatment Steps
West
East
South Down 1.000 uG
East Down 0.100 uG
N
W
E
S

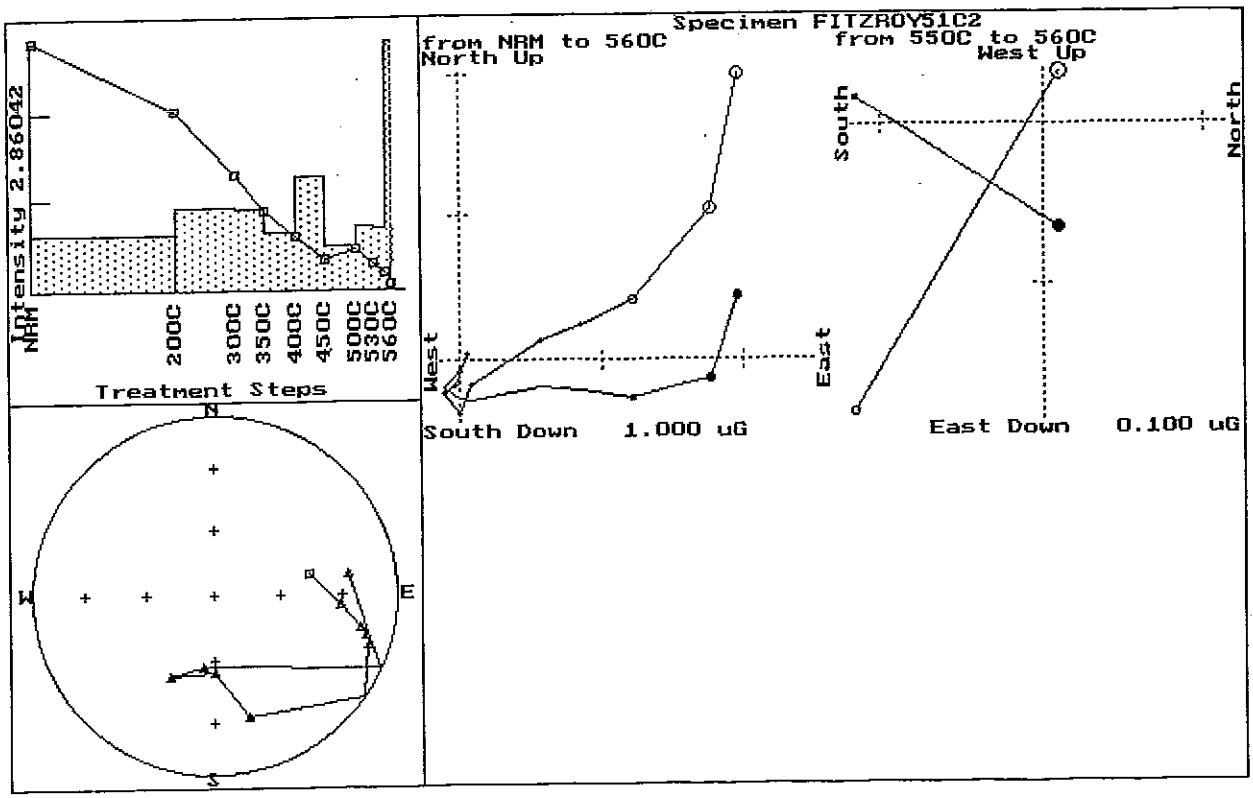
Specimen FITZROY51C2
from NRM to 560C
North Up
from 550C to 560C
West Up
Intensity 2.86042
NRM
200C
300C
350C
400C
450C
500C
530C
560C
Treatment Steps
N
W
E
S
West
East
South
North
South Down 1.000 uG
East Down 0.100 uG

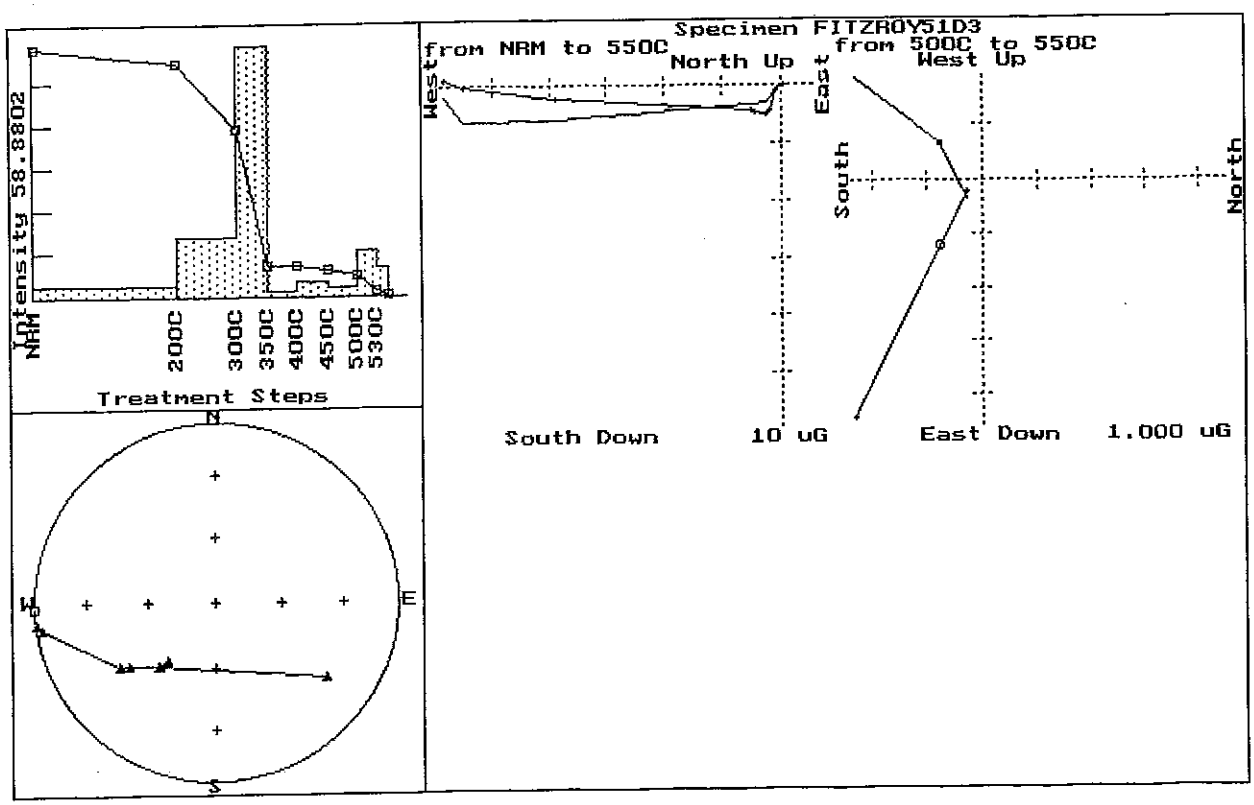
Specimen FITZROY51D3
from NRM to 550C
North Up
from 500C to 550C
West Up
Intensity 58.8802
NRM
200C
300C
350C
400C
450C
500C
530C
Treatment Steps
N
W
E
S
West
East
South
North
South Down 10 uG
East Down 1.000 uG

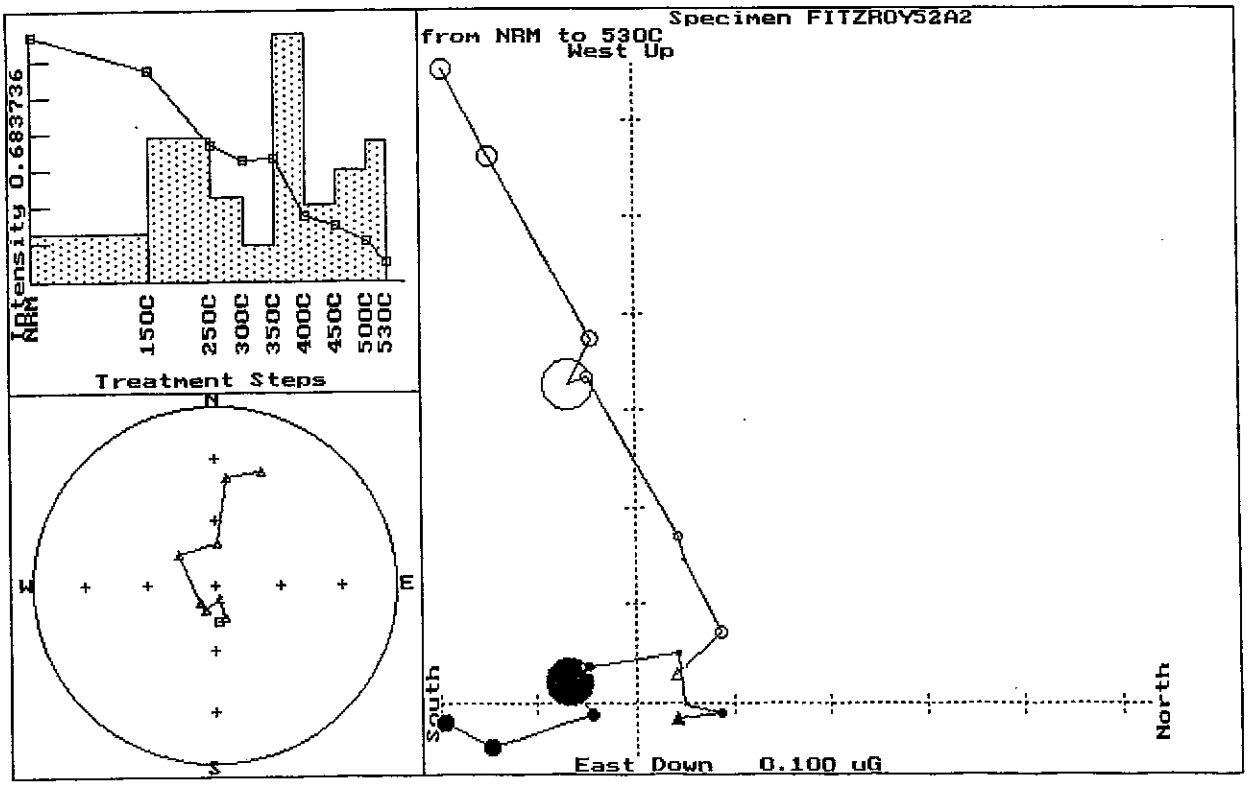
Intensity 0.683736
NRM
150C
250C
300C
350C
400C
450C
500C
530C
Treatment Steps
N
W
E
S
Specimen FITZROY52A2
from NRM to 530C
West Up
South
North
East Down
0.100 uG

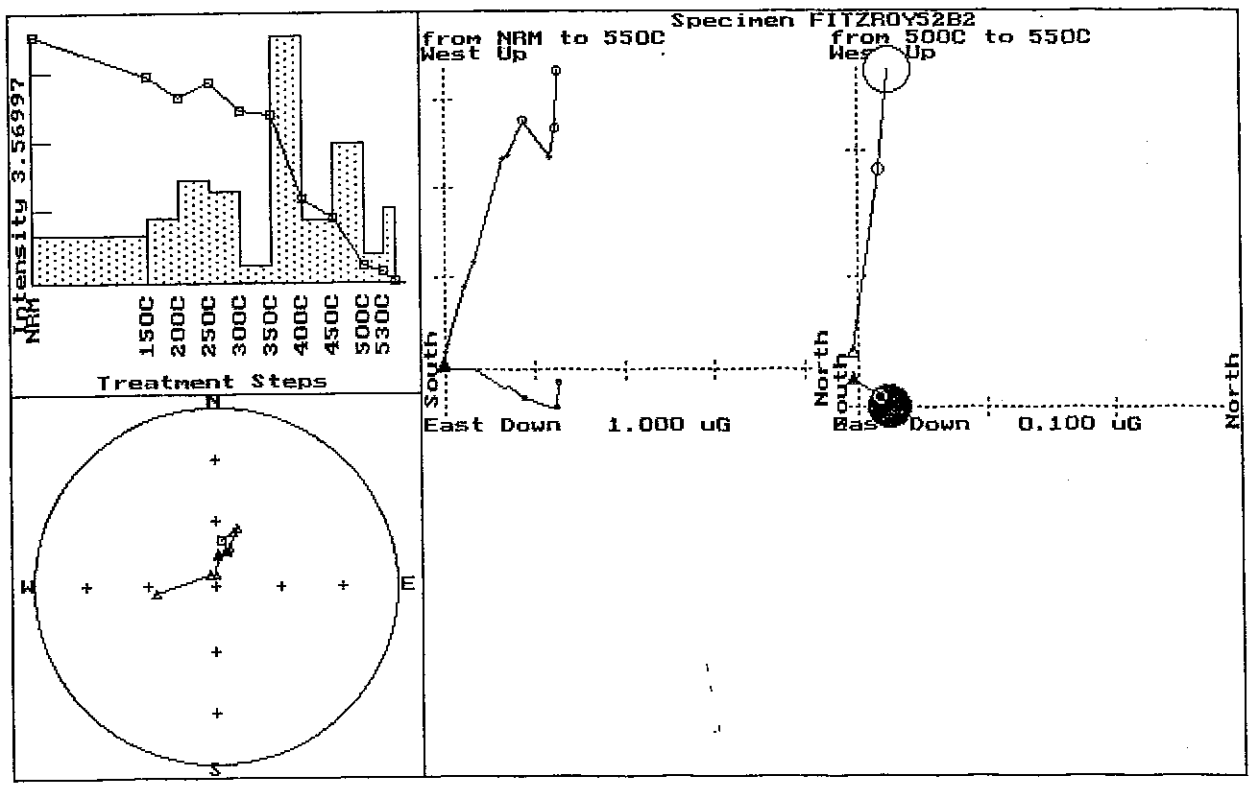
Intensity 3.56997
NRM
150C
200C
250C
300C
350C
400C
450C
500C
530C
Treatment Steps
N
W
E
S
Specimen FITZROY52B2
from NRM to 550C
from 500C to 550C
West Up
South
North
East Down
1.000 uG
Down
0.100 uG

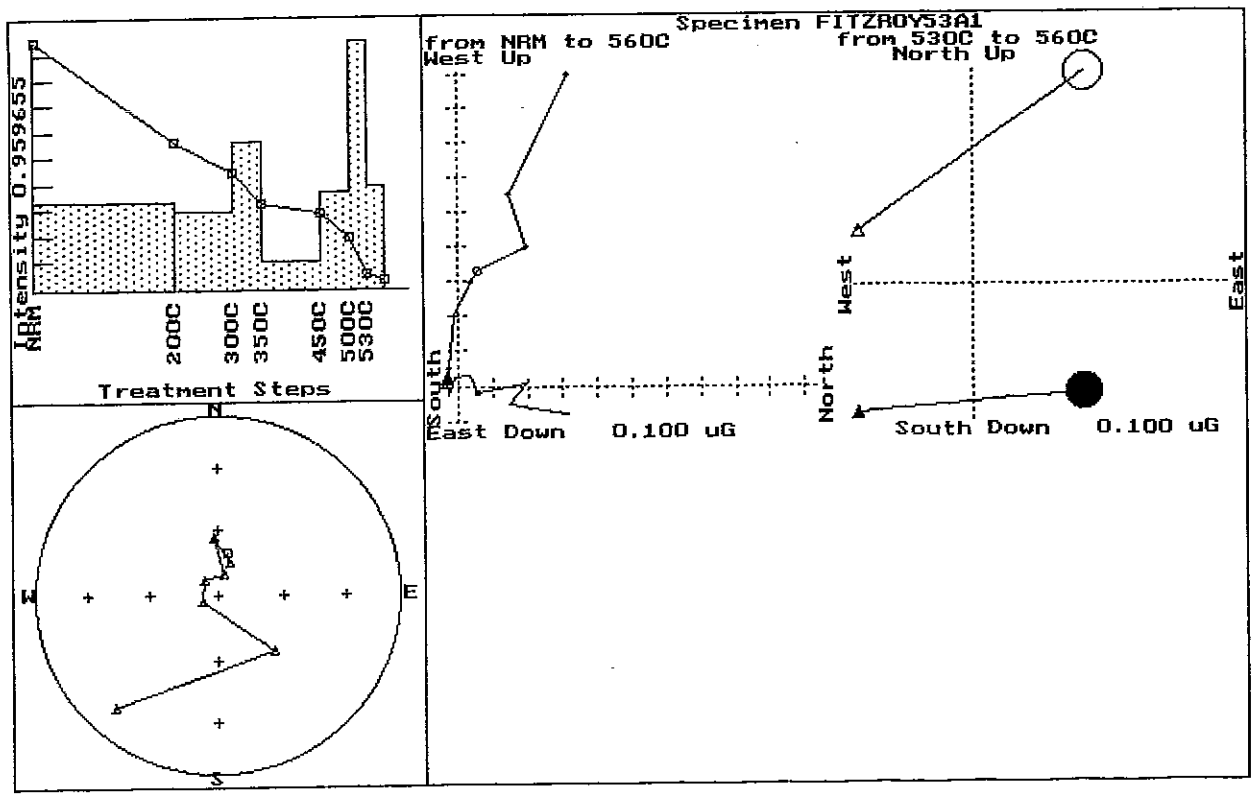
Intensity 0.959655
NRM
200C
300C
350C
450C
500C
530C
Treatment Steps
N
W
E
S
Specimen FITZROY53A1
from NRM to 560C
West Up
South
East Down 0.100 uG
from 530C to 560C
North Up
West
East
North
South Down 0.100 uG

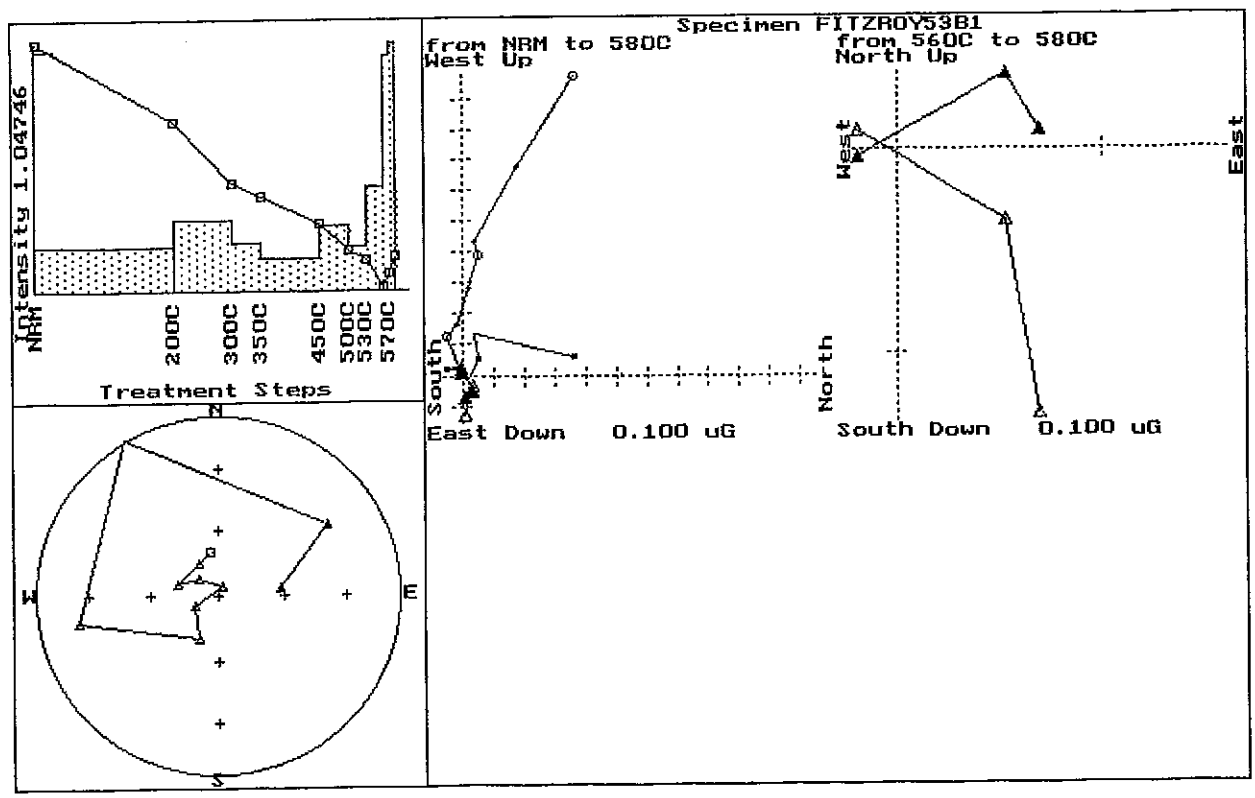
Intensity 1.04746
NRM
200C
300C
350C
450C
500C
530C
570C
Treatment Steps
N
W
E
S
Specimen FITZROY53B1
from NRM to 580C
West Up
South
East Down 0.100 uG
from 560C to 580C
North Up
West
East
North
South Down 0.100 uG

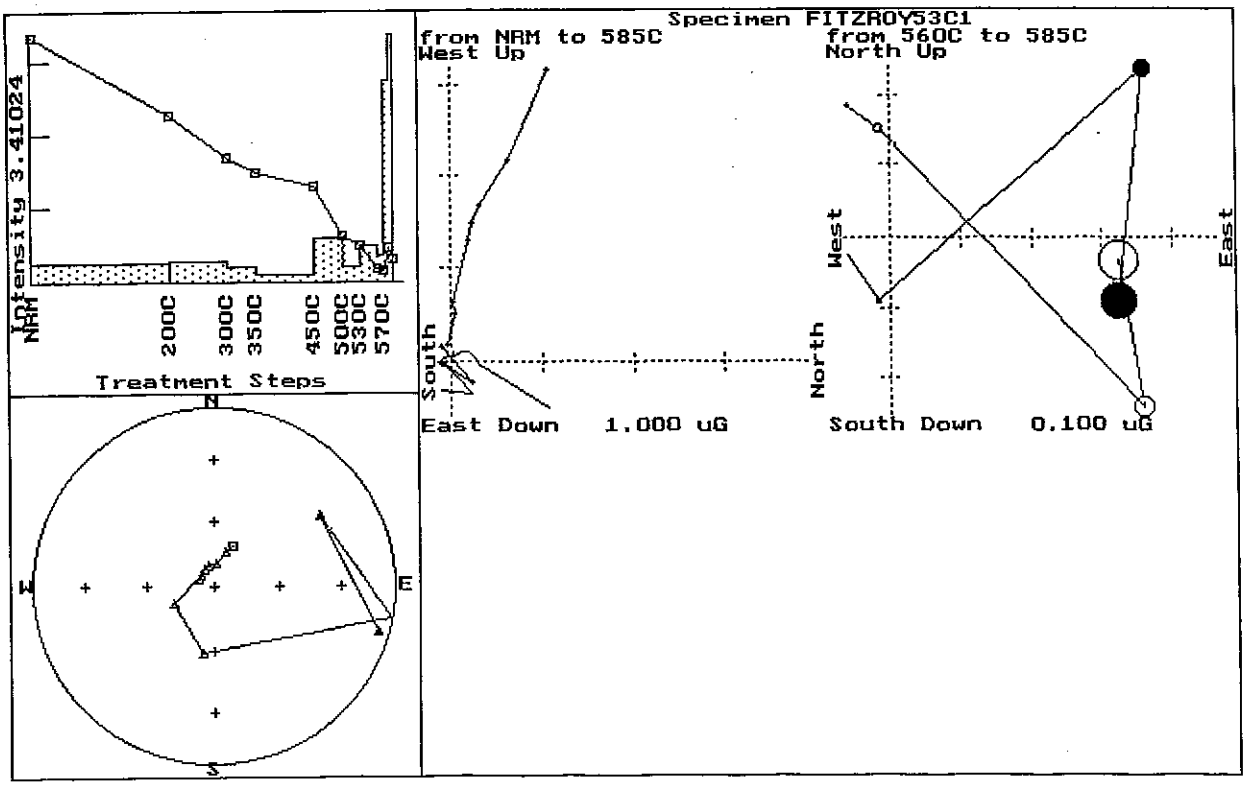
Specimen FITZROY53C1
from NRM to 585C
West Up
from 560C to 585C
North Up
Intensity 3.41024
NRM
200C
300C
350C
450C
500C
530C
570C
Treatment Steps
N
W
E
S
South
North
West
East
East Down 1.000 uG
South Down 0.100 uG

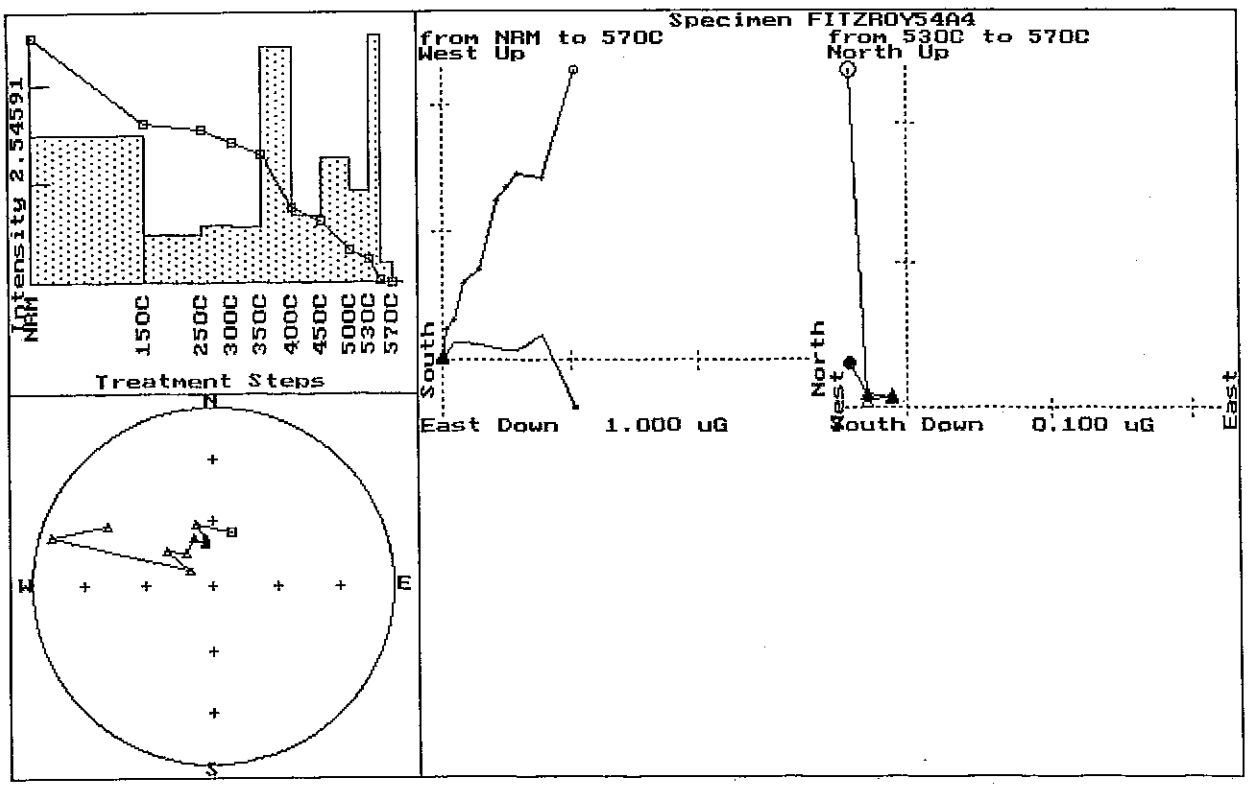
Specimen FITZROY54A4
from NRM to 570C
West Up
from 530C to 570C
North Up
Intensity 2.54591
NRM
150C
250C
300C
350C
400C
450C
500C
530C
570C
Treatment Steps
N
W
E
S
South
North
West
East
East Down 1.000 uG
South Down 0.100 uG

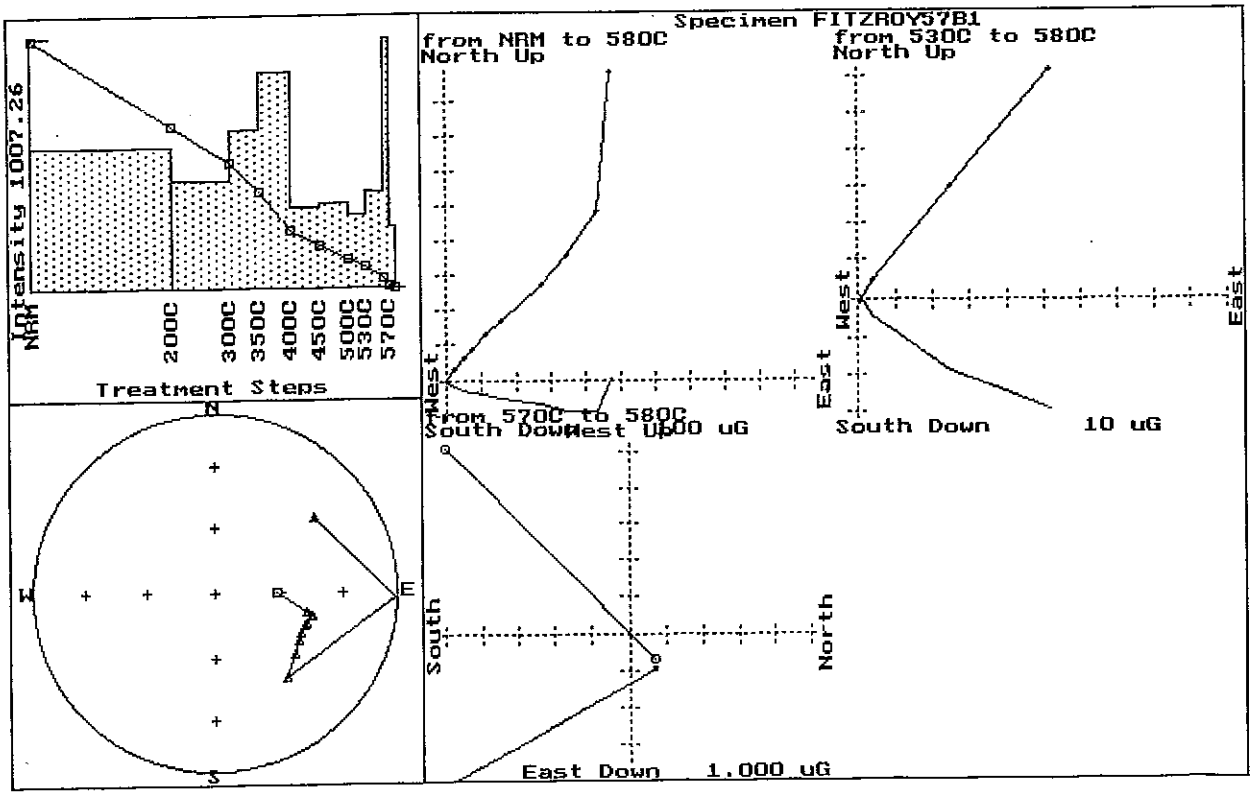
Specimen FITZROY57B1
from NRM to 580C
North Up
from 530C to 580C
North Up
Intensity 1007.26
NRM
200C
300C
350C
400C
450C
500C
530C
570C
Treatment Steps
N
E
S
W
West
East
from 570C to 580C
South Down
West Up
South Down
10 uG
South
North
East Down
1.000 uG

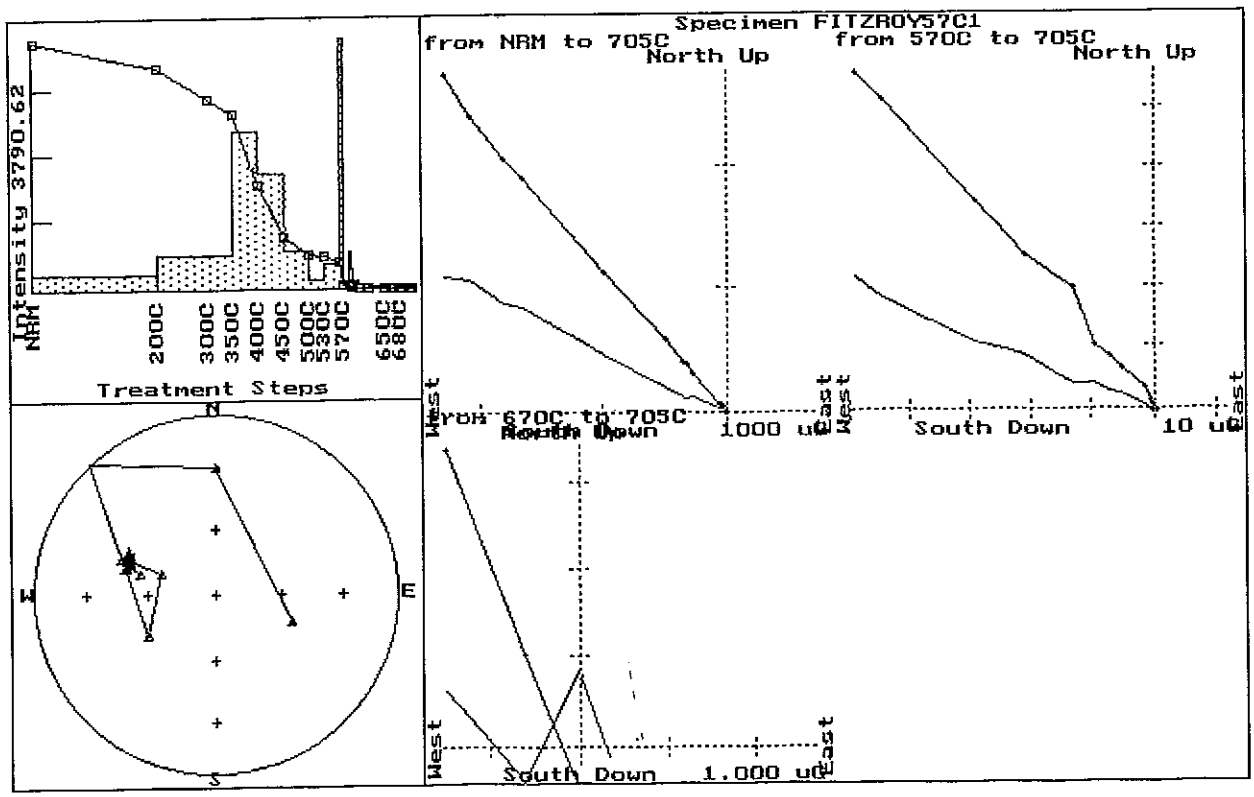
Specimen FITZROY57C1
from NRM to 705C
North Up
from 570C to 705C
North Up
Intensity 3790.62
NRM
200C
300C
350C
400C
450C
500C
530C
570C
650C
680C
Treatment Steps
N
E
S
W
West
East
from 670C to 705C
South Down
1000 uG
South Down
10 uG
West
East
South Down
1.000 uG

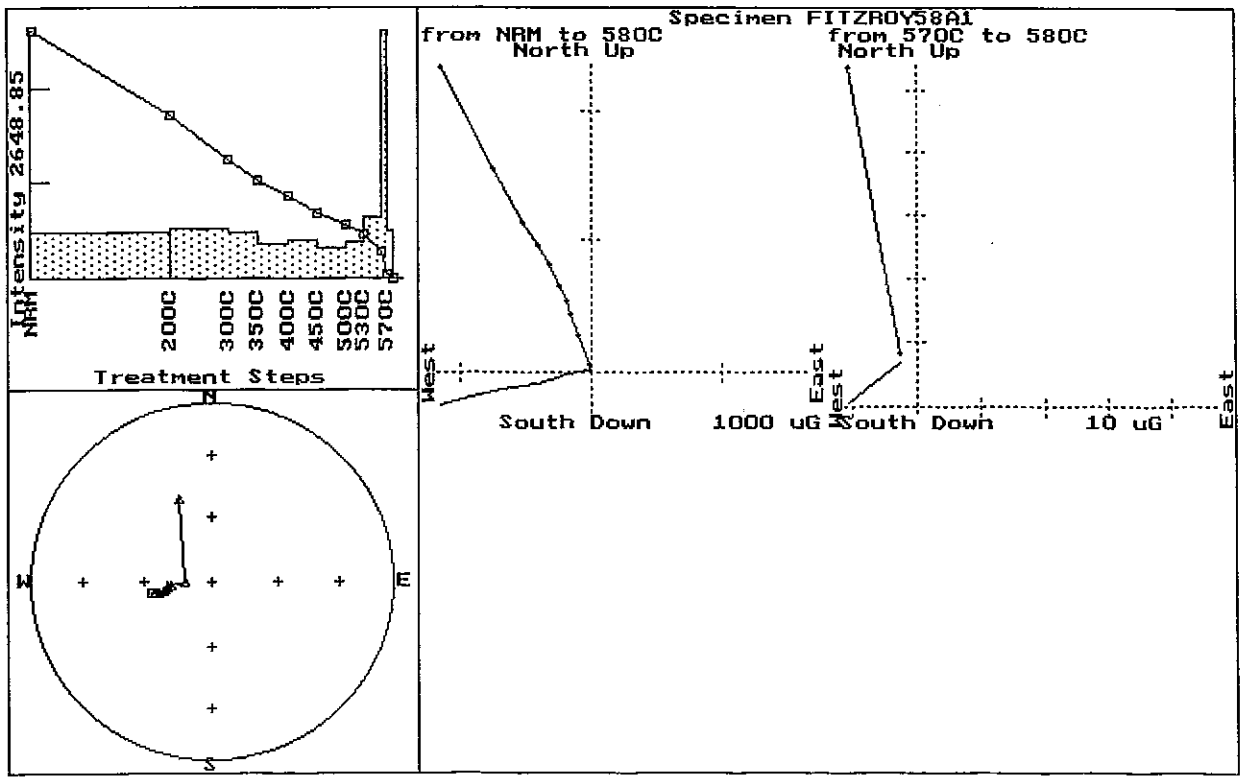
Specimen FITZROY58A1
from NRM to 580C
North Up
from 570C to 580C
North Up
Intensity 2648.85
NRM
200C
300C
350C
400C
450C
500C
530C
570C
Treatment Steps
N
E
S
W
West
East
South Down
1000 uG
10 uG

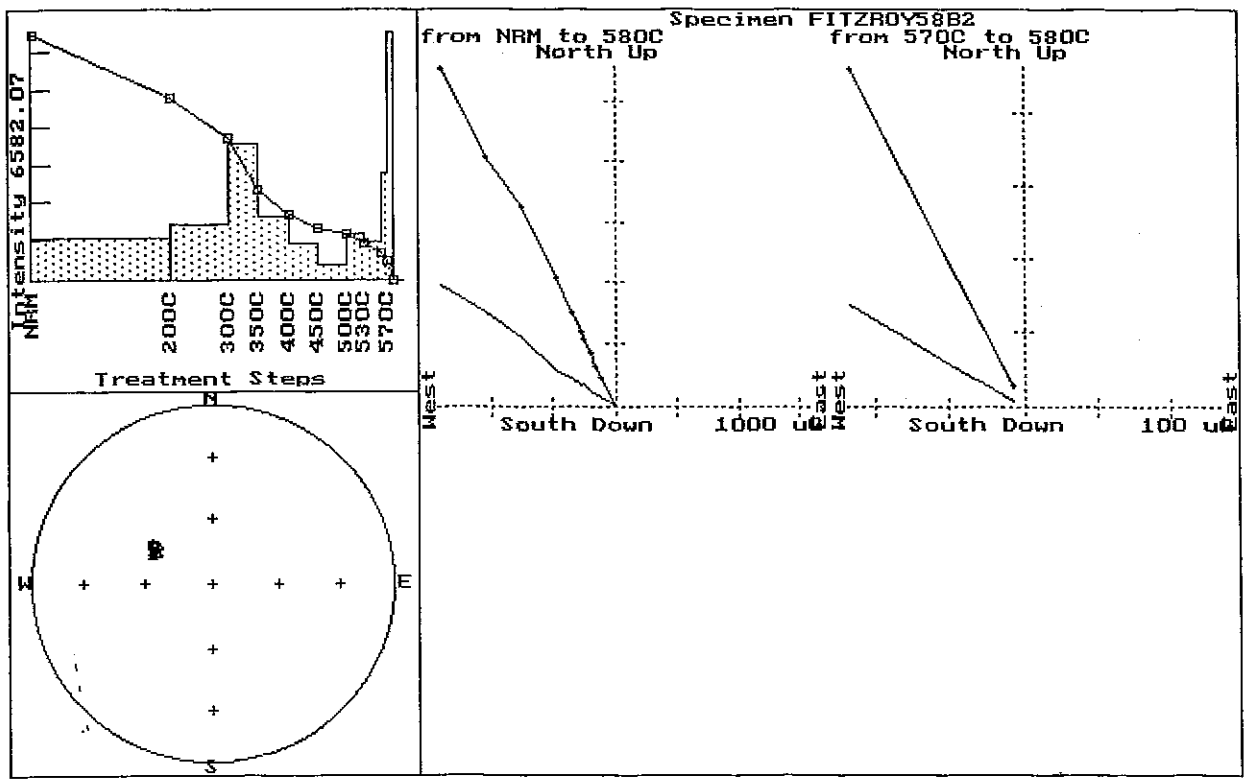
Specimen FITZROY58B2
from NRM to 580C
North Up
from 570C to 580C
North Up
Intensity 6582.07
NRM
200C
300C
350C
400C
450C
500C
530C
570C
Treatment Steps
N
E
S
W
West
East
South Down
1000 uG
100 uG

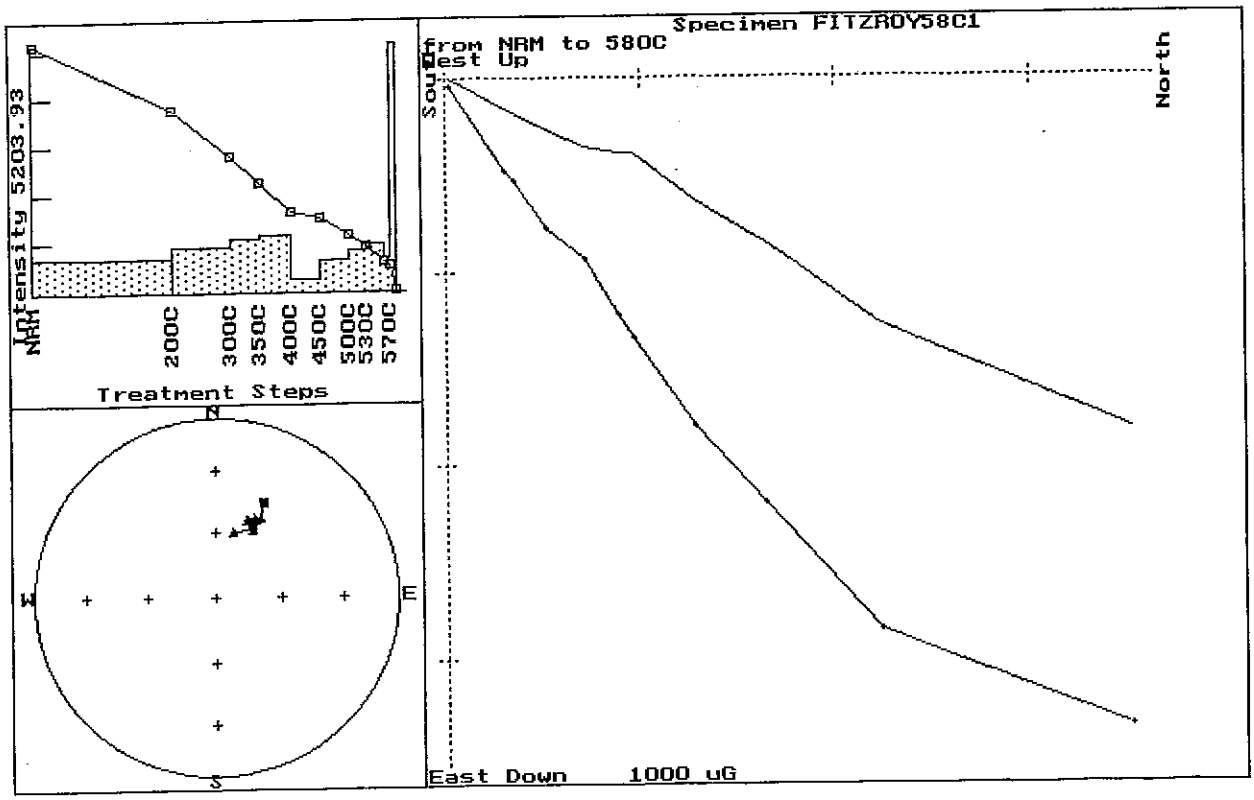
Specimen FITZROY58C1
from NRM to 580C
West Up
South
North
Intensity 5203.93
NRM
200C
300C
350C
400C
450C
500C
530C
570C
Treatment Steps
N
E
S
W
East Down
1000 uG

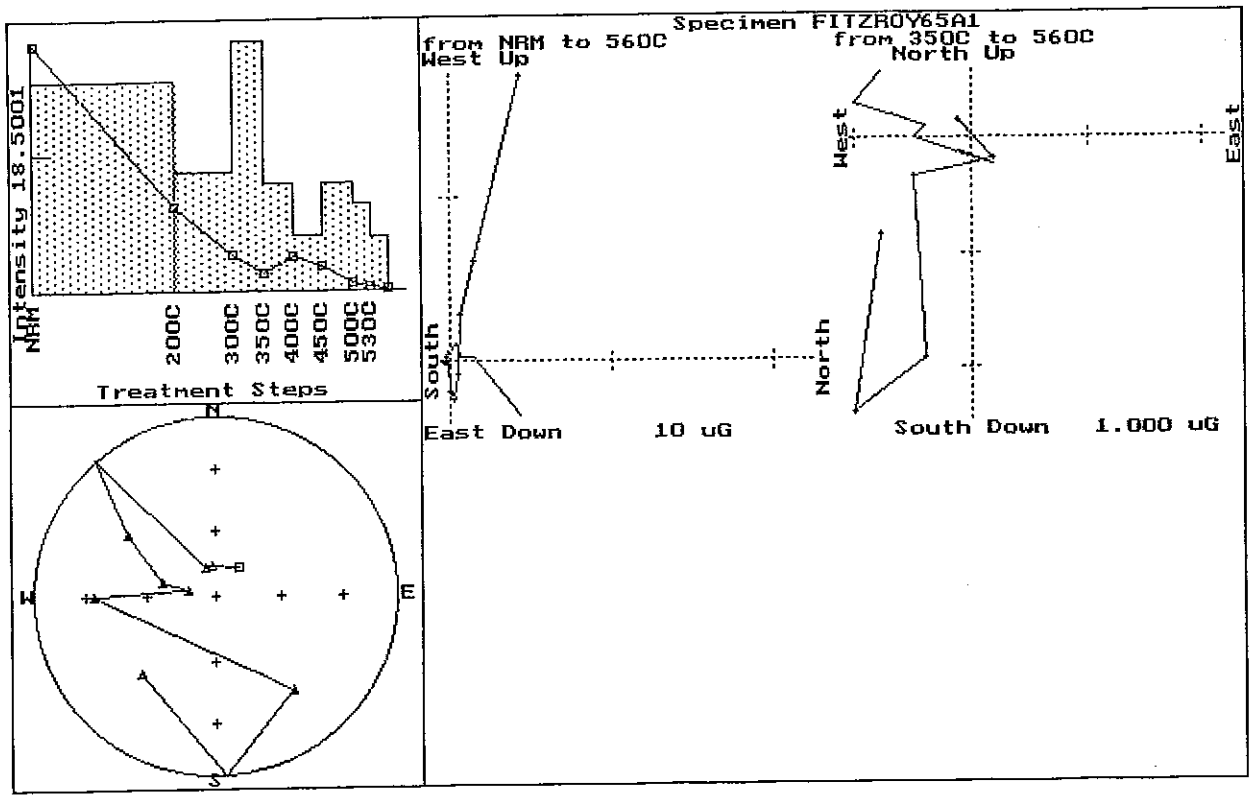
Specimen FITZROY65A1
from NRM to 560C
West Up
from 350C to 560C
North Up
Intensity 18.5001
NRM
200C
300C
350C
400C
450C
500C
530C
Treatment Steps
N
E
S
W
South
North
West
East
East Down
10 uG
South Down
1.000 uG

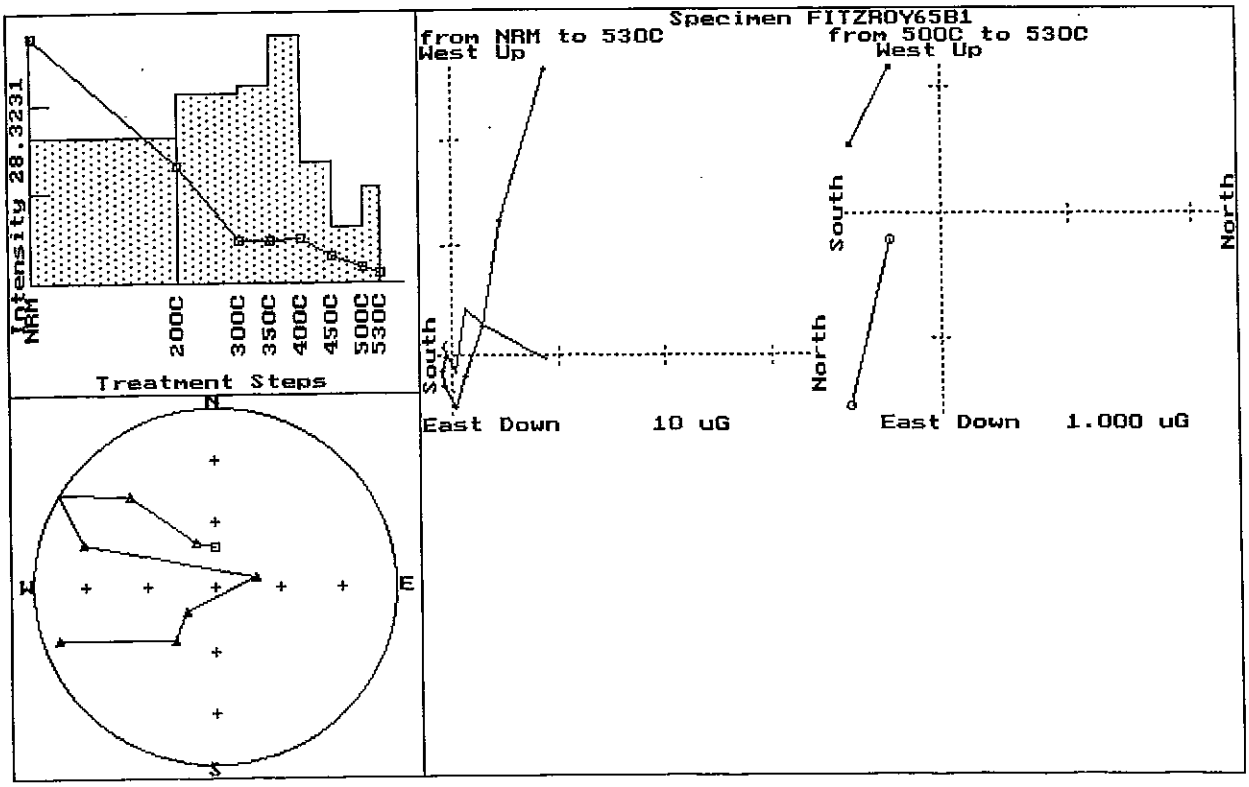
Specimen FITZROY65B1
from NRM to 530C
West Up
from 500C to 530C
West Up
Intensity 28.3231
NRM
200C
300C
350C
400C
450C
500C
530C
Treatment Steps
South
North
East Down
10 uG
East Down
1.000 uG
N
W
E
S

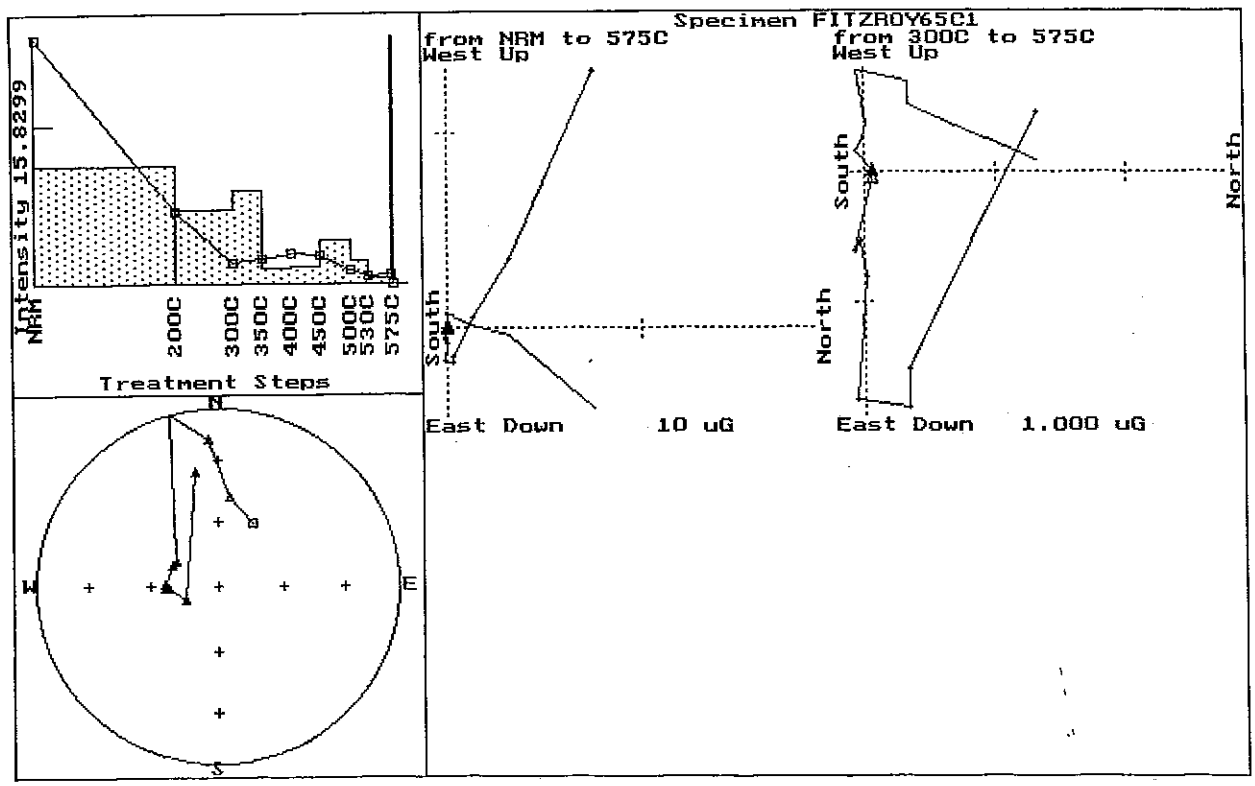
Specimen FITZROY65C1
from NRM to 575C
West Up
from 300C to 575C
West Up
Intensity 15.8299
NRM
200C
300C
350C
400C
450C
500C
530C
575C
Treatment Steps
South
North
East Down
10 uG
East Down
1.000 uG
N
W
E
S

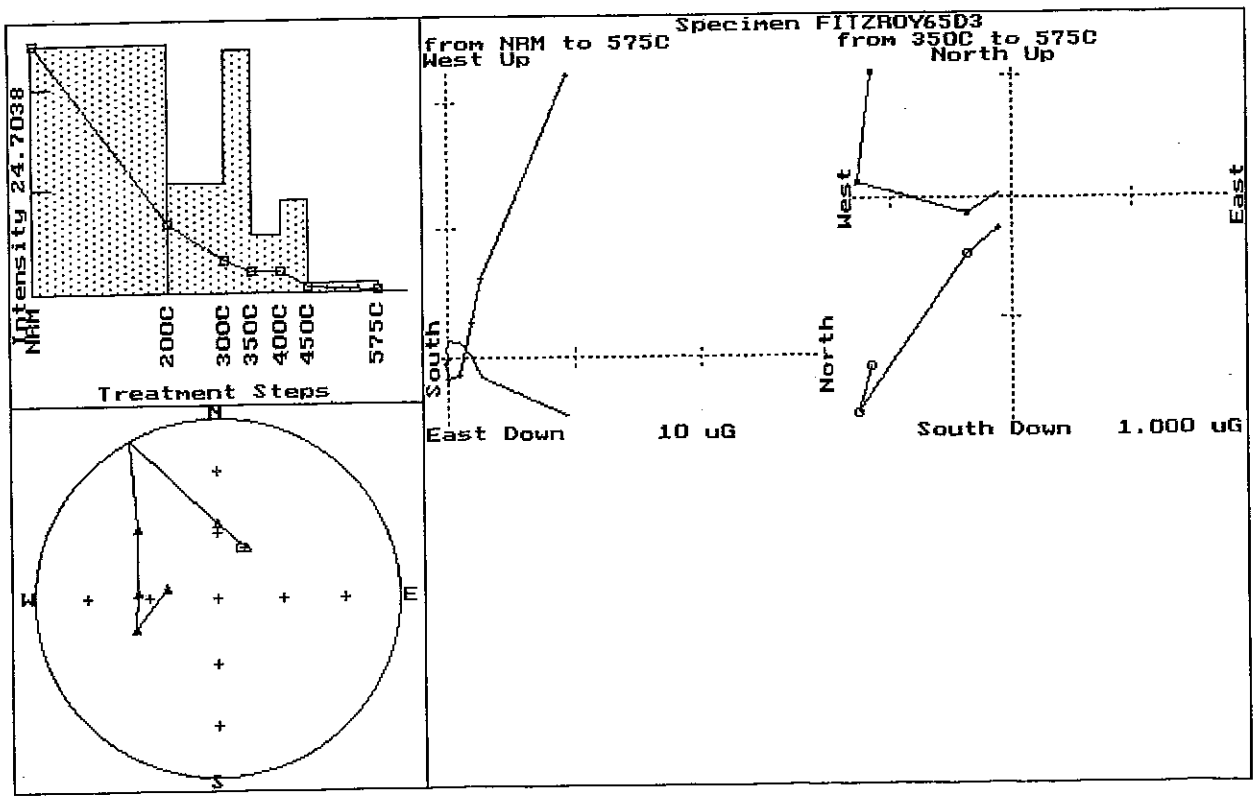
Intensity 24.7038
NRM
200C
300C
350C
400C
450C
575C
Treatment Steps
N
W
E
S
Specimen FITZROY65D3
from NRM to 575C
West Up
South
East Down
10 uG
from 350C to 575C
North Up
West
East
North
South Down
1.000 uG

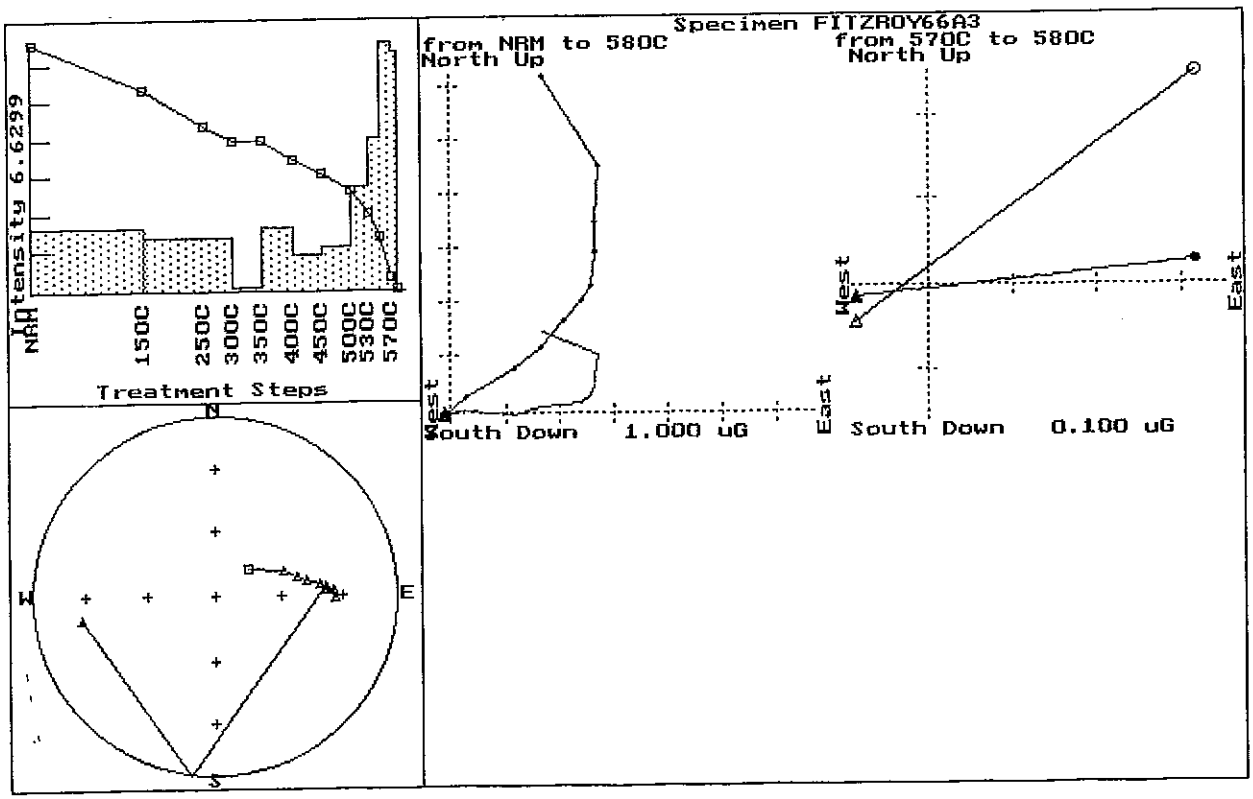
Intensity 6.6299
NRM
150C
250C
300C
350C
400C
450C
500C
530C
570C
Treatment Steps
N
W
E
S
Specimen FITZROY66A3
from NRM to 580C
North Up
West
South Down
1.000 uG
from 570C to 580C
North Up
West
East
South Down
0.100 uG

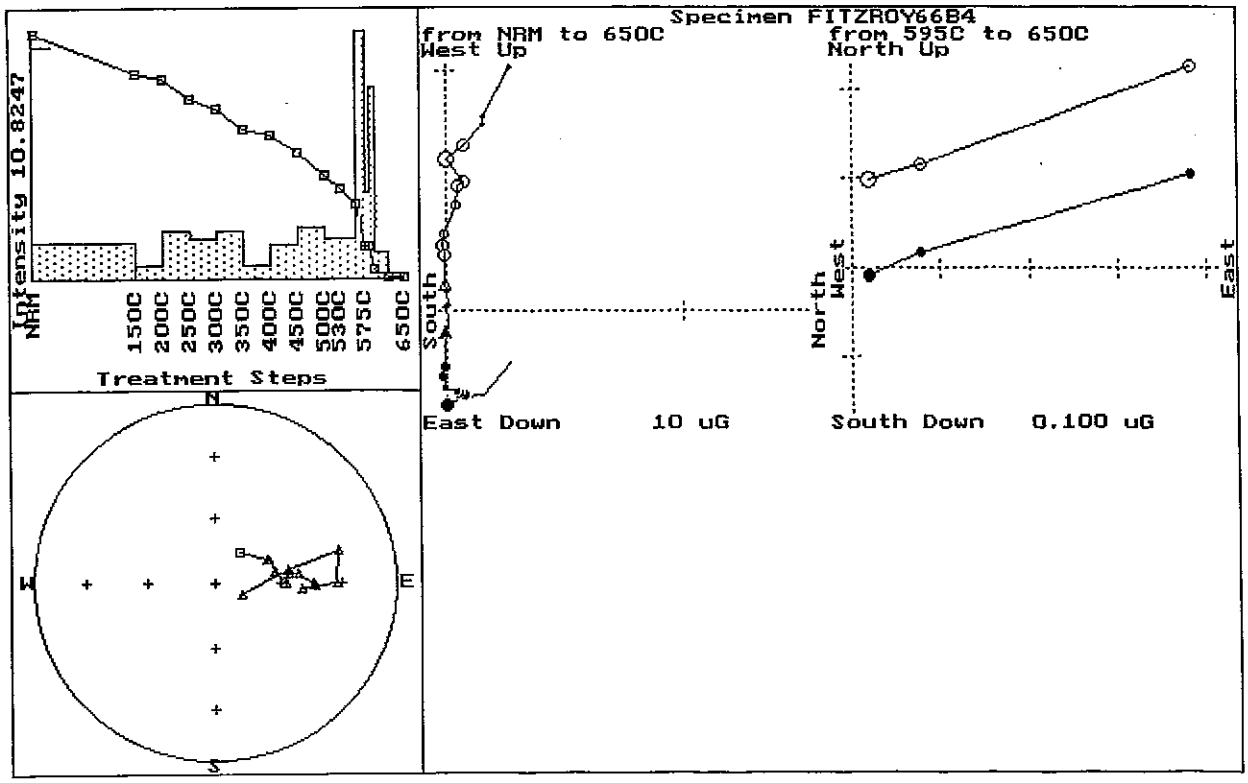
Specimen FITZROY66B4
from NRM to 650C
West Up
from 595C to 650C
North Up
Intensity 10.8247
NRM
150C 200C 250C 300C 350C 400C 450C 500C 530C 575C 650C
Treatment Steps
N
E
S
W
South
North
West
East
East Down 10 uG
South Down 0.100 uG

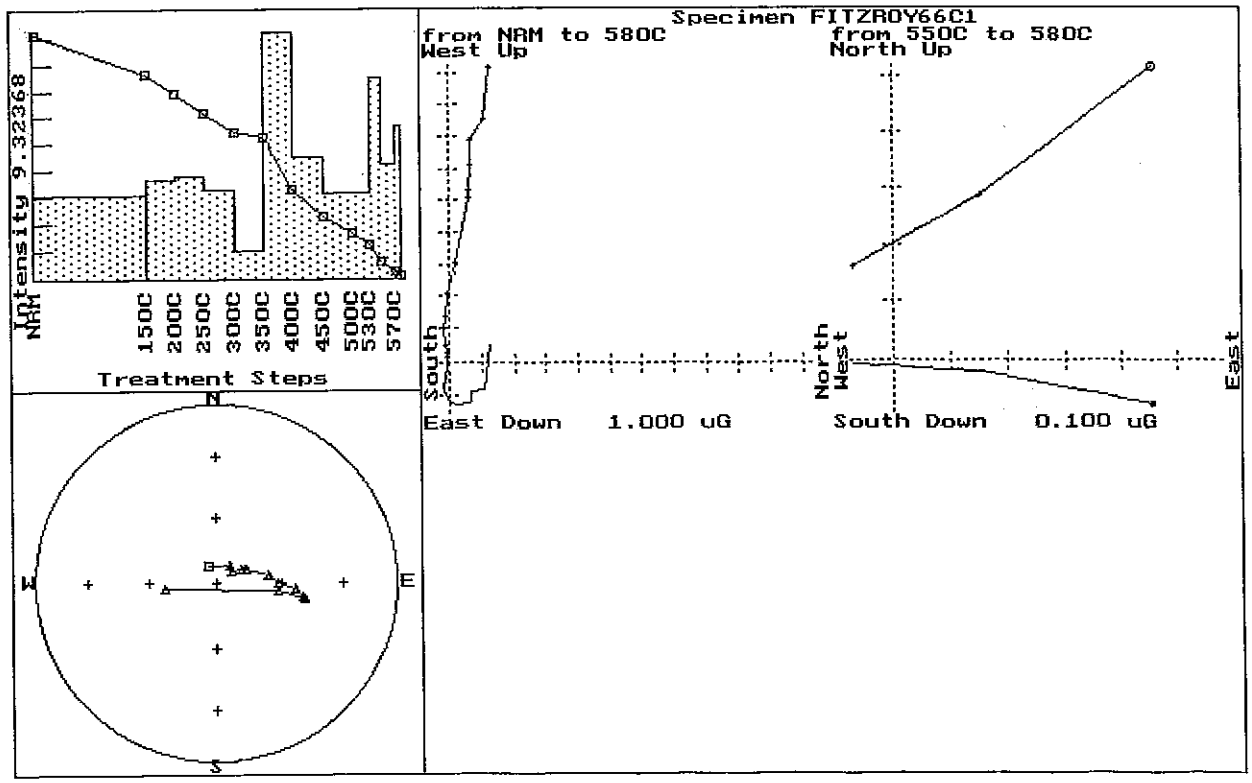
Specimen FITZROY66C1
from NRM to 580C
West Up
from 550C to 580C
North Up
Intensity 9.32368
NRM
150C 200C 250C 300C 350C 400C 450C 500C 530C 570C
Treatment Steps
N
E
S
W
South
North
West
East
East Down 1.000 uG
South Down 0.100 uG

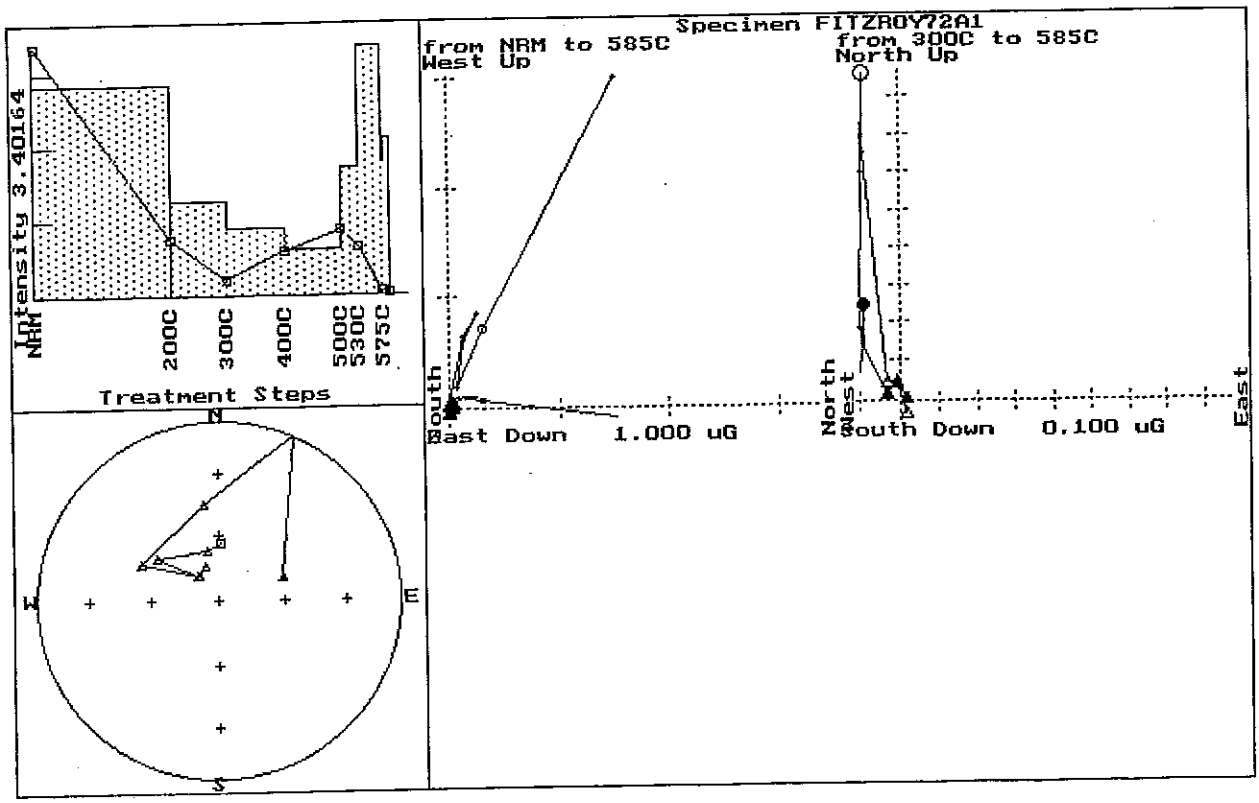
Intensity 3.40164
NRM
200C
300C
400C
500C
530C
575C
Treatment Steps
N
W
E
S
Specimen FITZROY72A1
from NRM to 585C
West Up
from 300C to 585C
North Up
South
East Down 1.000 uG
North
West
South Down 0.100 uG
East

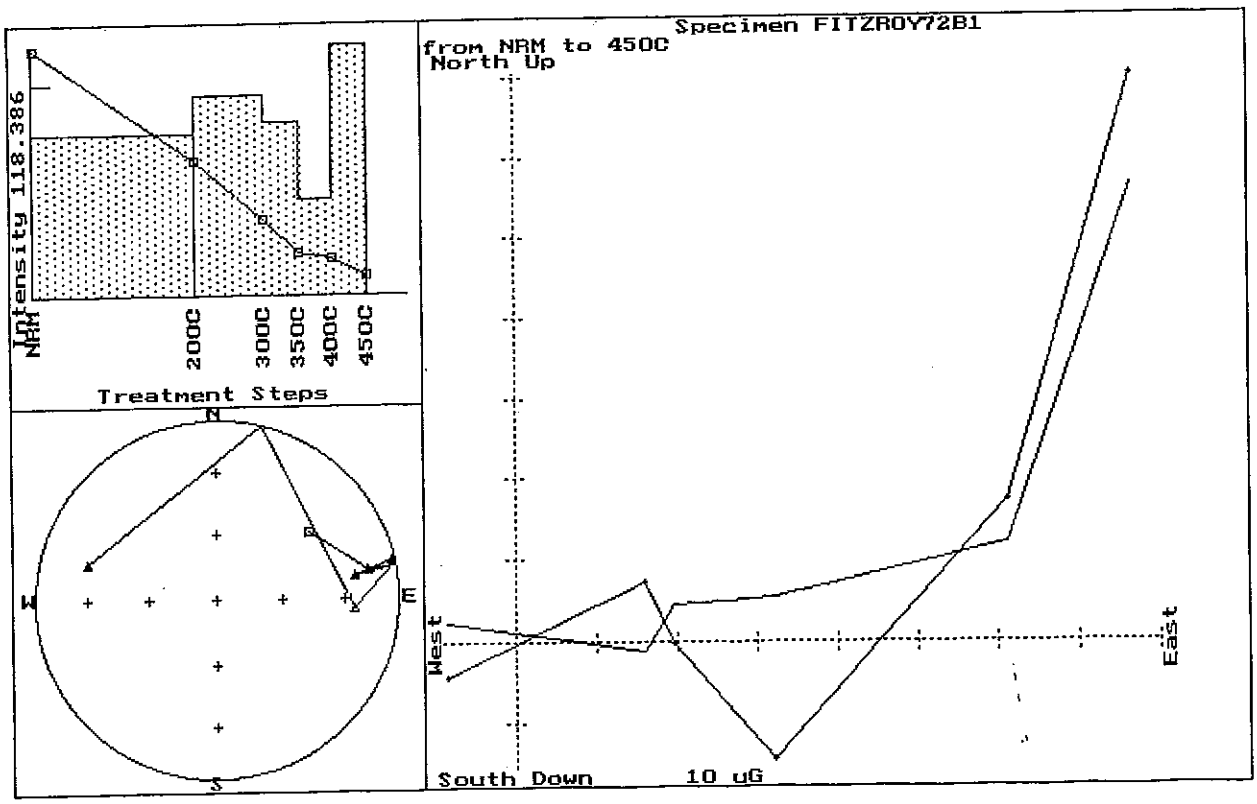
Intensity 118.386
NRM
200C
300C
350C
400C
450C
Treatment Steps
N
W
E
S
Specimen FITZROY72B1
from NRM to 450C
North Up
West
East
South Down 10 uG

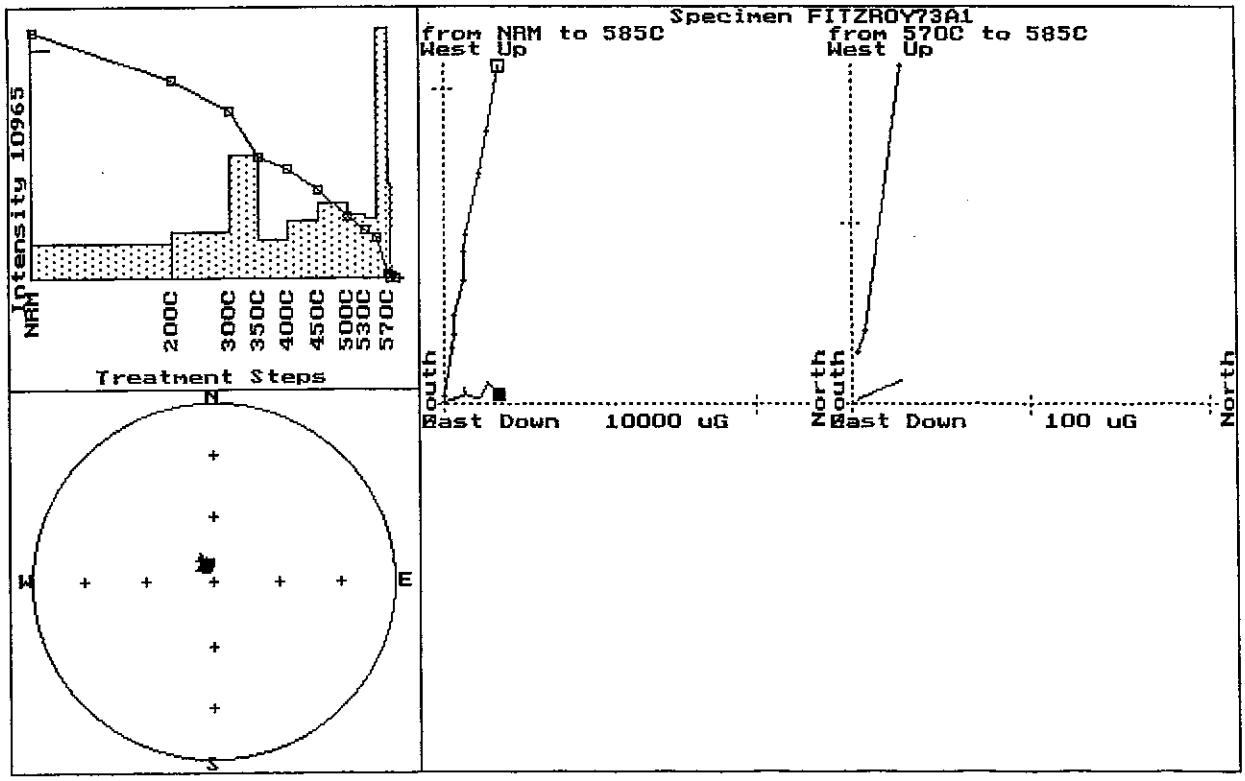
Specimen FITZROY73A1
from NRM to 585C
West Up
from 570C to 585C
West Up
Intensity 10965
NRM
200C
300C
350C
400C
450C
500C
530C
570C
Treatment Steps
N
W
E
S
South
East Down
10000 uG
North
South
East Down
100 uG
North

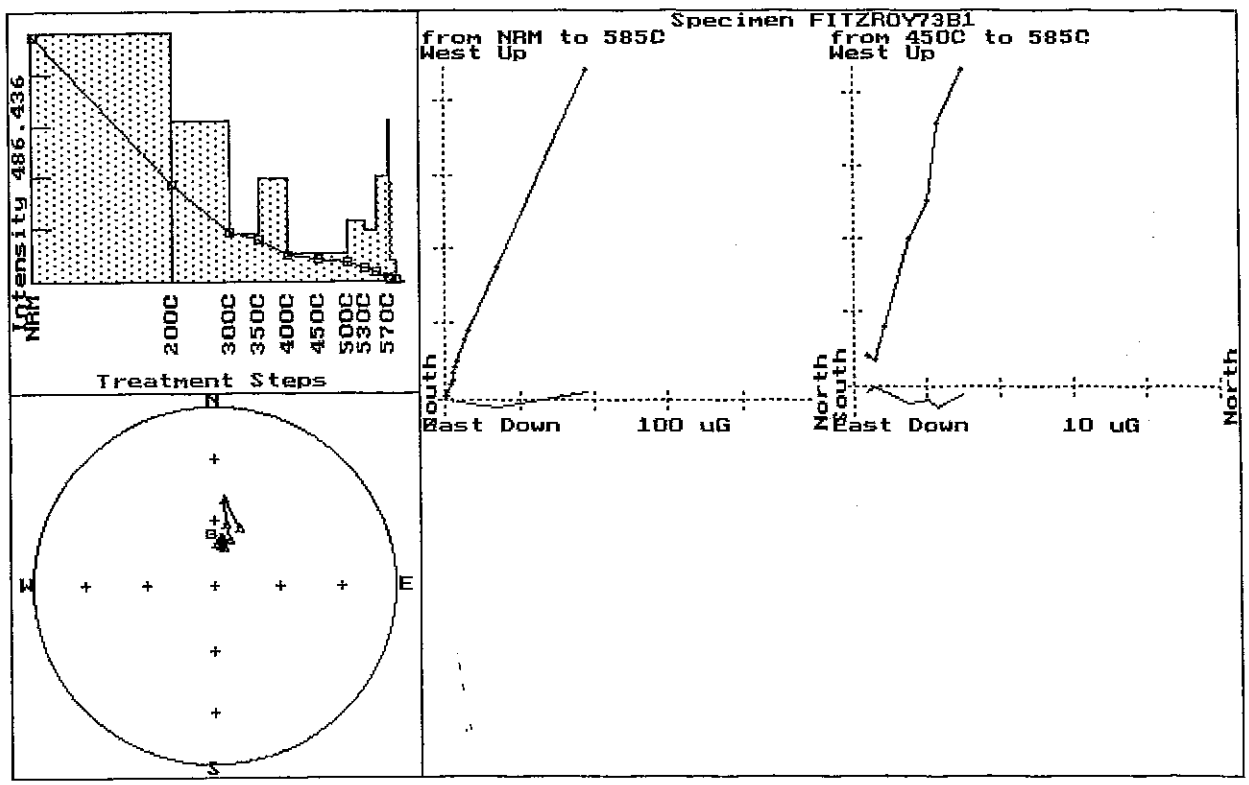
Specimen FITZROY73B1
from NRM to 585C
West Up
from 450C to 585C
West Up
Intensity 486.436
NRM
200C
300C
350C
400C
450C
500C
530C
570C
Treatment Steps
N
W
E
S
South
East Down
100 uG
North
South
East Down
10 uG
North

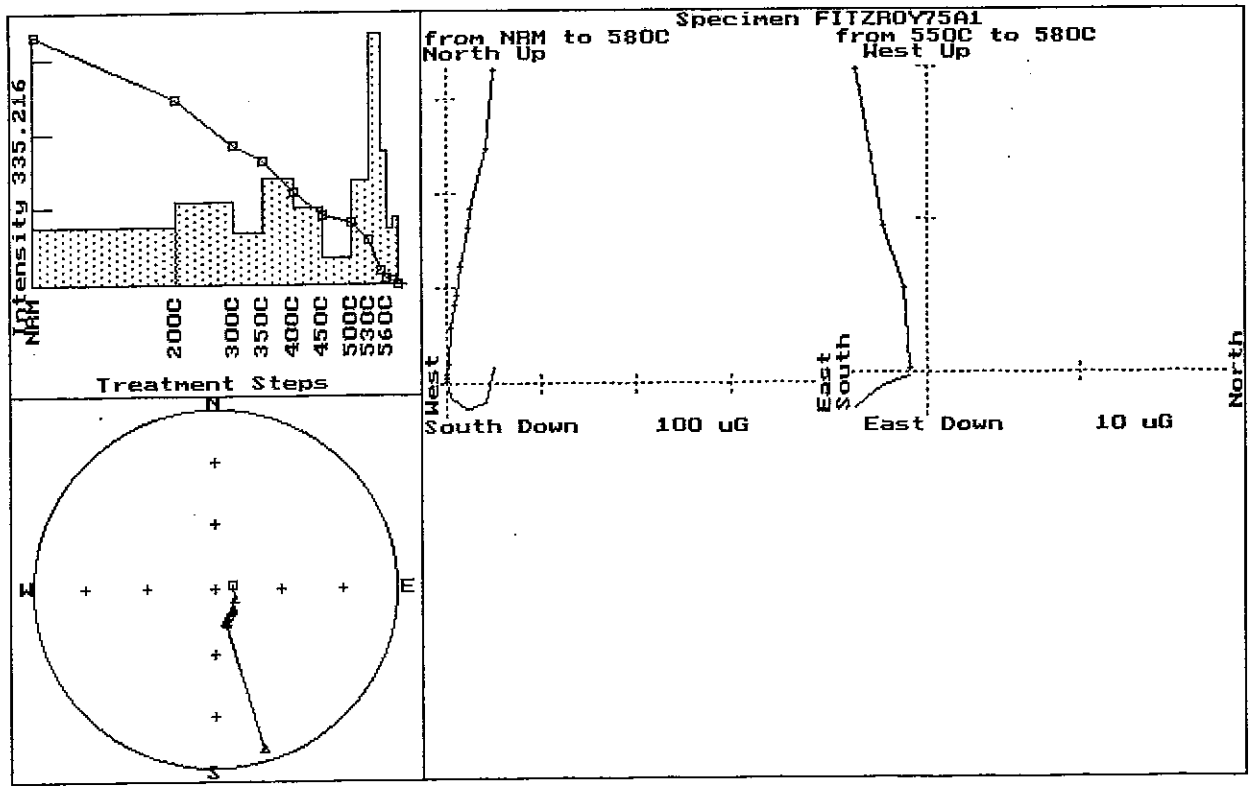
Specimen FITZROY75A1
from NRM to 580C
North Up
from 550C to 580C
West Up
Intensity 335.216
NRM
200C
300C
350C
400C
450C
500C
530C
560C
Treatment Steps
N
E
S
W
West
East
South
North
South Down
100 uG
East Down
10 uG

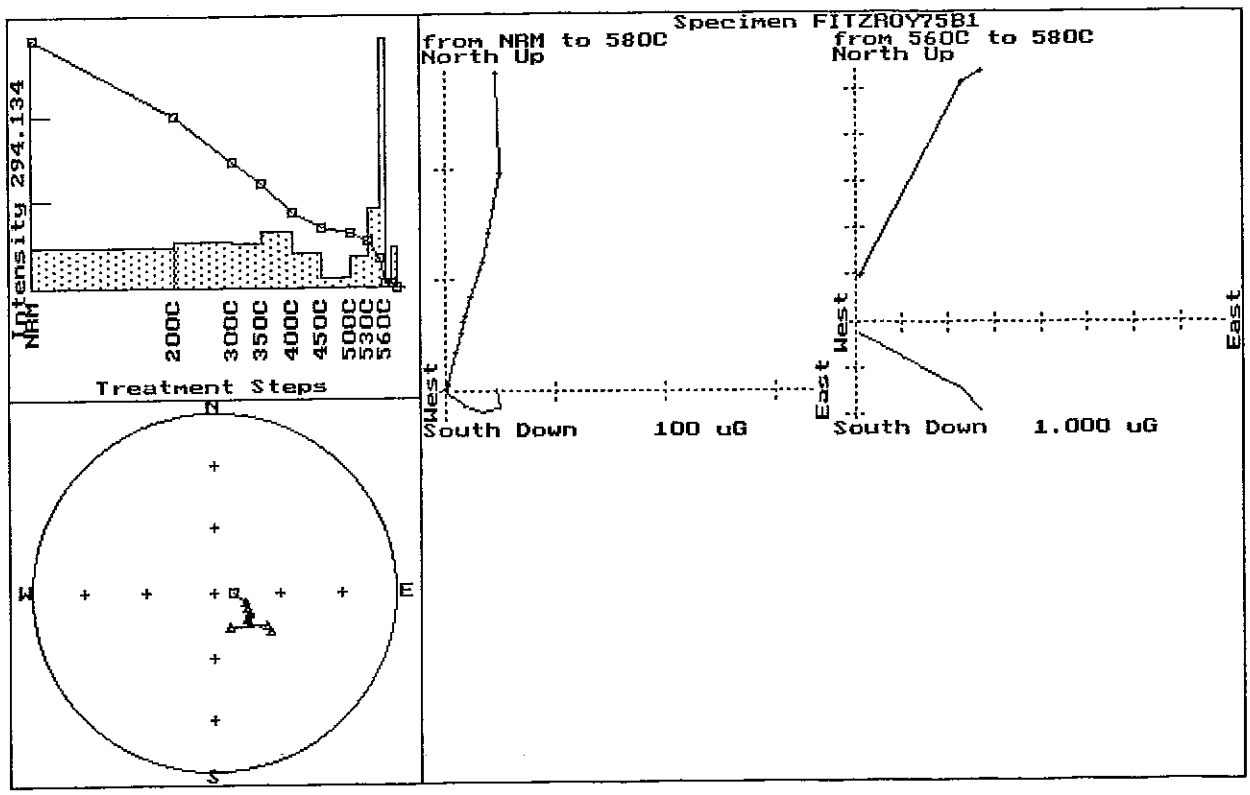
Specimen FITZROY75B1
from NRM to 580C
North Up
from 560C to 580C
North Up
Intensity 294.134
NRM
200C
300C
350C
400C
450C
500C
530C
560C
Treatment Steps
N
E
S
W
West
East
South Down
100 uG
South Down
1.000 uG

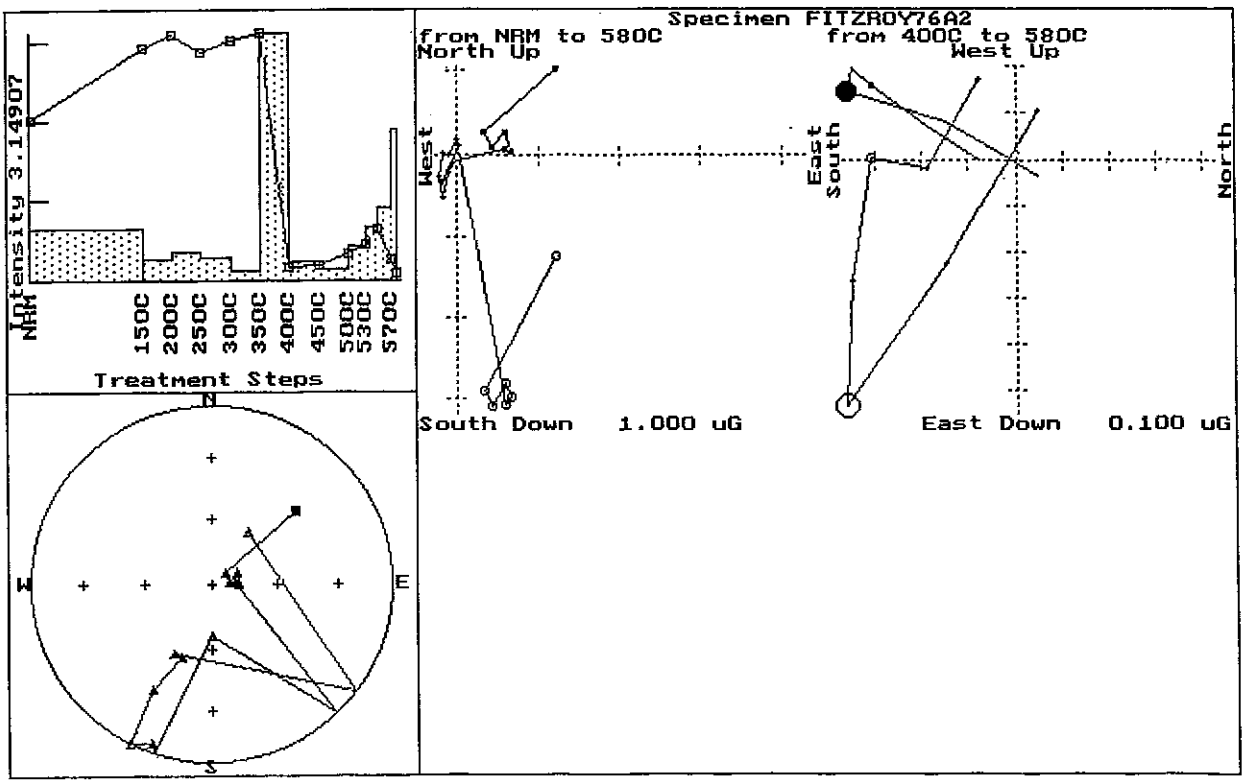
Intensity 3.14907
NRM
150C
200C
250C
300C
350C
400C
450C
500C
530C
570C
Treatment Steps
N
W
E
S
Specimen FITZROY76A2
from NRM to 580C
North Up
West
East
South
from 400C to 580C
West Up
North
South Down 1.000 uG
East Down 0.100 uG

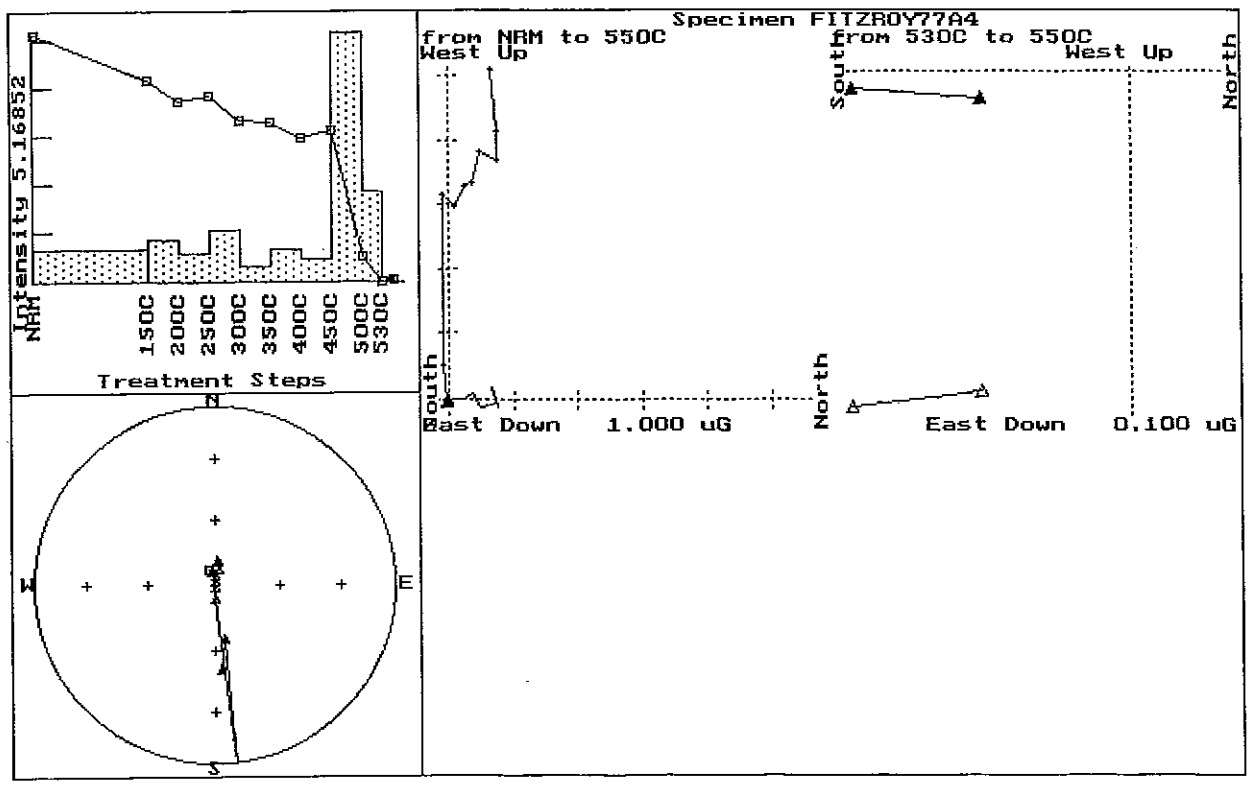
Intensity 5.16852
NRM
150C
200C
250C
300C
350C
400C
450C
500C
530C
Treatment Steps
N
W
E
S
Specimen FITZROY77A4
from NRM to 550C
West Up
South
East
from 530C to 550C
West Up
South
North
East Down 1.000 uG
East Down 0.100 uG

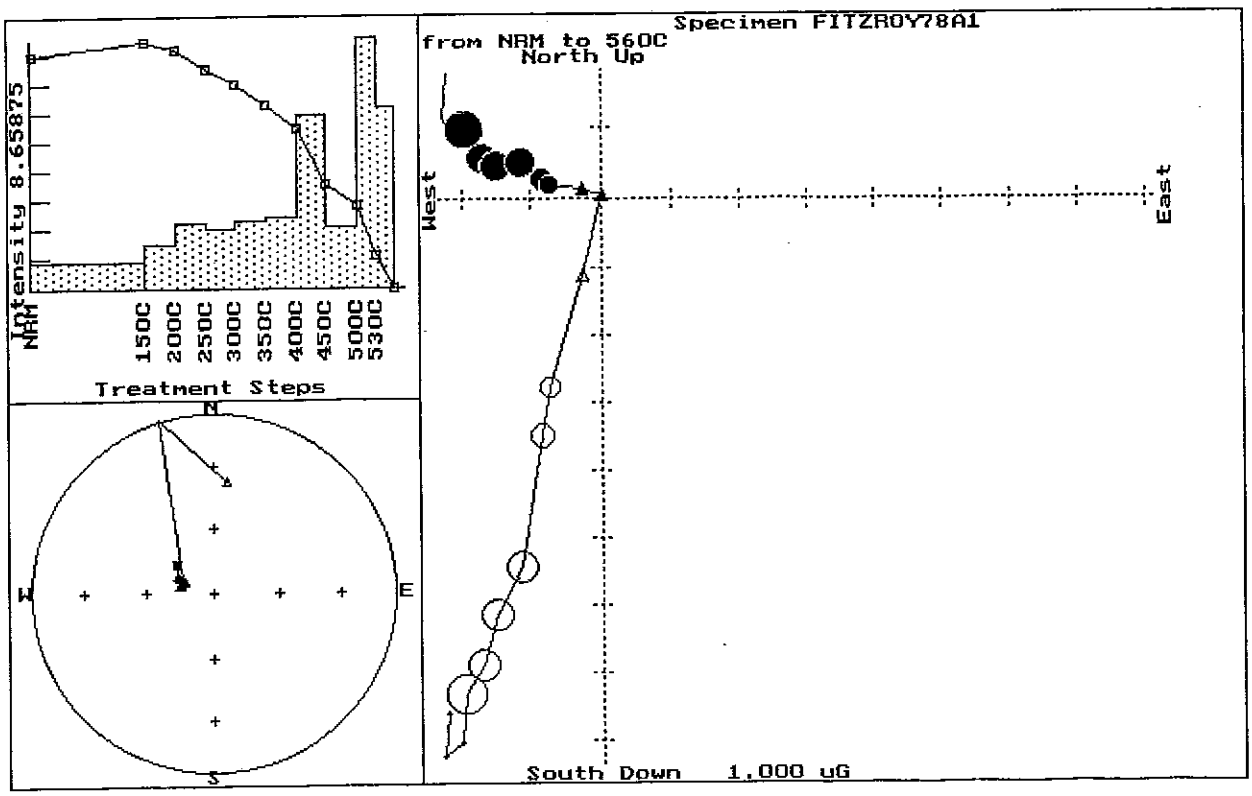
Specimen FITZROY78A1
from NRM to 560C
North Up
Intensity 8.65875
NRM
150C 200C 250C 300C 350C 400C 450C 500C 530C
Treatment Steps
N
W
E
S
West
East
South Down 1,000 uG

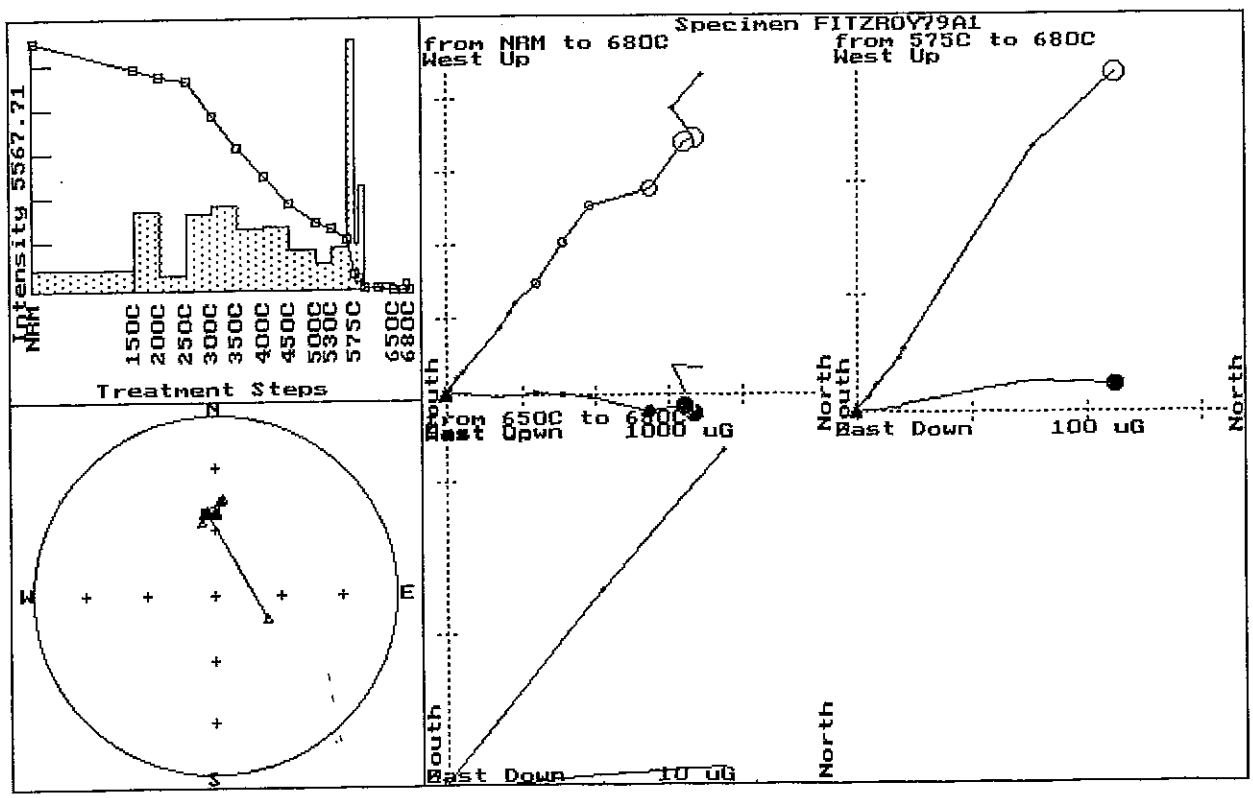
Specimen FITZROY79A1
from NRM to 680C
West Up
from 575C to 680C
West Up
Intensity 5567.71
NRM
150C 200C 250C 300C 350C 400C 450C 500C 530C 575C 650C 680C
Treatment Steps
N
W
E
S
South
North
East Down 1000 uG
East Down 100 uG
East Down 10 uG

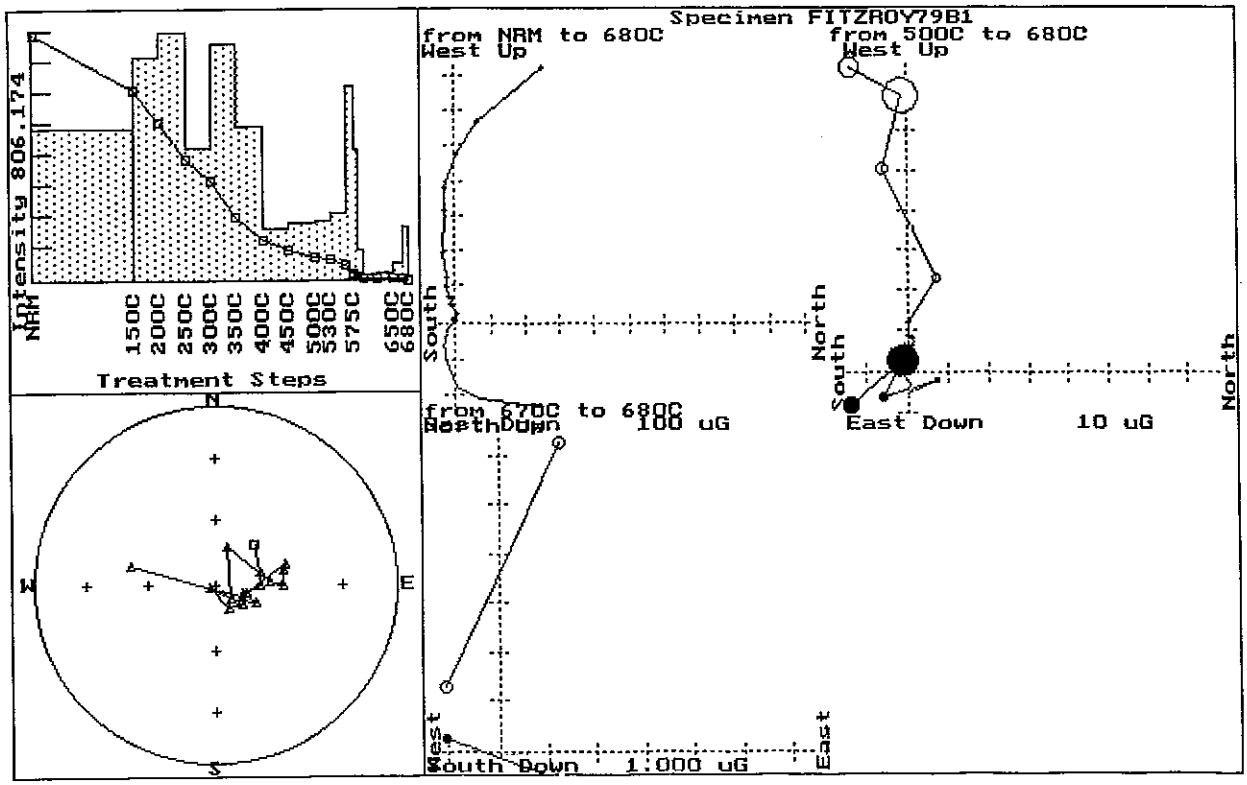
Intensity 806.174
NRM
150C
200C
250C
300C
350C
400C
450C
500C
530C
575C
650C
680C
Treatment Steps
N
W
E
S
Specimen FITZROY79B1
from NRM to 680C
West Up
South
North
from 500C to 680C
West Up
South
North
from 570C to 680C
North Down
100 uG
East Down
10 uG
West
East
South Down
1.000 uG

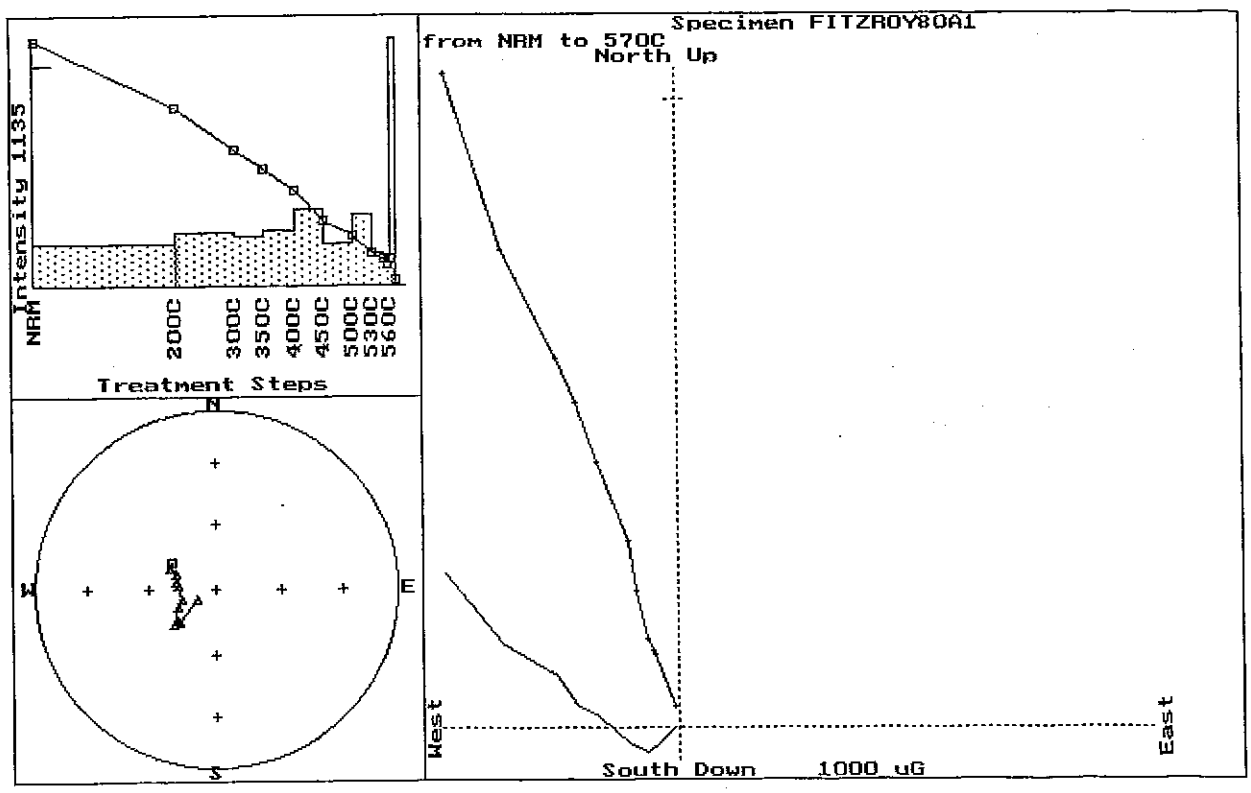
Intensity 1135
NRM
200C
300C
350C
400C
450C
500C
530C
560C
Treatment Steps
N
W
E
S
Specimen FITZROY80A1
from NRM to 570C
North Up
West
East
South Down
1000 uG

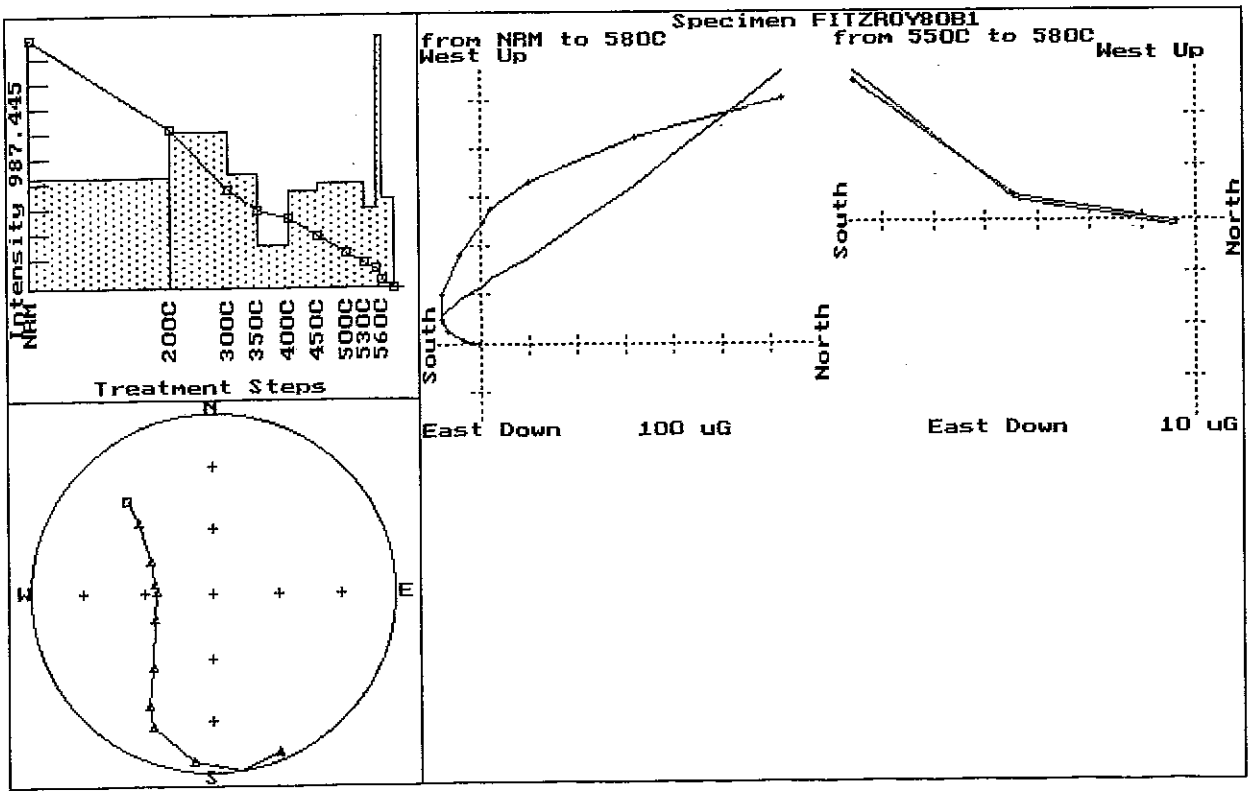
Intensity 987.445
NRM
200C
300C
350C
400C
450C
500C
530C
560C
Treatment Steps
N
W
E
S
Specimen FITZROY80B1
from NRM to 580C
West Up
South
North
East Down
100 uG
from 550C to 580C
West Up
South
North
East Down
10 uG

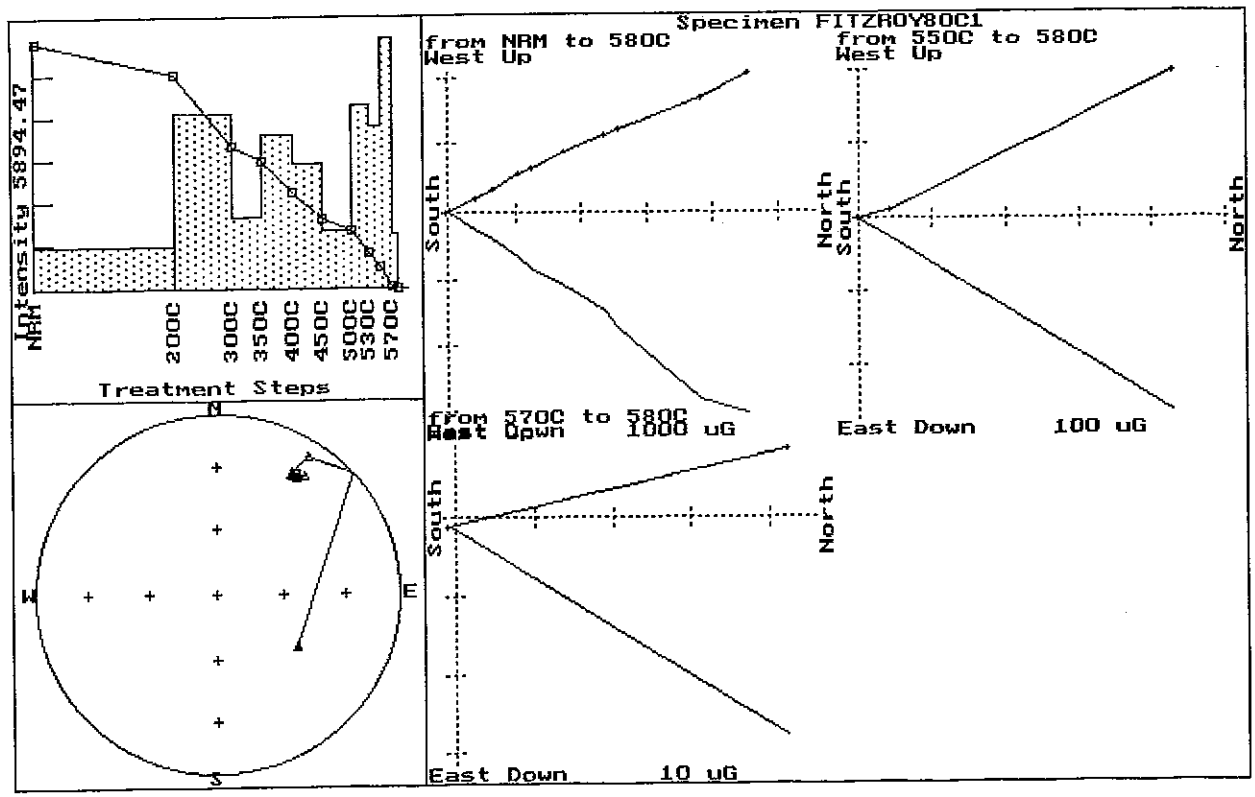
Intensity 5894.47
NRM
200C
300C
350C
400C
450C
500C
530C
570C
Treatment Steps
N
W
E
S
Specimen FITZROY80C1
from NRM to 580C
West Up
South
North
East Down
100 uG
from 550C to 580C
West Up
North
South
North
from 570C to 580C
West Down
1000 uG
South
North
East Down
10 uG

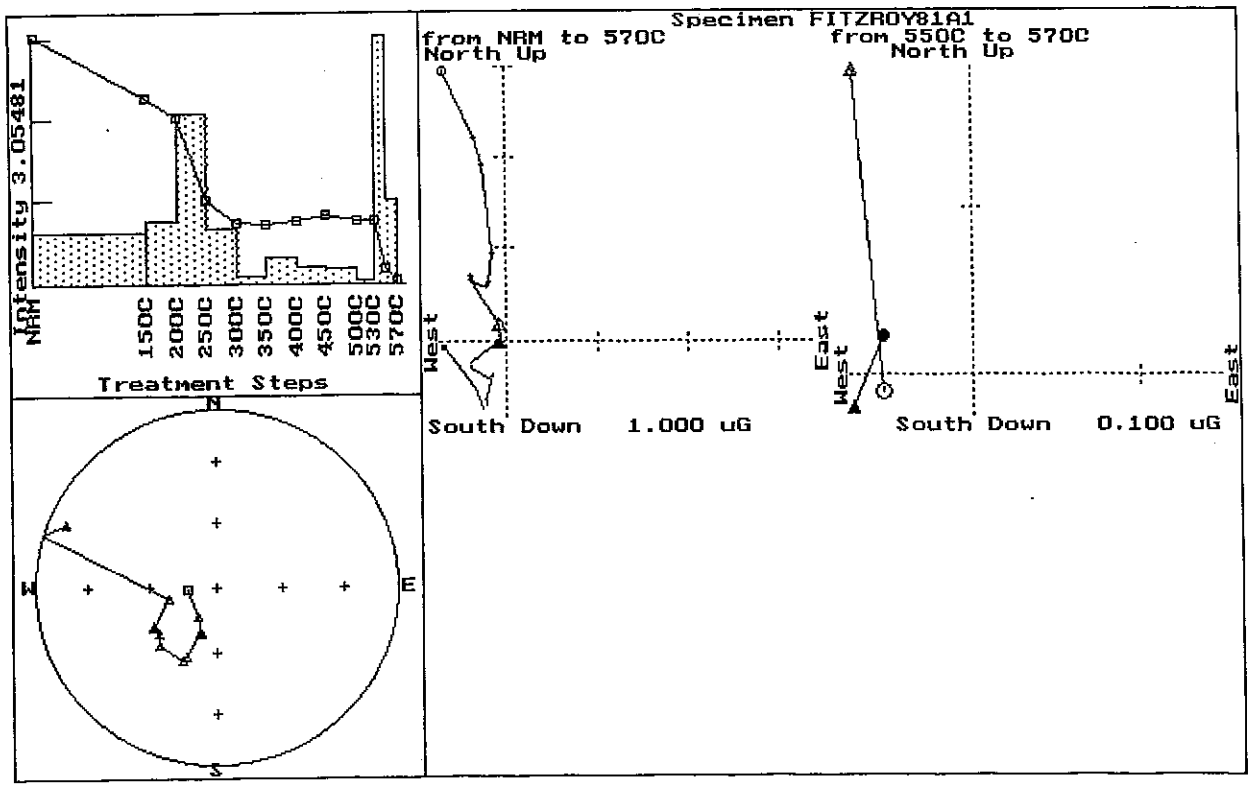
Intensity 3.05481
NRM
150C
200C
250C
300C
350C
400C
450C
500C
530C
570C
Treatment Steps
N
E
S
W
Specimen FITZROY81A1
from NRM to 570C
North Up
West
East
South Down 1.000 uG
from 550C to 570C
North Up
West
East
South Down 0.100 uG

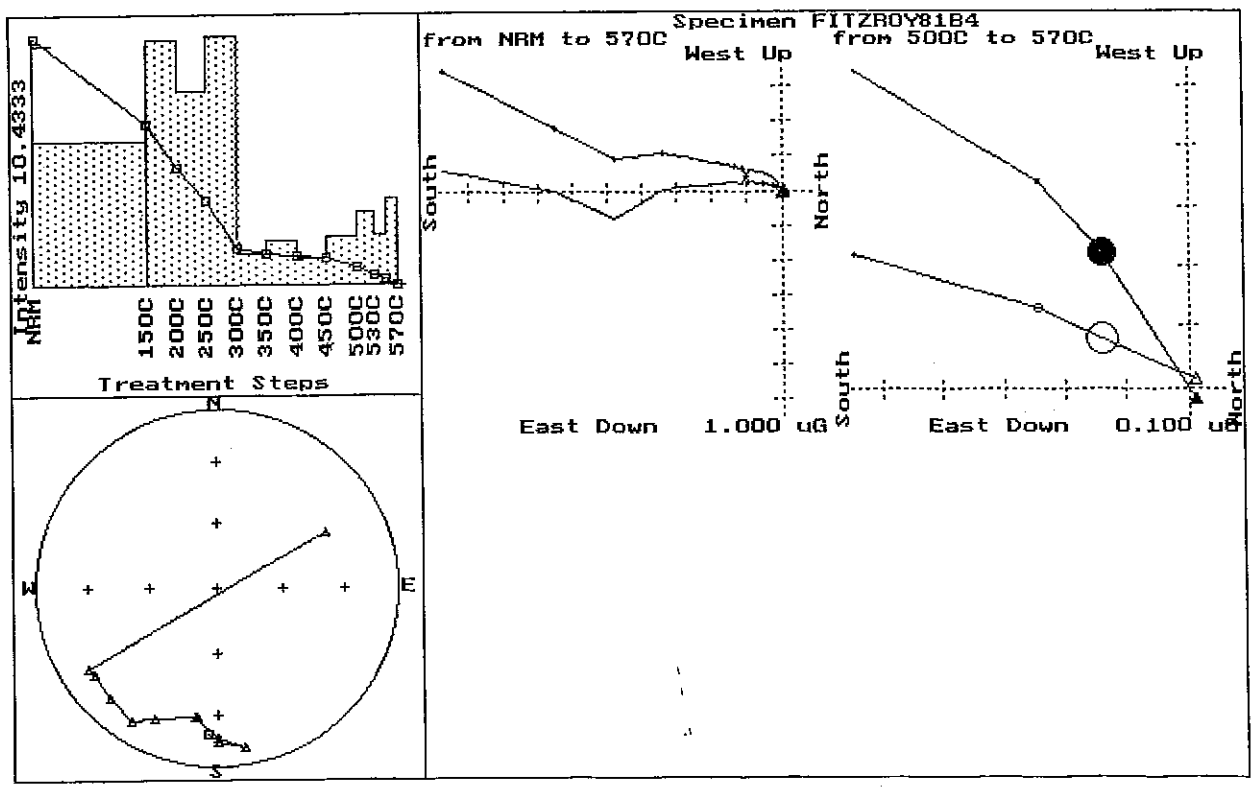
Intensity 10.4333
NRM
150C
200C
250C
300C
350C
400C
450C
500C
530C
570C
Treatment Steps
N
E
S
W
Specimen FITZROY81B4
from NRM to 570C
West Up
South
North
East Down 1.000 uG
from 500C to 570C
West Up
South
North
East Down 0.100 uG

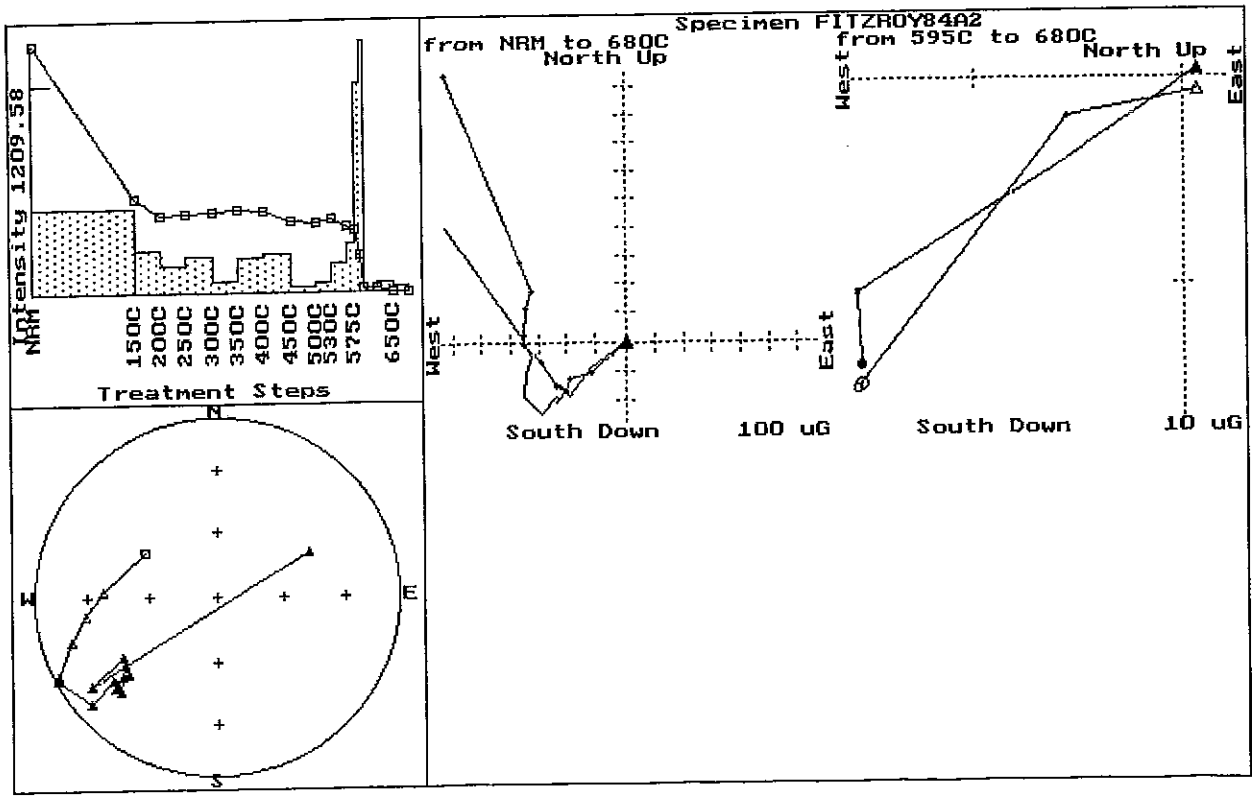
Specimen FITZROY84A2
from NRM to 680C
North Up
from 595C to 680C
North Up
Intensity 1209.58
NRM
150C
200C
250C
300C
350C
400C
450C
500C
530C
575C
650C
Treatment Steps
West
East
South Down
100 uG
South Down
10 uG

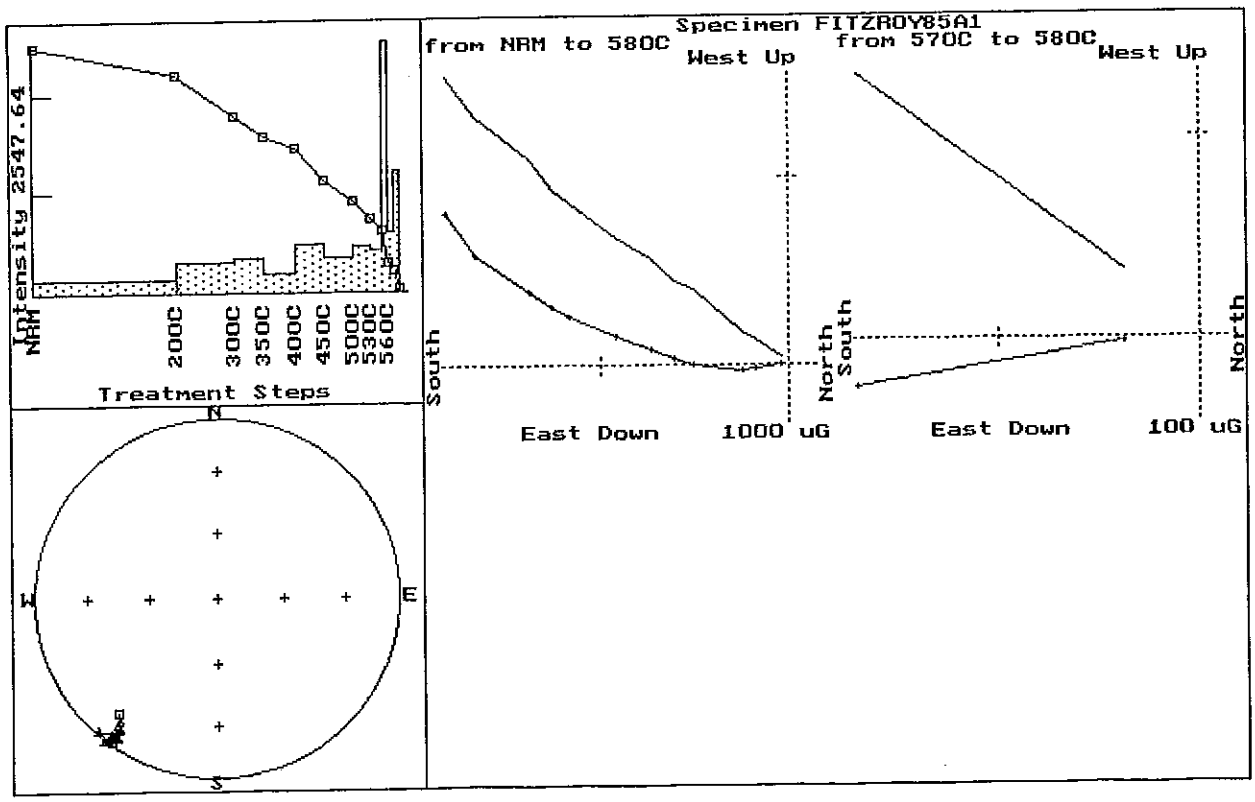
Specimen FITZROY85A1
from NRM to 580C
West Up
from 570C to 580C
West Up
Intensity 2547.64
NRM
200C
300C
350C
400C
450C
500C
530C
560C
Treatment Steps
South
North
East Down
1000 uG
East Down
100 uG

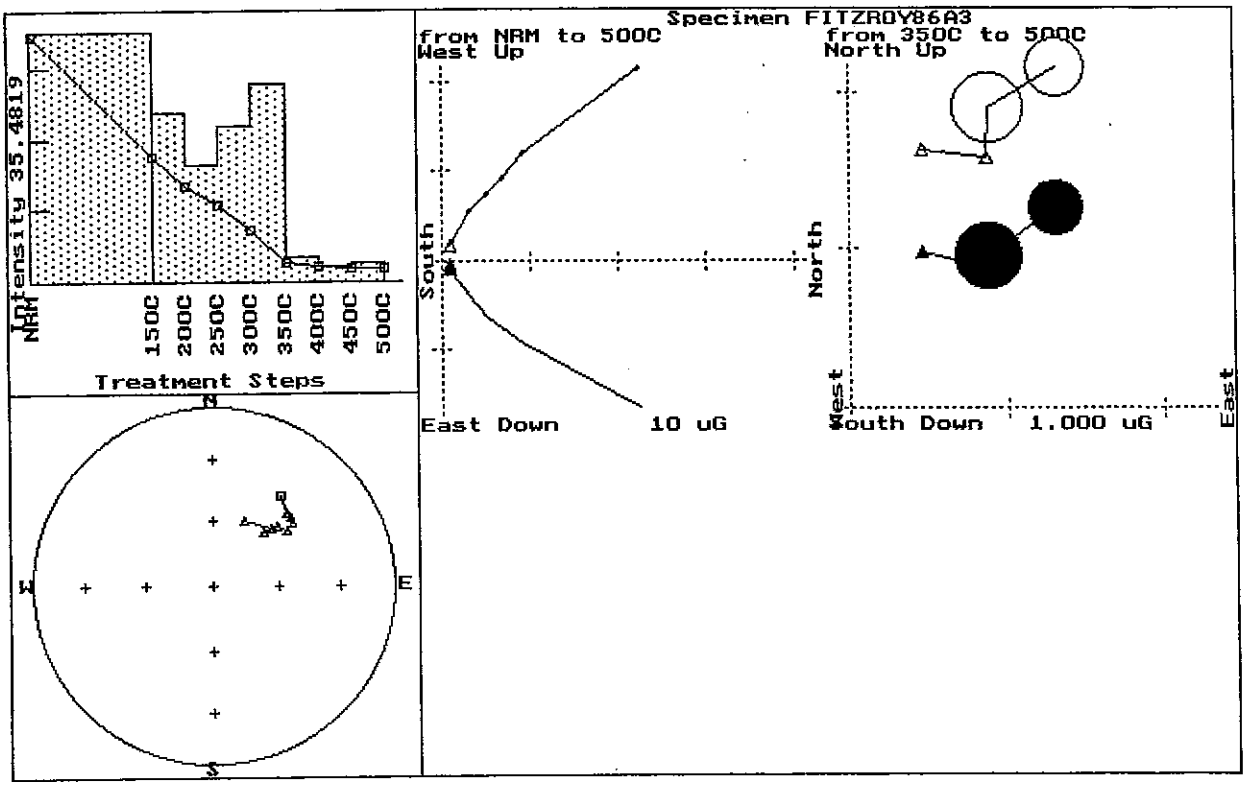
Specimen FITZROY86A3
from NRM to 500C
West Up
from 350C to 500C
North Up
Intensity 35.4819
NRM
150C 200C 250C 300C 350C 400C 450C 500C
Treatment Steps
N
E
S
W
South
North
West
East
East Down 10 uG
South Down 1.000 uG

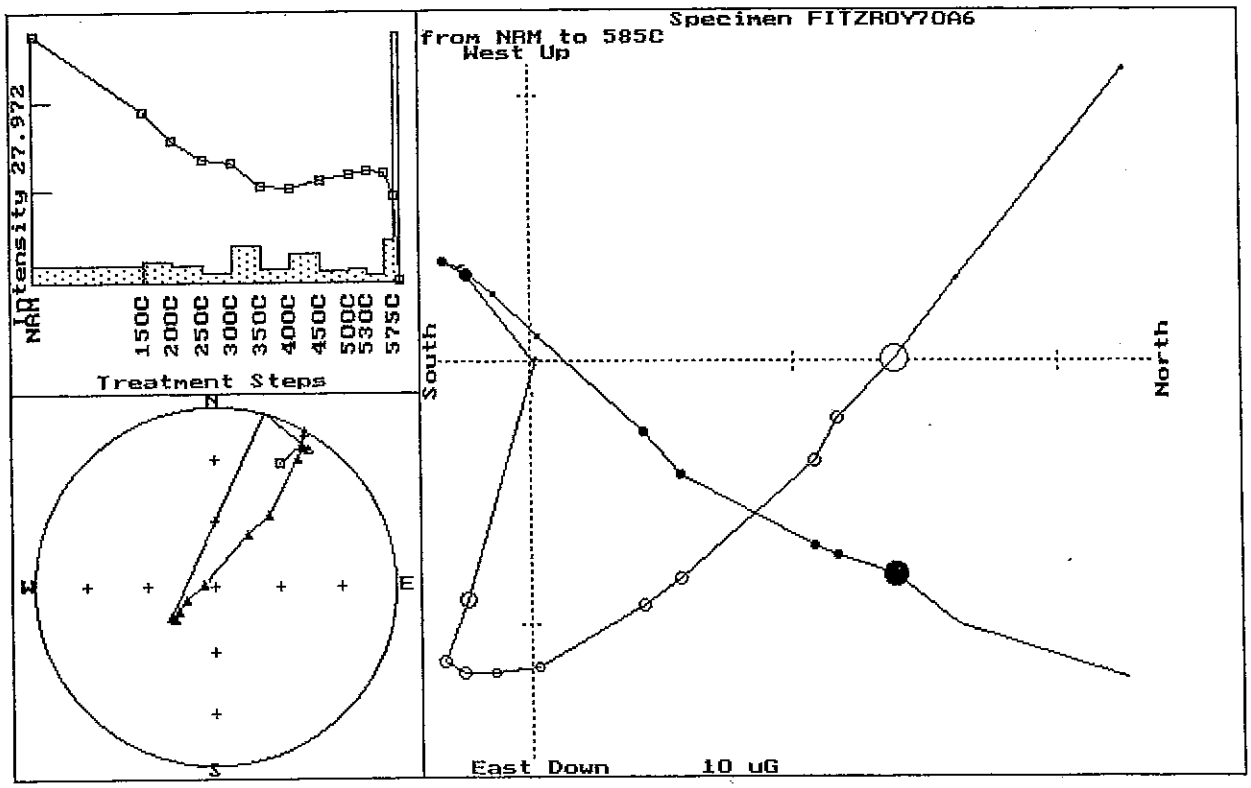
Specimen FITZROY70A6
from NRM to 585C
West Up
Intensity 27.972
NRM
150C 200C 250C 300C 350C 400C 450C 500C 530C 575C
Treatment Steps
N
E
S
W
South
North
East Down 10 uG

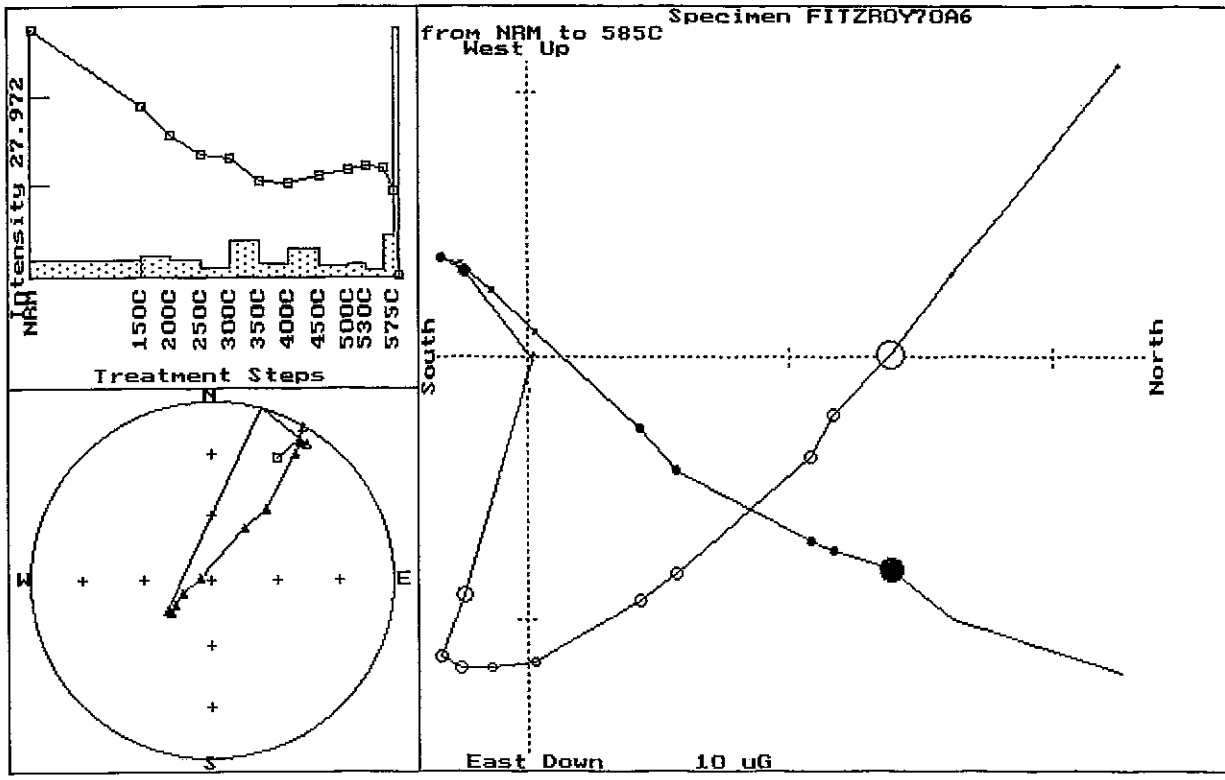
Specimen FITZROY70A6
from NRM to 585C
West Up
Intensity 27.972
NRM
150C
200C
250C
300C
350C
400C
450C
500C
530C
575C
Treatment Steps
N
W
E
S
South
North
East Down
10 uG

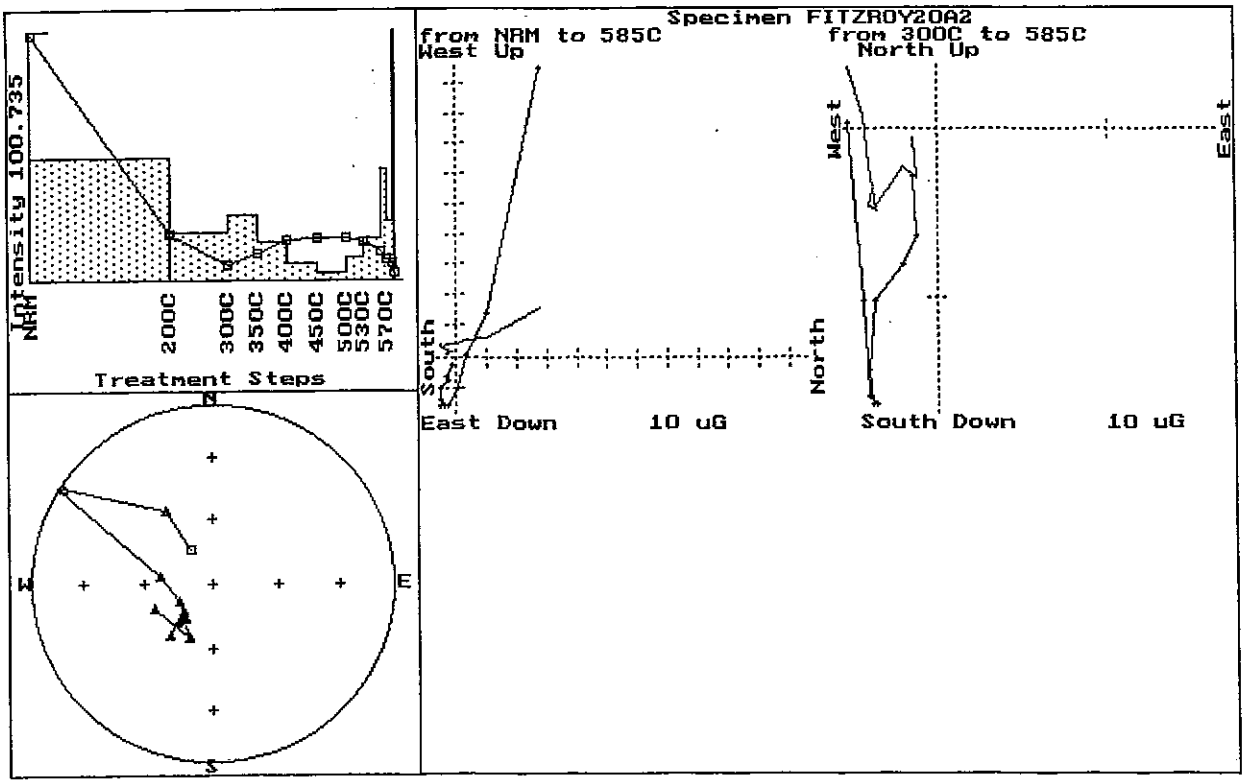
Specimen FITZROY20A2
from NRM to 585C
West Up
from 300C to 585C
North Up
Intensity 100.735
NRM
200C
300C
350C
400C
450C
500C
530C
570C
Treatment Steps
West
East
South
North
East Down
10 uG
South Down
10 uG

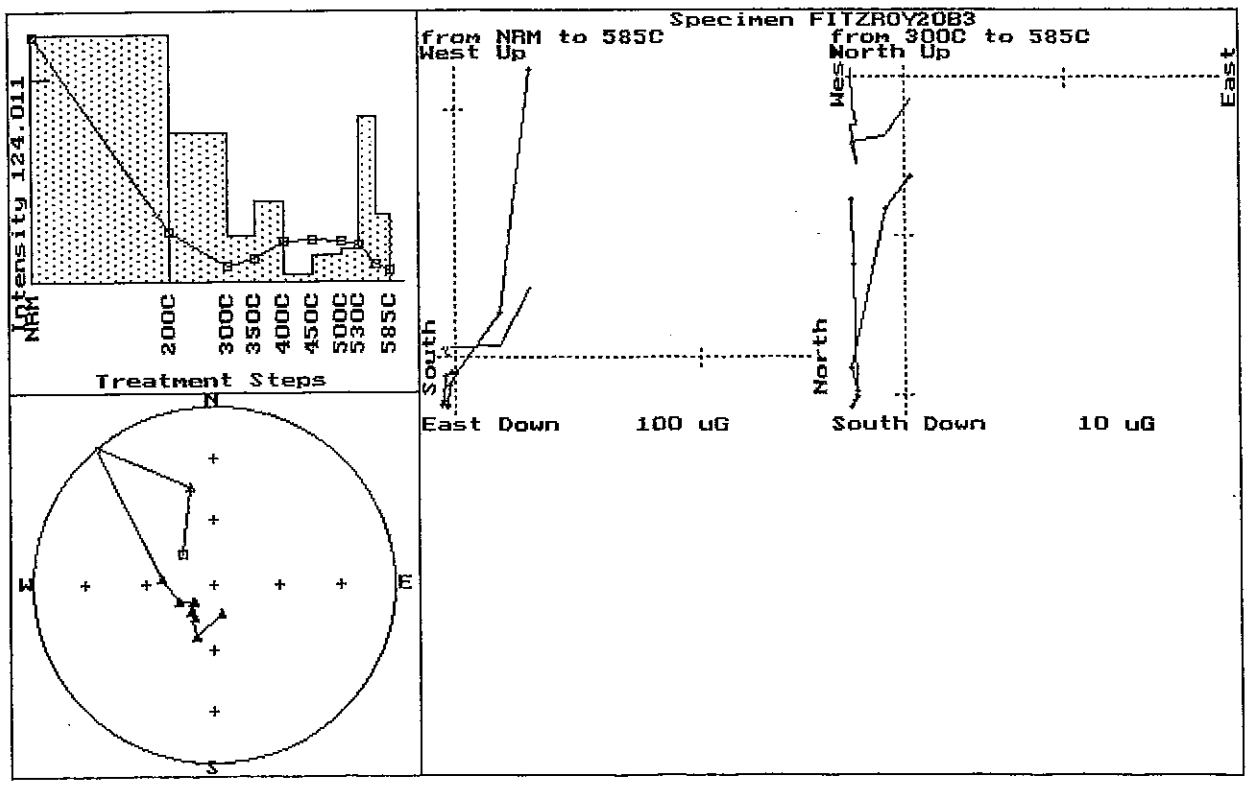
Specimen FITZROY20B3
from NRM to 585C
West Up
from 300C to 585C
North Up
Intensity 124.011
NRM
200C
300C
350C
400C
450C
500C
530C
585C
Treatment Steps
West
East
South
North
East Down
100 uG
South Down
10 uG

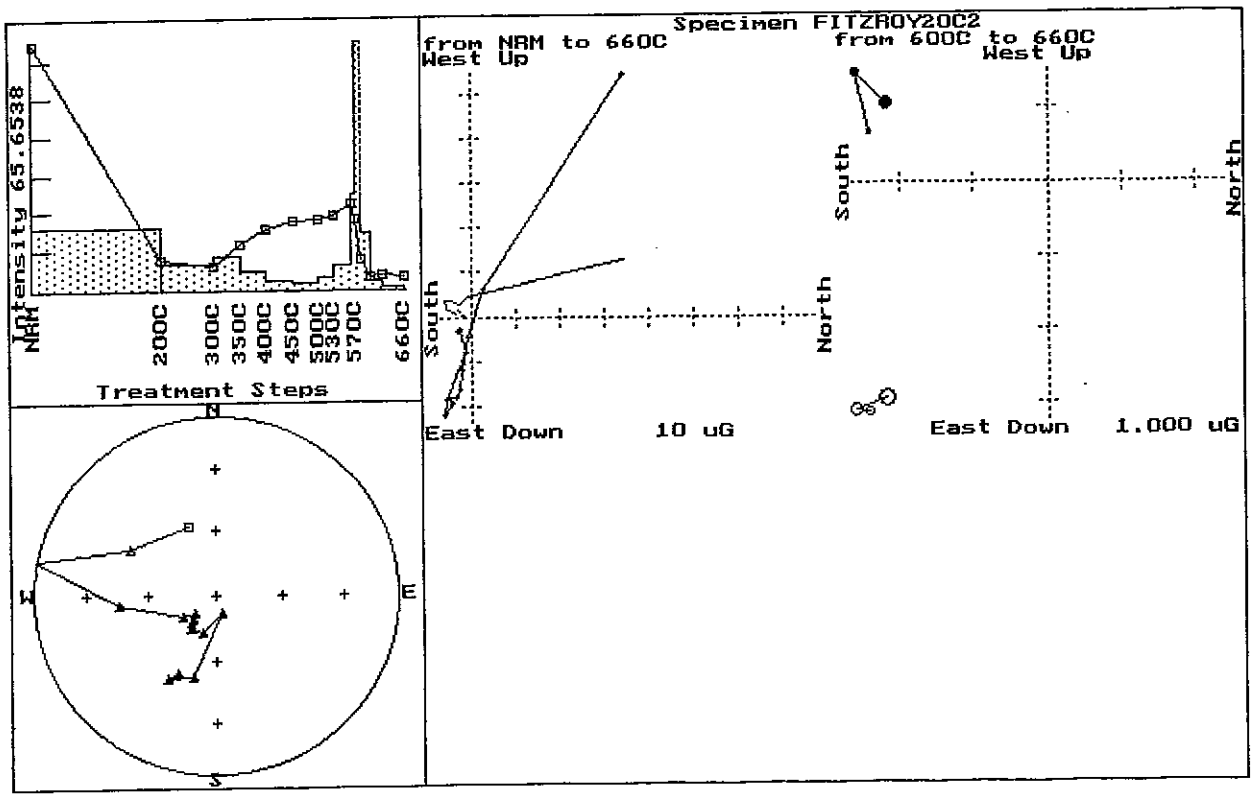
Intensity 65.6538
NRM
200C
300C
350C
400C
450C
500C
530C
570C
660C
Treatment Steps
N
E
S
W
Specimen FITZROY20C2
from NRM to 660C
West Up
South
North
East Down
10 uG
from 600C to 660C
West Up
South
North
East Down
1.000 uG

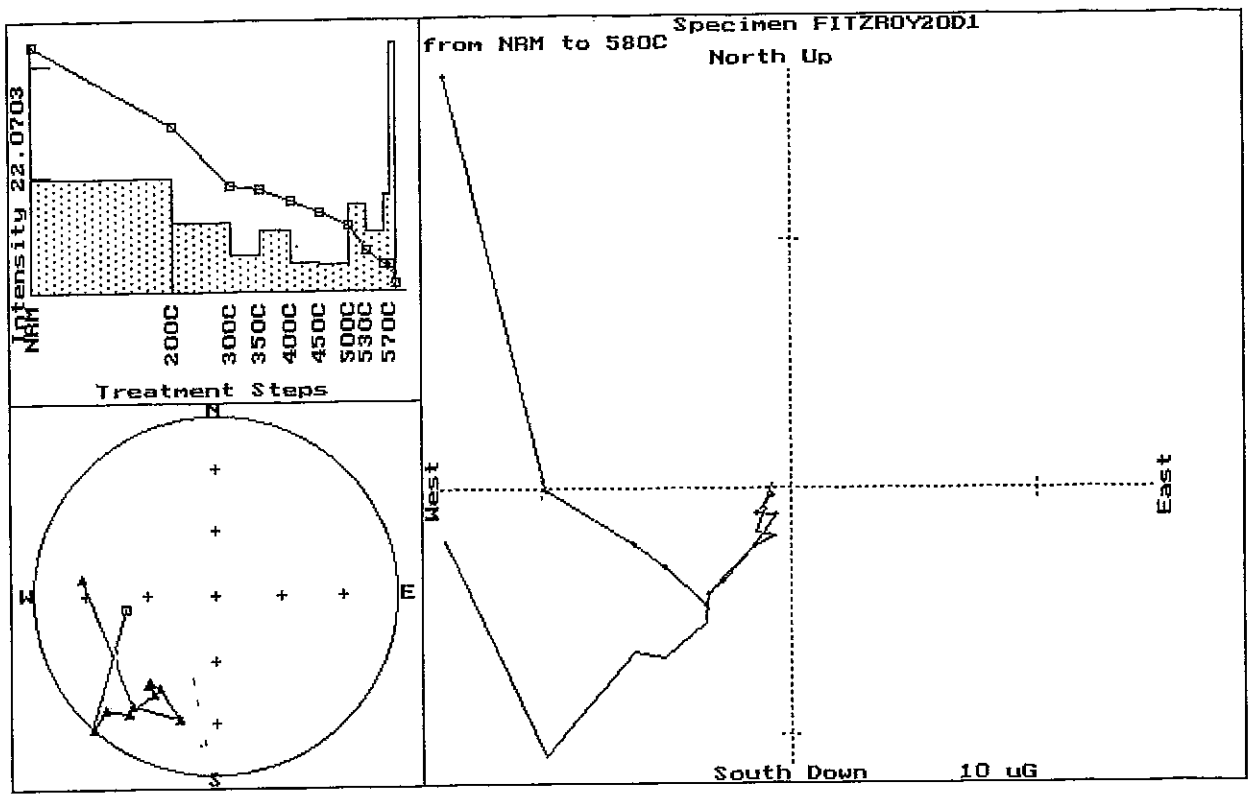
Intensity 22.0703
NRM
200C
300C
350C
400C
450C
500C
530C
570C
Treatment Steps
N
E
S
W
Specimen FITZROY20D1
from NRM to 580C
North Up
West
East
South Down
10 uG

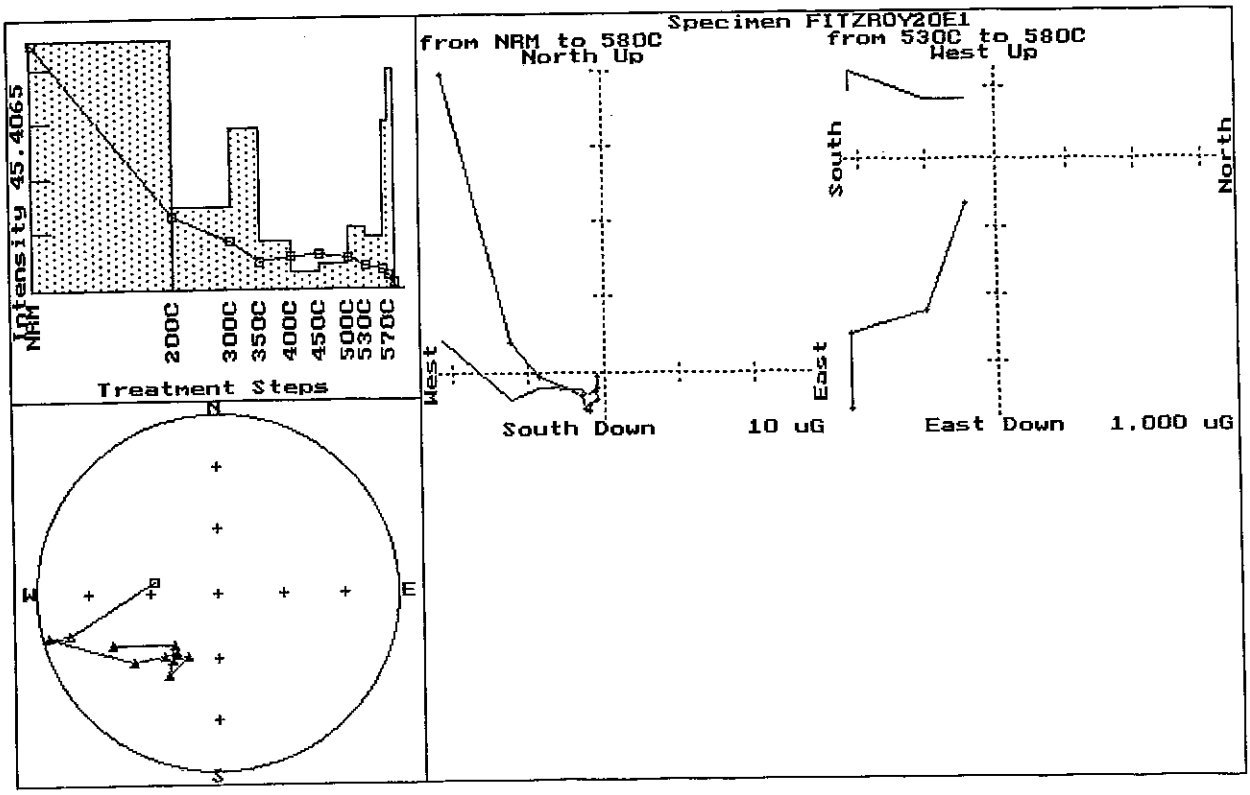
Specimen FITZROY20E1
from NRM to 580C
North Up
from 530C to 580C
West Up
Intensity 45.4065
NRM
200C
300C
350C
400C
450C
500C
530C
570C
Treatment Steps
West
East
South
North
South Down
10 uG
East Down
1.000 uG
N
E
S
W

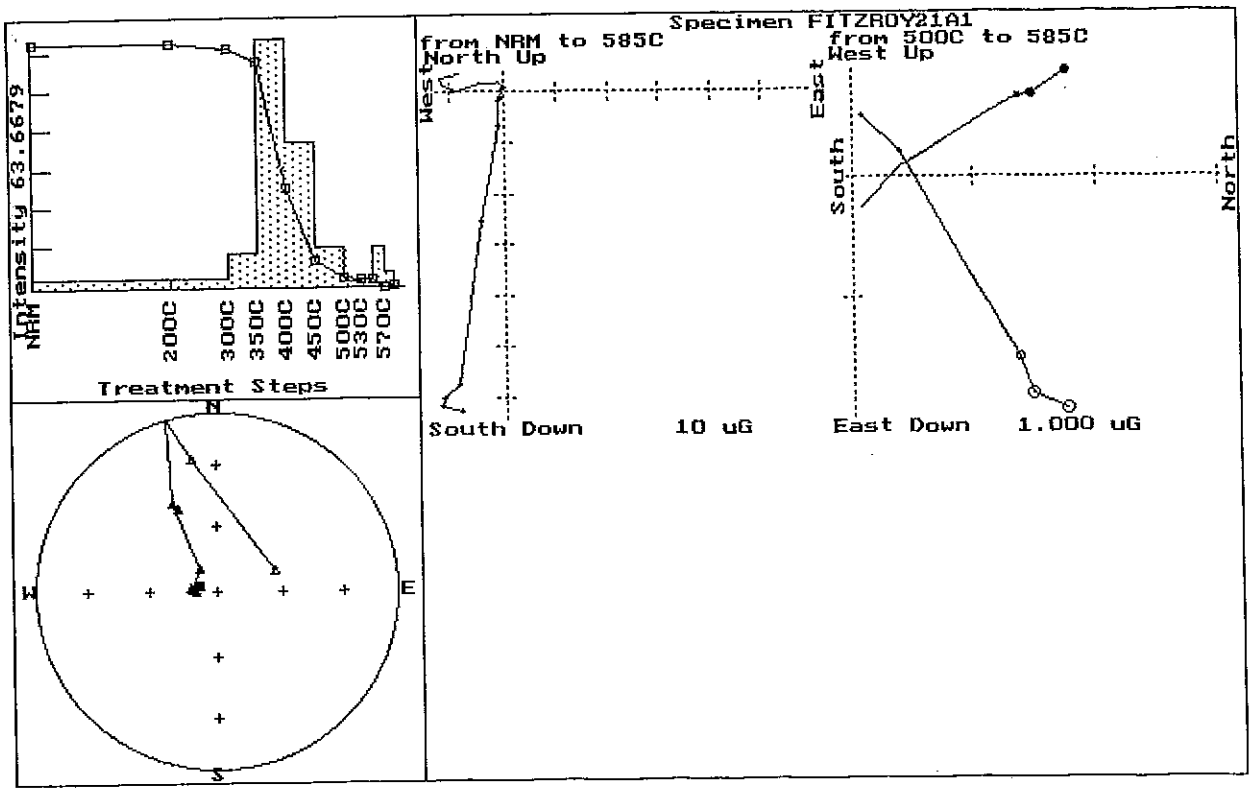
Specimen FITZROY21A1
from NRM to 585C
North Up
from 500C to 585C
West Up
Intensity 63.6679
NRM
200C
300C
350C
400C
450C
500C
530C
570C
Treatment Steps
West
East
South
North
South Down
10 uG
East Down
1.000 uG
N
E
S
W

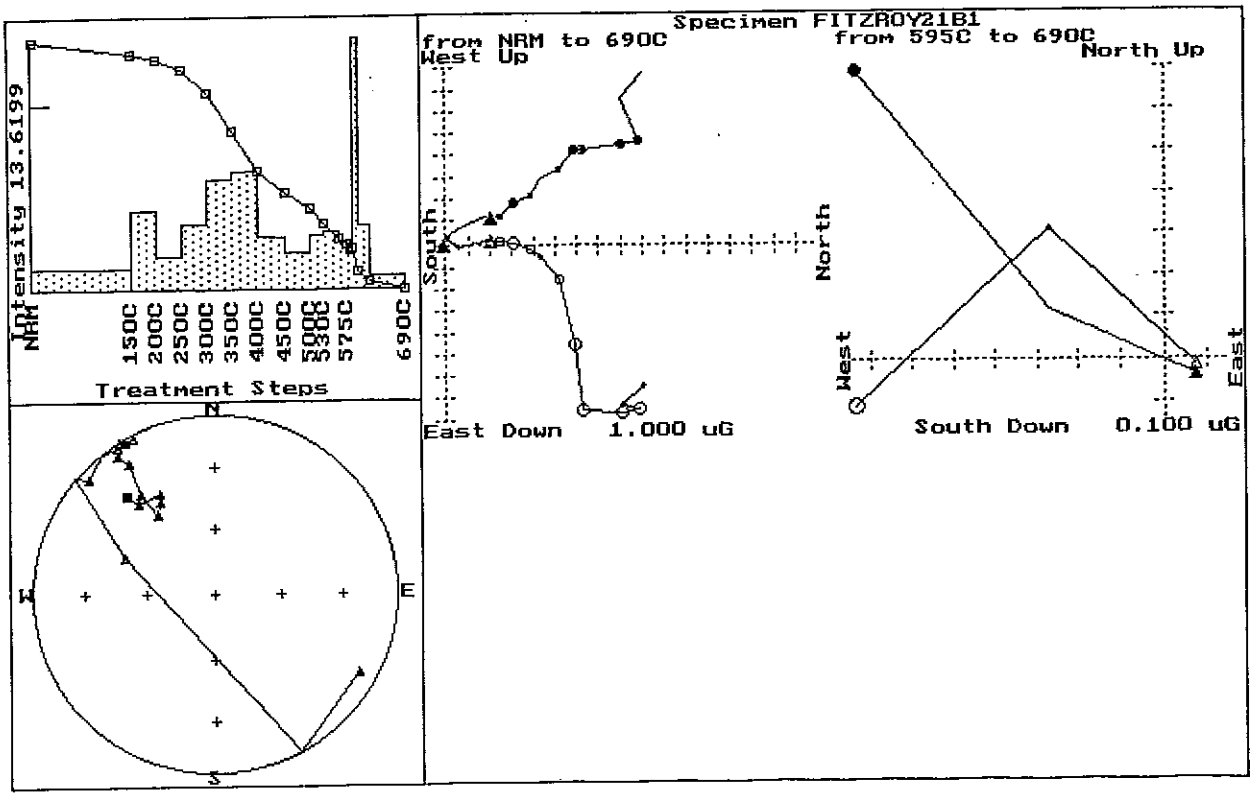
Specimen FITZROY21B1
from NRM to 690C
West Up
from 595C to 690C
North Up
Intensity 13.6199
NRM
150C
200C
250C
300C
350C
400C
450C
500C
530C
575C
690C
Treatment Steps
South
North
West
East
East Down 1.000 uG
South Down 0.100 uG
N
E
S
W

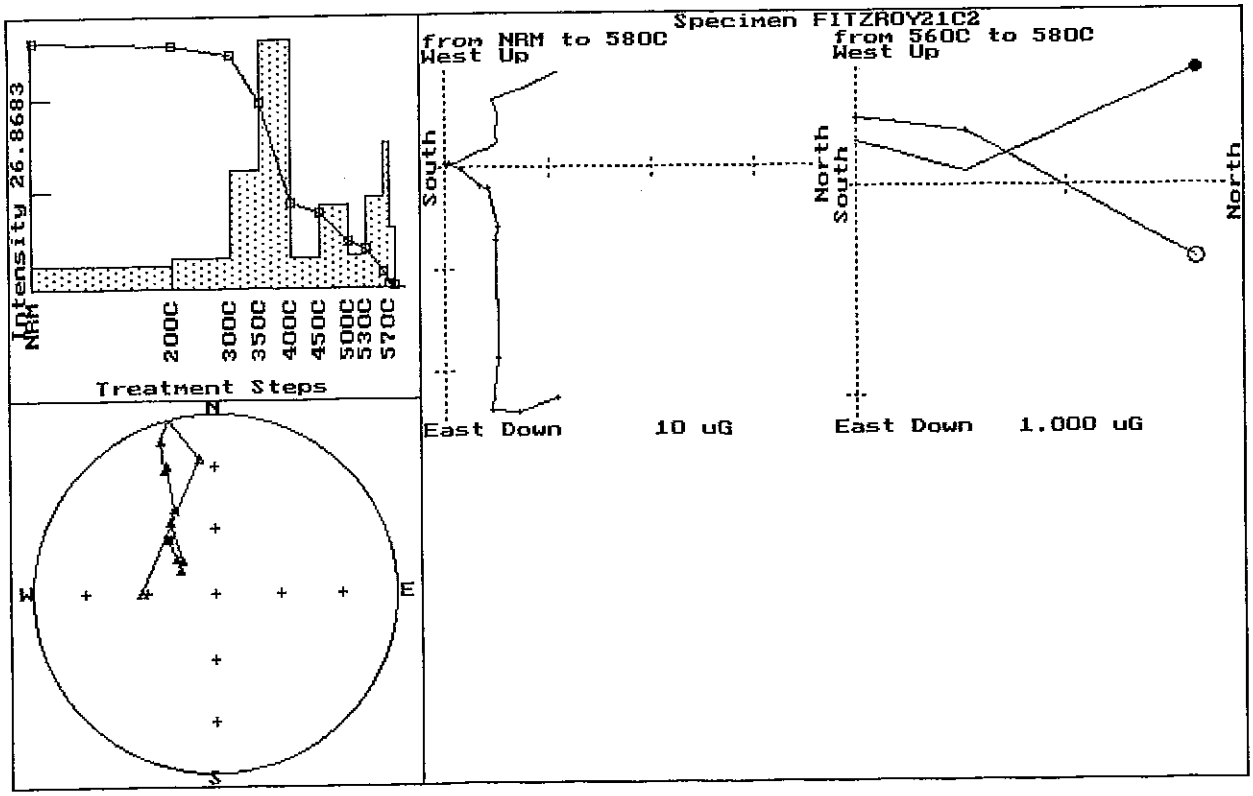
Specimen FITZROY21C2
from NRM to 580C
West Up
from 560C to 580C
West Up
Intensity 26.8683
NRM
200C
300C
350C
400C
450C
500C
530C
570C
Treatment Steps
South
North
South
North
East Down 10 uG
East Down 1.000 uG
N
E
S
W

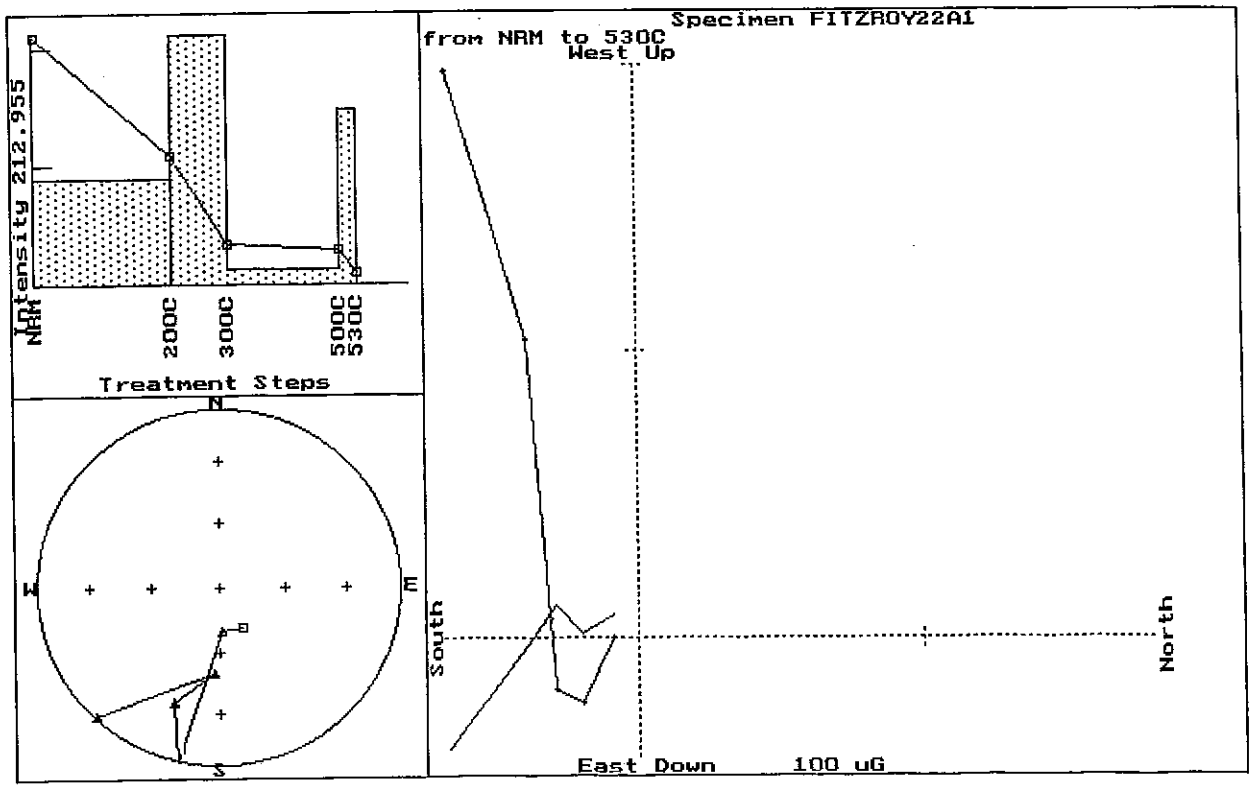
Intensity 212.955
NRM
200C
300C
500C
530C
Treatment Steps
N
E
S
W
Specimen FITZROY22A1
from NRM to 530C
West Up
South
North
East Down
100 uG

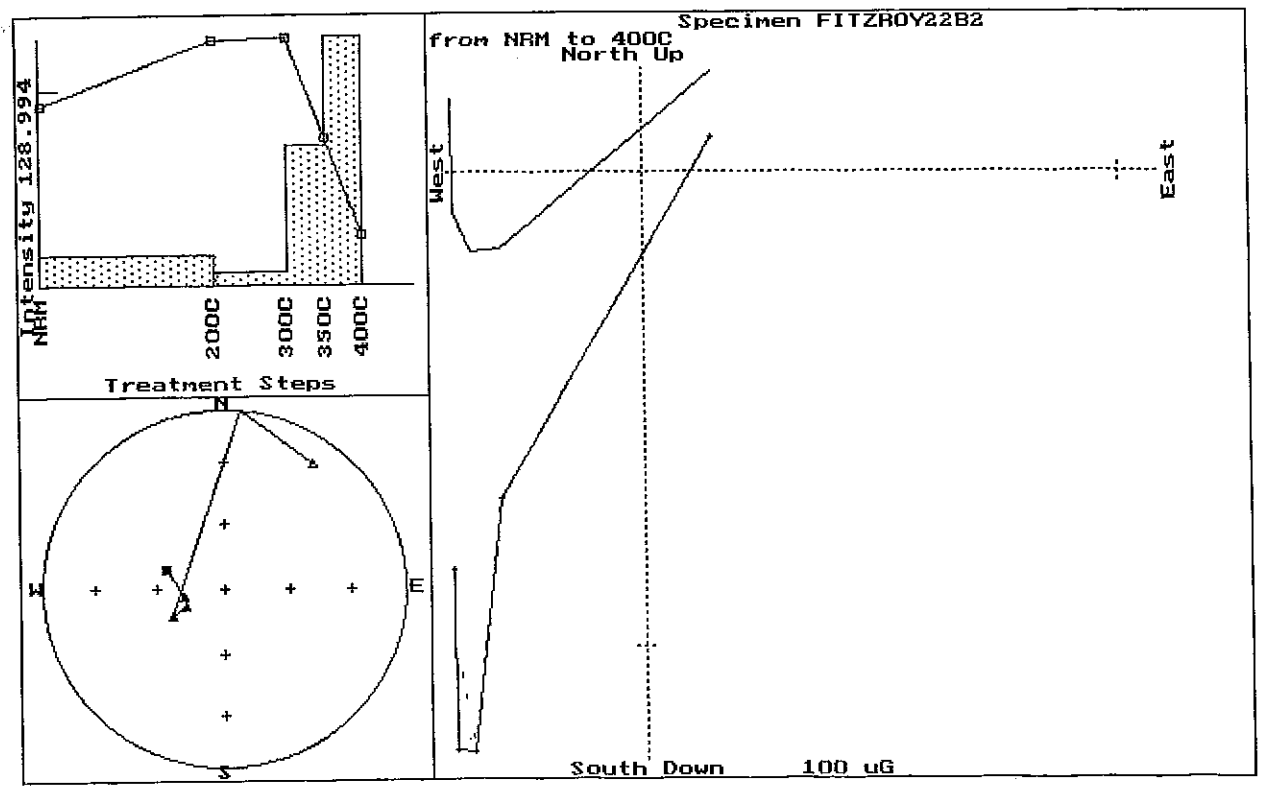
Intensity 128.994
NRM
200C
300C
350C
400C
Treatment Steps
N
E
S
W
Specimen FITZROY22B2
from NRM to 400C
North Up
West
East
South Down
100 uG

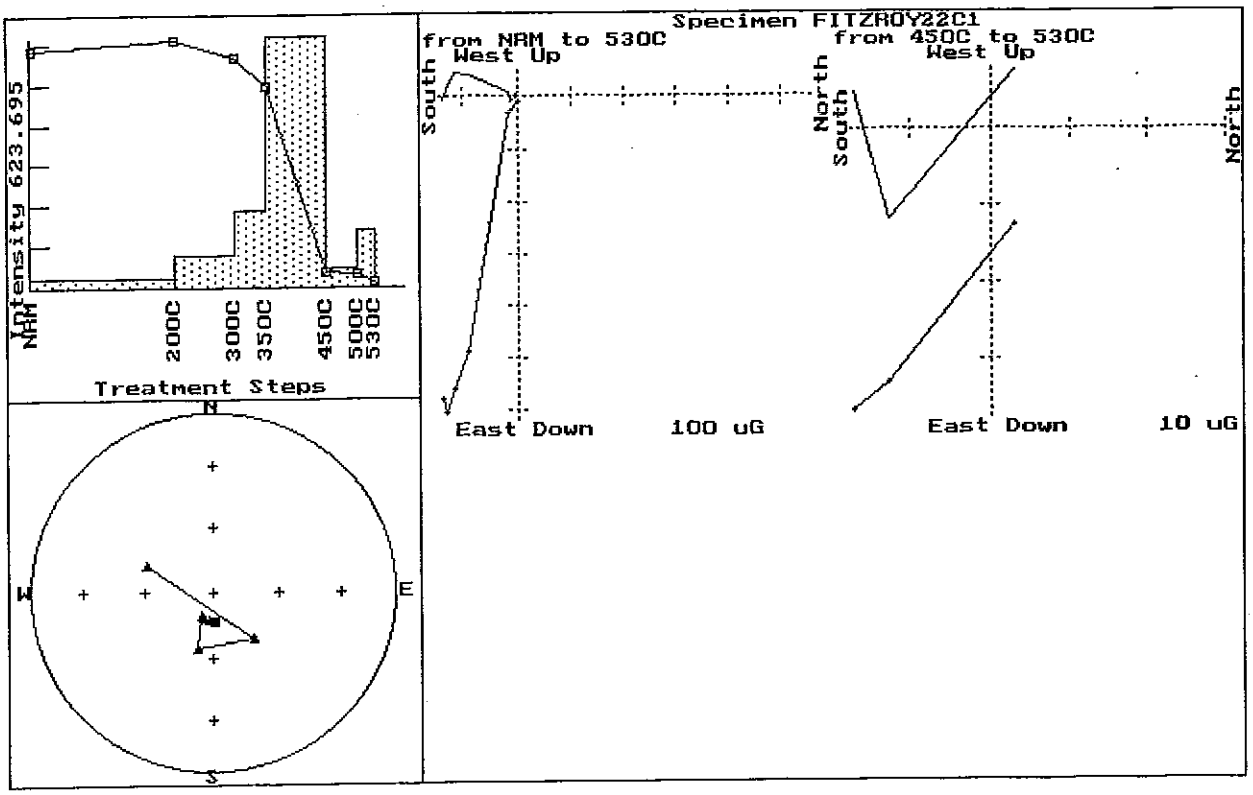
Intensity 623.695
NRM
200C
300C
350C
450C
500C
530C
Treatment Steps
N
W
E
S
Specimen FITZROY22C1
from NRM to 530C
West Up
South
East Down
100 uG
from 450C to 530C
West Up
North
South
East Down
10 uG
North

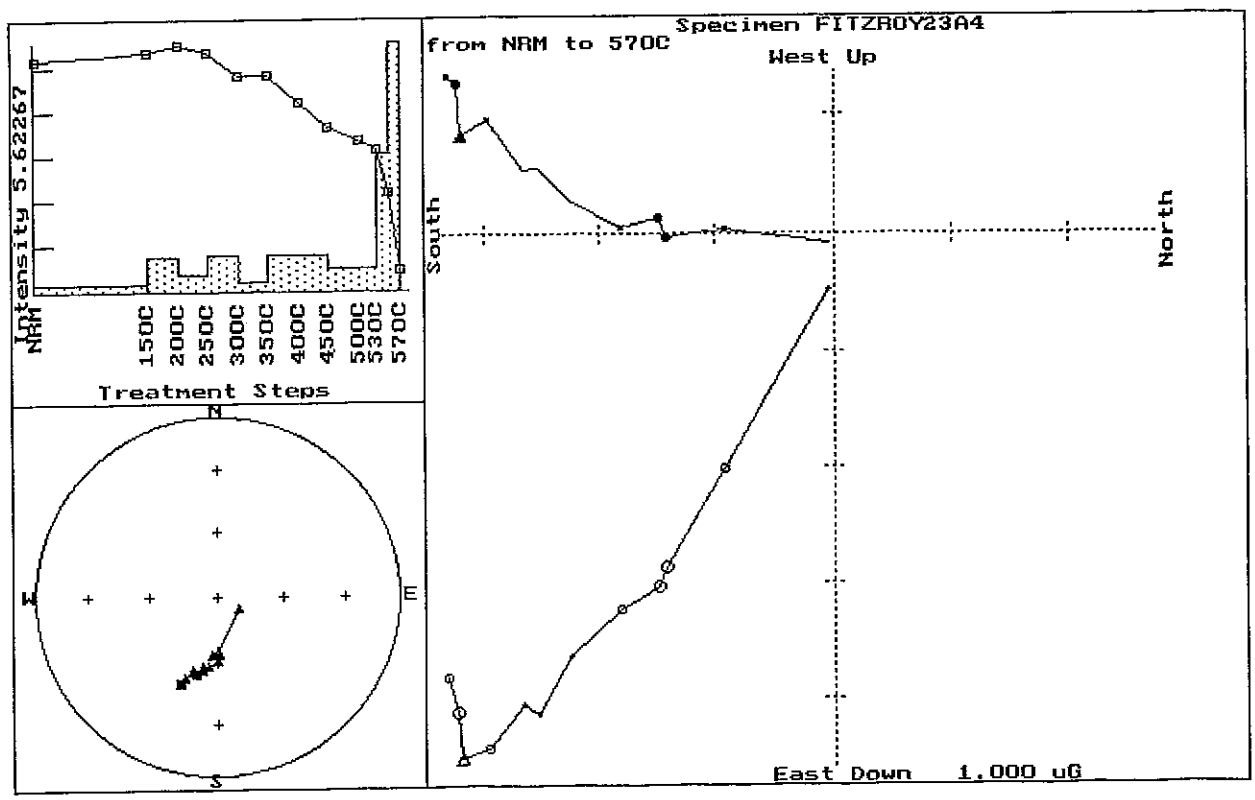
Intensity 5.62267
NRM
150C
200C
250C
300C
350C
400C
450C
500C
530C
570C
Treatment Steps
N
W
E
S
Specimen FITZROY23A4
from NRM to 570C
West Up
South
North
East Down
1.000 uG

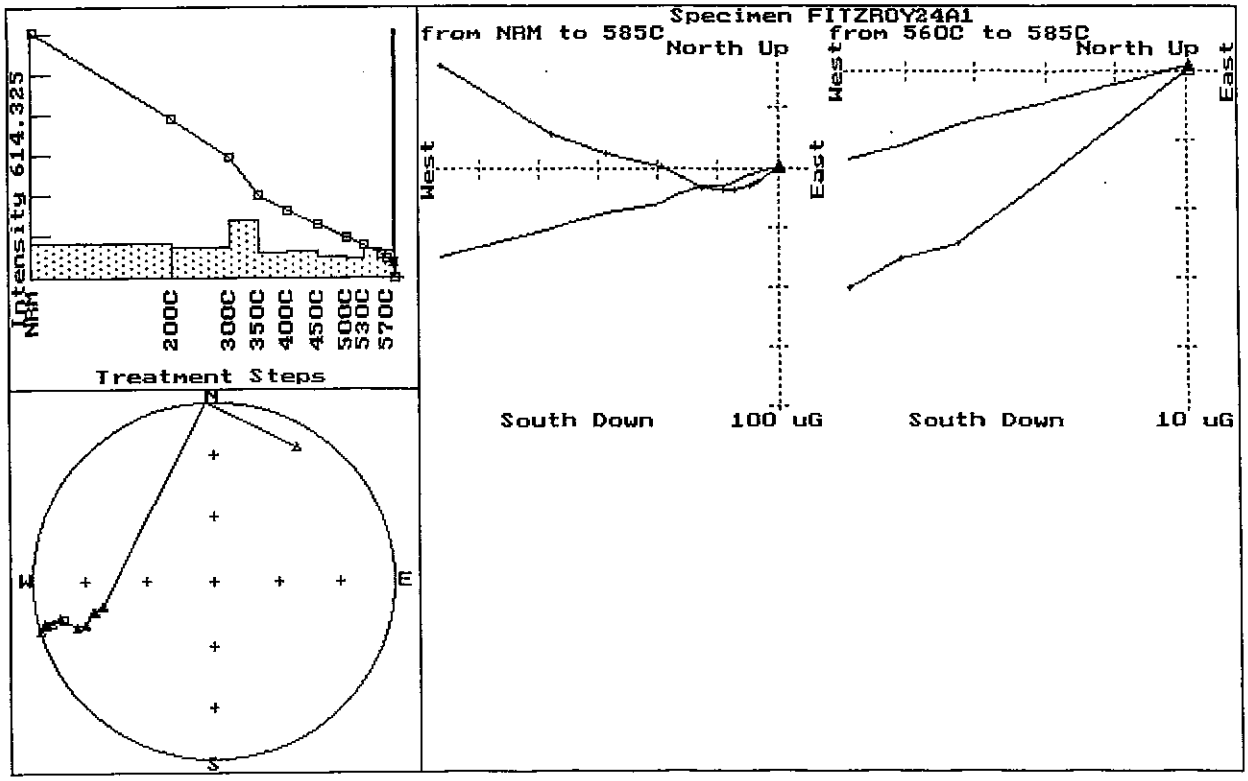
Specimen FITZROY24A1
from NRM to 585C
North Up
West
East
South Down
100 uG
from 560C to 585C
North Up
West
East
South Down
10 uG
Intensity 614.325
NRM
200C
300C
350C
400C
450C
500C
530C
570C
Treatment Steps
N
E
W
S

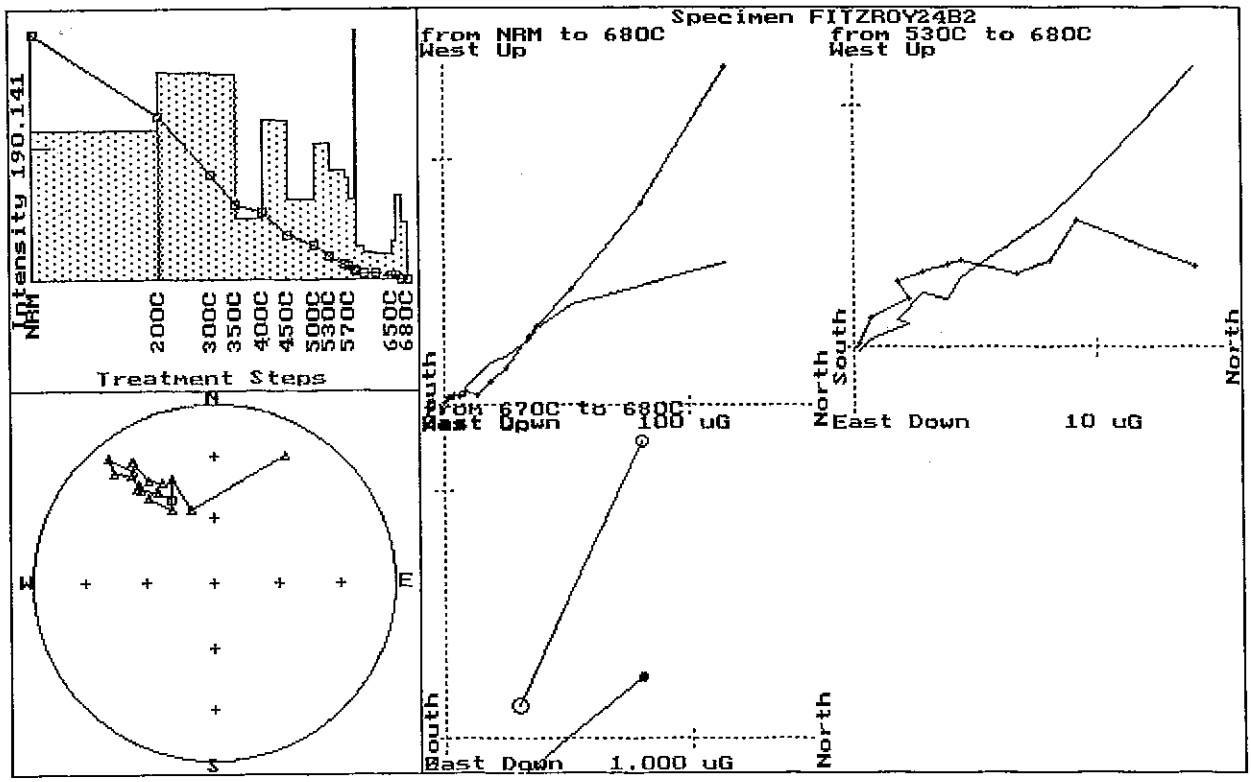
Specimen FITZROY24B2
from NRM to 680C
West Up
South
East Down
100 uG
from 530C to 680C
West Up
North
South
East Down
10 uG
from 670C to 680C
South
North
East Down
1.000 uG
Intensity 190.141
NRM
200C
300C
350C
400C
450C
500C
530C
570C
650C
680C
Treatment Steps
N
E
W
S

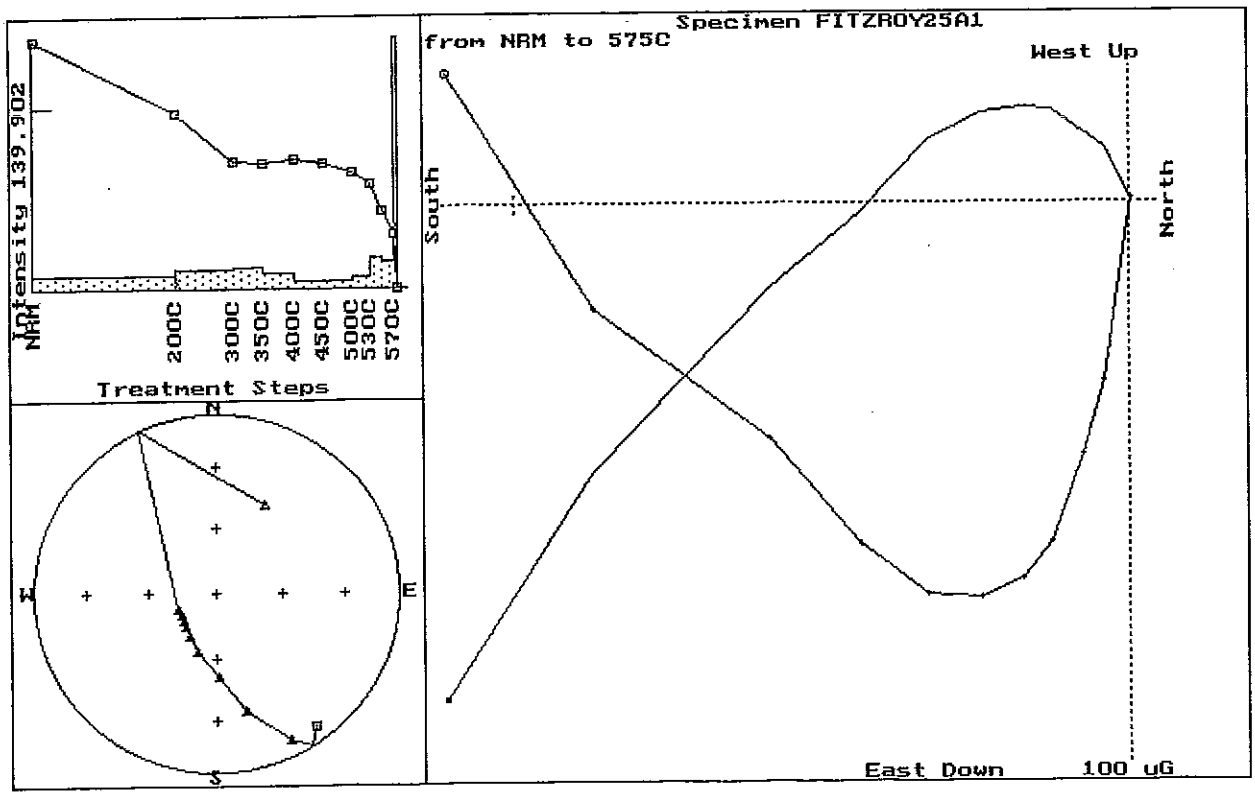
Intensity 139.902
NRM
200C
300C
350C
400C
450C
500C
530C
570C
Treatment Steps
N
W
E
S
Specimen FITZROY25A1
from NRM to 575C
West Up
South
North
East Down
100 uG

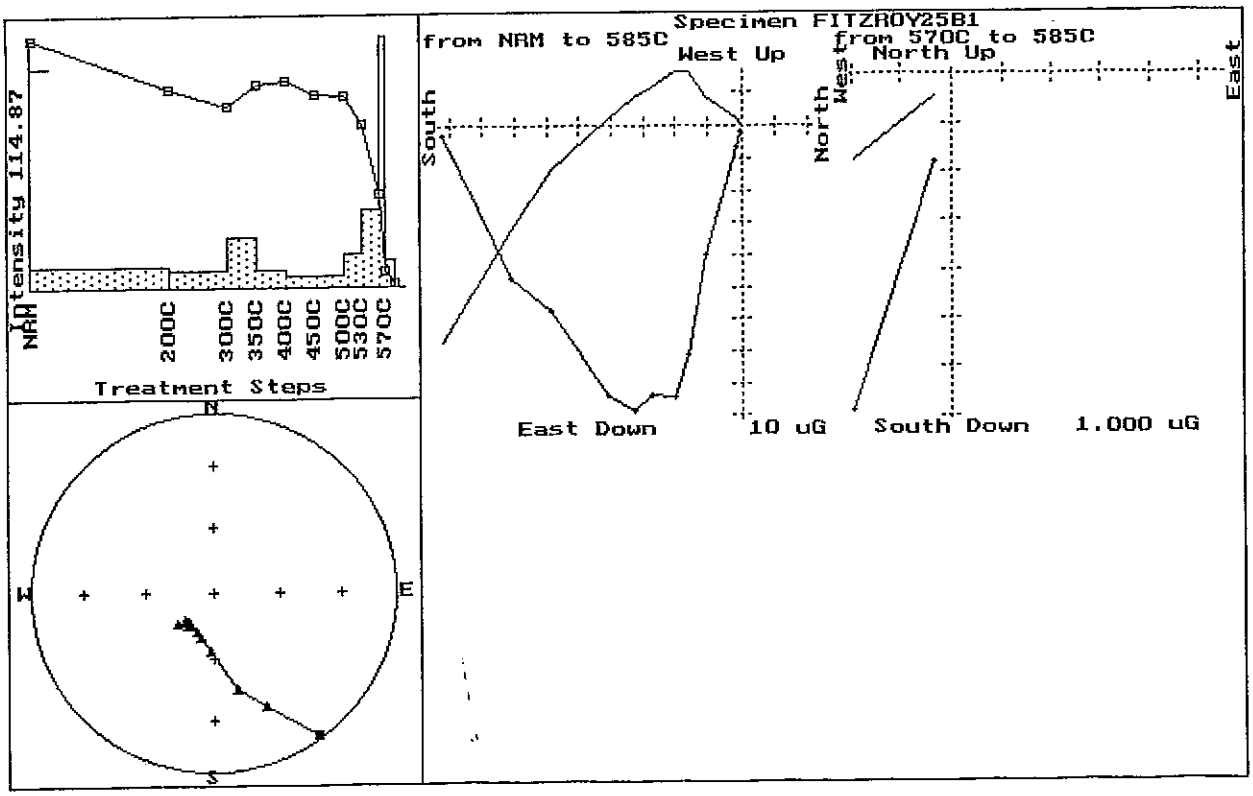
Intensity 114.87
NRM
200C
300C
350C
400C
450C
500C
530C
570C
Treatment Steps
N
W
E
S
Specimen FITZROY25B1
from NRM to 585C
from 570C to 585C
West Up
North Up
South
North
West
East
East Down
10 uG
South Down
1.000 uG

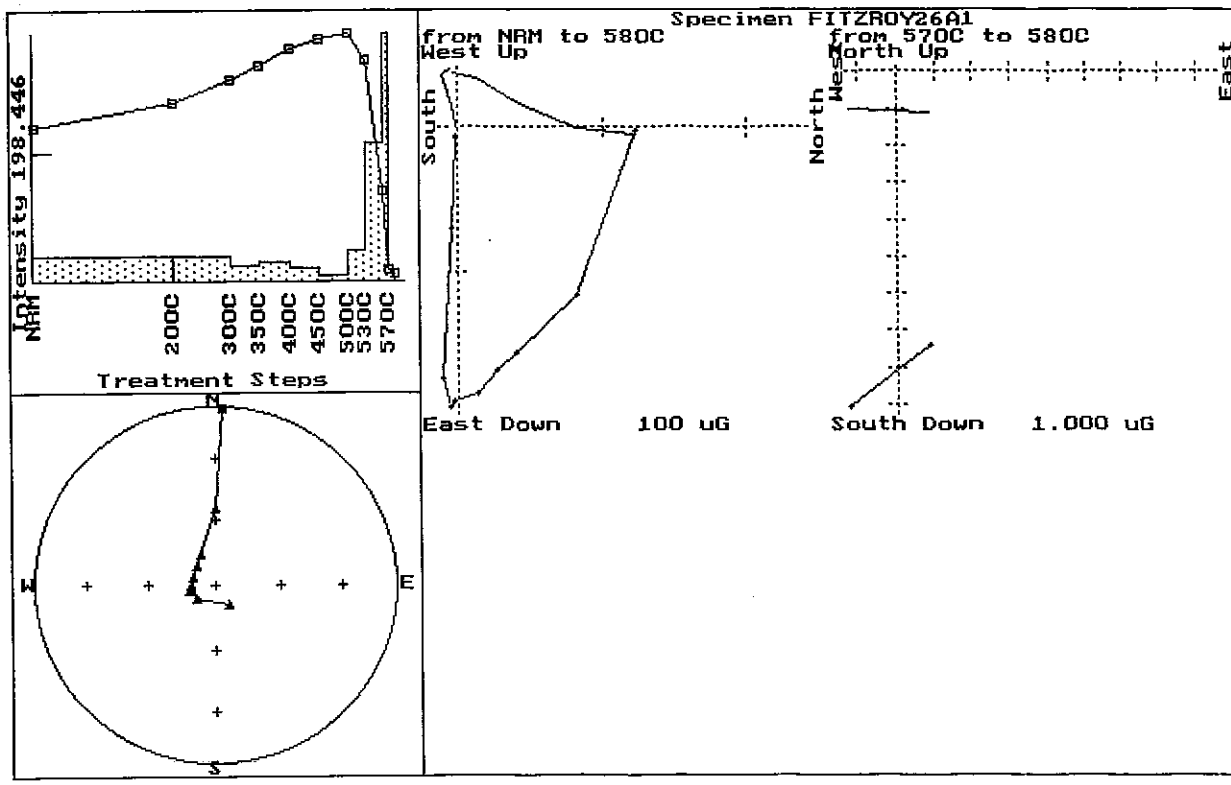
Specimen FITZROY26A1
from NRM to 580C
West Up
from 570C to 580C
North Up
Intensity 198.446
NRM
200C
300C
350C
400C
450C
500C
530C
570C
Treatment Steps
South
North
West
East
East Down
100 uG
South Down
1.000 uG
N
E
S
W

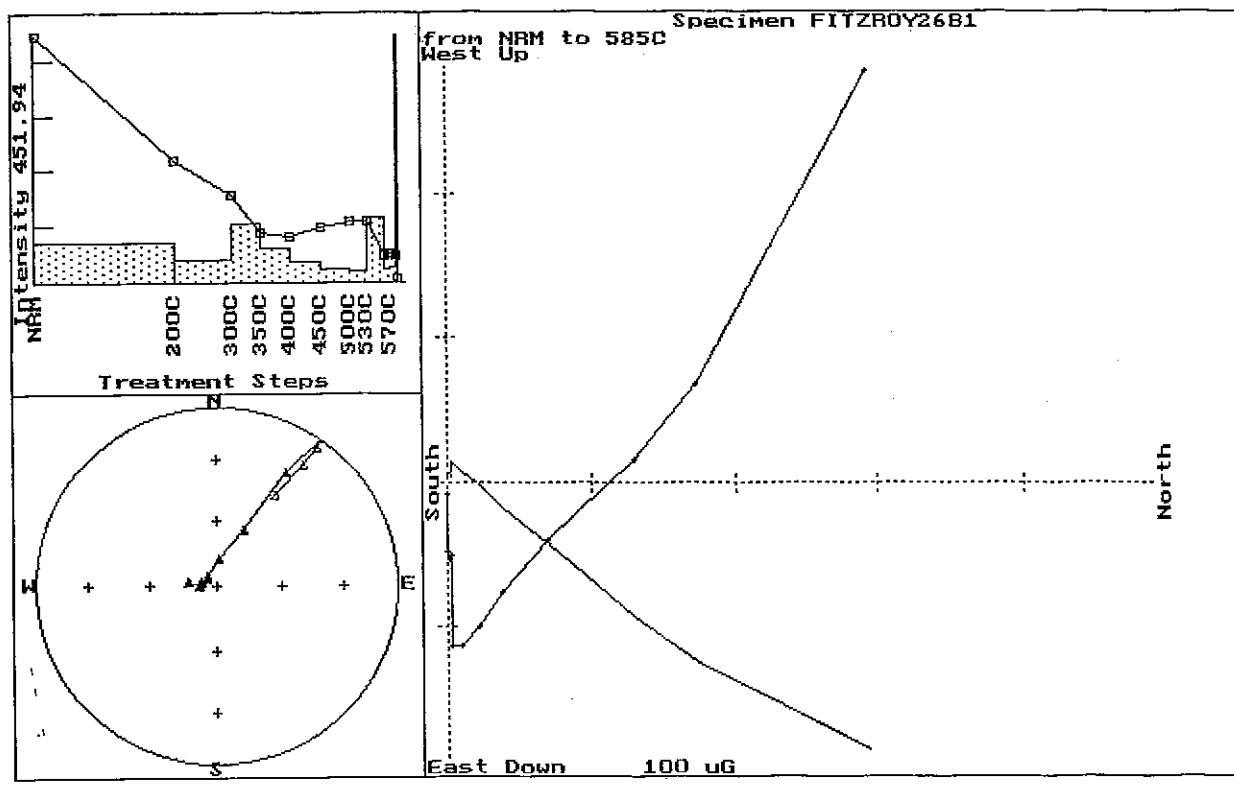
Specimen FITZROY26B1
from NRM to 585C
West Up
Intensity 451.94
NRM
200C
300C
350C
400C
450C
500C
530C
570C
Treatment Steps
South
North
East Down
100 uG
N
E
S
W

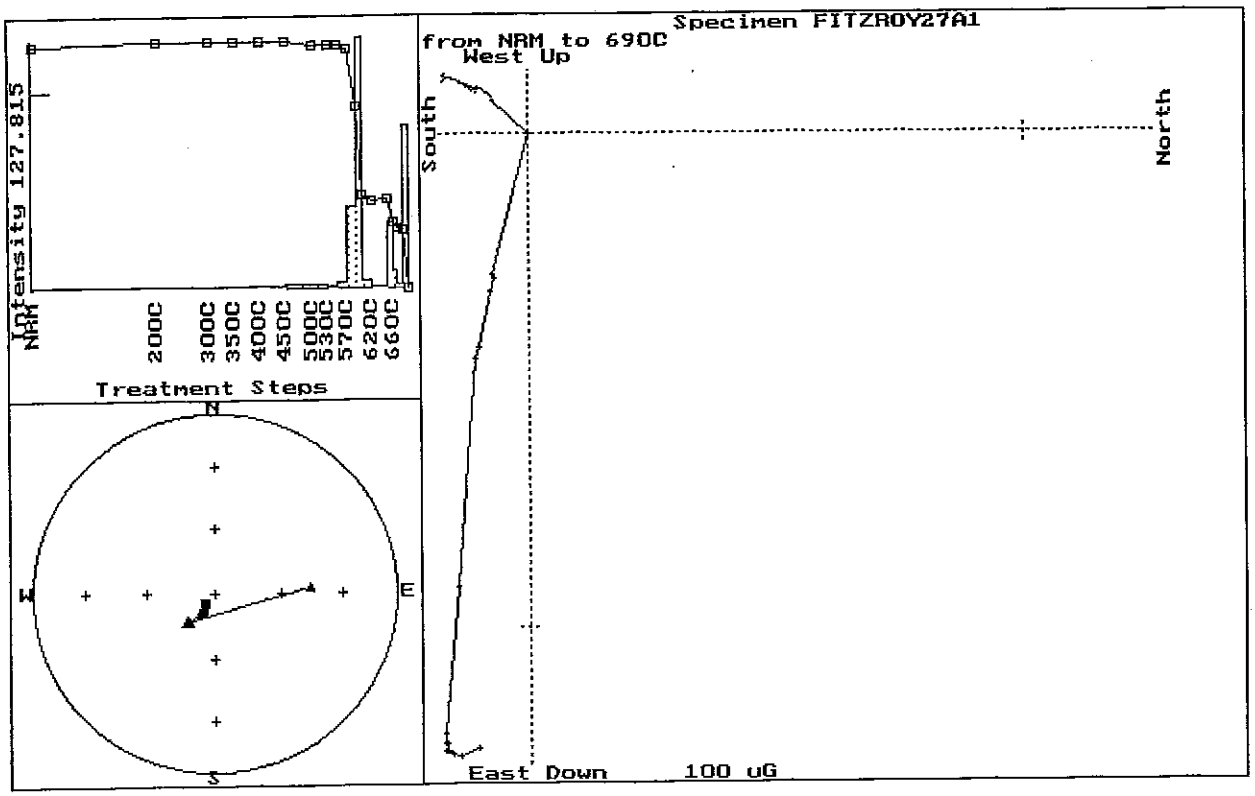
Specimen FITZROY27A1
from NRM to 690C
West Up
South
North
Intensity 127.815
NRM
200C
300C
350C
400C
450C
500C
530C
570C
620C
660C
Treatment Steps
N
E
S
East Down
100 uG

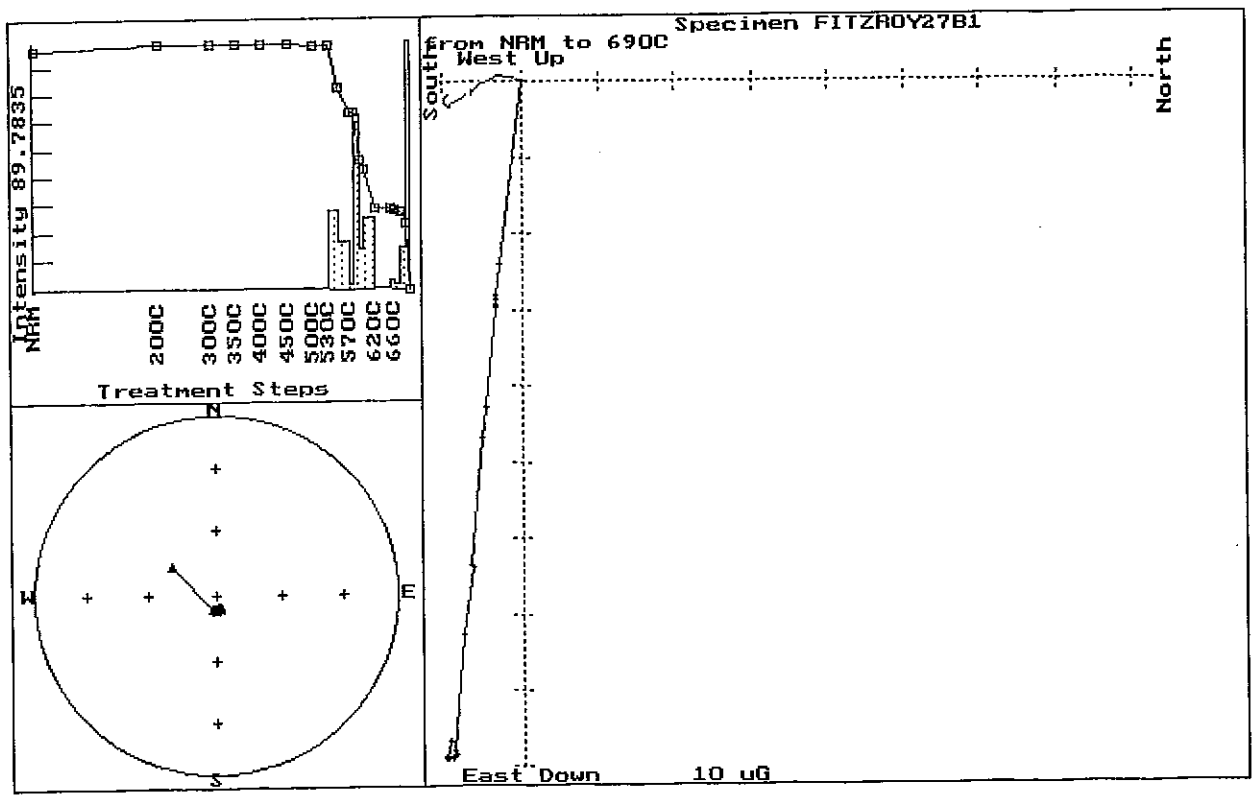
Specimen FITZROY27B1
from NRM to 690C
West Up
South
North
Intensity 89.7835
NRM
200C
300C
350C
400C
450C
500C
530C
570C
620C
660C
Treatment Steps
N
E
S
East Down
10 uG

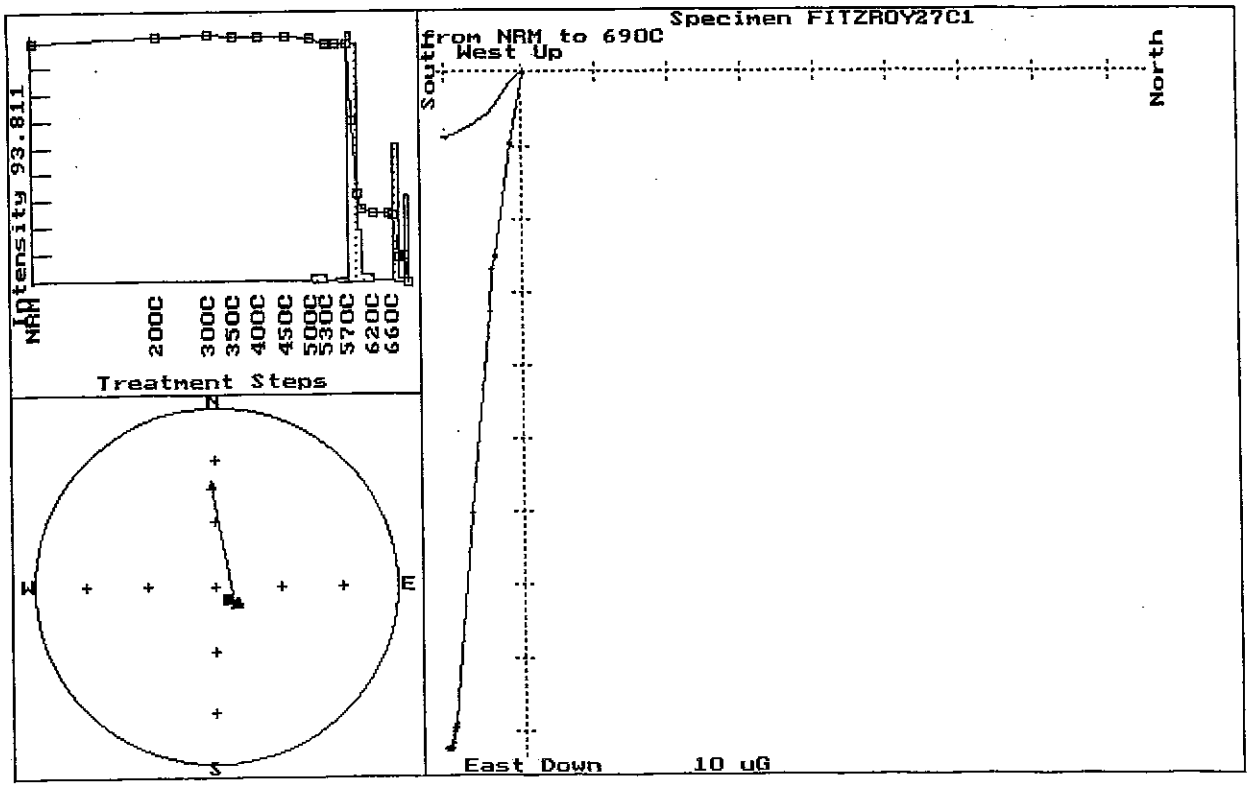
Specimen FITZROY27C1
from NRM to 690C
West Up
South
North
Intensity 93.811
NRM
200C
300C
350C
400C
450C
500C
530C
570C
620C
660C
Treatment Steps
N
W
E
S
East Down
10 uG

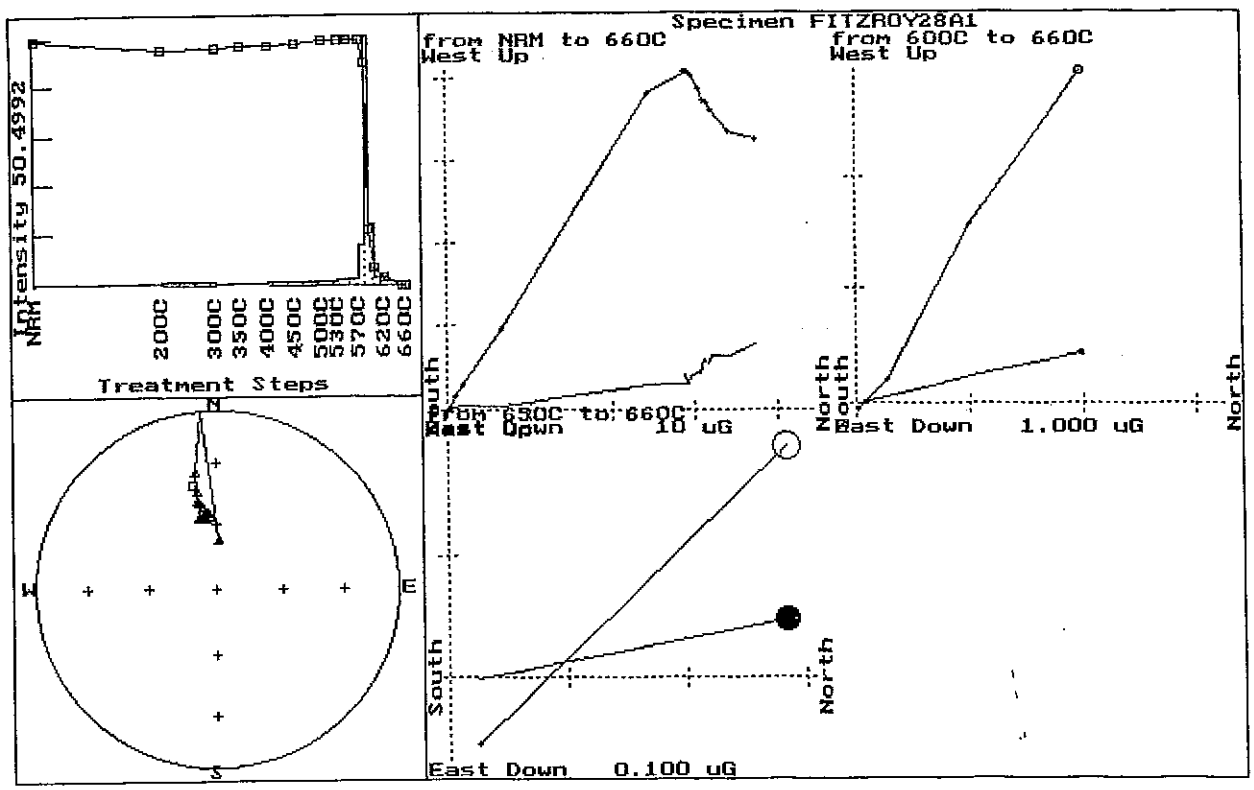
Specimen FITZROY28A1
from NRM to 660C
West Up
from 600C to 660C
West Up
Intensity 50.4992
NRM
200C
300C
350C
400C
450C
500C
530C
570C
620C
660C
Treatment Steps
N
W
E
S
South
North
East Down
10 uG
East Down
1.000 uG
East Down
0.100 uG

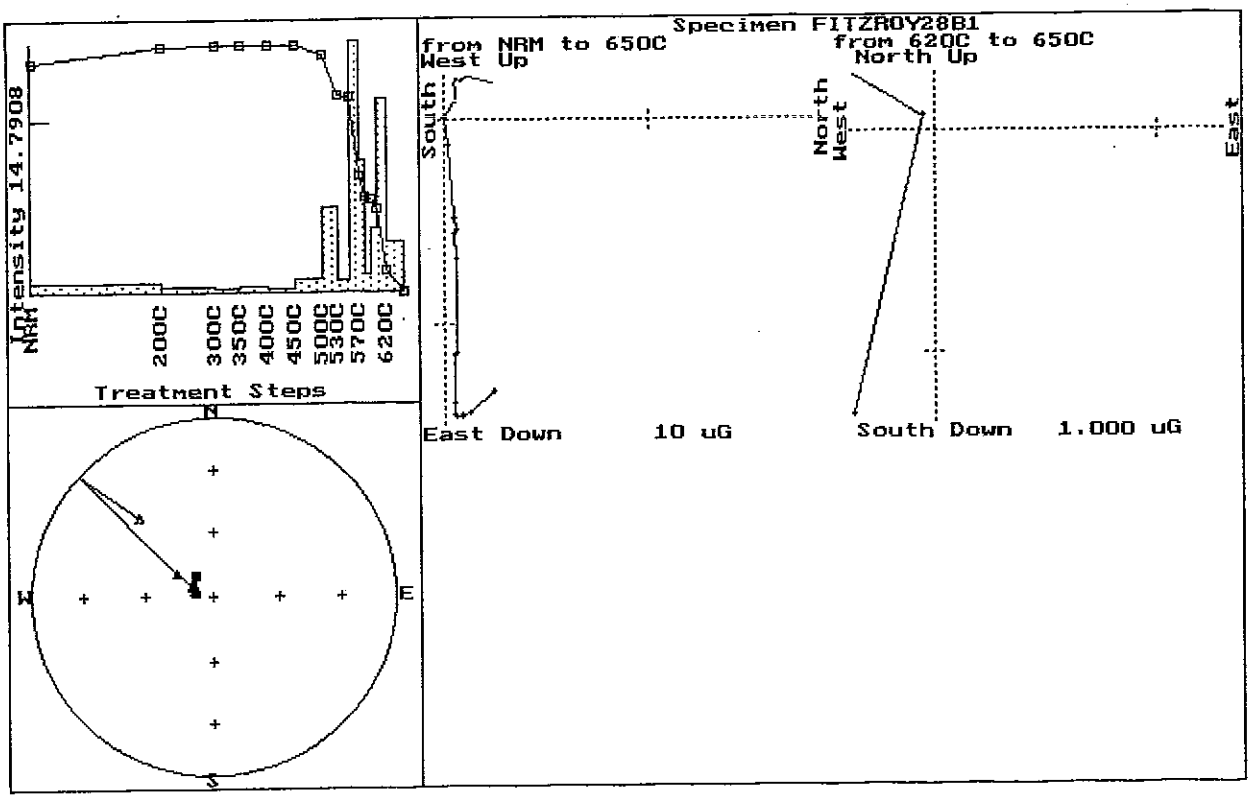
Specimen FITZROY28B1
from NRM to 650C
West Up
from 620C to 650C
North Up
Intensity 14.7908
NRM
200C
300C
350C
400C
450C
500C
530C
570C
620C
Treatment Steps
South
North
West
East
East Down
10 uG
South Down
1.000 uG
N
W
E
S

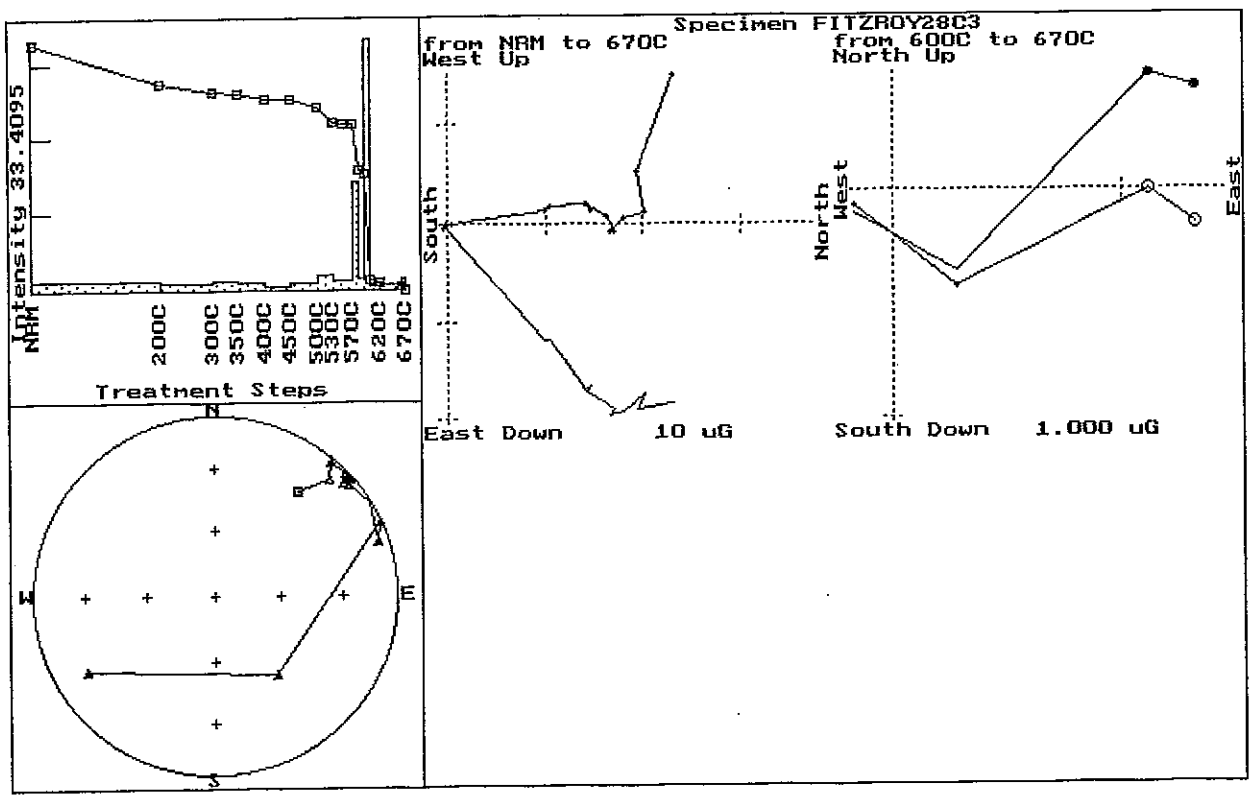
Specimen FITZROY28C3
from NRM to 670C
West Up
from 600C to 670C
North Up
Intensity 33.4095
NRM
200C
300C
350C
400C
450C
500C
530C
570C
620C
670C
Treatment Steps
South
North
West
East
East Down
10 uG
South Down
1.000 uG
N
W
E
S

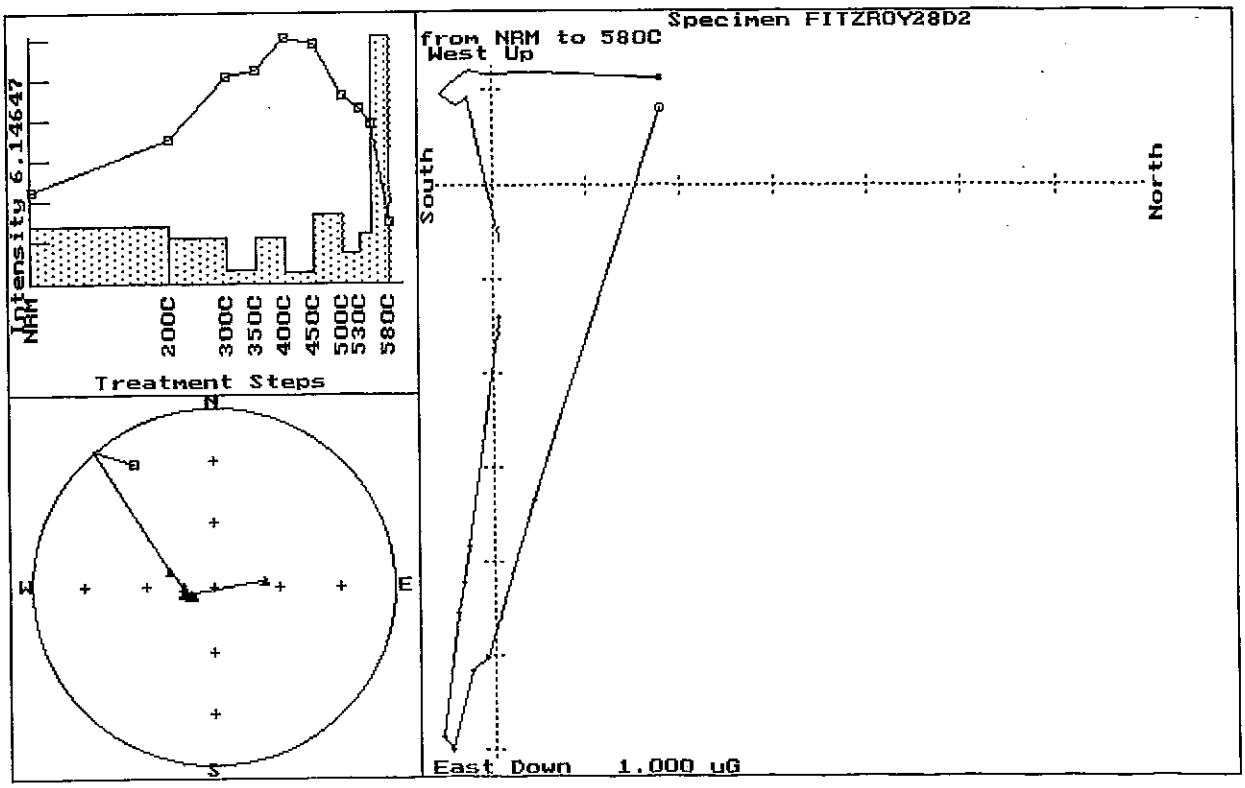
Specimen FITZROY28D2
from NRM to 580C
West Up
South
North
East Down 1.000 uG
Intensity 6.14647
NRM
200C
300C
350C
400C
450C
500C
530C
580C
Treatment Steps
N
E
S
W

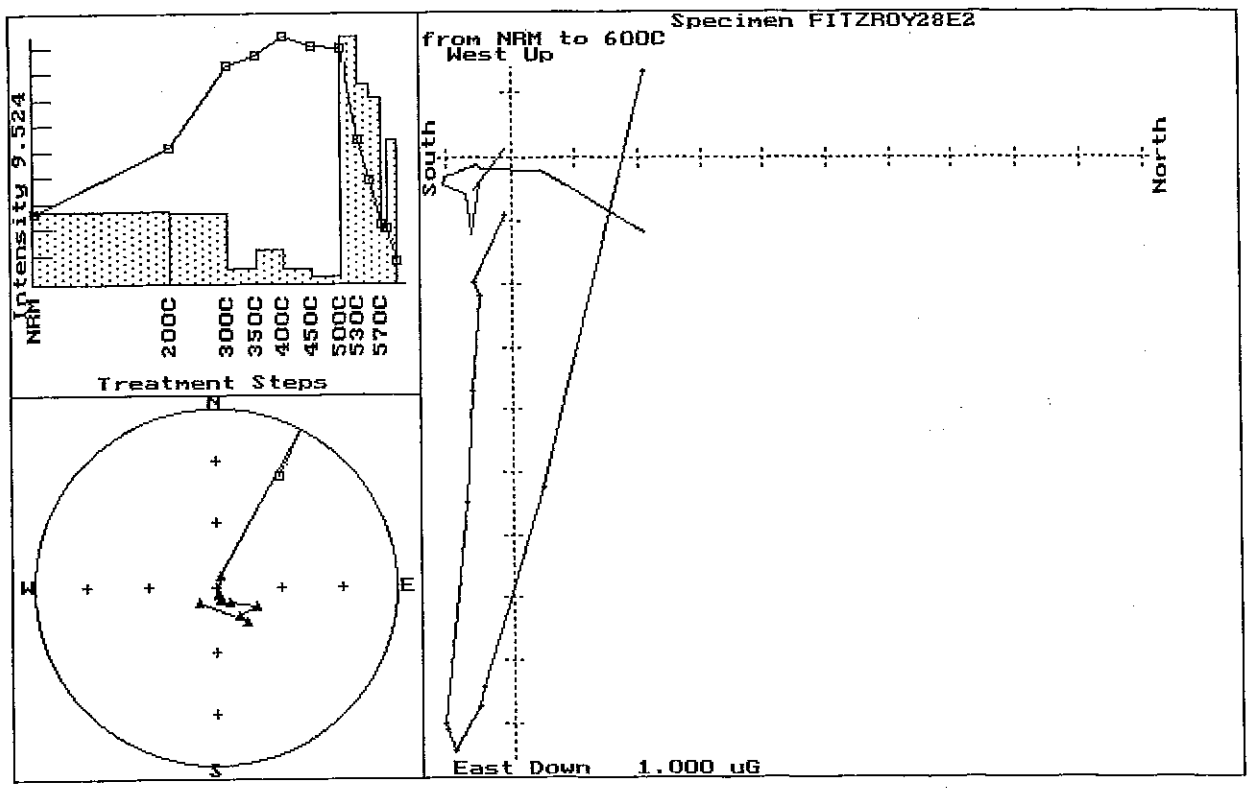
Specimen FITZROY28E2
from NRM to 600C
West Up
South
North
East Down 1.000 uG
Intensity 9.524
NRM
200C
300C
350C
400C
450C
500C
530C
570C
Treatment Steps
N
E
S
W

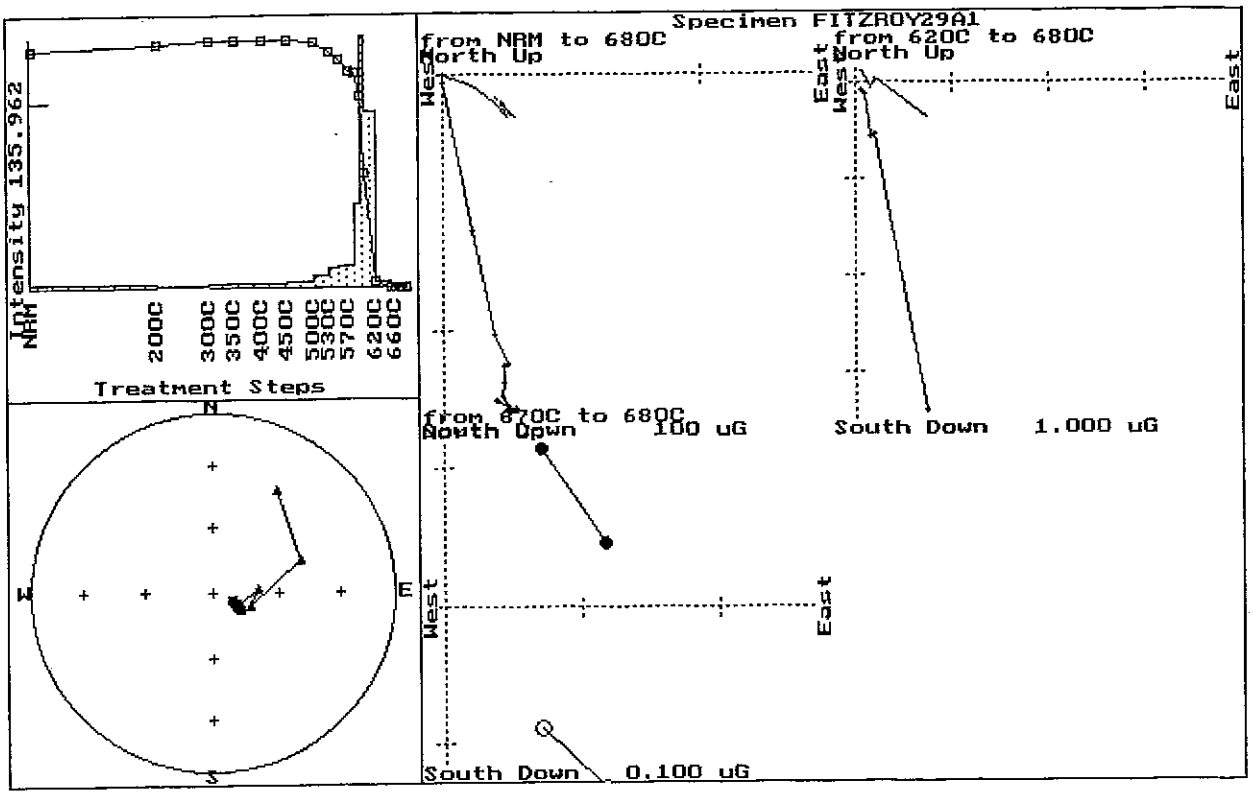
Intensity 135.962
NRM
200C
300C
350C
400C
450C
500C
530C
570C
620C
660C
Treatment Steps
N
E
S
Specimen FITZROY29A1
from NRM to 680C
North Up
West
East
from 620C to 680C
North Up
West
East
from 670C to 680C
North Down
100 uG
West
East
South Down
1.000 uG
South Down
0.100 uG

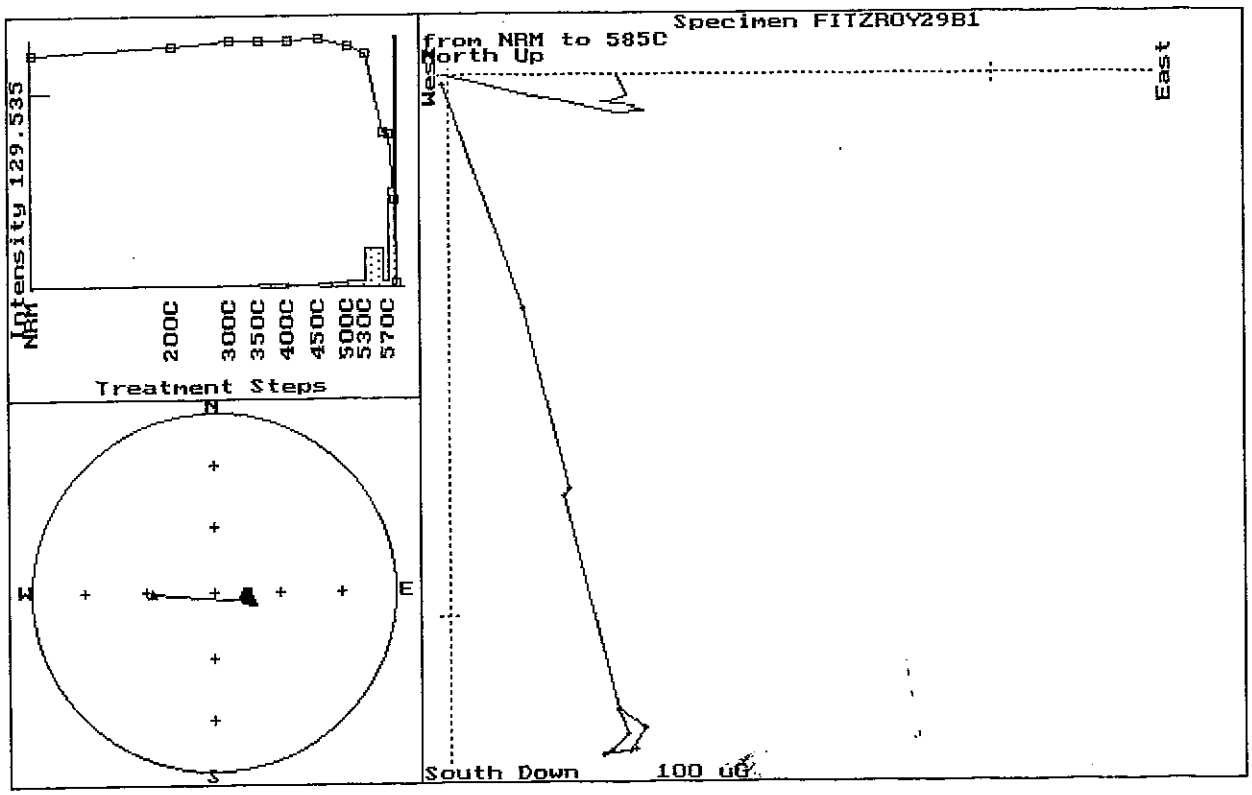
Intensity 129.535
NRM
200C
300C
350C
400C
450C
500C
530C
570C
Treatment Steps
N
E
S
Specimen FITZROY29B1
from NRM to 585C
North Up
West
East
South Down
100 uG

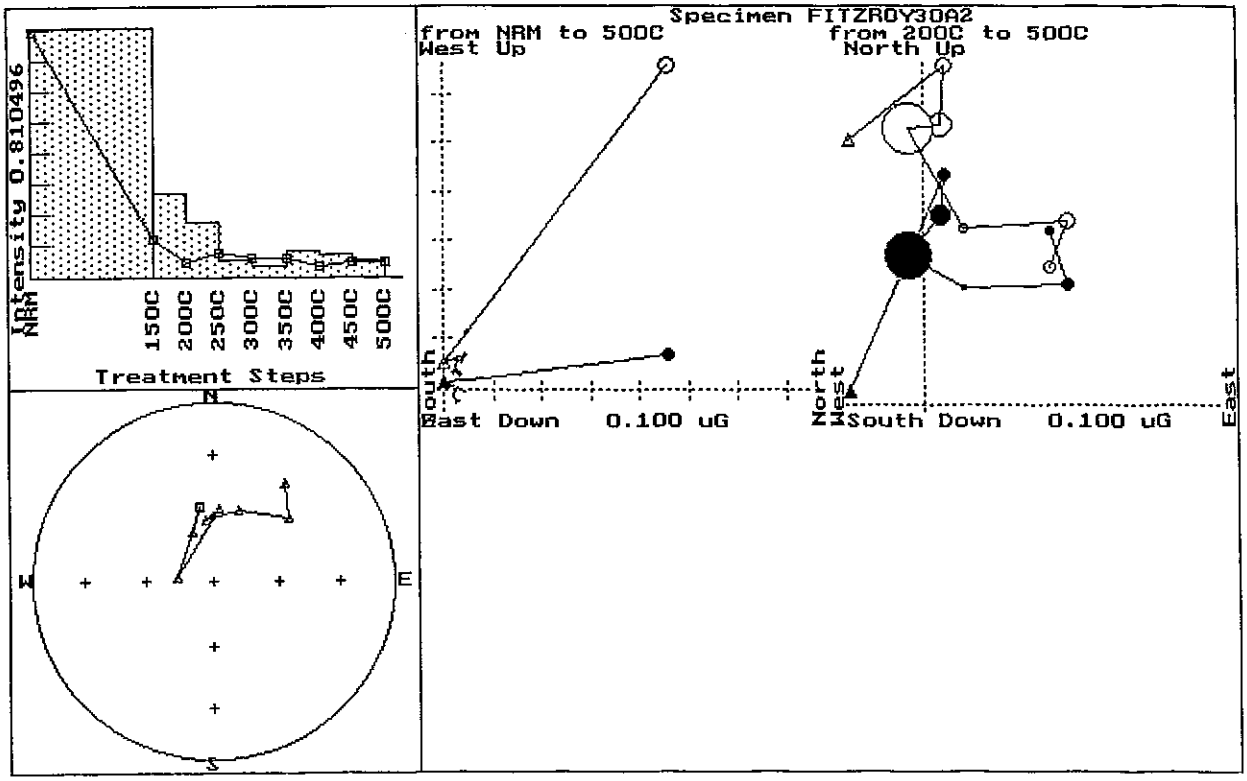
Specimen FITZROY30A2
from NRM to 500C
West Up
from 200C to 500C
North Up
Intensity 0.810496
NRM
150C
200C
250C
300C
350C
400C
450C
500C
Treatment Steps
N
E
S
South
East Down 0.100 uG
North
West
South Down 0.100 uG
East

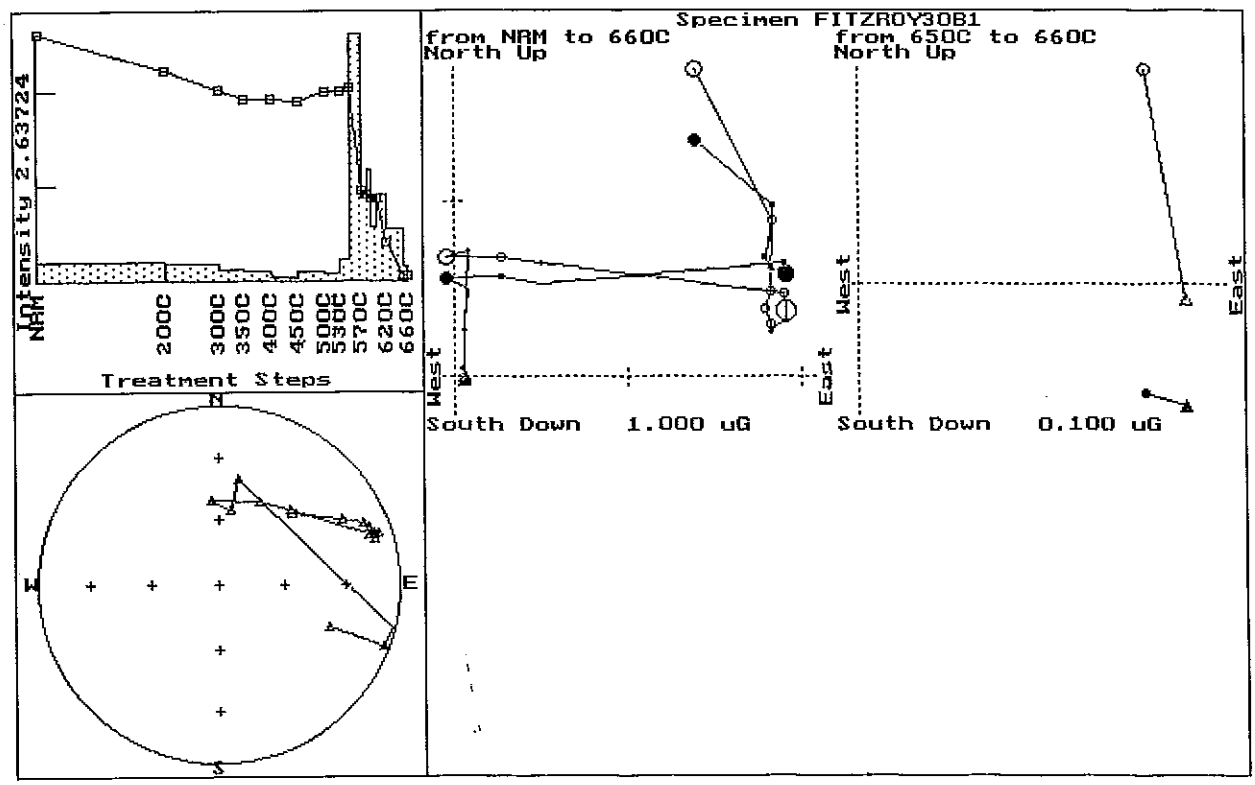
Specimen FITZROY30B1
from NRM to 660C
North Up
from 650C to 660C
North Up
Intensity 2.63724
NRM
200C
300C
350C
400C
450C
500C
530C
570C
620C
660C
Treatment Steps
N
W
E
S
West
East
South Down 1.000 uG
West
East
South Down 0.100 uG

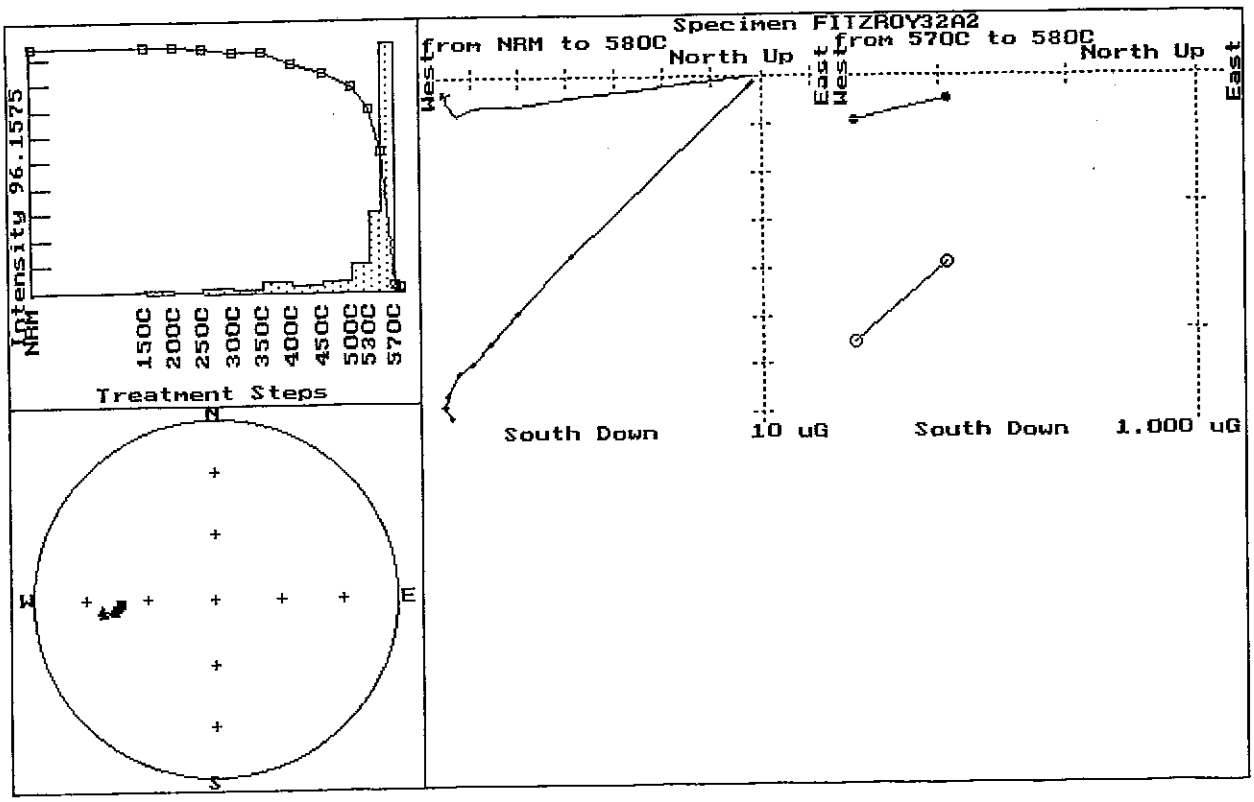
Specimen FITZROY32A2
from NRM to 580C
North Up
West
East
from 570C to 580C
North Up
West
East
Intensity 96.1575
NRM
150C
200C
250C
300C
350C
400C
450C
500C
530C
570C
Treatment Steps
N
W
E
S
South Down
10 uG
South Down
1.000 uG

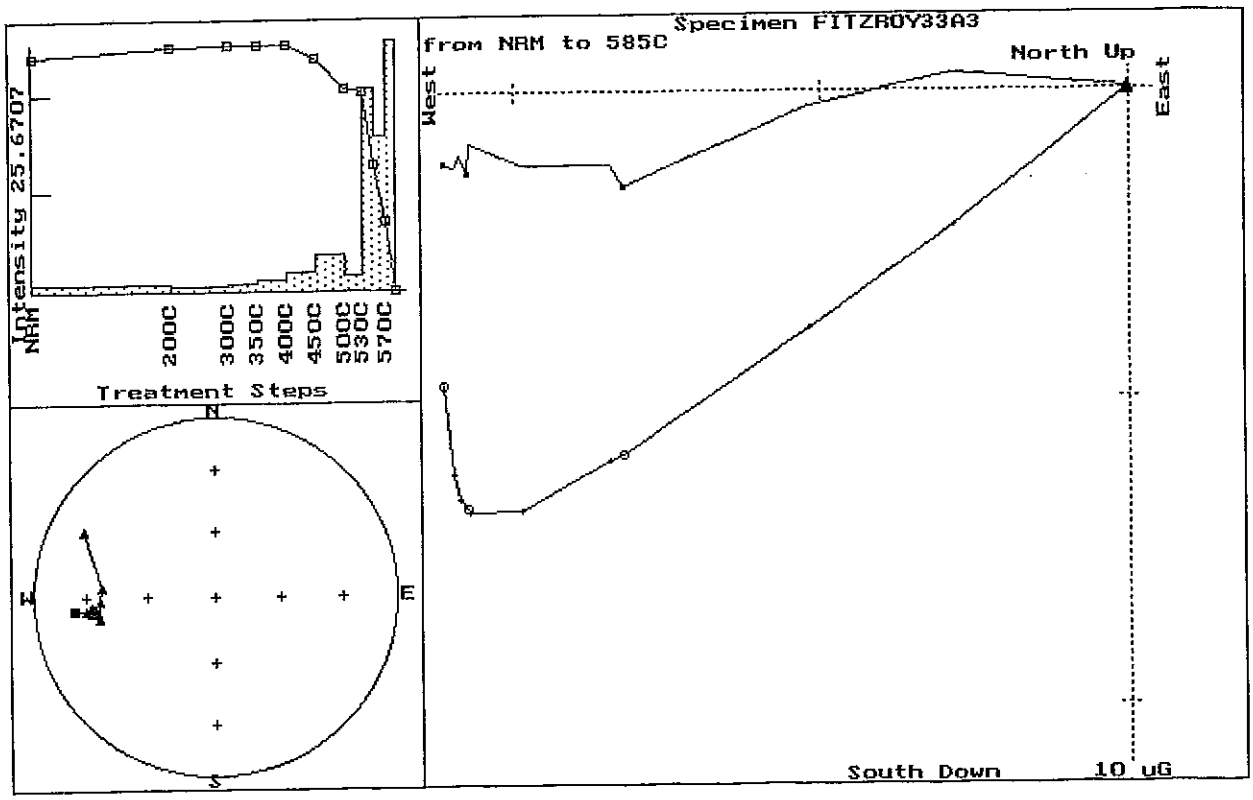
Specimen FITZROY33A3
from NRM to 585C
North Up
West
East
Intensity 25.6707
NRM
200C
300C
350C
400C
450C
500C
530C
570C
Treatment Steps
N
W
E
S
South Down
10 uG

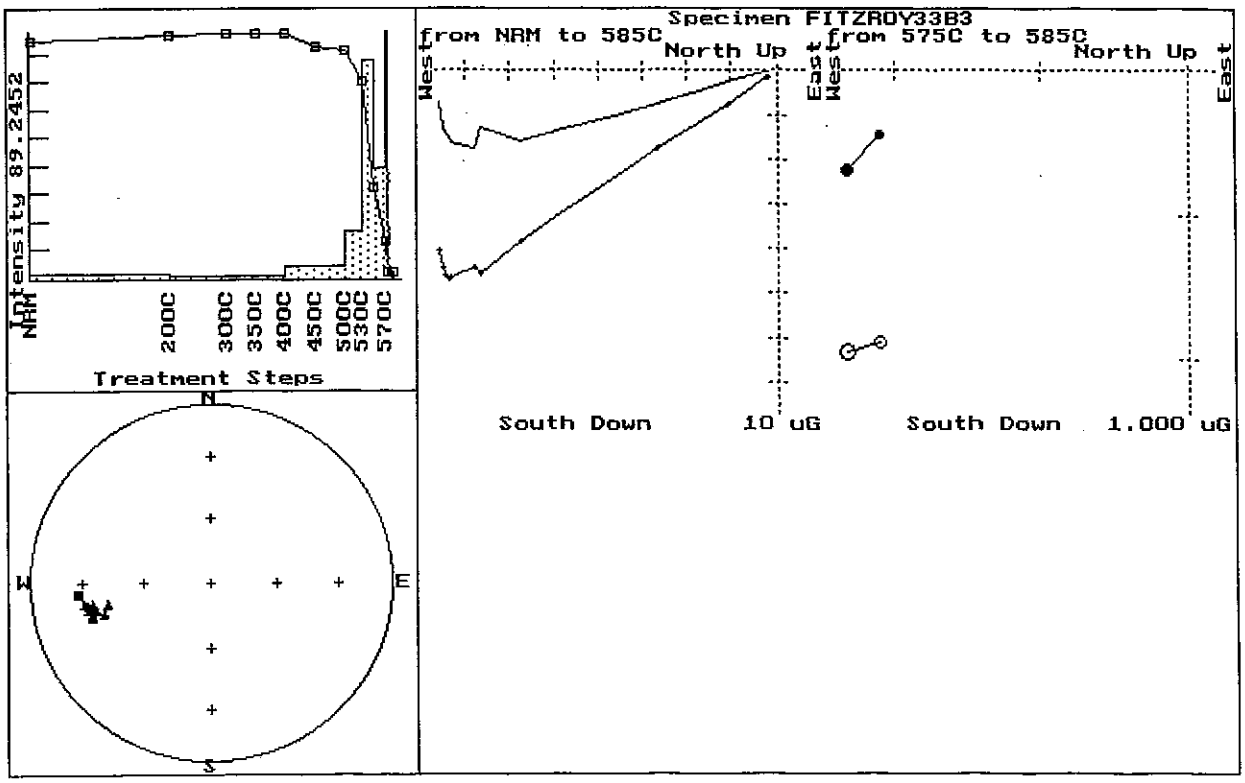
Intensity 89.2452
NRM
200C
300C
350C
400C
450C
500C
530C
570C
Treatment Steps
N
E
S
W
Specimen FITZROY33B3
from NRM to 585C
North Up
West
East
South Down
10 uG
from 575C to 585C
North Up
West
East
South Down
1.000 uG

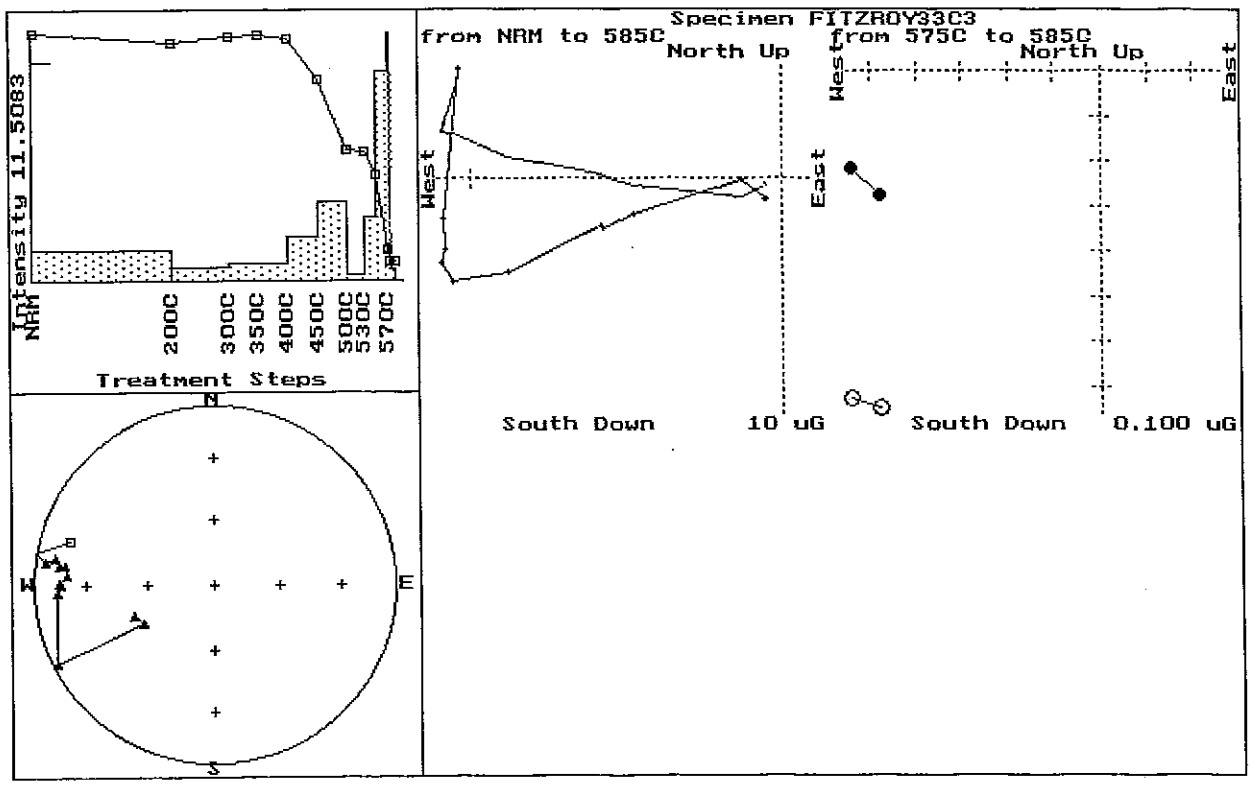
Intensity 11.5083
NRM
200C
300C
350C
400C
450C
500C
530C
570C
Treatment Steps
N
E
S
W
Specimen FITZROY33C3
from NRM to 585C
North Up
West
East
South Down
10 uG
from 575C to 585C
North Up
West
East
South Down
0.100 uG

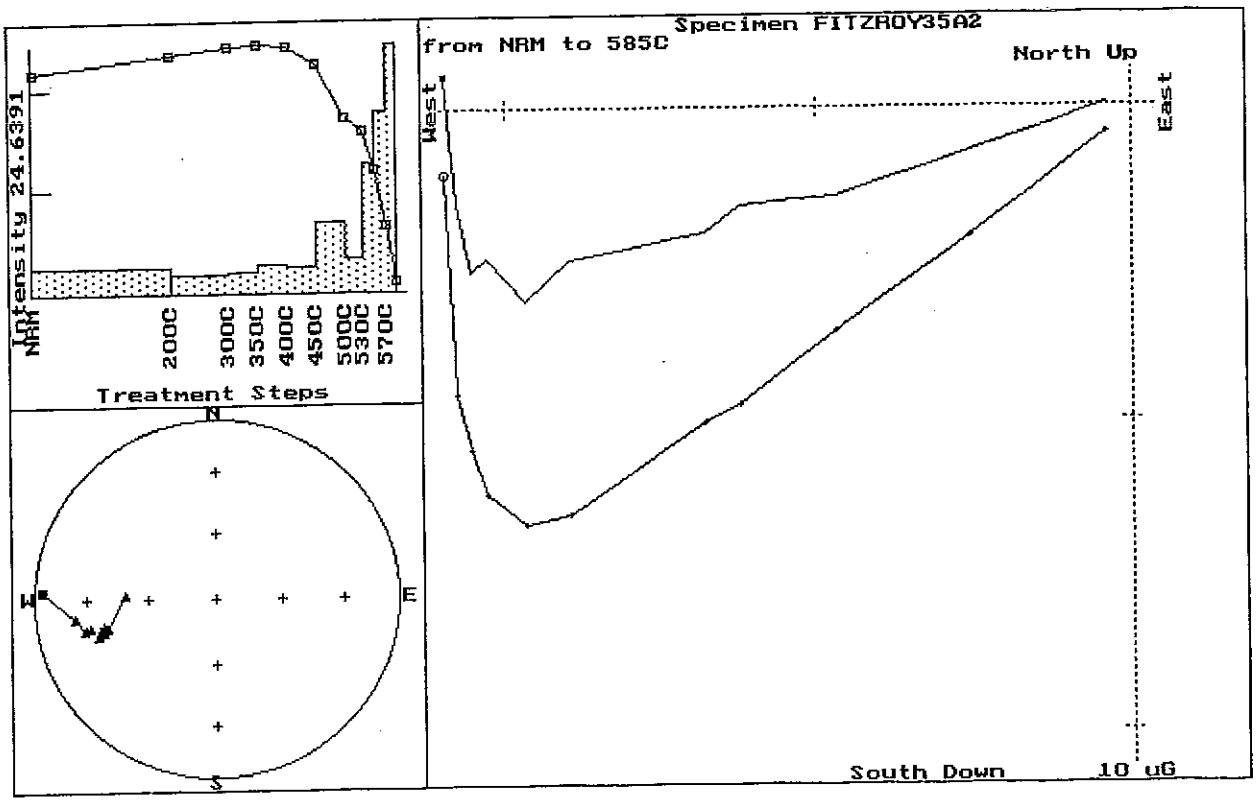
Specimen FITZROY35A2
from NRM to 585C
North Up
West
East
Intensity 24.6391
NRM
200C
300C
350C
400C
450C
500C
530C
570C
Treatment Steps
N
E
S
South Down
10 uG

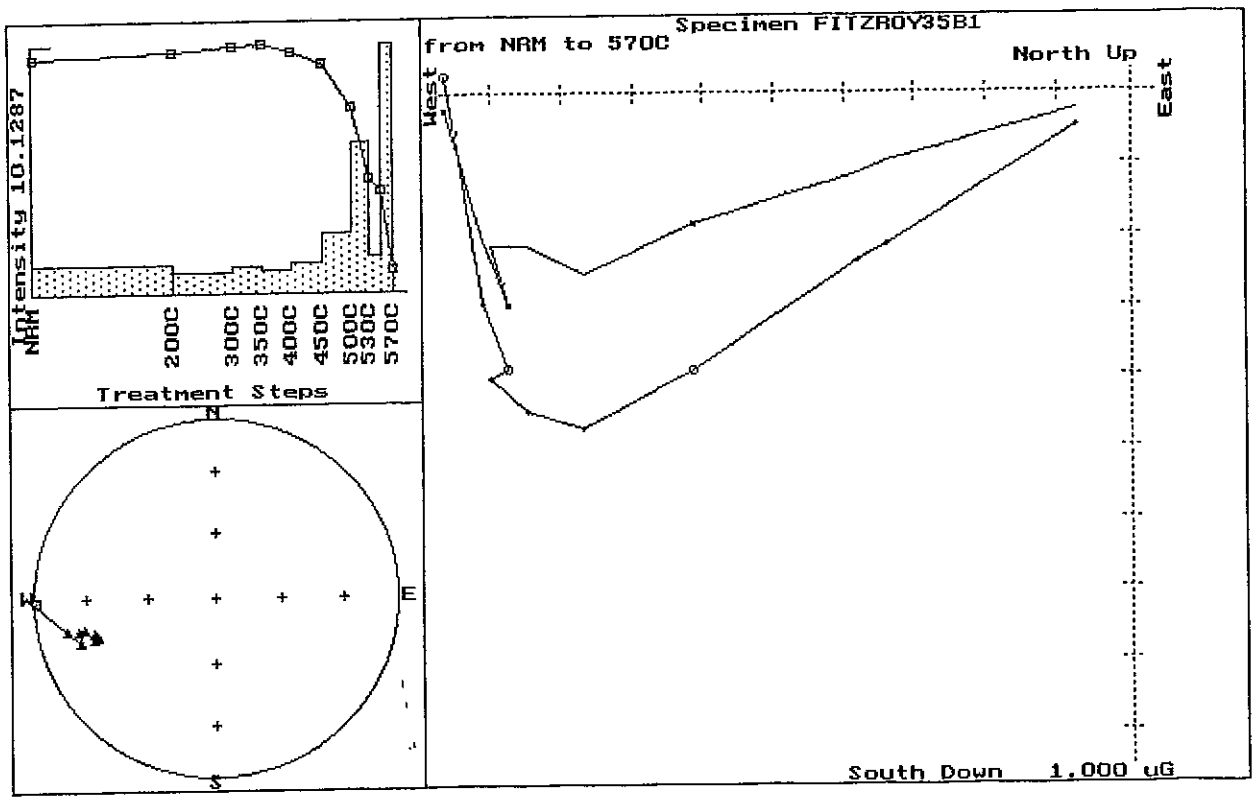
Specimen FITZROY35B1
from NRM to 570C
North Up
West
East
Intensity 10.1287
NRM
200C
300C
350C
400C
450C
500C
530C
570C
Treatment Steps
N
E
S
South Down
1.000 uG

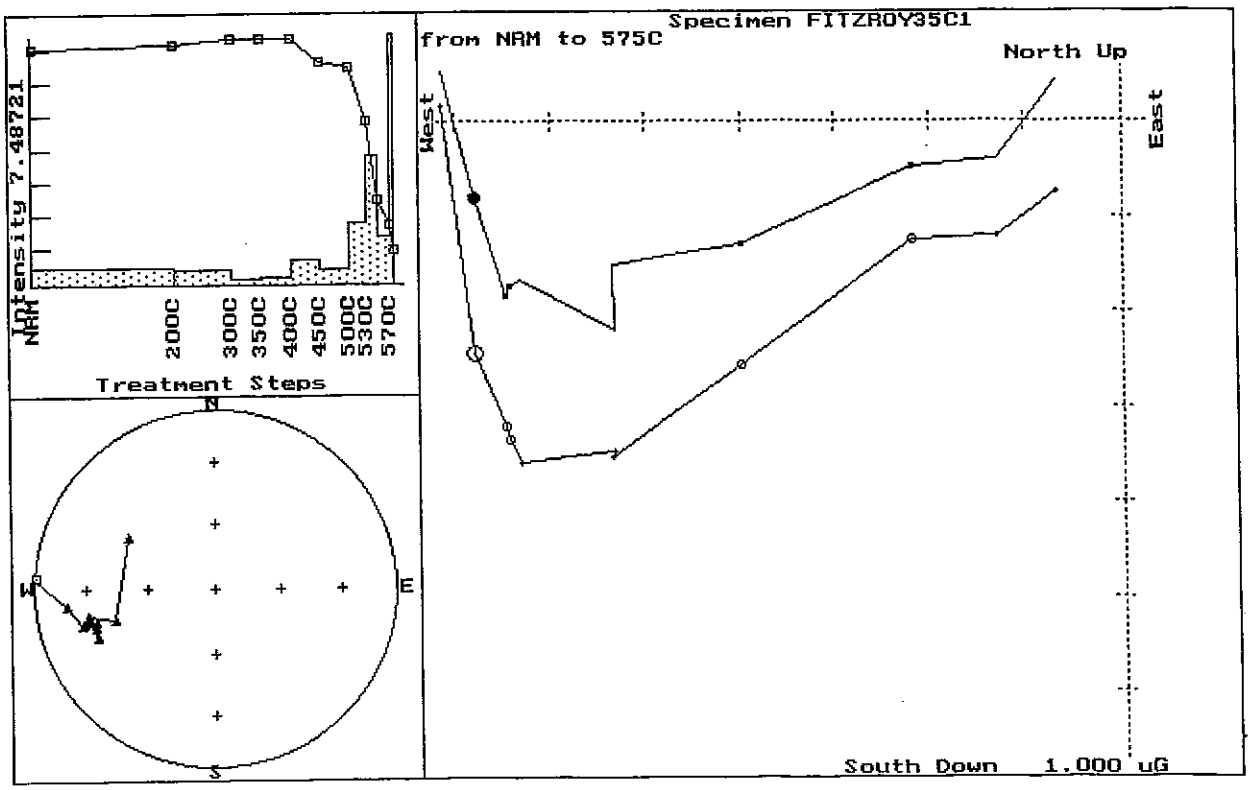
Specimen FITZROY35C1
from NRM to 575C
North Up
West
East
Intensity 7.48721
NRM
200C
300C
350C
400C
450C
500C
530C
570C
Treatment Steps
N
E
S
South Down
1.000 uG

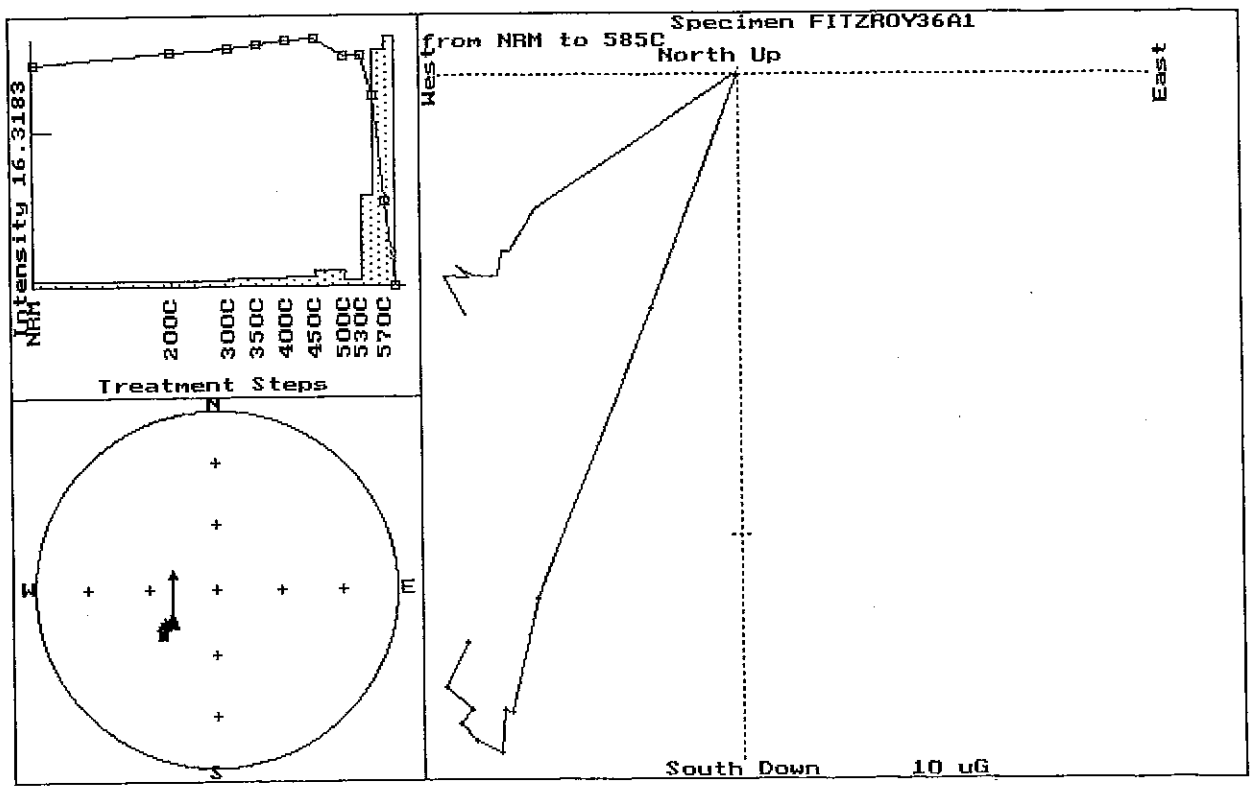
Specimen FITZROY36A1
from NRM to 585C
North Up
West
East
Intensity 16.3183
NRM
200C
300C
350C
400C
450C
500C
530C
570C
Treatment Steps
N
E
S
South Down
10 uG

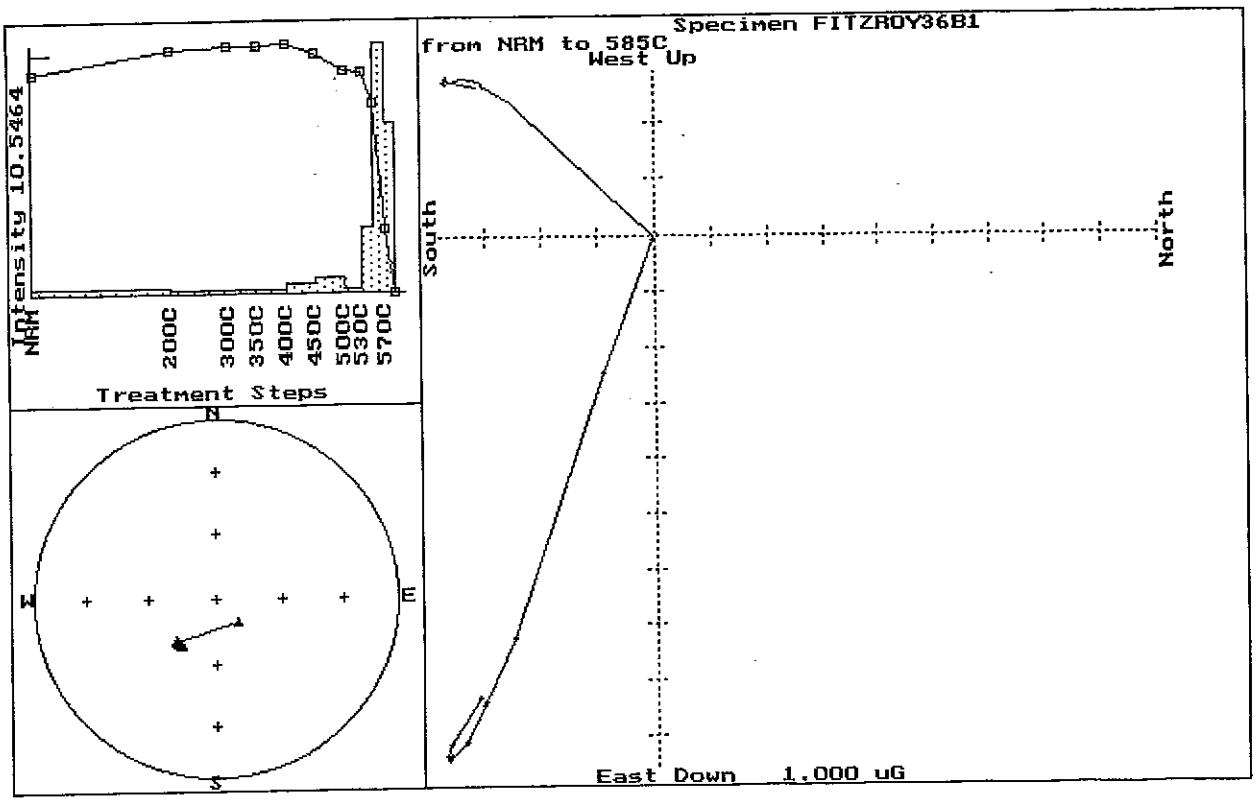
Specimen FITZROY36B1
from NRM to 585C
West Up
South
North
East Down 1.000 uG
Intensity 10.5464
NRM
200C
300C
350C
400C
450C
500C
530C
570C
Treatment Steps
N
E
S
W

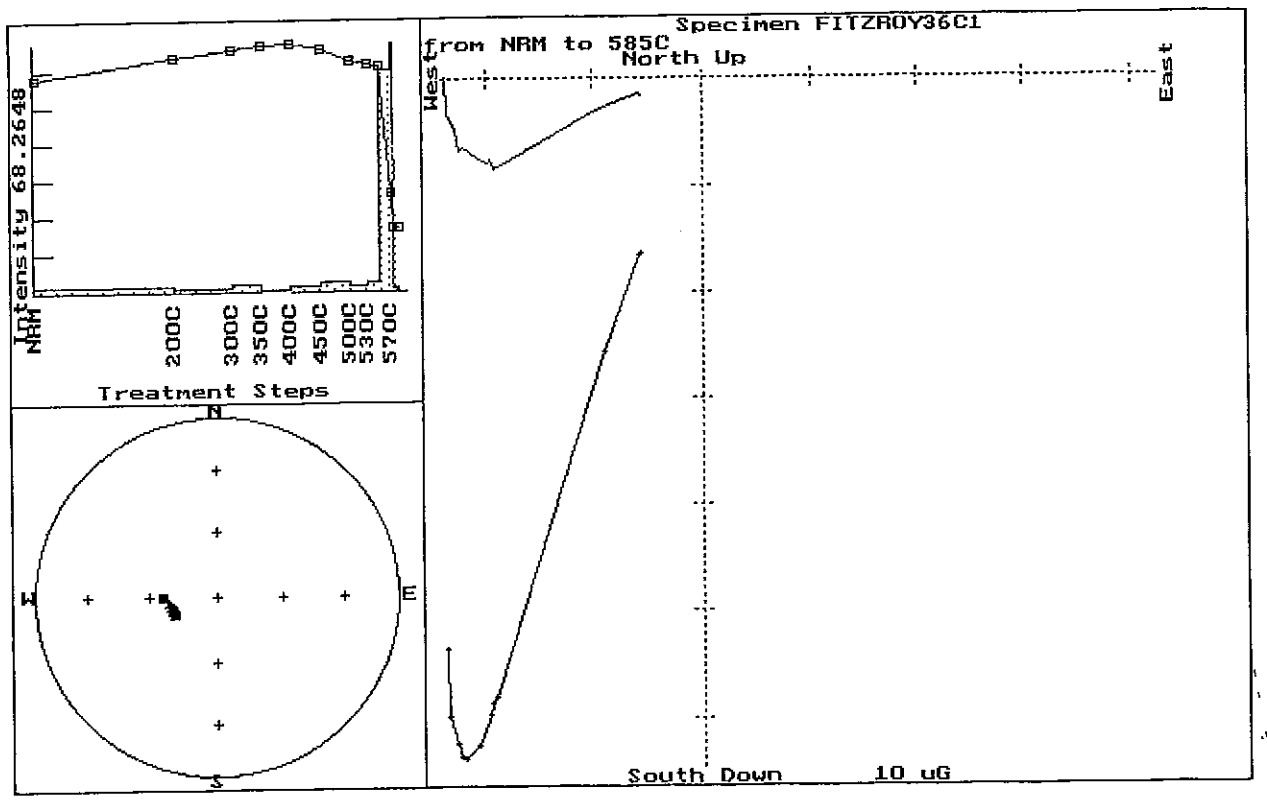
Specimen FITZROY36C1
from NRM to 585C
North Up
West
East
South Down 10 uG
Intensity 68.2648
NRM
200C
300C
350C
400C
450C
500C
530C
570C
Treatment Steps
N
E
S
W

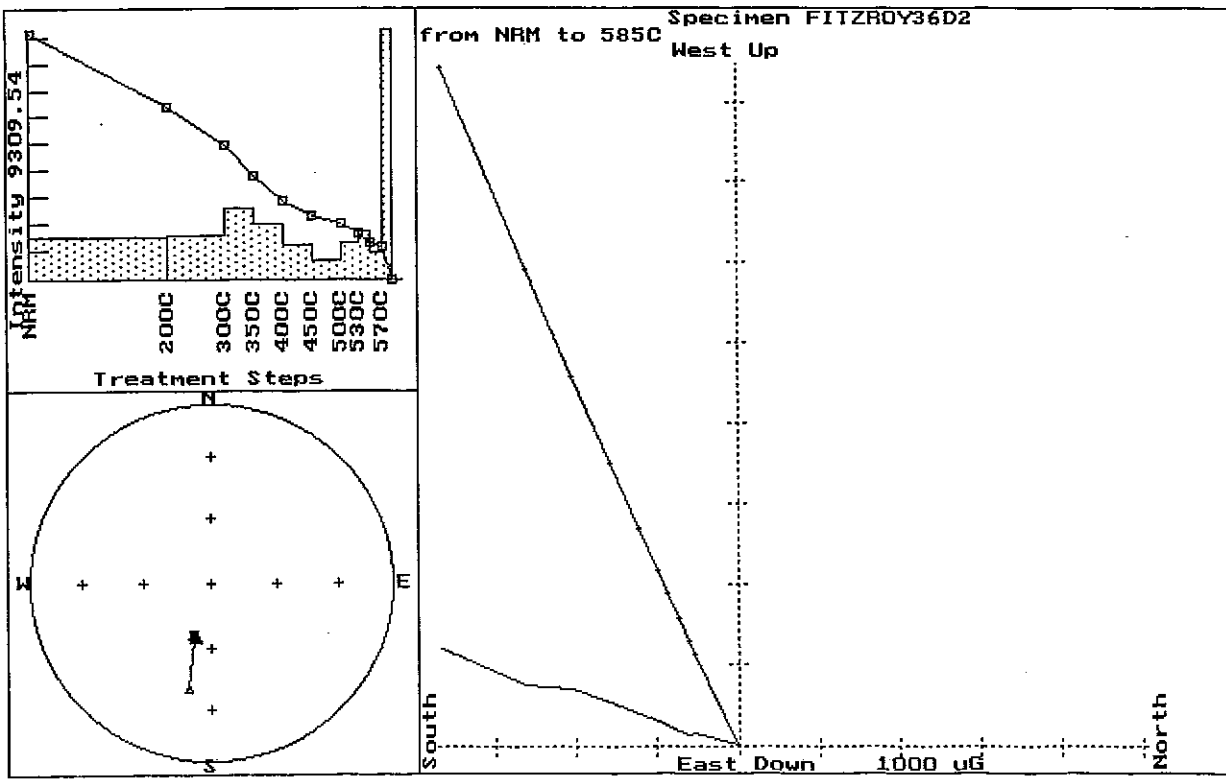
Intensity 9309.54
NRM
200C
300C
350C
400C
450C
500C
530C
570C
Treatment Steps
N
W
E
S
Specimen FITZROY36D2
from NRM to 585C
West Up
South
North
East Down
1000 uG

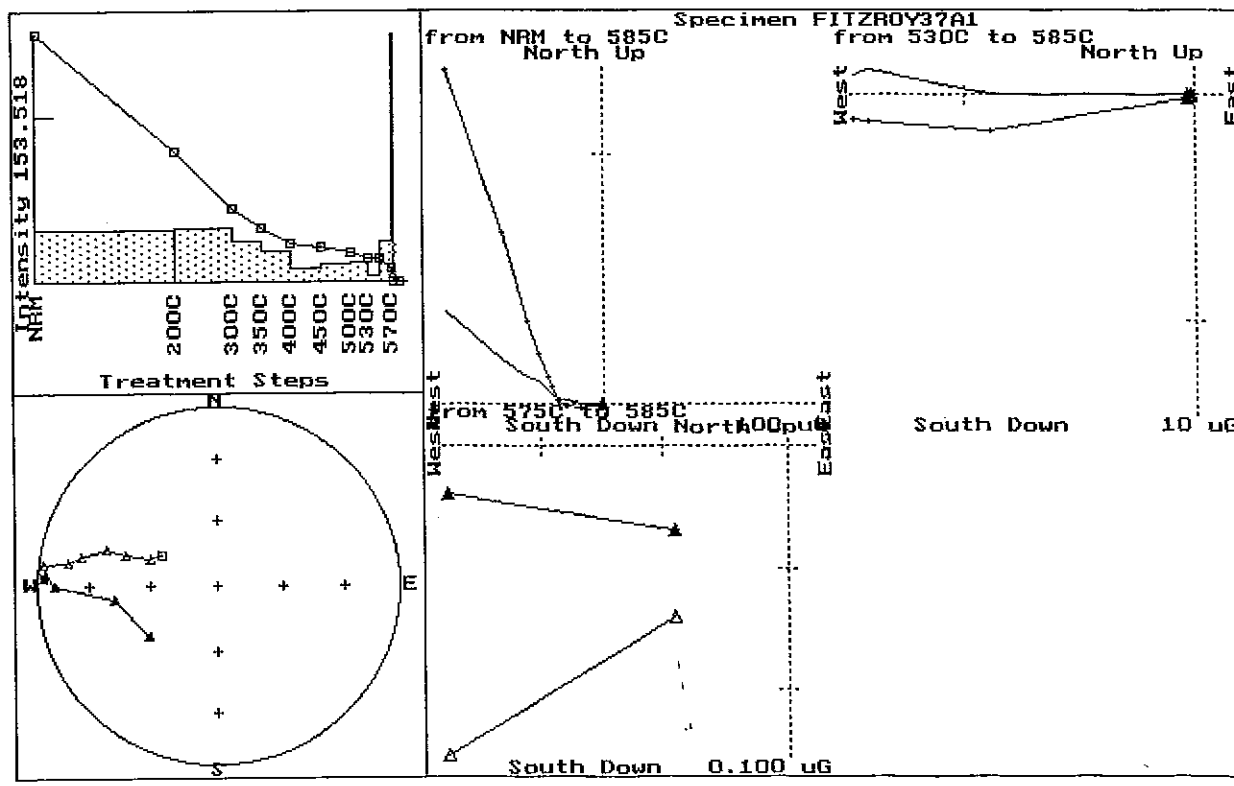
Intensity 153.518
NRM
200C
300C
350C
400C
450C
500C
530C
570C
Treatment Steps
N
W
E
S
Specimen FITZROY37A1
from NRM to 585C
North Up
from 530C to 585C
North Up
West
East
from 575C to 585C
South Down North
West
East
South Down
10 uG
South Down
0.100 uG

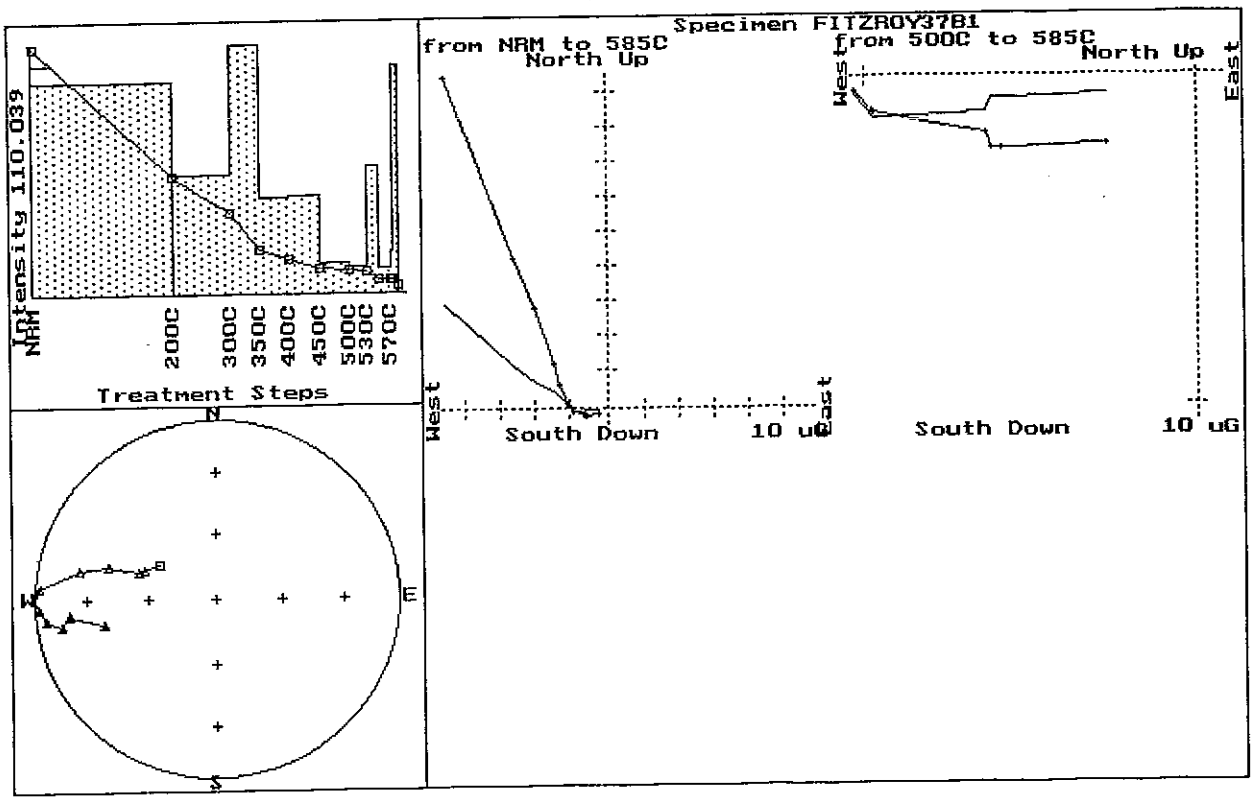
Specimen FITZROY37B1
from NRM to 585C
North Up
from 500C to 585C
North Up
Intensity 110.039
NRM
200C
300C
350C
400C
450C
500C
530C
570C
Treatment Steps
N
E
S
West
East
South Down
10 uG
South Down
10 uG

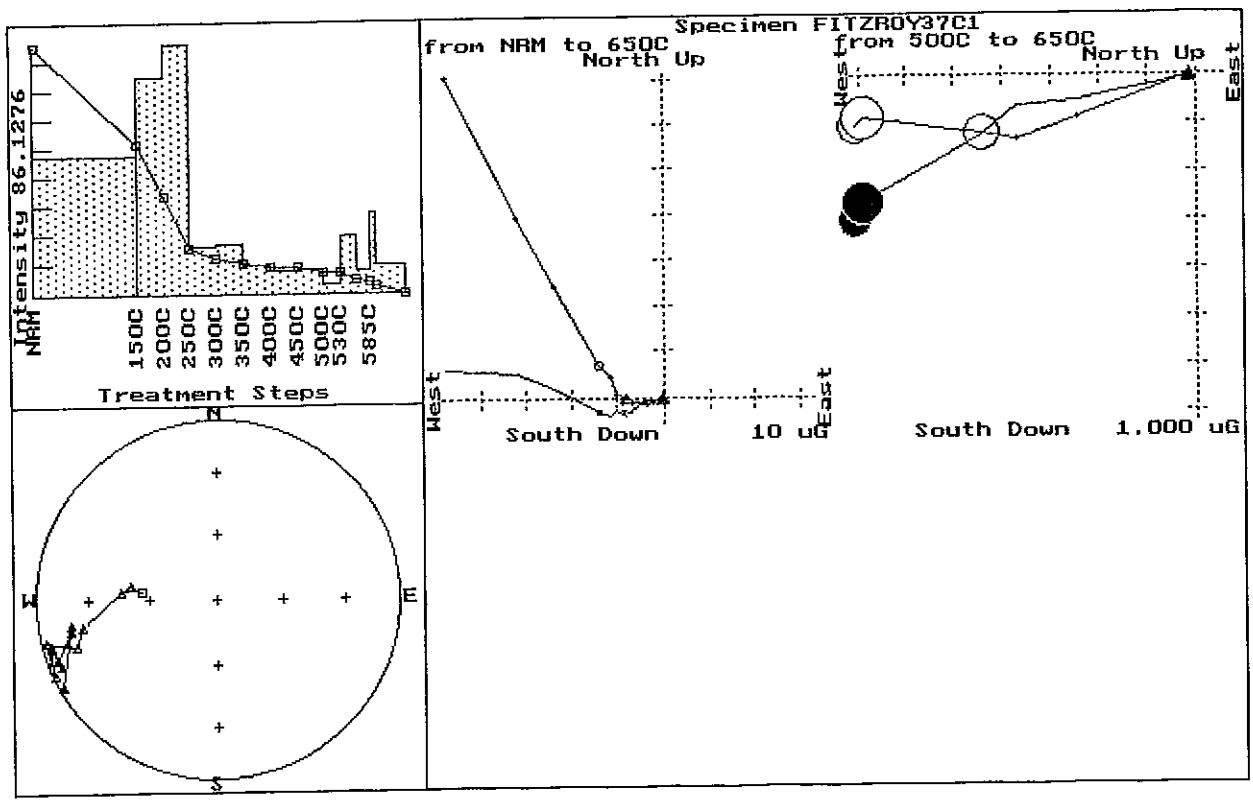
Specimen FITZROY37C1
from NRM to 650C
North Up
from 500C to 650C
North Up
Intensity 86.1276
NRM
150C
200C
250C
300C
350C
400C
450C
500C
530C
585C
Treatment Steps
N
E
S
West
East
South Down
10 uG
South Down
1.000 uG

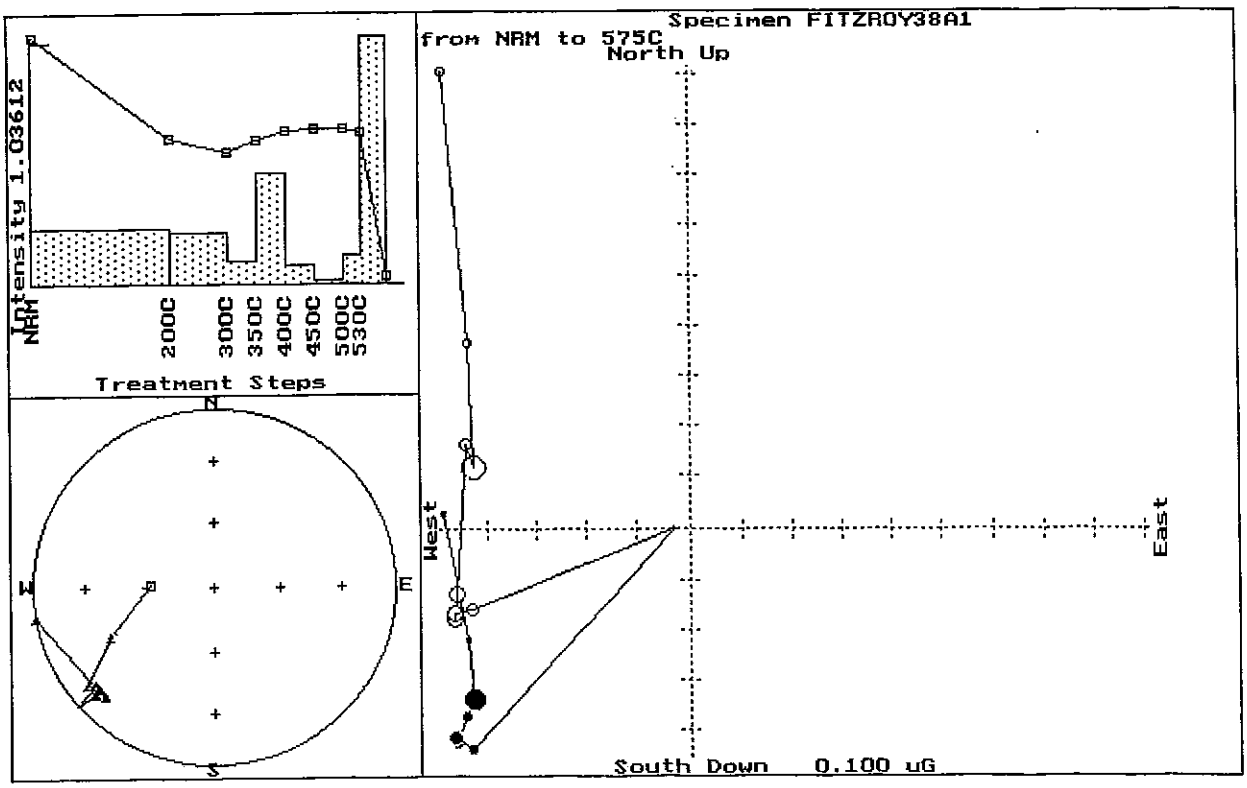
Specimen FITZROY38A1
from NRM to 575C
North Up
Intensity 1.03612
NRM
200C
300C
350C
400C
450C
500C
530C
Treatment Steps
N
E
S
W
West
East
South Down
0.100 uG

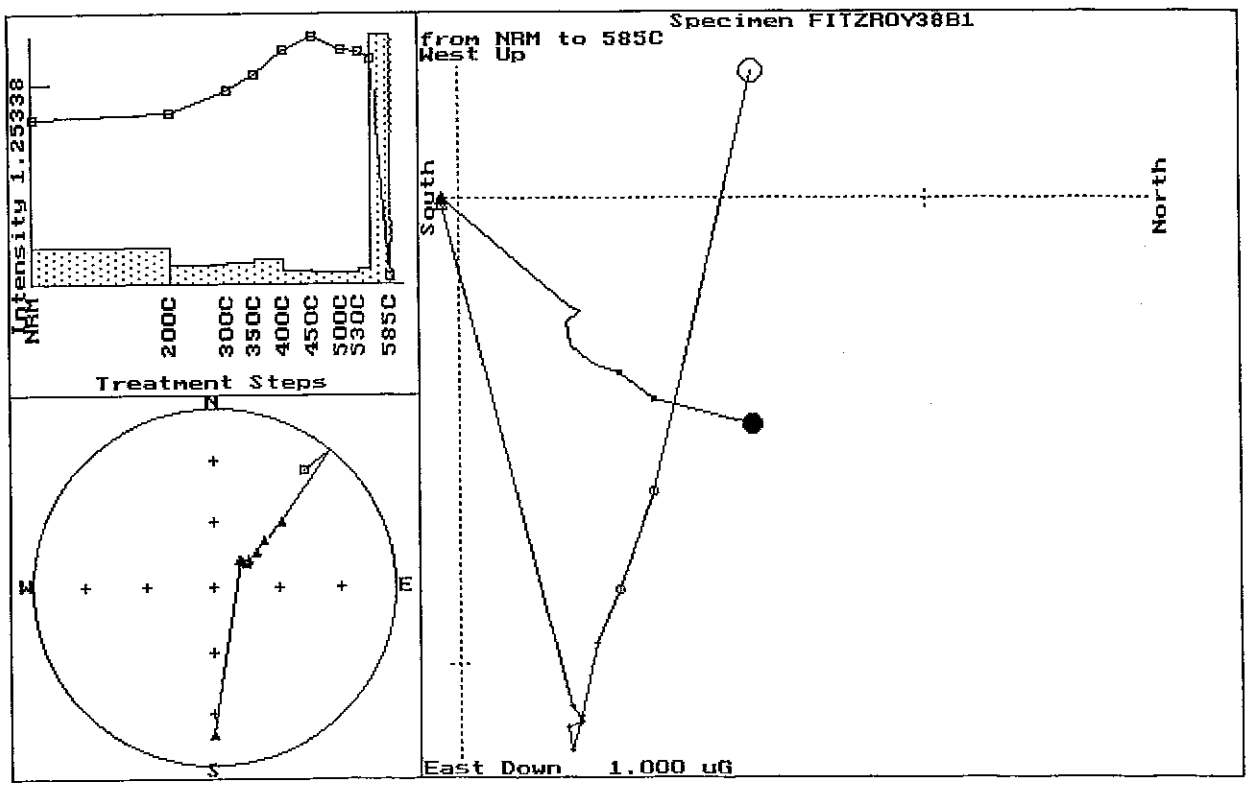
Specimen FITZROY38B1
from NRM to 585C
West Up
Intensity 1.25338
NRM
200C
300C
350C
400C
450C
500C
530C
585C
Treatment Steps
N
E
S
W
South
North
East Down
1.000 uG

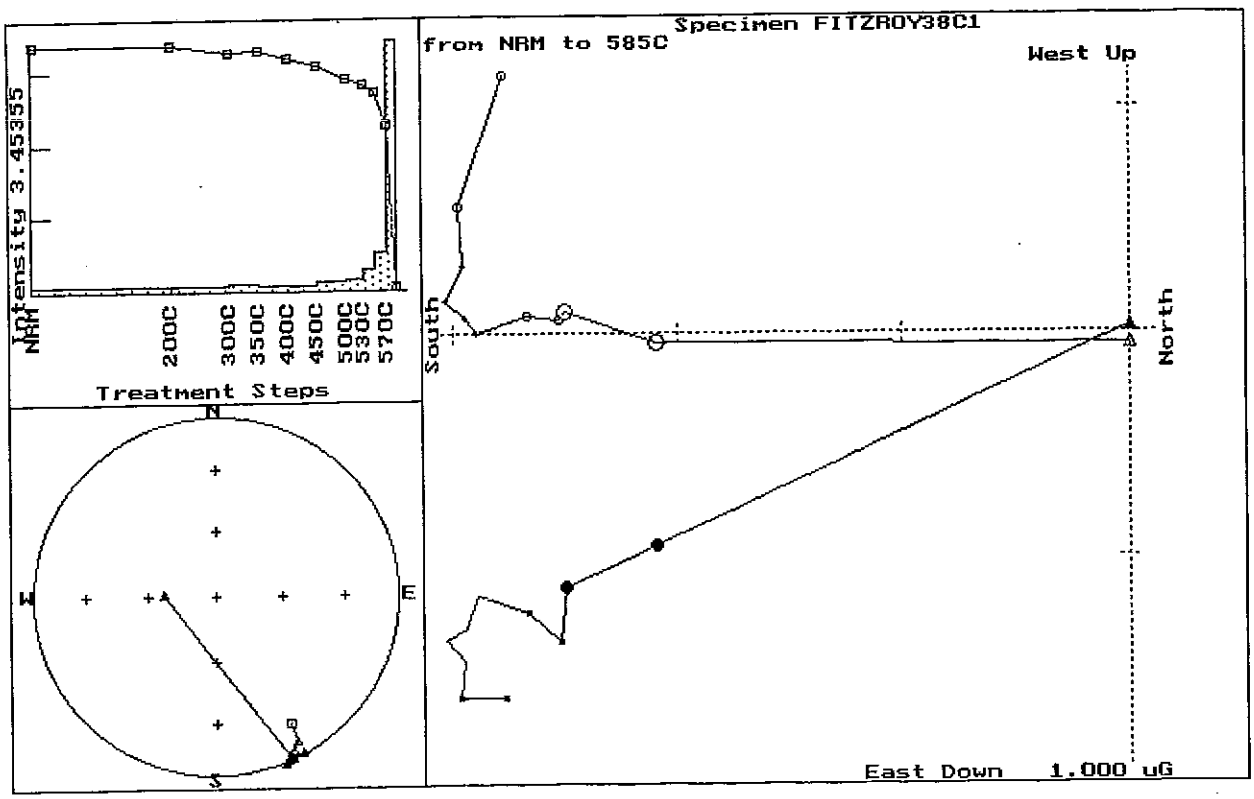
Intensity 3.45355
NRM
200C
300C
350C
400C
450C
500C
530C
570C
Treatment Steps
N
W
E
S
Specimen FITZROY38C1
from NRM to 585C
West Up
South
North
East Down 1.000 uG

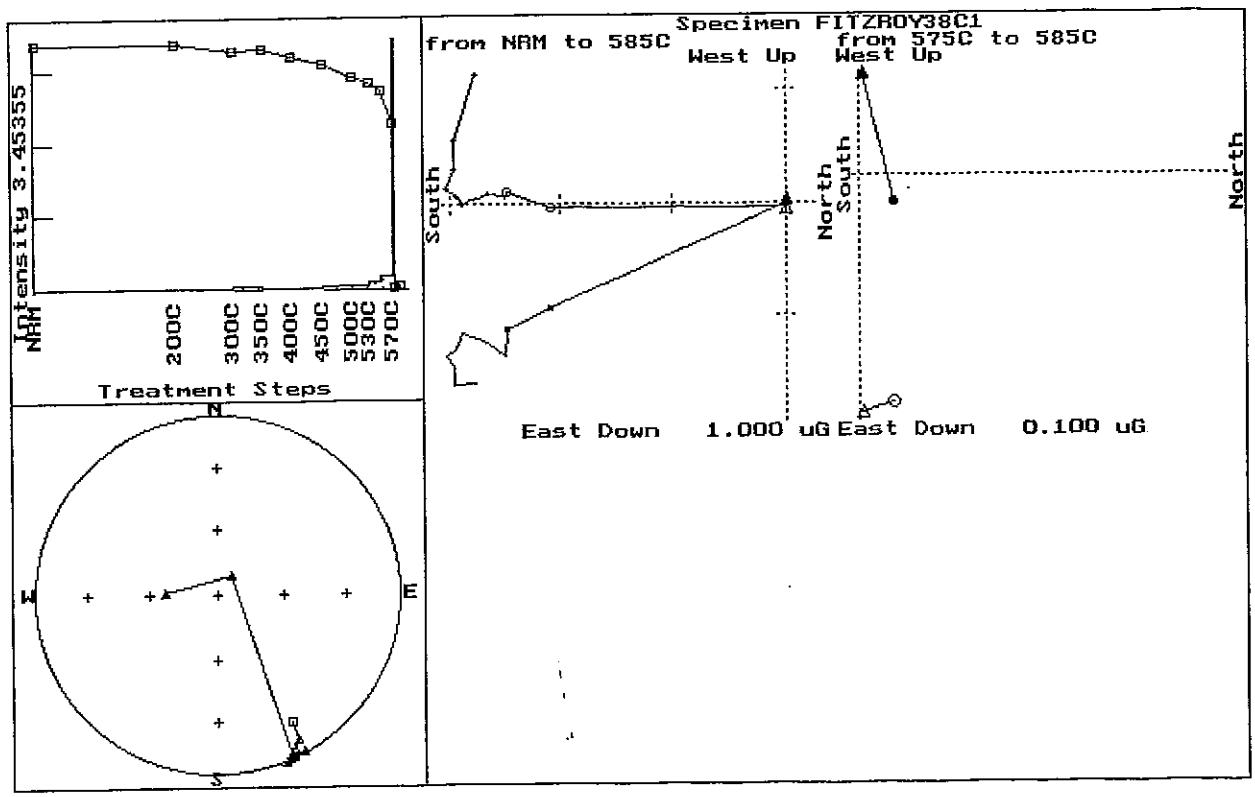
Intensity 3.45355
NRM
200C
300C
350C
400C
450C
500C
530C
570C
Treatment Steps
N
W
E
S
Specimen FITZROY38C1
from NRM to 585C
from 575C to 585C
West Up
West Up
South
North
South
North
East Down 1.000 uG
East Down 0.100 uG

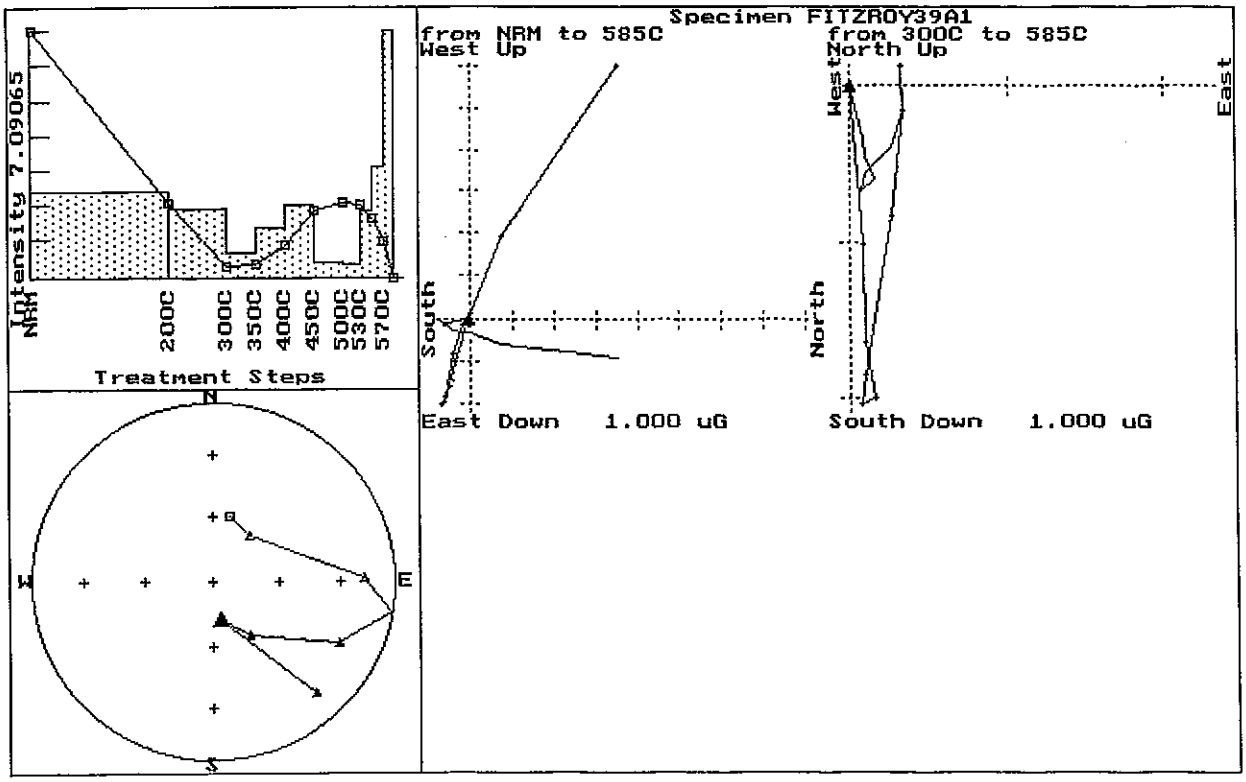
Specimen FITZROY39A1
from NRM to 585C
West Up
from 300C to 585C
North Up
Intensity 7.09065
NRM
200C
300C
350C
400C
450C
500C
530C
570C
Treatment Steps
N
E
S
W
South
North
West
East
East Down 1.000 uG
South Down 1.000 uG

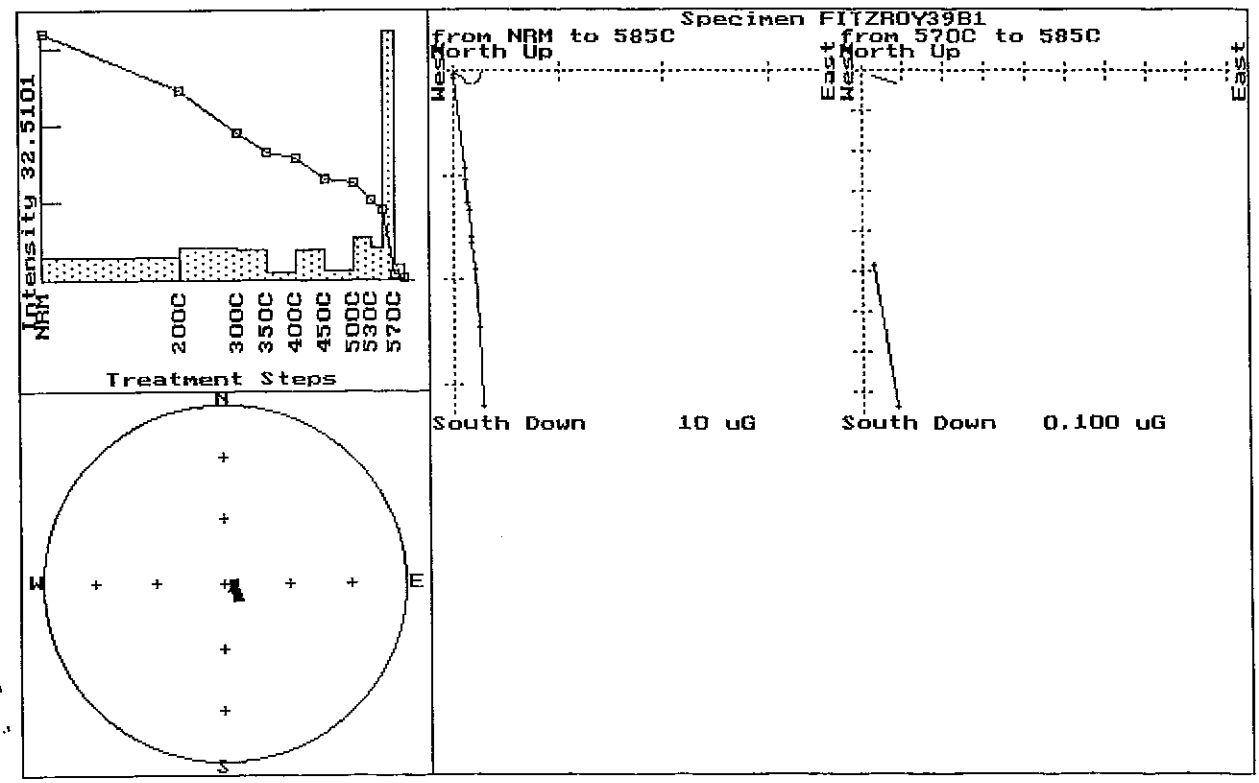
Specimen FITZROY39B1
from NRM to 585C
North Up
from 570C to 585C
North Up
Intensity 32.5101
NRM
200C
300C
350C
400C
450C
500C
530C
570C
Treatment Steps
N
E
S
W
West
East
South Down 10 uG
South Down 0.100 uG

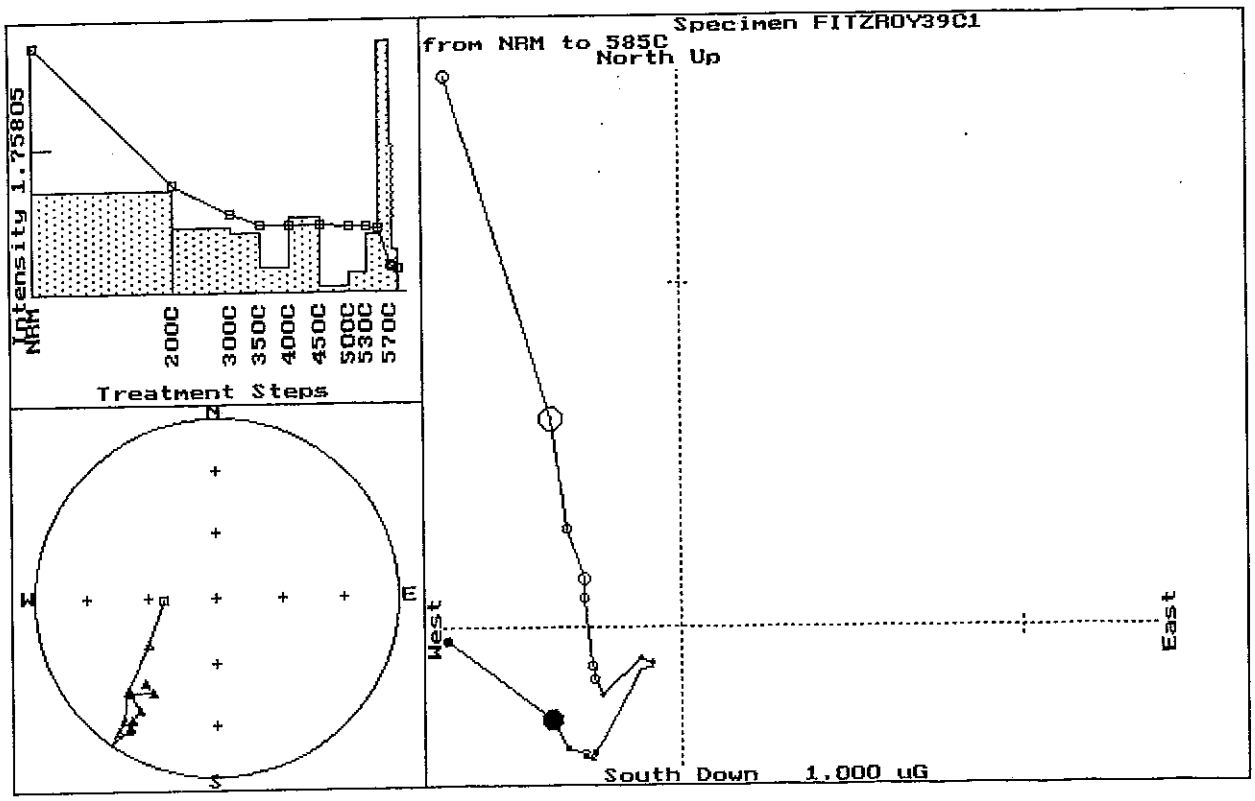
Specimen FITZROY39C1
from NRM to 585C
North Up
Intensity 1.75805
NRM
200C
300C
350C
400C
450C
500C
530C
570C
Treatment Steps
N
E
S
W
West
East
South Down
1.000 uG

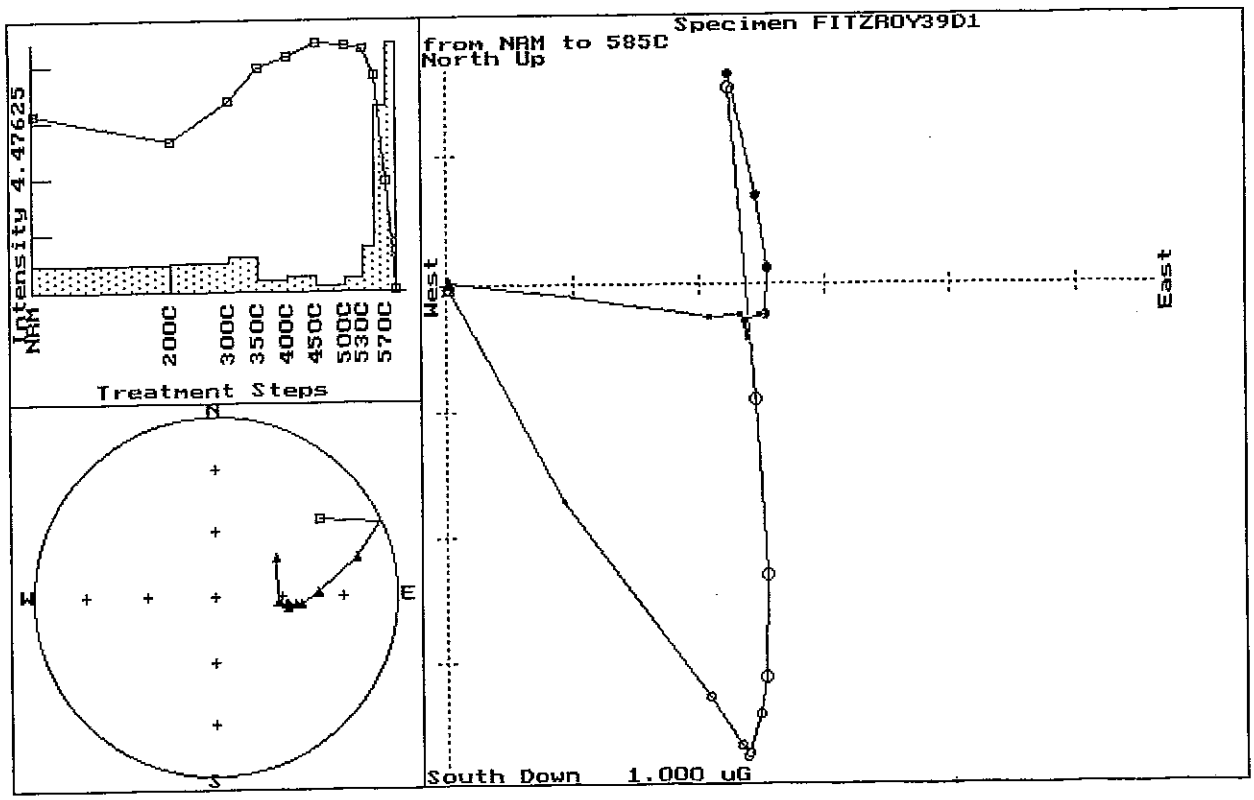
Specimen FITZROY39D1
from NRM to 585C
North Up
Intensity 4.47625
NRM
200C
300C
350C
400C
450C
500C
530C
570C
Treatment Steps
N
E
S
W
West
East
South Down
1.000 uG

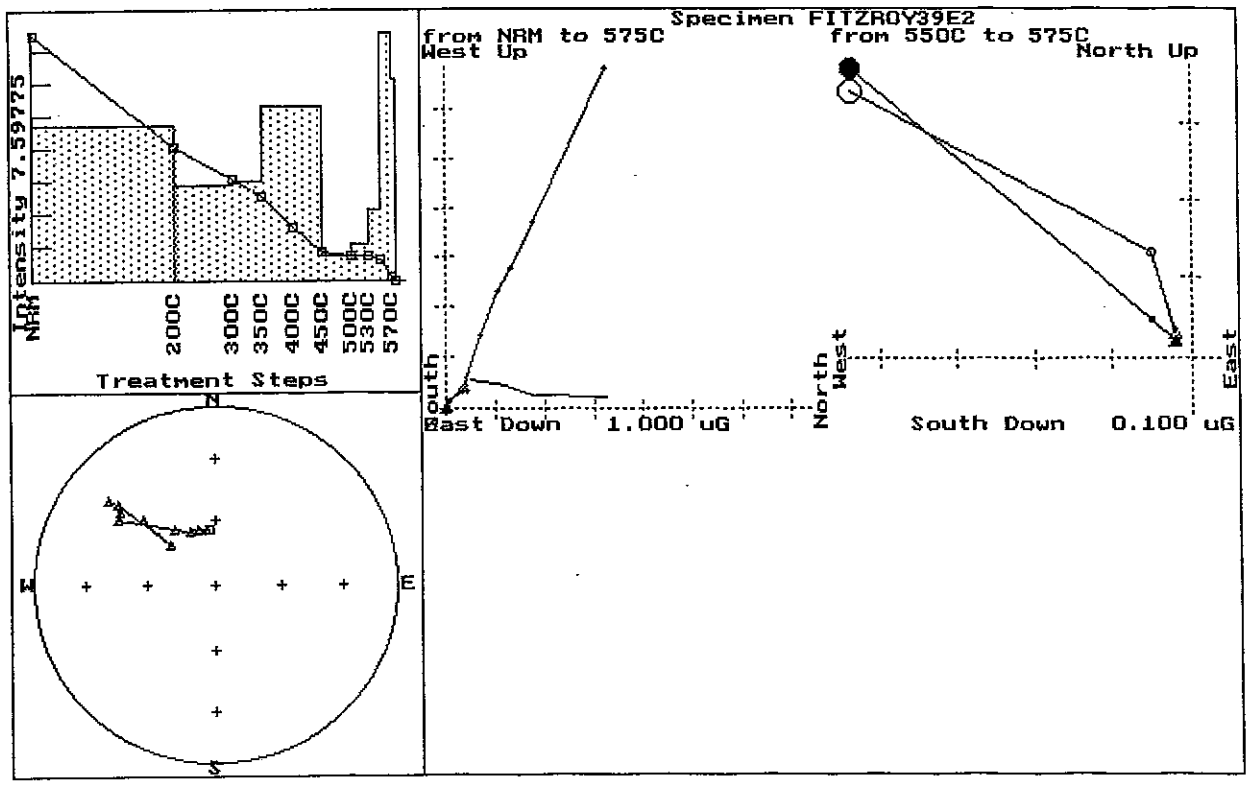
Specimen FITZROY39E2
from NRM to 575C
West Up
from 550C to 575C
North Up
Intensity 7.59775
NRM
200C
300C
350C
400C
450C
500C
530C
570C
Treatment Steps
N
E
S
W
South
East Down 1.000 uG
North
West
East
South Down 0.100 uG

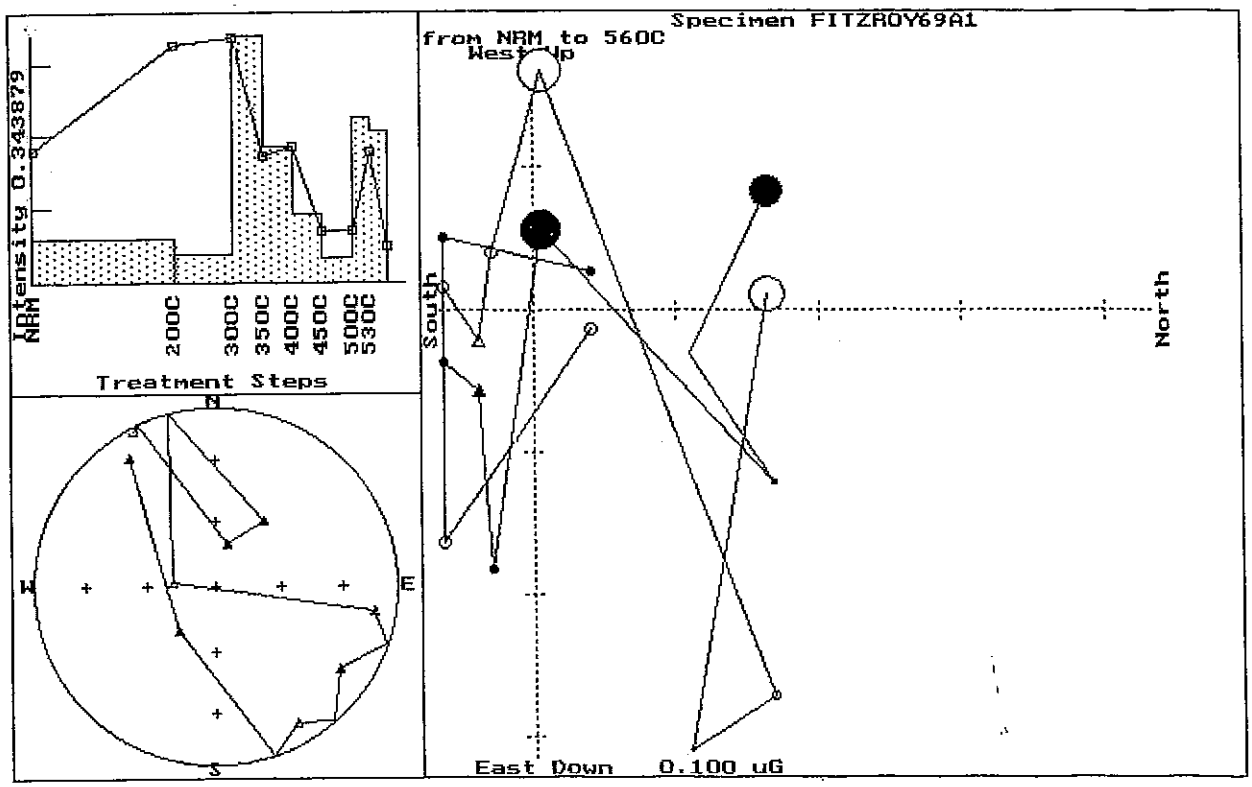
Specimen FITZROY69A1
from NRM to 560C
West Up
Intensity 0.343879
NRM
200C
300C
350C
400C
450C
500C
530C
Treatment Steps
N
E
S
W
South
North
East Down 0.100 uG

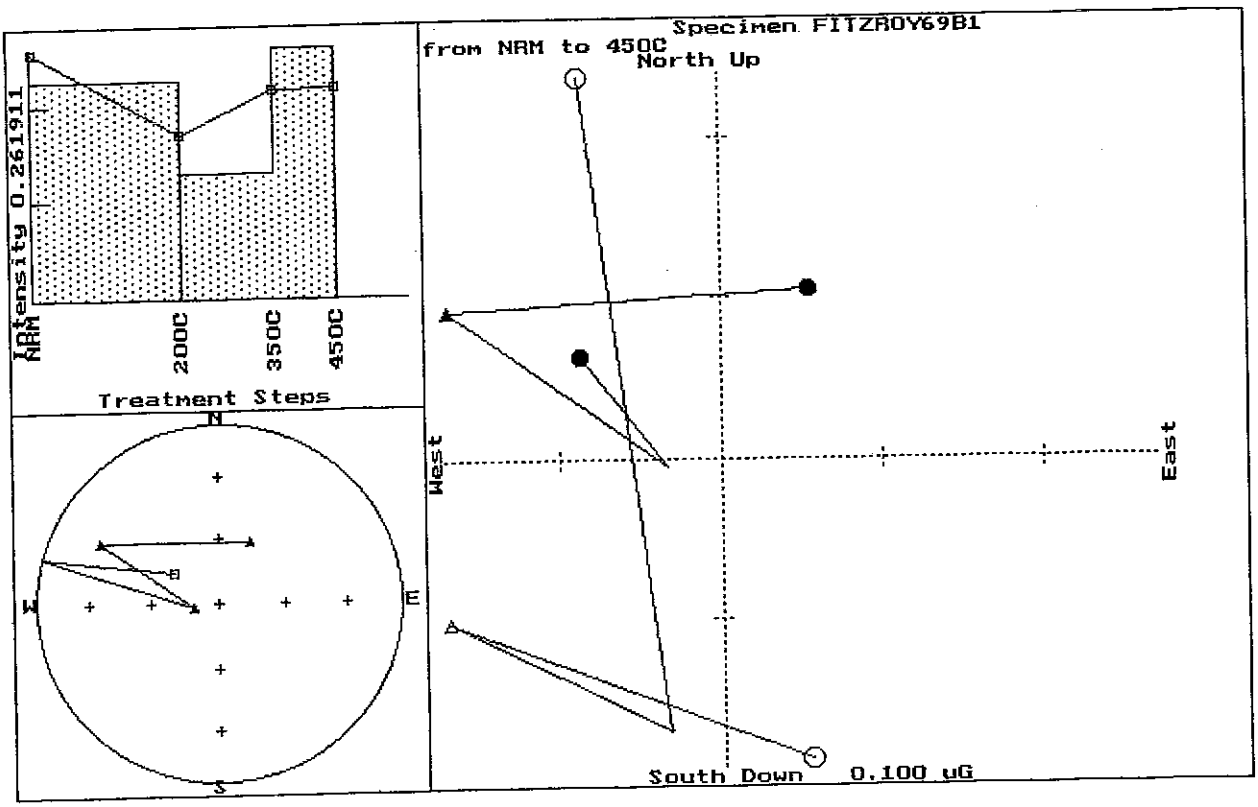
Specimen FITZROY69B1
from NRM to 450C
North Up
Intensity 0.261911
NRM
200C
350C
450C
Treatment Steps
N
E
S
W
West
East
South Down
0.100 uG

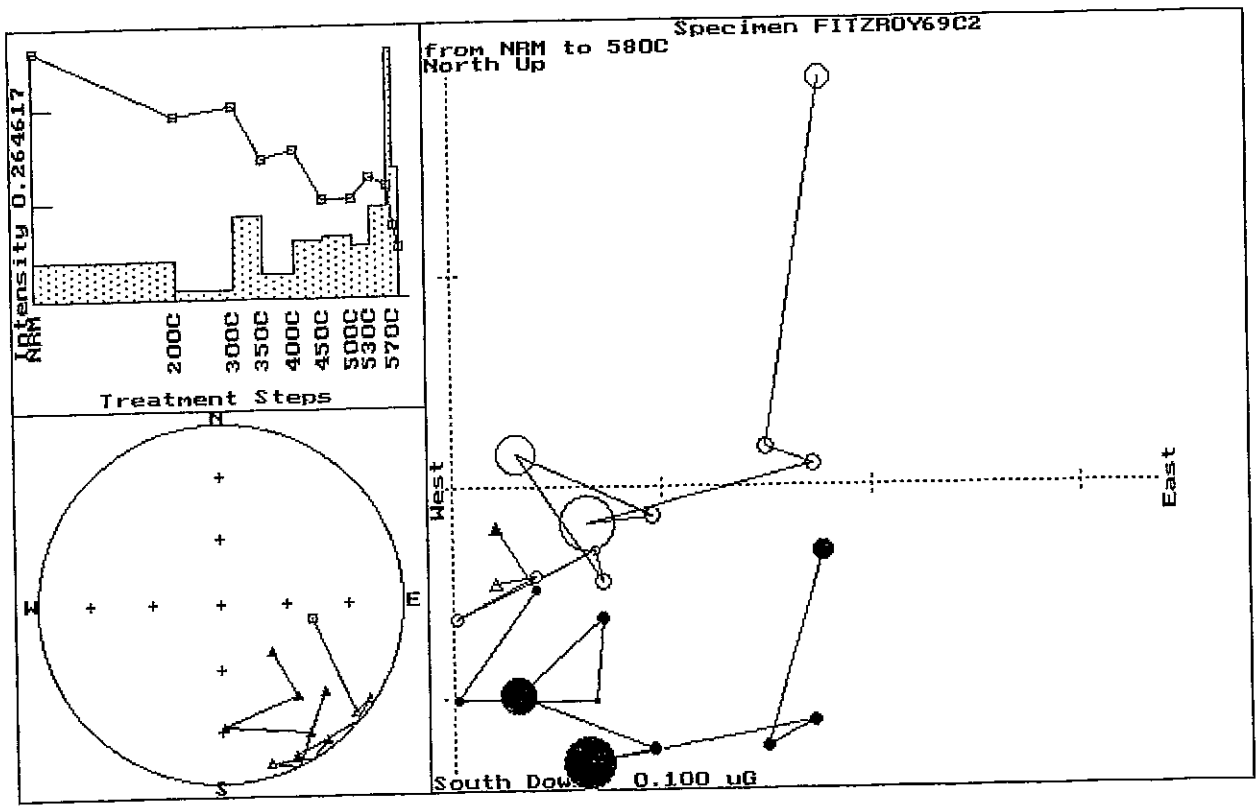
Specimen FITZROY69C2
from NRM to 580C
North Up
Intensity 0.264617
NRM
200C
300C
350C
400C
450C
500C
530C
570C
Treatment Steps
N
E
S
W
West
East
South Down
0.100 uG

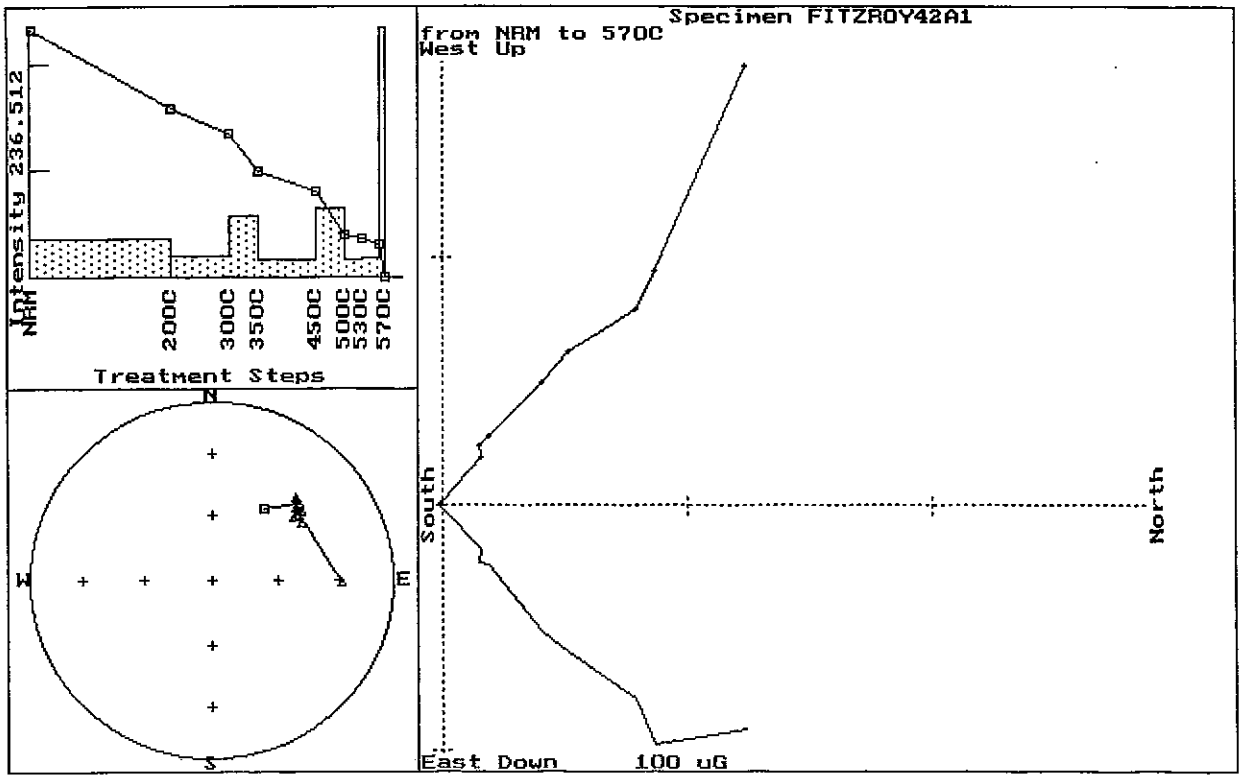
Specimen FITZROY42A1
from NRM to 570C
West Up
Intensity 236.512
NRM
200C
300C
350C
450C
500C
530C
570C
Treatment Steps
N
W
E
S
South
North
East Down
100 uG

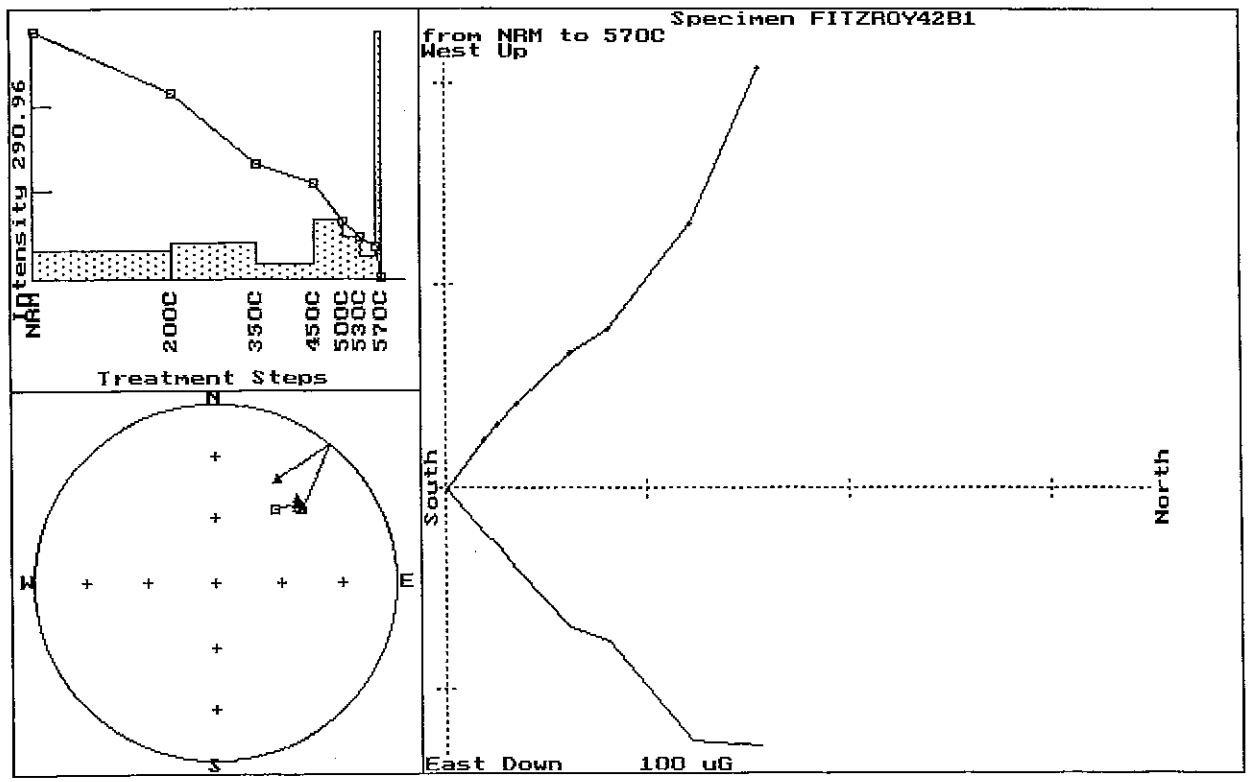
Specimen FITZROY42B1
from NRM to 570C
West Up
Intensity 290.96
NRM
200C
350C
450C
500C
530C
570C
Treatment Steps
N
W
E
S
South
North
East Down
100 uG

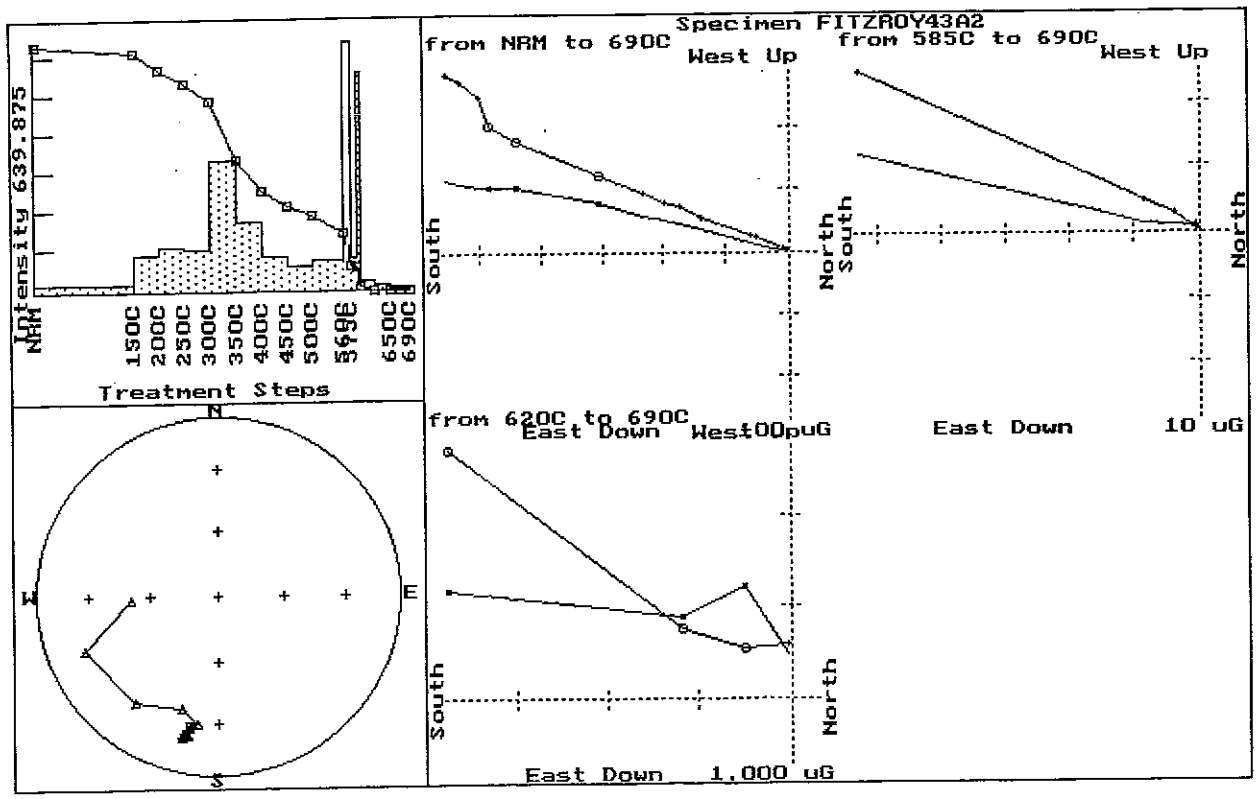
Specimen FITZROY43A2
Intensity 639.875
NRM
150C
200C
250C
300C
350C
400C
450C
500C
650C
690C
Treatment Steps
from NRM to 690C
West Up
South
North
East Down
from 585C to 690C
West Up
South
North
East Down
10 uG
from 620C to 690C
East Down
West
South
North
East Down
1.000 uG
N
E
S
W

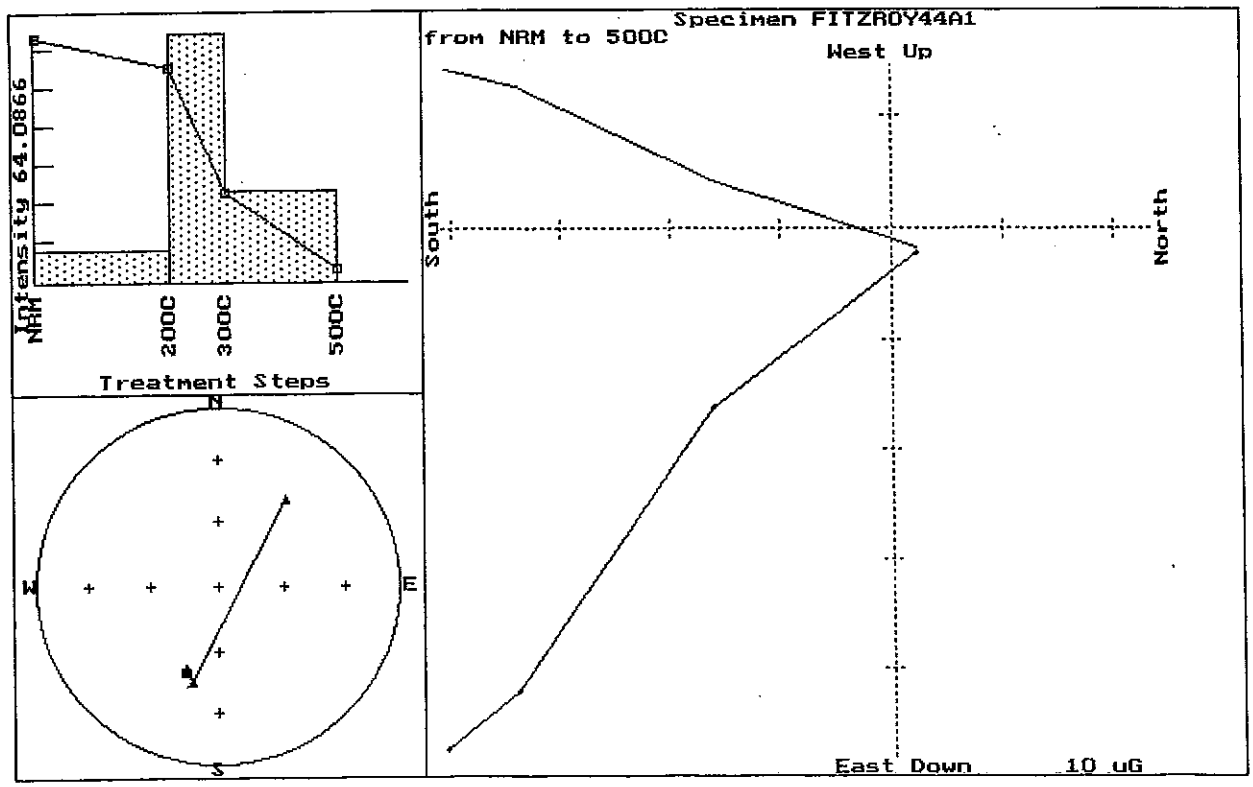
Specimen FITZROY44A1
from NRM to 500C
West Up
South
North
East Down
10 uG
Intensity 64.0866
NRM
200C
300C
500C
Treatment Steps
N
E
S
W

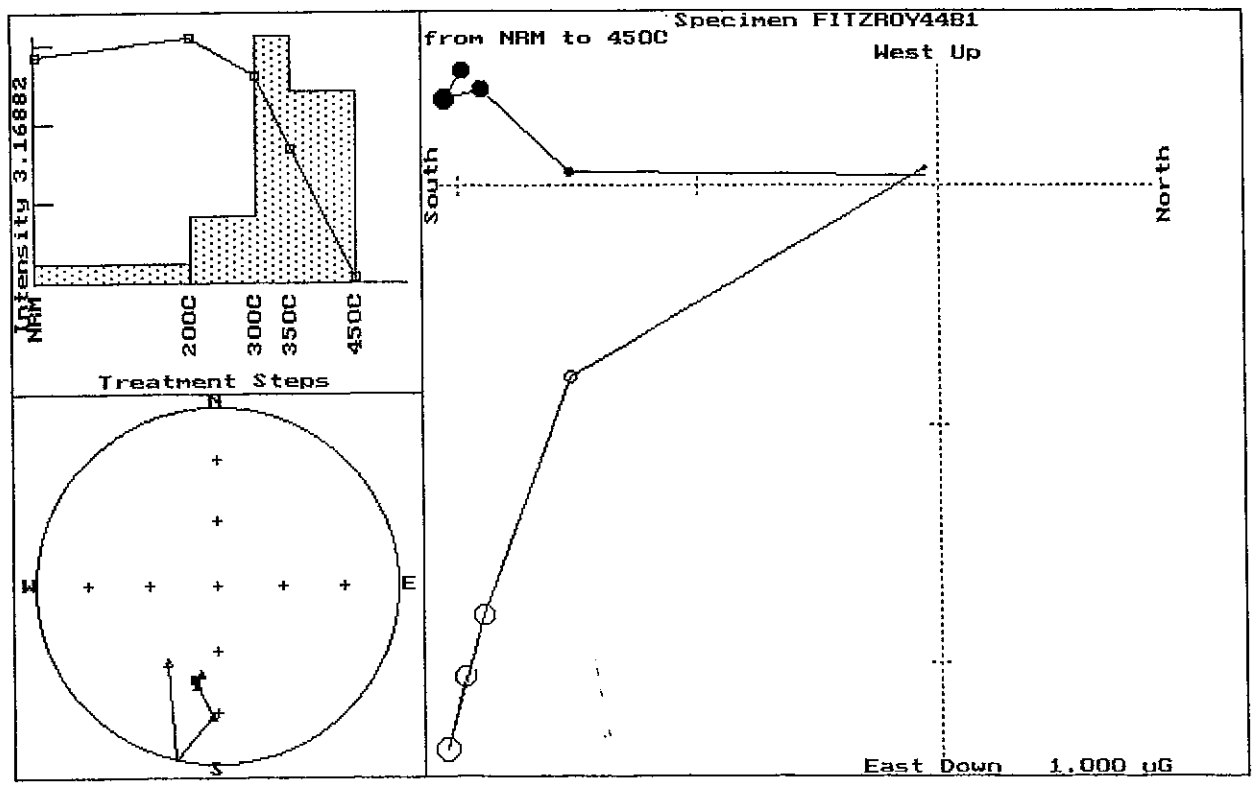
Specimen FITZROY44B1
from NRM to 450C
West Up
South
North
East Down
1.000 uG
Intensity 3.16882
NRM
200C
300C
350C
450C
Treatment Steps
N
E
S
W

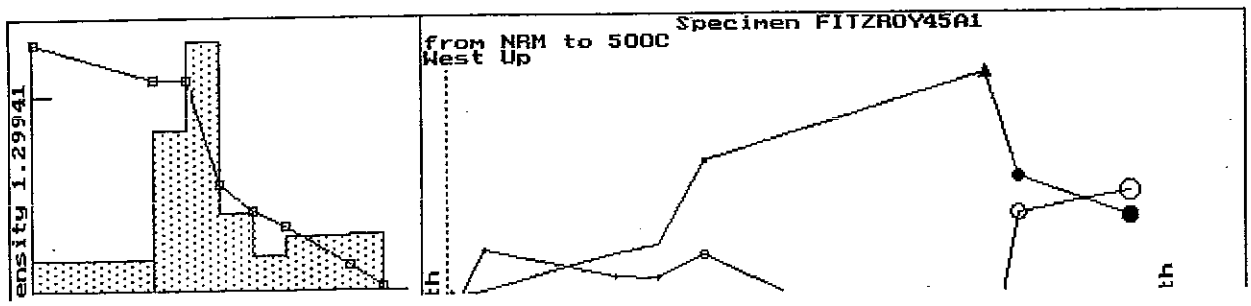
ensity 1.29941
Specimen FITZROY45A1
from NRM to 500C
West Up
th
th

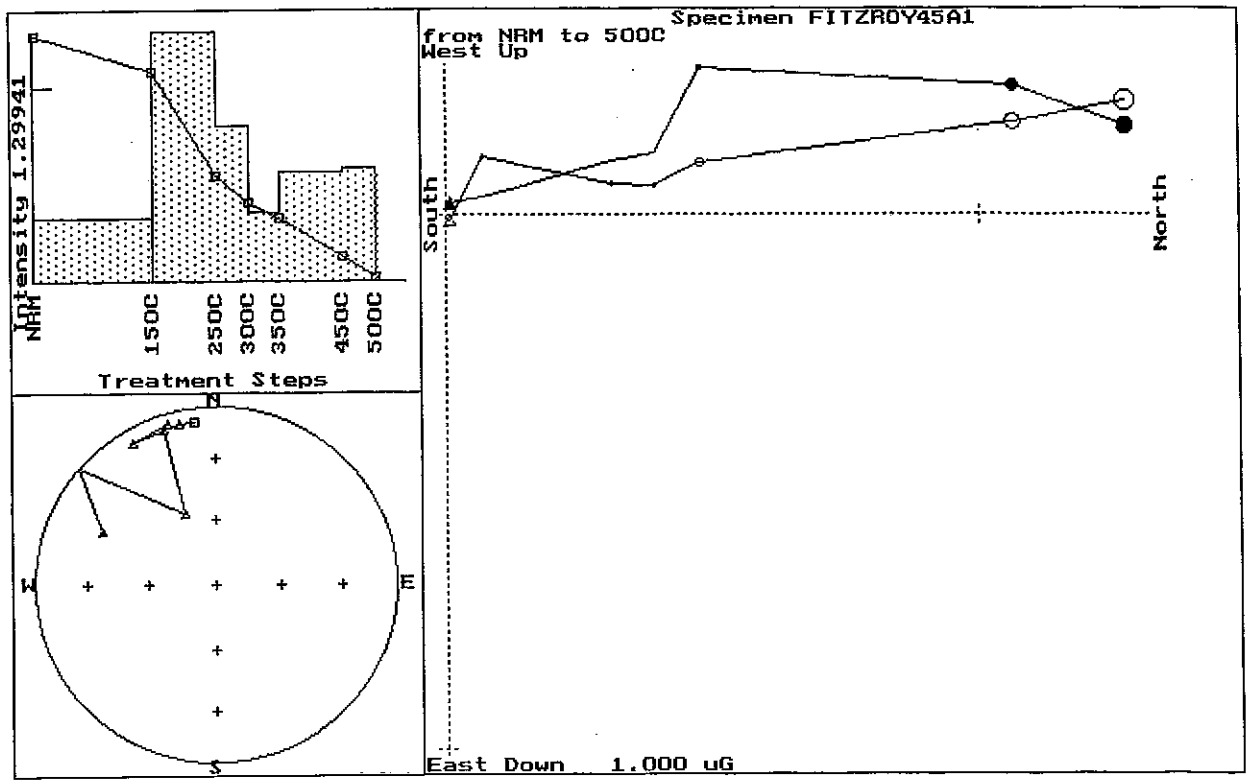
Specimen FITZROY45A1
from NRM to 500C
West Up
Intensity 1.29941
NRM
150C
250C
300C
350C
450C
500C
Treatment Steps
N
E
S
W
South
North
East Down 1.000 uG

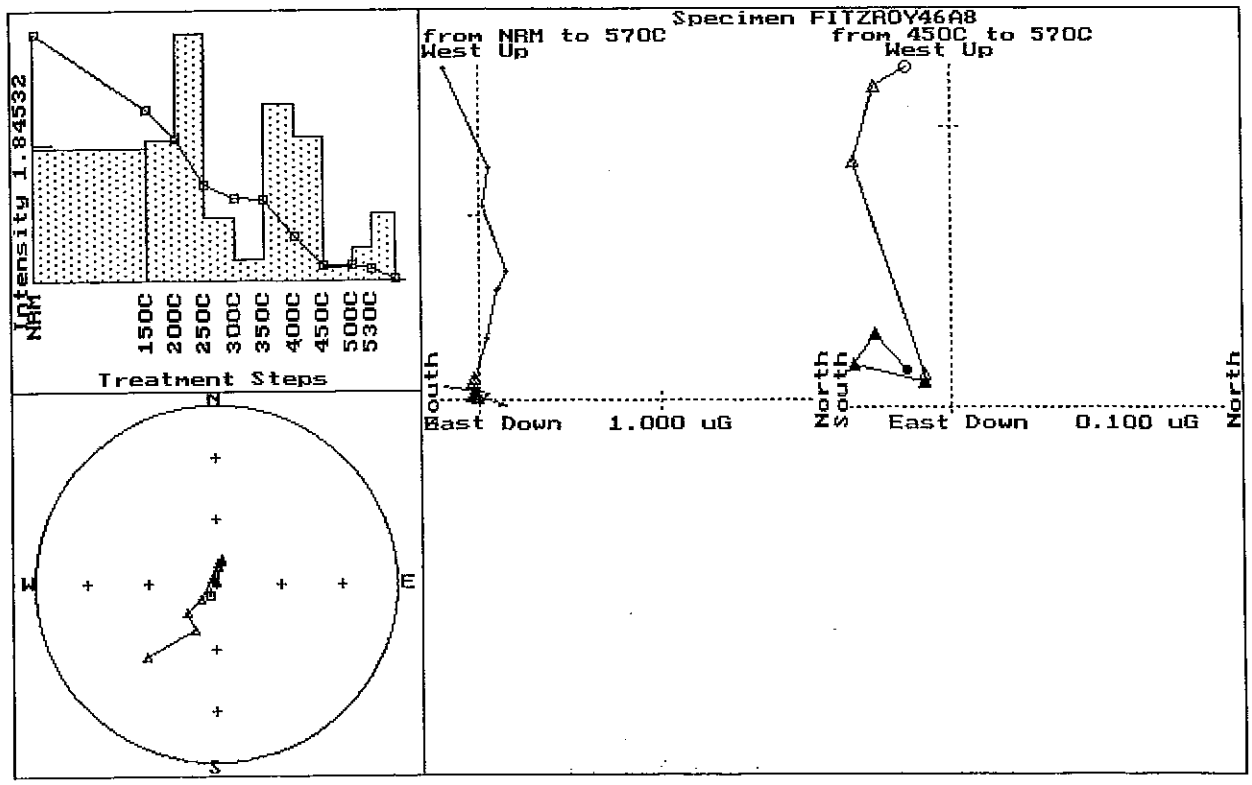
Specimen FITZROY46A8
from NRM to 570C
West Up
from 450C to 570C
West Up
Intensity 1.84532
NRM
150C
200C
250C
300C
350C
400C
450C
500C
530C
Treatment Steps
N
E
S
W
South
East Down 1.000 uG
North
South
East Down 0.100 uG
North

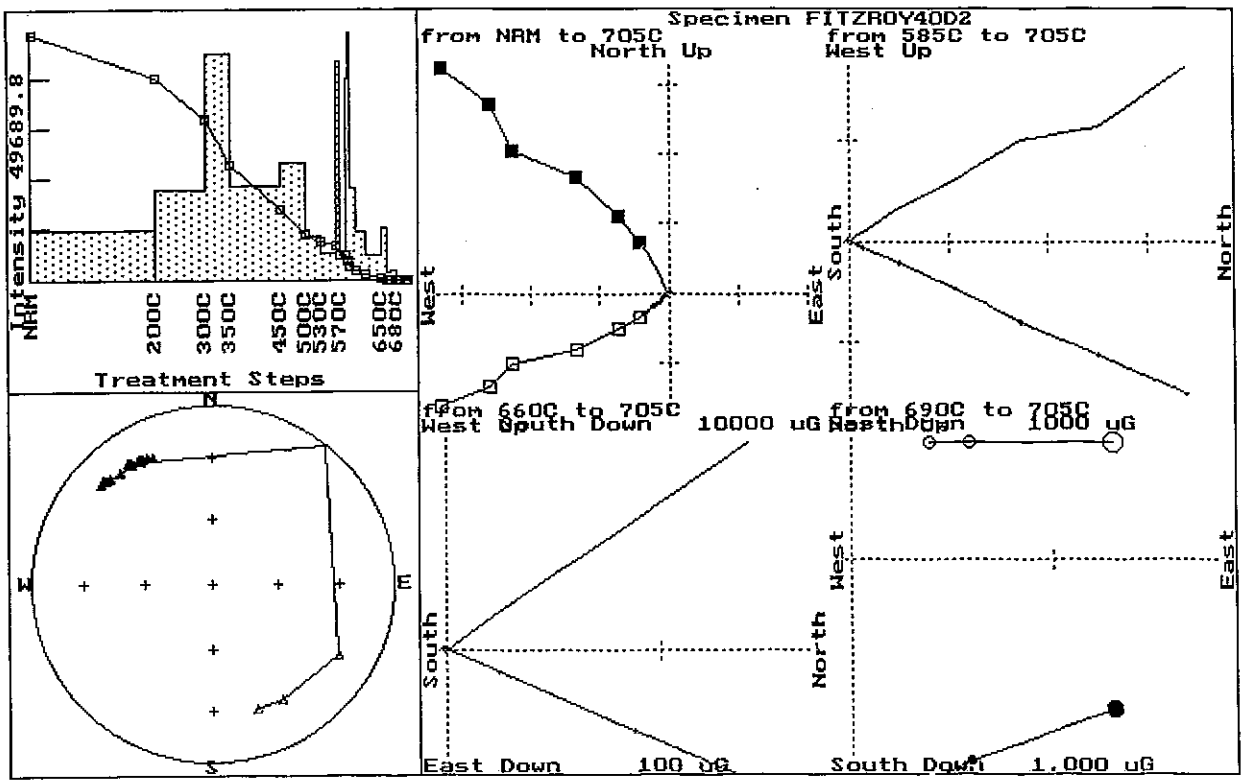
Specimen FITZROY40D2
Intensity 49689.8
NRM
200C
300C
350C
450C
500C
530C
570C
650C
680C
Treatment Steps
N
E
S
W
from NRM to 705C
North Up
West
East
from 585C to 705C
West Up
South
North
from 660C to 705C
West Up
South
East
10000 uG
from 690C to 705C
North Up
1000 uG
West
East
South
North
East Down
100 uG
South Down
1.000 uG

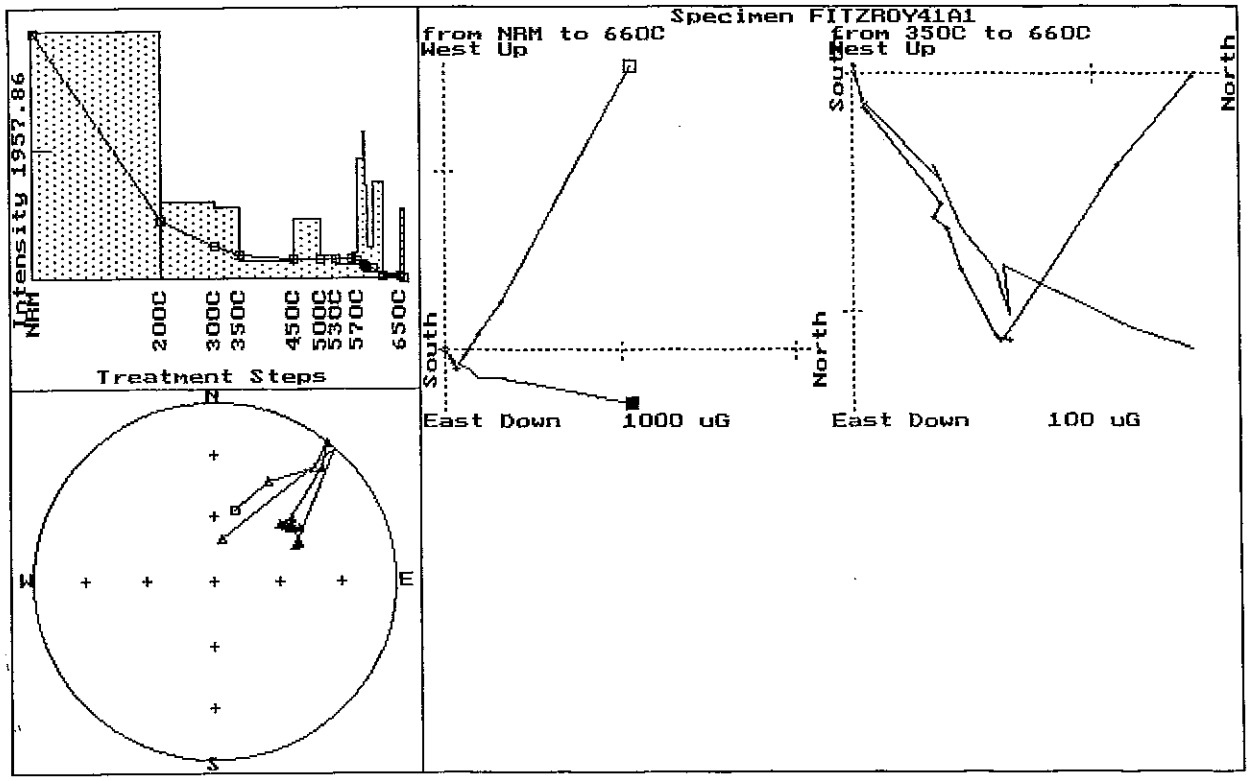
Specimen FITZROY41A1
Intensity 1957.86
NRM
200C
300C
350C
450C
500C
530C
570C
650C
Treatment Steps
N
E
S
W
from NRM to 660C
West Up
South
North
East Down
1000 uG
from 350C to 660C
West Up
South
North
East Down
100 uG

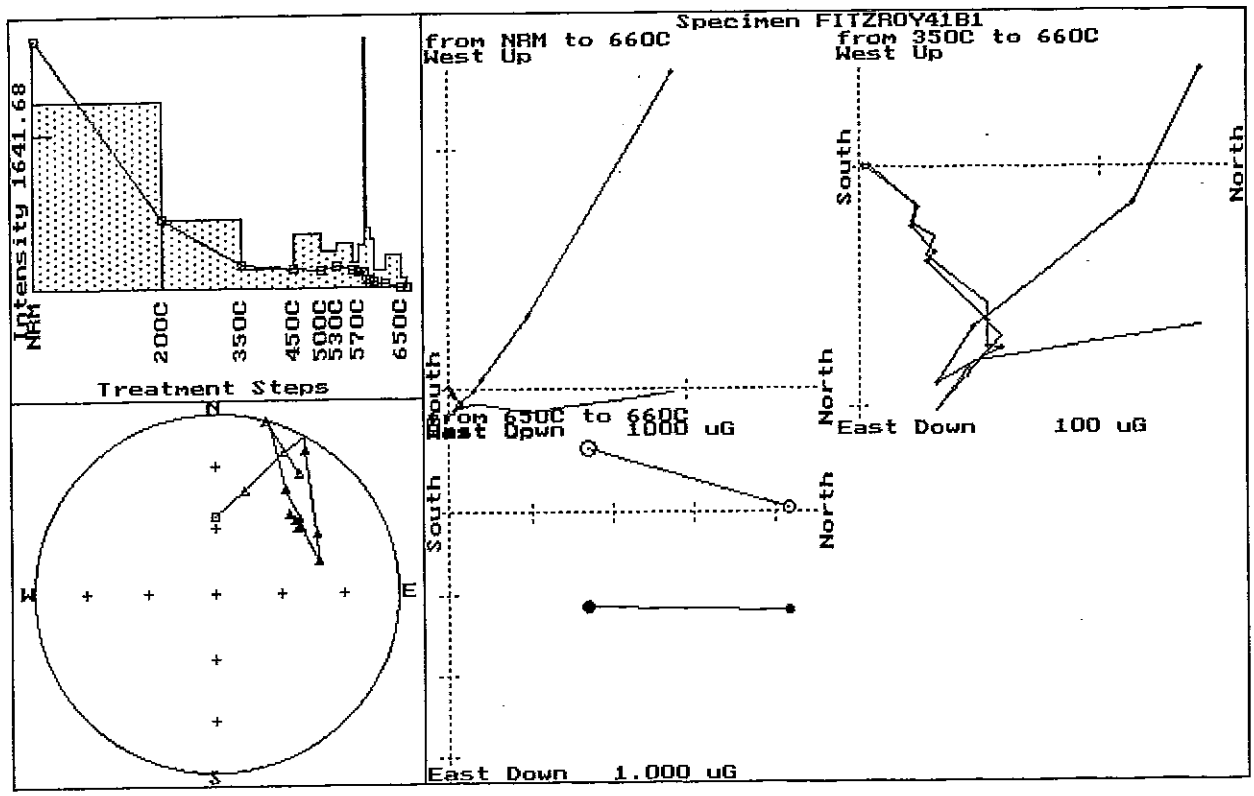
Specimen FITZROY41B1
Intensity 1641.68
NRM
200C
350C
450C
500C
530C
570C
650C
Treatment Steps
N
W
E
S
from NRM to 660C
West Up
South
North
East Down 1.000 uG
from 350C to 660C
West Up
South
North
East Down 100 uG
from 650C to 660C
East Down 1000 uG
South
North

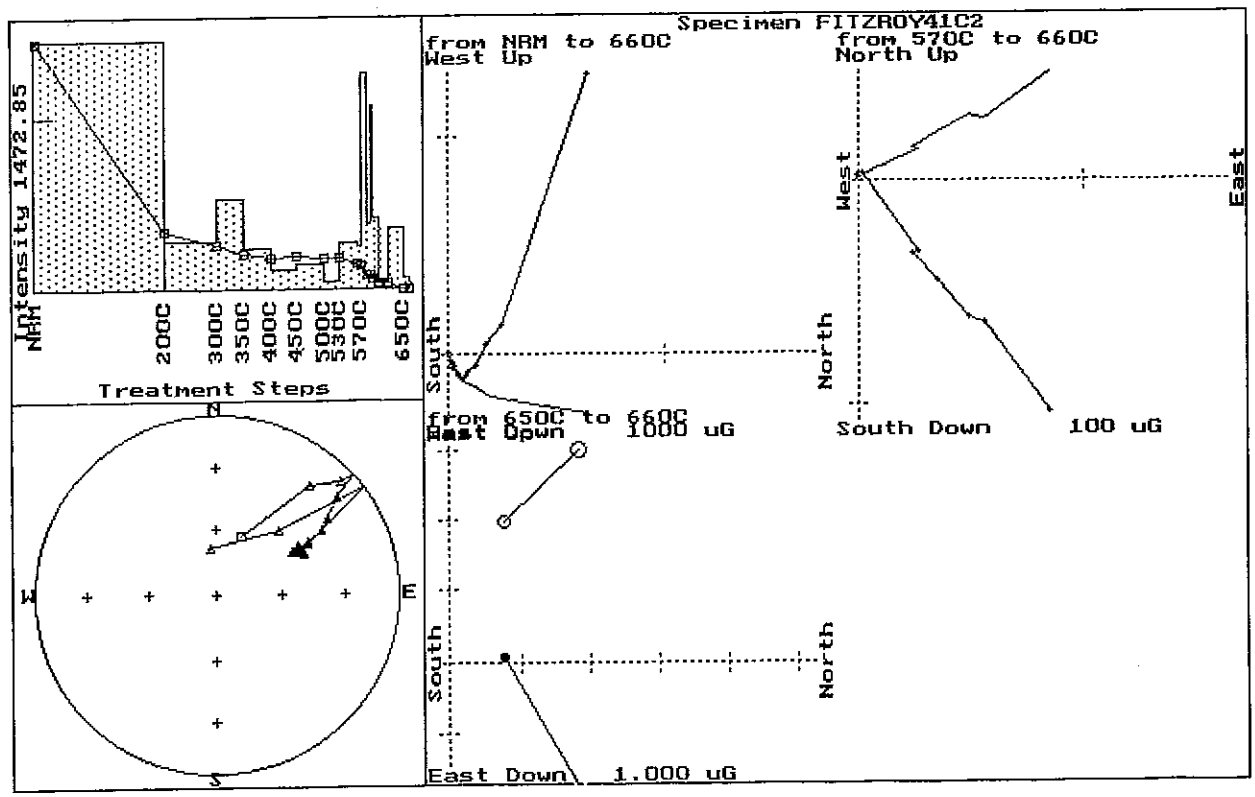
Specimen FITZROY41C2
Intensity 1472.85
NRM
200C
300C
350C
400C
450C
500C
530C
570C
650C
Treatment Steps
N
W
E
S
from NRM to 660C
West Up
South
North
East Down 1.000 uG
from 570C to 660C
North Up
West
East
South Down 100 uG
from 650C to 660C
East Down 1000 uG
South
North

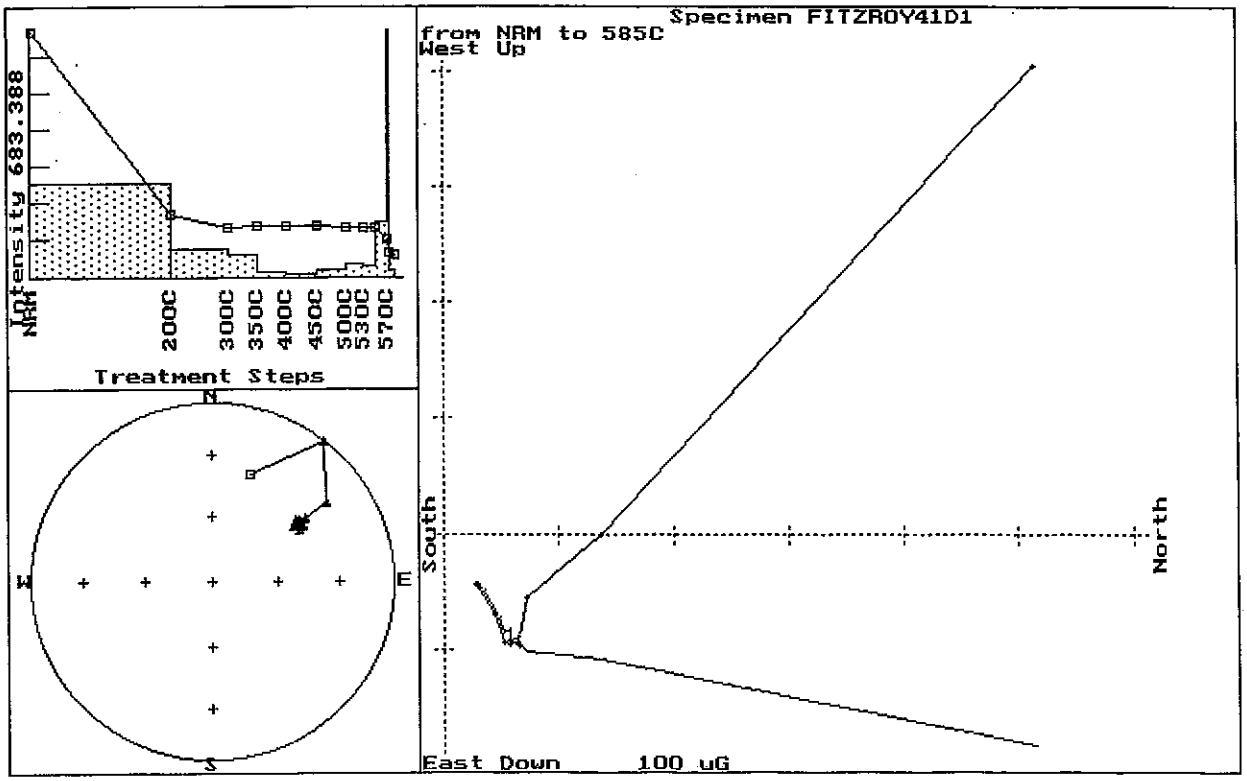
Specimen FITZROY41D1
from NRM to 585C
West Up
Intensity 683.388
NRM
200C
300C
350C
400C
450C
500C
530C
570C
Treatment Steps
N
W
E
S
South
North
East Down
100 uG

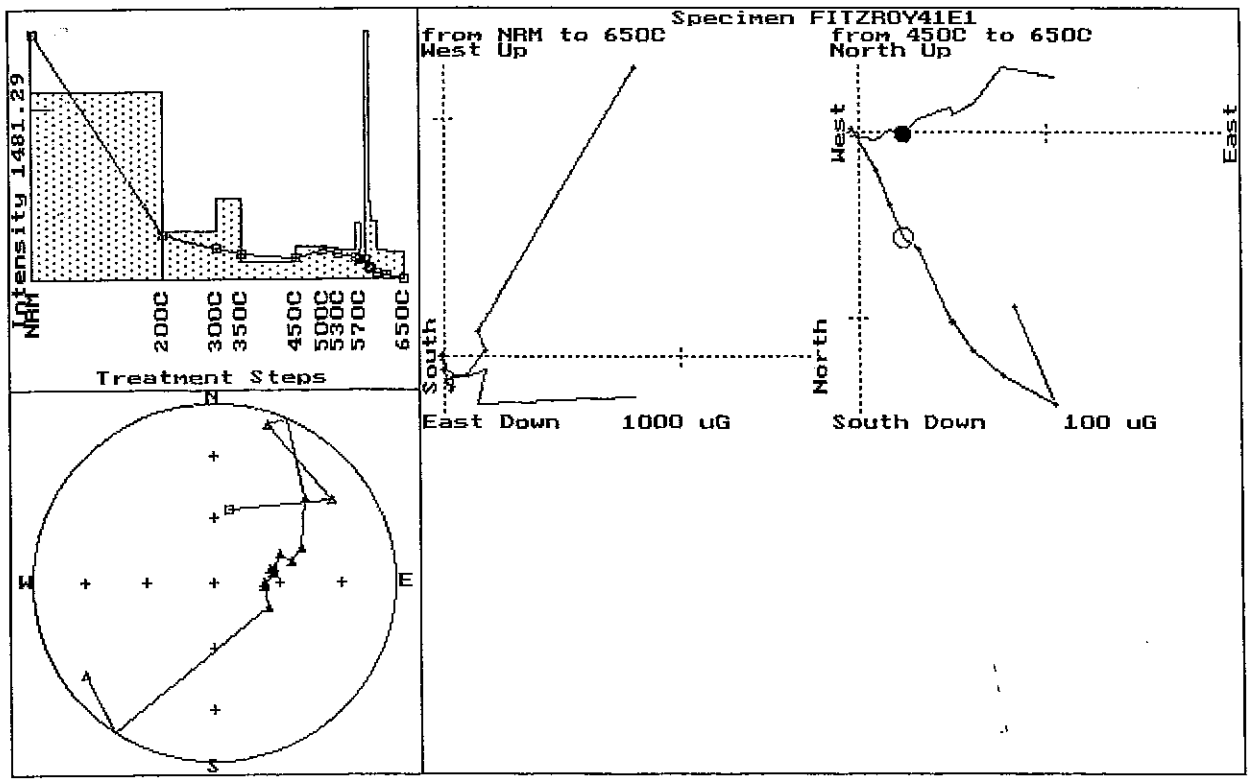
Specimen FITZROY41E1
from NRM to 650C
West Up
from 450C to 650C
North Up
Intensity 1481.29
NRM
200C
300C
350C
450C
500C
530C
570C
650C
Treatment Steps
N
W
E
S
South
North
West
East
East Down
1000 uG
South Down
100 uG

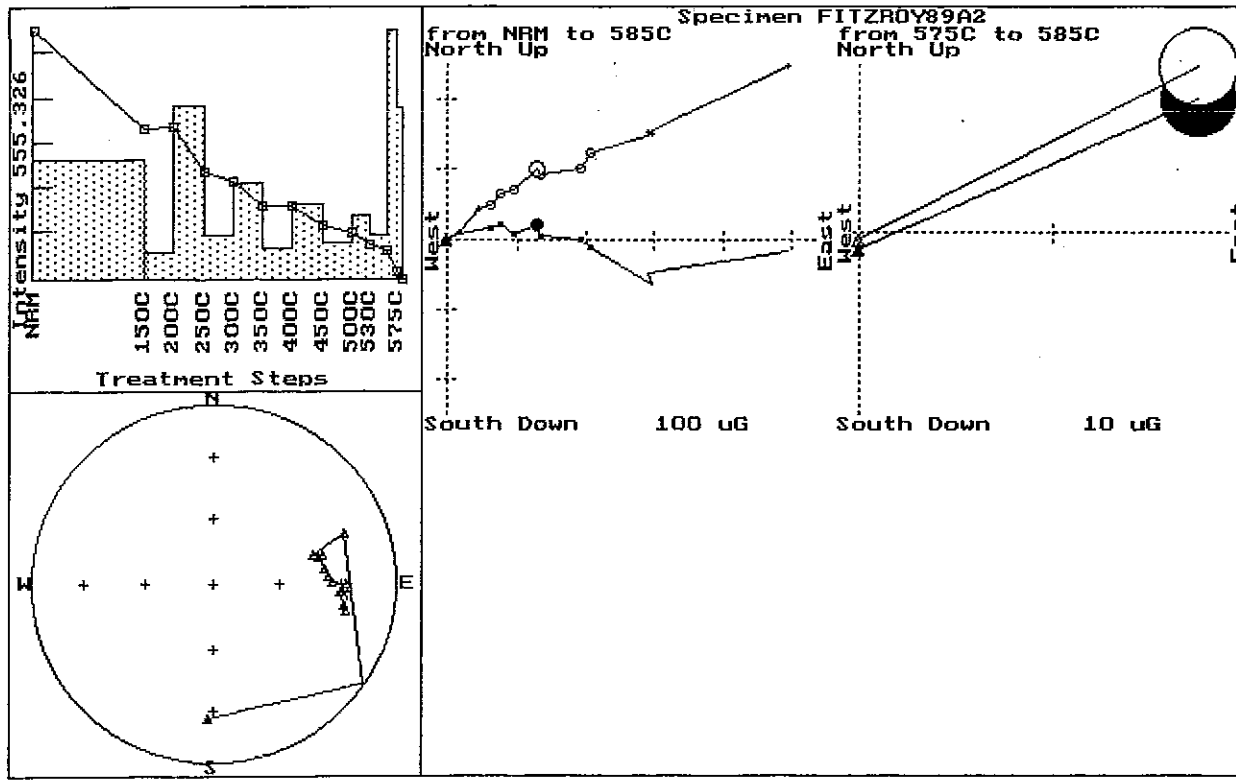
Specimen FITZROY89A2
from NRM to 585C
North Up
from 575C to 585C
North Up
Intensity 555.326
NRM
150C
200C
250C
300C
350C
400C
450C
500C
530C
575C
Treatment Steps
N
W
E
S
West
East
West
East
South Down
100 uG
South Down
10 uG

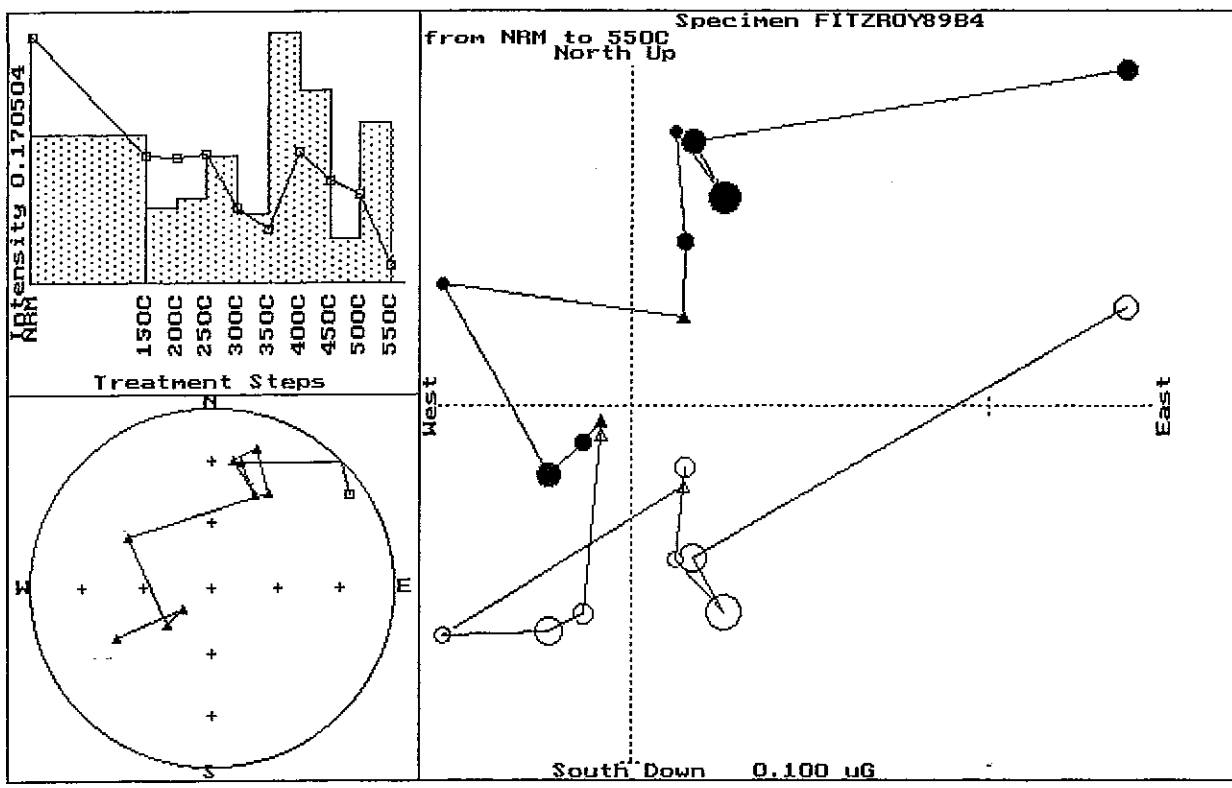
Specimen FITZROY89B4
from NRM to 550C
North Up
Intensity 0.170504
NRM
150C
200C
250C
300C
350C
400C
450C
500C
550C
Treatment Steps
N
W
E
S
West
East
South Down
0.100 uG

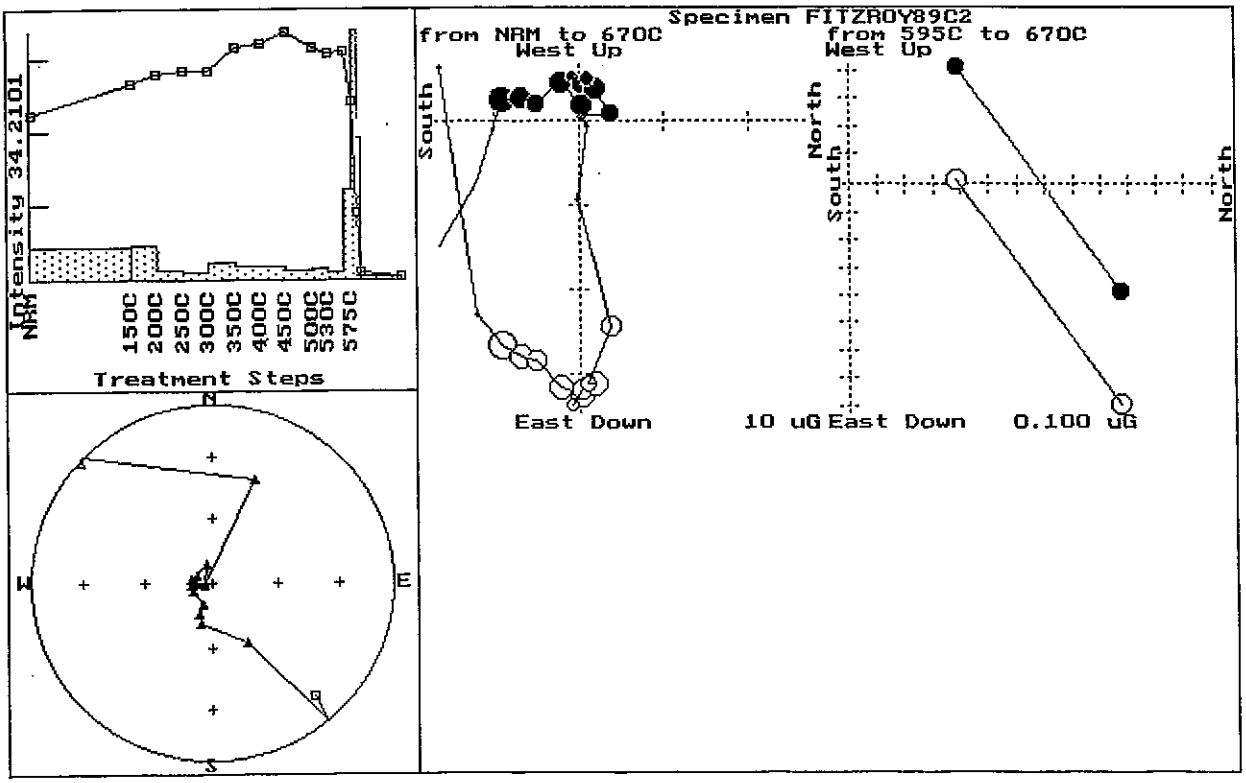
Intensity 34.2101
NRM
150C
200C
250C
300C
350C
400C
450C
500C
530C
575C
Treatment Steps
N
E
S
W
Specimen FITZROY89C2
from NRM to 670C
West Up
South
East Down
10 uG
from 595C to 670C
West Up
North
South
East Down
0.100 uG

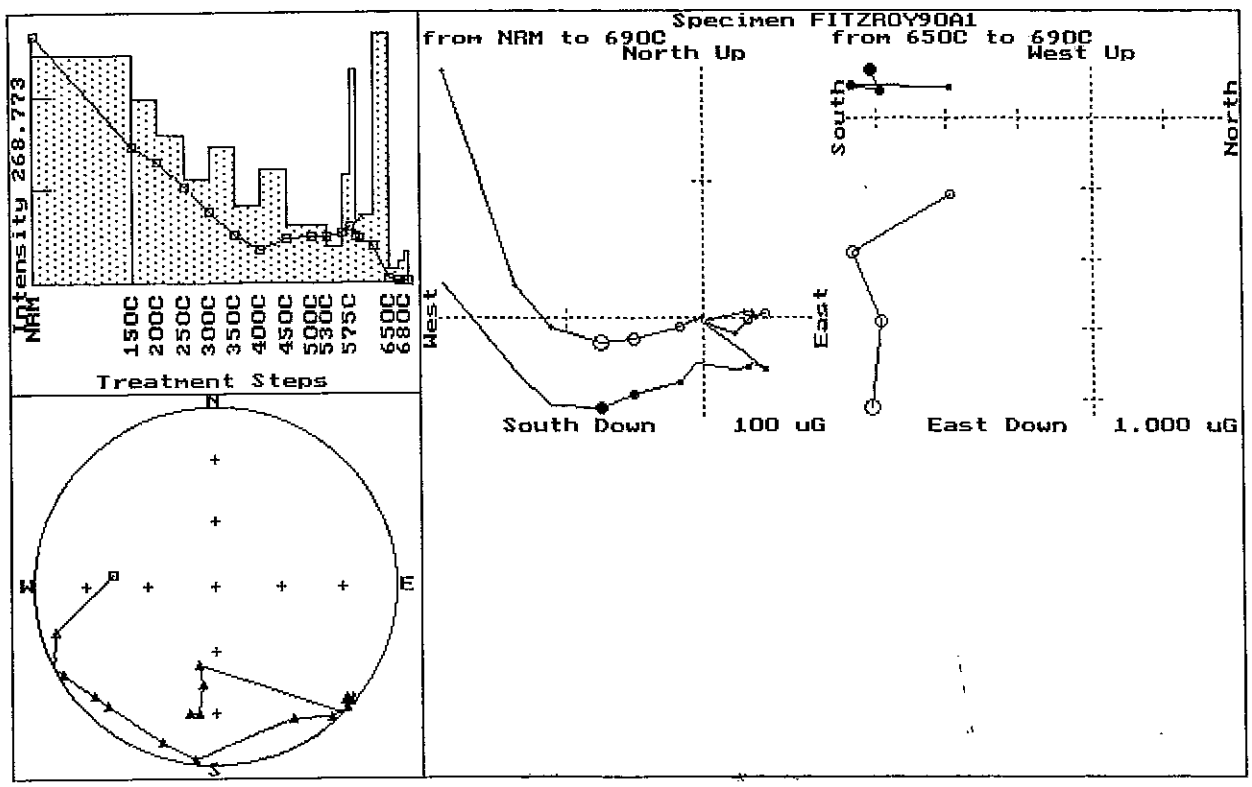
Intensity 268.773
NRM
150C
200C
250C
300C
350C
400C
450C
500C
530C
575C
650C
680C
Treatment Steps
N
E
S
W
Specimen FITZROY90A1
from NRM to 690C
North Up
South Down
100 uG
from 650C to 690C
West Up
South
North
East Down
1.000 uG

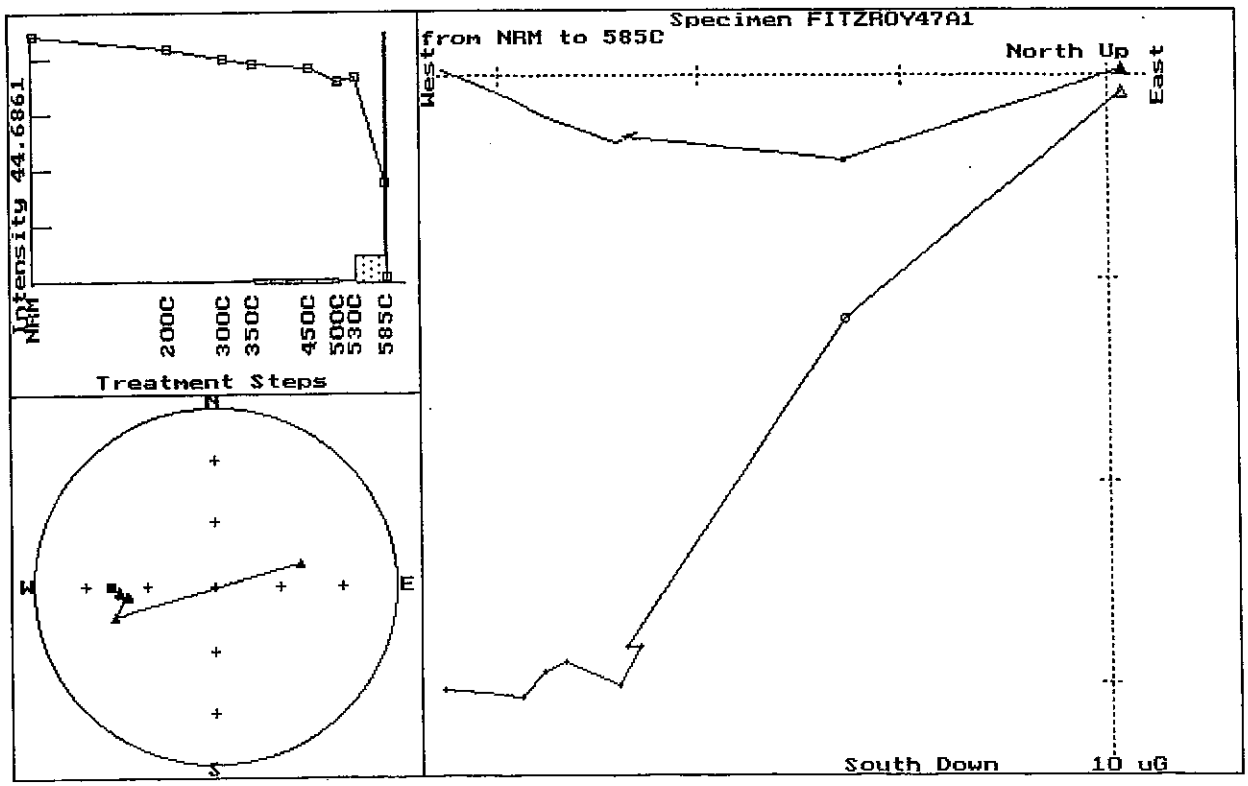
Specimen FITZROY47A1
from NRM to 585C
North Up
West
East
Intensity 44.6861
NRM
200C
300C
350C
450C
500C
530C
585C
Treatment Steps
N
E
S
W
South Down
10 uG

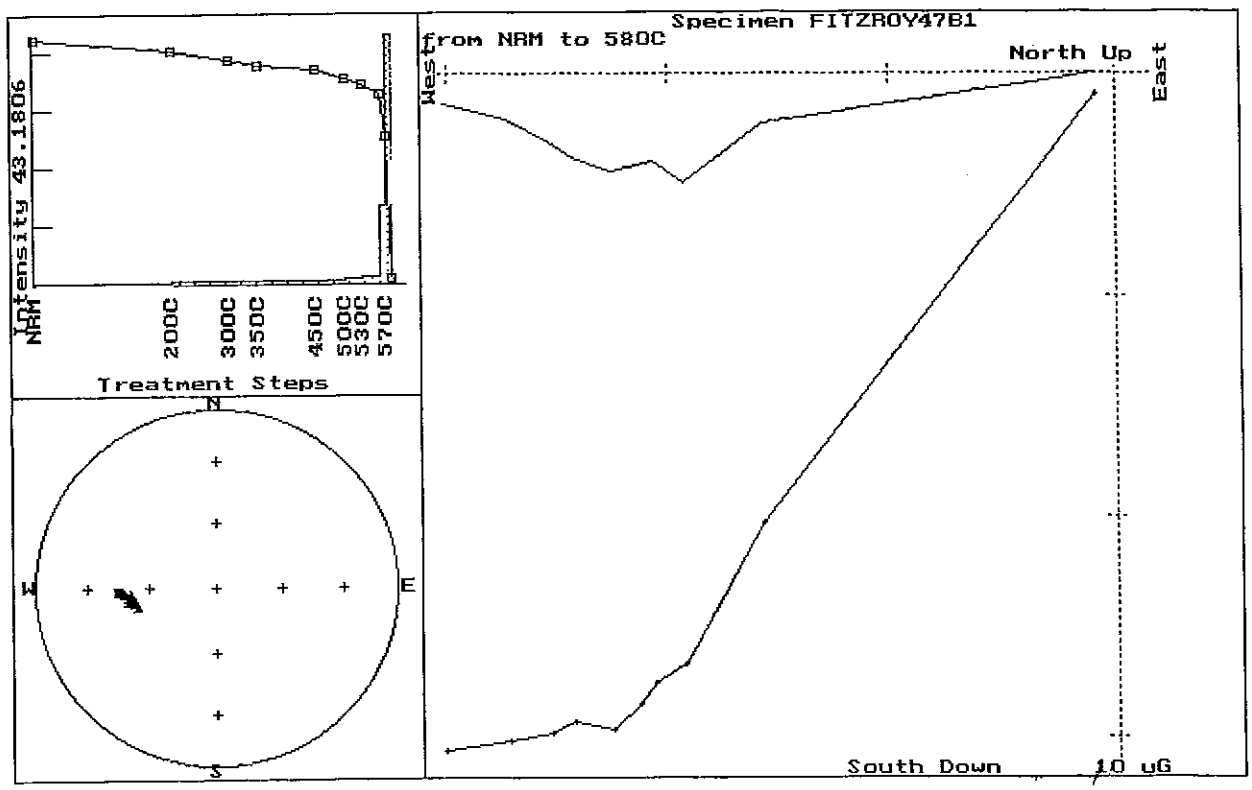
Specimen FITZROY47B1
from NRM to 580C
North Up
West
East
Intensity 43.1806
NRM
200C
300C
350C
450C
500C
530C
570C
Treatment Steps
N
E
S
W
South Down
10 uG

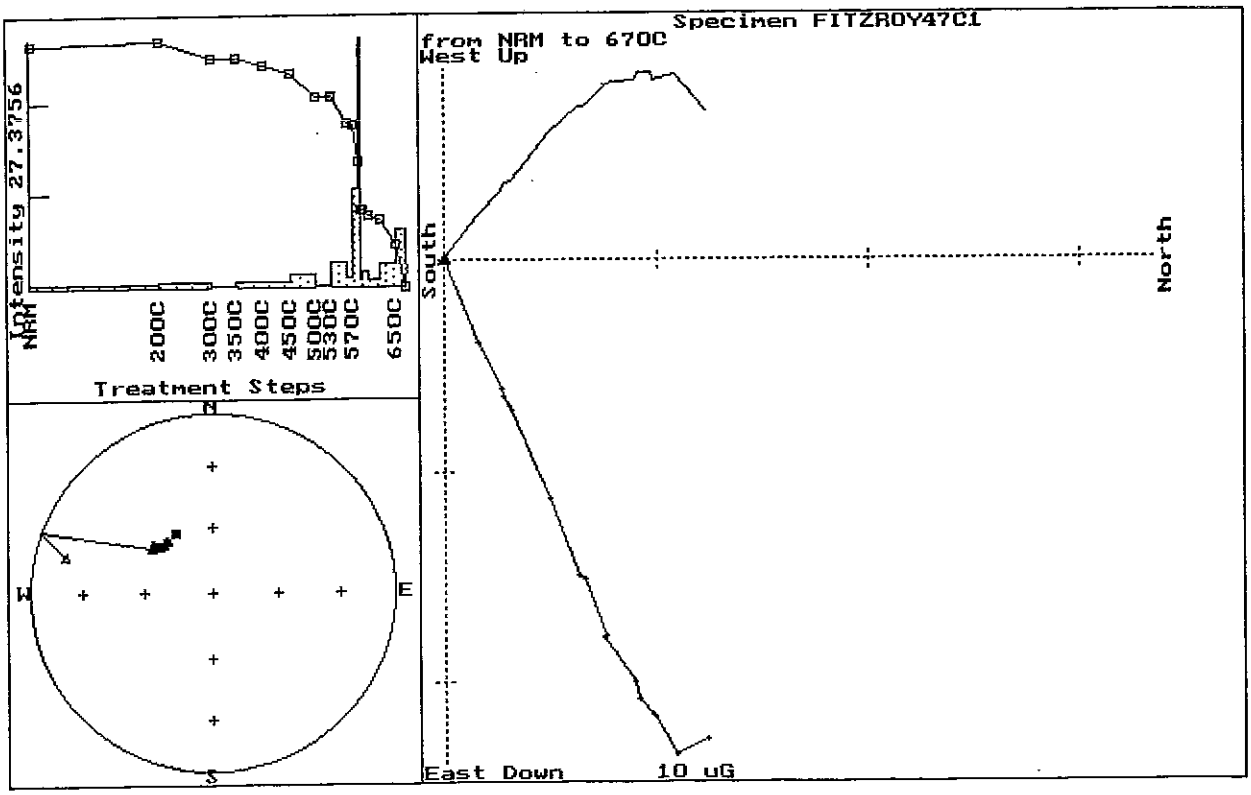
Specimen FITZROY47C1
from NRM to 670C
West Up
Intensity 27.3756
NRM
200C
300C
350C
400C
450C
500C
530C
570C
650C
Treatment Steps
N
W
E
S
South
North
East Down
10 uG

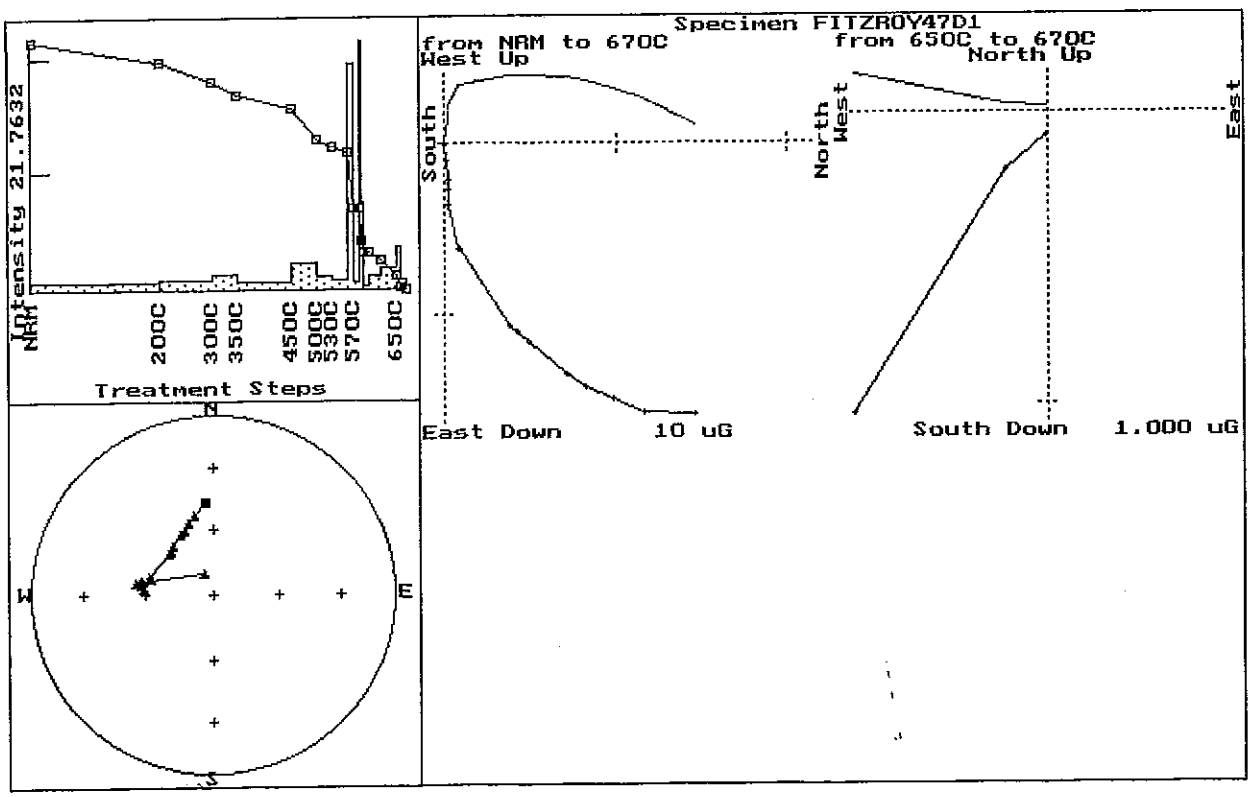
Specimen FITZROY47D1
from NRM to 670C
West Up
from 650C to 670C
North Up
Intensity 21.7632
NRM
200C
300C
350C
450C
500C
530C
570C
650C
Treatment Steps
N
W
E
S
South
North
West
East
East Down
10 uG
South Down
1.000 uG

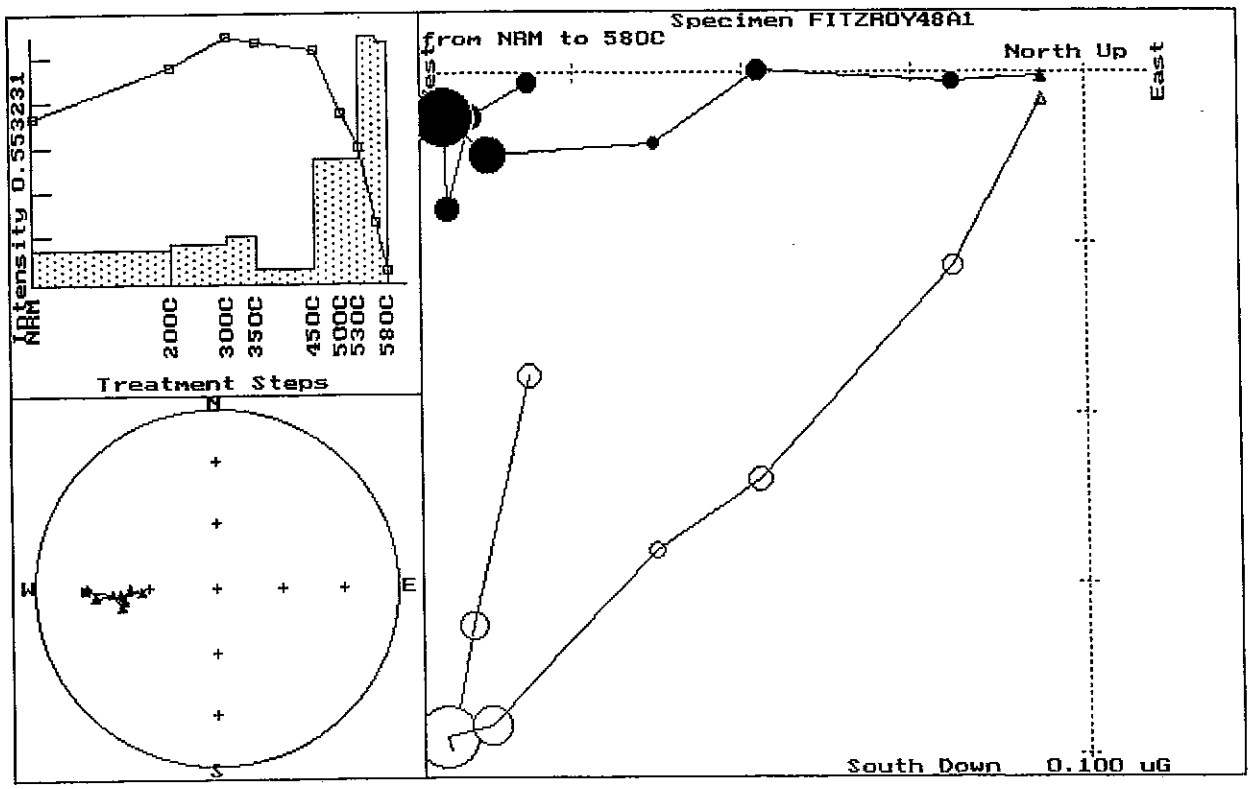
Specimen FITZROY48A1
from NRM to 580C
North Up
East
West
Intensity 0.553231
NRM
200C
300C
350C
450C
500C
530C
580C
Treatment Steps
N
S
E
W
South Down
0.100 uG

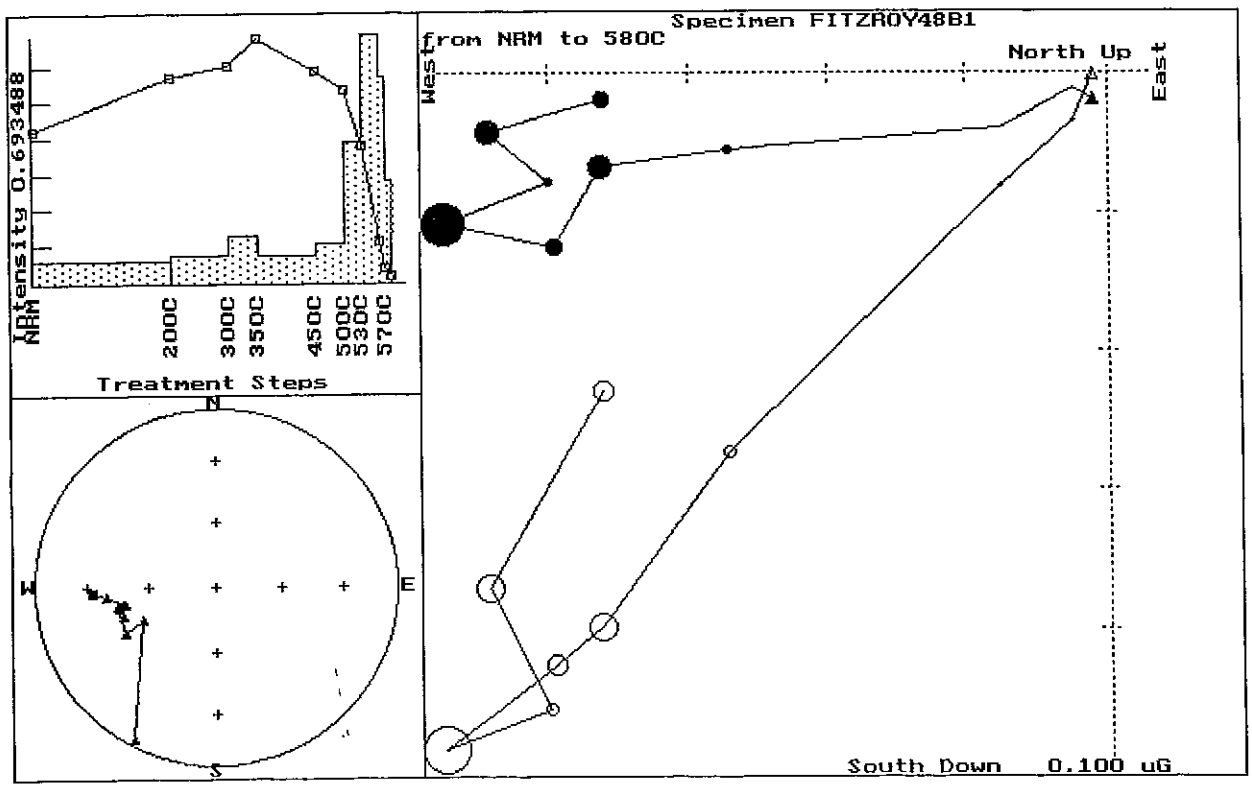
Specimen FITZROY48B1
from NRM to 580C
North Up
East
West
Intensity 0.693488
NRM
200C
300C
350C
450C
500C
530C
570C
Treatment Steps
N
S
E
W
South Down
0.100 uG

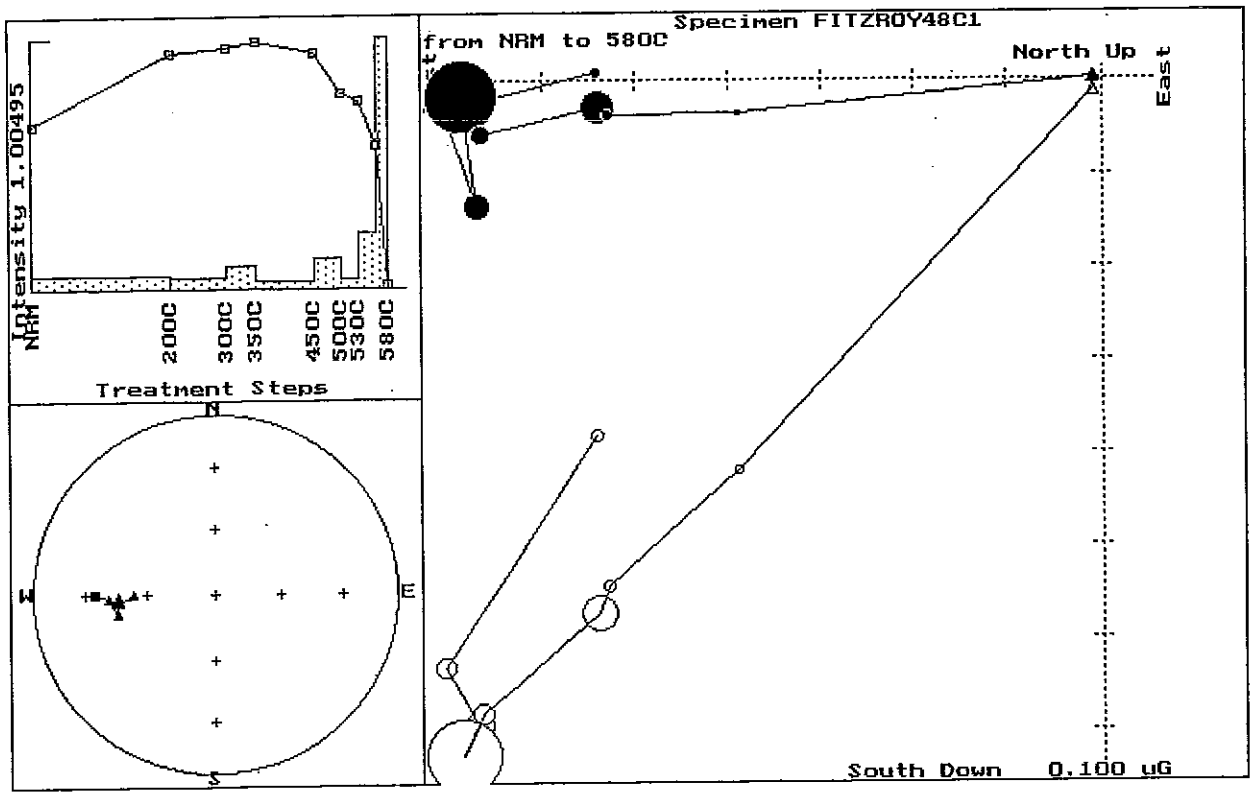
Intensity 1.00495
NRM
200C
300C
350C
450C
500C
530C
580C
Treatment Steps
N
W
E
S
Specimen FITZROY48C1
from NRM to 580C
North Up
East
South Down
0.100 uG

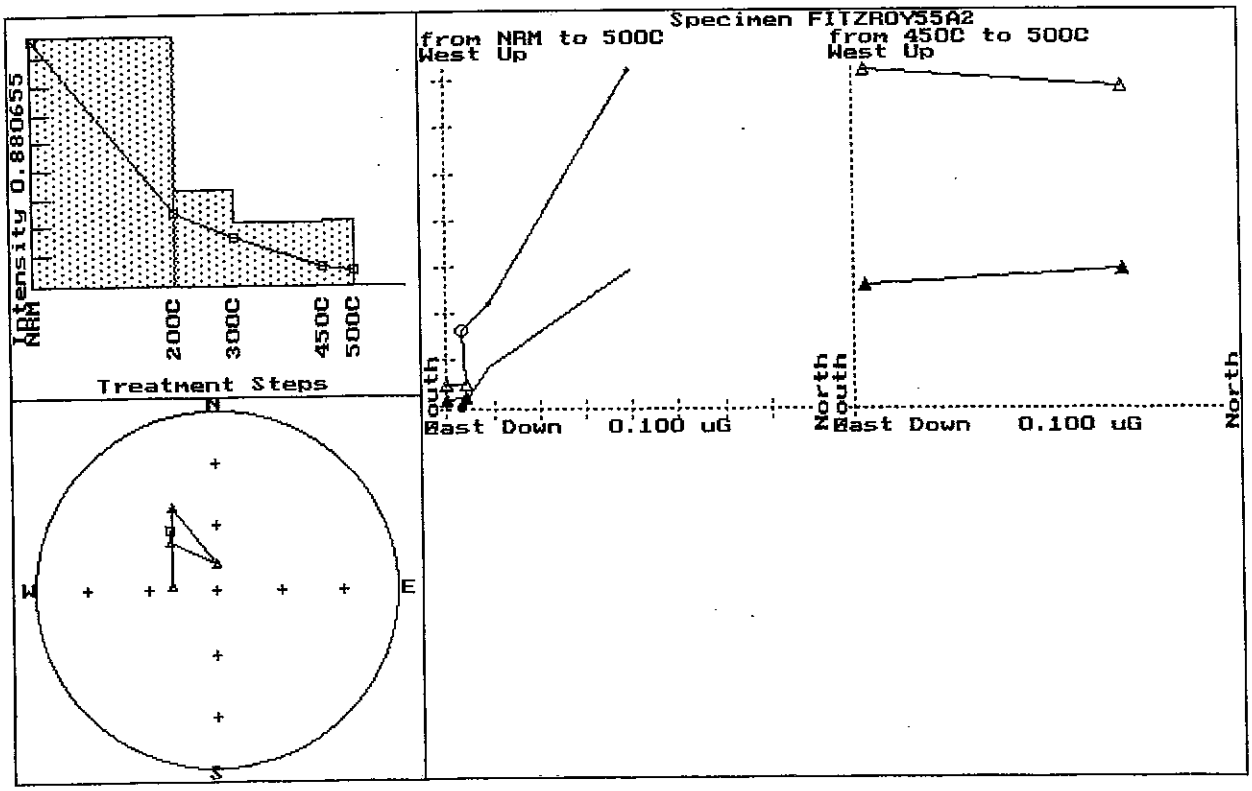
Specimen FITZROY55A2
from NRM to 500C
West Up
from 450C to 500C
West Up
Intensity 0.880655
NRM
200C
300C
450C
500C
Treatment Steps
N
W
E
S
South
East Down
0.100 uG
North
South
East Down
0.100 uG
North

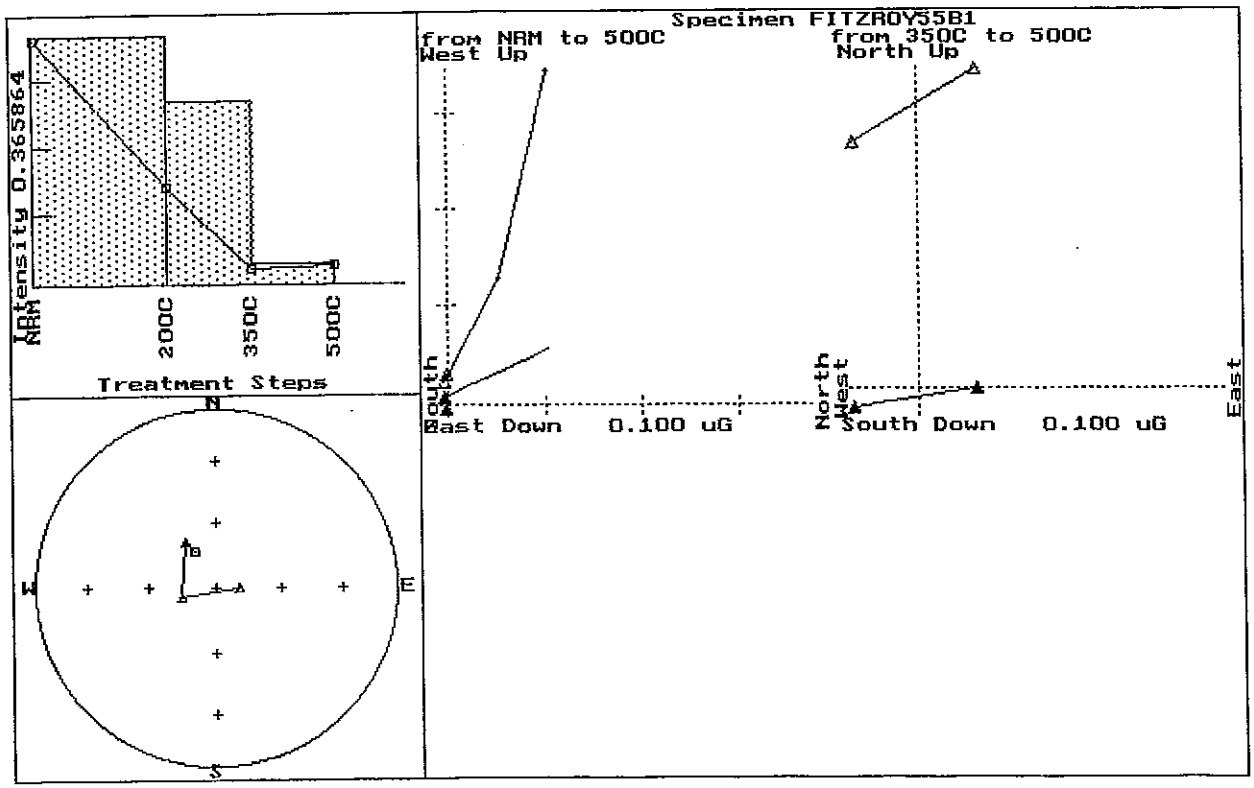
Specimen FITZROY55B1
from NRM to 500C
West Up
from 350C to 500C
North Up
Intensity 0.365864
NRM
200C
350C
500C
Treatment Steps
N
W
E
S
South
East Down
0.100 uG
North
West
South Down
0.100 uG
East

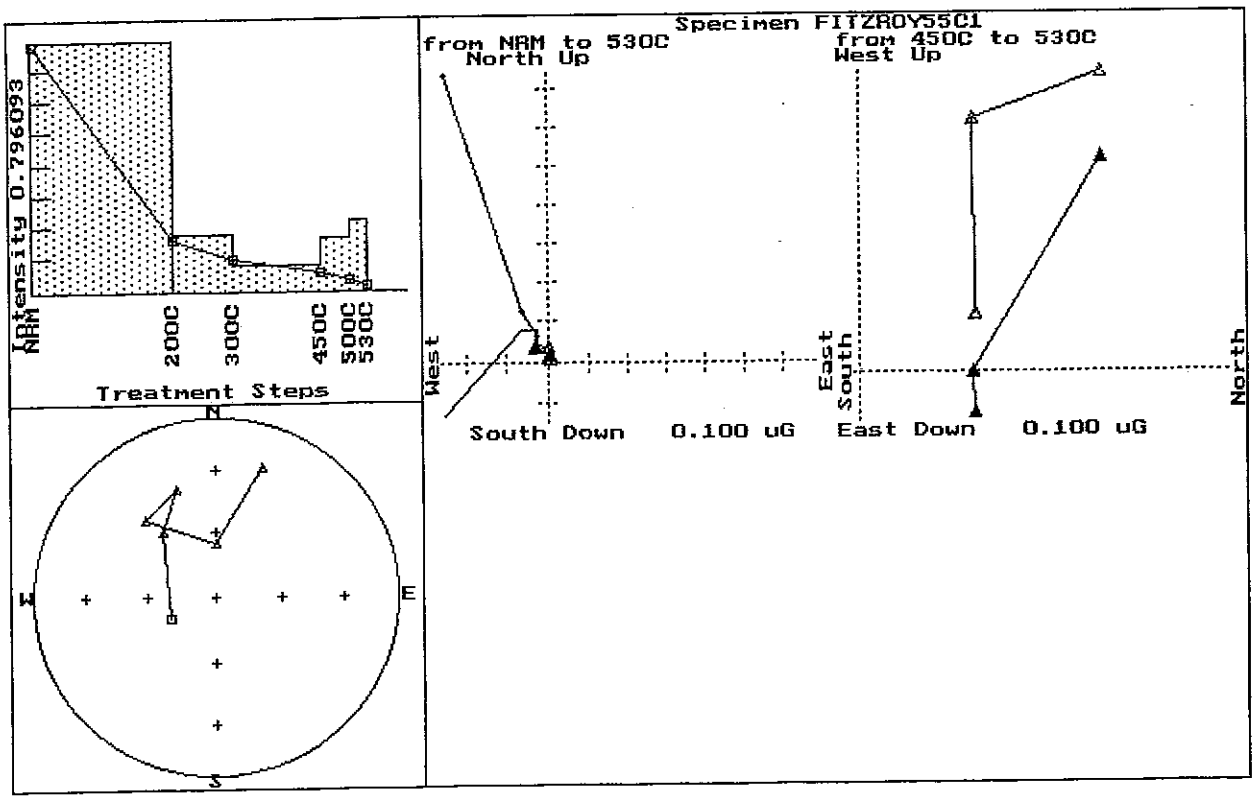
Intensity 0.796093
NRM
200C
300C
450C
500C
530C
Treatment Steps
N
W
E
S
Specimen FITZROY55C1
from NRM to 530C
North Up
West
East
South Down 0.100 uG
from 450C to 530C
West Up
South
North
East Down 0.100 uG

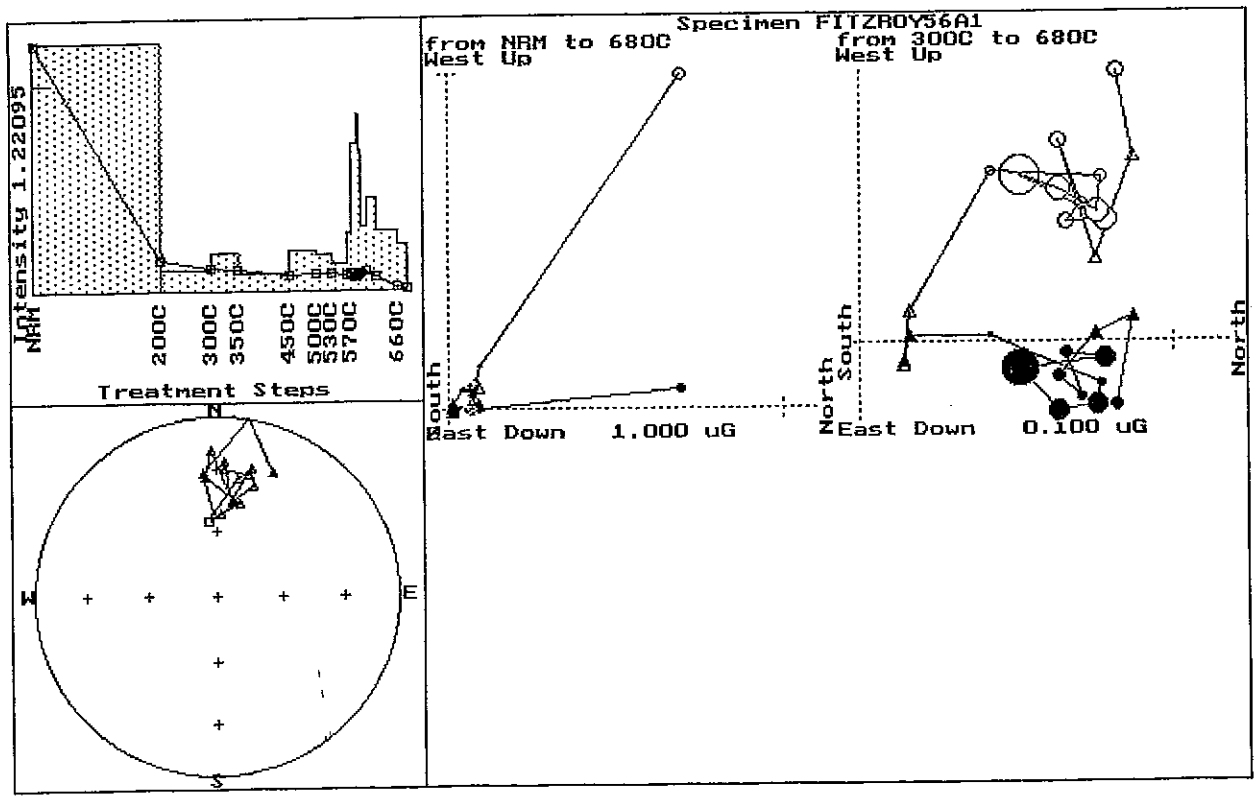
Intensity 1.22095
NRM
200C
300C
350C
450C
500C
530C
570C
660C
Treatment Steps
N
W
E
S
Specimen FITZROY56A1
from NRM to 680C
West Up
South
East Down 1.000 uG
from 300C to 680C
West Up
North
South
East Down 0.100 uG

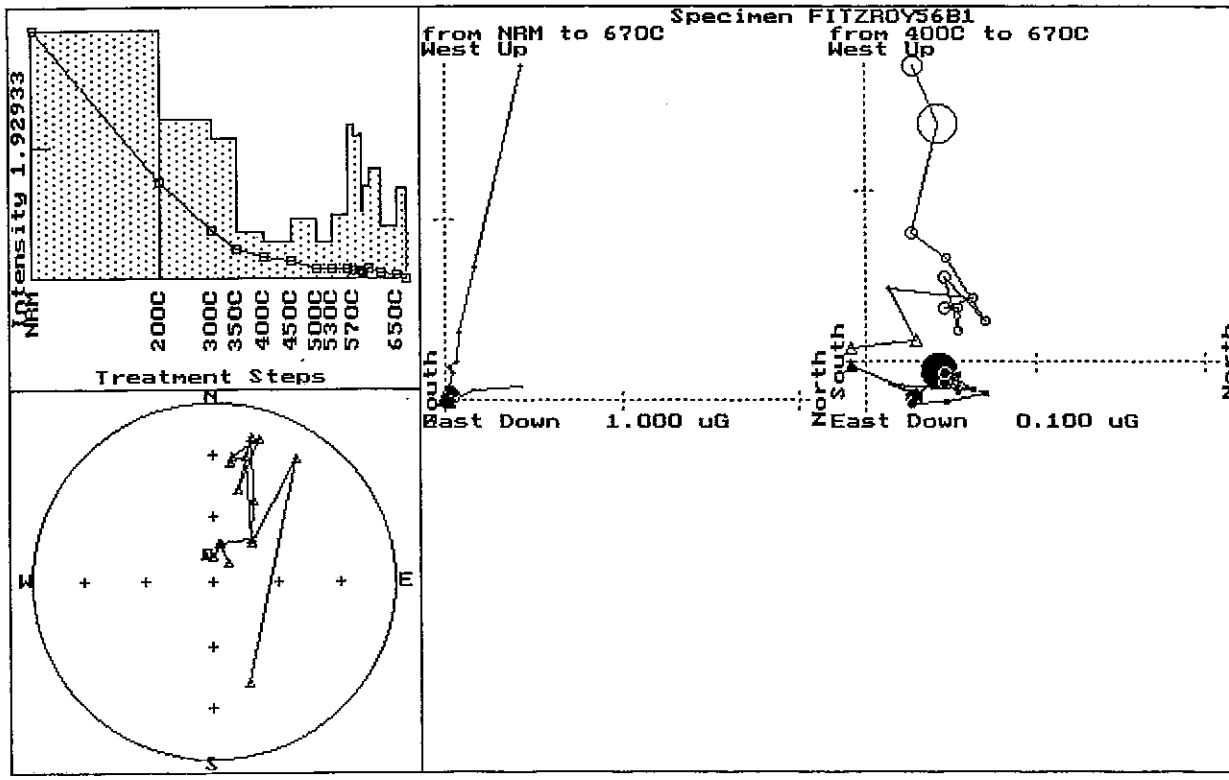
Specimen FITZROY56B1
from NRM to 670C
West Up
from 400C to 670C
West Up
Intensity 1.92933
NRM
200C
300C
350C
400C
450C
500C
530C
570C
650C
Treatment Steps
N
W
E
S
South
East Down
1.000 uG
North
South
East Down
0.100 uG
North

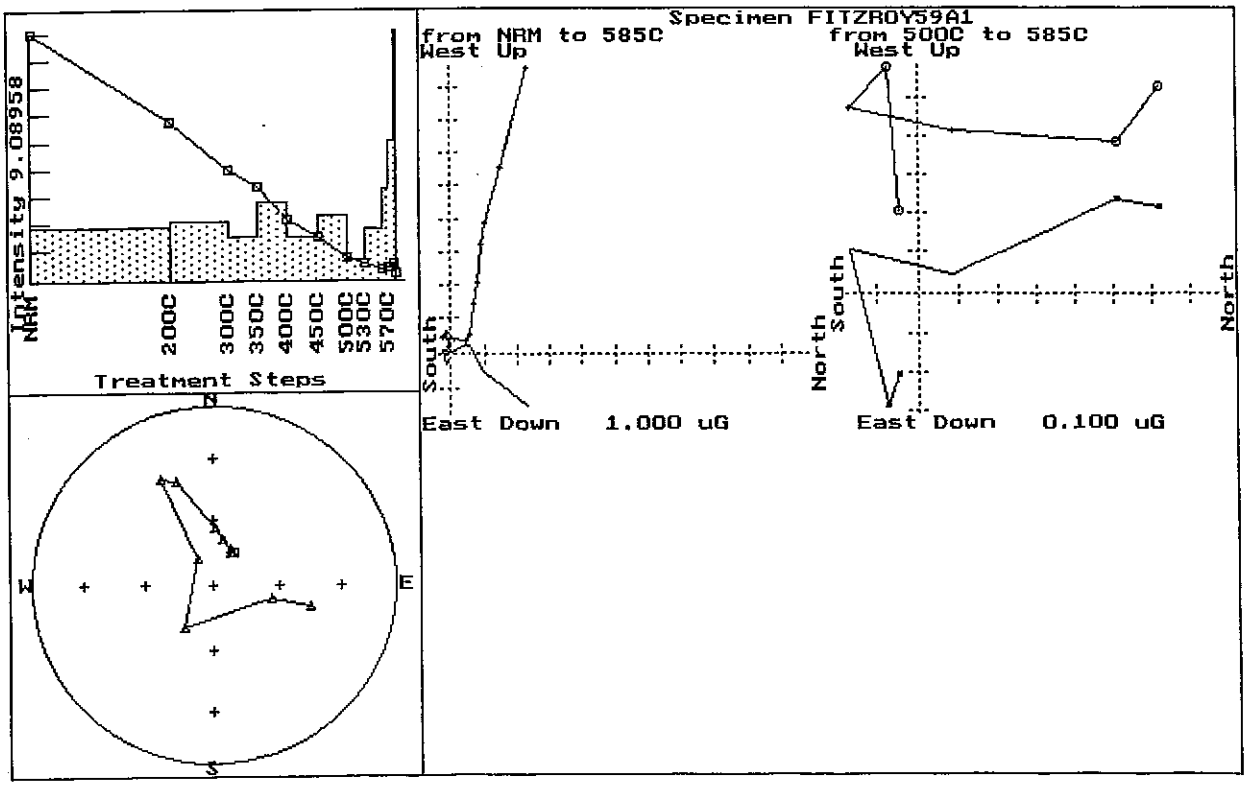
Specimen FITZROY59A1
Intensity 9.08958
NRM
200C
300C
350C
400C
450C
500C
530C
570C
Treatment Steps
N
W
E
S
from NRM to 585C
West Up
South
North
East Down 1.000 uG
from 500C to 585C
West Up
South
North
East Down 0.100 uG

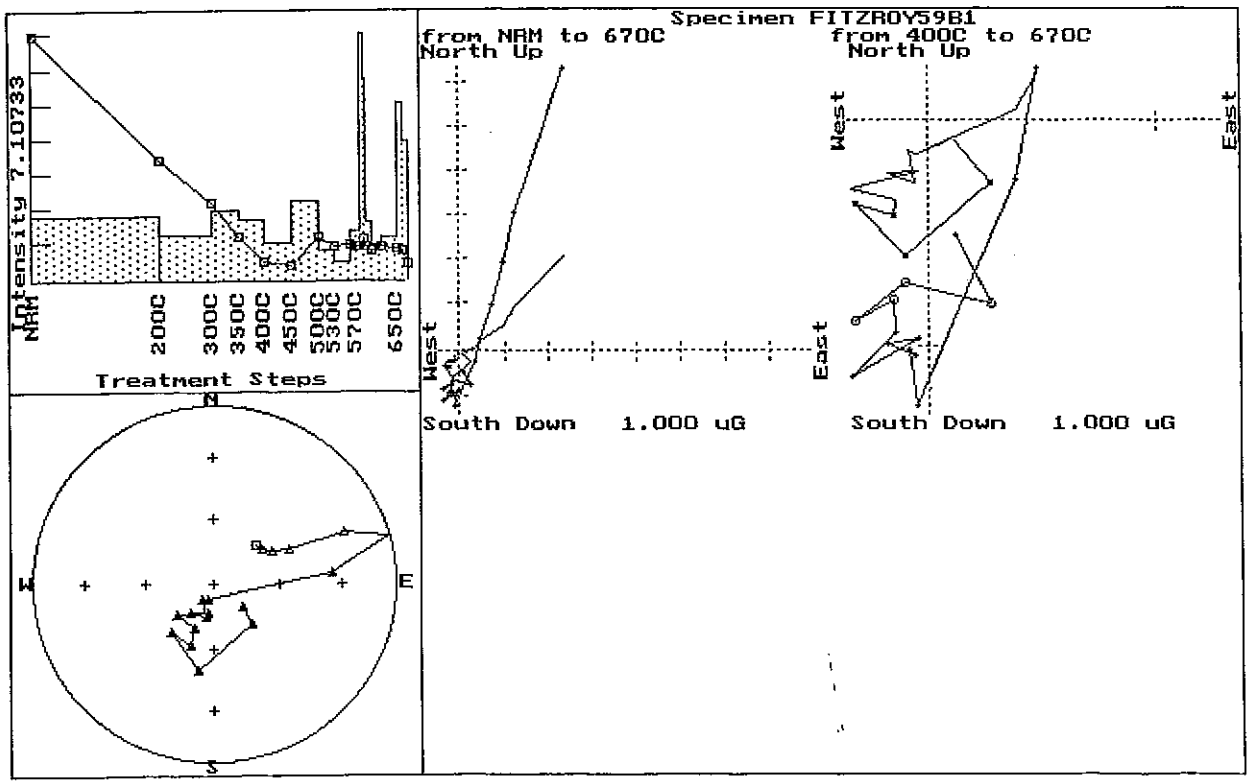
Specimen FITZROY59B1
Intensity 7.10733
NRM
200C
300C
350C
400C
450C
500C
530C
570C
650C
Treatment Steps
N
W
E
S
from NRM to 670C
North Up
West
East
South Down 1.000 uG
from 400C to 670C
North Up
West
East
South Down 1.000 uG

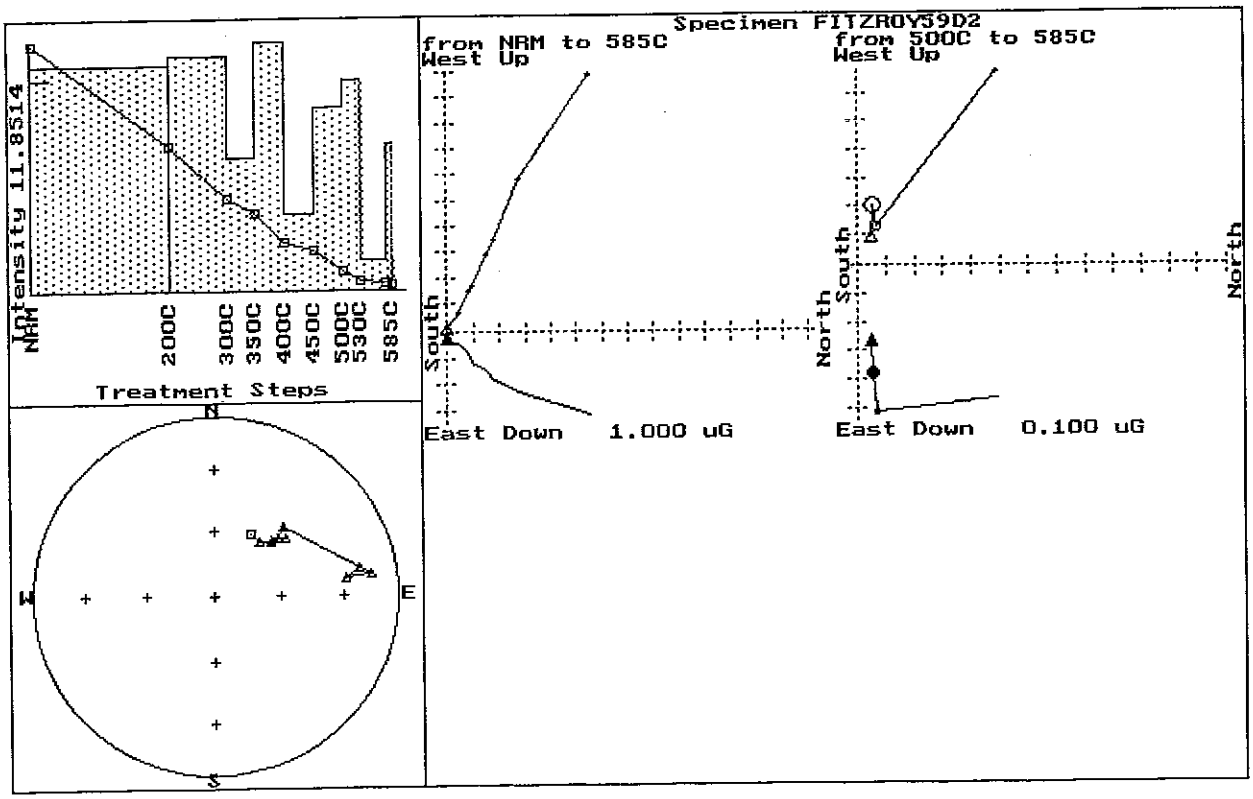
Intensity 11.8514
NRM
200C
300C
350C
400C
450C
500C
530C
585C
Treatment Steps
N
W
E
S
Specimen FITZROY59D2
from NRM to 585C
West Up
South
East Down
1.000 uG
from 500C to 585C
West Up
South
North
North
East Down
0.100 uG

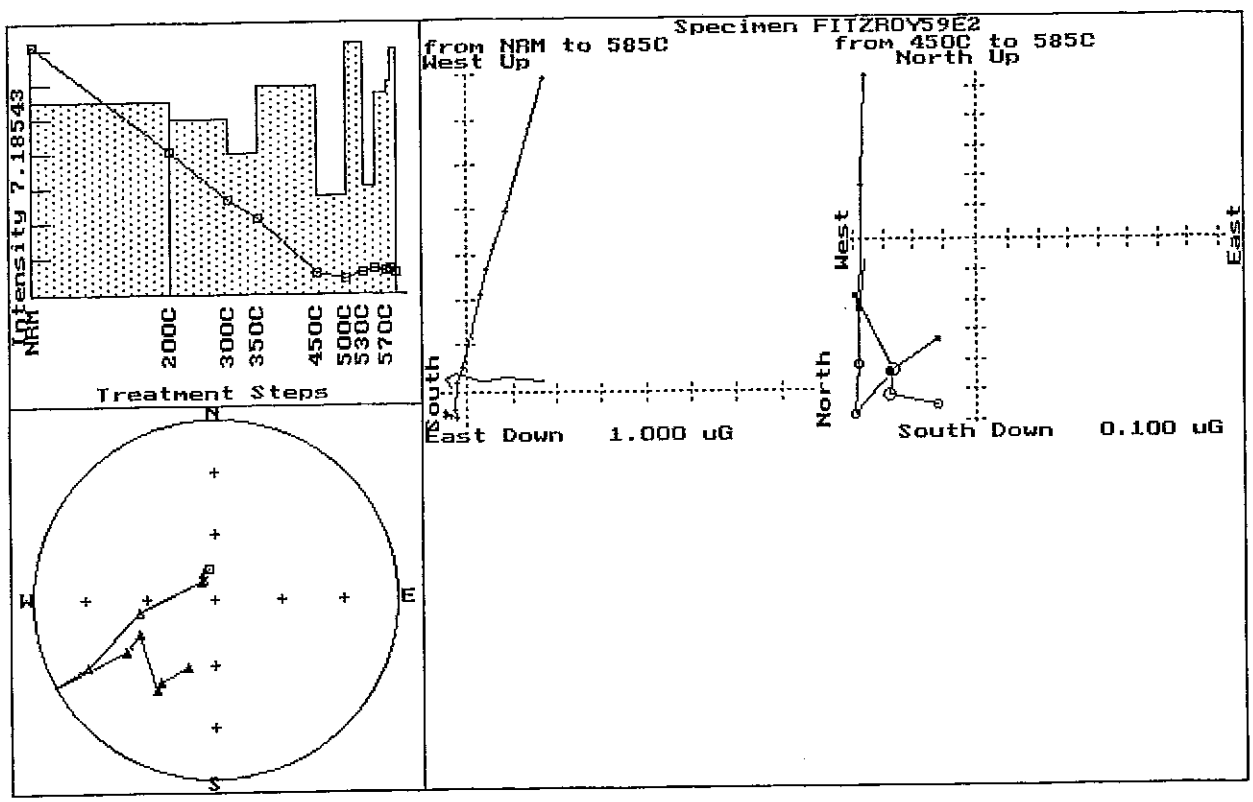
Intensity 7.18543
NRM
200C
300C
350C
450C
500C
530C
570C
Treatment Steps
N
W
E
S
Specimen FITZROY59E2
from NRM to 585C
West Up
South
East Down
1.000 uG
from 450C to 585C
North Up
West
East
North
South Down
0.100 uG

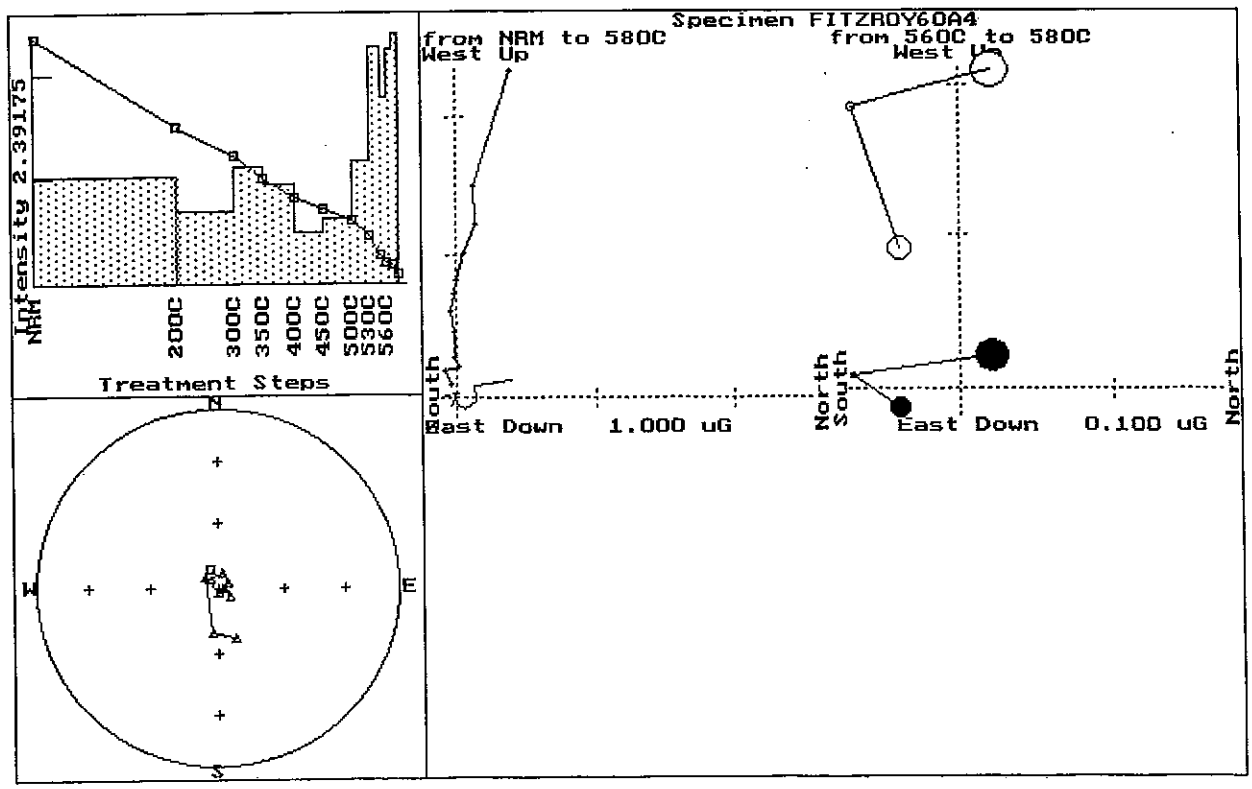
Specimen FITZROY60A4
from NRM to 580C
West Up
from 560C to 580C
West Up
Intensity 2.39175
NRM
200C
300C
350C
400C
450C
500C
530C
560C
Treatment Steps
N
E
S
W
South
East Down 1.000 uG
North
South
East Down 0.100 uG
North

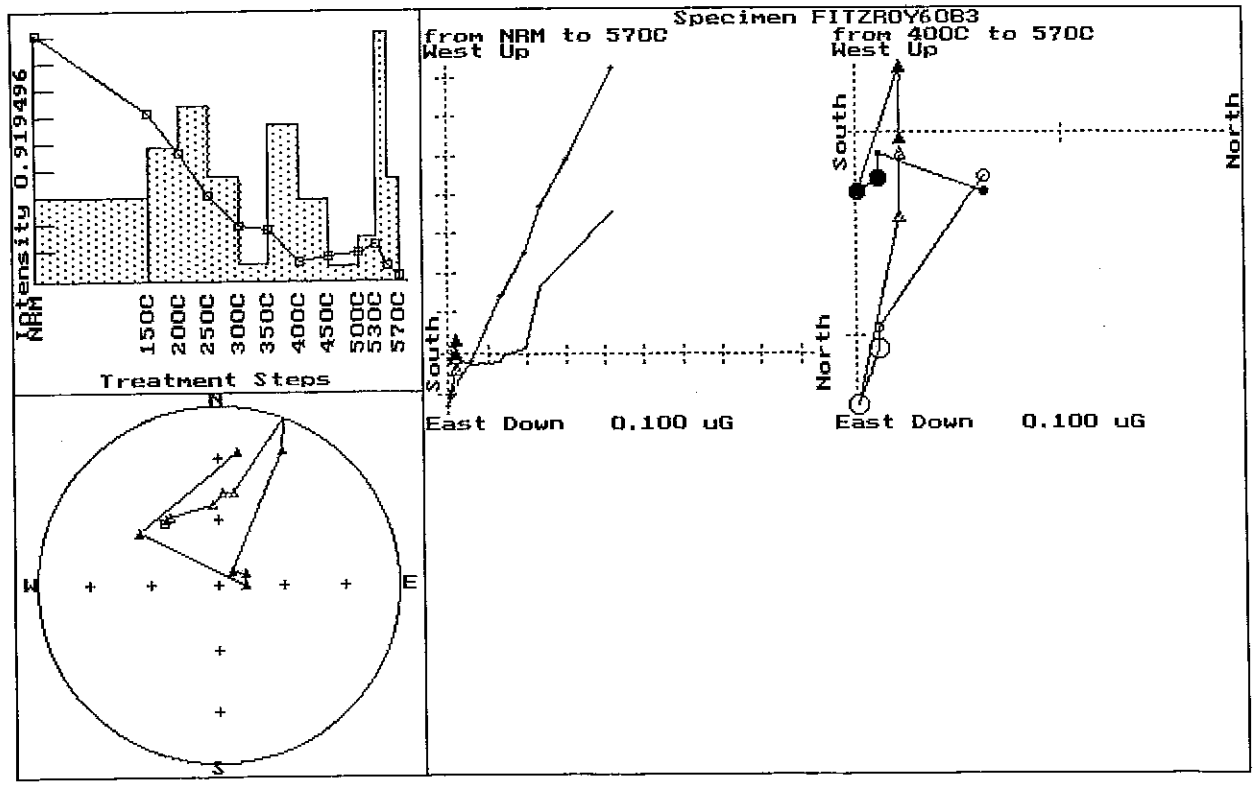
Specimen FITZROY60B3
from NRM to 570C
West Up
from 400C to 570C
West Up
Intensity 0.919496
NRM
150C
200C
250C
300C
350C
400C
450C
500C
530C
570C
Treatment Steps
N
E
S
W
South
East Down 0.100 uG
North
South
East Down 0.100 uG
North

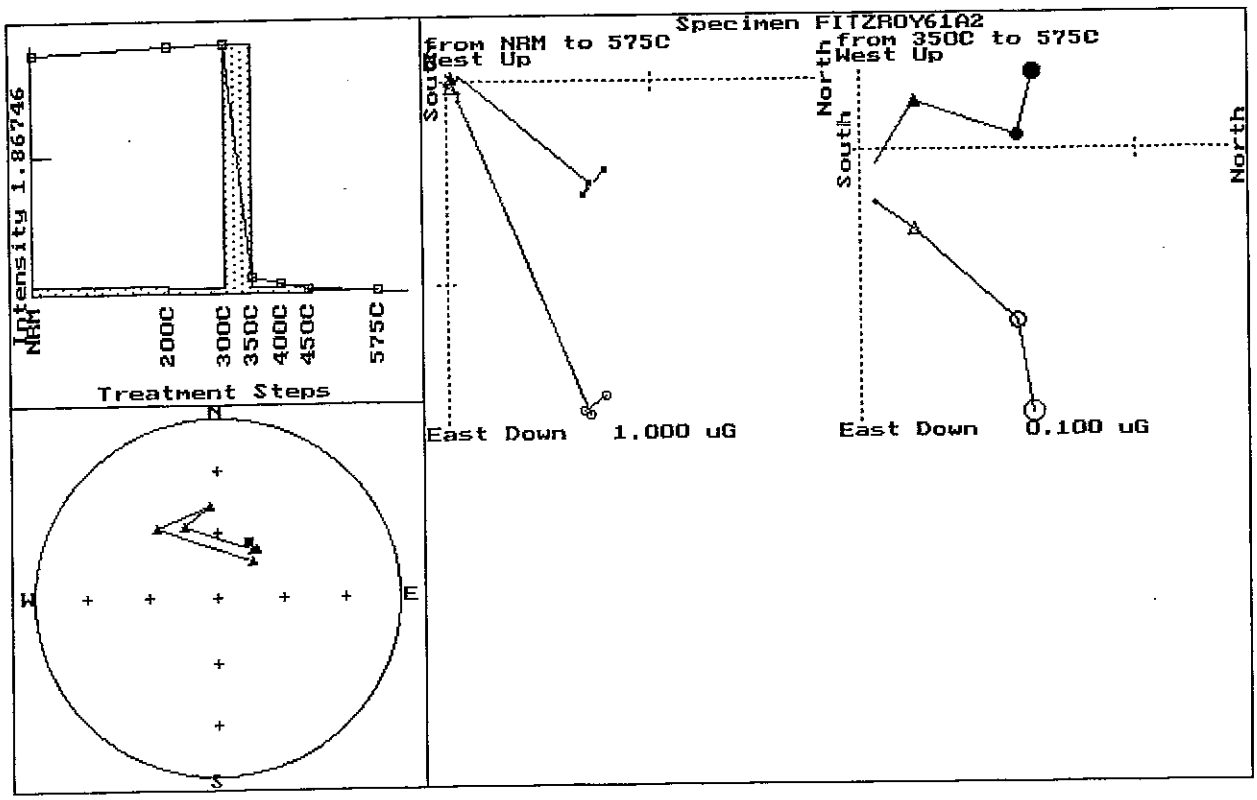
Intensity 1.86746
NRM
200C
300C
350C
400C
450C
575C
Treatment Steps
N
W
E
S
Specimen FITZROY61A2
from NRM to 575C
West Up
South
East Down 1.000 uG
from 350C to 575C
West Up
North
South
North
East Down 0.100 uG

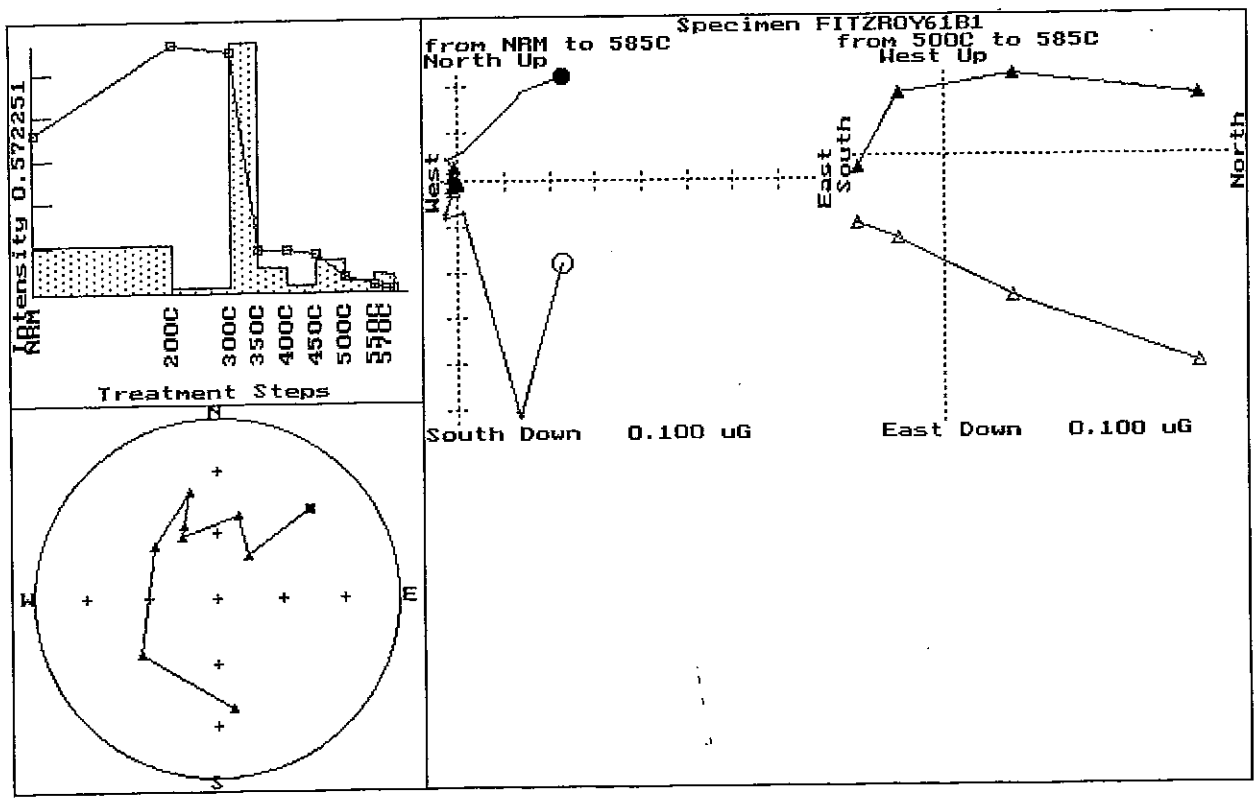
Intensity 0.572251
NRM
200C
300C
350C
400C
450C
500C
575C
Treatment Steps
N
W
E
S
Specimen FITZROY61B1
from NRM to 585C
North Up
West
East
South Down 0.100 uG
from 500C to 585C
West Up
South
North
East Down 0.100 uG

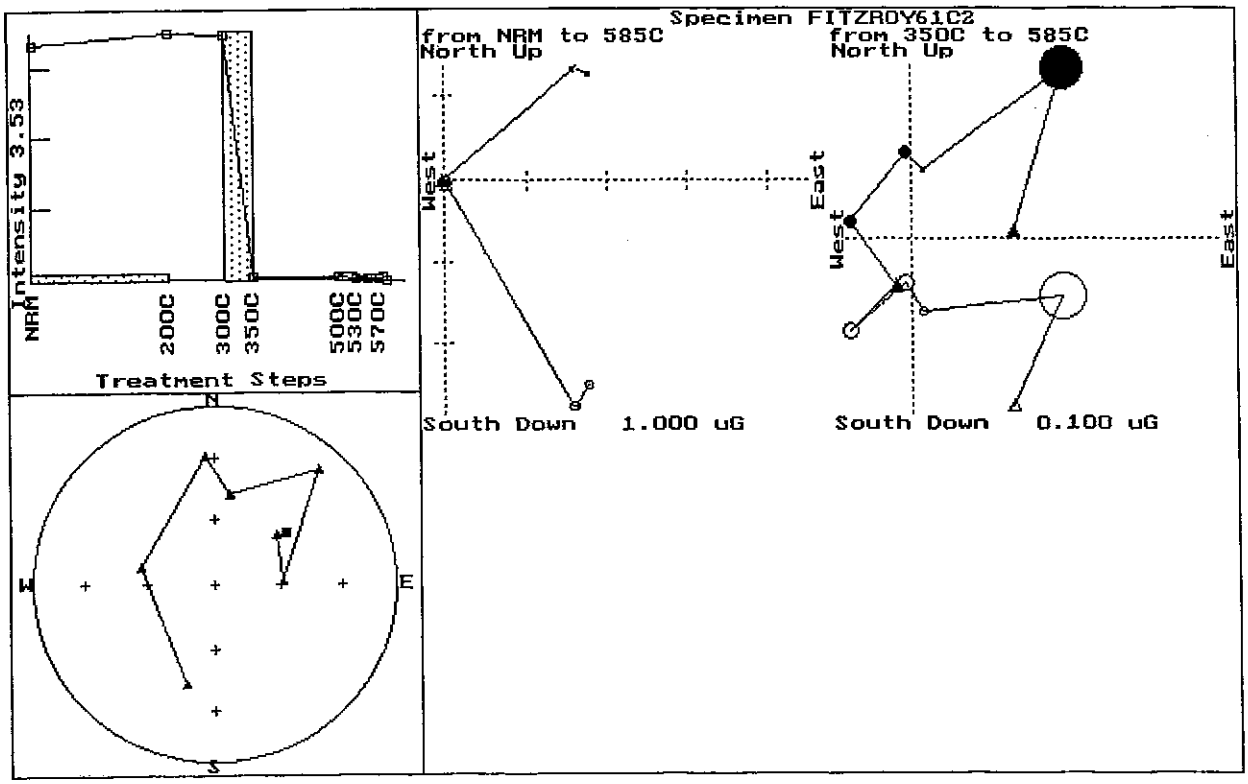
Specimen FITZROY61C2
Intensity 3.53
NRM
200C
300C
350C
500C
530C
570C
Treatment Steps
from NRM to 585C
North Up
West
East
South Down
1.000 uG
from 350C to 585C
North Up
West
East
South Down
0.100 uG
N
W
E
S

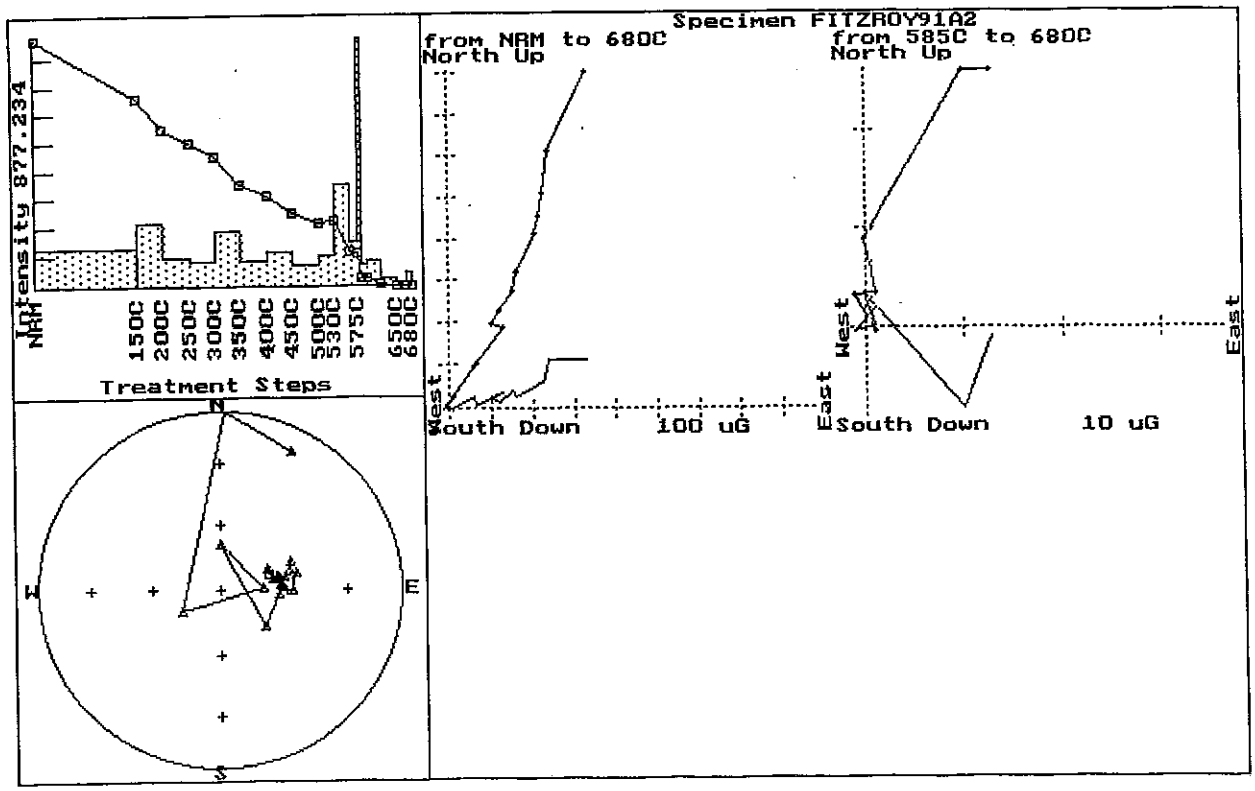
Specimen FITZROY91A2
from NRM to 680C
North Up
from 585C to 680C
North Up
Intensity 877.234
NRM
150C 200C 250C 300C 350C 400C 450C 500C 530C 575C 650C 680C
Treatment Steps
N
W
E
S
West
South Down
100 uG
East
West
East
South Down
10 uG

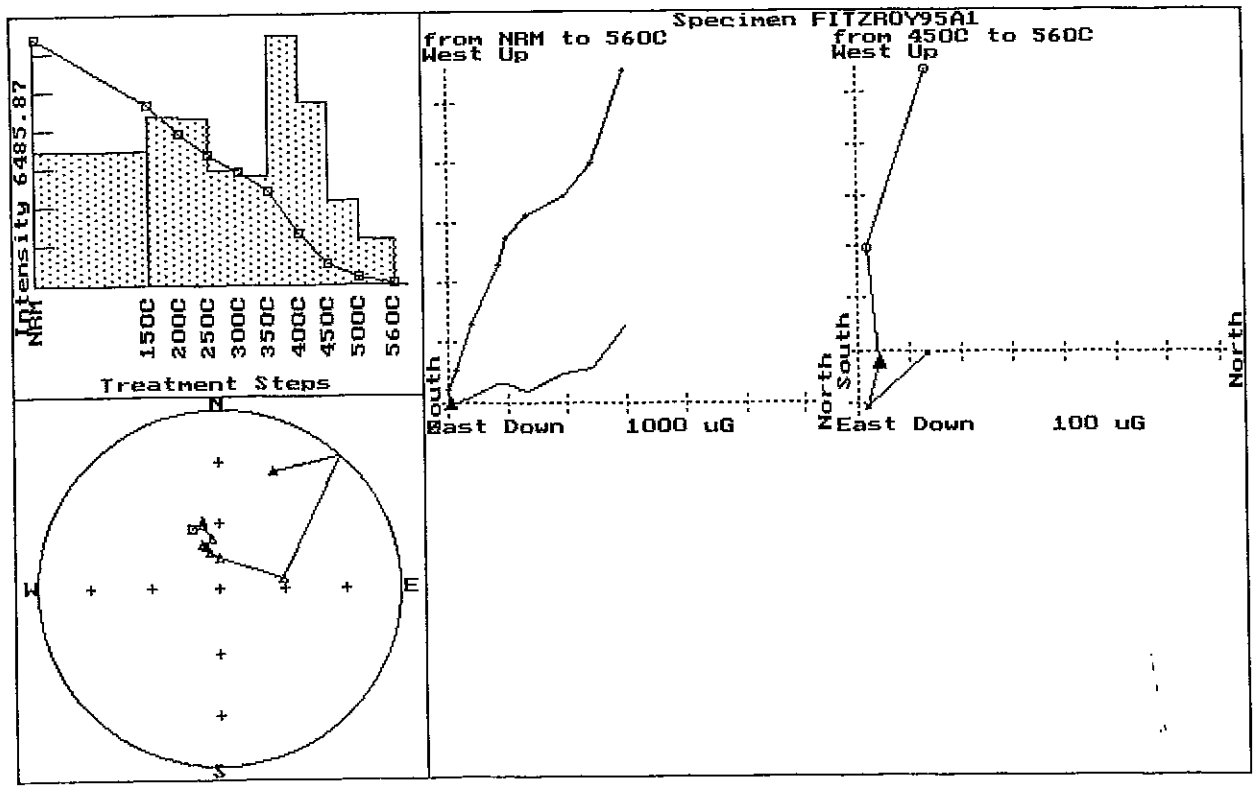
Specimen FITZROY95A1
from NRM to 560C
West Up
from 450C to 560C
West Up
Intensity 6485.87
NRM
150C 200C 250C 300C 350C 400C 450C 500C 560C
Treatment Steps
N
W
E
S
South
East Down
1000 uG
North
South
North
East Down
100 uG

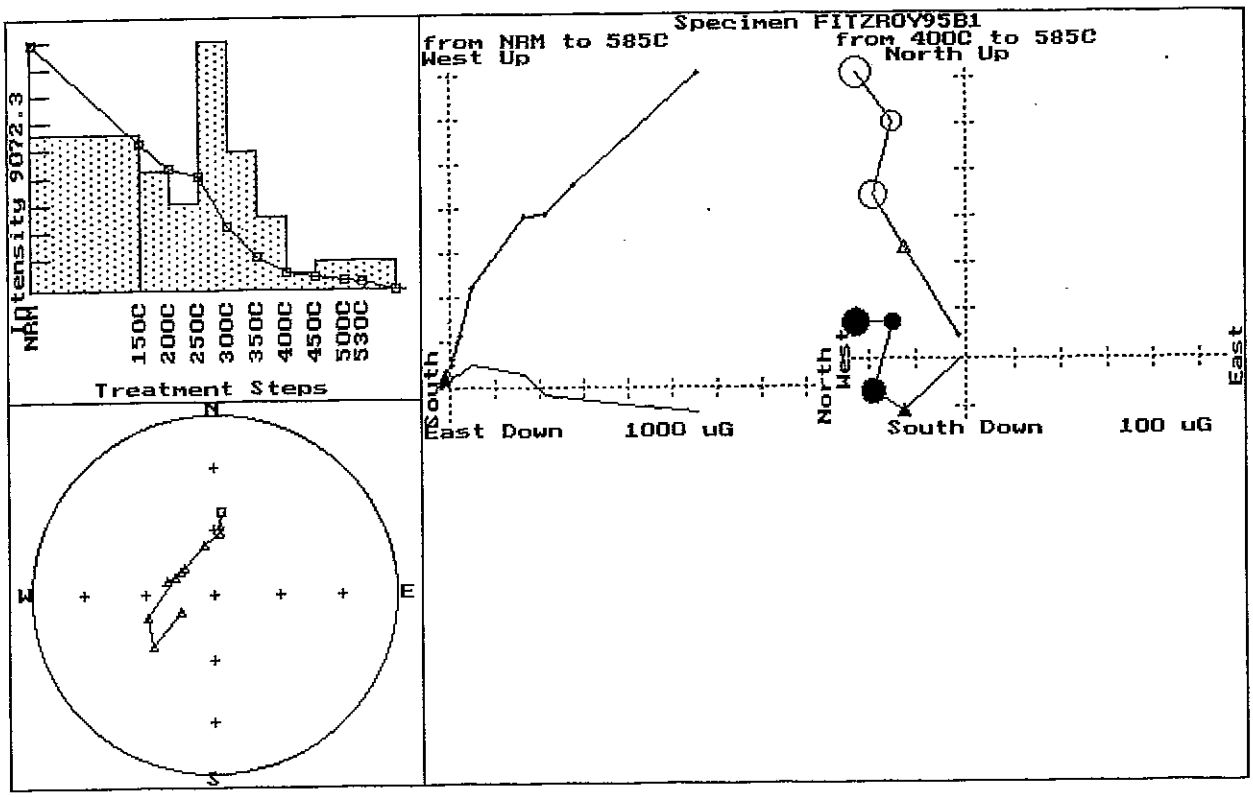
Intensity 9072.3
NRM
150C
200C
250C
300C
350C
400C
450C
500C
530C
Treatment Steps
N
W
E
S
Specimen FITZROY95B1
from NRM to 585C
West Up
South
East Down
1000 uG
from 400C to 585C
North Up
North
West
East
South Down
100 uG

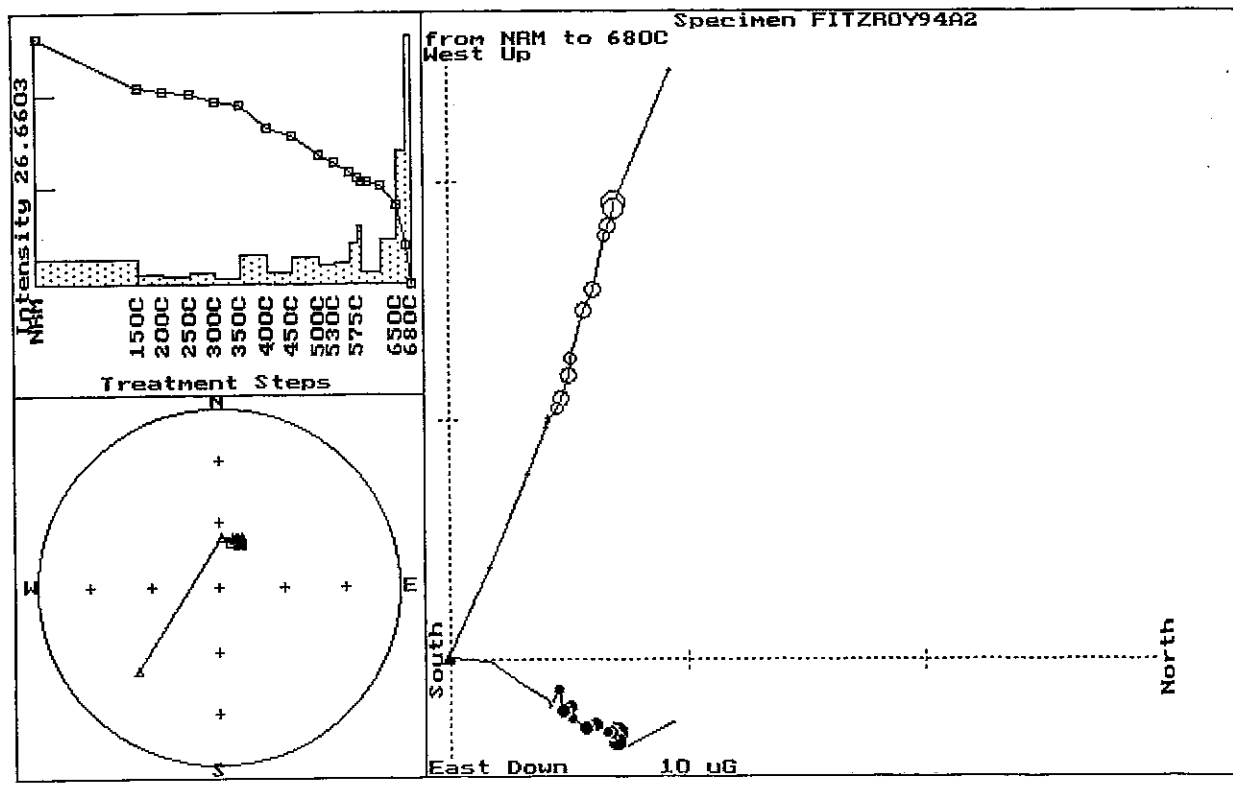
Specimen FITZROY94A2
from NRM to 680C
West Up
Intensity 26.6603
NRM
150C
200C
250C
300C
350C
400C
450C
500C
530C
575C
650C
680C
Treatment Steps
N
W
E
S
South
North
East Down
10 uG

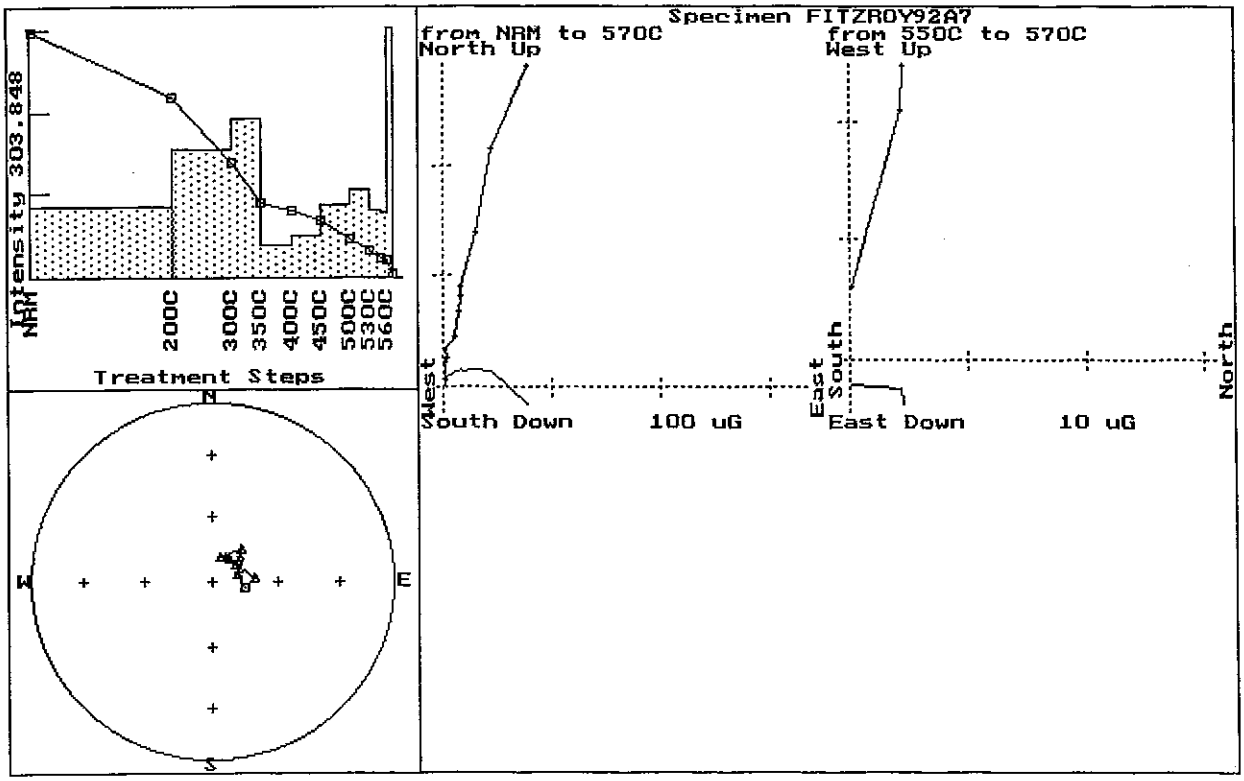
Specimen FITZROY92A7
from NRM to 570C
North Up
from 550C to 570C
West Up
Intensity 303.848
NRM
200C
300C
350C
400C
450C
500C
530C
560C
Treatment Steps
N
W
E
S
West
South Down
100 uG
East
South
East Down
10 uG
North

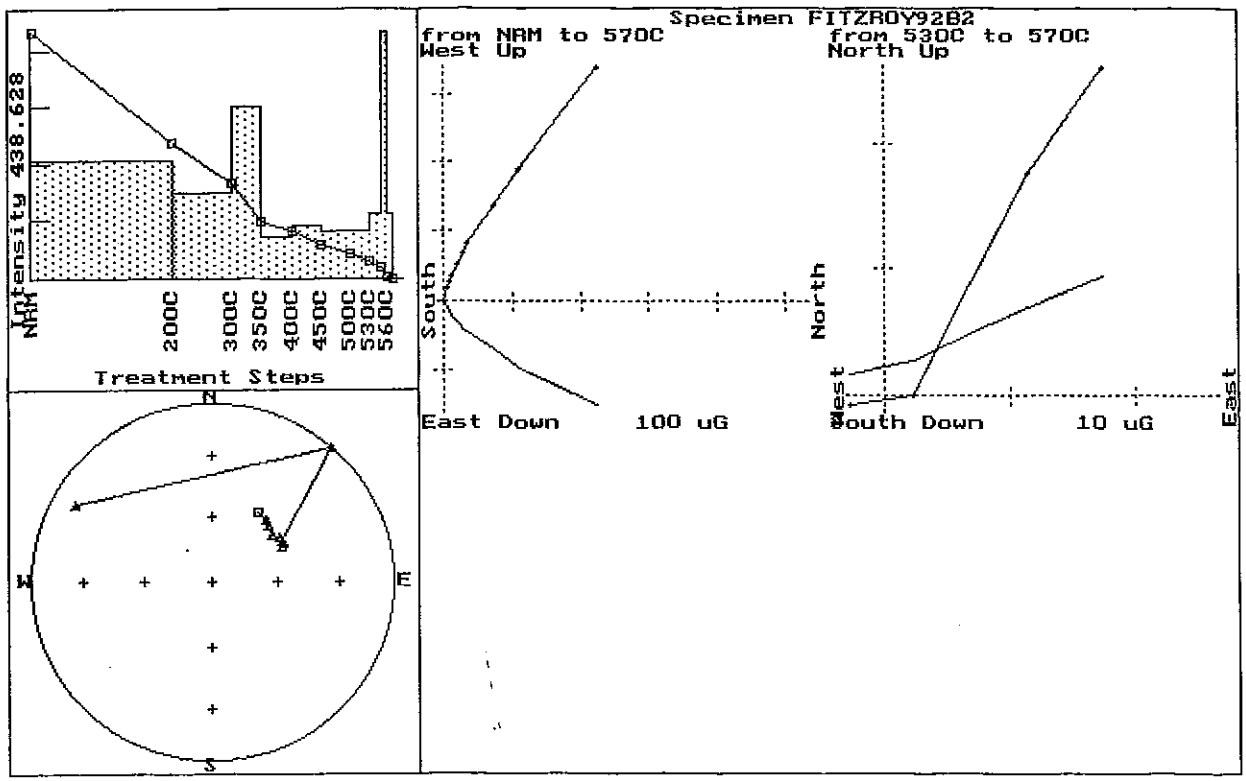
Specimen FITZROY92B2
from NRM to 570C
West Up
from 530C to 570C
North Up
Intensity 438.628
NRM
200C
300C
350C
400C
450C
500C
530C
560C
Treatment Steps
N
W
E
S
South
East Down
100 uG
North
West
South Down
10 uG
East

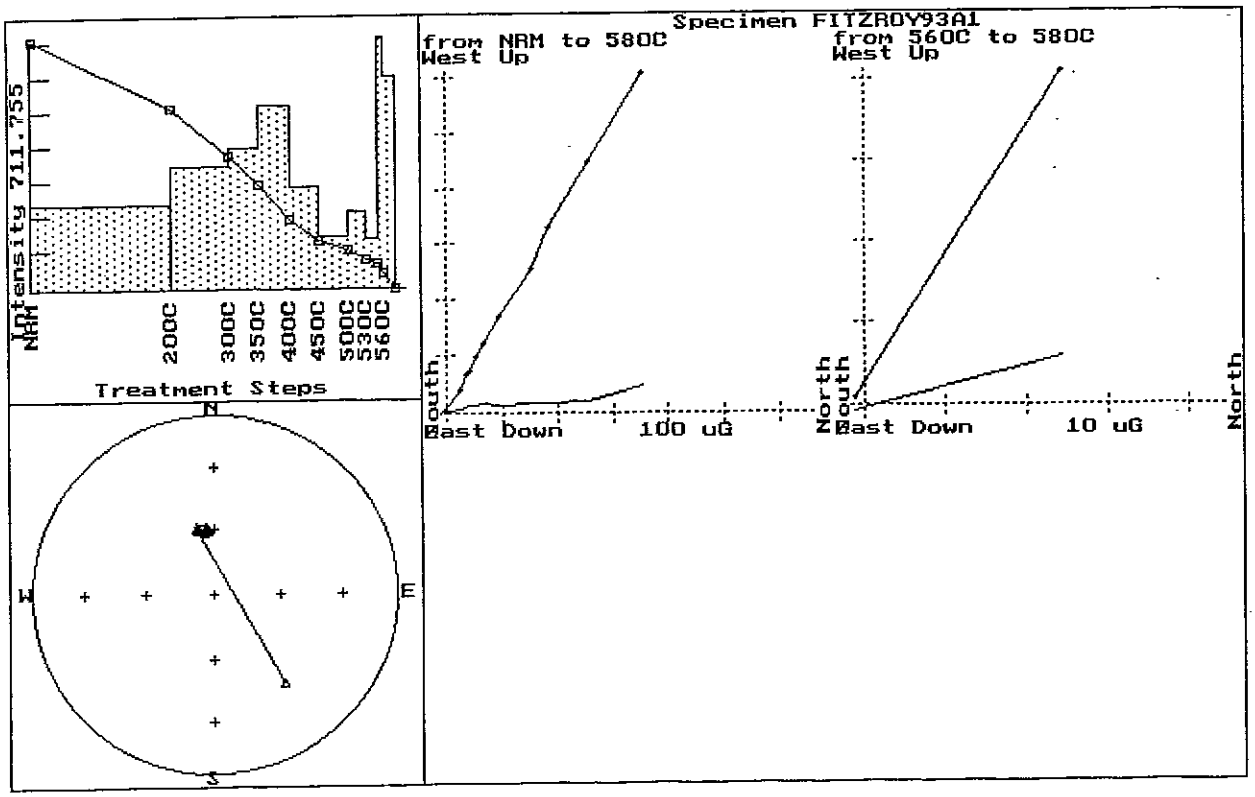
Specimen FITZROY93A1
from NRM to 580C
West Up
from 560C to 580C
West Up
Intensity 711.755
NRM
200C
300C
350C
400C
450C
500C
530C
560C
Treatment Steps
N
W
E
S
South
East Down
100 uG
North
South
East Down
10 uG
North

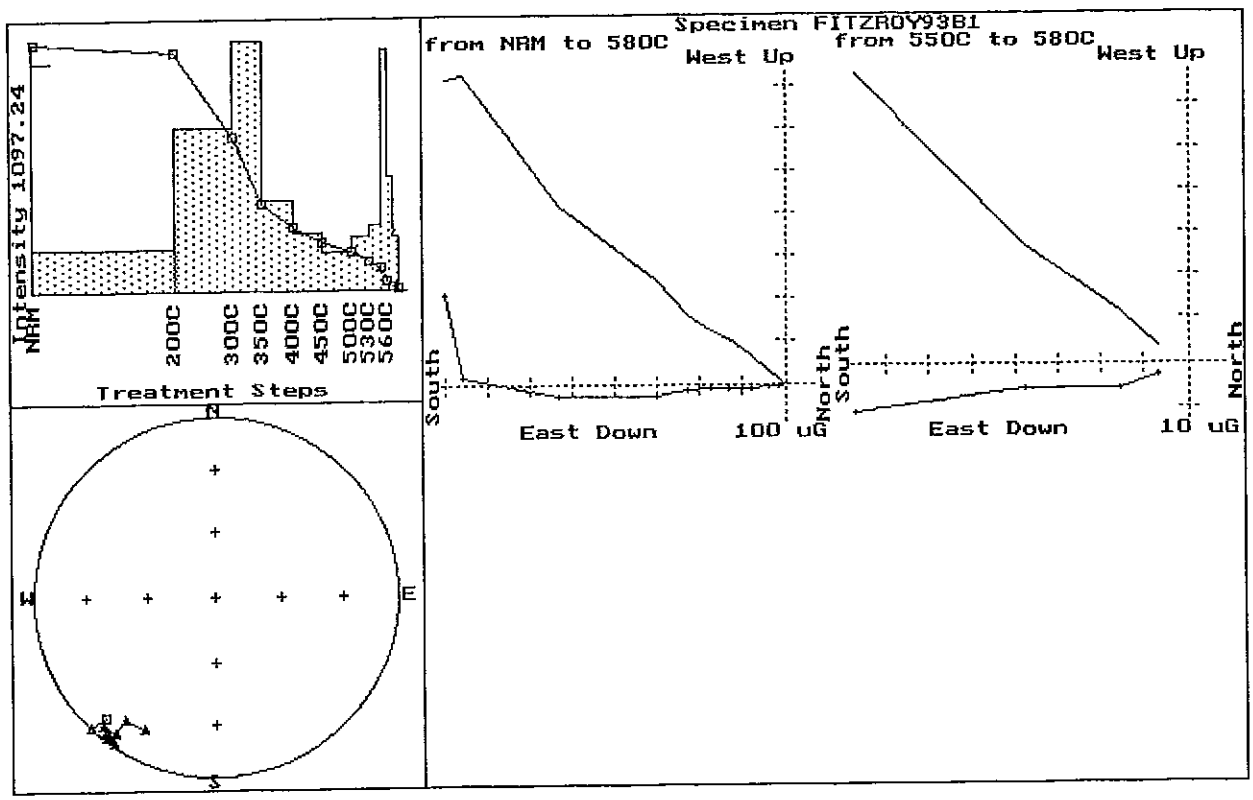
Specimen FITZROY93B1
from NRM to 580C
West Up
from 550C to 580C
West Up
Intensity 1097.24
NRM
200C
300C
350C
400C
450C
500C
530C
560C
Treatment Steps
N
W
E
S
South
East Down
100 uG
North
South
East Down
10 uG
North

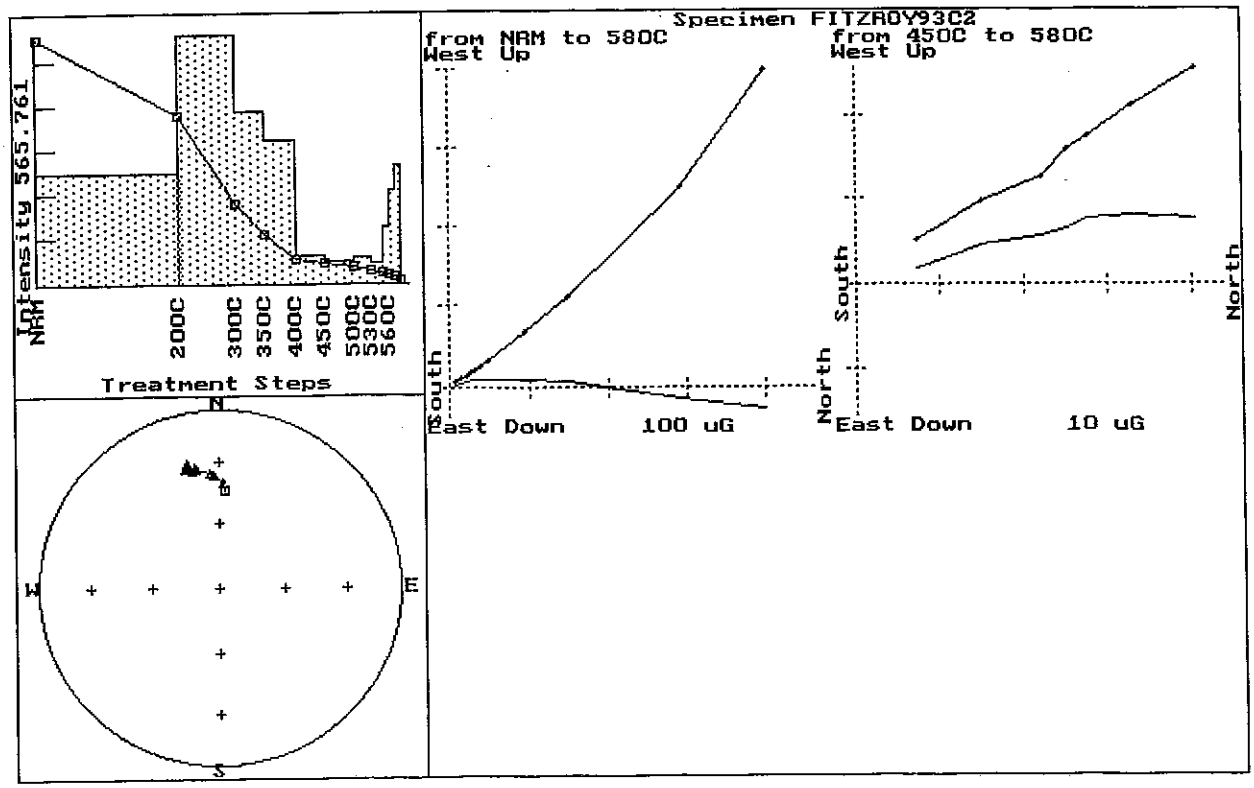
Intensity 565.761
NRM
200C
300C
350C
400C
450C
500C
530C
560C
Treatment Steps
N
W
E
S
Specimen FITZROY93C2
from NRM to 580C
West Up
South
East Down
100 uG
from 450C to 580C
West Up
South
North
East Down
10 uG
North

Appendix II

Magnetic fabric plots for all sites. The susceptibility anisotropy defines an ellipsoid with axes corresponding to three principal susceptibilities: major, intermediate and minor (k1, k2, k3).

The anisotropy ratio is k1/k3.
Bulk susceptibility = (k1+k2+k3)/3.
Lineation = k1/k2.
Foliation = k2/k3.
T factor characterises the ellipsoid shape ($-1 < T < 1$; $T < 0$ for prolate ellipsoids, $T > 0$ for oblate ellipsoids.

In the equal area lower hemisphere stereonets, squares denote major axes (magnetic lineations), triangles denote intermediate axes and dots denote minor axes (magnetic foliation poles).

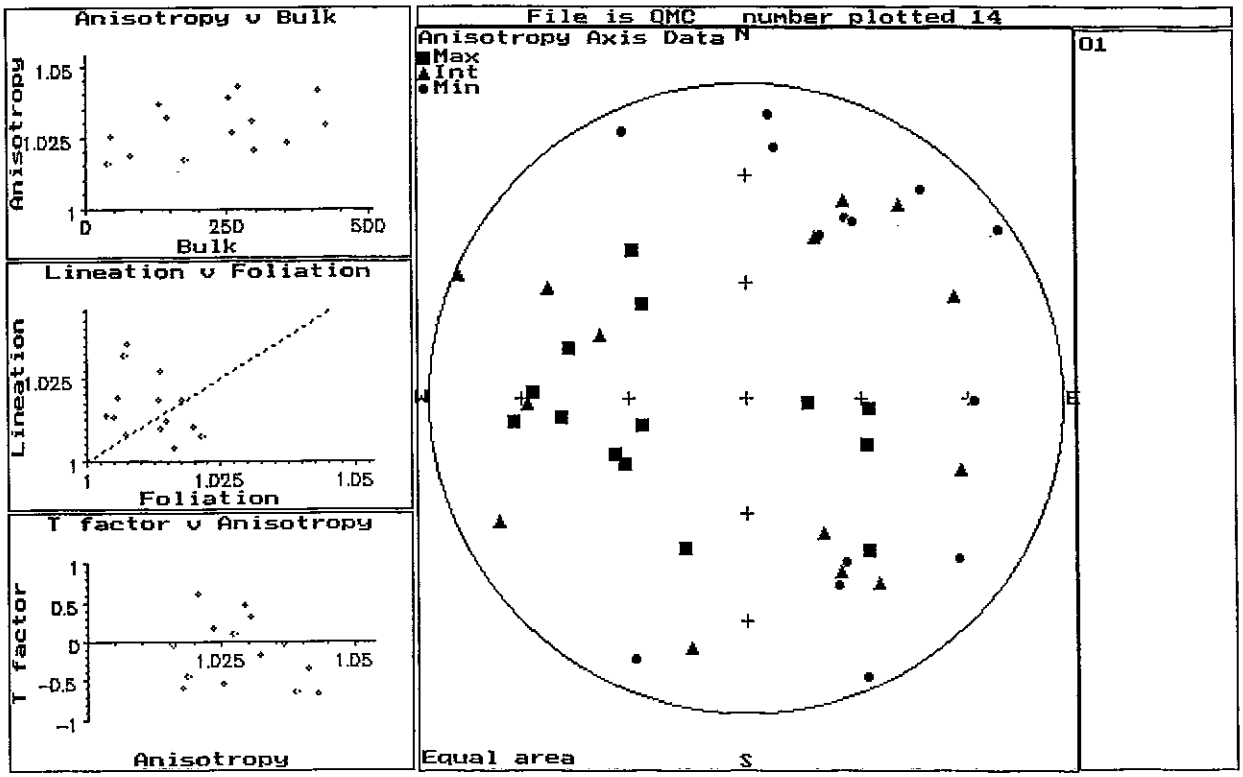
Anisotropy v Bulk
Anisotropy
1.05
1.025
1
0
250
500
Bulk
Lineation v Foliation
Lineation
1.025
1
1
1.025
1.05
Foliation
T factor v Anisotropy
T factor
1
0.5
0
-0.5
-1
1.025
1.05
Anisotropy
File is QMC number plotted 14
Anisotropy Axis Data
Max
Int
Min
N
W
E
S
Equal area
01

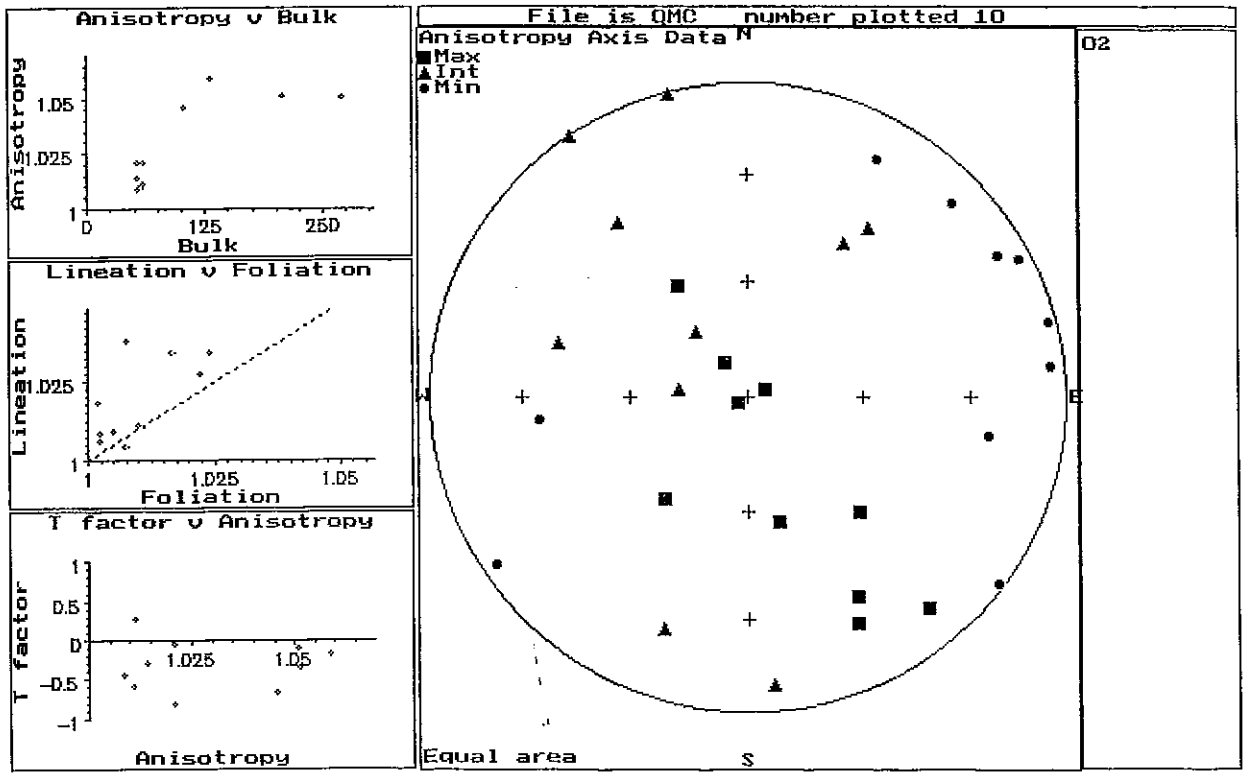
Anisotropy v Bulk
Anisotropy
1.05
1.025
1
0
125
250
Bulk
Lineation v Foliation
Lineation
1.025
1
1
1.025
1.05
Foliation
T factor v Anisotropy
T factor
1
0.5
0
-0.5
-1
1.025
1.05
Anisotropy
File is QMC number plotted 10
Anisotropy Axis Data
Max
Int
Min
N
W
E
S
Equal area
02

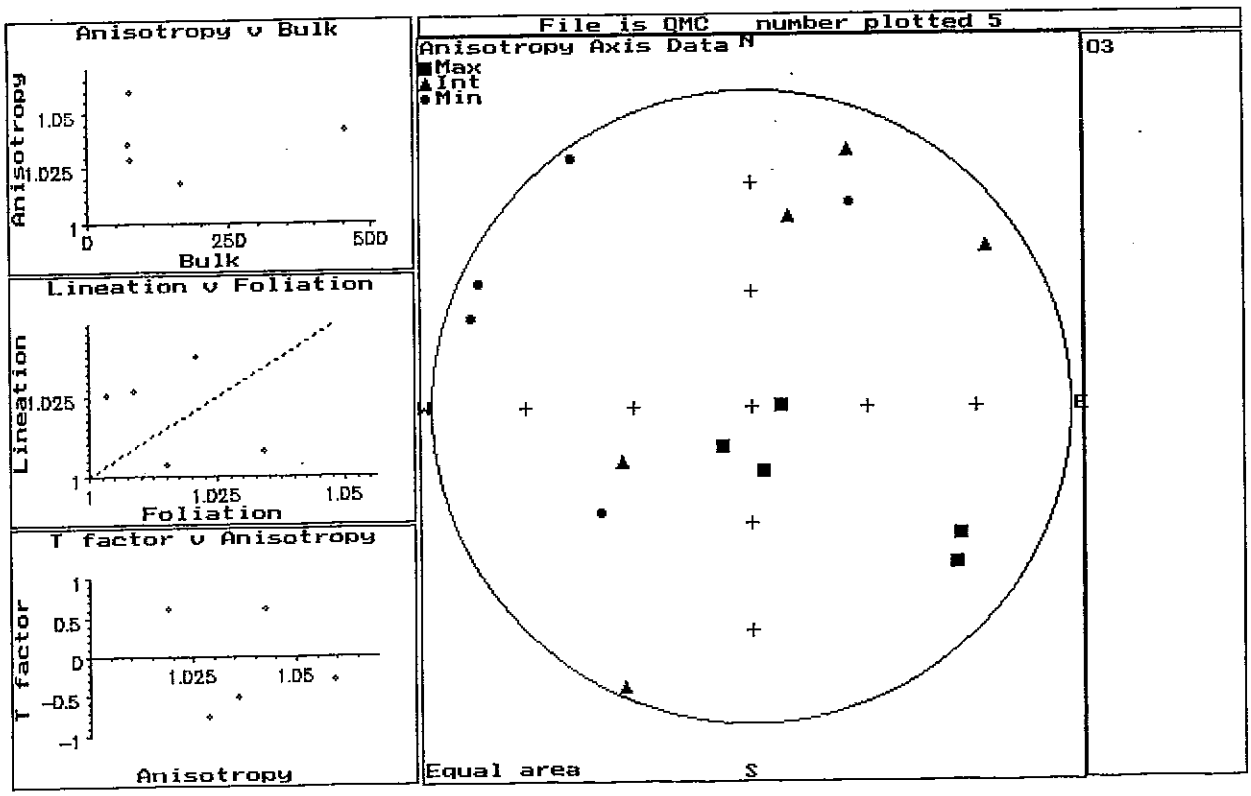
Anisotropy v Bulk
Anisotropy
1.05
1.025
1
0
250
500
Bulk
Lineation v Foliation
Lineation
1.025
1
1
1.025
1.05
Foliation
T factor v Anisotropy
T factor
1
0.5
0
-0.5
-1
1.025
1.05
Anisotropy
File is QMC number plotted 5
Anisotropy Axis Data
Max
Int
Min
N
E
S
Equal area
03

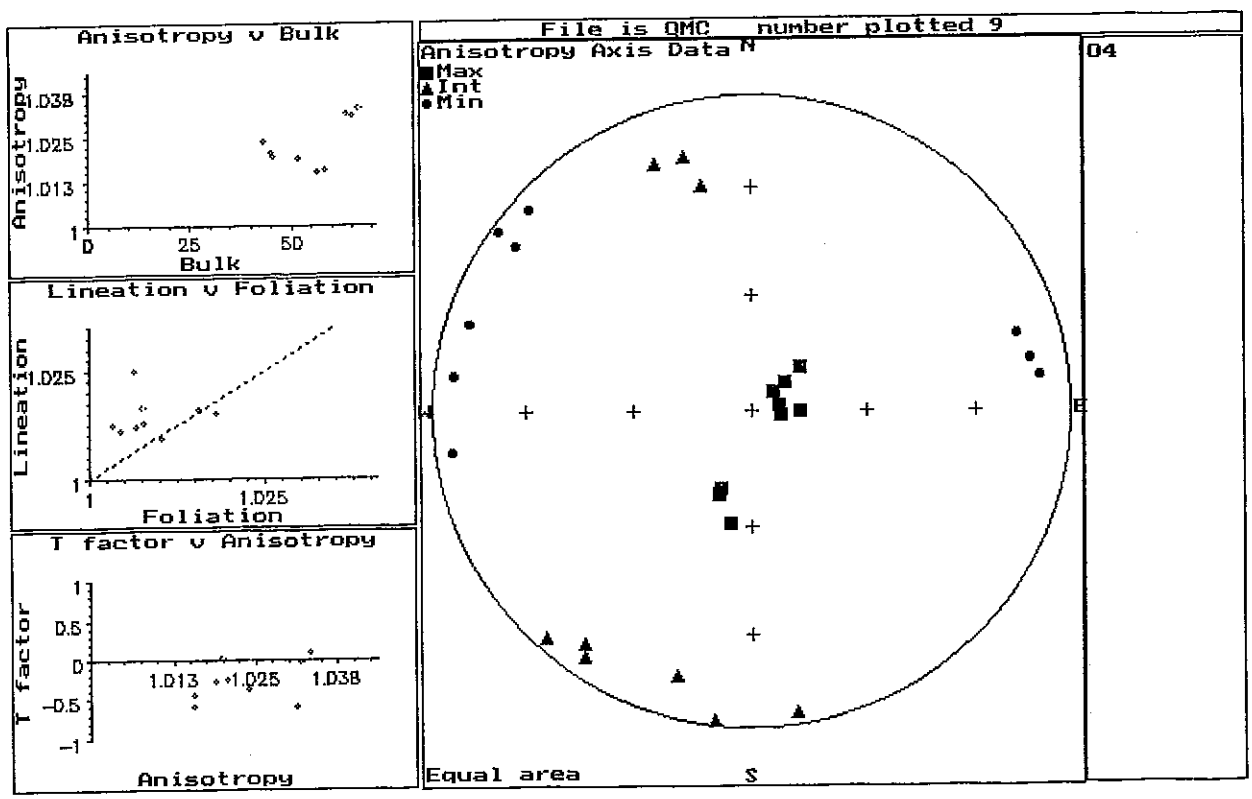
Anisotropy v Bulk
Anisotropy
1.038
1.025
1.013
1
0
25
50
Bulk
Lineation v Foliation
Lineation
1.025
1
1
1.025
Foliation
T factor v Anisotropy
T factor
1
0.5
0
-0.5
-1
1.013
1.025
1.038
Anisotropy
File is QMC number plotted 9
Anisotropy Axis Data
Max
Int
Min
N
E
S
Equal area
04

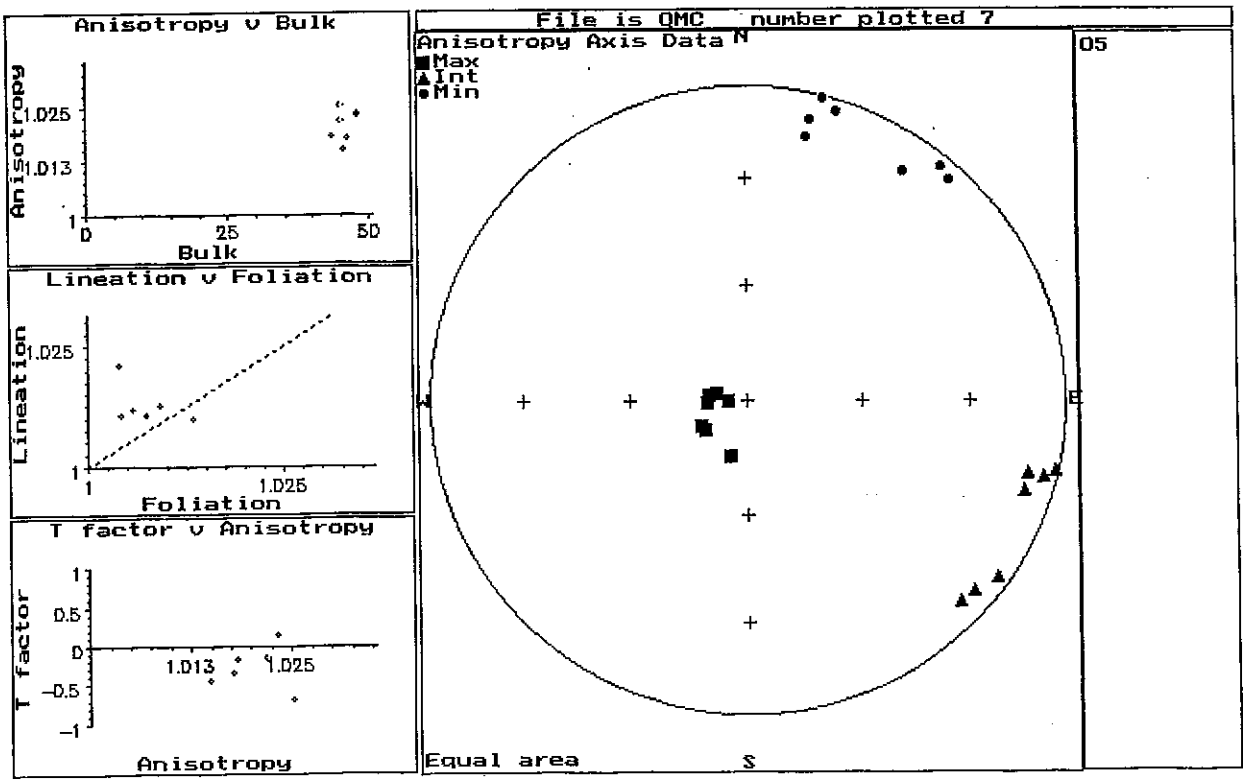
Anisotropy v Bulk
Anisotropy
1.025
1.013
1
0
25
50
Bulk
Lineation v Foliation
Lineation
1.025
1
1
1.025
Foliation
T factor v Anisotropy
T factor
1
0.5
0
−0.5
−1
1.013
1.025
Anisotropy
File is QMC number plotted 7
Anisotropy Axis Data
Max
Int
Min
N
E
S
Equal area
05

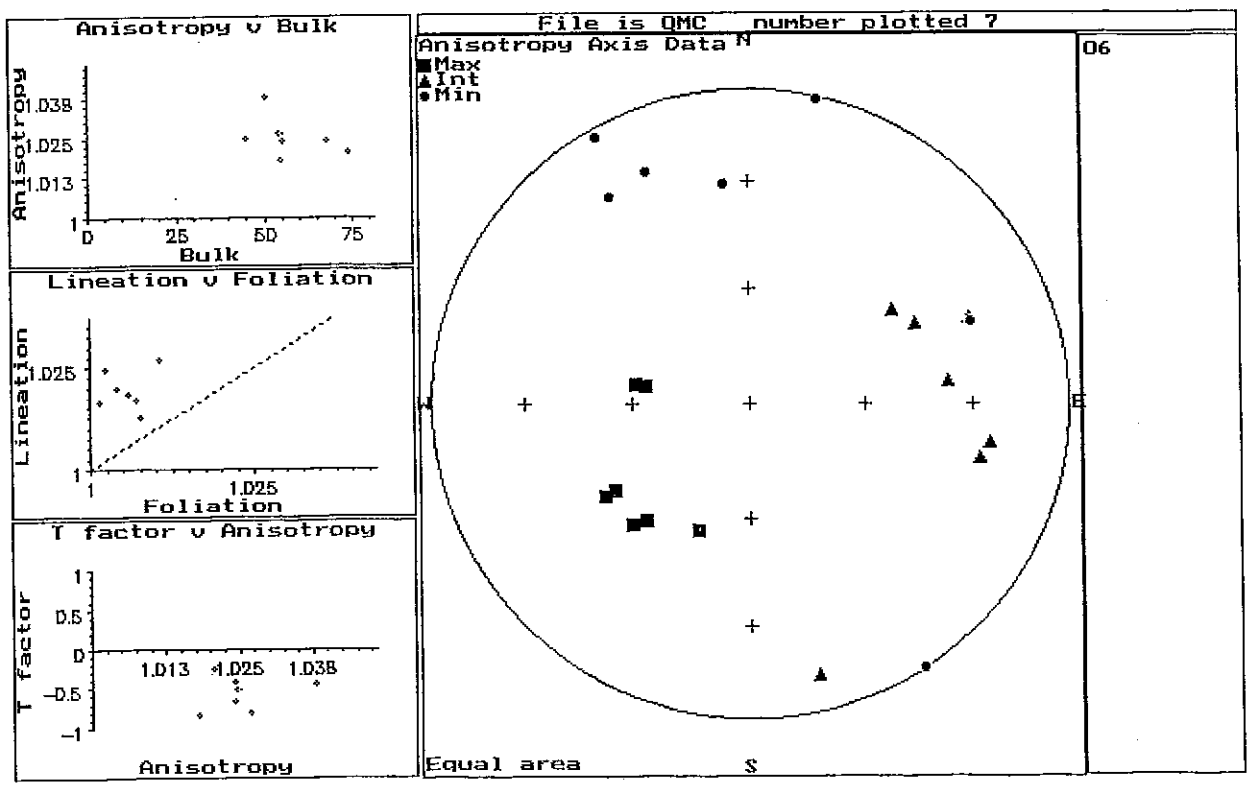
Anisotropy v Bulk
Anisotropy
1.038
1.025
1.013
1
0
25
50
75
Bulk
Lineation v Foliation
Lineation
1.025
1
1
1.025
Foliation
T factor v Anisotropy
T factor
1
0.5
0
−0.5
−1
1.013
1.025
1.038
Anisotropy
File is QMC number plotted 7
Anisotropy Axis Data
Max
Int
Min
N
E
S
Equal area
06

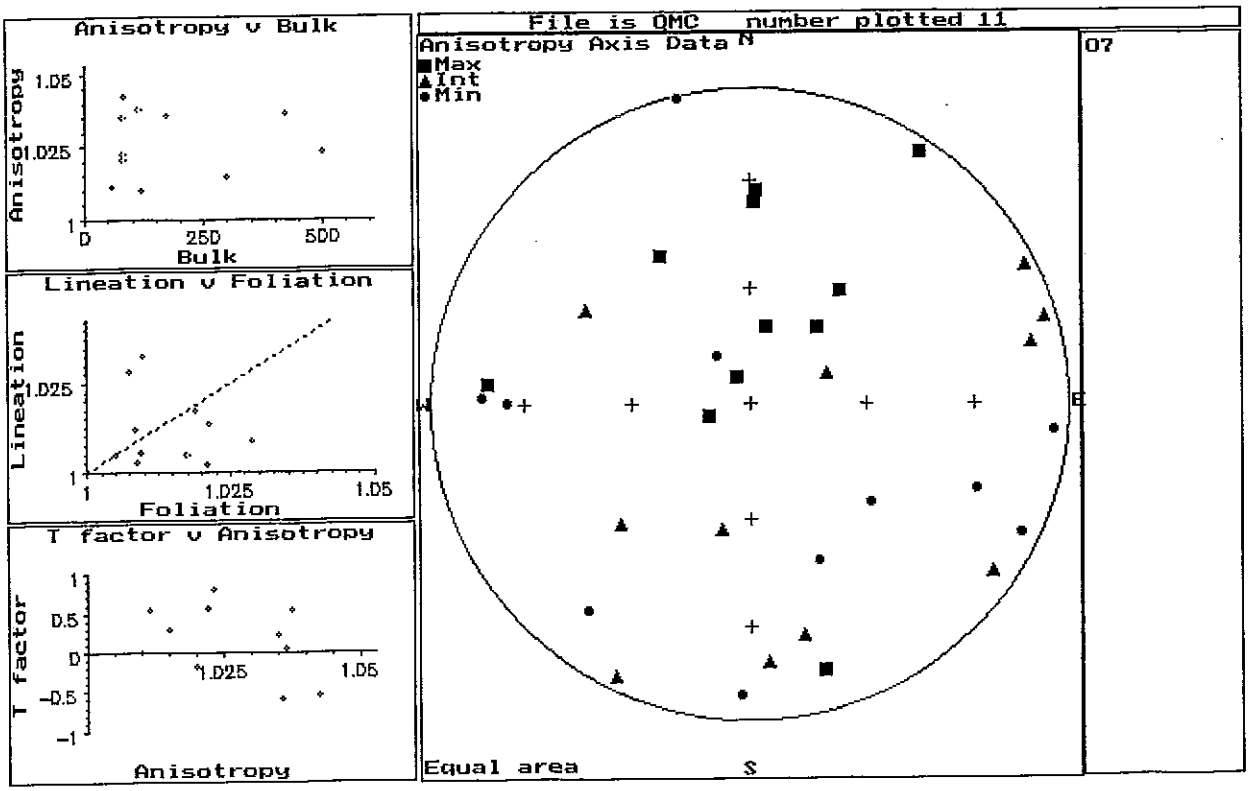
Anisotropy v Bulk
Anisotropy
1.05
1.025
1
0
250
500
Bulk
Lineation v Foliation
Lineation
1.025
1
1
1.025
1.05
Foliation
T factor v Anisotropy
T factor
1
0.5
0
-0.5
-1
1.025
1.05
Anisotropy
File is QMC number plotted 11
Anisotropy Axis Data
Max
Int
Min
N
W
E
S
Equal area
07

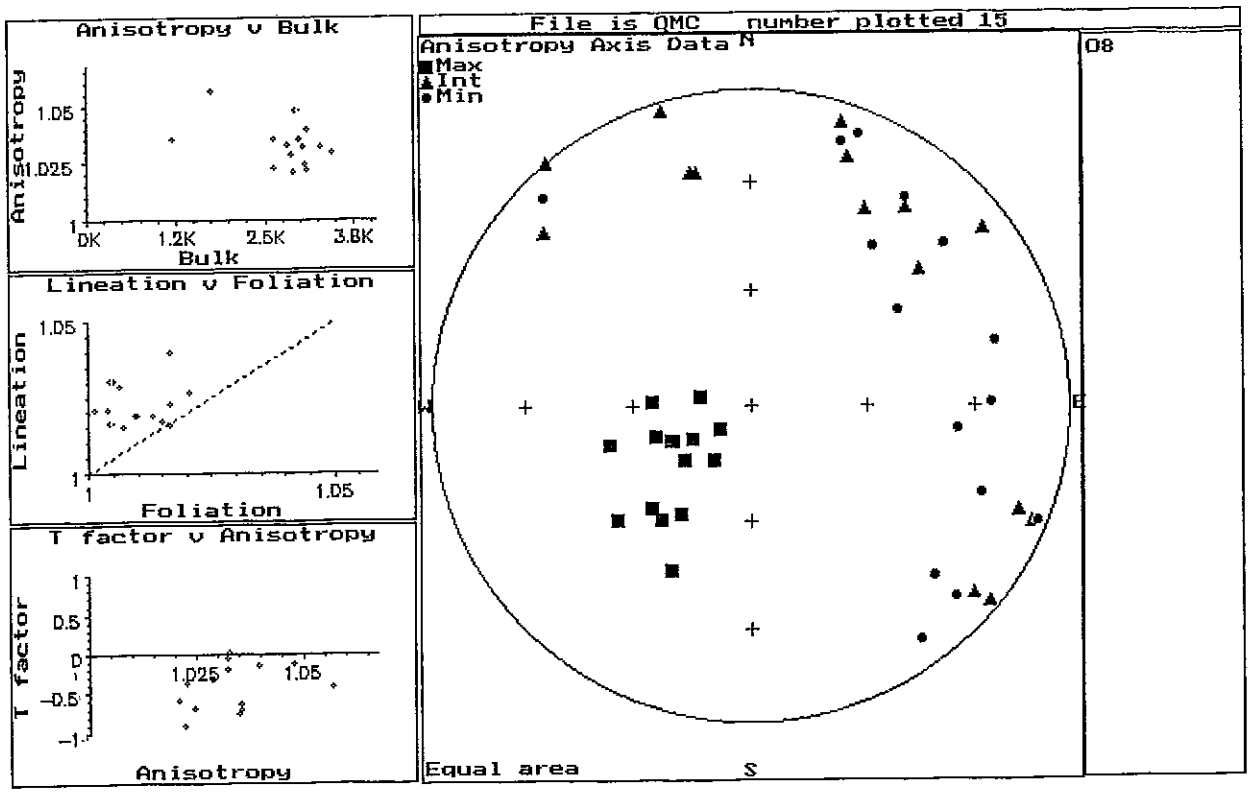
Anisotropy v Bulk
Anisotropy
1.05
1.025
1
0K
1.2K
2.5K
3.8K
Bulk
Lineation v Foliation
Lineation
1.05
1
1
1.05
Foliation
T factor v Anisotropy
T factor
1
0.5
0
-0.5
-1
1.025
1.05
Anisotropy
File is QMC number plotted 15
Anisotropy Axis Data
Max
Int
Min
N
W
E
S
Equal area
08

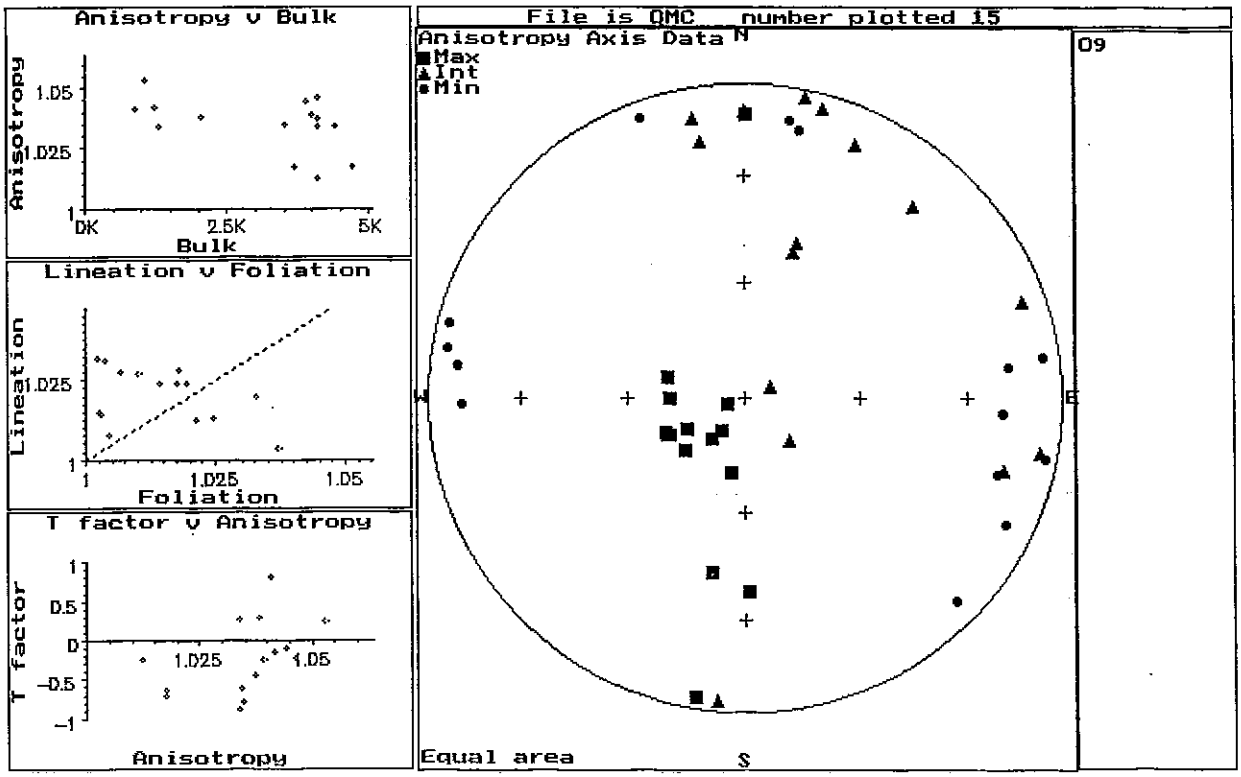
Anisotropy v Bulk
Anisotropy
1.05
1.025
1
0K
2.5K
5K
Bulk
Lineation v Foliation
Lineation
1.025
1
1
1.025
1.05
Foliation
T factor v Anisotropy
T factor
1
0.5
0
-0.5
-1
1.025
1.05
Anisotropy
File is QMC number plotted 15
Anisotropy Axis Data
Max
Int
Min
N
W
E
S
Equal area
09

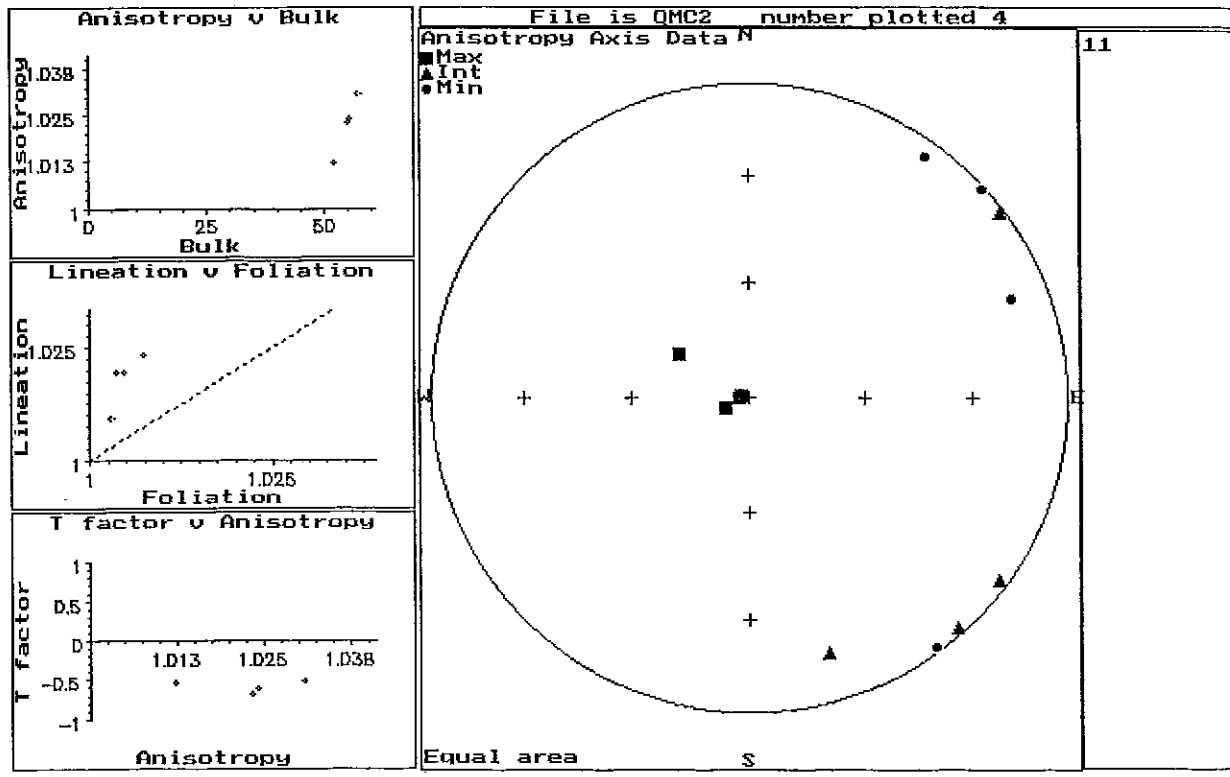
Anisotropy v Bulk
Anisotropy
1.038
1.025
1.013
1
0
25
50
Bulk
Lineation v Foliation
Lineation
1.025
1
1
1.025
Foliation
T factor v Anisotropy
T factor
1
0.5
0
-0.5
-1
1.013
1.025
1.038
Anisotropy
File is QMC2 number plotted 4
Anisotropy Axis Data
Max
Int
Min
N
W
E
S
Equal area
11

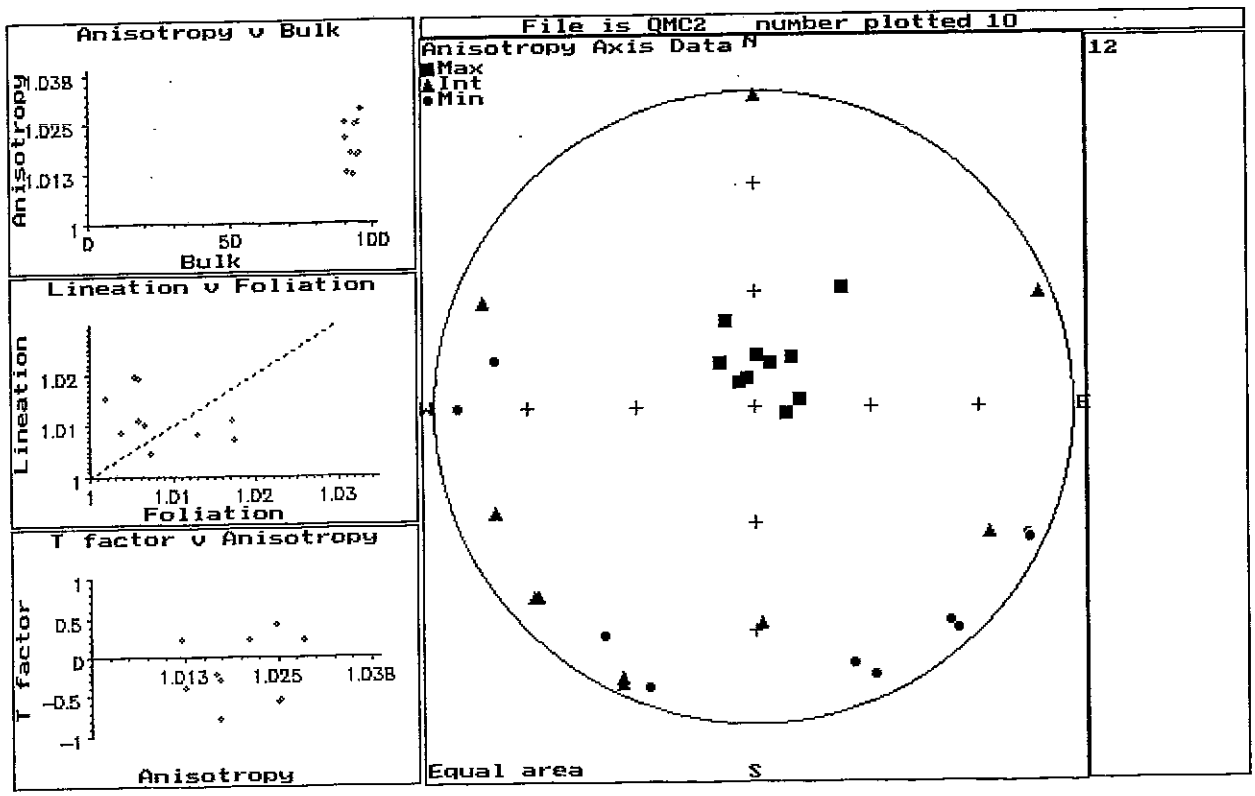
Anisotropy v Bulk
Anisotropy
1.038
1.025
1.013
1
0
50
100
Bulk
Lineation v Foliation
Lineation
1.02
1.01
1
1
1.01
1.02
1.03
Foliation
T factor v Anisotropy
T factor
1
0.5
0
−0.5
−1
1.013
1.025
1.038
Anisotropy
File is QMC2 number plotted 10
Anisotropy Axis Data
Max
Int
Min
N
E
S
Equal area
12

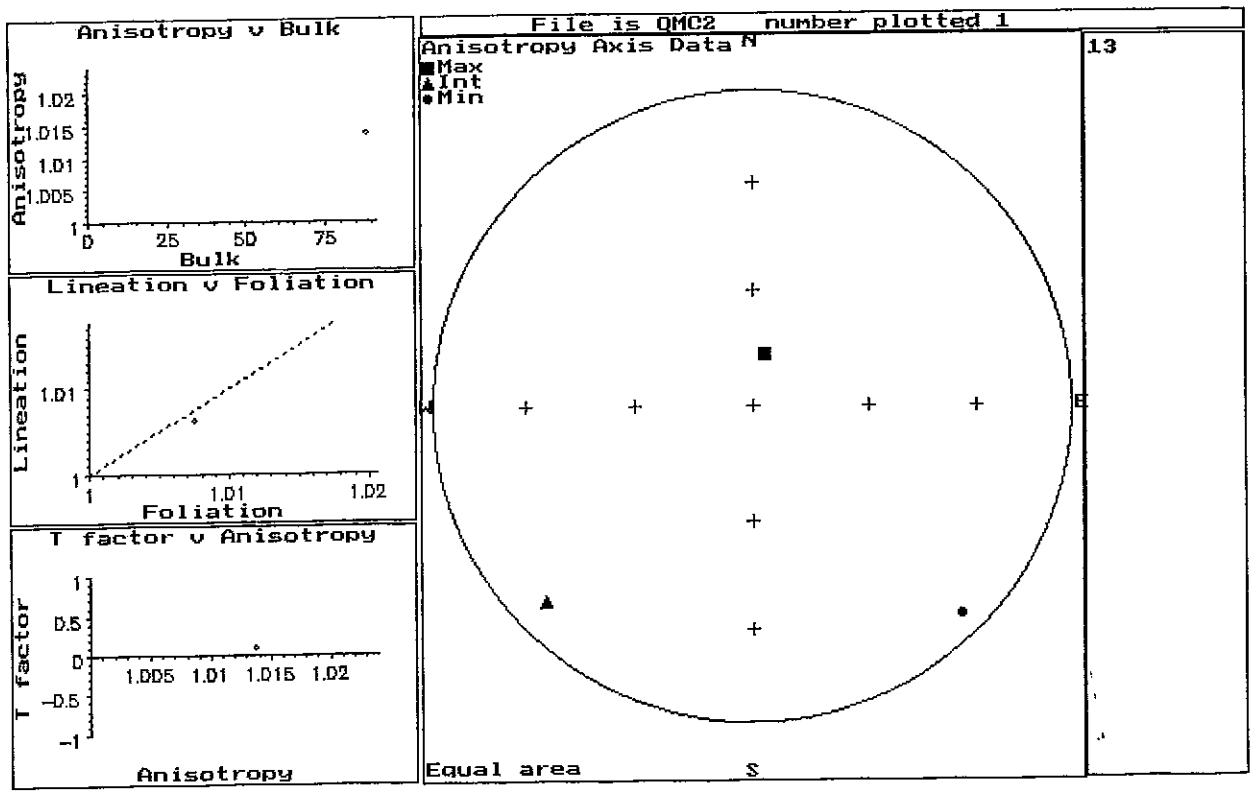
Anisotropy v Bulk
Anisotropy
1.02
1.015
1.01
1.005
1
0
25
50
75
Bulk
Lineation v Foliation
Lineation
1.01
1
1
1.01
1.02
Foliation
T factor v Anisotropy
T factor
1
0.5
0
−0.5
−1
1.005
1.01
1.015
1.02
Anisotropy
File is QMC2 number plotted 1
Anisotropy Axis Data
Max
Int
Min
N
E
S
Equal area
13

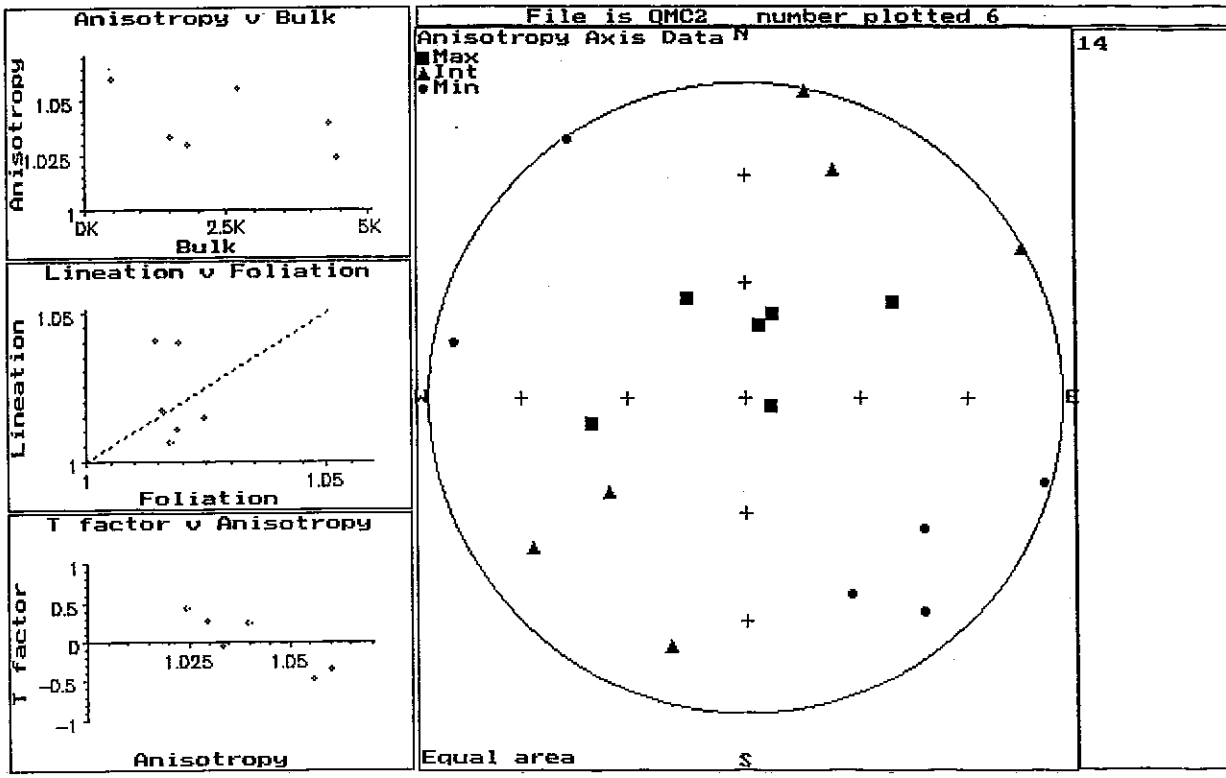
Anisotropy v Bulk
Anisotropy
1.05
1.025
1
0K
2.5K
5K
Bulk
Lineation v Foliation
Lineation
1.05
1
1
1.05
Foliation
T factor v Anisotropy
T factor
1
0.5
0
-0.5
-1
1.025
1.05
Anisotropy
File is QMC2 number plotted 6
Anisotropy Axis Data
N
Max
Int
Min
W
E
S
Equal area
14

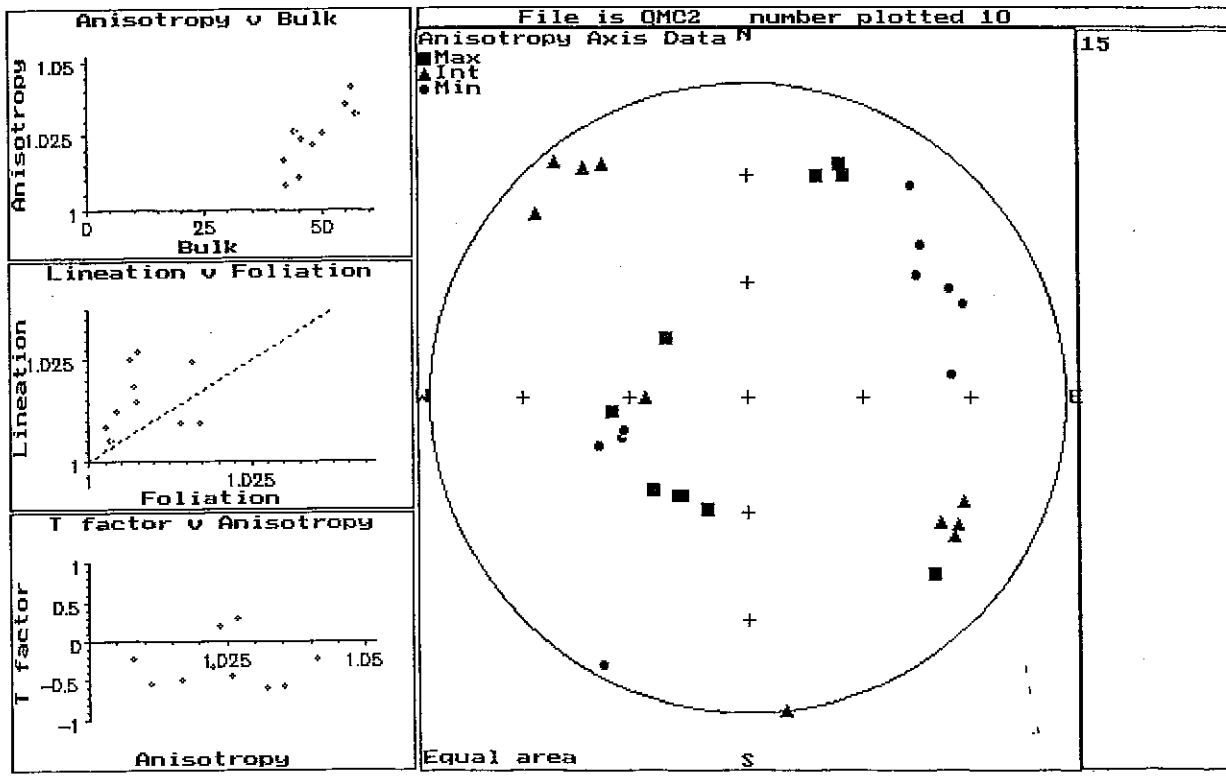
Anisotropy v Bulk
Anisotropy
1.05
1.025
1
0
25
50
Bulk
Lineation v Foliation
Lineation
1.025
1
1
1.025
Foliation
T factor v Anisotropy
T factor
1
0.5
0
-0.5
-1
1.025
1.05
Anisotropy
File is QMC2 number plotted 10
Anisotropy Axis Data
N
Max
Int
Min
W
E
S
Equal area
15

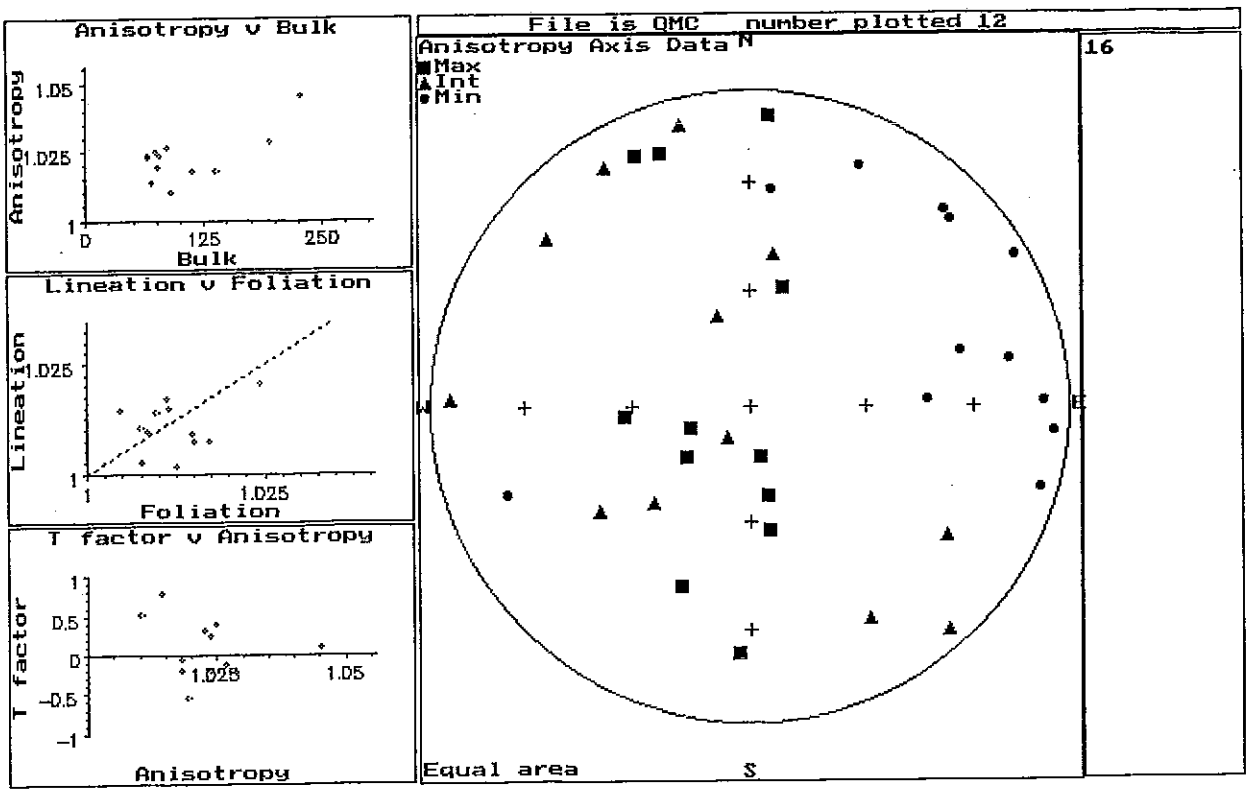
Anisotropy v Bulk
Anisotropy
1.05
1.025
1
D
125
25D
Bulk
Lineation v Foliation
Lineation
1.025
1
1.025
Foliation
T factor v Anisotropy
T factor
1
0.5
0
-0.5
-1
1.025
1.05
Anisotropy
File is QMC number plotted 12
Anisotropy Axis Data
Max
Int
Min
N
W
E
S
Equal area
16

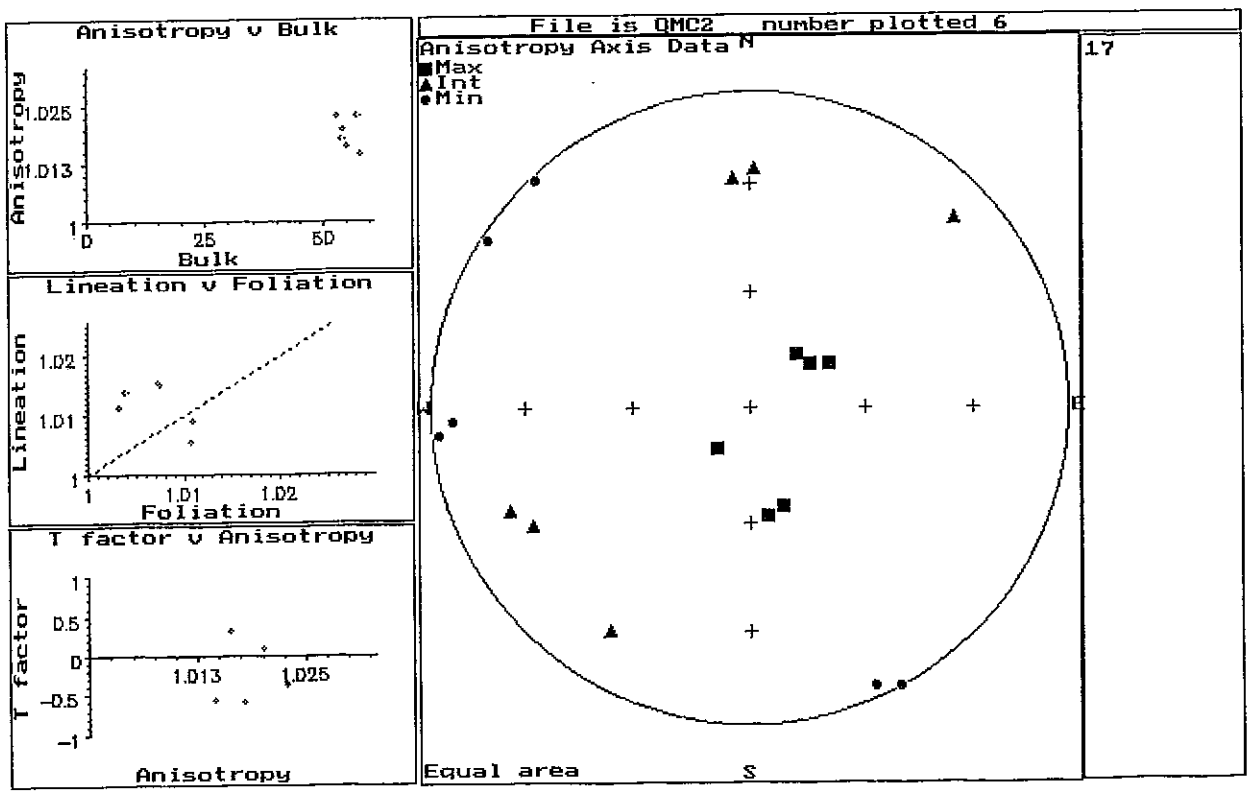
Anisotropy v Bulk
Anisotropy
1.025
1.013
1
D
25
50
Bulk
Lineation v Foliation
Lineation
1.02
1.01
1
1
1.01
1.02
Foliation
T factor v Anisotropy
T factor
1
0.5
0
-0.5
-1
1.013
1.025
Anisotropy
File is QMC2 number plotted 6
Anisotropy Axis Data
Max
Int
Min
N
W
E
S
Equal area
17

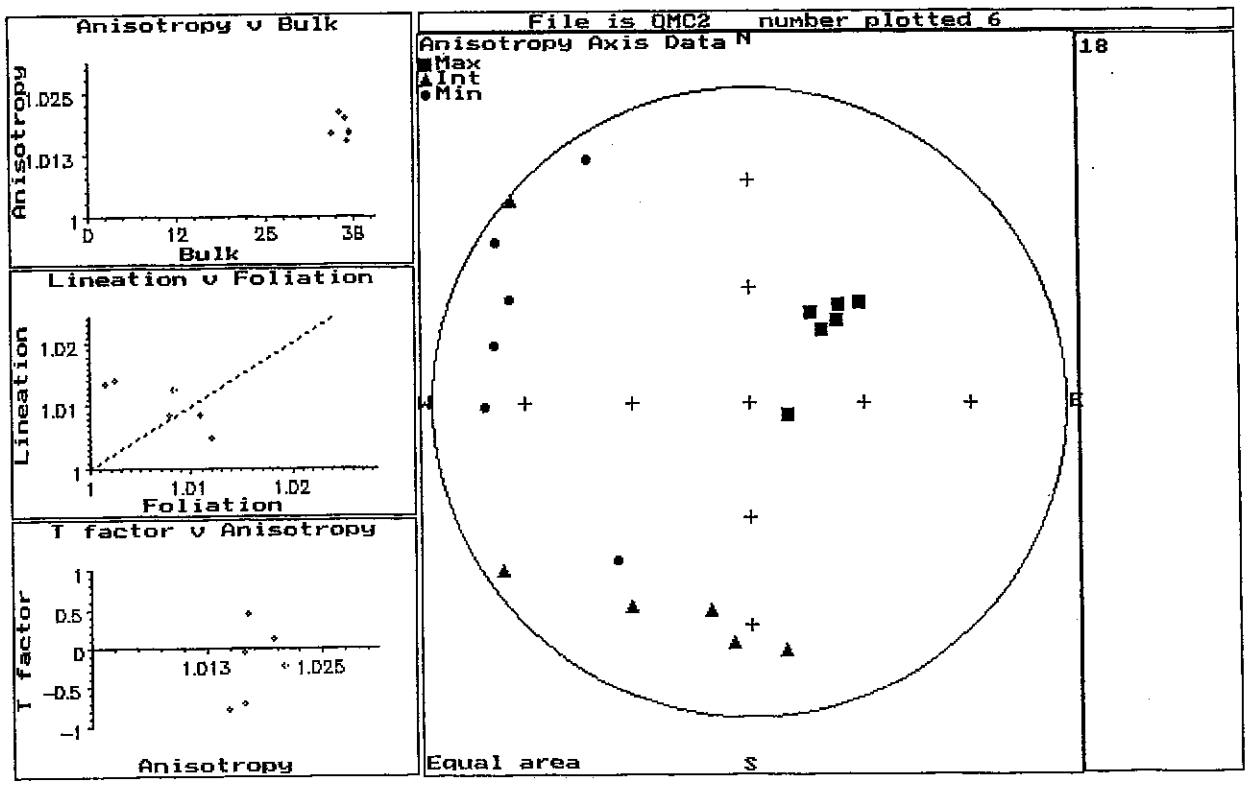
Anisotropy v Bulk
Anisotropy
1.025
1.013
1
0
12
25
38
Bulk
Lineation v Foliation
Lineation
1.02
1.01
1
1
1.01
1.02
Foliation
T factor v Anisotropy
T factor
1
0.5
0
−0.5
−1
1.013
1.025
Anisotropy
File is QMC2 number plotted 6
Anisotropy Axis Data
Max
Int
Min
N
W
E
S
Equal area
18

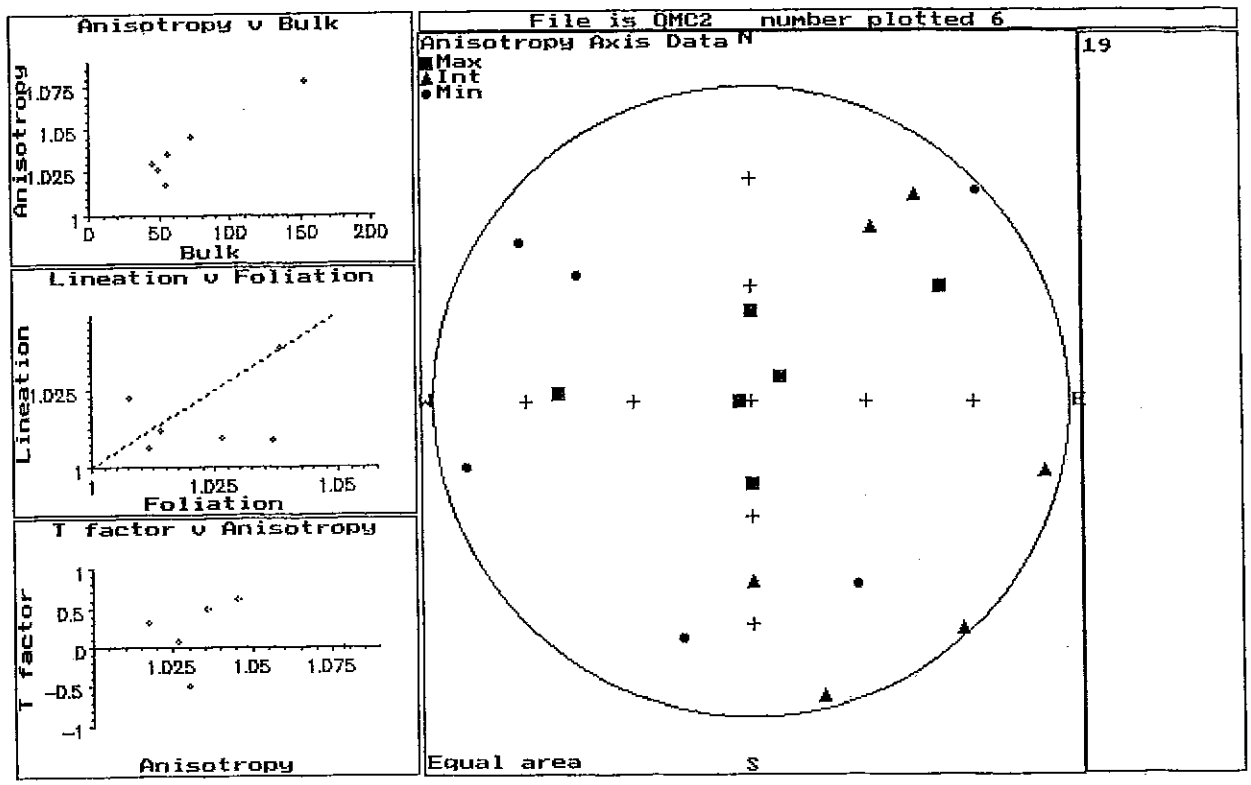
Anisptropy v Bulk
Anisotropy
1.075
1.05
1.025
1
0
50
100
150
200
Bulk
Lineation v Foliation
Lineation
1.025
1
1
1.025
1.05
Foliation
T factor v Anisotropy
T factor
1
0.5
0
−0.5
−1
1.025
1.05
1.075
Anisotropy
File is QMC2 number plotted 6
Anisotropy Axis Data
Max
Int
Min
N
W
E
S
Equal area
19

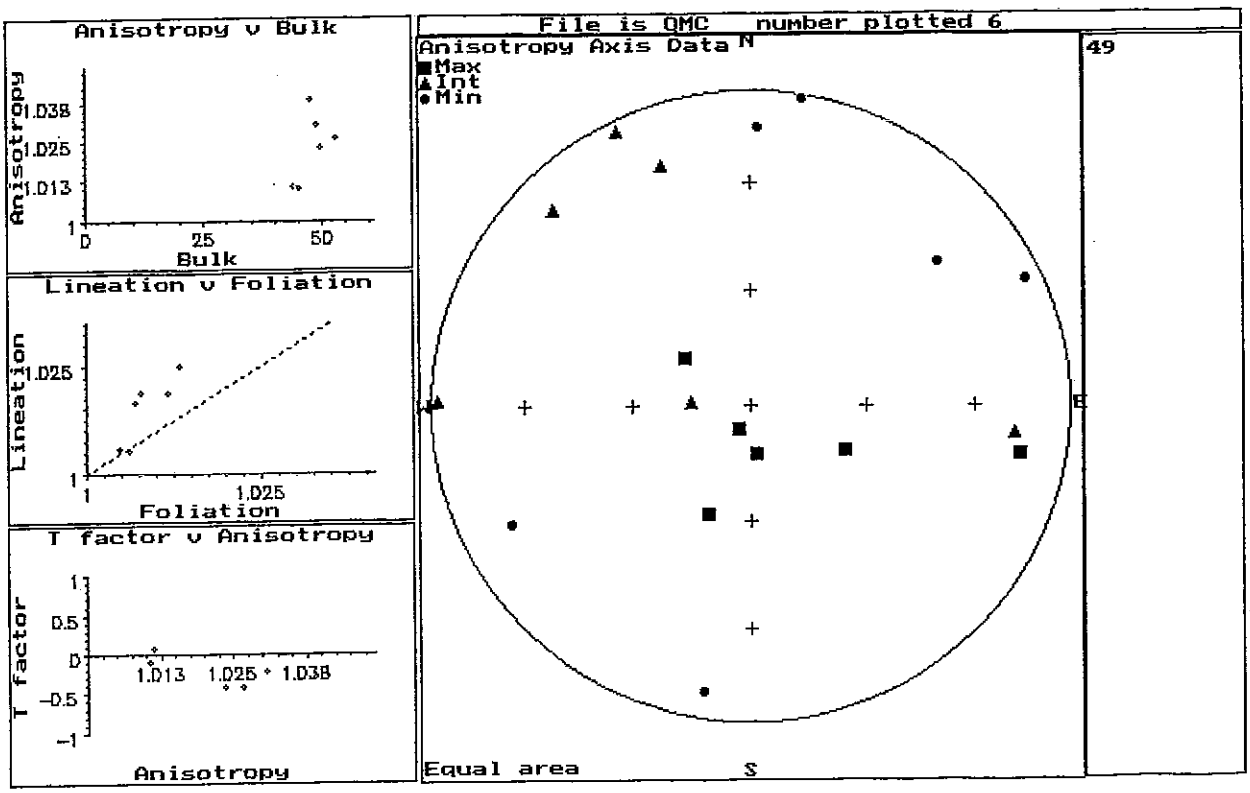
Anisotropy v Bulk
Anisotropy
1.038
1.025
1.013
1
0
25
50
Bulk
Lineation v Foliation
Lineation
1.025
1
1
1.025
Foliation
T factor v Anisotropy
T factor
1
0.5
0
−0.5
−1
1.013
1.025
1.038
Anisotropy
File is QMC number plotted 6
Anisotropy Axis Data
Max
Int
Min
N
E
S
Equal area
49

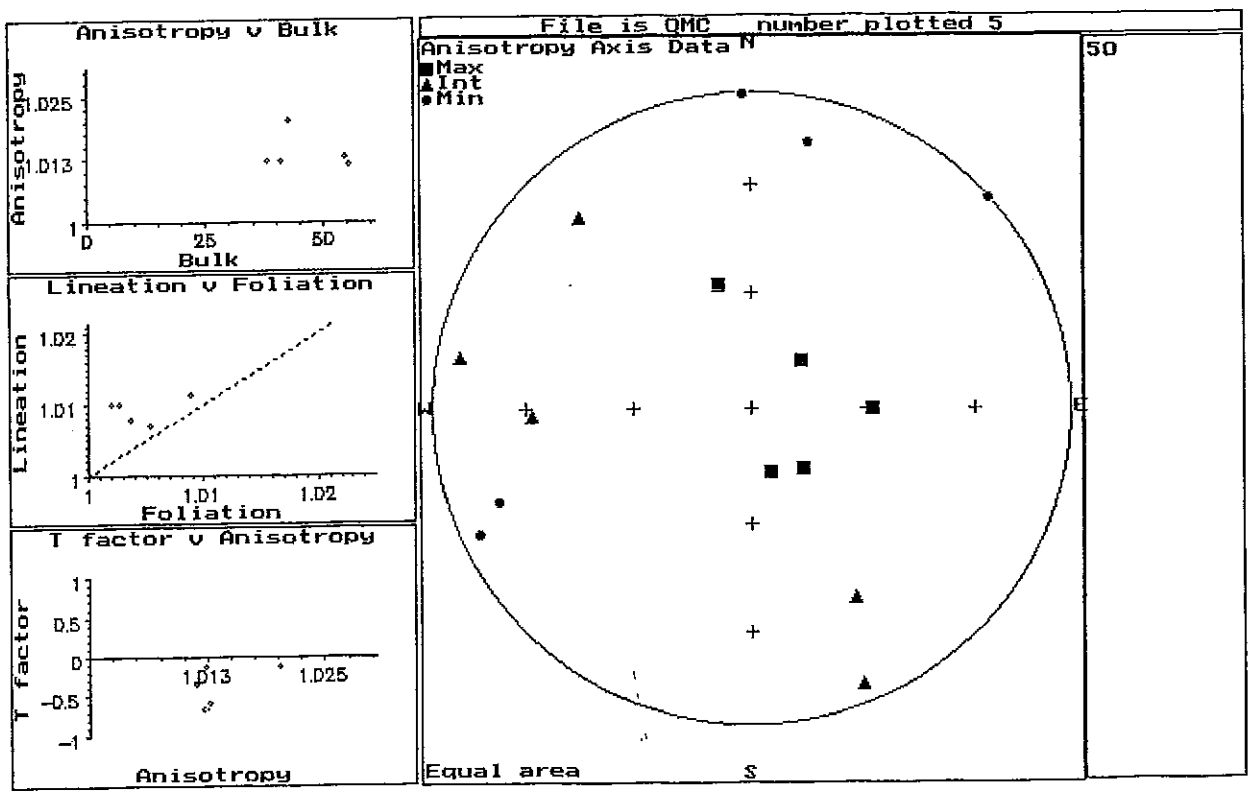
Anisotropy v Bulk
Anisotropy
1.025
1.013
1
0
25
50
Bulk
Lineation v Foliation
Lineation
1.02
1.01
1
1
1.01
1.02
Foliation
T factor v Anisotropy
T factor
1
0.5
0
−0.5
−1
1.013
1.025
Anisotropy
File is QMC number plotted 5
Anisotropy Axis Data
Max
Int
Min
N
E
S
Equal area
50

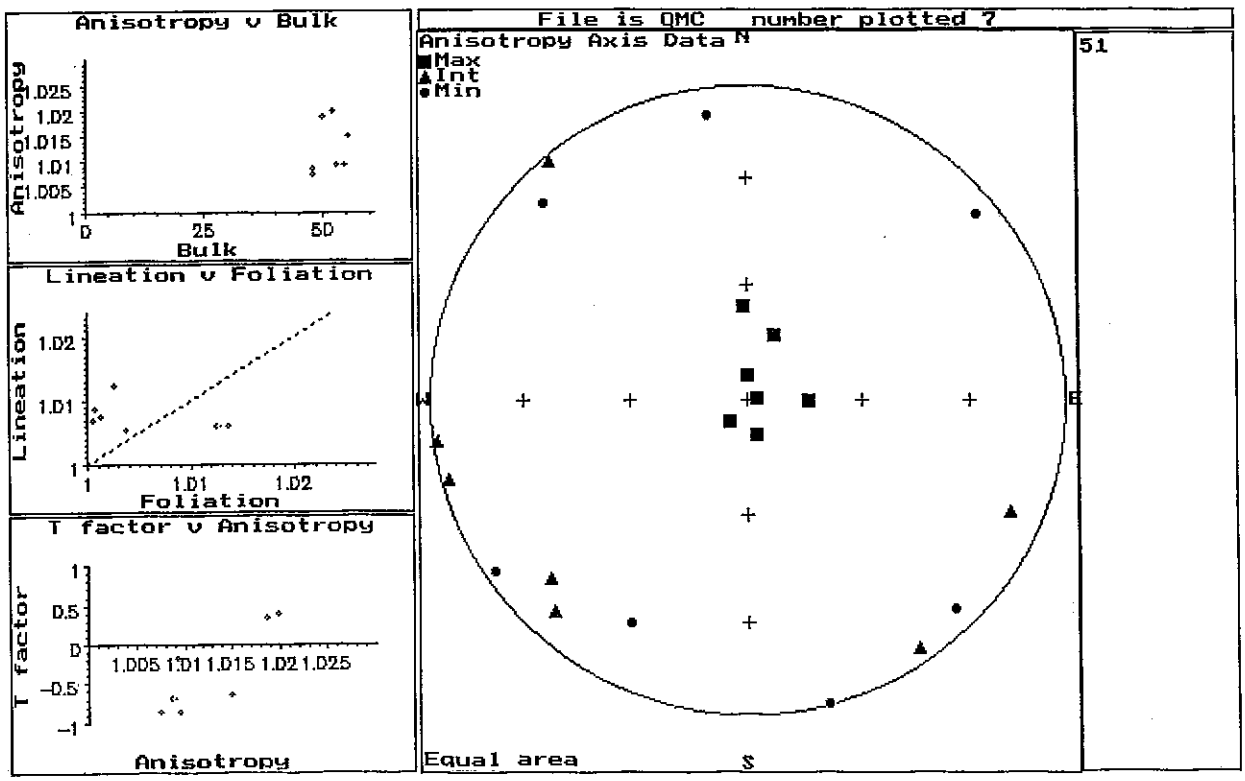
Anisotropy v Bulk
Anisotropy
1.D25
1.D2
1.D15
1.D1
1.DD5
1
D
25
5D
Bulk
Lineation v Foliation
Lineation
1.D2
1.D1
1
1.D1
1.D2
Foliation
T factor v Anisotropy
T factor
1
D.5
D
−D.5
−1
1.DD5 1.D1 1.D15 1.D2 1.D25
Anisotropy
File is QMC number plotted 7
Anisotropy Axis Data
Max
Int
Min
N
W
E
S
Equal area
51

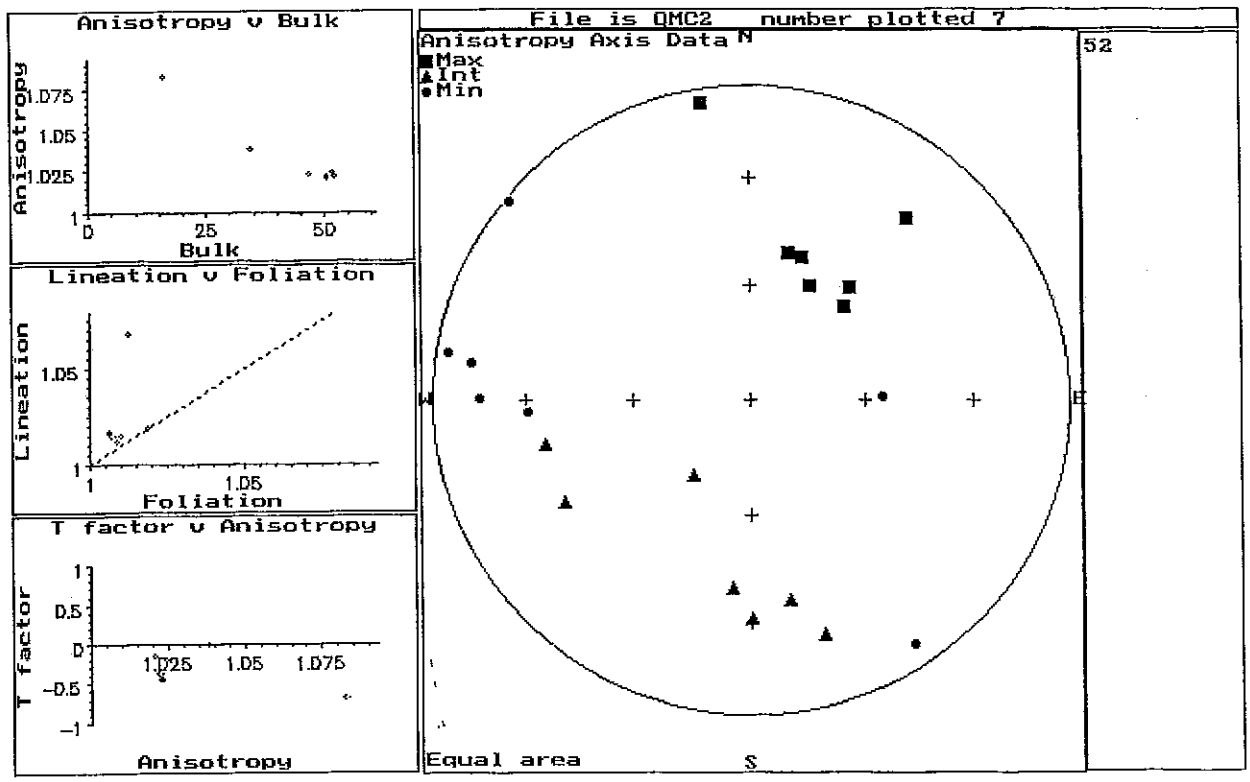
Anisotropy v Bulk
Anisotropy
1.D75
1.D5
1.D25
1
D
25
5D
Bulk
Lineation v Foliation
Lineation
1.D5
1
1
1.D5
Foliation
T factor v Anisotropy
T factor
1
D.5
D
−D.5
−1
1.D25
1.D5
1.D75
Anisotropy
File is QMC2 number plotted 7
Anisotropy Axis Data
Max
Int
Min
N
W
E
S
Equal area
52

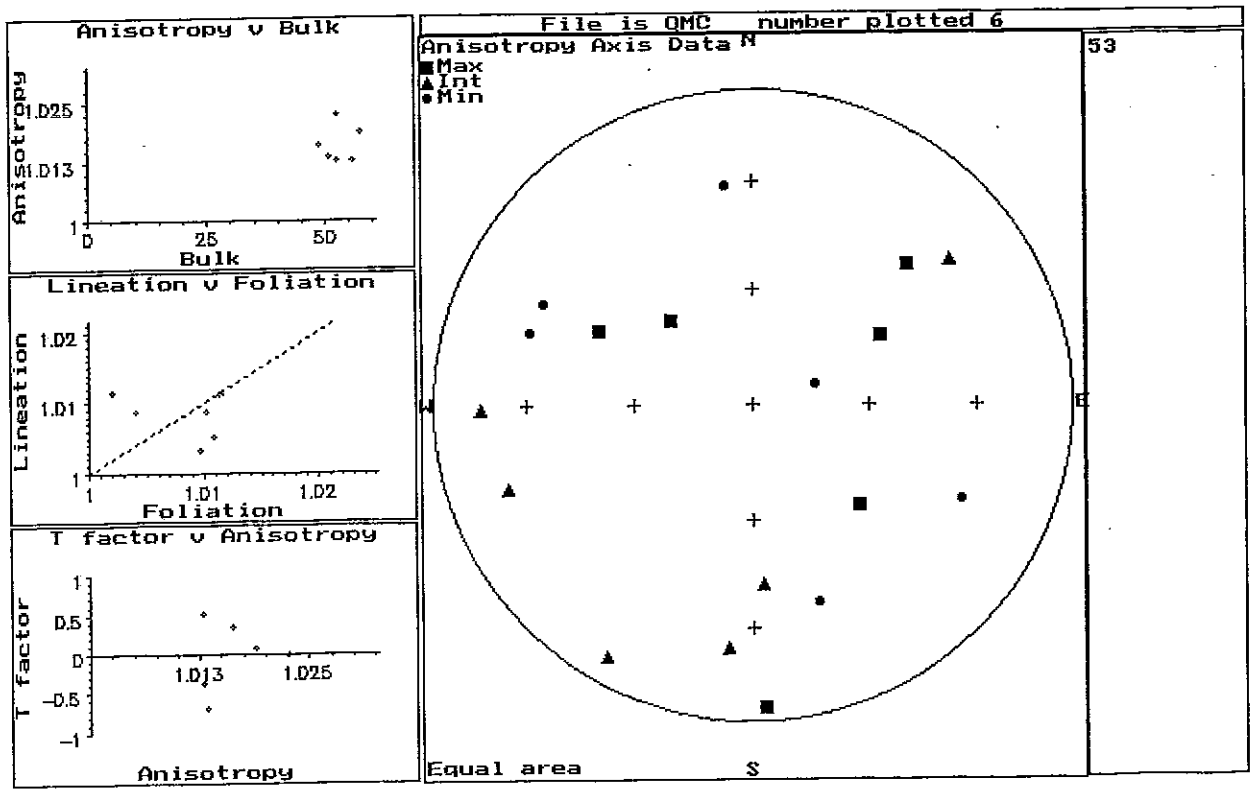
Anisotropy v Bulk
Anisotropy
1.025
1.013
1
0
25
50
Bulk
Lineation v Foliation
Lineation
1.02
1.01
1
1
1.01
1.02
Foliation
T factor v Anisotropy
T factor
1
0.5
0
-0.5
-1
1.013
1.025
Anisotropy
File is QMC number plotted 6
Anisotropy Axis Data
Max
Int
Min
N
W
E
S
Equal area
53

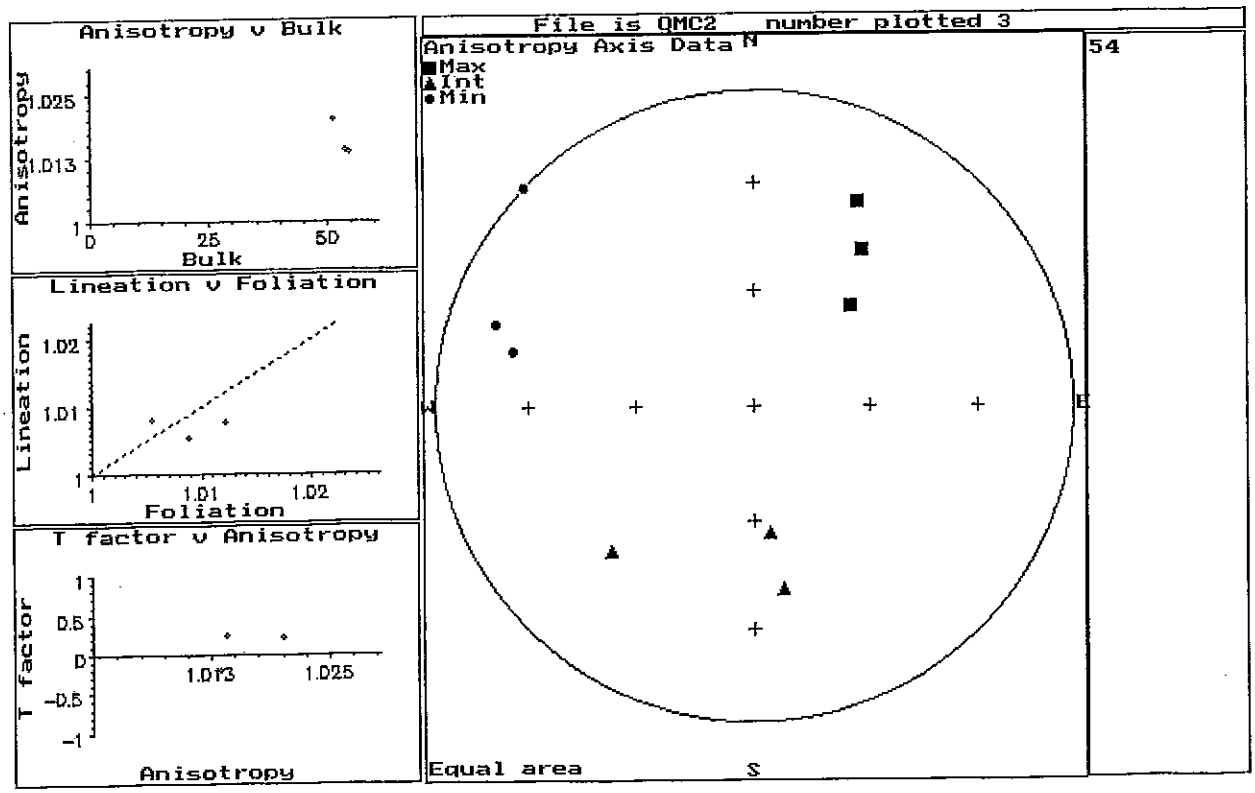
Anisotropy v Bulk
Anisotropy
1.025
1.013
1
0
25
50
Bulk
Lineation v Foliation
Lineation
1.02
1.01
1
1
1.01
1.02
Foliation
T factor v Anisotropy
T factor
1
0.5
0
-0.5
-1
1.013
1.025
Anisotropy
File is QMC2 number plotted 3
Anisotropy Axis Data
Max
Int
Min
N
W
E
S
Equal area
54

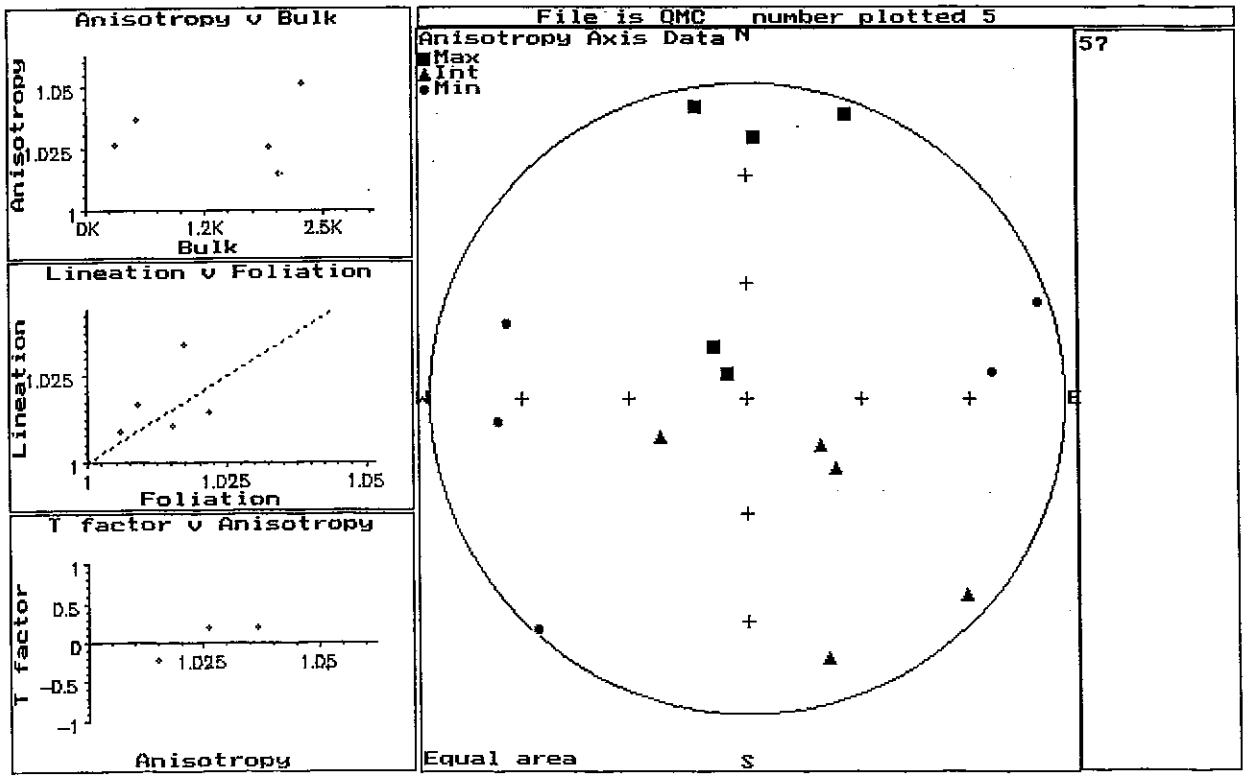
Anisotropy v Bulk
Anisotropy
1.05
1.025
1
DK
1.2K
2.5K
Bulk
Lineation v Foliation
Lineation
1.025
1
1.025
1.05
Foliation
T factor v Anisotropy
T factor
1
0.5
0
-0.5
-1
1.025
1.05
Anisotropy
File is QMC number plotted 5
Anisotropy Axis Data
Max
Int
Min
N
W
E
S
Equal area
57

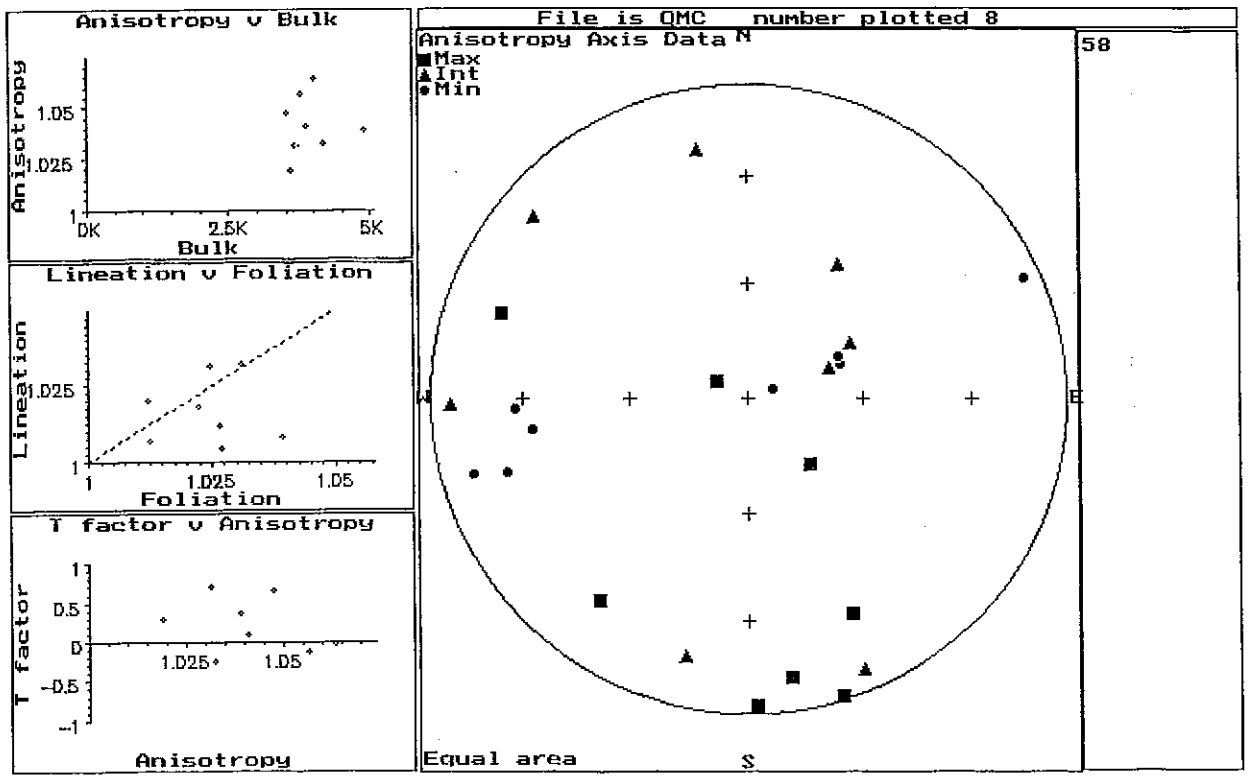
Anisotropy v Bulk
Anisotropy
1.05
1.025
1
DK
2.5K
5K
Bulk
Lineation v Foliation
Lineation
1.025
1
1.025
1.05
Foliation
T factor v Anisotropy
T factor
1
0.5
0
-0.5
-1
1.025
1.05
Anisotropy
File is QMC number plotted 8
Anisotropy Axis Data
Max
Int
Min
N
W
E
S
Equal area
58

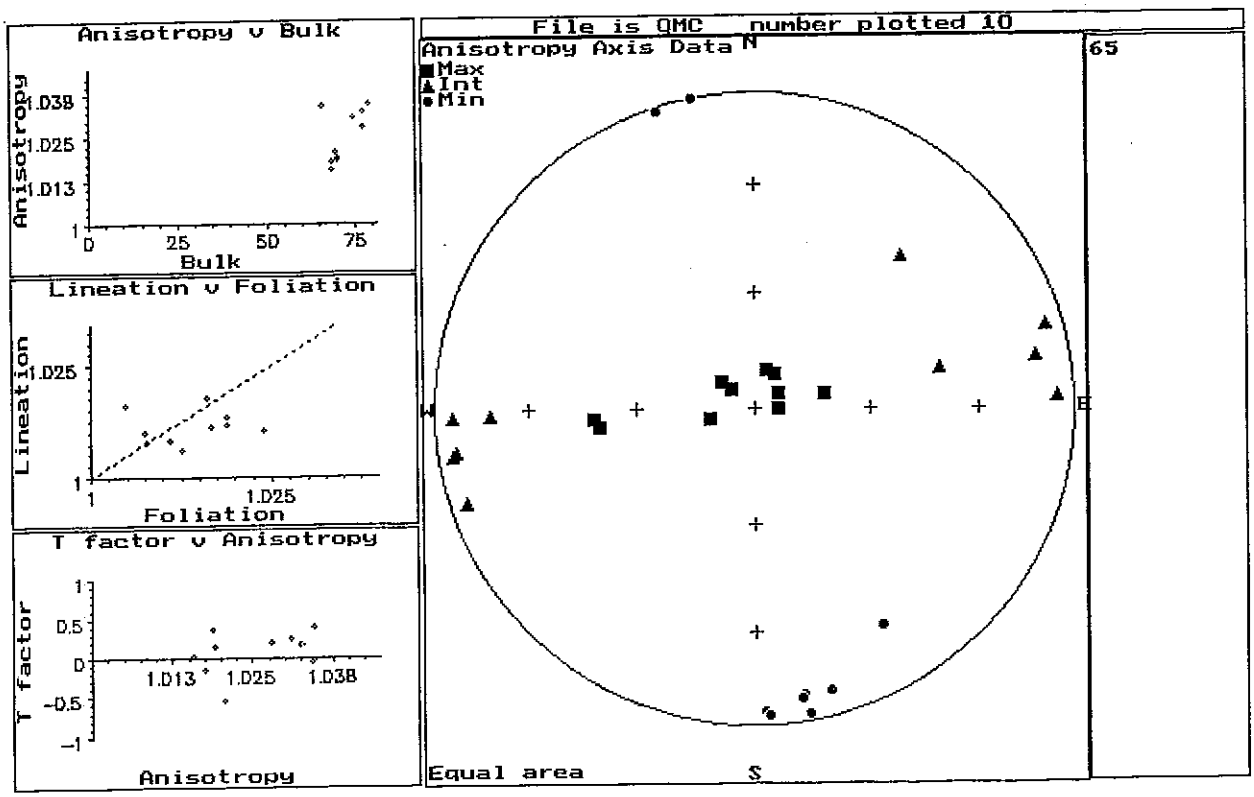
Anisotropy v Bulk
Anisotropy
1.038
1.025
1.013
1
0
25
50
75
Bulk
Lineation v Foliation
Lineation
1.025
1
1
1.025
Foliation
T factor v Anisotropy
T factor
1
0.5
0
-0.5
-1
1.013
1.025
1.038
Anisotropy
File is QMC number plotted 10
Anisotropy Axis Data
Max
Int
Min
N
W
E
S
Equal area
65

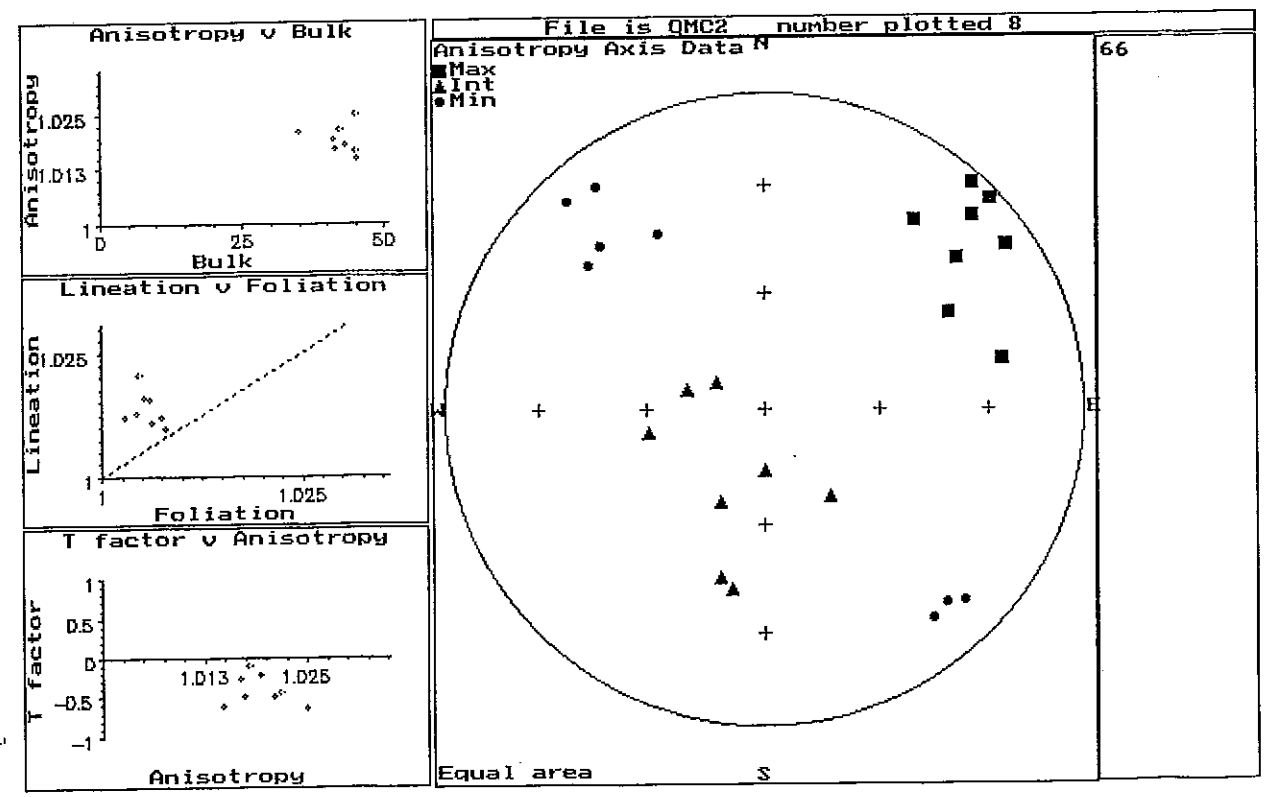
Anisotropy v Bulk
Anisotropy
1.025
1.013
1
0
25
50
Bulk
Lineation v Foliation
Lineation
1.025
1
1
1.025
Foliation
T factor v Anisotropy
T factor
1
0.5
0
-0.5
-1
1.013
1.025
Anisotropy
File is QMC2 number plotted 8
Anisotropy Axis Data
Max
Int
Min
N
W
E
S
Equal area
66

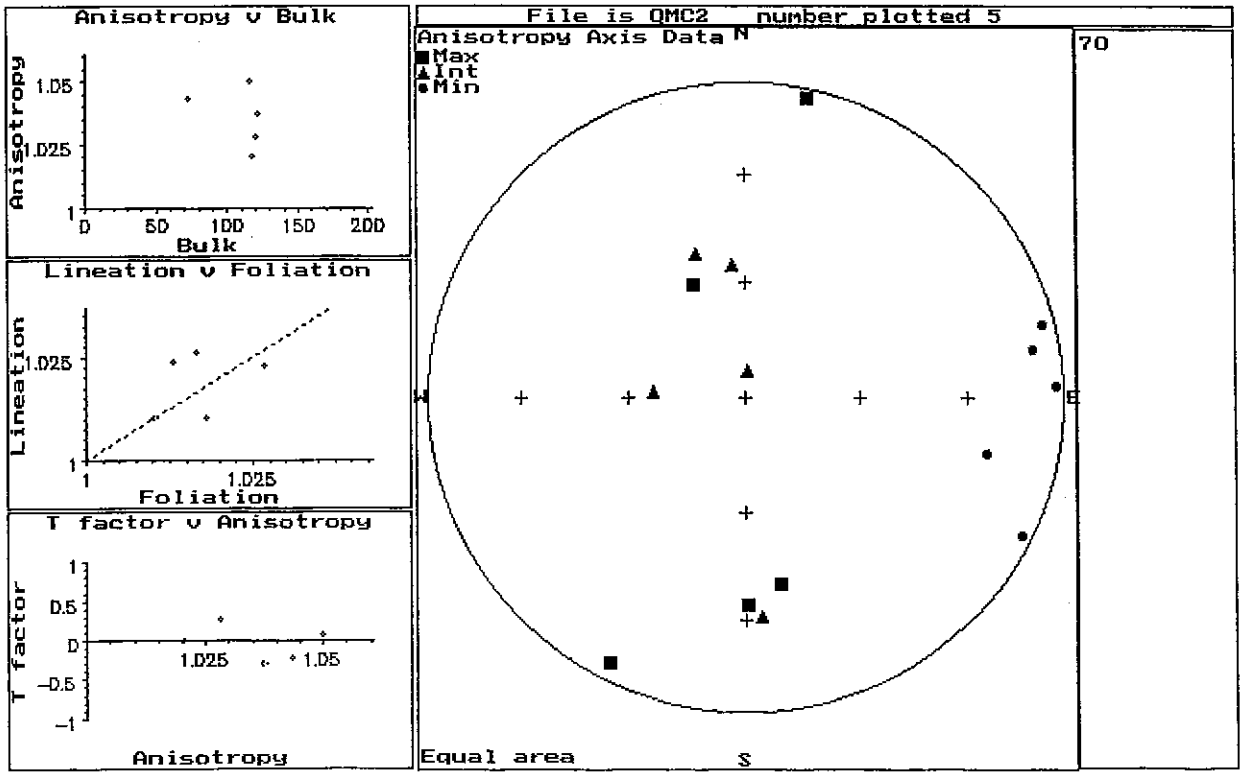
Anisotropy v Bulk
Anisotropy
1.05
1.025
1
0
50
100
150
200
Bulk
Lineation v Foliation
Lineation
1.025
1
1
1.025
Foliation
T factor v Anisotropy
T factor
1
0.5
0
-0.5
-1
1.025
1.05
Anisotropy
File is QMC2 number plotted 5
Anisotropy Axis Data
Max
Int
Min
N
W
E
S
Equal area
70

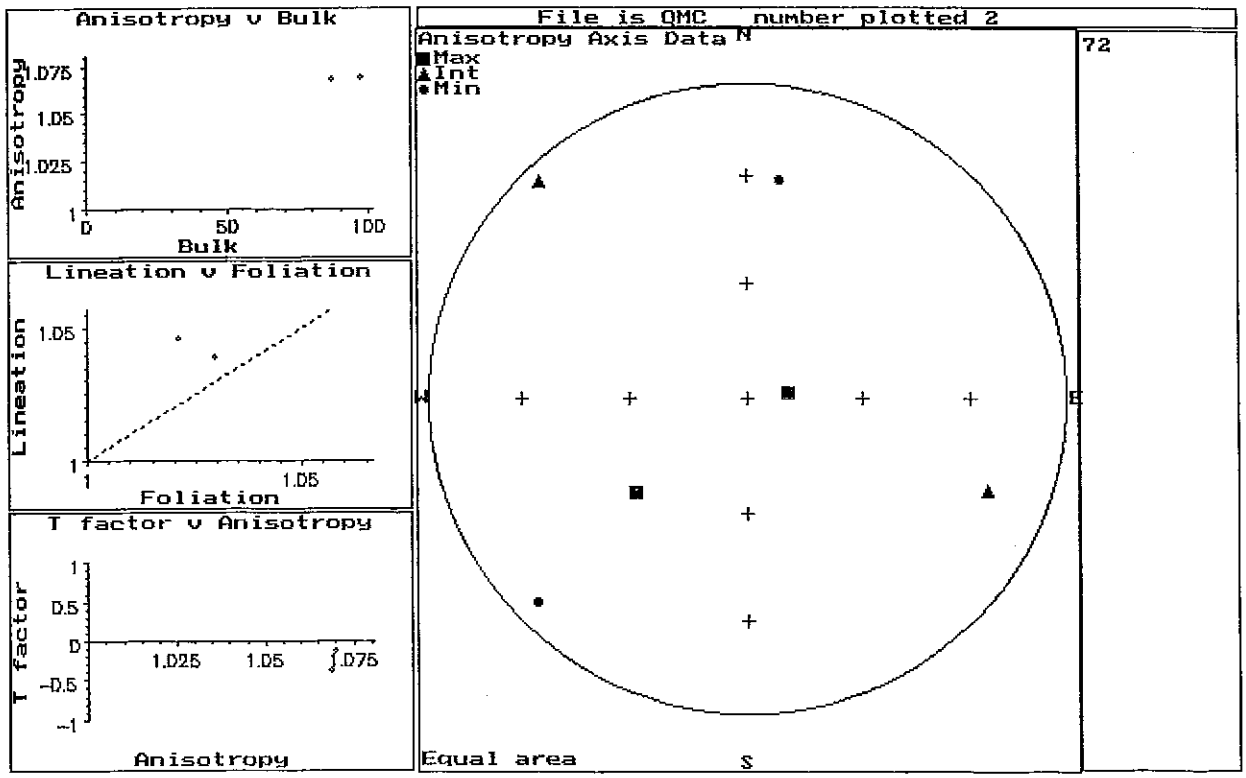
Anisotropy v Bulk
Anisotropy
1.075
1.05
1.025
1
0
50
100
Bulk
Lineation v Foliation
Lineation
1.05
1
1
1.05
Foliation
T factor v Anisotropy
T factor
1
0.5
0
-0.5
-1
1.025
1.05
1.075
Anisotropy
File is QMC number plotted 2
Anisotropy Axis Data
Max
Int
Min
N
W
E
S
Equal area
72

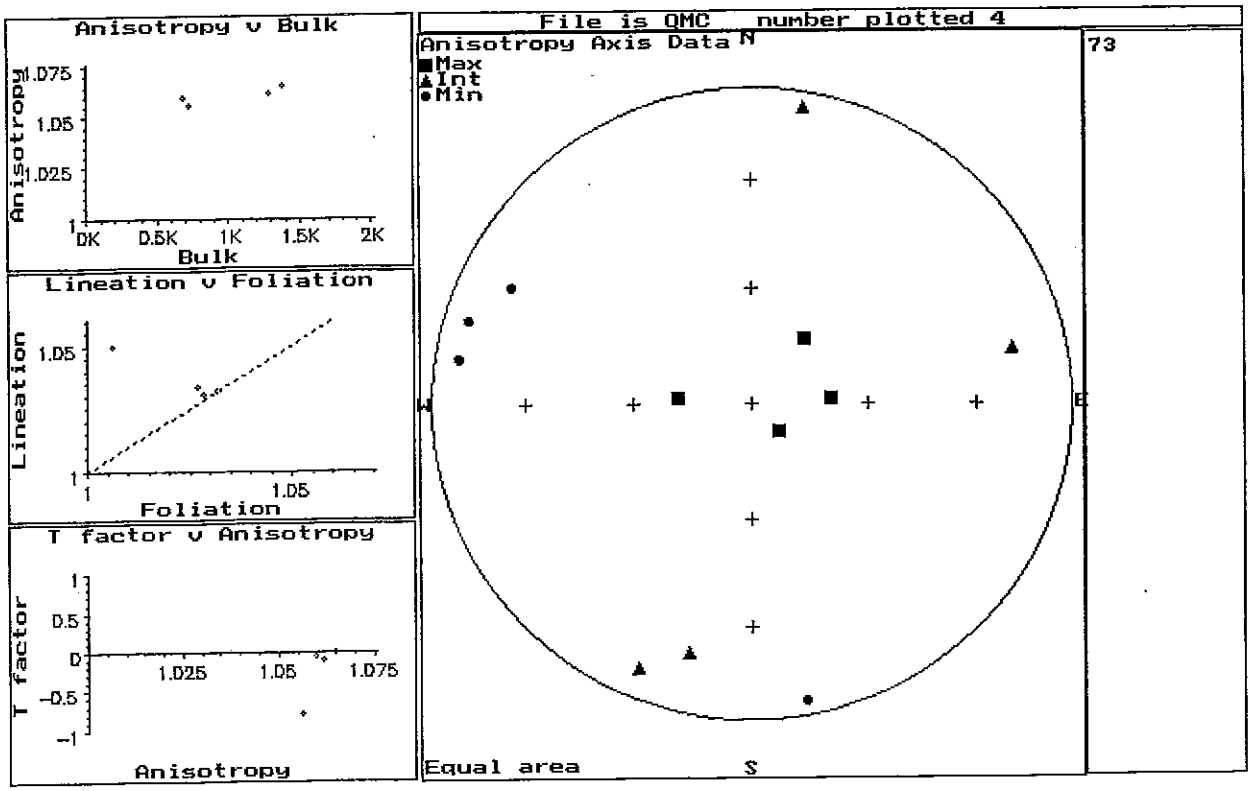
Anisotropy v Bulk
Anisotropy
1.075
1.05
1.025
1
0K
0.5K
1K
1.5K
2K
Bulk
Lineation v Foliation
Lineation
1.05
1
1
1.05
Foliation
T factor v Anisotropy
T factor
1
0.5
0
-0.5
-1
1.025
1.05
1.075
Anisotropy
File is QMC number plotted 4
Anisotropy Axis Data
Max
Int
Min
N
W
E
S
Equal area
73

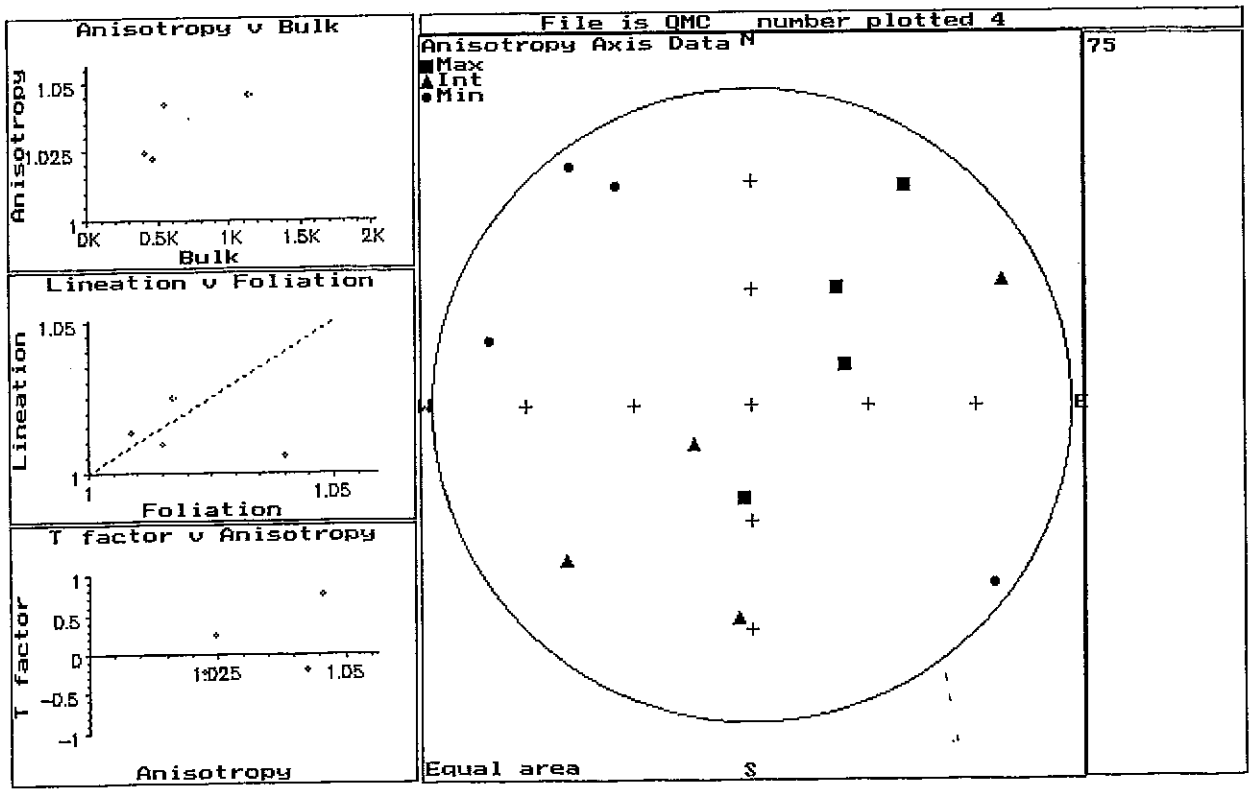
Anisotropy v Bulk
Anisotropy
1.05
1.025
1
0K
0.5K
1K
1.5K
2K
Bulk
Lineation v Foliation
Lineation
1.05
1
1
1.05
Foliation
T factor v Anisotropy
T factor
1
0.5
0
-0.5
-1
1.025
1.05
Anisotropy
File is QMC number plotted 4
Anisotropy Axis Data
Max
Int
Min
N
W
E
S
Equal area
75

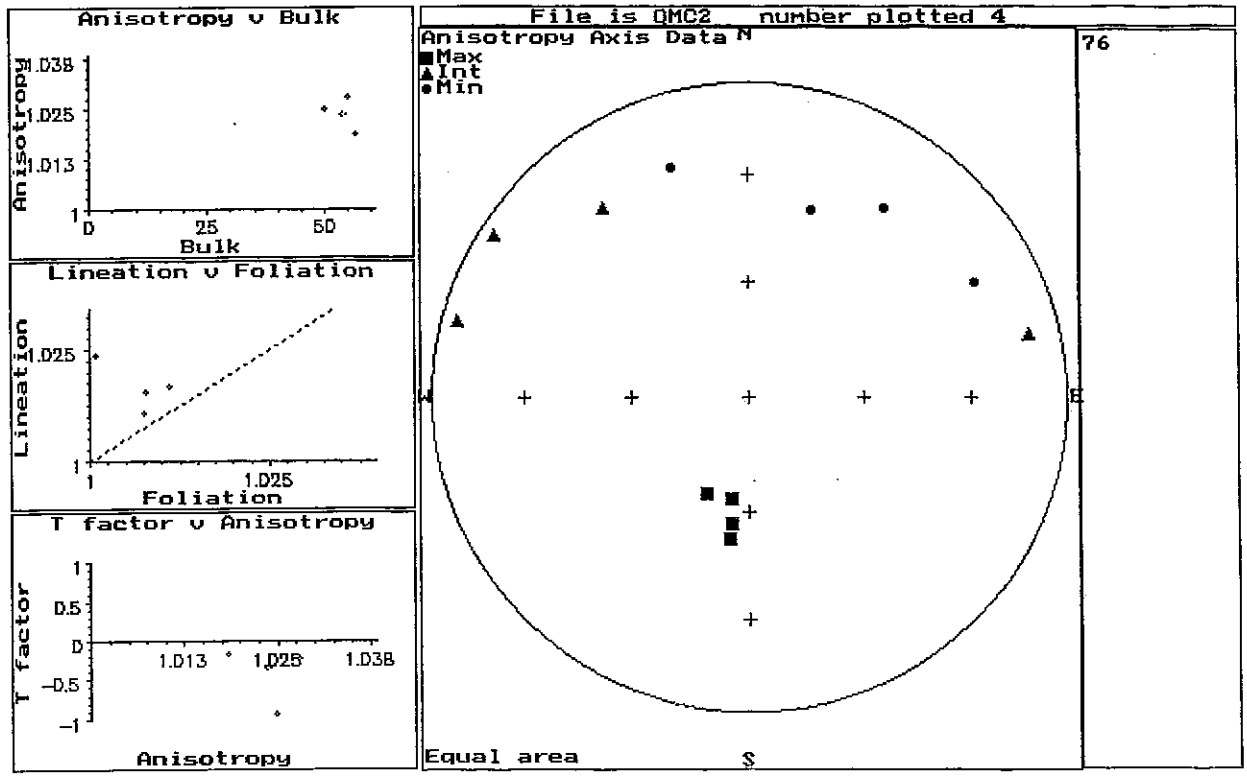
Anisotropy v Bulk
Anisotropy
1.038
1.025
1.013
1
D
25
50
Bulk
Lineation v Foliation
Lineation
1.025
1
1
1.025
Foliation
T factor v Anisotropy
T factor
1
0.5
0
−0.5
−1
1.013
1.025
1.038
Anisotropy
File is QMC2 number plotted 4
Anisotropy Axis Data
Max
Int
Min
N
E
S
Equal area
76

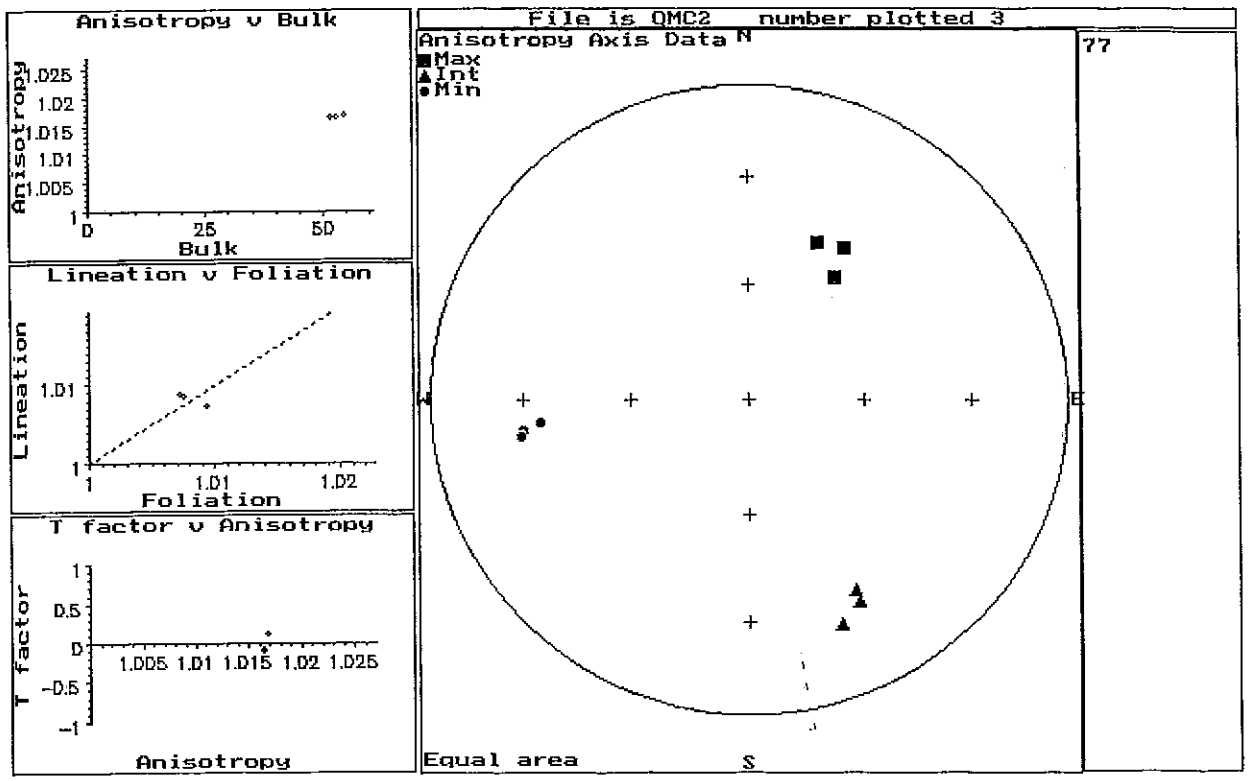
Anisotropy v Bulk
Anisotropy
1.025
1.02
1.015
1.01
1.005
1
D
25
50
Bulk
Lineation v Foliation
Lineation
1.01
1
1
1.01
1.02
Foliation
T factor v Anisotropy
T factor
1
0.5
0
−0.5
−1
1.005
1.01
1.015
1.02
1.025
Anisotropy
File is QMC2 number plotted 3
Anisotropy Axis Data
Max
Int
Min
N
E
S
Equal area
77

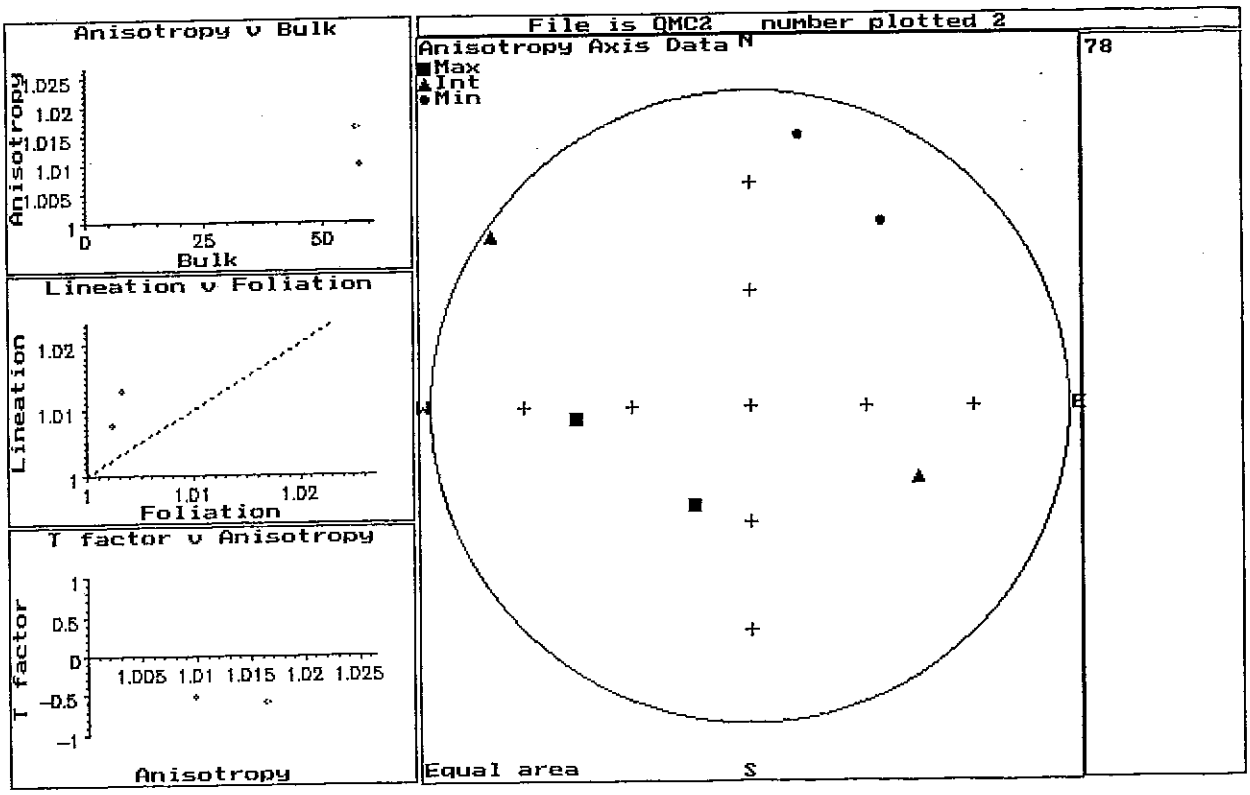
Anisotropy v Bulk
Anisotropy
1.025
1.02
1.015
1.01
1.005
1
0
25
50
Bulk
Lineation v Foliation
Lineation
1.02
1.01
1
1
1.01
1.02
Foliation
T factor v Anisotropy
T factor
1
0.5
0
−0.5
−1
1.005 1.01 1.015 1.02 1.025
Anisotropy
File is QMC2 number plotted 2
Anisotropy Axis Data
Max
Int
Min
N
W
E
S
Equal area
78

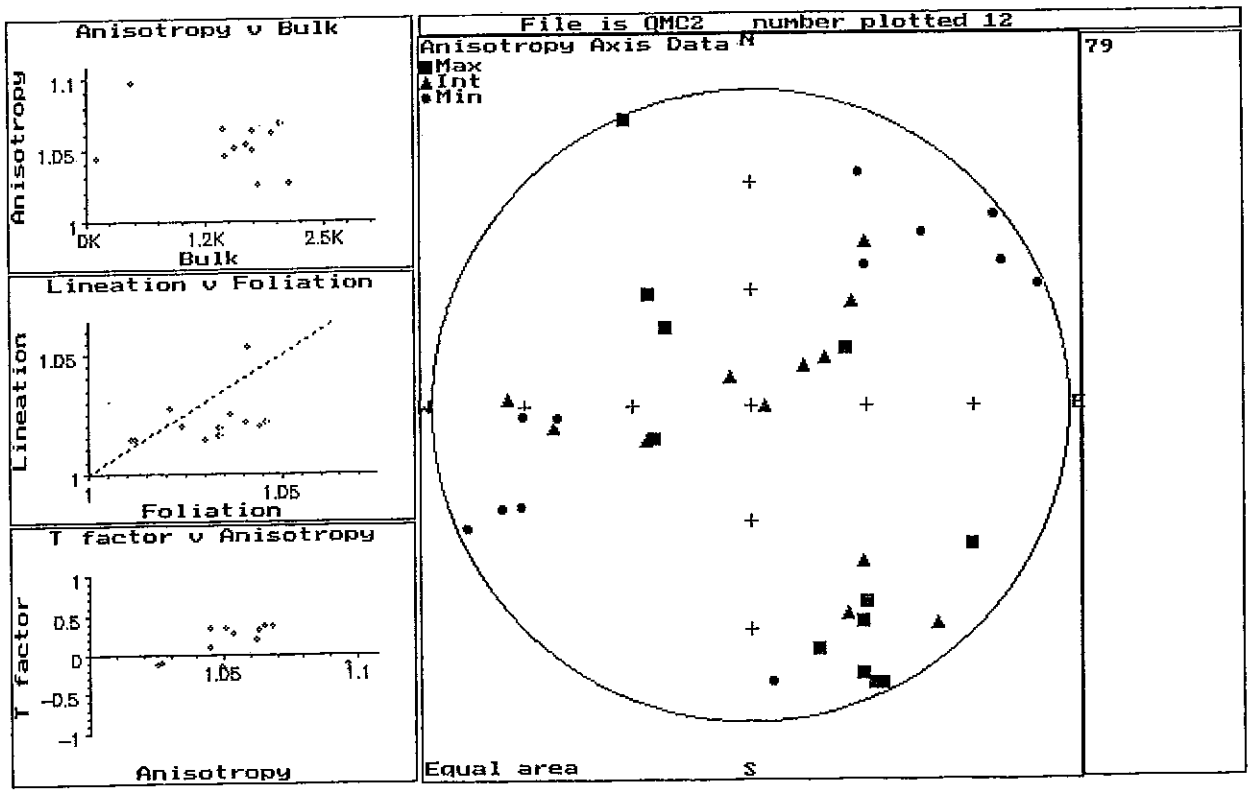
Anisotropy v Bulk
Anisotropy
1.1
1.05
1
0K
1.2K
2.5K
Bulk
Lineation v Foliation
Lineation
1.05
1
1
1.05
Foliation
T factor v Anisotropy
T factor
1
0.5
0
−0.5
−1
1.05
1.1
Anisotropy
File is QMC2 number plotted 12
Anisotropy Axis Data
Max
Int
Min
N
W
E
S
Equal area
79

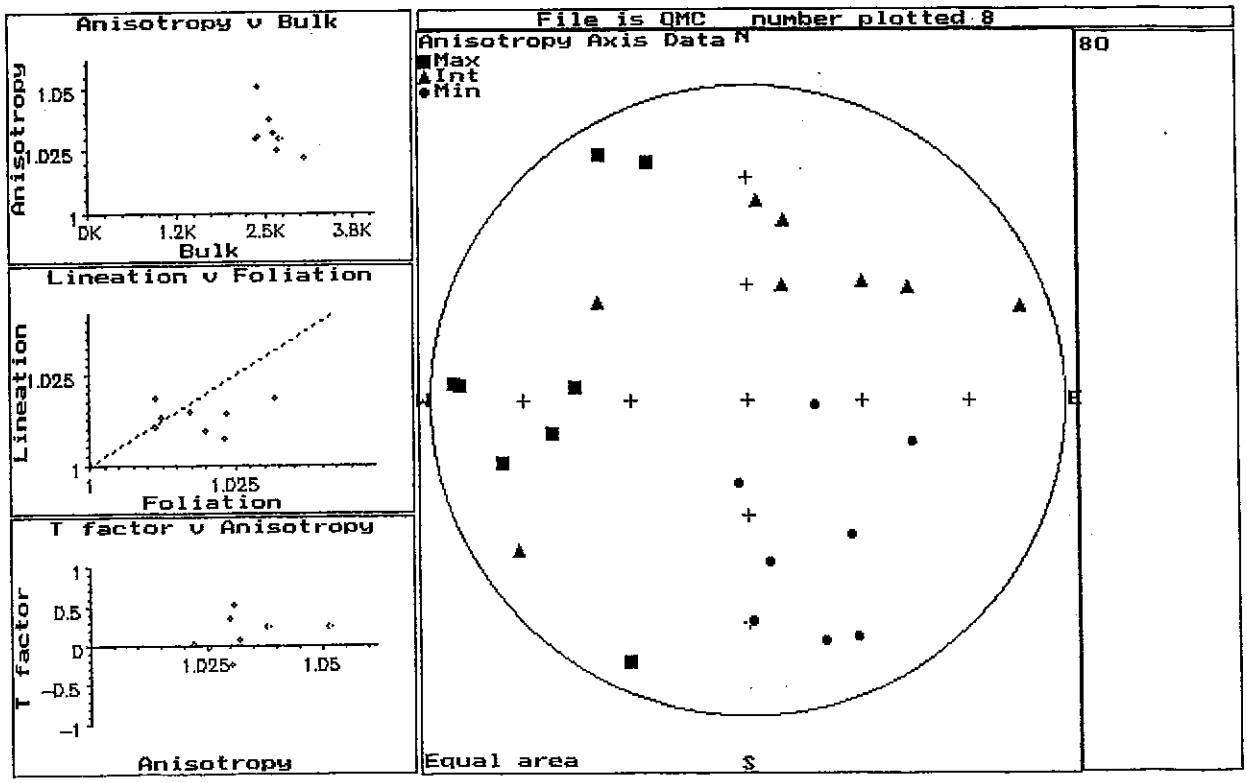
Anisotropy v Bulk
Anisotropy
1.05
1.025
1
DK
1.2K
2.5K
3.8K
Bulk
Lineation v Foliation
Lineation
1.025
1
1
1.025
Foliation
T factor v Anisotropy
T factor
1
0.5
0
-0.5
-1
1.025
1.05
Anisotropy
File is QMC number plotted 8
Anisotropy Axis Data
Max
Int
Min
N
W
E
S
Equal area
80

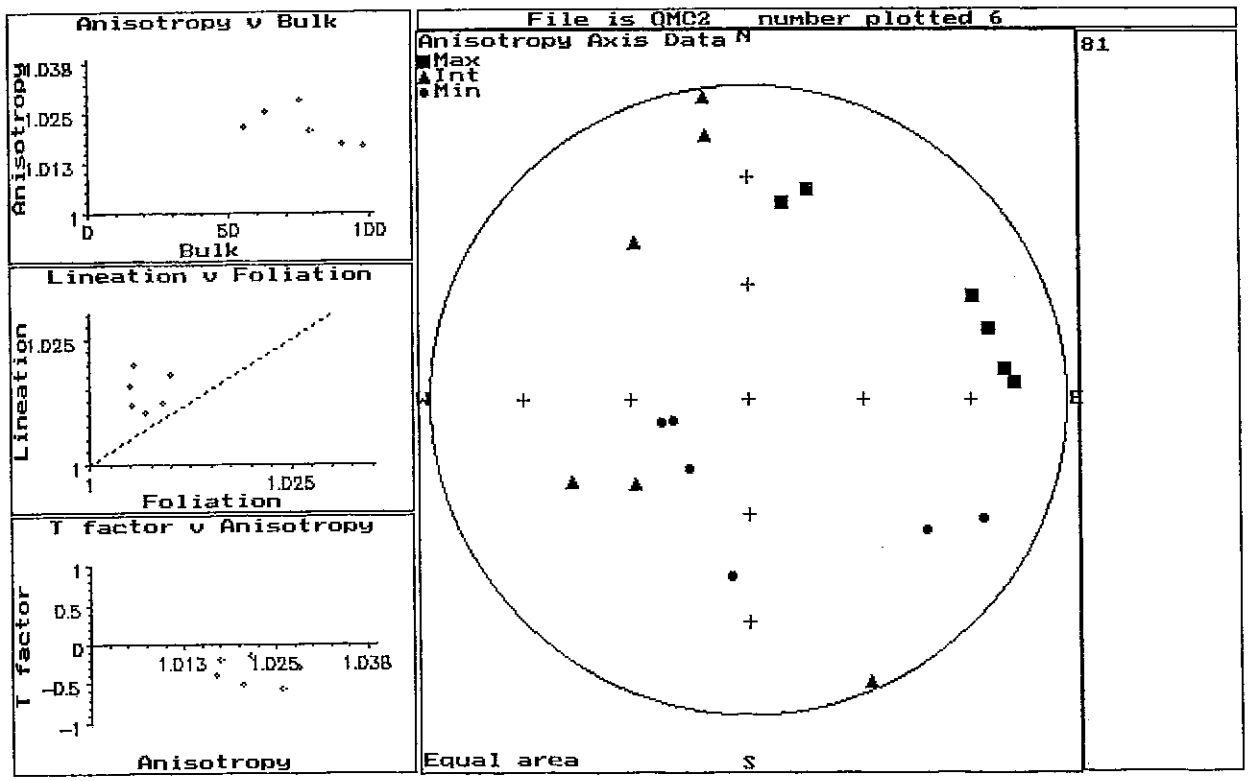
Anisotropy v Bulk
Anisotropy
1.038
1.025
1.013
1
D
5D
1DD
Bulk
Lineation v Foliation
Lineation
1.025
1
1
1.025
Foliation
T factor v Anisotropy
T factor
1
0.5
0
-0.5
-1
1.013
1.025
1.038
Anisotropy
File is QMC2 number plotted 6
Anisotropy Axis Data
Max
Int
Min
N
W
E
S
Equal area
81

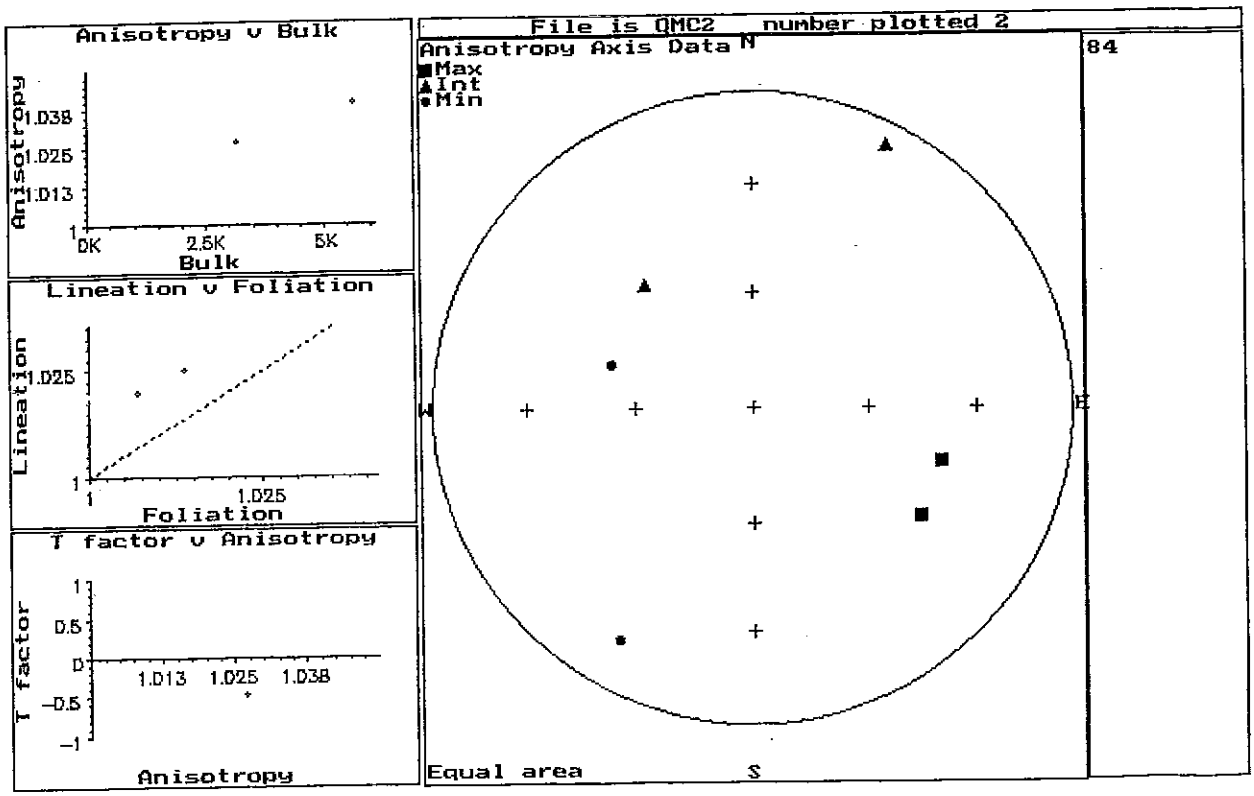
Anisotropy v Bulk
Anisotropy
1.038
1.025
1.013
1
0K
2.5K
5K
Bulk
Lineation v Foliation
Lineation
1.025
1
1
1.025
Foliation
T factor v Anisotropy
T factor
1
0.5
0
-0.5
-1
1.013
1.025
1.038
Anisotropy
File is QMC2 number plotted 2
Anisotropy Axis Data N
Max
Int
Min
84
W
E
Equal area
S

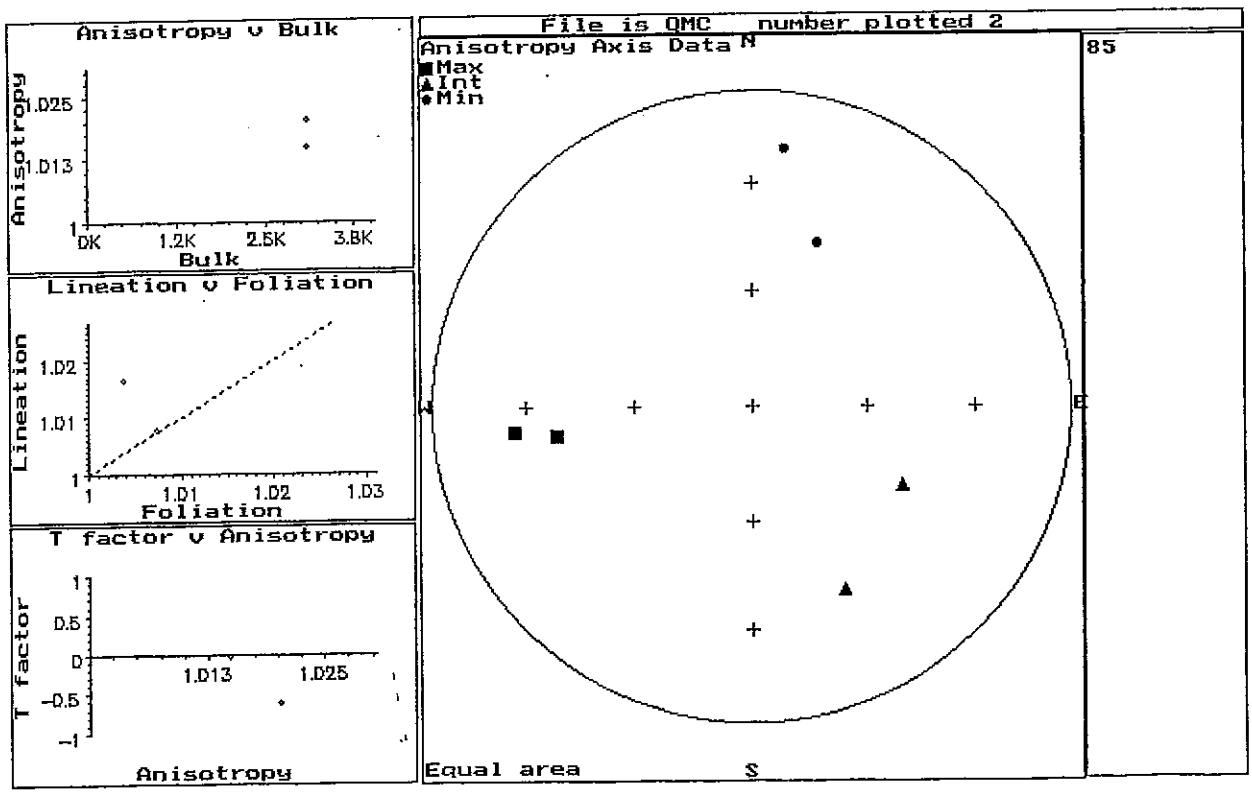
Anisotropy v Bulk
Anisotropy
1.025
1.013
1
0K
1.2K
2.5K
3.8K
Bulk
Lineation v Foliation
Lineation
1.02
1.01
1
1
1.01
1.02
1.03
Foliation
T factor v Anisotropy
T factor
1
0.5
0
-0.5
-1
1.013
1.025
Anisotropy
File is QMC number plotted 2
Anisotropy Axis Data N
Max
Int
Min
85
W
E
Equal area
S

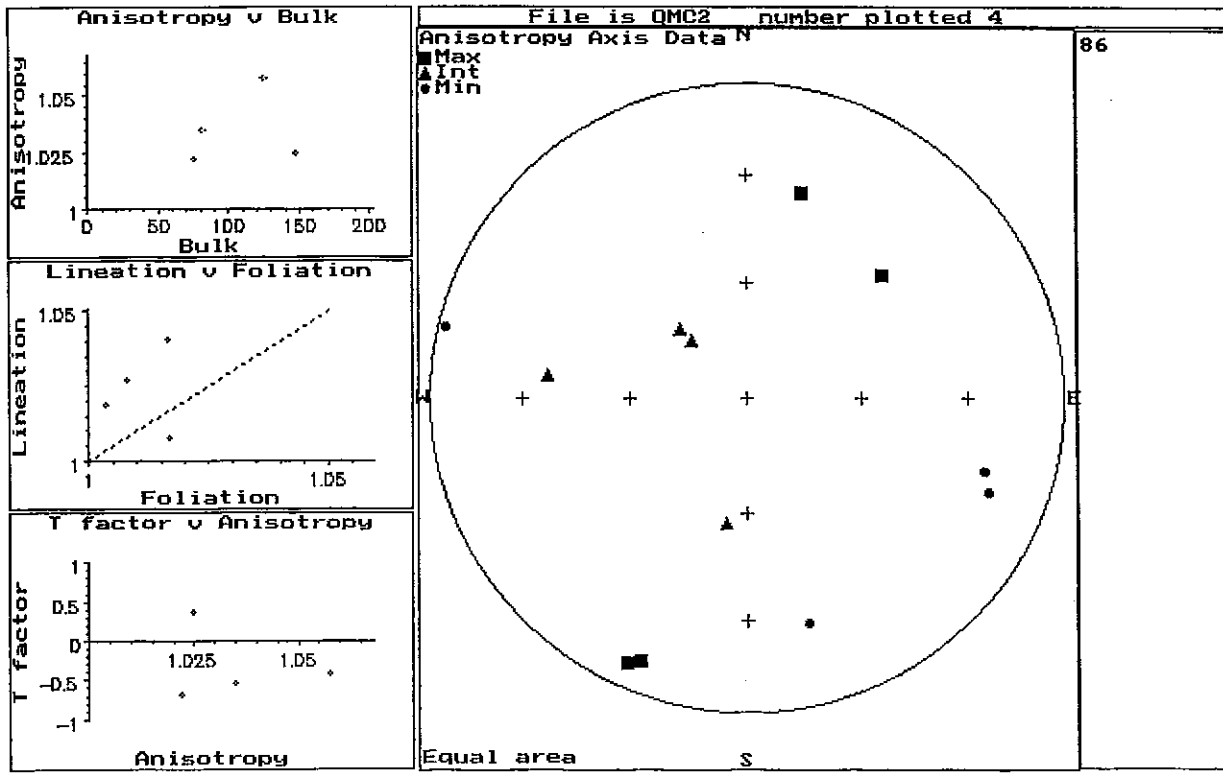
Anisotropy v Bulk
Anisotropy
1.05
1.025
1
0
50
100
150
200
Bulk
Lineation v Foliation
Lineation
1.05
1
1
1.05
Foliation
T factor v Anisotropy
T factor
1
0.5
0
-0.5
-1
1.025
1.05
Anisotropy
File is QMC2 number plotted 4
Anisotropy Axis Data
Max
Int
Min
N
E
S
Equal area
86

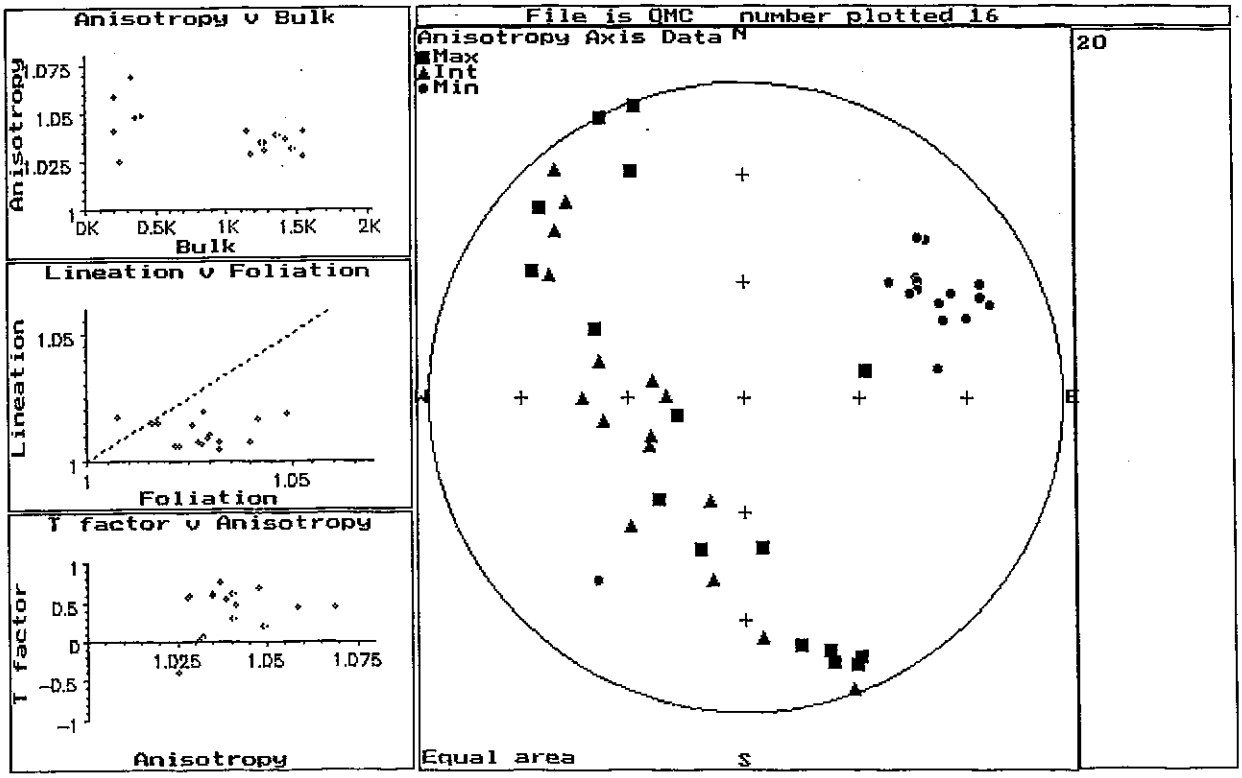
Anisotropy v Bulk
Anisotropy
1.075
1.05
1.025
1
0K
0.5K
1K
1.5K
2K
Bulk
Lineation v Foliation
Lineation
1.05
1
1
1.05
Foliation
T factor v Anisotropy
T factor
1
0.5
0
−0.5
−1
1.025
1.05
1.075
Anisotropy
File is QMC number plotted 16
Anisotropy Axis Data
Max
Int
Min
N
E
S
Equal area
20

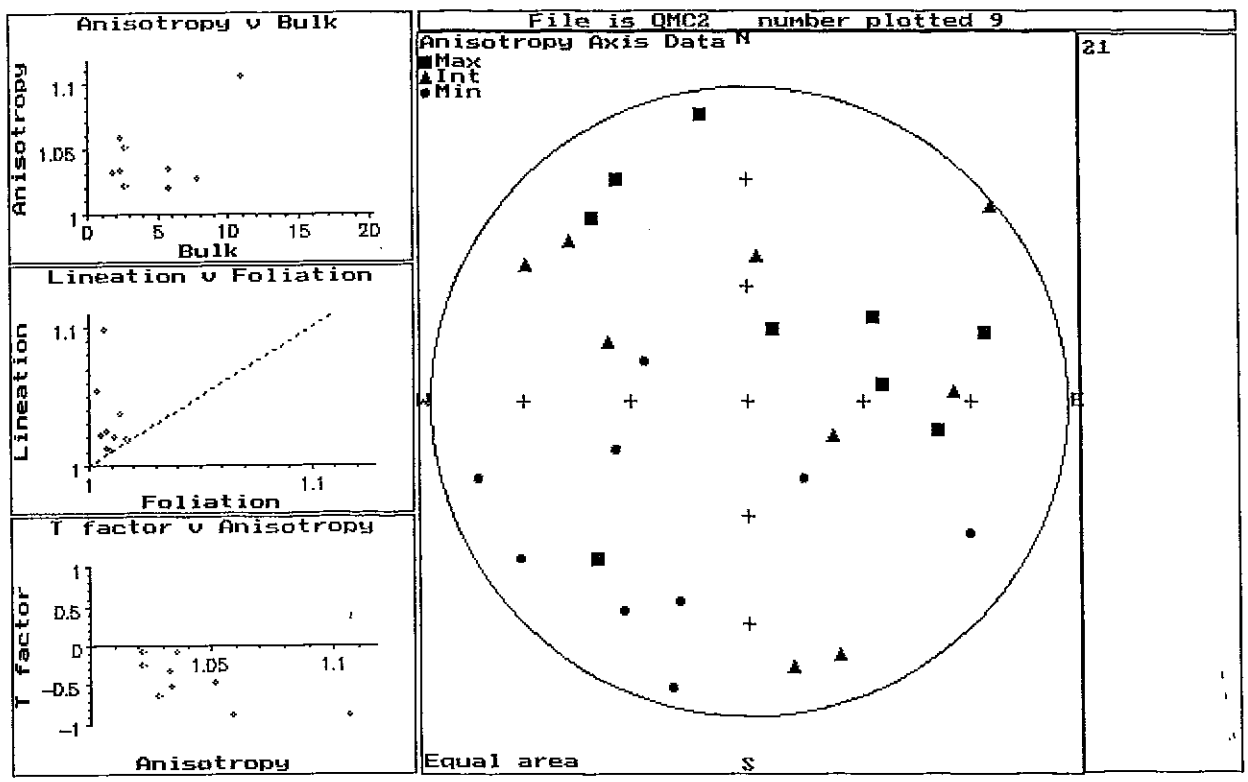
Anisotropy v Bulk
Anisotropy
1.1
1.05
1
0
5
10
15
20
Bulk
Lineation v Foliation
Lineation
1.1
1
1
1.1
Foliation
T factor v Anisotropy
T factor
1
0.5
0
−0.5
−1
1.05
1.1
Anisotropy
File is QMC2 number plotted 9
Anisotropy Axis Data
Max
Int
Min
N
E
S
Equal area
21

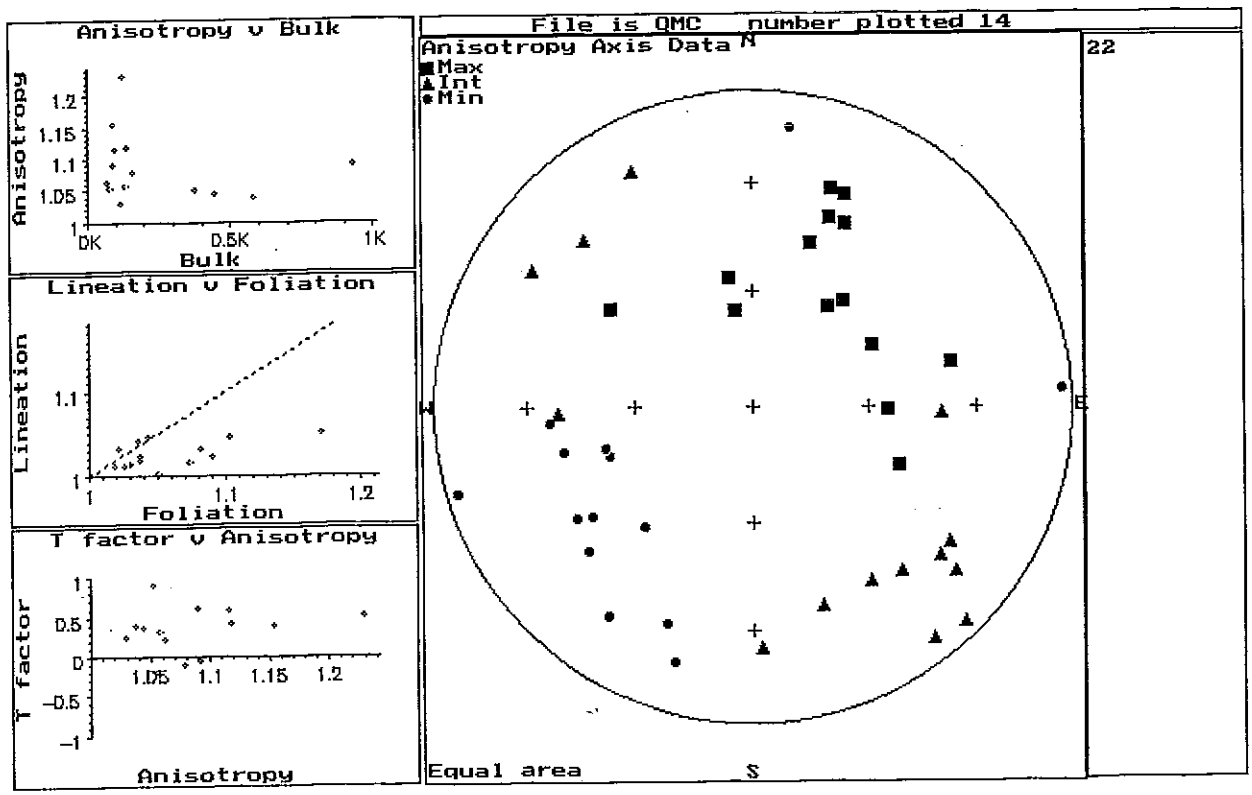
Anisotropy v Bulk
Anisotropy
1.2
1.15
1.1
1.05
1
0K
0.5K
1K
Bulk
Lineation v Foliation
Lineation
1.1
1
1
1.1
1.2
Foliation
T factor v Anisotropy
T factor
1
0.5
0
-0.5
-1
1.05
1.1
1.15
1.2
Anisotropy
File is QMC number plotted 14
Anisotropy Axis Data
Max
Int
Min
N
W
E
S
Equal area
22

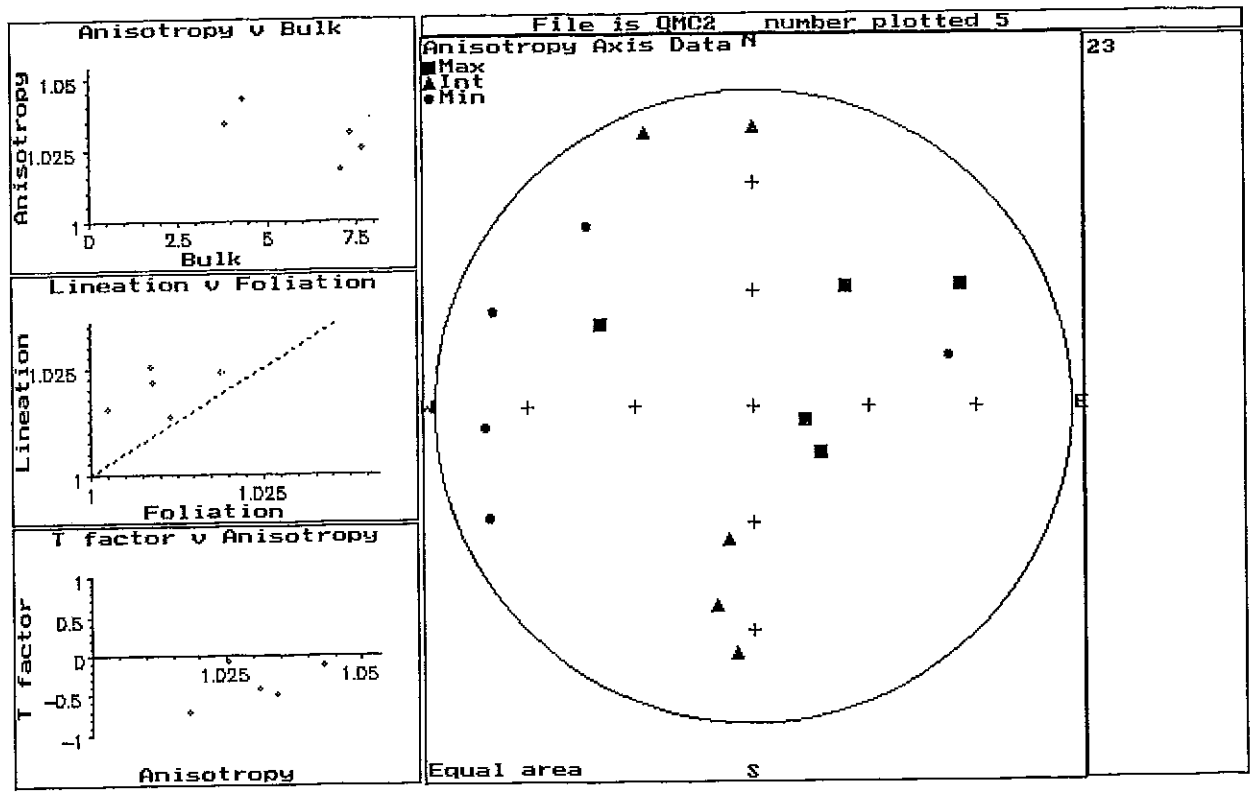
Anisotropy v Bulk
Anisotropy
1.05
1.025
1
0
2.5
5
7.5
Bulk
Lineation v Foliation
Lineation
1.025
1
1
1.025
Foliation
T factor v Anisotropy
T factor
1
0.5
0
-0.5
-1
1.025
1.05
Anisotropy
File is QMC2 number plotted 5
Anisotropy Axis Data
Max
Int
Min
N
W
E
S
Equal area
23

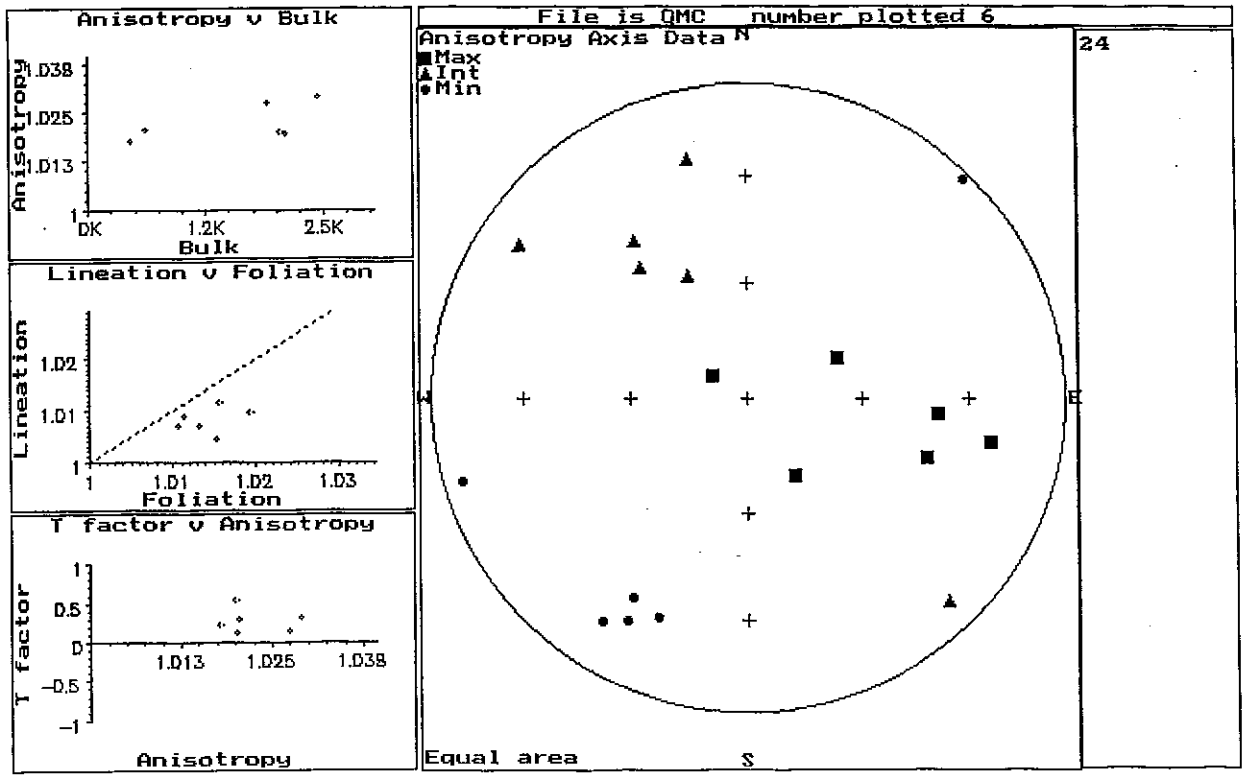
Anisotropy v Bulk
Anisotropy
1.038
1.025
1.013
1
DK
1.2K
2.5K
Bulk
Lineation v Foliation
Lineation
1.02
1.01
1
1
1.01
1.02
1.03
Foliation
T factor v Anisotropy
T factor
1
0.5
0
-0.5
-1
1.013
1.025
1.038
Anisotropy
File is QMC number plotted 6
Anisotropy Axis Data
Max
Int
Min
N
W
E
S
Equal area
24

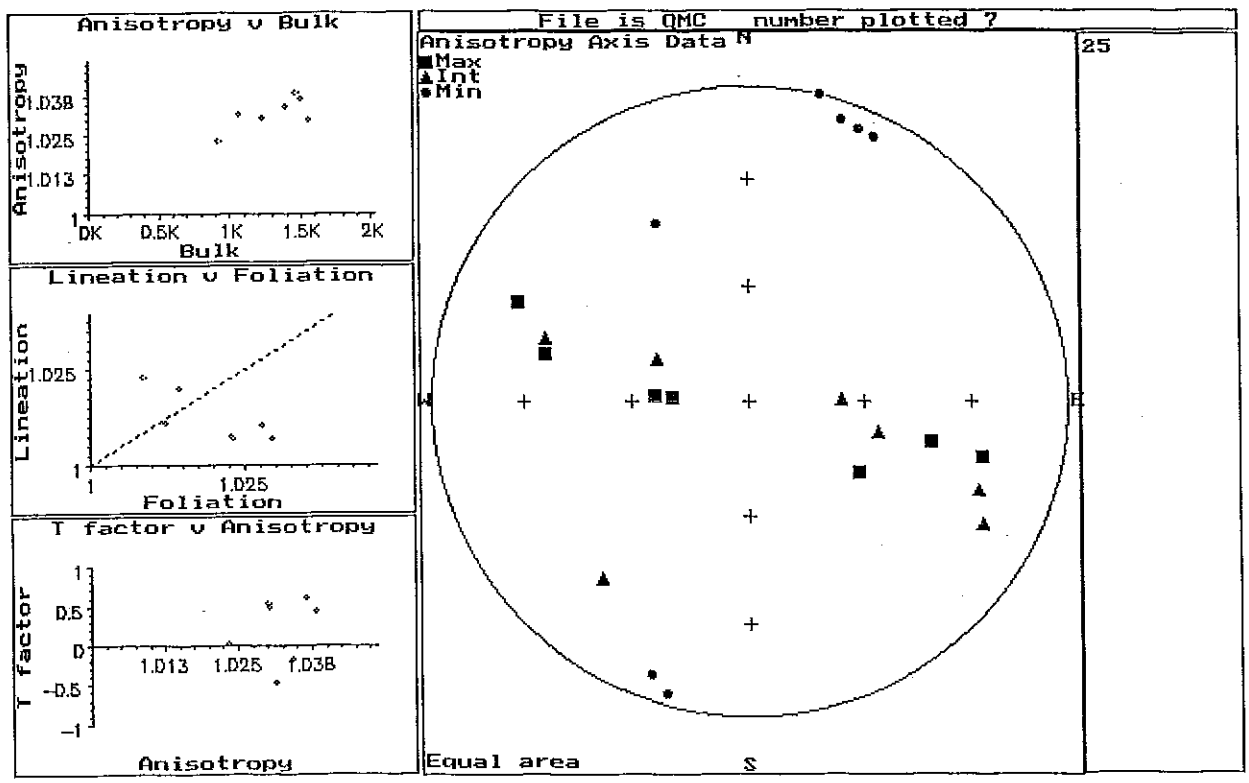
Anisotropy v Bulk
Anisotropy
1.038
1.025
1.013
1
DK
0.5K
1K
1.5K
2K
Bulk
Lineation v Foliation
Lineation
1.025
1
1
1.025
Foliation
T factor v Anisotropy
T factor
1
0.5
0
-0.5
-1
1.013
1.025
1.038
Anisotropy
File is QMC number plotted 7
Anisotropy Axis Data
Max
Int
Min
N
W
E
S
Equal area
25

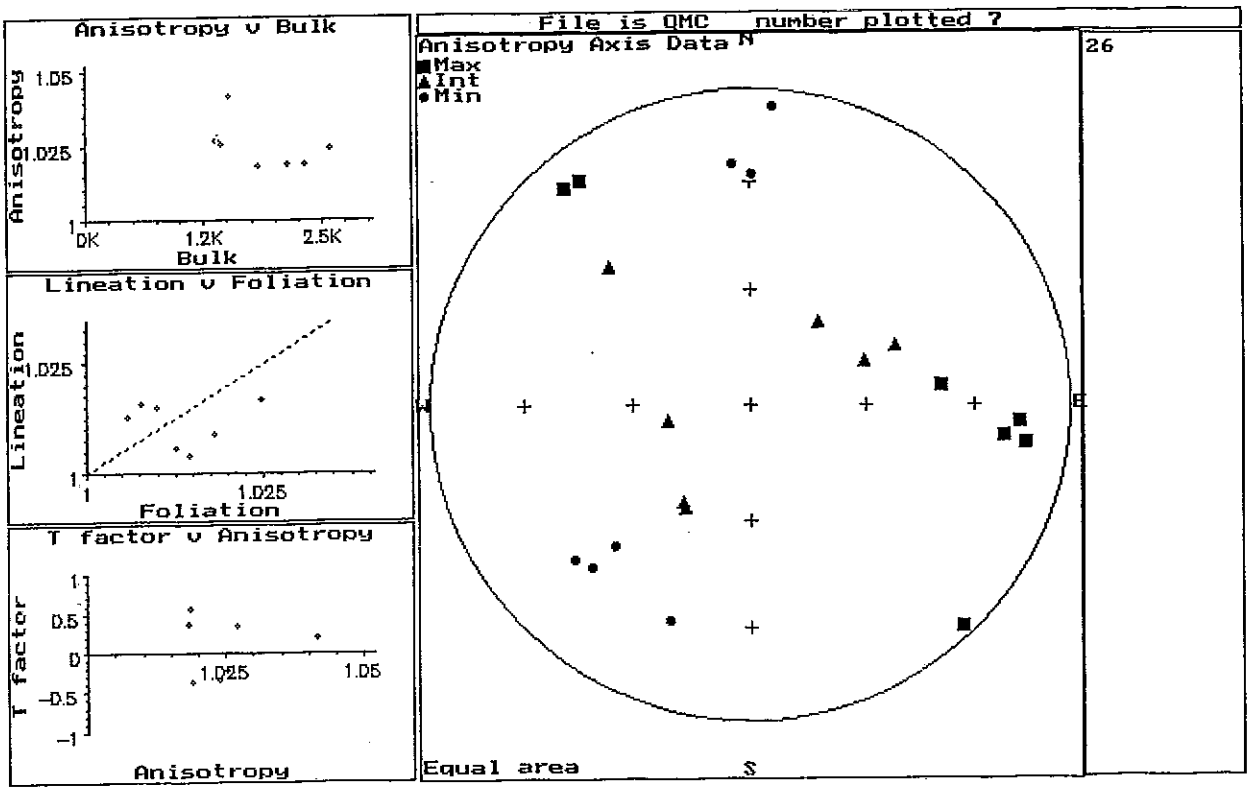
Anisotropy v Bulk
Anisotropy
1.05
1.025
1
0K
1.2K
2.5K
Bulk
Lineation v Foliation
Lineation
1.025
1
1
1.025
Foliation
T factor v Anisotropy
T factor
1
0.5
0
-0.5
-1
1.025
1.05
Anisotropy
File is QMC number plotted 7
Anisotropy Axis Data
Max
Int
Min
N
W
E
S
Equal area
26

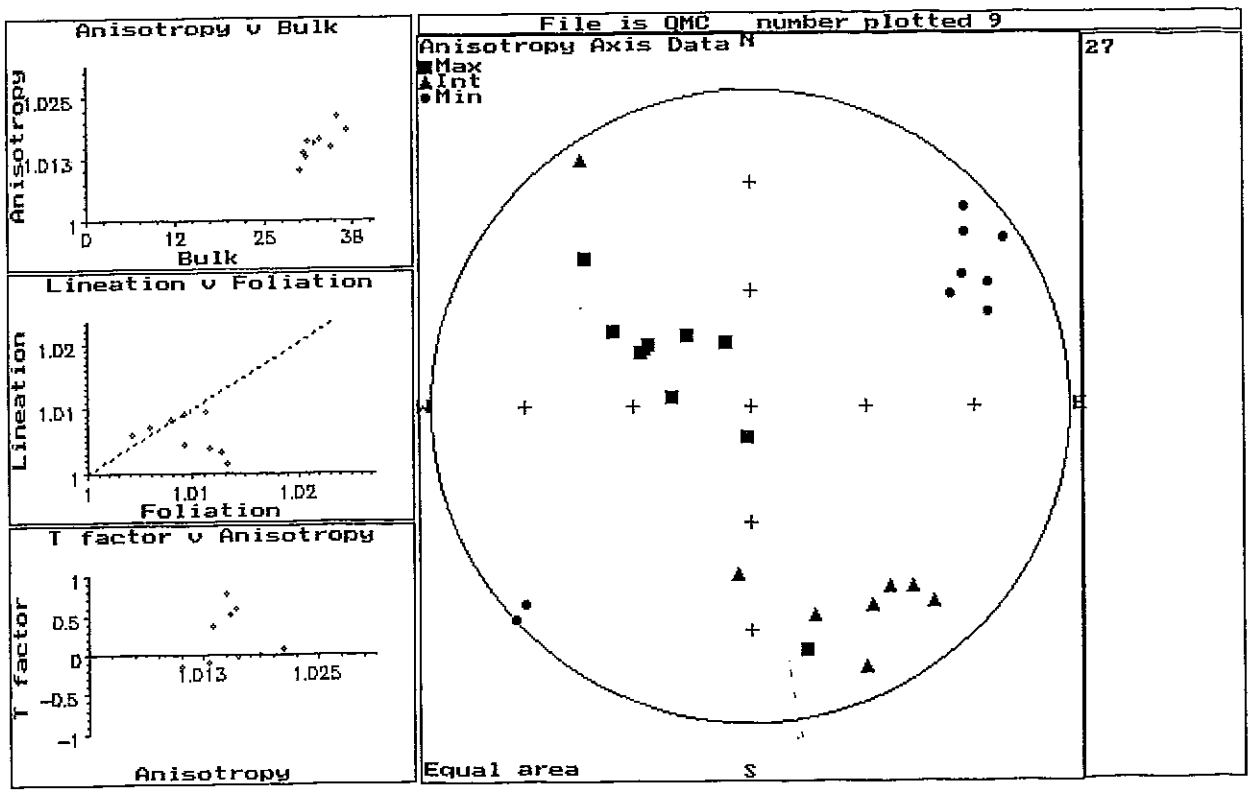
Anisotropy v Bulk
Anisotropy
1.025
1.013
1
0
12
25
38
Bulk
Lineation v Foliation
Lineation
1.02
1.01
1
1
1.01
1.02
Foliation
T factor v Anisotropy
T factor
1
0.5
0
-0.5
-1
1.013
1.025
Anisotropy
File is QMC number plotted 9
Anisotropy Axis Data
Max
Int
Min
N
W
E
S
Equal area
27

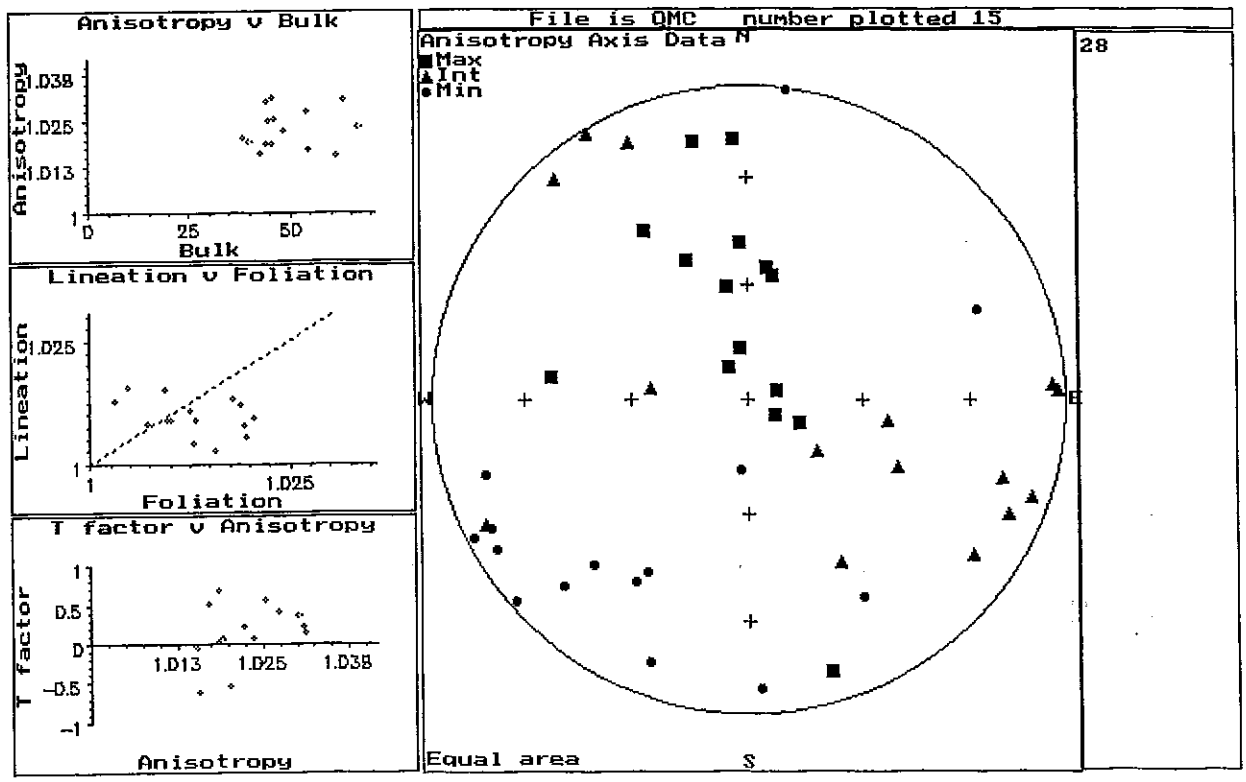
Anisotropy v Bulk
Anisotropy
1.038
1.025
1.013
1
D
25
5D
Bulk
Lineation v Foliation
Lineation
1.025
1
1
1.025
Foliation
T factor v Anisotropy
T factor
1
0.5
D
−0.5
−1
1.013
1.025
1.038
Anisotropy
File is QMC number plotted 15
Anisotropy Axis Data
Max
Int
Min
N
E
S
Equal area
28

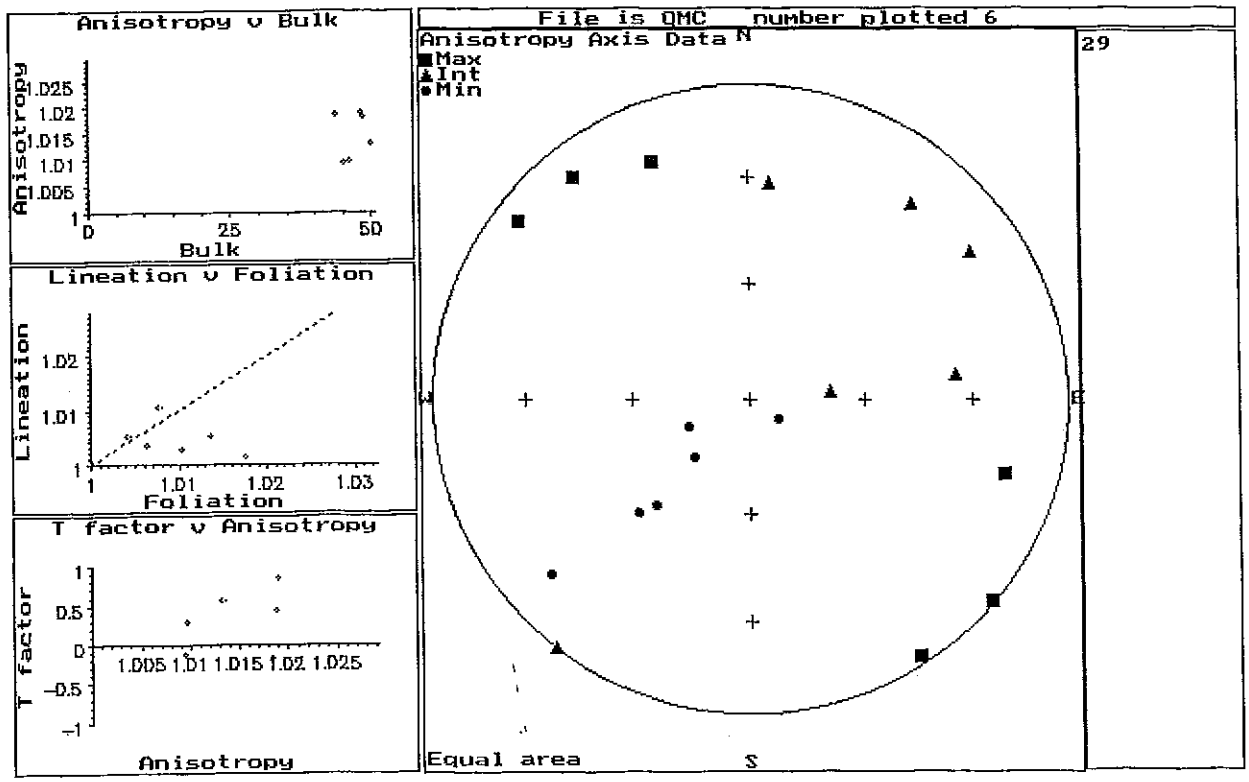
Anisotropy v Bulk
Anisotropy
1.025
1.02
1.015
1.01
1.005
1
D
25
5D
Bulk
Lineation v Foliation
Lineation
1.02
1.01
1
1
1.01
1.02
1.03
Foliation
T factor v Anisotropy
T factor
1
0.5
D
−0.5
−1
1.005 1.01 1.015 1.02 1.025
Anisotropy
File is QMC number plotted 6
Anisotropy Axis Data
Max
Int
Min
N
E
S
Equal area
29

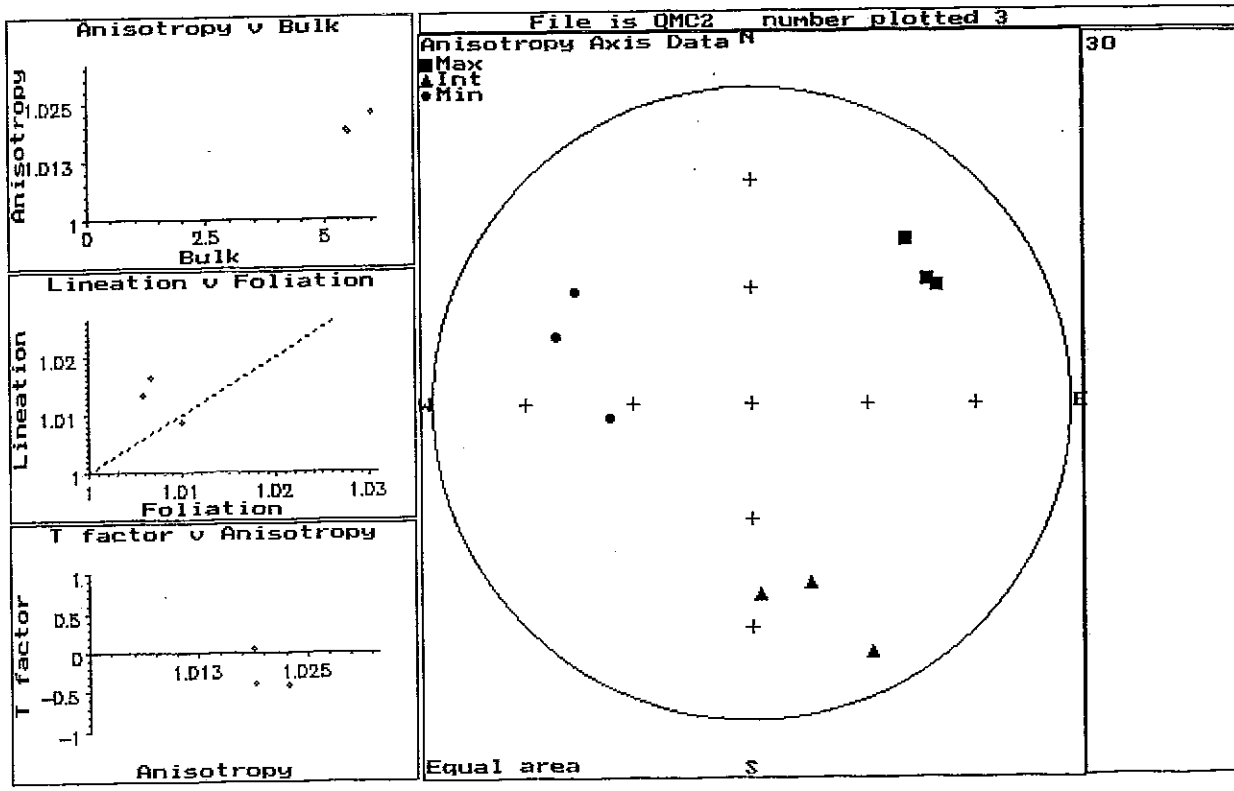
Anisotropy v Bulk
Anisotropy
1.025
1.013
1
0
2.5
5
Bulk
Lineation v Foliation
Lineation
1.02
1.01
1
1.01
1.02
1.03
Foliation
T factor v Anisotropy
T factor
1
0.5
0
−0.5
−1
1.013
1.025
Anisotropy
File is QMC2 number plotted 3
Anisotropy Axis Data
Max
Int
Min
N
E
S
30
Equal area

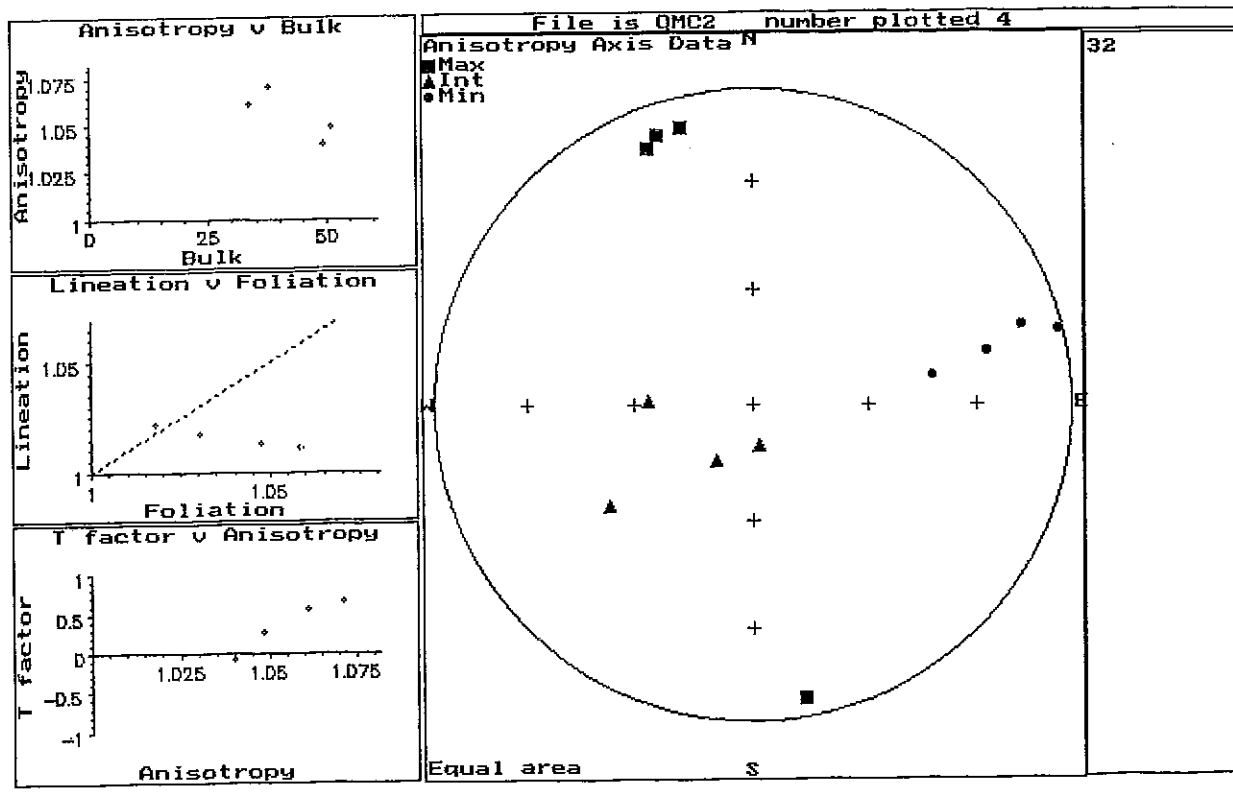
Anisotropy v Bulk
Anisotropy
1.075
1.05
1.025
1
0
25
50
Bulk
Lineation v Foliation
Lineation
1.05
1
1
1.05
Foliation
T factor v Anisotropy
T factor
1
0.5
0
−0.5
−1
1.025
1.05
1.075
Anisotropy
File is QMC2 number plotted 4
Anisotropy Axis Data
Max
Int
Min
N
E
S
32
Equal area

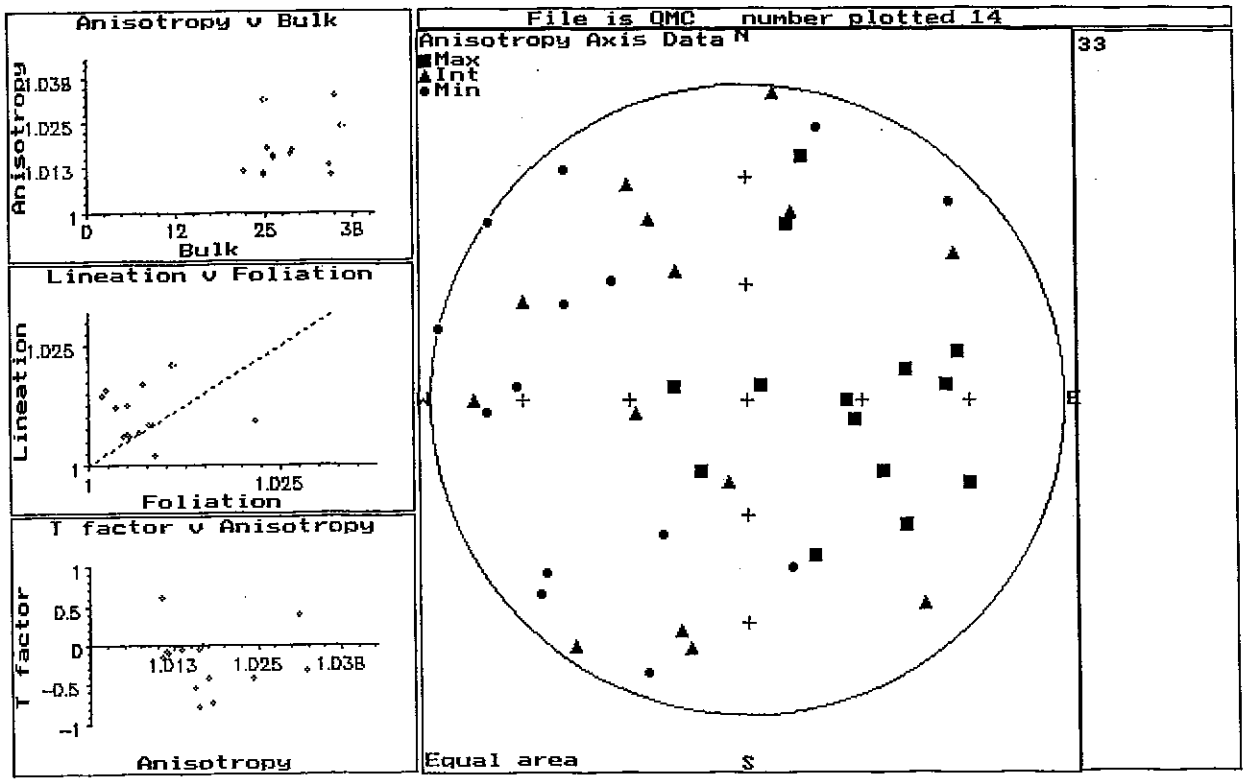
Anisotropy v Bulk
Anisotropy
1.038
1.025
1.013
1
0
12
25
38
Bulk
Lineation v Foliation
Lineation
1.025
1
1
1.025
Foliation
T factor v Anisotropy
T factor
1
0.5
0
-0.5
-1
1.013
1.025
1.038
Anisotropy
File is QMC number plotted 14
Anisotropy Axis Data
Max
Int
Min
N
E
S
Equal area
33

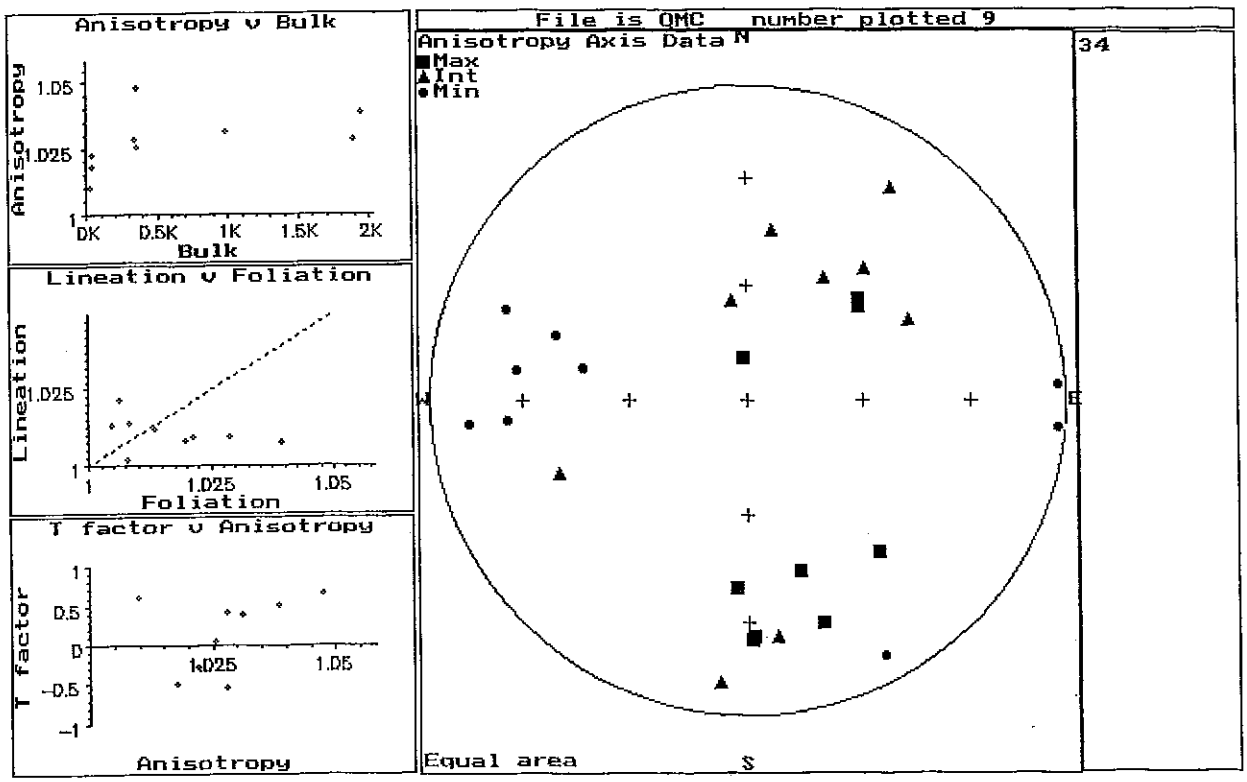
Anisotropy v Bulk
Anisotropy
1.05
1.025
1
0K
0.5K
1K
1.5K
2K
Bulk
Lineation v Foliation
Lineation
1.025
1
1
1.025
1.05
Foliation
T factor v Anisotropy
T factor
1
0.5
0
-0.5
-1
1.025
1.05
Anisotropy
File is QMC number plotted 9
Anisotropy Axis Data
Max
Int
Min
N
E
S
Equal area
34

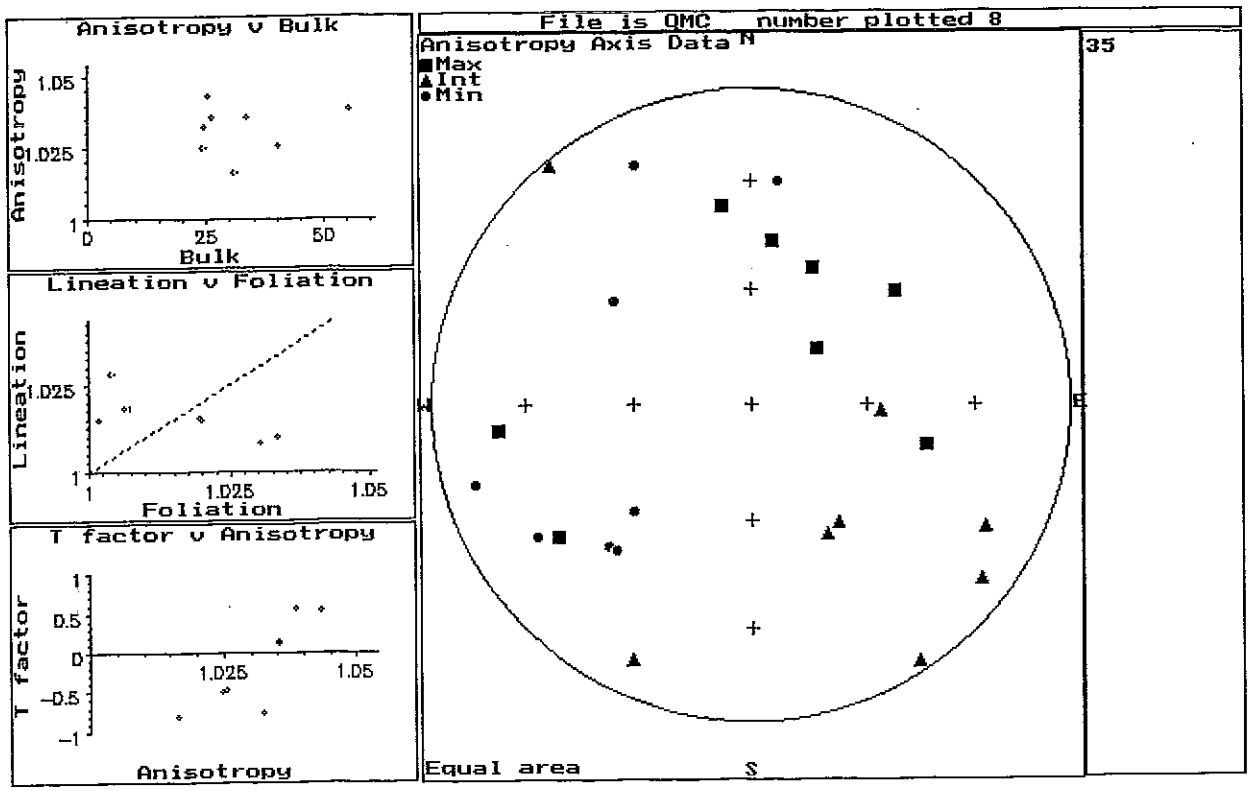
Anisotropy v Bulk
Anisotropy
1.05
1.025
1
0
25
50
Bulk
Lineation v Foliation
Lineation
1.025
1
1
1.025
1.05
Foliation
T factor v Anisotropy
T factor
1
0.5
0
−0.5
−1
1.025
1.05
Anisotropy
File is QMC number plotted 8
Anisotropy Axis Data
Max
Int
Min
N
E
S
Equal area
35

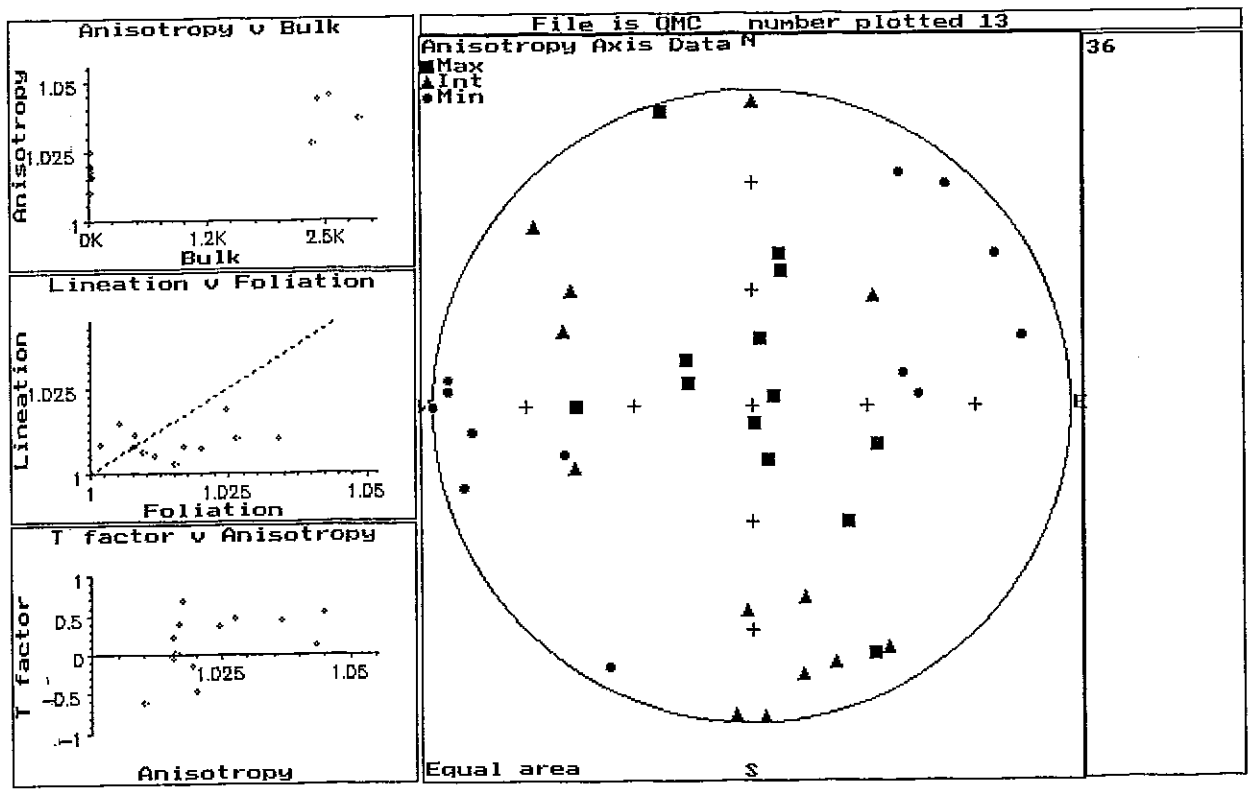
Anisotropy v Bulk
Anisotropy
1.05
1.025
1
0K
1.2K
2.5K
Bulk
Lineation v Foliation
Lineation
1.025
1
1
1.025
1.05
Foliation
T factor v Anisotropy
T factor
1
0.5
0
−0.5
−1
1.025
1.05
Anisotropy
File is QMC number plotted 13
Anisotropy Axis Data
Max
Int
Min
N
E
S
Equal area
36

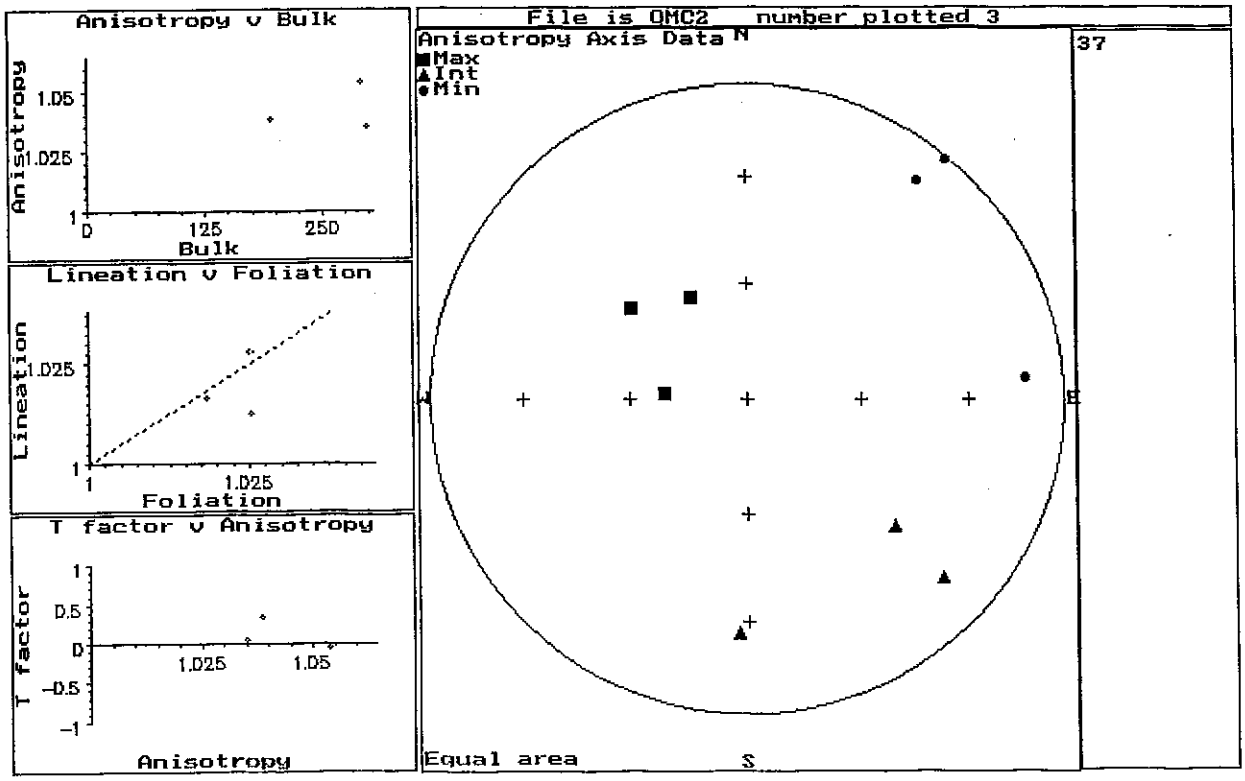
Anisotropy v Bulk
Anisotropy
1.05
1.025
1
0
125
250
Bulk
Lineation v Foliation
Lineation
1.025
1
1
1.025
Foliation
T factor v Anisotropy
T factor
1
0.5
0
-0.5
-1
1.025
1.05
Anisotropy
File is OMC2 number plotted 3
Anisotropy Axis Data
Max
Int
Min
N
W
E
S
37
Equal area

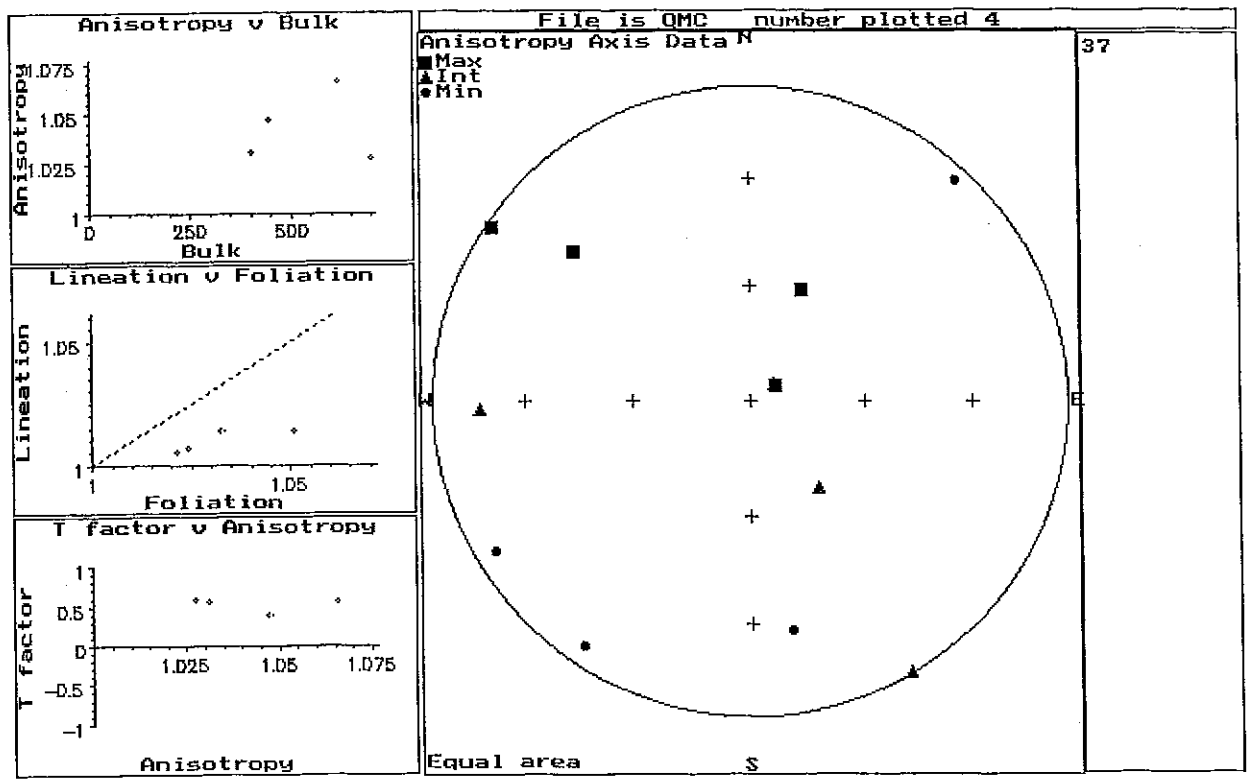
Anisotropy v Bulk
Anisotropy
1.075
1.05
1.025
1
0
250
500
Bulk
Lineation v Foliation
Lineation
1.05
1
1
1.05
Foliation
T factor v Anisotropy
T factor
1
0.5
0
-0.5
-1
1.025
1.05
1.075
Anisotropy
File is OMC number plotted 4
Anisotropy Axis Data
Max
Int
Min
N
W
E
S
37
Equal area

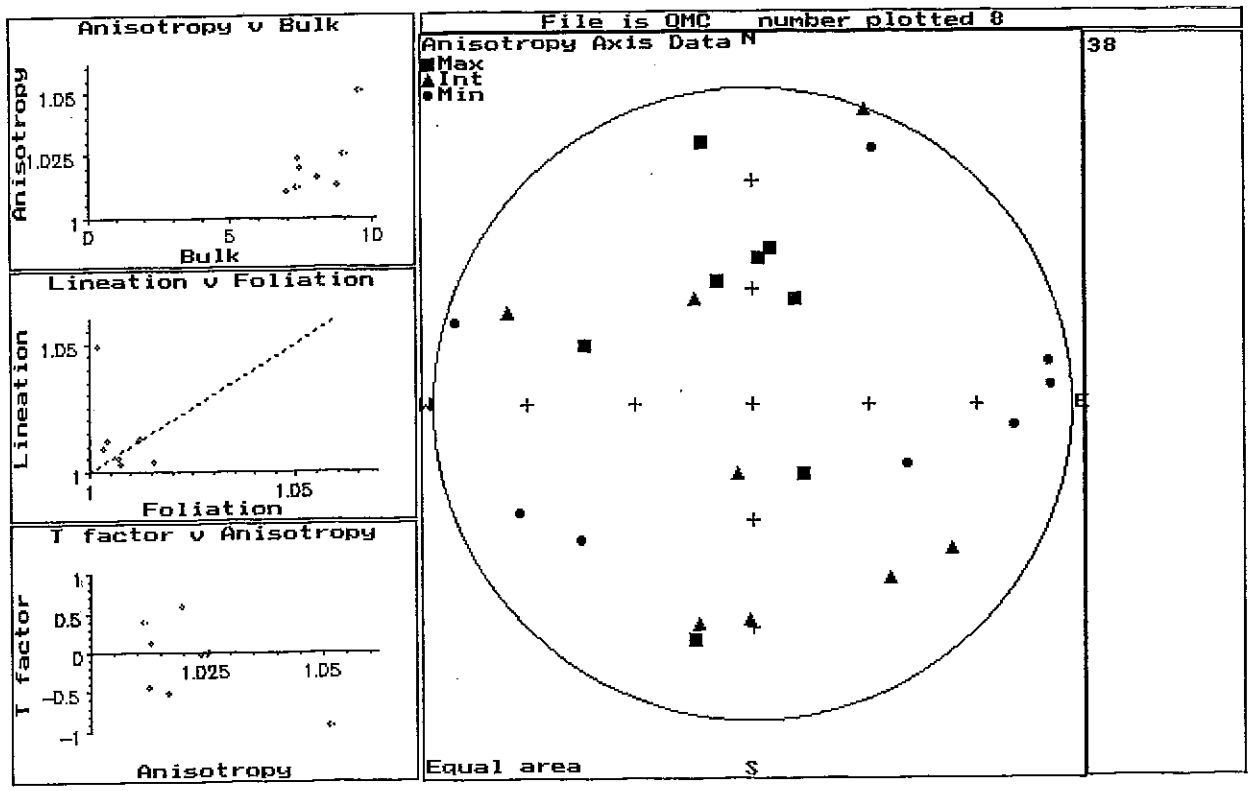
Anisotropy v Bulk
Anisotropy
1.05
1.025
1
0
5
10
Bulk
Lineation v Foliation
Lineation
1.05
1
1
1.05
Foliation
T factor v Anisotropy
T factor
0.5
0
−0.5
−1
1.025
1.05
Anisotropy
File is QMC number plotted 8
Anisotropy Axis Data
Max
Int
Min
N
E
S
Equal area
38

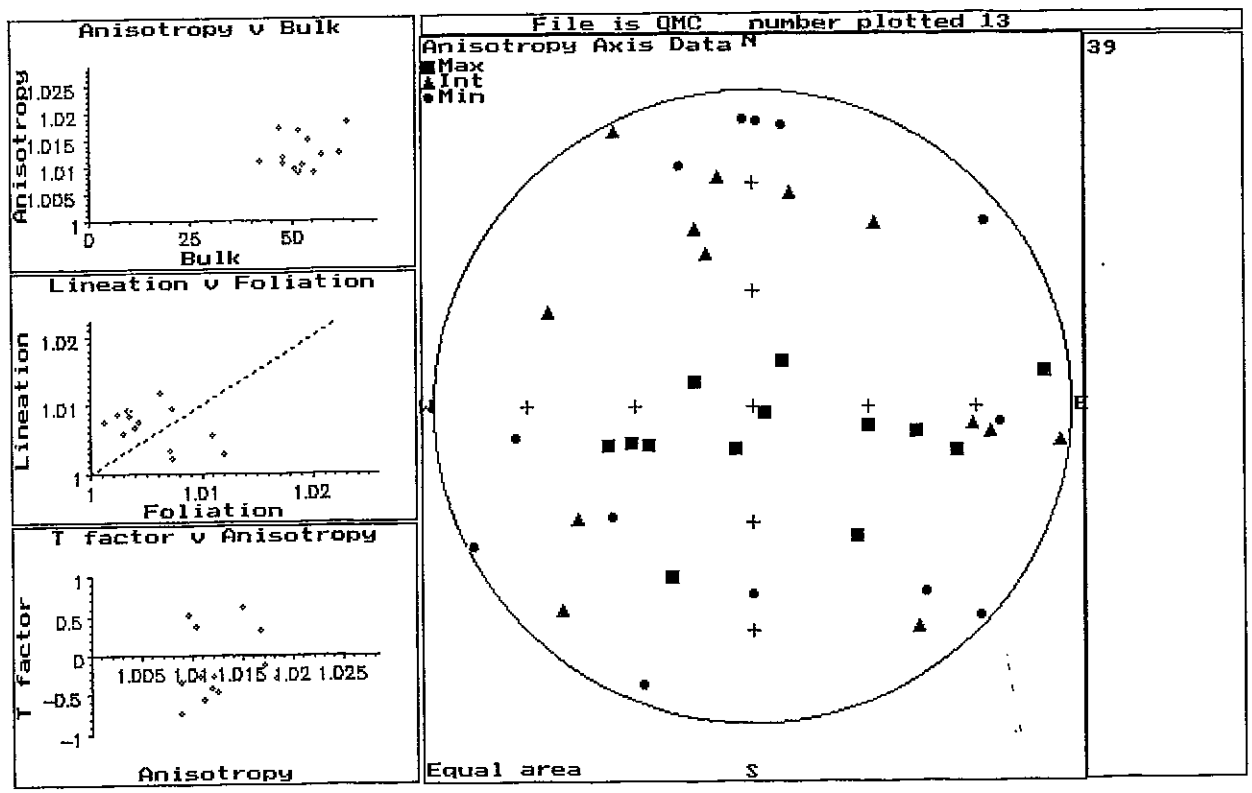
Anisotropy v Bulk
Anisotropy
1.025
1.02
1.015
1.01
1.005
1
0
25
50
Bulk
Lineation v Foliation
Lineation
1.02
1.01
1
1
1.01
1.02
Foliation
T factor v Anisotropy
T factor
0.5
0
−0.5
−1
1.005
1.01
1.015
1.02
1.025
Anisotropy
File is QMC number plotted 13
Anisotropy Axis Data
Max
Int
Min
N
E
S
Equal area
39

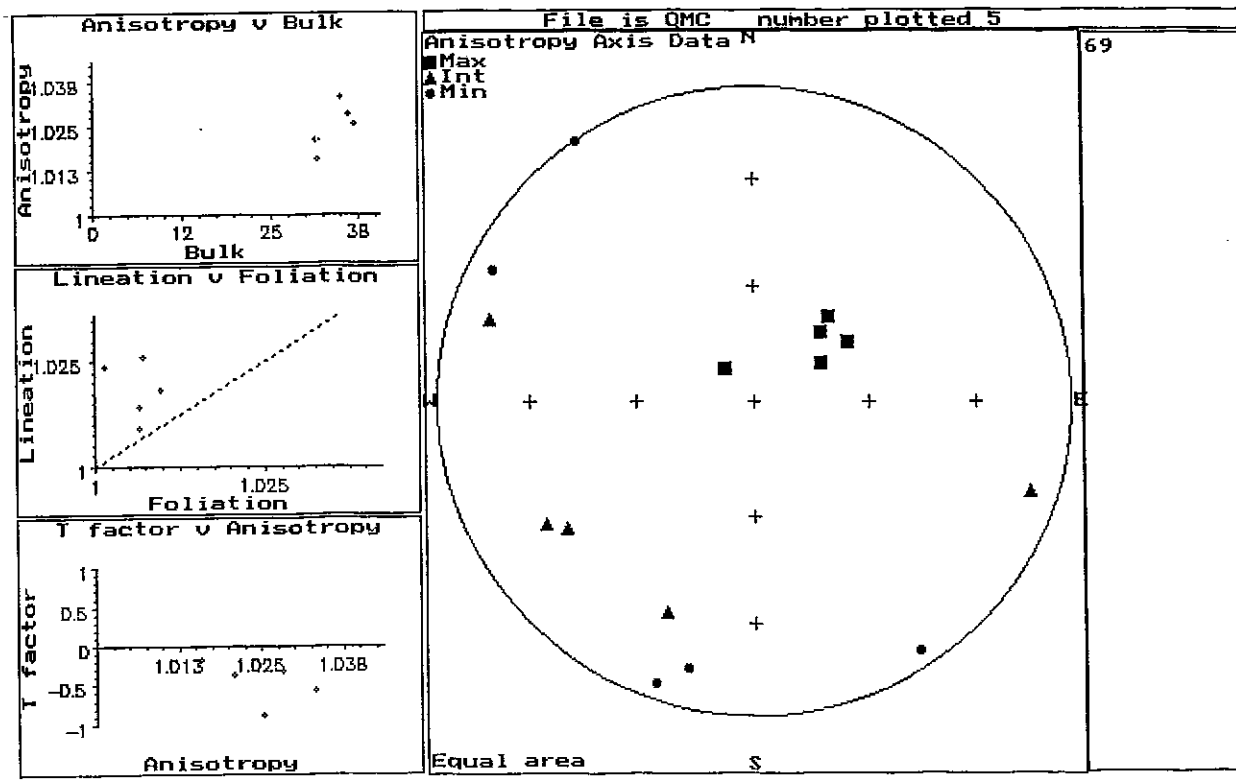
Anisotropy v Bulk
Anisotropy
1.038
1.025
1.013
1
0
12
25
38
Bulk
Lineation v Foliation
Lineation
1.025
1
1
1.025
Foliation
T factor v Anisotropy
T factor
1
0.5
0
-0.5
-1
1.013
1.025
1.038
Anisotropy
File is QMC number plotted 5
Anisotropy Axis Data
Max
Int
Min
N
W
E
S
Equal area
69

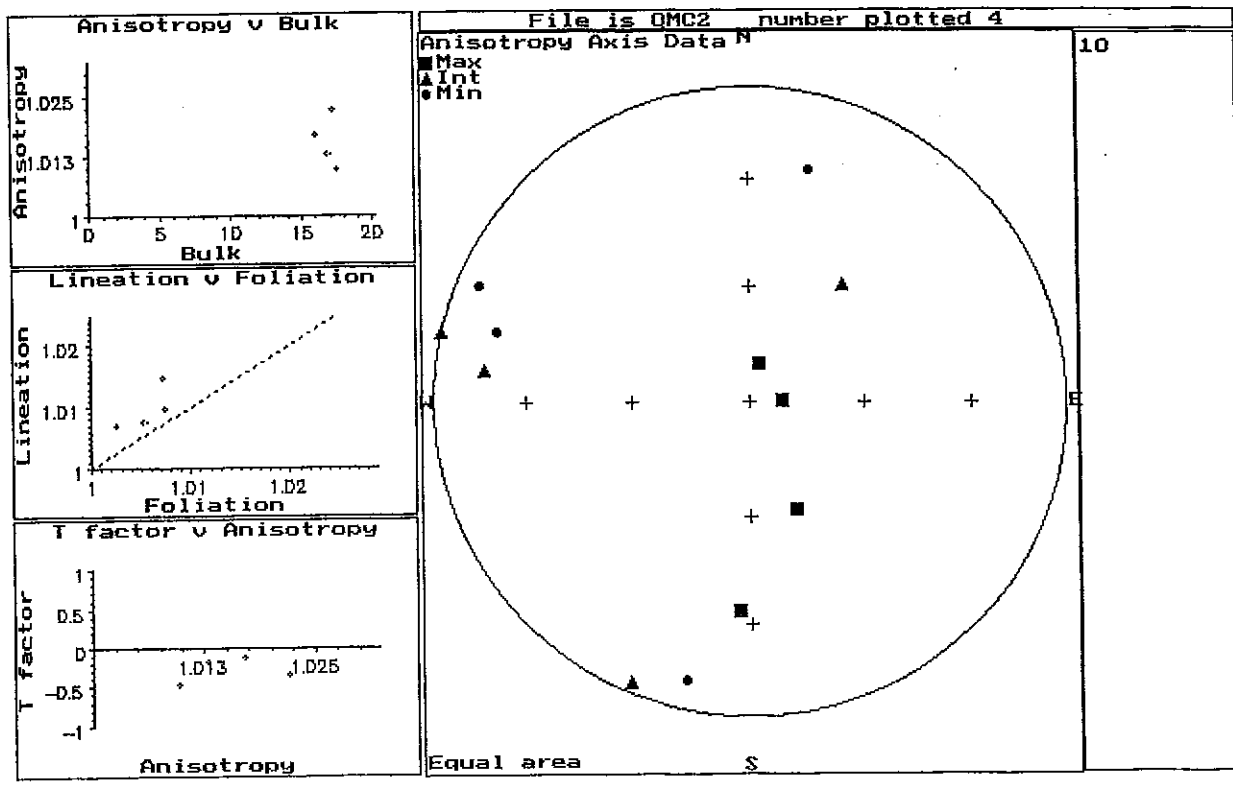
Anisotropy v Bulk
Anisotropy
1.025
1.013
1
0
5
10
15
20
Bulk
Lineation v Foliation
Lineation
1.02
1.01
1
1
1.01
1.02
Foliation
T factor v Anisotropy
T factor
1
0.5
0
-0.5
-1
1.013
1.025
Anisotropy
File is QMC2 number plotted 4
Anisotropy Axis Data
Max
Int
Min
N
W
E
S
Equal area
10

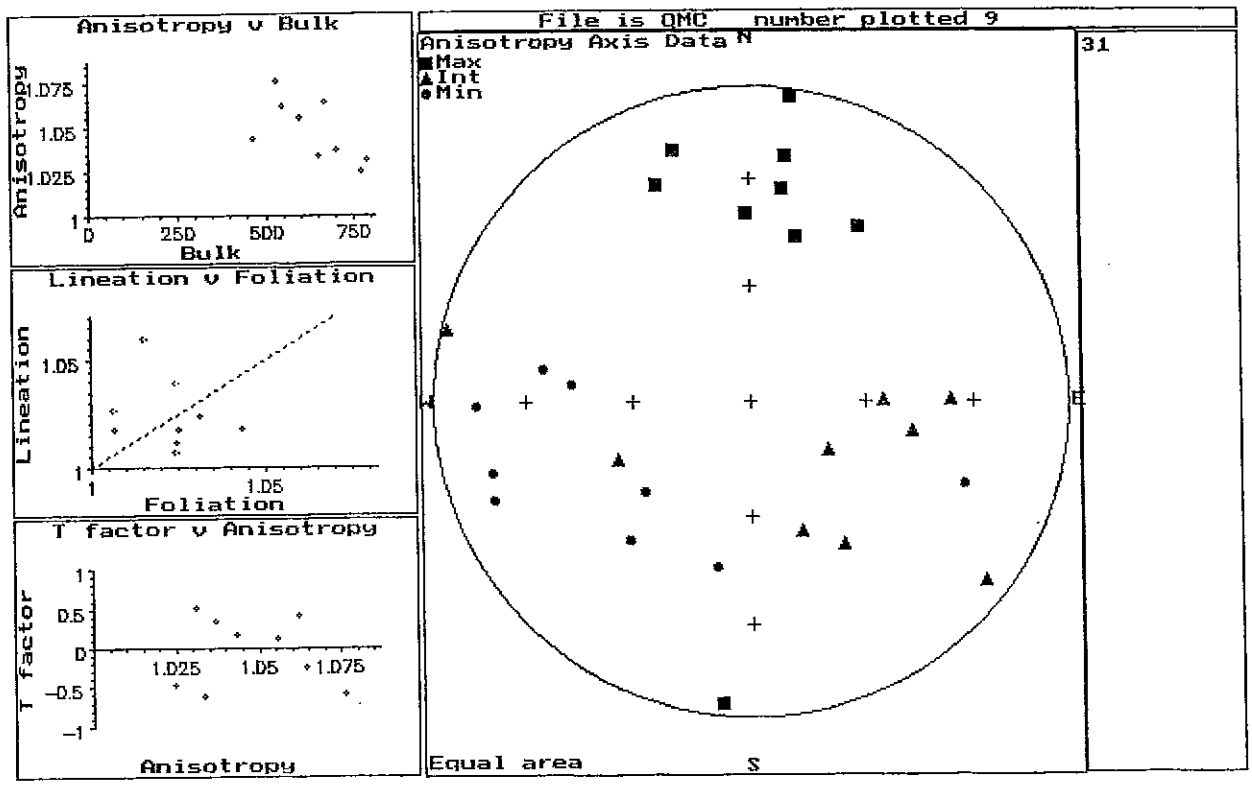
Anisotropy v Bulk
Anisotropy
1.075
1.05
1.025
1
0
250
500
750
Bulk
Lineation v Foliation
Lineation
1.05
1
1
1.05
Foliation
T factor v Anisotropy
T factor
1
0.5
0
-0.5
-1
1.025
1.05
1.075
Anisotropy
File is QMC_ number plotted 9
Anisotropy Axis Data
Max
Int
Min
N
W
E
S
Equal area
31

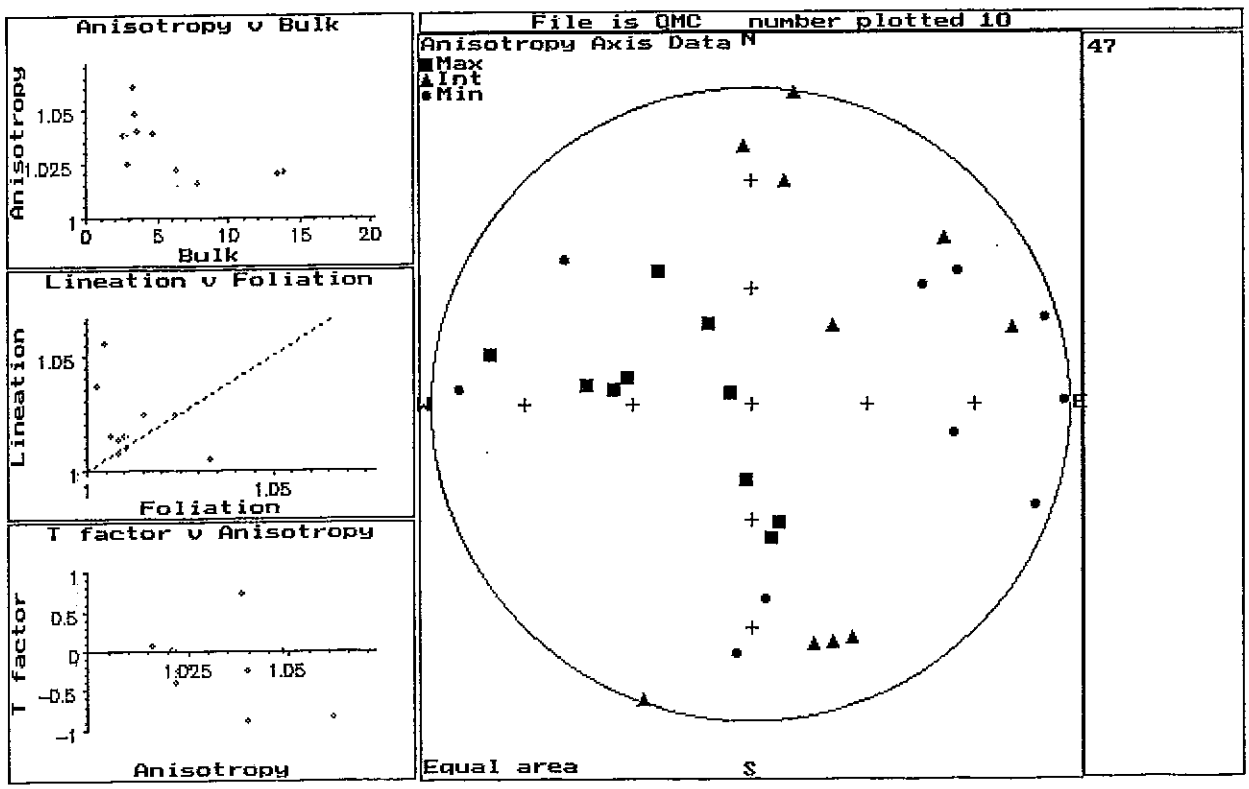
Anisotropy v Bulk
Anisotropy
1.05
1.025
1
0
5
10
15
20
Bulk
Lineation v Foliation
Lineation
1.05
1
1
1.05
Foliation
T factor v Anisotropy
T factor
1
0.5
0
-0.5
-1
1.025
1.05
Anisotropy
File is QMC number plotted 10
Anisotropy Axis Data
Max
Int
Min
N
E
S
Equal area
47

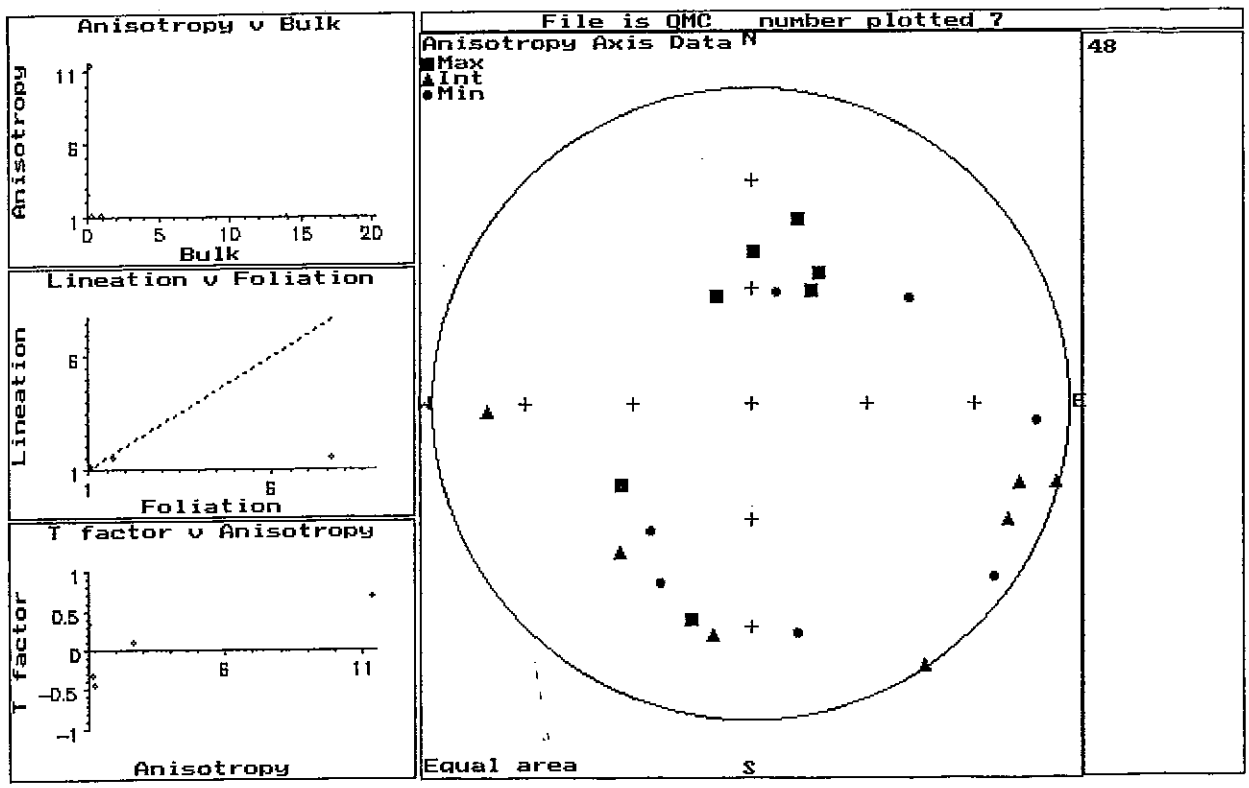
Anisotropy v Bulk
Anisotropy
11
6
1
0
5
10
15
20
Bulk
Lineation v Foliation
Lineation
6
1
1
6
Foliation
T factor v Anisotropy
T factor
1
0.5
0
-0.5
-1
6
11
Anisotropy
File is QMC number plotted 7
Anisotropy Axis Data
Max
Int
Min
N
E
S
Equal area
48

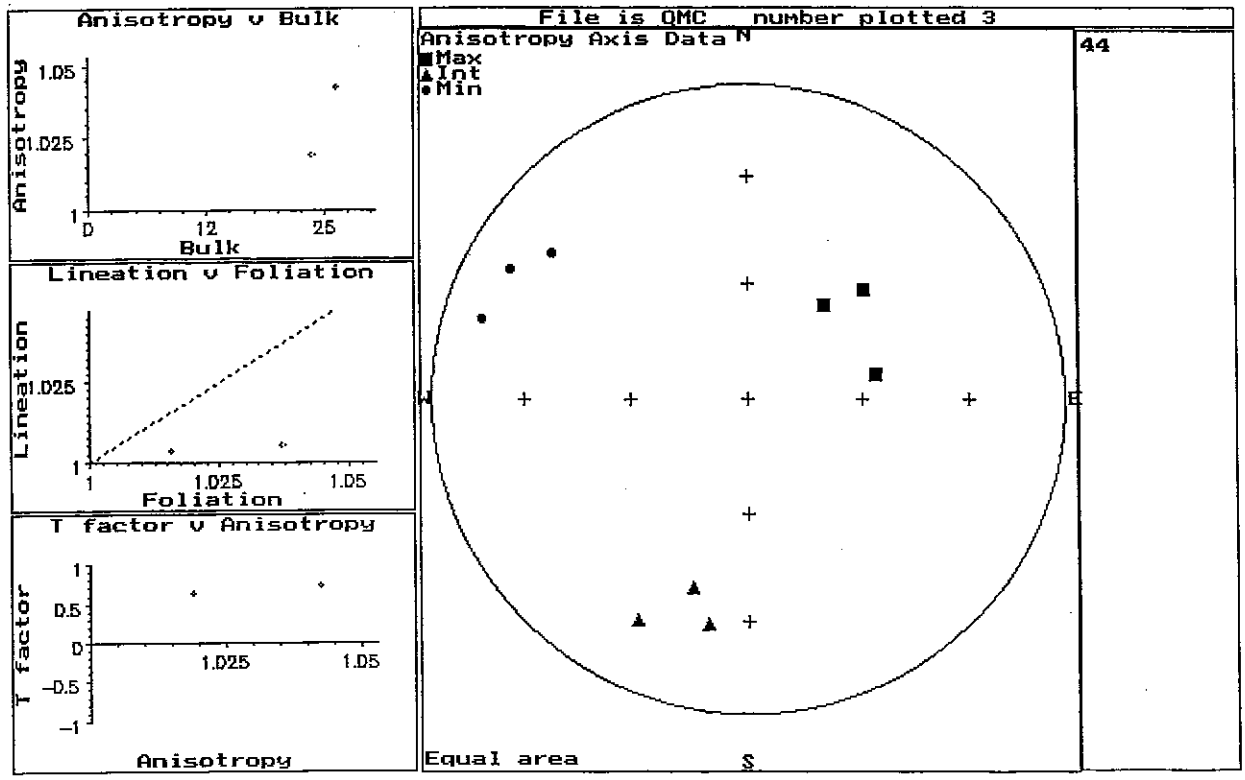
Anisotropy v Bulk
Anisotropy
1.05
1.025
1
0
12
25
Bulk
Lineation v Foliation
Lineation
1.025
1
1
1.025
1.05
Foliation
T factor v Anisotropy
T factor
0.5
0
-0.5
-1
1.025
1.05
Anisotropy
File is QMC number plotted 3
Anisotropy Axis Data
Max
Int
Min
N
W
E
S
Equal area
44

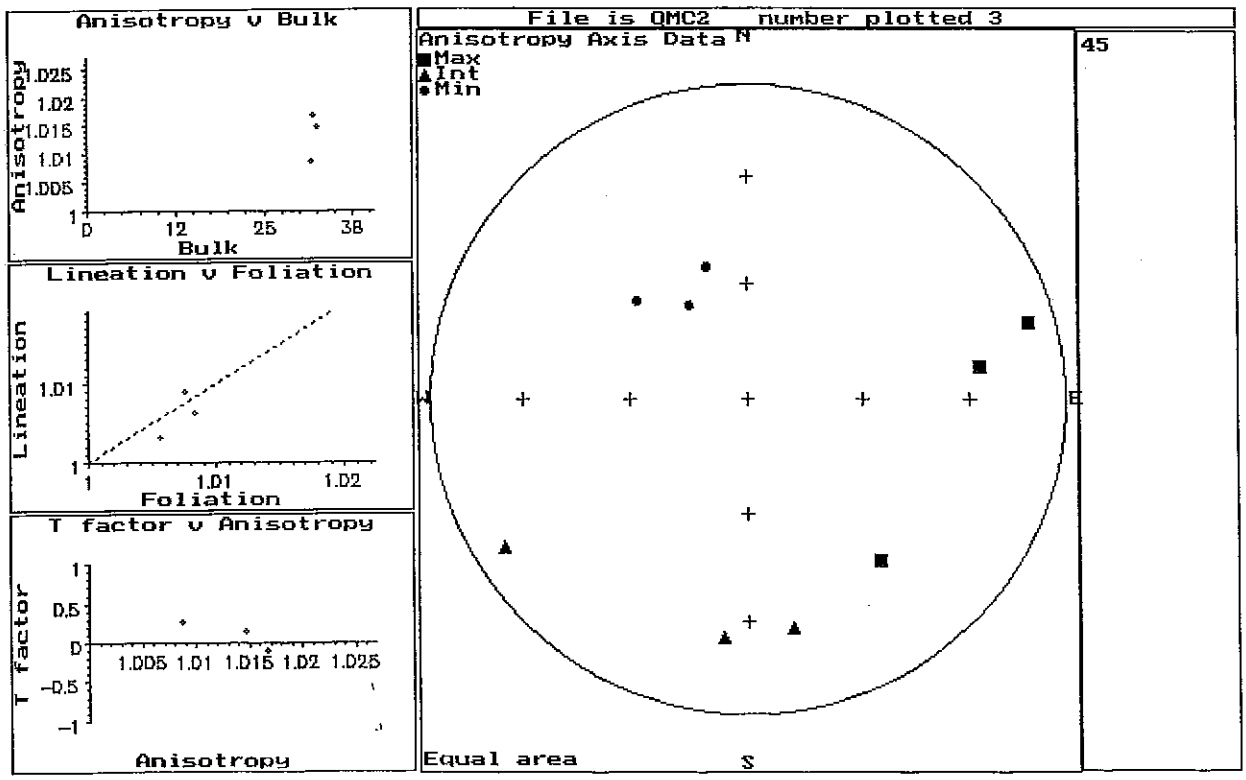
Anisotropy v Bulk
Anisotropy
1.025
1.02
1.015
1.01
1.005
1
0
12
25
38
Bulk
Lineation v Foliation
Lineation
1.01
1
1
1.01
1.02
Foliation
T factor v Anisotropy
T factor
0.5
0
-0.5
-1
1.005
1.01
1.015
1.02
1.025
Anisotropy
File is QMC2 number plotted 3
Anisotropy Axis Data
Max
Int
Min
N
W
E
S
Equal area
45

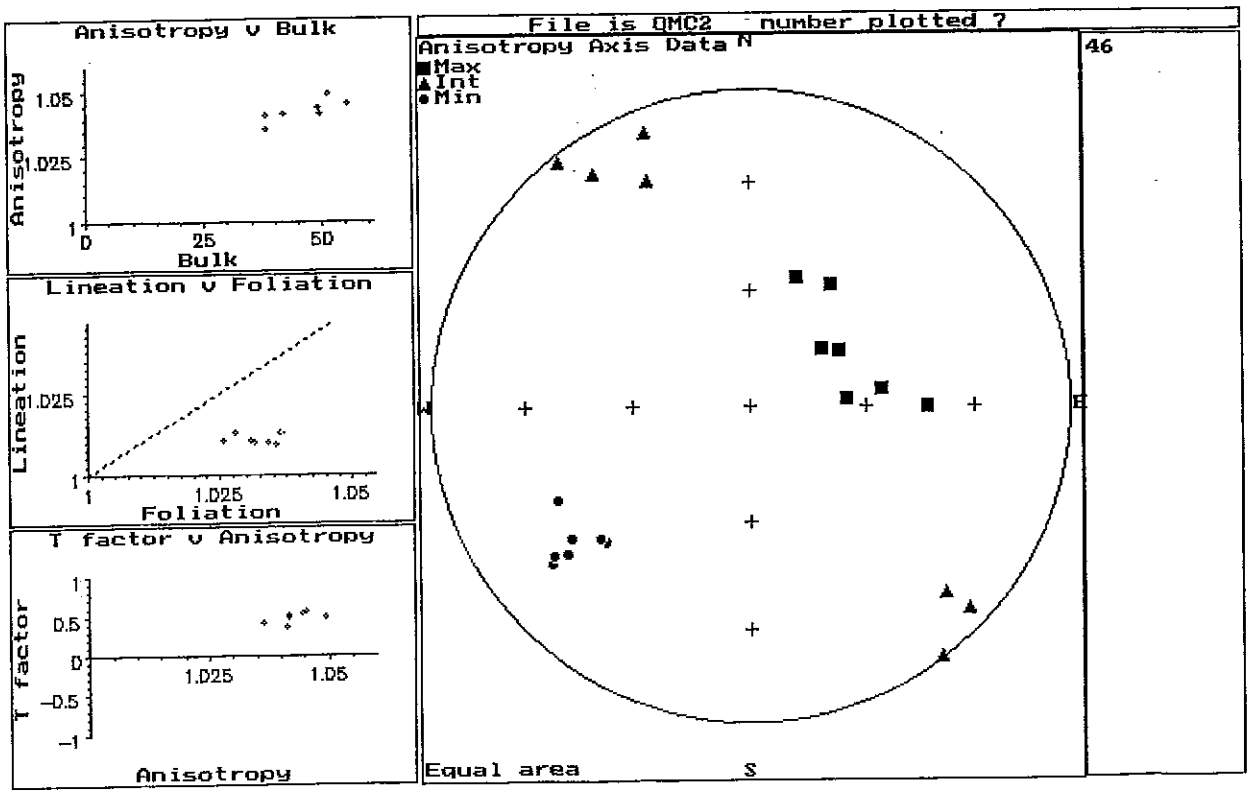
Anisotropy v Bulk
Anisotropy
1.05
1.025
1
D
25
50
Bulk
Lineation v Foliation
Lineation
1.025
1
1
1.025
1.05
Foliation
T factor v Anisotropy
T factor
1
0.5
0
−0.5
−1
1.025
1.05
Anisotropy
File is QMC2 number plotted 7
Anisotropy Axis Data
Max
Int
Min
N
E
S
Equal area
46

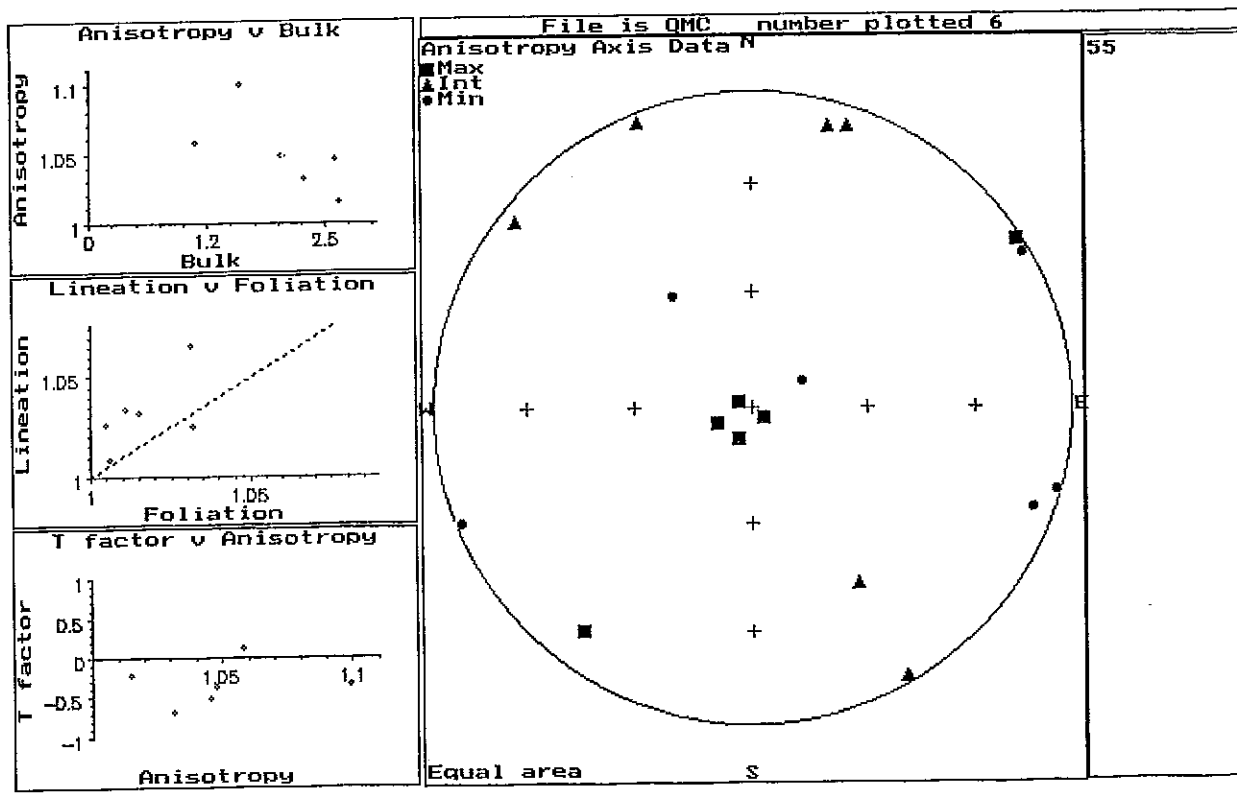
Anisotropy v Bulk
Anisotropy
1.1
1.05
1
D
1.2
2.5
Bulk
Lineation v Foliation
Lineation
1.05
1
1
1.05
Foliation
T factor v Anisotropy
T factor
1
0.5
0
−0.5
−1
1.05
1.1
Anisotropy
File is QMC number plotted 6
Anisotropy Axis Data
Max
Int
Min
N
E
S
Equal area
55

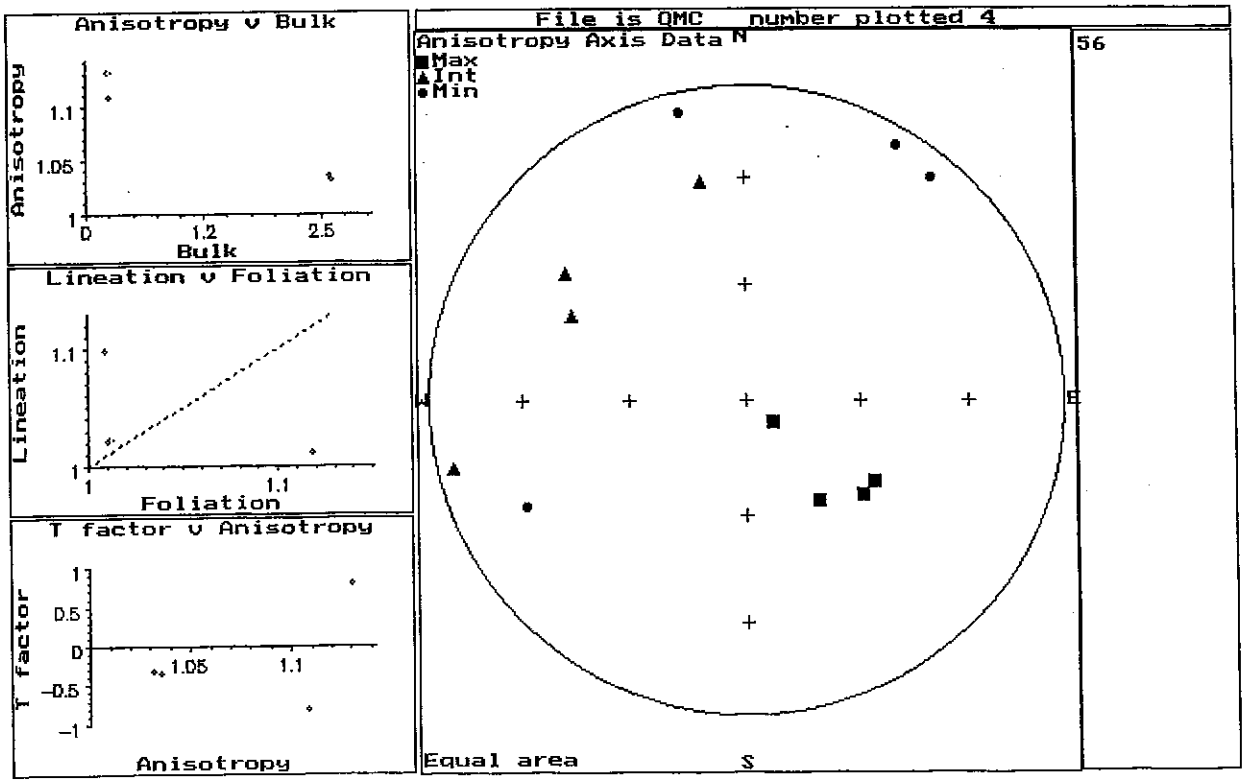
Anisotropy v Bulk
Anisotropy
1.1
1.05
1
0
1.2
2.5
Bulk
Lineation v Foliation
Lineation
1.1
1
1
1.1
Foliation
T factor v Anisotropy
T factor
1
0.5
0
−0.5
−1
1.05
1.1
Anisotropy
File is QMC number plotted 4
Anisotropy Axis Data
Max
Int
Min
N
W
E
S
Equal area
56

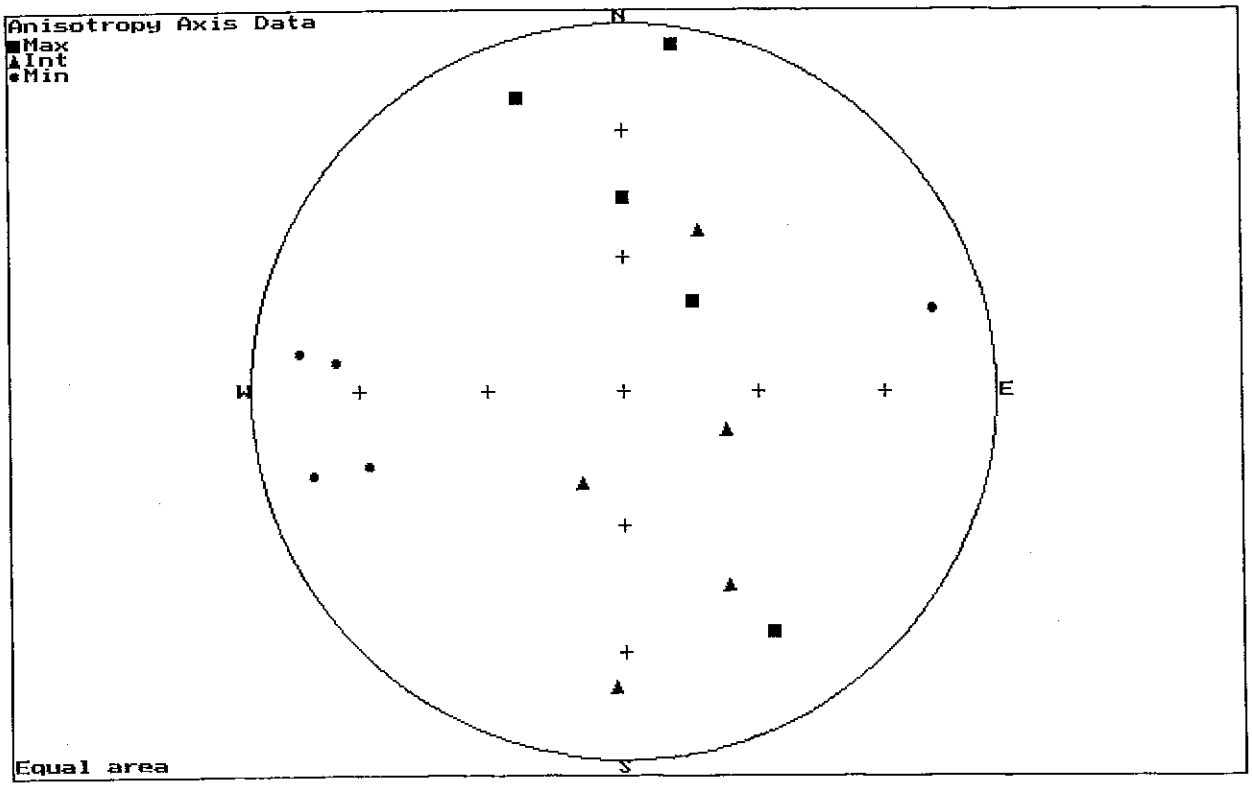
Anisotropy Axis Data
Max
Int
Min
N
W
E
S
Equal area

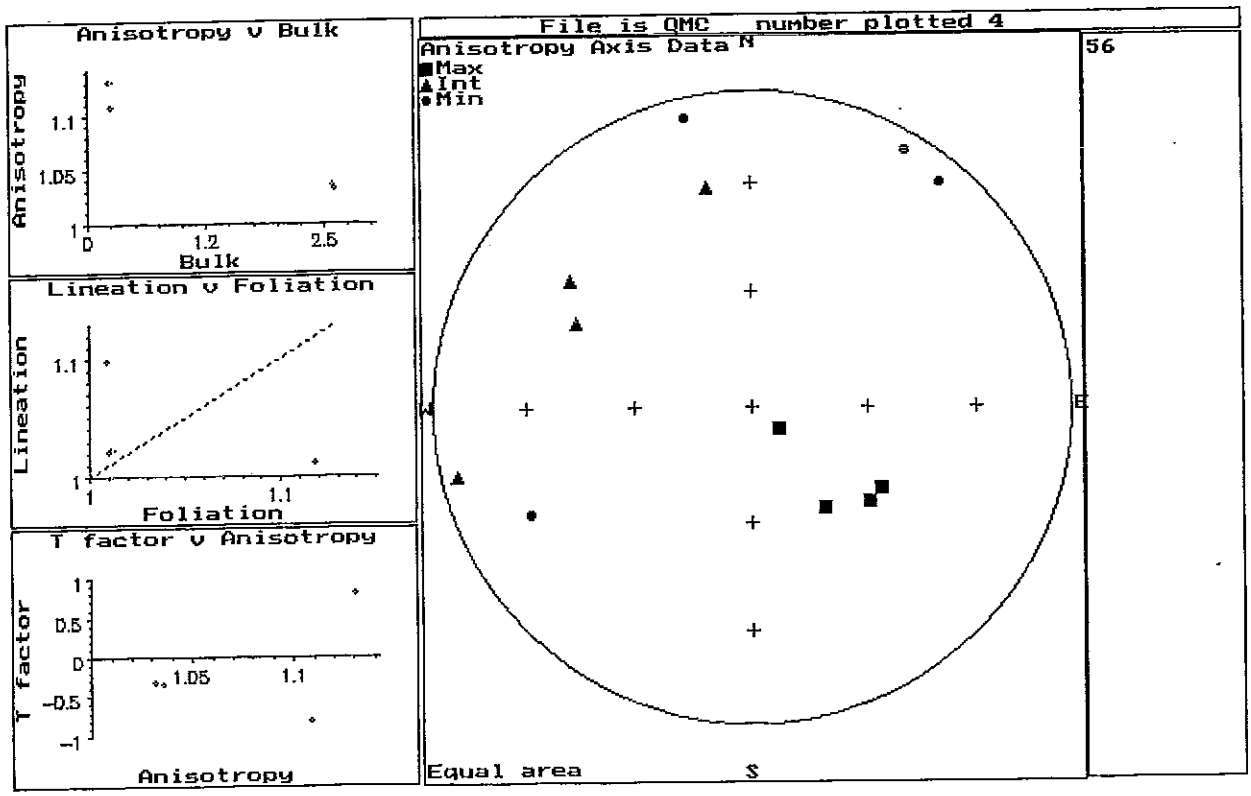
Anisotropy v Bulk
Anisotropy
1.1
1.05
1
0
1.2
2.5
Bulk
Lineation v Foliation
Lineation
1.1
1
1
1.1
Foliation
T factor v Anisotropy
T factor
1
0.5
0
-0.5
-1
1.05
1.1
Anisotropy
File is QMC number plotted 4
Anisotropy Axis Data N
Max
Int
Min
56
E
S
Equal area

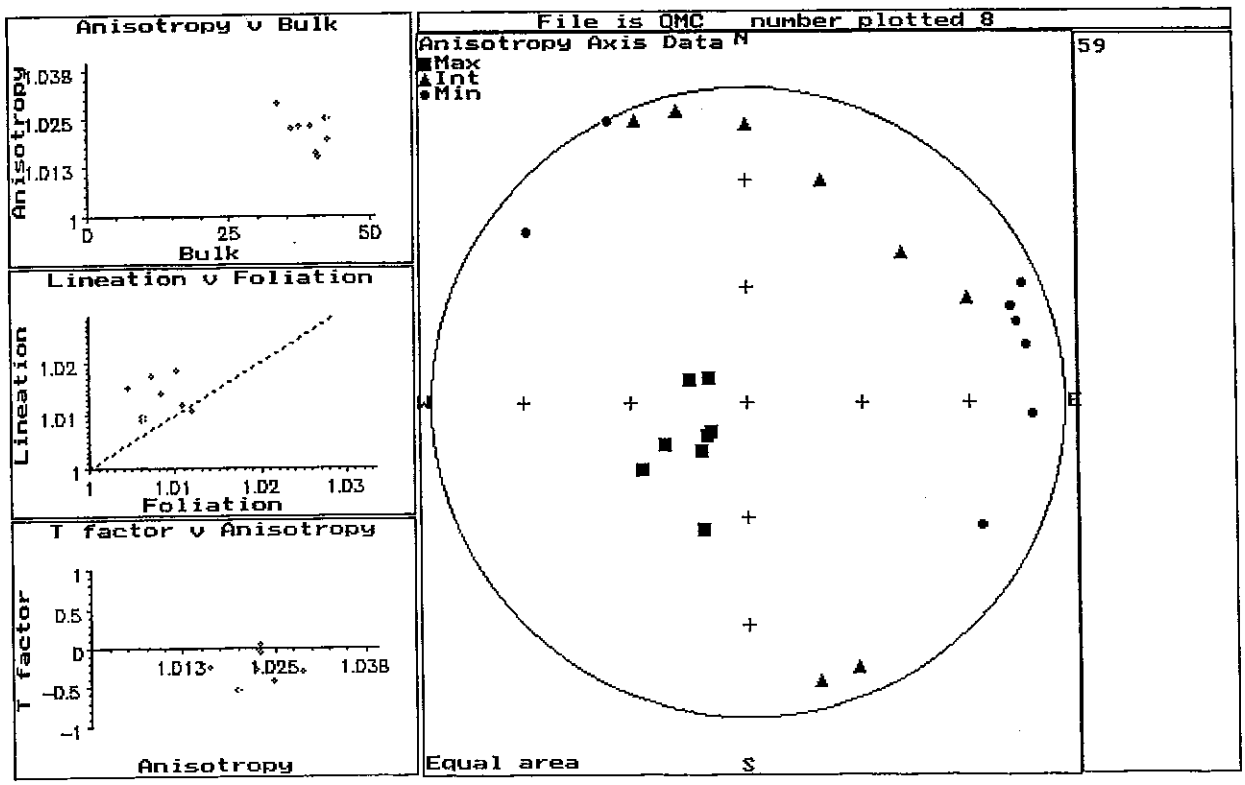
Anisotropy v Bulk
Anisotropy
1.038
1.025
1.013
1
0
25
50
Bulk
Lineation v Foliation
Lineation
1.02
1.01
1
1
1.01
1.02
1.03
Foliation
T factor v Anisotropy
T factor
0.5
0
-0.5
-1
1.013
1.025
1.038
Anisotropy
File is QMC number plotted 8
Anisotropy Axis Data
Max
Int
Min
N
W
E
S
Equal area
59

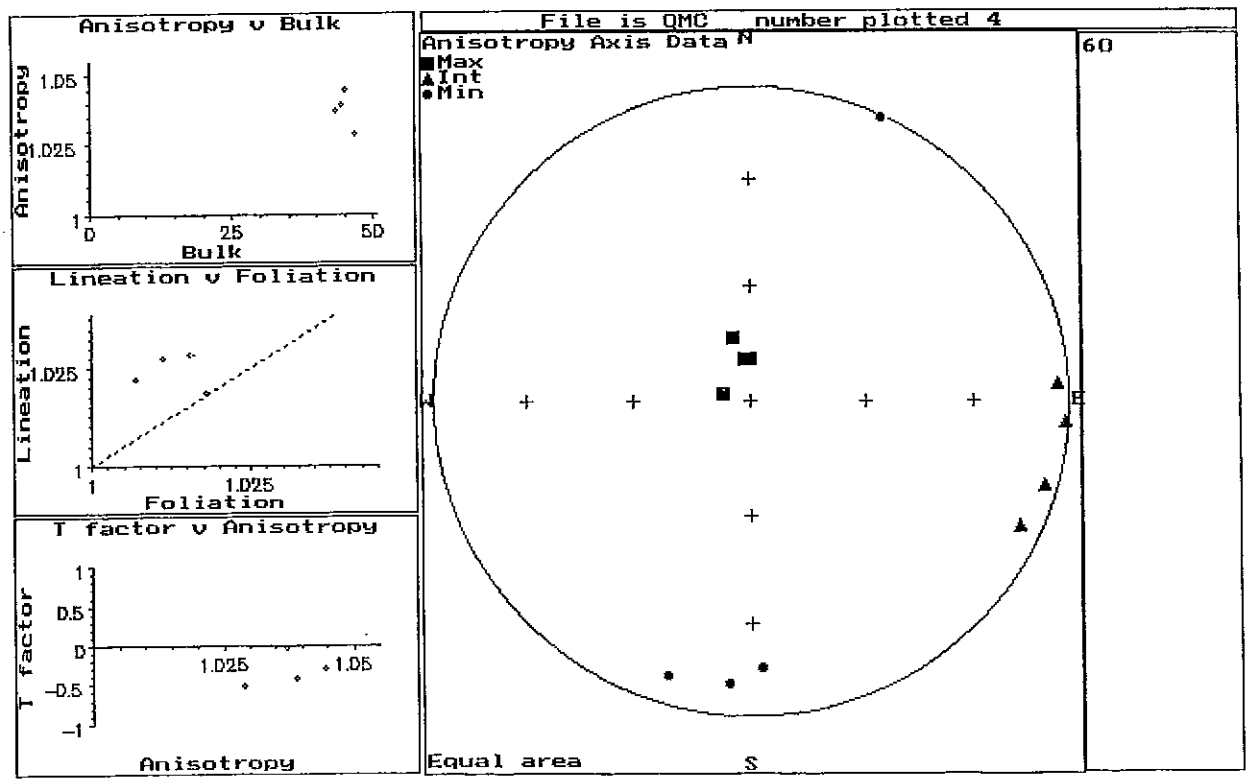
Anisotropy v Bulk
Anisotropy
1.05
1.025
1
0
25
50
Bulk
Lineation v Foliation
Lineation
1.025
1
1
1.025
Foliation
T factor v Anisotropy
T factor
0.5
0
-0.5
-1
1.025
1.05
Anisotropy
File is QMC number plotted 4
Anisotropy Axis Data
Max
Int
Min
N
W
E
S
Equal area
60

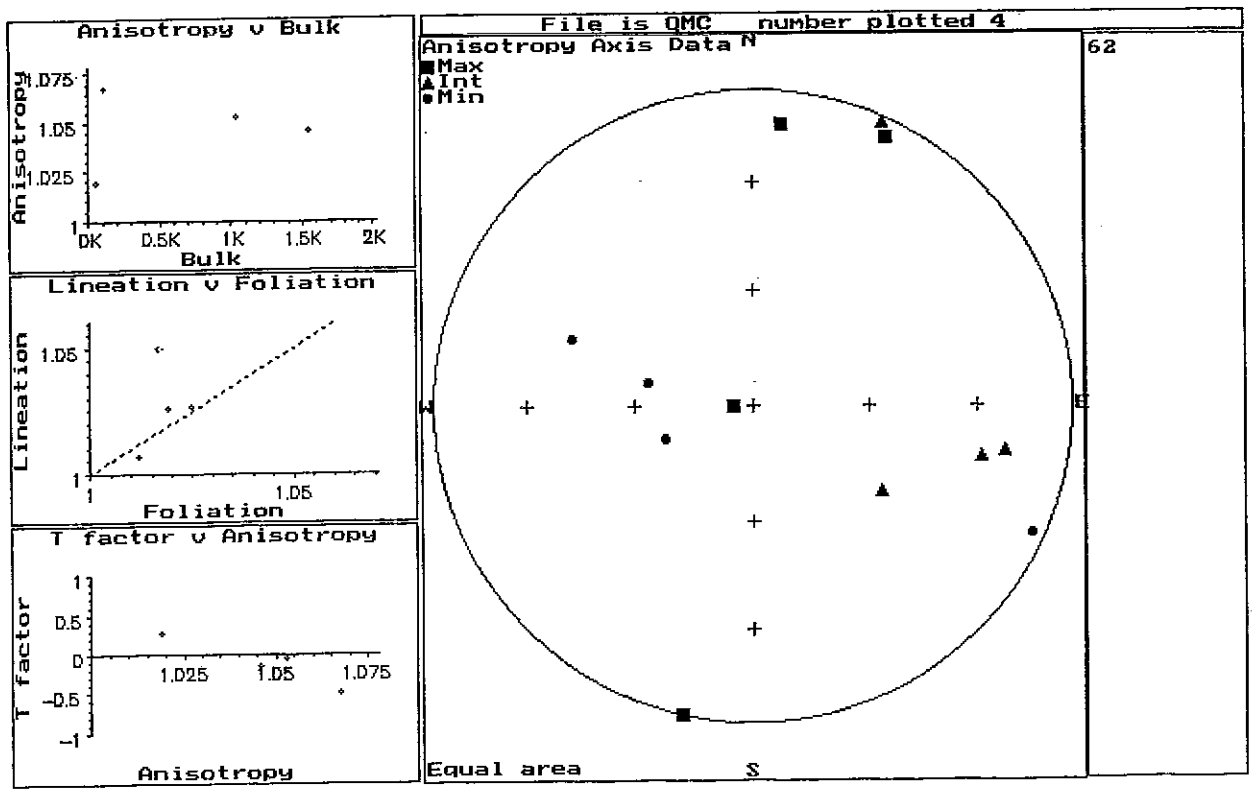
Anisotropy v Bulk
Anisotropy
1.075
1.05
1.025
1
0K
0.5K
1K
1.5K
2K
Bulk
Lineation v Foliation
Lineation
1.05
1
1
1.05
Foliation
T factor v Anisotropy
T factor
1
0.5
0
-0.5
-1
1.025
1.05
1.075
Anisotropy
File is QMC number plotted 4
Anisotropy Axis Data
Max
Int
Min
N
W
E
S
Equal area
62

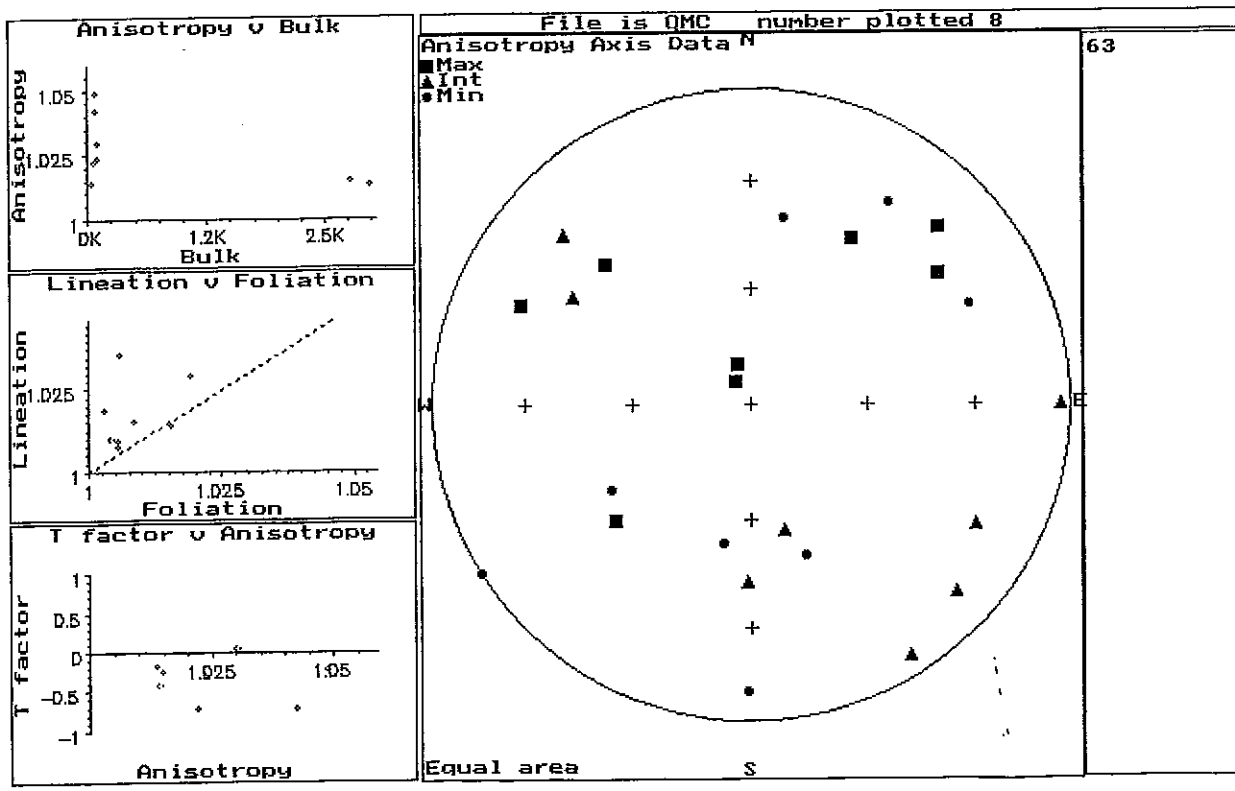
Anisotropy v Bulk
Anisotropy
1.05
1.025
1
0K
1.2K
2.5K
Bulk
Lineation v Foliation
Lineation
1.025
1
1
1.025
1.05
Foliation
T factor v Anisotropy
T factor
1
0.5
0
-0.5
-1
1.025
1.05
Anisotropy
File is QMC number plotted 8
Anisotropy Axis Data
Max
Int
Min
N
W
E
S
Equal area
63

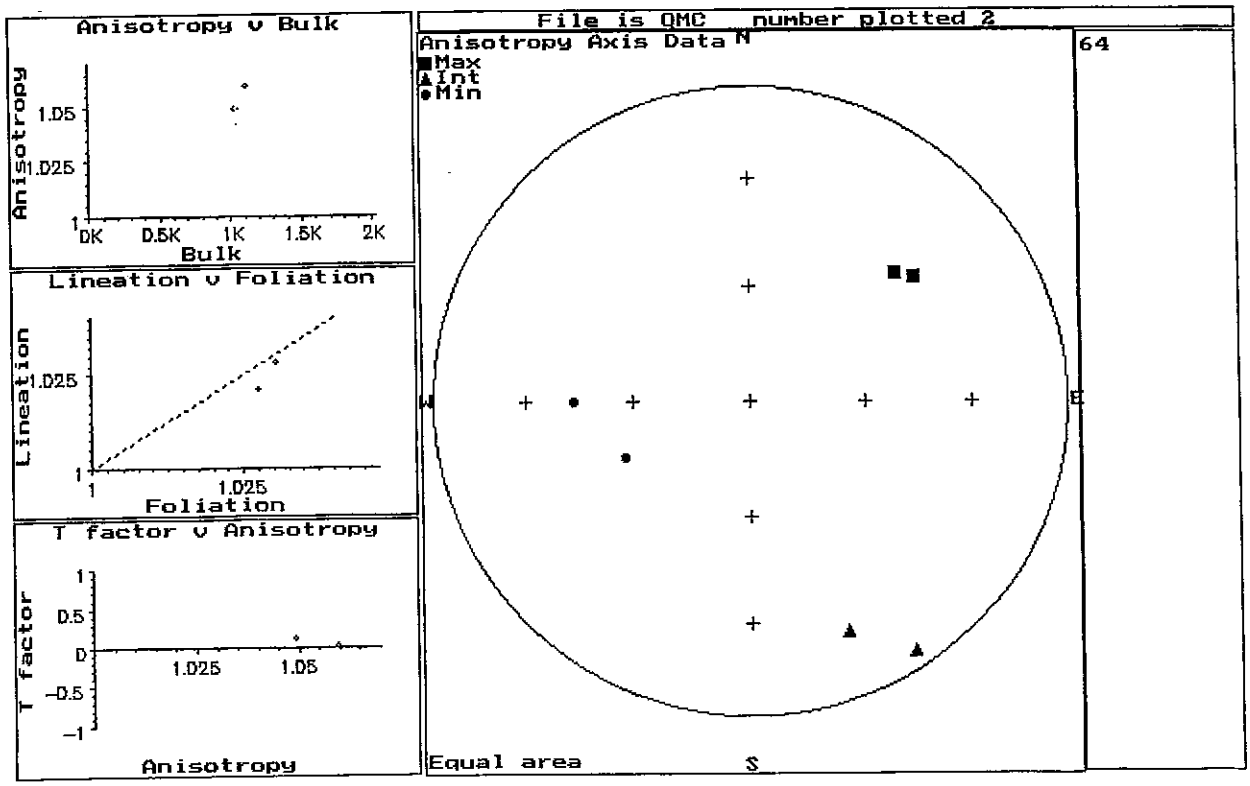
Anisotropy v Bulk
Anisotropy
1.05
1.025
1
0K
0.5K
1K
1.5K
2K
Bulk
Lineation v Foliation
Lineation
1.025
1
1
1.025
Foliation
T factor v Anisotropy
T factor
1
0.5
0
-0.5
-1
1.025
1.05
Anisotropy
File is QMC number plotted 2
Anisotropy Axis Data
Max
Int
Min
N
W
E
S
64
Equal area

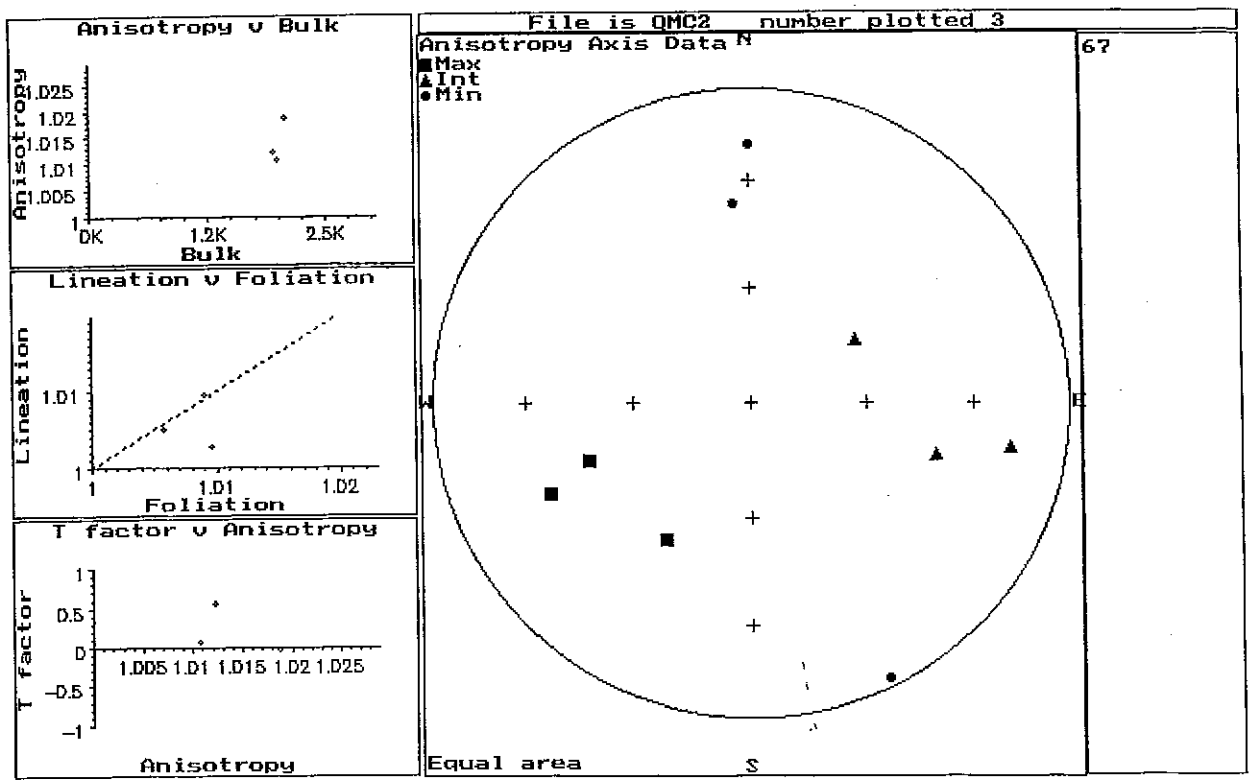
Anisotropy v Bulk
Anisotropy
1.025
1.02
1.015
1.01
1.005
1
0K
1.2K
2.5K
Bulk
Lineation v Foliation
Lineation
1.01
1
1
1.01
1.02
Foliation
T factor v Anisotropy
T factor
1
0.5
0
-0.5
-1
1.005 1.01 1.015 1.02 1.025
Anisotropy
File is QMC2 number plotted 3
Anisotropy Axis Data
Max
Int
Min
N
W
E
S
67
Equal area

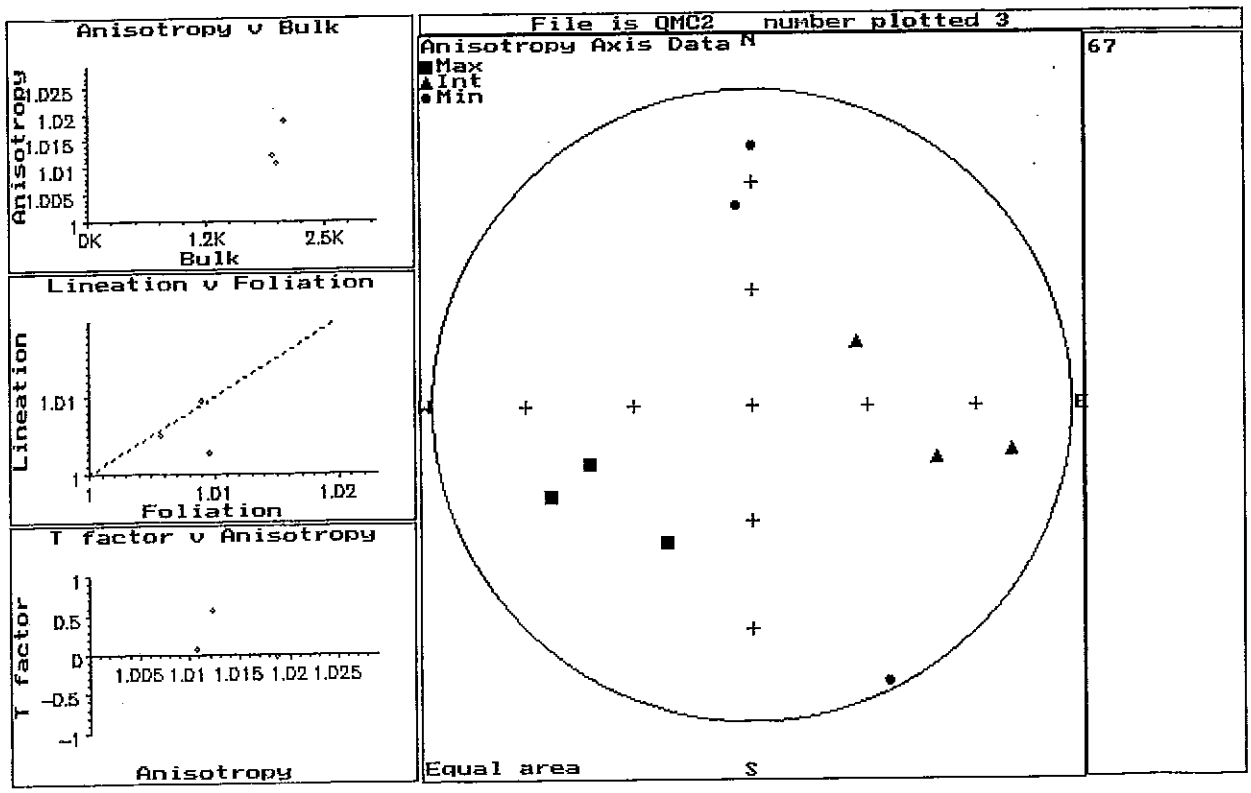
Anisotropy v Bulk
Anisotropy
1.025
1.02
1.015
1.01
1.005
1
0K
1.2K
2.5K
Bulk
Lineation v Foliation
Lineation
1.01
1
1
1.01
1.02
Foliation
T factor v Anisotropy
T factor
1
0.5
0
-0.5
-1
1.005 1.01 1.015 1.02 1.025
Anisotropy
File is QMC2 number plotted 3
Anisotropy Axis Data
Max
Int
Min
N
E
S
Equal area
67

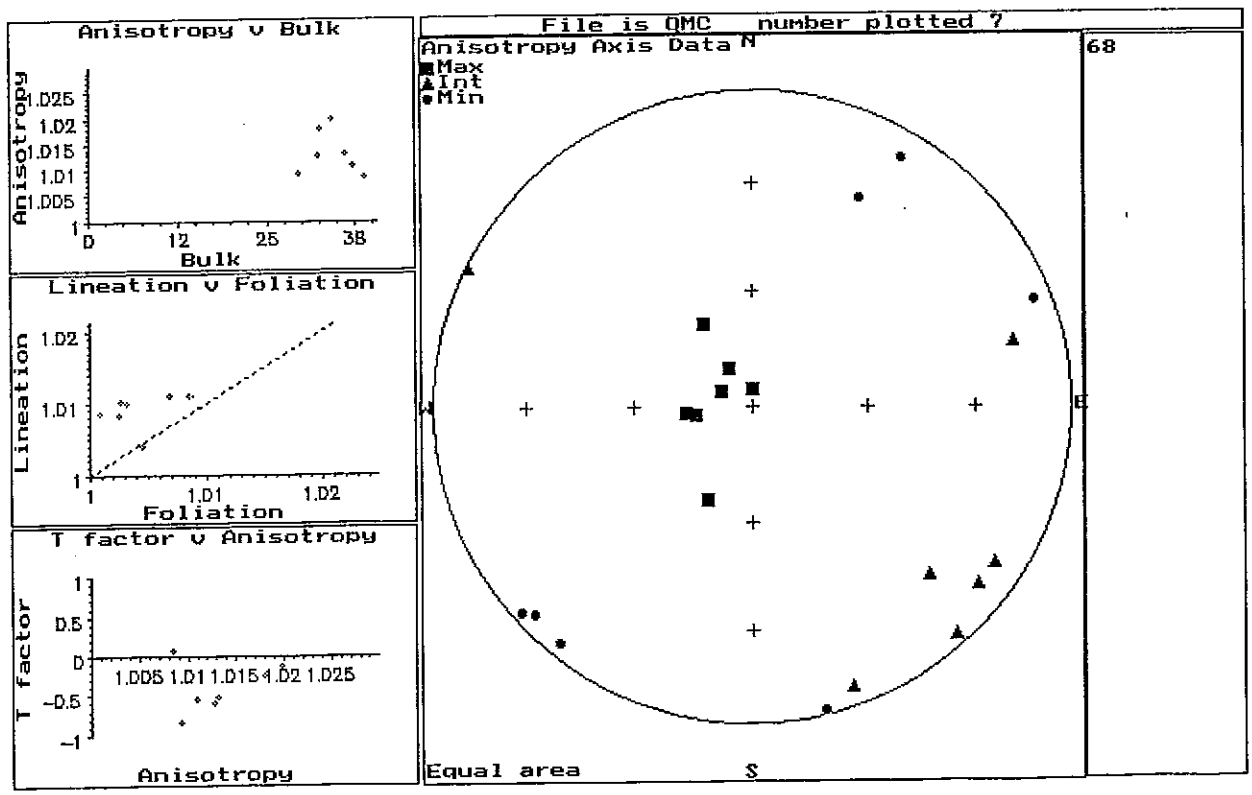
Anisotropy v Bulk
Anisotropy
1.025
1.02
1.015
1.01
1.005
1
0
12
25
38
Bulk
Lineation v Foliation
Lineation
1.02
1.01
1
1
1.01
1.02
Foliation
T factor v Anisotropy
T factor
1
0.5
0
-0.5
-1
1.005 1.01 1.015 1.02 1.025
Anisotropy
File is QMC number plotted 7
Anisotropy Axis Data
Max
Int
Min
N
E
S
Equal area
68

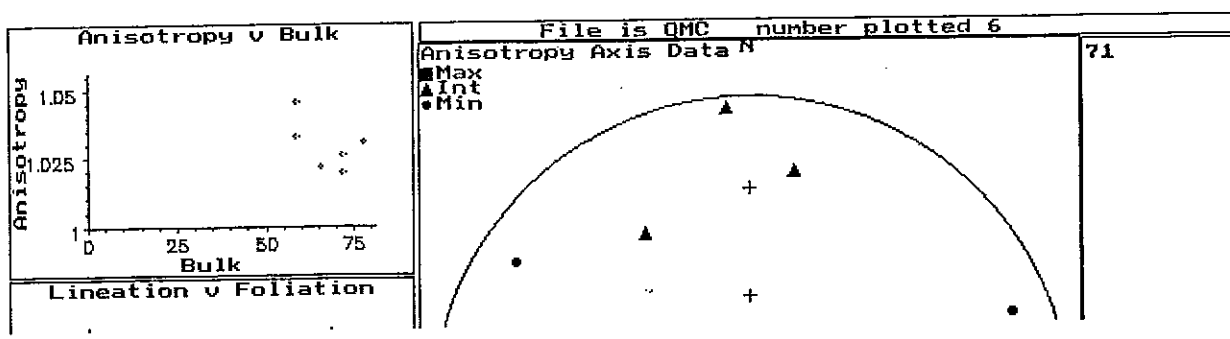
Anisotropy v Bulk
Anisotropy
1.05
1.025
1
0
25
50
75
Bulk
Lineation v Foliation
File is QMC number plotted 6
Anisotropy Axis Data
Max
Int
Min
N
71

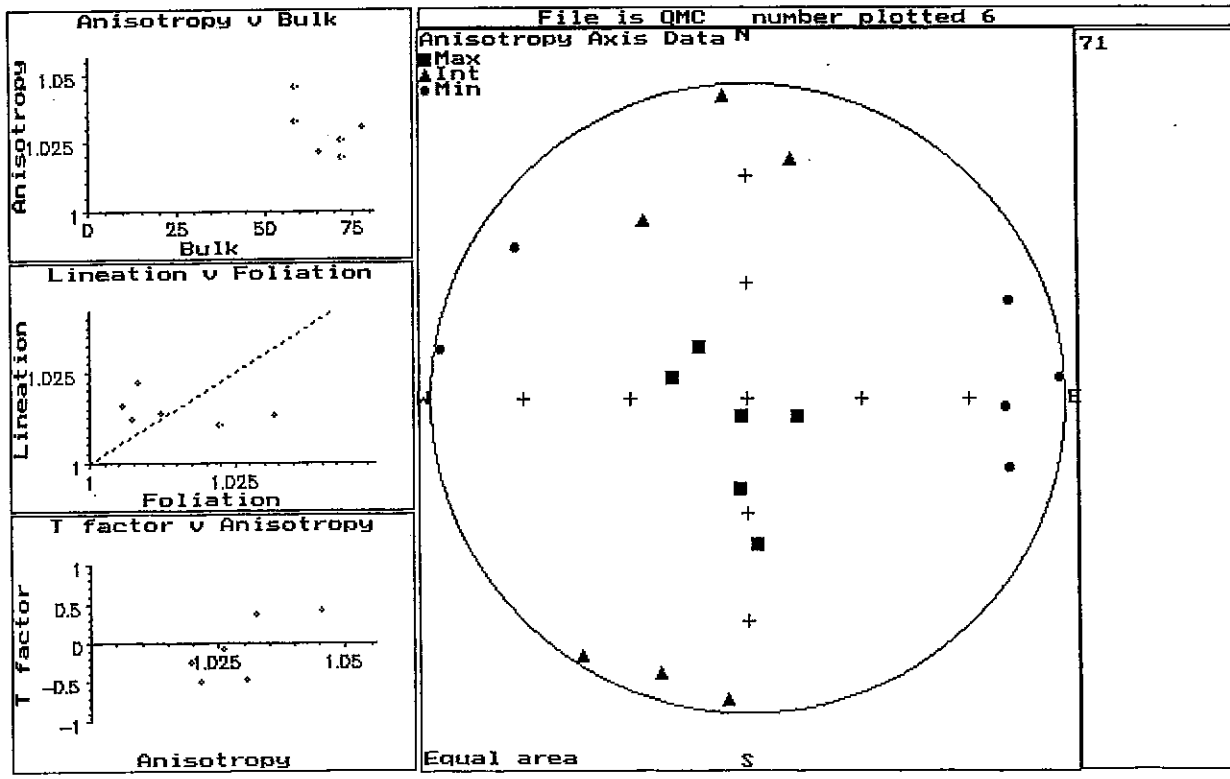
Anisotropy v Bulk
Anisotropy
1.05
1.025
1
0
25
50
75
Bulk
Lineation v Foliation
Lineation
1.025
1
1
1.025
Foliation
T factor v Anisotropy
T factor
1
0.5
0
-0.5
-1
1.025
1.05
Anisotropy
File is QMC number plotted 6
Anisotropy Axis Data
Max
Int
Min
N
W
E
S
Equal area
71

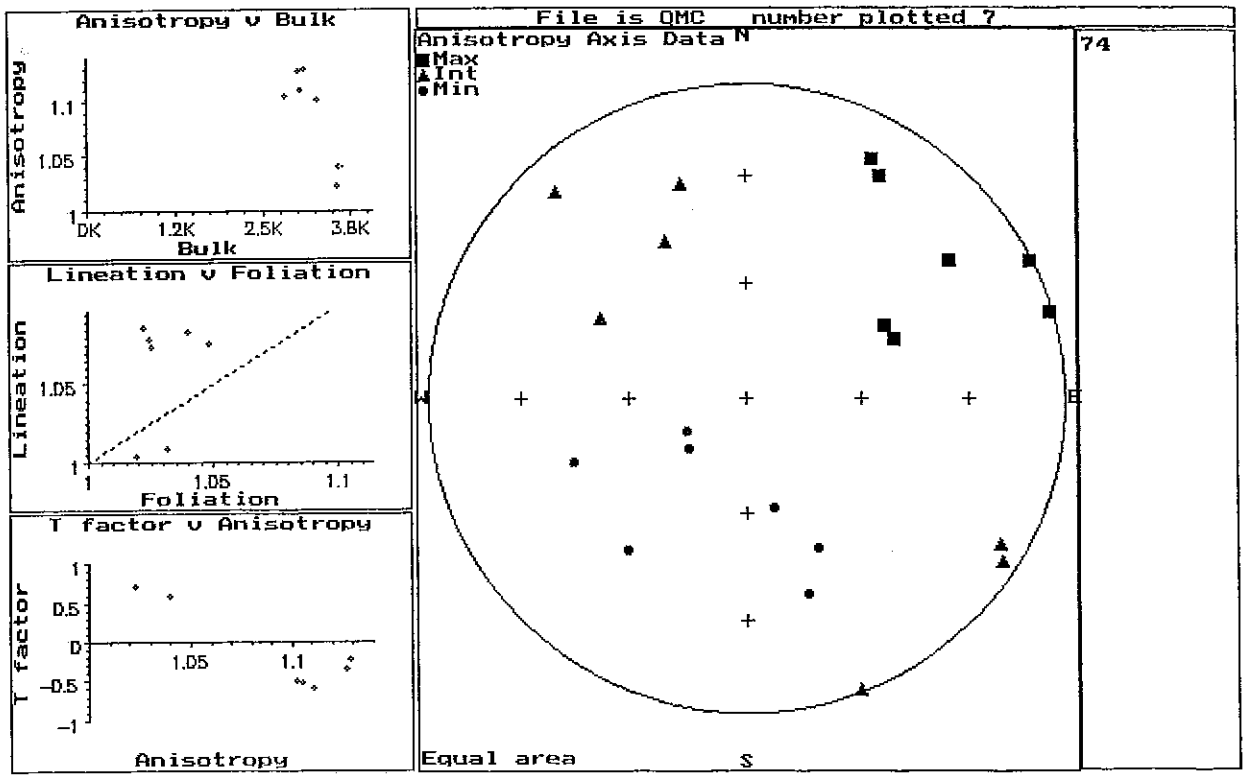
Anisotropy v Bulk
Anisotropy
1.1
1.05
1
0K
1.2K
2.5K
3.8K
Bulk
Lineation v Foliation
Lineation
1.05
1
1
1.05
1.1
Foliation
T factor v Anisotropy
T factor
1
0.5
0
-0.5
-1
1.05
1.1
Anisotropy
File is QMC number plotted 7
Anisotropy Axis Data
Max
Int
Min
N
W
E
S
Equal area
74

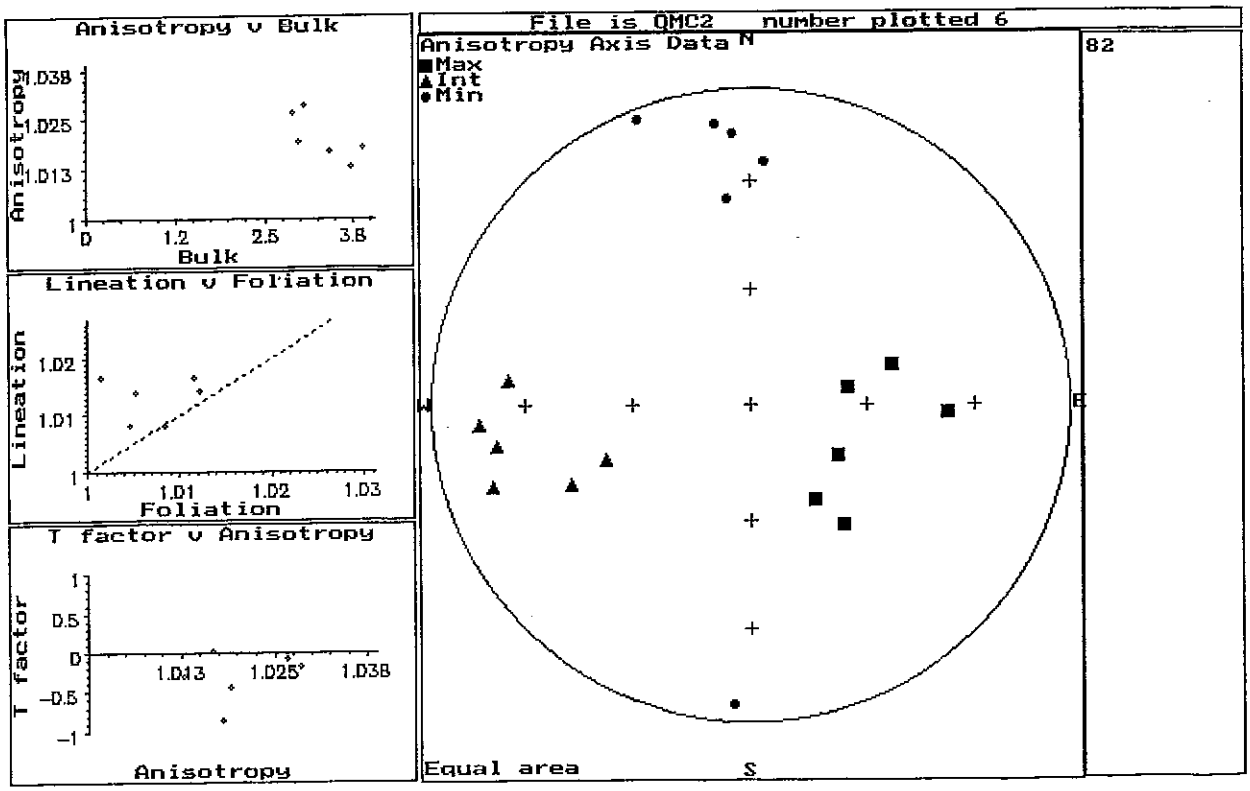
Anisotropy v Bulk
Anisotropy
1.038
1.025
1.013
1
1
1.2
2.5
3.8
Bulk
Lineation v Foliation
Lineation
1.02
1.01
1
1
1.01
1.02
1.03
Foliation
T factor v Anisotropy
T factor
1
0.5
0
-0.5
-1
1.013
1.025
1.038
Anisotropy
File is QMC2 number plotted 6
Anisotropy Axis Data
Max
Int
Min
N
W
E
S
Equal area
82

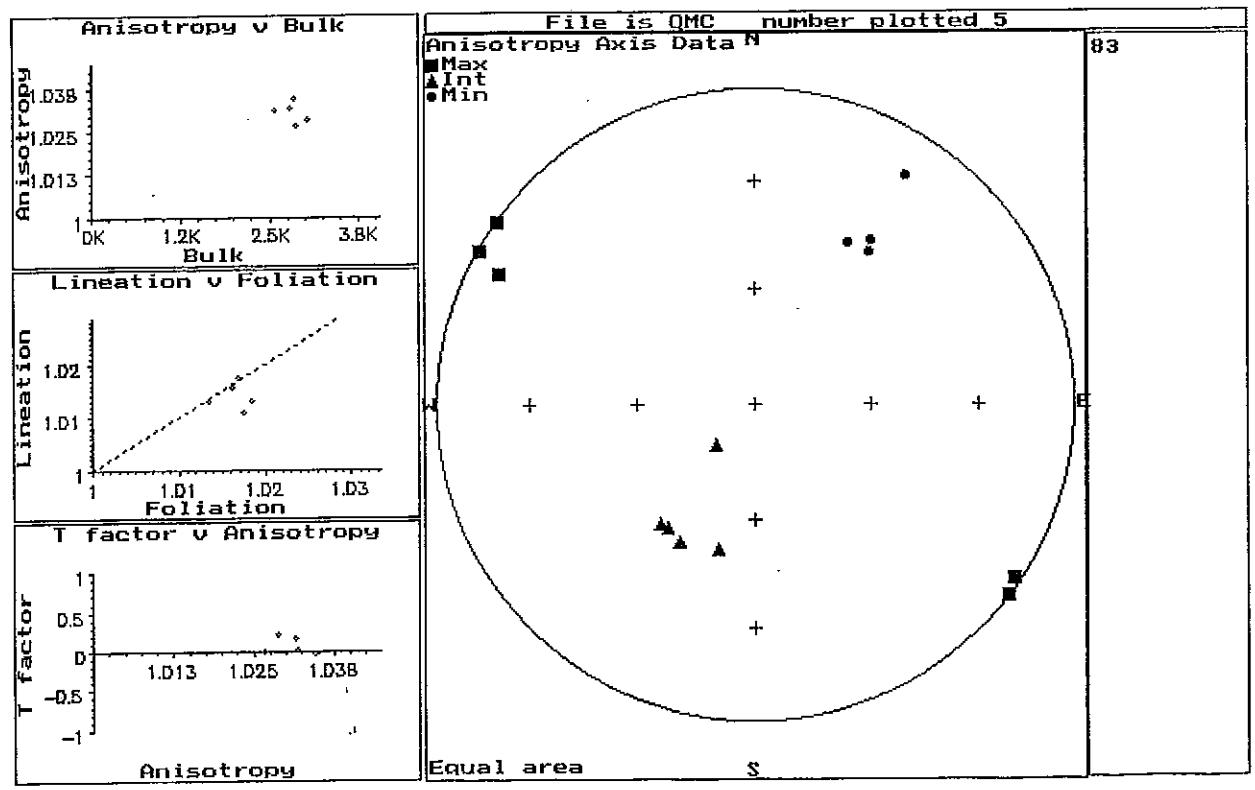
Anisotropy v Bulk
Anisotropy
1.038
1.025
1.013
1
1K
1.2K
2.5K
3.8K
Bulk
Lineation v Foliation
Lineation
1.02
1.01
1
1
1.01
1.02
1.03
Foliation
T factor v Anisotropy
T factor
1
0.5
0
-0.5
-1
1.013
1.025
1.038
Anisotropy
File is QMC number plotted 5
Anisotropy Axis Data
Max
Int
Min
N
W
E
S
Equal area
83

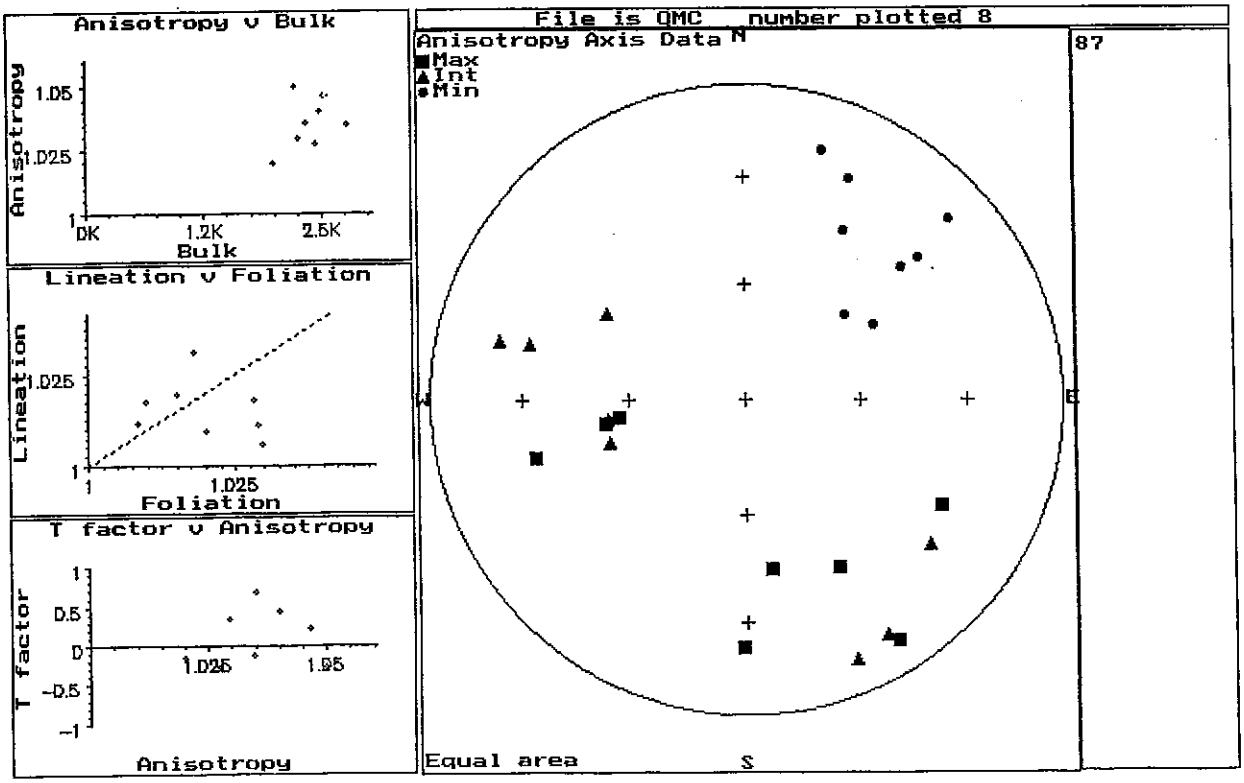
Anisotropy v Bulk
Anisotropy
1.05
1.025
1
0K
1.2K
2.5K
Bulk
Lineation v Foliation
Lineation
1.025
1
1.025
Foliation
T factor v Anisotropy
T factor
1
0.5
0
-0.5
-1
1.025
1.05
Anisotropy
File is QMC number plotted 8
Anisotropy Axis Data
Max
Int
Min
N
87
W
E
Equal area
S

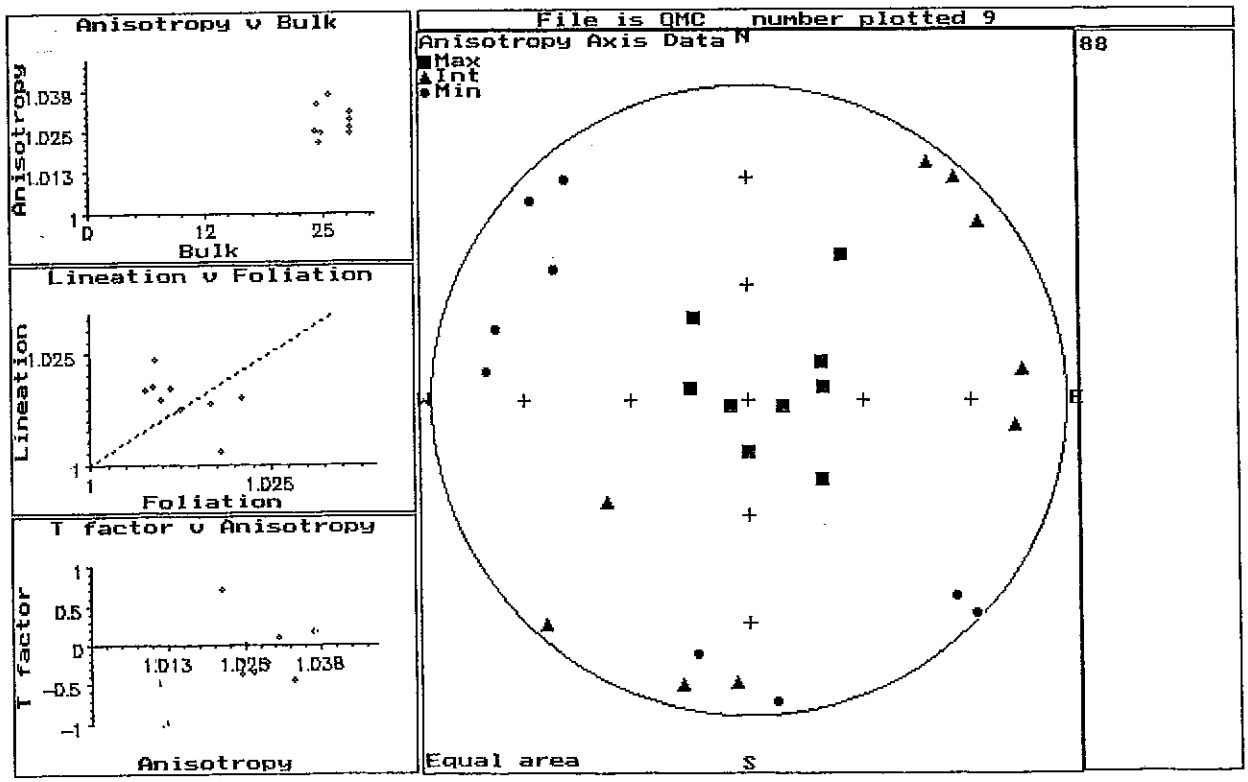
Anisotropy v Bulk
Anisotropy
1.038
1.025
1.013
1
0
12
25
Bulk
Lineation v Foliation
Lineation
1.025
1
1
1.025
Foliation
T factor v Anisotropy
T factor
1
0.5
0
-0.5
-1
1.013
1.025
1.038
Anisotropy
File is QMC number plotted 9
Anisotropy Axis Data
Max
Int
Min
N
88
W
E
Equal area
S

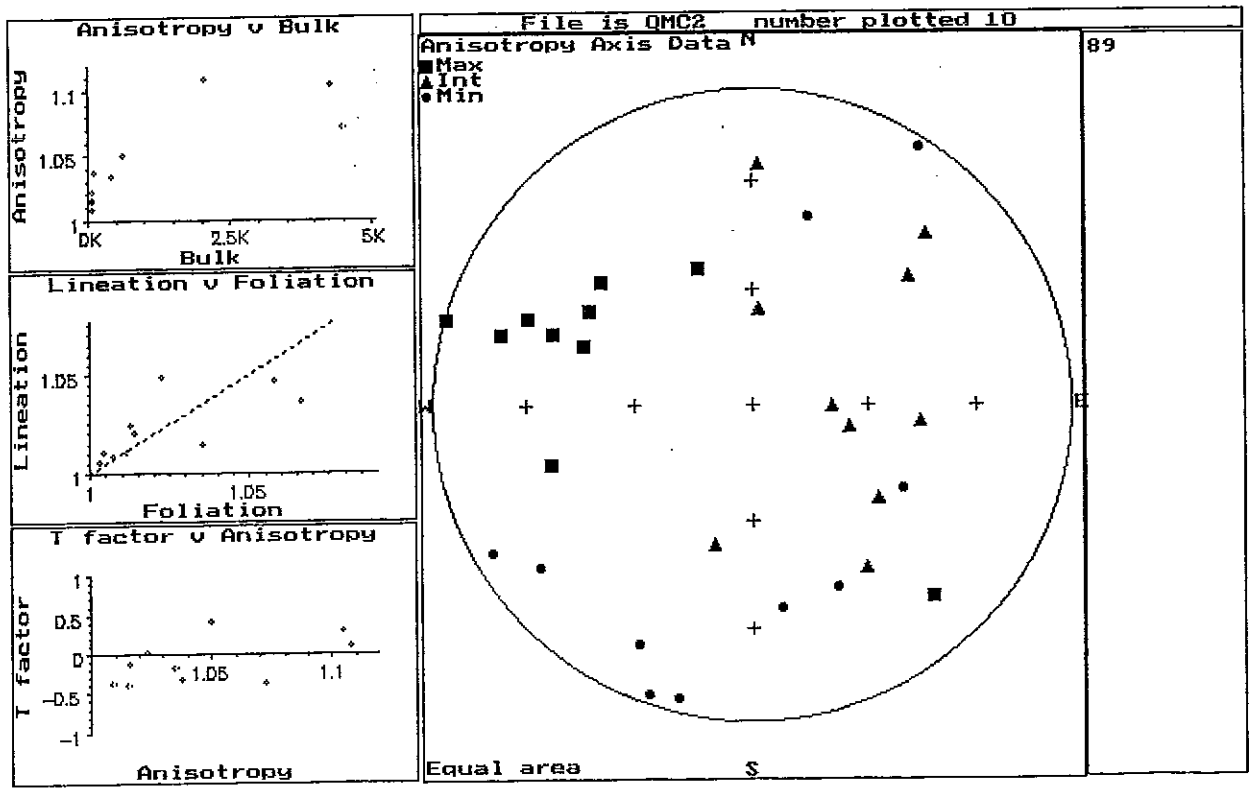
Anisotropy v Bulk
Anisotropy
1.1
1.05
1
0K
2.5K
5K
Bulk
Lineation v Foliation
Lineation
1.05
1
1
1.05
Foliation
T factor v Anisotropy
T factor
1
0.5
0
−0.5
−1
1.05
1.1
Anisotropy
File is QMC2 number plotted 10
Anisotropy Axis Data N
Max
Int
Min
89
E
Equal area
S

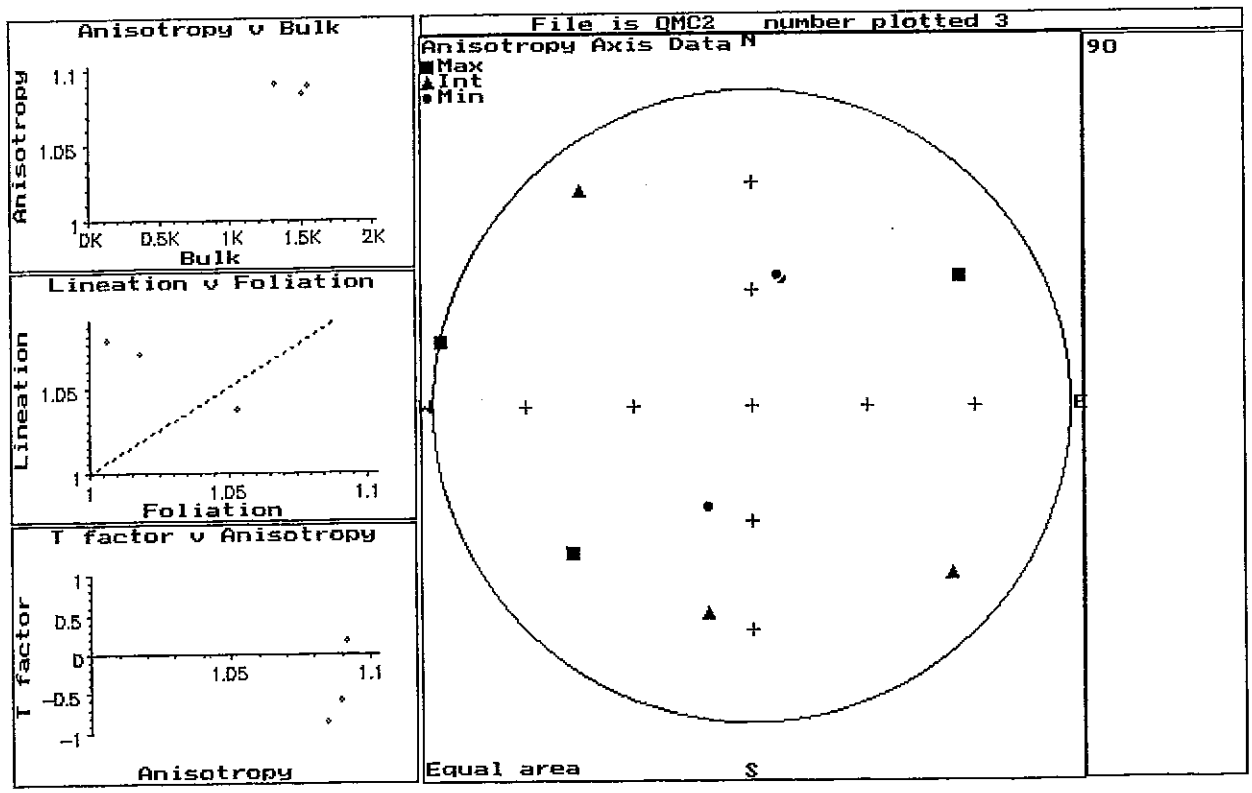
Anisotropy v Bulk
Anisotropy
1.1
1.05
1
0K
0.5K
1K
1.5K
2K
Bulk
Lineation v Foliation
Lineation
1.05
1
1
1.05
1.1
Foliation
T factor v Anisotropy
T factor
1
0.5
0
−0.5
−1
1.05
1.1
Anisotropy
File is QMC2 number plotted 3
Anisotropy Axis Data N
Max
Int
Min
90
E
Equal area
S

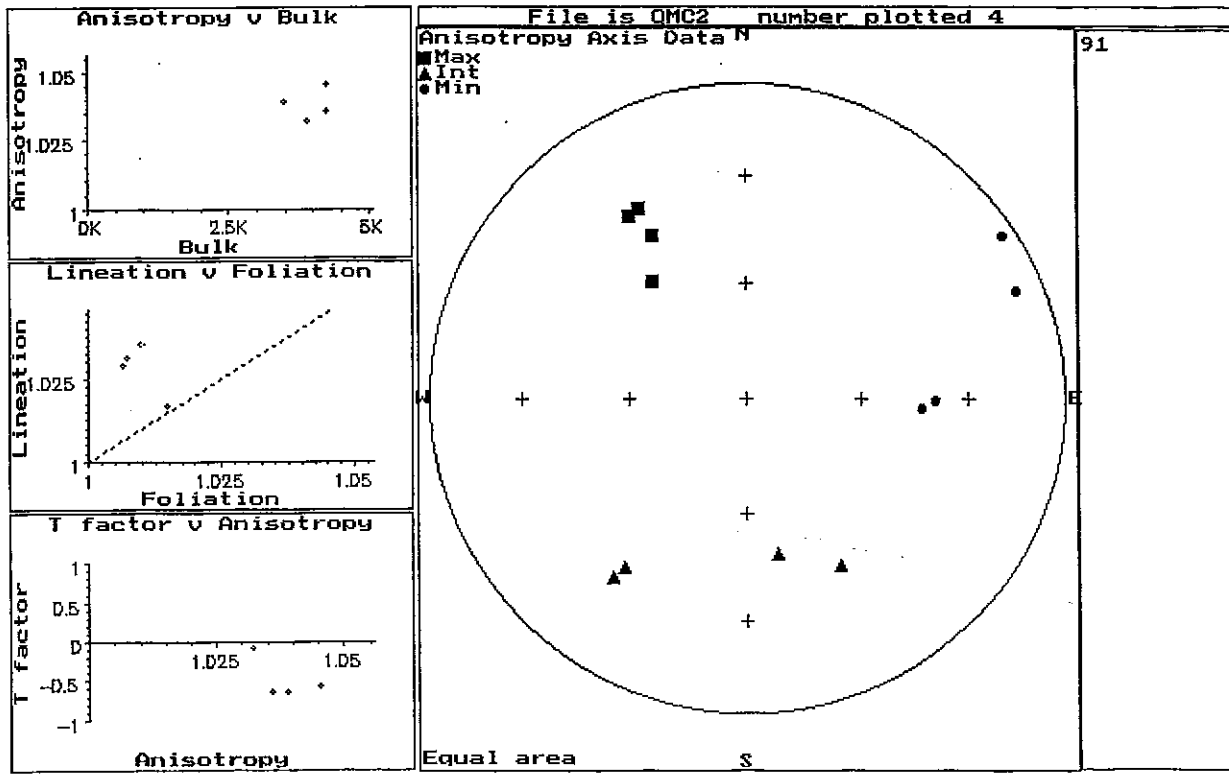
Anisotropy v Bulk
Anisotropy
1.05
1.025
1
0K
2.5K
5K
Bulk
Lineation v Foliation
Lineation
1.025
1
1
1.025
1.05
Foliation
T factor v Anisotropy
T factor
1
0.5
0
-0.5
-1
1.025
1.05
Anisotropy
File is QMC2 number plotted 4
Anisotropy Axis Data
Max
Int
Min
N
W
E
S
Equal area
91

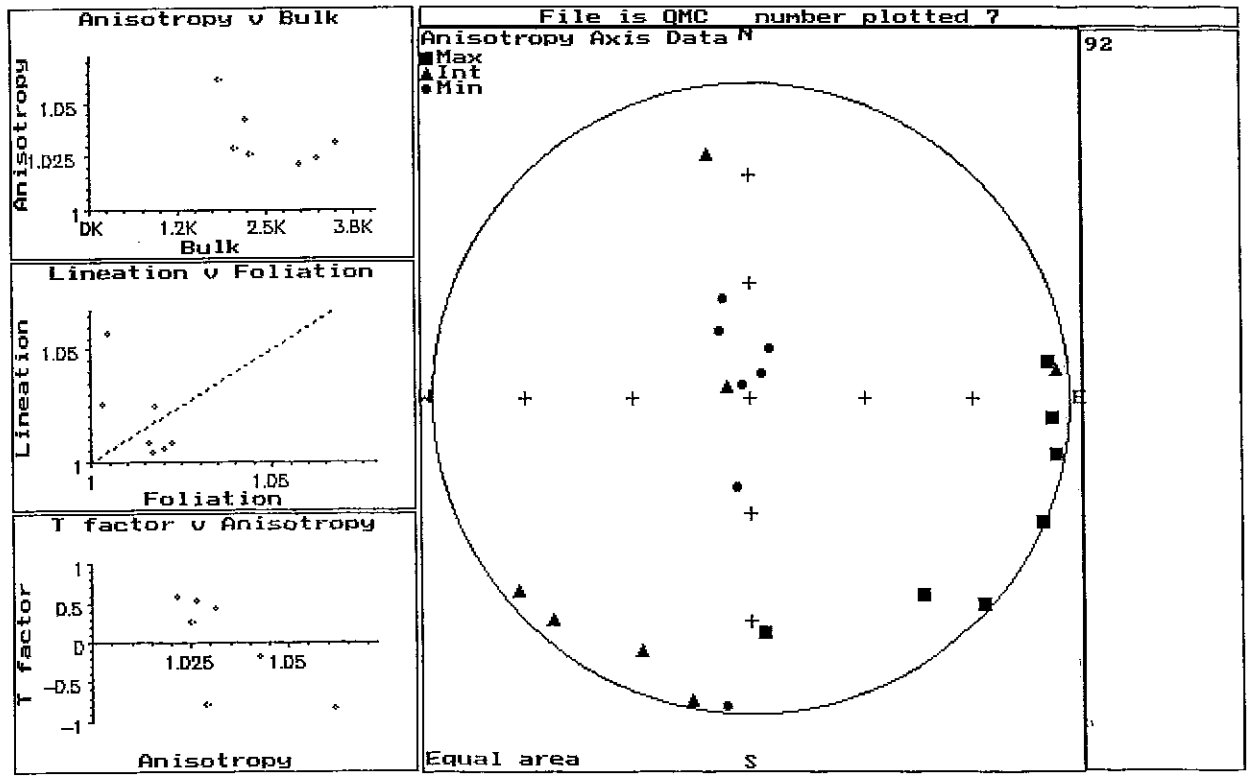
Anisotropy v Bulk
Anisotropy
1.05
1.025
1
0K
1.2K
2.5K
3.8K
Bulk
Lineation v Foliation
Lineation
1.05
1
1
1.05
Foliation
T factor v Anisotropy
T factor
1
0.5
0
-0.5
-1
1.025
1.05
Anisotropy
File is QMC number plotted 7
Anisotropy Axis Data
Max
Int
Min
N
W
E
S
Equal area
92

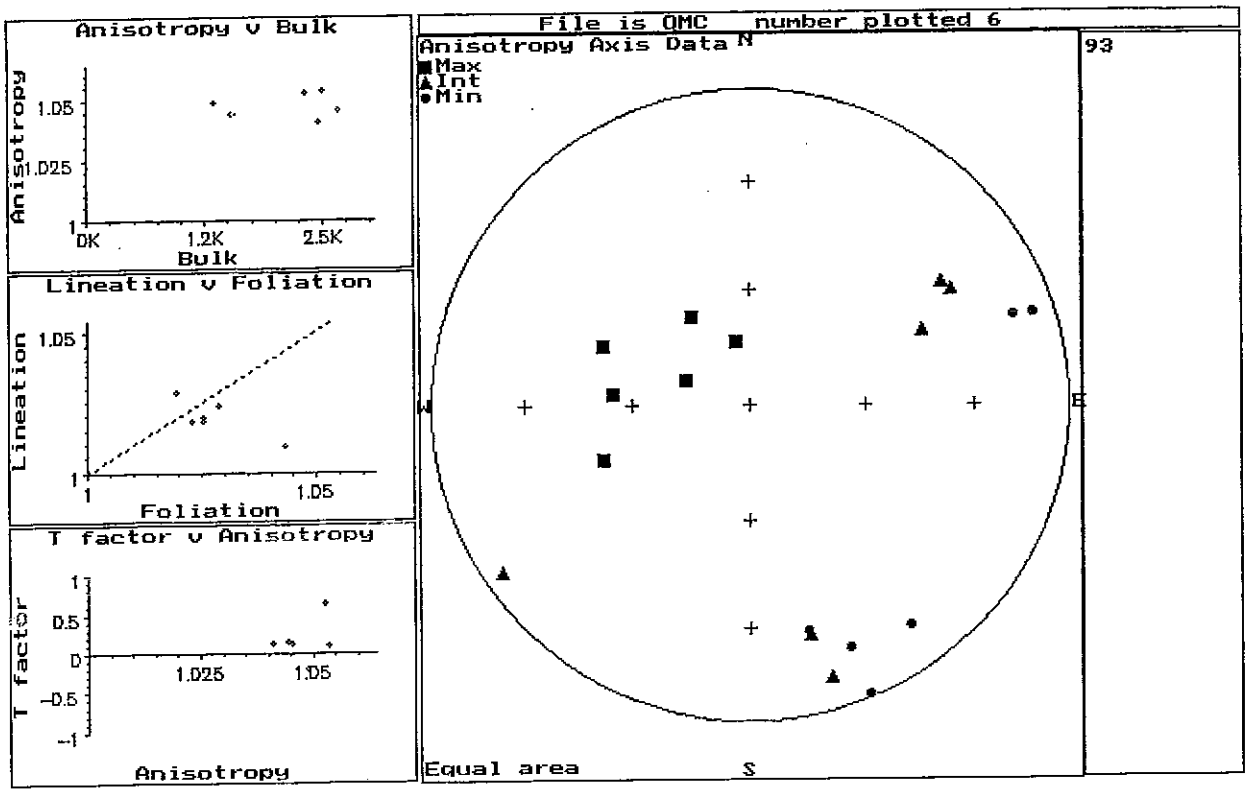
Anisotropy v Bulk
Anisotropy
1.05
1.025
1
0K
1.2K
2.5K
Bulk
Lineation v Foliation
Lineation
1.05
1
1
1.05
Foliation
T factor v Anisotropy
T factor
1
0.5
0
-0.5
-1
1.025
1.05
Anisotropy
File is OMC number plotted 6
Anisotropy Axis Data
Max
Int
Min
N
93
W
E
Equal area
S

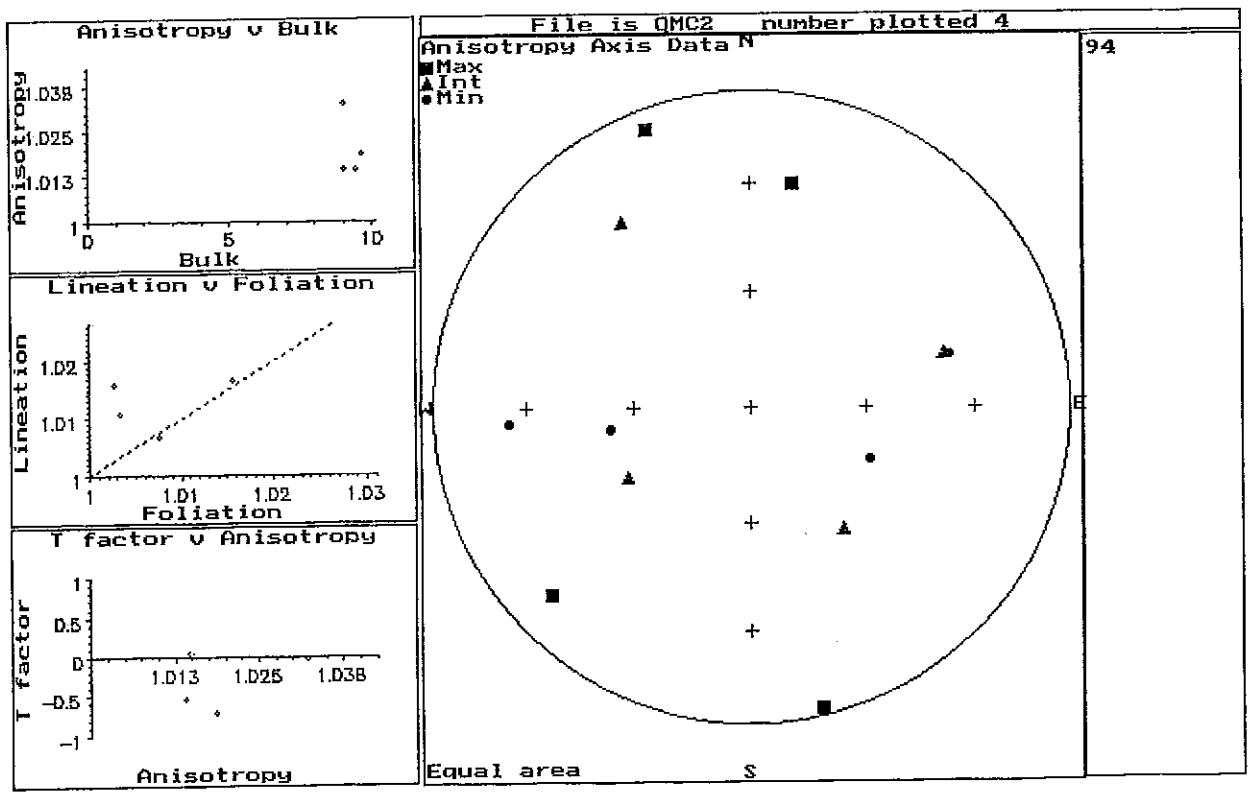
Anisotropy v Bulk
Anisotropy
1.038
1.025
1.013
1
0
5
10
Bulk
Lineation v Foliation
Lineation
1.02
1.01
1
1
1.01
1.02
1.03
Foliation
T factor v Anisotropy
T factor
1
0.5
0
-0.5
-1
1.013
1.025
1.038
Anisotropy
File is OMC2 number plotted 4
Anisotropy Axis Data
Max
Int
Min
N
94
W
E
Equal area
S

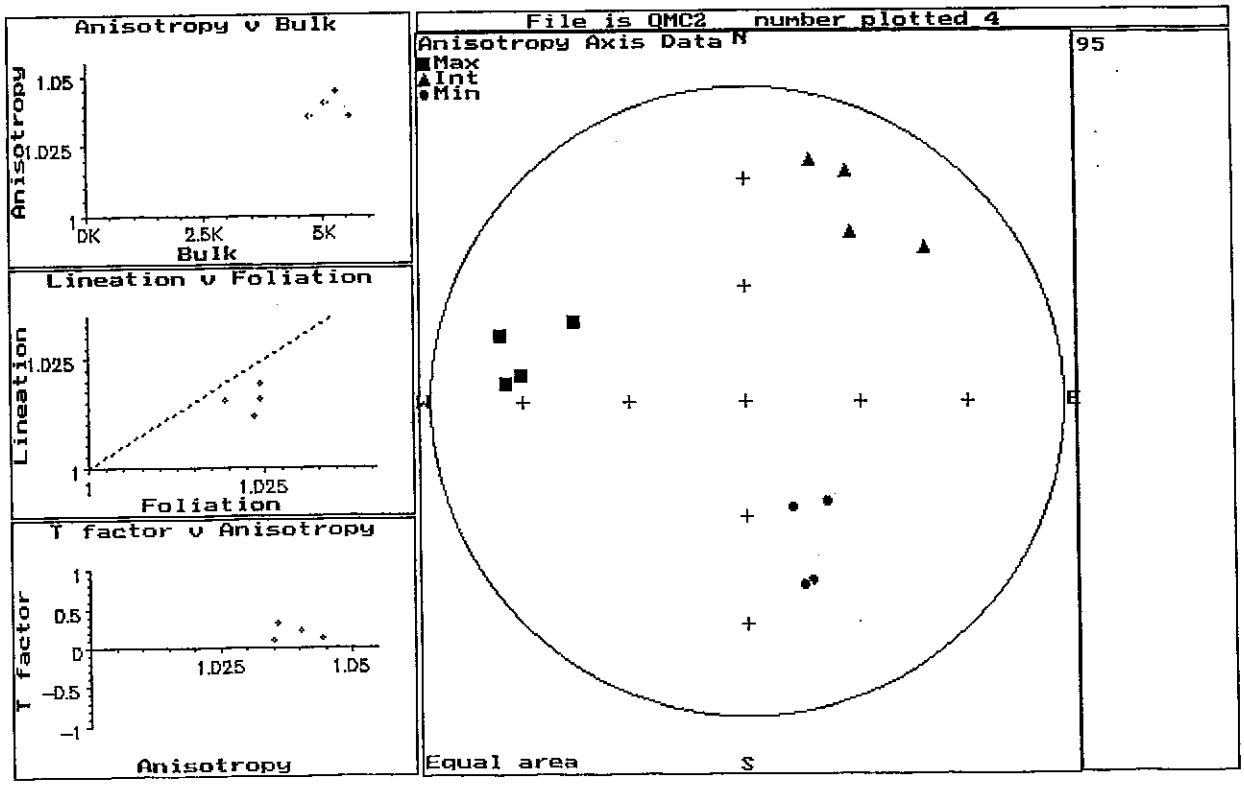
Anisotropy v Bulk
Anisotropy
1.05
1.025
1
0K
2.5K
5K
Bulk
Lineation v Foliation
Lineation
1.025
1
1
1.025
Foliation
T factor v Anisotropy
T factor
1
0.5
0
-0.5
-1
1.025
1.05
Anisotropy
File is QMC2 number plotted 4
Anisotropy Axis Data
N
Max
Int
Min
W
E
S
Equal area
95

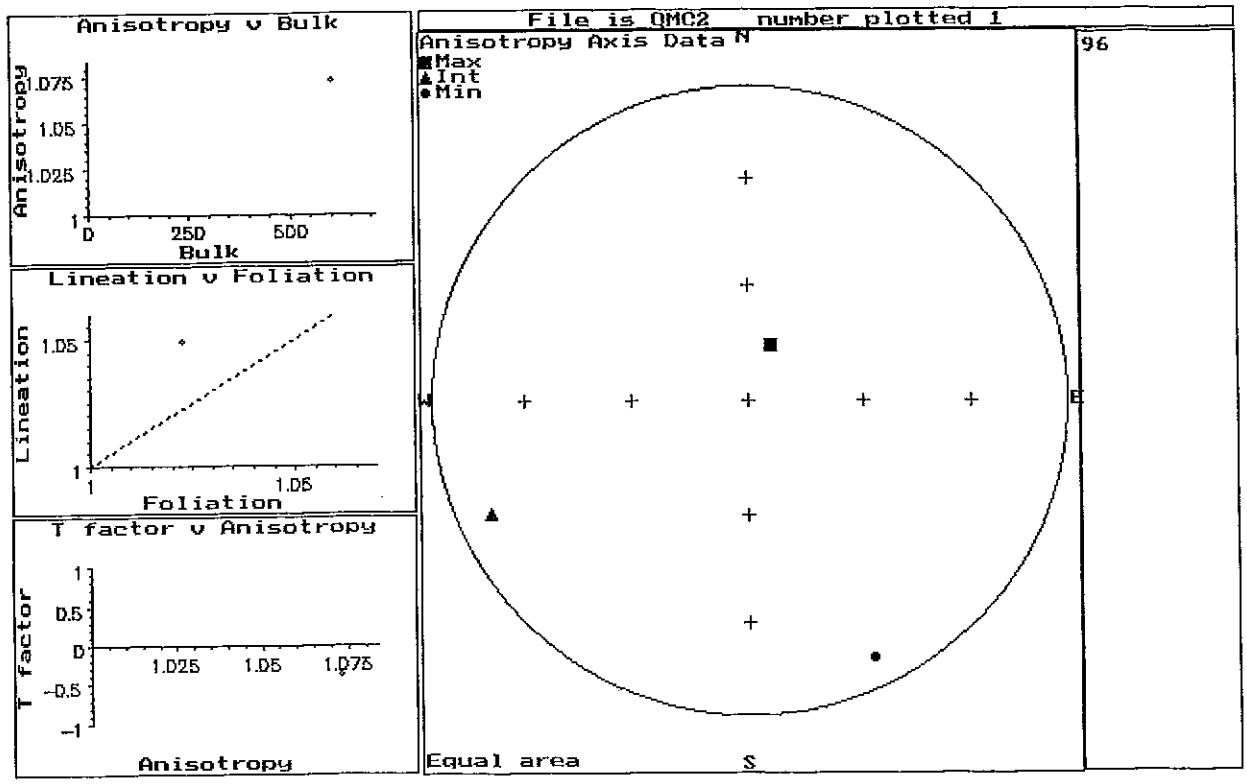
Anisotropy v Bulk
Anisotropy
1.075
1.05
1.025
1
0
250
500
Bulk
Lineation v Foliation
Lineation
1.05
1
1
1.05
Foliation
T factor v Anisotropy
T factor
1
0.5
0
-0.5
-1
1.025
1.05
1.075
Anisotropy
File is QMC2 number plotted 1
Anisotropy Axis Data
N
Max
Int
Min
W
E
S
Equal area
96

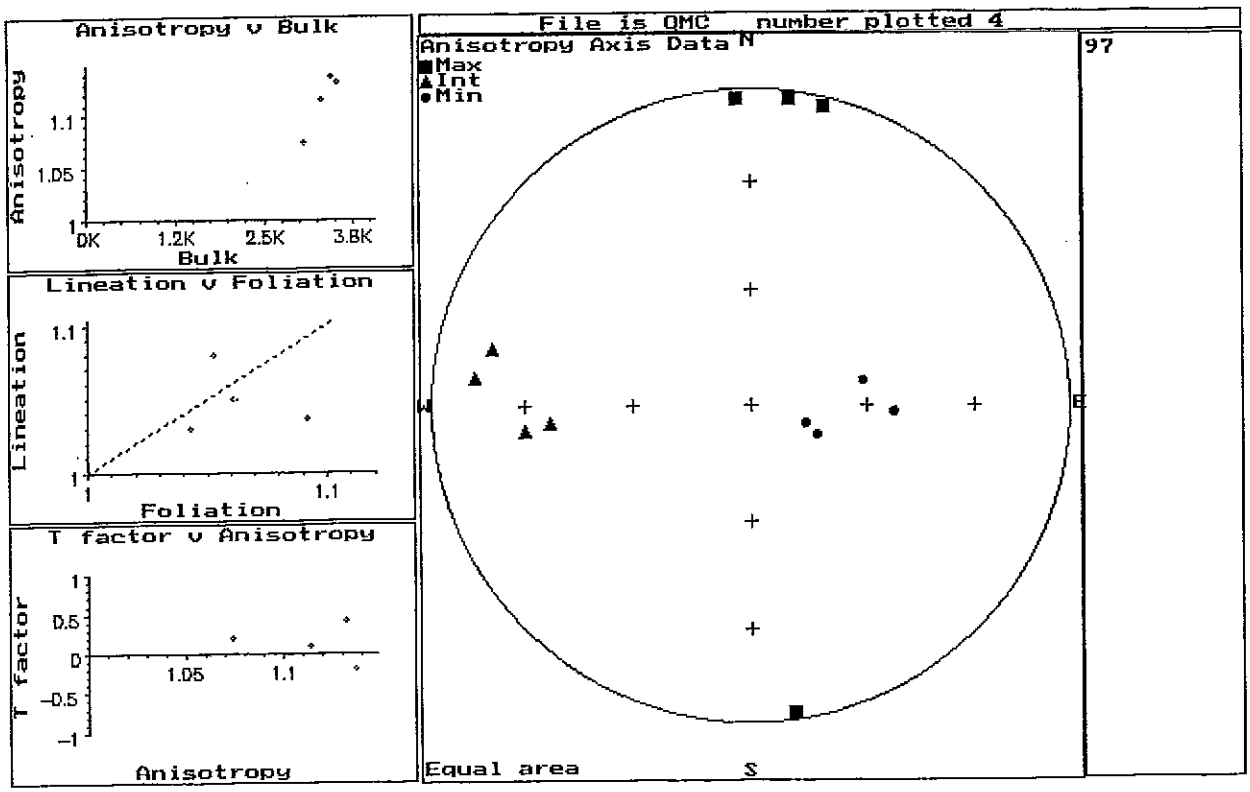
Anisotropy v Bulk
Anisotropy
1.1
1.05
1
0K
1.2K
2.5K
3.8K
Bulk
Lineation v Foliation
Lineation
1.1
1
1
1.1
Foliation
T factor v Anisotropy
T factor
1
0.5
0
-0.5
-1
1.05
1.1
Anisotropy
File is QMC number plotted 4
Anisotropy Axis Data
Max
Int
Min
N
W
E
S
Equal area
97